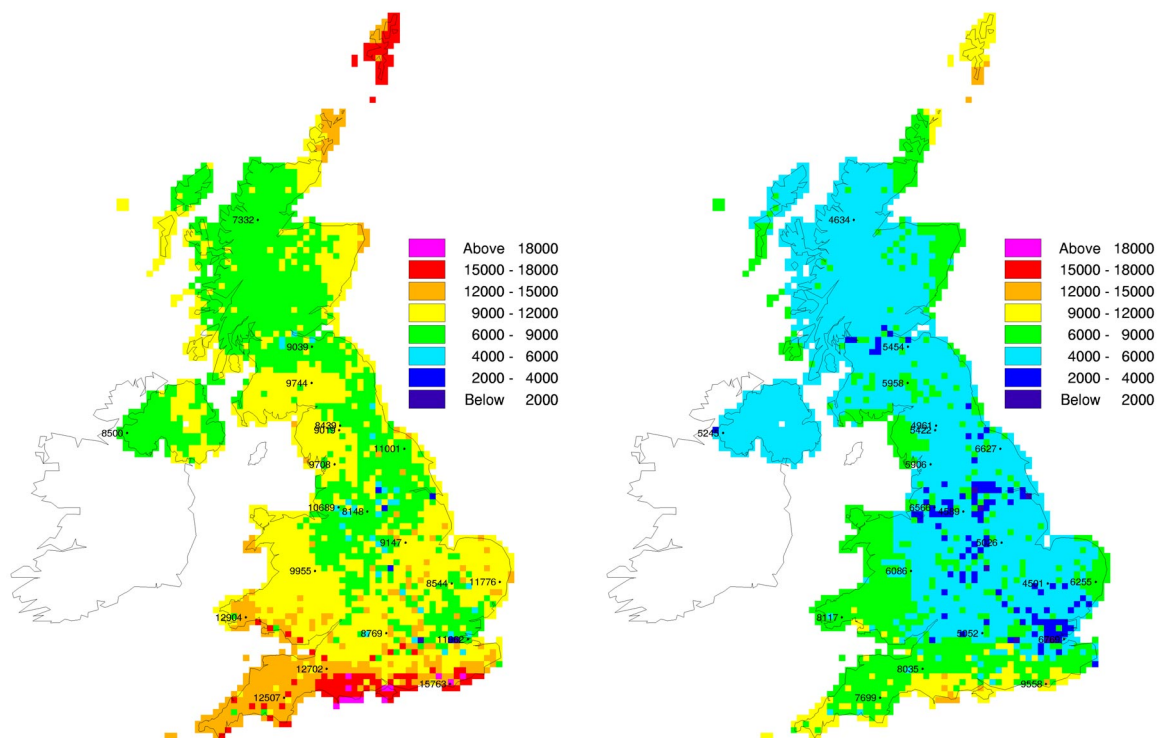


Modelling of Tropospheric Ozone

A report produced for the Department for Environment, Food and Rural Affairs, the Scottish Executive, Welsh Assembly Government and the Department of the Environment Northern Ireland



**AOT40 Crops for the 2020 Base Case Run
with and without Changing Atmospheric Composition arising from Climate Change**

Title	Modelling of Tropospheric Ozone
Customer	Department for Environment, Food and Rural Affairs, the Scottish Executive, Welsh Assembly Government and the Department of the Environment Northern Ireland
Customer reference	EPG 1/3/200
Confidentiality, copyright and reproduction	
File reference	
Report number	AEAT/ENV/R/2100
Report status	Issue 1

AEA Technology plc
netcen
 551 Harwell
 Didcot
 Oxon., OX11 0QJ

Telephone: 0870-190-6488
 Facsimile 0870-190-6607

netcen is an operating division of AEA Technology plc
 AEA Technology is certificated to BS EN ISO9001:(2001)

	Name	Signature	Date
Author	Garry Hayman John Abbott Claire Thomson Tony Bush Andrew Kent Dick Derwent Mike Jenkin Mike Pilling Andrew Rickard Louise Whitehead		12/2005
Reviewed by	Garry Hayman Geoff Dollard		12/2005
Approved by	Garry Hayman		12/2005 03/2006

Version History

Version	Version Number	Date Available
Initial Draft	AEAT/ENV/R/2100 Draft	2 nd December 2005
Draft reviewed by Geoff Dollard	AEAT/ENV/R/2100 Draft 2	9 th December 2005
Draft submitted for external review by Defra, Devolved Administrations and Project Partners	AEAT/ENV/R/2100 Draft 3 for External Comment	13 th December 2005
Release Issue (including comments from Defra)	AEAT/ENV/R/2100 Issue 1	31 st March 2006

Executive Summary

The Department for Environment, Food and Rural Affairs (Defra) and the Devolved Administrations (the Scottish Executive, Welsh Assembly Government and the Department of the Environment Northern Ireland) awarded the contract **Modelling of Tropospheric Ozone** (EPG 1/3/200) to a consortium led by **netcen** (part of AEA Technology). The contract addresses ground-level ozone, its formation, impacts and control.

The non-linear nature of ground-level ozone production requires the use of sophisticated chemical transport models to understand its production and subsequent control. The Department and the Devolved Administrations (DAs) have funded the development of a number of models over the years. They seek to build on this work but now require a modelling capability to treat ozone formation (a) on all spatial scales from urban areas at high spatial resolution to the global scale so that ozone production on the regional and global scales is linked and (b) from timescales of hours to reproduce the diurnal behaviour of ozone to decades so that the influence of climate change can be assessed. The Ozone Source-receptor Model (OSRM) will be the main tool used to meet these requirements.

As part of their ozone research programme, Defra and the Devolved Administrations have supported the development of near explicit chemical mechanisms, especially that of the Master Chemical Mechanism. This was in recognition that a more targeted approach on ozone precursor emissions would bring greater environmental benefits than a simple percentage mass reduction. The Department and the DAs are continuing their support for this work.

The new project is not a simple continuation of earlier work. There is a stronger emphasis on model application to evaluate planned and proposed policies. In addition, new tasks have been identified: Technical assistance is required to fulfil commitments arising from the implementation of European Directives and in particular, the 3rd Daughter Directive on Ozone. Work is also in progress to move from the current AOT metrics for protection of ecosystems to a more realistic flux-based approach.

The principal aims of the project are:

- to maintain, develop and apply tools for modelling tropospheric ozone formation over a range of spatial scales
- to support and guide policy on emission reductions and objectives, and to verify compliance

To meet these aims and to address the intended applications, the programme of work had 5 main objectives or tasks:

- ❑ Objective 1 - **Development and Application of Ozone Models**
- ❑ Objective 2 - **Detailed Assessment of the Relationship between Ozone, NO and NO₂, and Factors Controlling Them**
- ❑ Objective 3 - **Policy Development and Scenario Analysis**
- ❑ Objective 4 - **Improvements to Photochemical Reaction Schemes**
- ❑ Objective 5 - **Development of Stomatal Flux Module for Crops and Semi-natural Vegetation**

This is the final report on the project. The report describes the work undertaken under the different project objectives, the results obtained and their significance for ozone air quality policy. The report draws on the work contained in the First and Second Annual project reports and the other reports prepared during the course of the project. It is large as it provides sufficient information to describe the many different studies undertaken during the project, without the need to refer to other documents.

Overall, the various studies have more than met the original objectives. The project has provided key technical input to the development of policies related to ozone air quality and has generated new insight into the factors controlling concentrations of ozone and of nitrogen oxides. The developments made to the Master Chemical Mechanism and its availability in other formats have confirmed its status

as a benchmark chemical mechanism for boundary-layer and tropospheric modelling and have improved its uptake.

The work will assist the development of UK actions and policies on ozone as follows:

- The realism and performance of the Ozone Source-receptor Model (OSRM) have been improved significantly through the modifications made to the model and by the introduction of a Surface Conversion algorithm (**Objective 1**). The performance of the OSRM has been compared to other models. These model developments and comparisons confirm that the OSRM is a robust model which can be used to assess the effectiveness of agreed or proposed actions and policies on ozone and oxides of nitrogen;
- Ambient levels of O₃ and NO₂ are strongly coupled (**Objective 2**). Thus, the response to reductions in the emissions of NO_x is highly non-linear. The success of proposed control strategies will depend on a complete understanding of the relationships between O₃, NO and NO₂ under atmospheric conditions. The extension of the previous analysis of O₃, NO and NO₂ measurements at relevant AURN sites to include more recent data has provided clear evidence that the fraction of NO_x emitted as NO₂ has increased significantly from the road vehicle fleets at a number of roadside and kerbside sites. At Marylebone Road, a number of factors may have contributed to the observed effect (such as an increase in the number of buses on routes running on Marylebone Road, and possibly by greater congestion resulting from Marylebone Road lying on the perimeter of the Congestion Charging zone). This will have implications for the attainment of the annual limit value for NO₂ (40 µg m⁻³, 20.9 ppb).

The analysis of hourly mean data for the site at Marylebone Road has provided insights into the seasonal and diurnal dependence of OX sources and their origins, and the conditions under which exceedences of the hourly mean NO₂ limit value (200 µg m⁻³, 104.5 ppb) are more probable. The present analysis demonstrates that the ambient concentration of OX at Marylebone Rd is sensitive to a number of factors, such as primary NO₂ emissions and regional background O₃ concentrations, and that variation in the magnitudes of these factors leads to substantial diurnal and seasonal differences in the level of NO_x required for the hourly mean NO₂ limit value of 104.5 ppb to be exceeded.

- The UK Photochemical Trajectory Model (UK PTM) and Ozone Source-receptor Model (OSRM) have been applied to evaluate a number of proposed ozone control measures (**Objective 3a**).

In the UK PTM model runs, a single linear trajectory was most often used. The trajectory had been selected to represent the air flow during an idealised photochemical episode over the UK (*i.e.*, anticyclonic meteorological situation of easterly winds, leading to a broad westerly air flow carrying photochemically-aged polluted air masses out of Europe towards the British Isles). This trajectory does not represent the conditions prevailing during a particular photochemical episode but represents a potential worst-case situation. For the OSRM model run, a calendar year is simulated and a wider range of realistic air mass trajectories is sampled, including those from other wind directions. These other trajectories may have little or no photochemical ozone production, especially if the trajectory has mainly passed over low emission areas (*e.g.*, the sea). There will be a chemical titration of the ozone in such air masses when these air masses pass over NO_x emission sources. It is therefore likely that the two models will give different response to NO_x and/or VOC emission controls (particularly NO_x control).

- The UK Photochemical Trajectory Model (PTM) was applied to evaluate the following proposed control measures:
 - **Petrol Volatility:** The policy question concerns the likely benefit arising from a 7 thousand tonne reduction in VOC emissions from petrol evaporation between 1st June and 31st August. Calculations by the UK PTM showed that this measure would have little impact on peak ozone concentrations.
 - **Petrol vs. Diesel:** There is strong pressure for policymakers to increase the penetration of new diesel vehicle technologies into the passenger car and LGV fleets to meet future targets for greenhouse gas emissions. The UK PTM has been used to assess the ozone benefit or dis-benefit to this policy from the implied increased NO_x emissions since the EURO IV emission standards imply higher NO_x emissions per kilometre travelled from diesel-engined cars compared with petrol-engined cars. The model results showed that the evaluation of the ozone benefits or dis-benefits depends markedly on whether just the

NO_x emission changes are considered or whether wider issues, such as the avoided emissions of volatile organic emissions from petrol-engined vehicles, are also taken into account.

- **Decorative Paints:** The European Commission has proposed a Directive to reduce the VOC content of decorative paints, varnishes and vehicle refinishing products. The OSRM and UK PTM have been used to assess the benefits to the UK of reductions in VOC emissions arising from within UK, and in UK + rest of Europe. Preliminary UK PTM calculations assuming a 40 ktonne per annum reduction in UK VOC emissions and proportional reduction in European emissions gave a noticeable reduction in peak ozone concentrations. Work undertaken as part of the Regulatory Impact Assessment indicated that the UK emission reduction would only be 2 ktonnes per annum over the current NAEI base case projection for 2010. These are significantly smaller than those proposed by the Commission as much of the reduction identified is already included in the current base case projection. OSRM calculations using the revised VOC emission reduction showed that UK action would have a negligible effect but that EU action would be more effective.
- **Post Gothenburg Controls:** Using its idealised episode trajectory, the UK PTM has shown that both VOC and NO_x control are effective in improving ozone air quality beyond 2010. Model runs, in which NO_x and VOC emissions were separately reduced by 30% across-the-board, suggested that the worst-case trajectory to central Wales was still VOC limited (*i.e.*, VOC control was more effective than NO_x control). Larger emission reductions indicated that the trajectory became NO_x limited.
- Older versions of the OSRM (Version 1.8a without Surface Conversion Algorithm and Version 2.2 with Surface Conversion Algorithm) were applied to evaluate a number of proposed ozone control measures (**Objective 3a**):
 - (a) Regulatory Impact Assessment of Directive on Decorative Paints (see also above)
 - (b) Proposed NO_x Emission Standards for Vehicles (EURO V Standards)
 - (c) Regulatory Impact Assessment of Directive on Petrol Vapour Recovery
 - (d) Post-Gothenburg Scenarios

These were UK-scale model runs. As the surface-conversion algorithm was not available for use in the version 1.8 model runs, the conclusions were based on the unconverted mid-boundary layer outputs. There appeared to be two counteracting effects (a) photochemical production of ozone involving oxides of nitrogen and volatile organic compounds and (b) chemical titration by NO_x removing ozone. These two effects respond differently to emission control. VOC emission control always seemed to improve ozone air quality while NO_x emission control gave a more complex response, which was metric and region specific. Generally, NO_x emission control had an adverse effect on ozone air quality. Thus, either VOC emission control alone or combined VOC and NO_x emission controls are needed to improve ozone air quality.

The OSRM outputs for the 2 Regulatory Impact Assessments were given to colleagues at netcen to undertake the cost-benefit analyses. A paper was prepared on all four series of model runs.

- The latest version of the OSRM (Version 2.2a with Surface Conversion Algorithm) was used to evaluate a number of ozone and NO_x control measures being considered within the **Review of the Air Quality Strategy** for future ozone and nitrogen dioxide air quality (**Objective 3a**). This review will assess progress towards the achievement of the AQS objectives and assess the costs and benefits of possible additional measures to improve air quality in the UK. The focus of this review of possible measures will be on the impact of measures on concentrations of particles, nitrogen dioxide and ozone, the pollutants for which the achievement of the objectives is likely to be the most challenging.

Model runs were undertaken to a 10 km x 10 km receptor grid covering the UK. The analysis of the various base case and scenario runs considered seven ozone and one nitrogen dioxide metrics. Population-weighted means were derived for the metrics associated with impacts on

human health. Area-weighted means were derived for the non-health effects metrics. The population- and area-weighted means have been determined for the following regions: All UK, Scotland, Wales, Northern Ireland, Inner London, Outer London and the Rest of England.

The key points to note from the model runs are that:

- The base case runs show a progressive worsening of ozone air quality for all metrics from 2003 to 2010 and beyond;
- There is however an improvement in nitrogen dioxide air quality as annual mean concentrations fall, especially for the NO_x control measures;
- The use of population-weighted means focuses the analysis on ozone in urban areas. In addition to the role of NO_x emissions in photochemical ozone production, lower NO_x emissions reduce the chemical titration effect, most notably in urban areas. This causes ozone concentrations to move towards the higher concentrations in surrounding rural areas. The reduced chemical titration is a major factor in the increase in the ozone metrics and the deterioration of ozone air quality;
- A second major factor leading to higher ozone concentrations is changing atmospheric composition arising from climate change. In the absence of such a change, the base case runs would have shown an improvement in ozone air quality for some metrics (AOT40 – Crops and AOT40 – Forests);
- The NO_x control measures generally increase ozone concentrations, although there are instances for some of the measures that ozone air quality is improved in 2020, as evidenced by a lower value of the ozone metric;
- The VOC control measures, on the other hand, lead to an improvement in ozone air quality for all ozone metrics;
- Meteorological effects and year-to-year variability in meteorology can have a larger effect on ozone air quality than some of the emission control measures considered.

As a result of the above, there will be widespread exceedences of ozone air quality standards and objectives in 2010 and beyond.

A paper was prepared on the ozone model runs for the Review of the Air Quality Strategy. This will be published as a supporting document to the Consultation Paper.

The UK-scale model runs undertaken for the Review of the Air Quality Strategy were largely based on specific emission control measures. Although desirable, the measures by themselves would not necessarily ensure attainment of ozone air quality targets or objectives. As a result, the Department has subsequently commissioned additional site-specific model runs, in which larger reductions of NO_x and/or VOC emissions were made. These runs will be reported in an addendum to this Final Report.

- A preliminary assessment has been prepared and submitted to the European Commission to meet the requirements of the third Daughter Directive on ozone (**Objective 3b**).

The Directive allows the use of supplementary assessment techniques to reduce the burden of monitoring. Work has been undertaken to assess the relative performance of the 2 ozone modelling techniques (OSRM and empirical mapping methods) and thus to recommend the preferred supplementary assessment technique to be used for the third Daughter Directive on ozone. From the analysis of the comparative performance of the two techniques, it was judged that the empirical modelling approach delivers least uncertainty in the model outputs. It was proposed that the empirical modelling approach should be taken forward as the preferred supplementary assessment technique for the reporting ozone levels in the 2004 calendar year.

The first annual air quality assessment for the third Daughter Directive pollutants has been prepared and submitted to the European Union. There are 28 agglomeration zones (large urban areas) and 15 non-agglomeration zones. The status of the zones has been determined from a combination of monitoring data and model results. The results of this assessment are summarised in the table below, in terms of exceedences of Target Values (TV) and Long-term Objectives (LTO).

Summary Results of Air Quality Assessment relative to the Target Values and Long-term Objectives for Ozone for 2010.

Target Value	Number of Zones exceeding
Max Daily 8-hour mean Target Value	none
AOT40 Target Value	none
Long-term Objective	Number of Zones exceeding
Max Daily 8-hour mean Long-term Objective	43 zones (36 measured + 7 modelled)
AOT40 Long-term Objective	7 zones (5 measured + 2 modelled)

- The Chemical Mechanism development (**Objective 4**) has less immediate policy relevance but it underpins the modelling tools used in the contract to assess ozone policy options. The reaction schemes for butane and isoprene in the MCM have been evaluated against chamber data. The evaluations have provided strong support for the MCM schemes for the most abundant components of emissions of anthropogenic and biogenic non-methane VOC, respectively.

The UK Photochemical Trajectory Model, incorporating (i) the Master Chemical Mechanism (v3.1), (ii) the Common Reactive Intermediate (CRI) mechanism or (iii) the Master Chemical Mechanism (v3.1) with the CRI-approach used for 37 new VOCs, has been used in a number of studies:

- **Multi-day Reactivity:** The results demonstrate the need for a comprehensive chemical mechanism as simplified mechanisms could potentially lead to different ozone source-receptor relationships being used in integrated assessment models.
- **Modelling of the 2003 TORCH Campaign:** THE UK PTM incorporating the CRI chemical mechanism has been used to simulate the concentrations of and other species measured at a site in the southern UK during the NERC Tropospheric Organic Chemistry Experiment (TORCH). The measurement campaign coincided with the August 2003 photochemical pollution episode. The comparison of the simulated and observed distributions of 34 emitted hydrocarbons provides strong support for the VOC speciation used in the NAEI, but is indicative of an under representation of the input of biogenic hydrocarbons, particularly at elevated temperatures. The MCM is one of the few chemical mechanisms available to predict the patterns and structures of oxidised products, such as simple and multifunctional carbonyls, thereby allowing a much more detailed examination of atmospheric chemical mechanisms. The comparison of modelled and measured products of VOC oxidation (carbonyl compounds) showed that the simulated distributions of four aldehydes and three ketones correlated well with observations for each class of compound. However, the simulated concentrations of the aldehydes were systematically lower than those observed, whereas those of the higher ketones were systematically higher. These results will be used to refine the MCM.

The relative contributions of VOC emissions from (a) man made and (b) natural sources to the modelled daily-average ozone concentration during the campaign were determined. The biogenic emissions were calculated to make a larger relative contribution at the higher temperatures prevailing during the episode. Although the magnitude of biogenic VOC emissions is subject to some uncertainty, these results support an important role for biogenic VOC oxidation in regional-scale ozone formation under heatwave conditions. 2003 may become a more typical year in the future, as a result of climate change.

The effects of 10% incremental reductions in the emissions of NO_x and anthropogenic VOC were examined for the emission years 1990, 2003 and 2020 to investigate whether ozone formation is limited by the availability of NO_x or VOC. The 1990 scenario demonstrates strong VOC limitation throughout the campaign period, with NO_x reductions almost always leading to an increase in ozone concentration. The results for 2003 and 2020 indicate that peak ozone formation for the photochemically-active conditions of this campaign is predominantly VOC-limited for the complete time series, but shows a trend towards NO_x-limitation. This sensitivity study also shows that VOC- and NO_x-limitation are not intrinsic properties of a location, and that it is possible to get events when either condition prevails.

- **Contribution of Different VOC Source Sectors:** Using the new NAEI VOC speciated emission inventories, the UK PTM has been updated and now contains as accurate a picture of the emissions of the major organic compounds as can be given with current understanding for the UK and, by assumption, the rest of Europe. A series of sensitivity experiments was performed

to calculate incremental reactivities for each of the 248 VOC source categories in the UK inventory. The largest contribution to the decline in episodic peak ozone concentrations between the years 2000 and 2010 came from the reduction in VOC emissions from the road transport sector. In 2020, because of the marked reductions in VOC emissions in the transport sector, a different range of source categories - chemical, oil and gas industries and the manufacturing industries that use solvents - will be responsible for the bulk of the ozone formation. This points to a major shift in policy if ozone levels are to be reduced beyond 2010 levels so that stationary VOC sources are targeted rather than motor vehicles.

- **Photochemical Ozone Creation Potentials:** The Photochemical Ozone Creation Potential is an index to rank volatile organic compounds according to their production of ground-level ozone. As a result of developments to the Master Chemical Mechanisms and because of improvements made to the speciation of the VOC emission inventories, updated or new POCPs have been determined for 177 selected organic compounds using the UK PTM and the standard 5-day trajectory scenario.

The work on Objective 4 and the improvements to the MCM website contribute to the Department's desired outcome to maintain the leading position of the Master Chemical Mechanism.

- A module to calculate ozone stomatal fluxes (**Objective 5**) has been developed for use with the OSRM. This will provide the Department with a more realistic tool to evaluate the impact of ozone on crops and vegetation for the forthcoming reviews of the European Union's National Emission Ceilings Directive and the Gothenburg Protocol to the UN ECE Convention on Long-range Transboundary Air Pollution.

The work described above will make an important contribution to the development of UK actions and policies on ozone.

Contents

1	INTRODUCTION	1
2	UK OZONE	3
2.1	INTRODUCTION	3
2.2	UK OZONE TRENDS	3
2.3	ANALYSIS OF OZONE MONITORING DATA AGAINST A HEALTH PROTECTION METRIC	5
2.4	OZONE IN 2003	10
3	OVERVIEW AND KEY FINDINGS	12
3.1	PROJECT AIMS AND STRUCTURE	12
3.2	PROJECT PARTNERS	13
3.3	ACHIEVEMENTS AND KEY RESULTS	13
3.4	POLICY RELEVANCE	27
4	DEVELOPMENT AND APPLICATION OF OZONE MODELS (OBJECTIVE 1)	32
4.1	INTRODUCTION	32
4.2	BRIEF OVERVIEW OF THE LATEST VERSION OF THE MODEL	32
4.3	MODEL DEVELOPMENTS	33
4.4	THE OSRM POST-PROCESSOR	36
4.4.1	Ozone and Nitrogen Oxide Metrics	36
4.4.2	Surface Conversion Algorithm	37
4.4.3	Review of the Surface Conversion Algorithm	40
4.5	OSRM PERFORMANCE	42
4.5.1	Comparison of Different Versions of OSRM	42
4.5.2	Comparison with Measurements	42
4.5.3	Comparison with Other Models	46
4.6	SUITABILITY OF THE OSRM	48
5	DETAILED ASSESSMENT OF THE RELATIONSHIP BETWEEN OZONE, NO AND NO₂, AND FACTORS CONTROLLING THEM (OBJECTIVE 2)	49
5.1	INTRODUCTION	49
5.2	THE CHEMICAL COUPLING OF O ₃ , NO AND NO ₂	49
5.3	ANALYSIS OF ANNUAL MEAN DATA	50
5.3.1	Regional OX levels in the UK	50
5.3.2	Site-dependent Local OX Contributions	51
5.3.3	Oxidant Partitioning as a Function of NO _x	53
5.3.4	Site-dependent [NO ₂] vs. [NO _x] and [O ₃] vs. [NO _x] relationships	55
5.3.5	Representative Expressions for Modelling Applications	56
5.3.6	Analysis of More Recent Annual Mean Data (2002-2005)	57
5.4	ANALYSIS OF 1998 AND 1999 HOURLY MEAN DATA AT MARYLEBONE RD	59
5.4.1	Methodology	59
5.4.2	Diurnal and Seasonal Dependence of Local and Regional OX Contributions	59
5.4.3	Estimation of Primary NO ₂ Emissions from Diesel and Petrol Vehicles	61
5.4.4	Conclusions	64
5.5	OSRM MODELLING OF URBAN OZONE, NITRIC OXIDE AND NITROGEN DIOXIDE	65
6	POLICY DEVELOPMENT AND SCENARIO ANALYSIS (OBJECTIVE 3A)	67
6.1	INTRODUCTION	67
6.2	UK PTM MODELLING	68
6.2.1	Petrol Volatility:	68
6.2.2	Petrol vs. Diesel	68
6.2.3	Decorative Paints	70
6.2.4	Post Gothenburg Emission Control	71
6.3	OSRM MODELLING	72
6.3.1	Using OSRM Version 1.8a	72
6.3.2	Using OSRM Version 2.2	77

6.4	OSRM MODELLING FOR THE REVIEW OF THE AIR QUALITY STRATEGY	79
6.4.1	Key Features of the Model Runs:	79
6.4.2	Model Outputs.....	83
6.4.3	Comparison with Air Quality Objectives.....	99
6.4.4	Calculation of Benefits.....	102
6.4.5	Summary	102
7	OZONE DAUGHTER DIRECTIVE (OBJECTIVE 3B)	103
7.1	INTRODUCTION	103
7.2	PRELIMINARY ASSESSMENT	103
7.2.1	Supplementary Information Techniques in the UK.....	104
7.2.2	Additional Monitoring Requirements.....	105
7.2.3	Achieving Compliance.....	110
7.3	EVALUATION OF SUPPLEMENTARY ASSESSMENT TECHNIQUES	111
7.4	SUPPORTING DOCUMENTATION FOR THE QUESTIONNAIRE.....	114
8	IMPROVEMENTS TO PHOTOCHEMICAL REACTION SCHEMES (OBJECTIVE 4)	116
8.1	MECHANISM DEVELOPMENT.....	116
8.1.1	Update of the Master Chemical Mechanism to MCMv3.1	116
8.1.2	Development and Evaluation of a Detailed Mechanism for the Atmospheric Oxidation of Aromatic Hydrocarbons 116	
8.1.3	Update to the Treatment of Photolysis Reactions in the MCM.....	119
8.1.4	Evaluation of Master Chemical Mechanism (MCM v3) using Environmental Chamber Data	126
8.1.5	The Common Representative Intermediates (CRI) Mechanism	129
8.2	THE NEW MCM WEBSITE.....	134
8.2.1	New Layout and Web Tools	135
8.2.2	Mechanism Reduction using the CRI mechanism.....	139
8.2.3	Under the Hood: New Design and Interactive Database.....	139
8.3	MULTI-DAY REACTIVITY SCALES DETERMINED BY THE UK PTM	140
8.3.1	Model Set-up.....	140
8.3.2	Aldehydes	140
8.3.3	Ketones.....	141
8.3.4	Alkenes	142
8.3.5	Multi-day Ozone Formation from Alkanes.....	144
8.3.6	Multi-day Ozone Formation from Aromatic VOCs.....	144
8.4	MODELLING THE AMBIENT DISTRIBUTION OF ORGANIC COMPOUNDS USING THE UK PTM.....	144
8.4.1	Introduction	144
8.4.2	Speciation and Temporal Variation of non-methane VOC Emissions.....	146
8.4.3	Simulations of Emitted Hydrocarbons using the CRI Mechanism.....	147
8.4.4	Simulations of Carbonyl Distributions with the MCM.....	149
8.4.5	Conclusions	151
8.5	UK PTM ANALYSIS OF OZONE FORMATION IN THE AUGUST 2003 HEATWAVE: SENSITIVITY TO CHANGES IN OZONE PRECURSOR EMISSIONS.....	151
8.5.1	Introduction	151
8.5.2	Contributions of Anthropogenic and Biogenic VOC to Ozone Formation	152
8.5.3	Sensitivity to Anthropogenic Emissions Variations over the Period 1990-2020	152
8.5.4	Effects of Incremental NO _x and VOC Emission Reductions.....	155
8.6	IMPLEMENTATION OF DEFRA'S VOC PROJECTIONS	156
8.6.1	Updating the UK PTM with the NAEI Speciated VOC Inventory.....	156
8.6.2	Contributions from Different Sources of Organic Compounds to Photochemical Ozone Formation.....	157
8.6.3	Application to Policy and the Defra VOC Projections to 2010 and 2020.....	159
8.7	PHOTOCHEMICAL OZONE CREATION POTENTIALS POCPs	160
9	DEVELOPMENT OF STOMATAL FLUX MODULE FOR CROPS AND SEMI-NATURAL VEGETATION (OBJECTIVE 5)	162
9.1	BACKGROUND	162
9.2	MODEL COMPONENTS	163
9.2.1	Surface Ozone-Flux Model.....	163
9.2.2	Meteorological Pre-processor.....	164
9.2.3	Ozone Flux Post-processor	164
9.3	OZONE FLUX CALCULATIONS	165
9.3.1	Upper-leaf Surface Conductance	165
9.3.2	Upper Leaf Stomatal Fluxes	166
9.3.3	Accumulated Ozone fluxes at UK Monitoring sites	167
9.3.4	UK MAPs of Accumulated Fluxes.....	169
9.4	SUMMARY	169

10	OTHER PROJECT ACTIVITIES	172
10.1	PROJECT MEETINGS.....	172
10.2	PROJECT OUTPUTS	173
10.3	PROJECT WEBSITE.....	174
10.4	PUBLICATIONS	174
10.4.1	Journal Publications.....	174
10.4.2	Other Publications	175
10.5	CONFERENCES/SEMINARS ATTENDED	176
11	REFERENCES	178
12	ACKNOWLEDGEMENTS	184

Appendices

Appendix 1	Programme of Work from Proposal
Appendix 2	Population or Area-weighted Means of the Selected O₃ and NO₂ Metrics
Appendix 3	Description of UK Photochemical Trajectory Model
Appendix 4	Percentage Contribution to Emissions, Incremental Reactivity and Photochemical Ozone Formation by VOC Source Sector.

1 Introduction

The Department for Environment, Food and Rural Affairs (Defra) and the Devolved Administrations (the Scottish Executive, Welsh Assembly Government and the Department of the Environment Northern Ireland) awarded the contract **Modelling of Tropospheric Ozone** (EPG 1/3/200) to a consortium led by **netcen** (part of AEA Technology). The contract addresses ground-level ozone, its formation, impacts and control.

The concentrations of ground-level ozone, a pollutant that affects human health, ecosystems and materials, widely exceed environmental quality standards across the UK and Europe. Ozone is not emitted directly into the atmosphere, but is a secondary photochemical pollutant formed in the lower atmosphere from the sunlight-initiated oxidation of volatile organic compounds (VOCs) in the presence of nitrogen oxides (NO_x). Elevated concentrations of ozone over the UK are especially generated when slow-moving or stagnant high pressure (anticyclonic) weather systems occurring in the spring or summer bring in photochemically reacting air masses from mainland Europe.

Under conditions characteristic of photochemical pollution episodes, the formation and transport of ozone can occur over hundreds of kilometres, with concentrations at a given location influenced by the history of the air mass over a period of up to several days. In addition to this, the increasing levels of ozone in the free troposphere on a global scale also influence regional scale photochemical processes by providing an increasing background ozone level upon which the regional and national scale formation is superimposed. This effect now has to be considered when assessing whether proposed air quality standards for ozone are likely to be achieved.

The non-linear nature of ground-level ozone production requires the use of sophisticated chemical transport models to understand the factors affecting its production and subsequent control. The Department and the Devolved Administrations (DAs) have funded the development of a number of models over the years. They seek to build on this work but now require a modelling capability to treat ozone formation (a) on all spatial scales from urban areas at high spatial resolution to the global scale so that ozone production on the regional and global scales is linked and (b) from timescales of hours to reproduce the diurnal behaviour of ozone to decades so that the influence of climate change can be assessed. The Ozone Source-receptor Model (OSRM), developed during the previous project on Modelling of Tropospheric Ozone Formation (EPG 1/3/143), will be the main tool used to address these requirements.

As part of their ozone research programme, Defra and the Devolved Administrations have supported the development of near explicit chemical mechanisms, especially that of the Master Chemical Mechanism. This was in recognition that a more targeted approach on ozone precursor emissions would bring greater environmental benefits than a simple percentage mass reduction. The Department and the DAs wish to continue their support for this work.

The new project is not a simple continuation of earlier work. There is a stronger emphasis on model application to evaluate planned and proposed policies. In addition, new tasks have been identified: Technical assistance is required to fulfil commitments arising from the implementation of European Directives and in particular, the 3rd Daughter Directive on Ozone. Work is also in progress to move from the current AOT metrics for protection of ecosystems to a more realistic flux-based approach. The Department desires to gain added value from its own research programme and the work currently in progress within the EMEP research programme on this specific topic.

This is the final report on the project. The report describes the work undertaken under the different project objectives, the results obtained and their significance for ozone air quality policy. The report draws on the work contained in the First and Second Annual project reports and the other reports prepared during the course of the project. It is large as it provides sufficient information to describe the many different studies undertaken during the project, without the need to refer to other documents.

The report is structured as follows:

Section	Content
Section 1 - Introduction	
Section 2 - UK Ozone	- Brief review of ozone measurements and trends
Section 3 - Overview and Key Findings	- Description of the project, its aims and structure. Summary of work and achievements. Policy Relevance
Section 4 - Development and Application of Ozone Models (Objective 1)	- Development of the Ozone Source-Receptor Model and its performance compared to measurements
Section 5 - Detailed Assessment of the Relationship between Ozone, NO and NO ₂ , and Factors Controlling Them (Objective 2)	- Analysis of co-located O ₃ , NO and NO ₂ measurements made at 65 UK monitoring sites. Relationship between these pollutants and comparison with those derived in the national empirical modelling.
Section 6 - Policy Development and Scenario Analysis (Objective 3a)	- Use of OSRM and the UK Photochemical Trajectory Model to evaluate a number of policy options and scenarios, especially the use of the OSRM for the Review of the Air Quality Strategy.
Section 7 - Ozone Daughter Directive (Objective 3b)	- Preliminary Assessment report for the 3 rd Daughter Directive on ozone.
Section 8 - Improvements to Photochemical Reaction Schemes (Objective 4)	- Oxidation schemes of 4 aromatic VOCs updated and compared to chamber data. Development of MCM website. Development of derived Common Reactive Intermediates mechanism. Use of UK PTM with MCM to study multi-day reactivity and to understand the measurements made during the TORCH campaign.
Section 9 - Development of Stomatal Flux Module for Crops and Semi-natural Vegetation (Objective 5)	- Background and approach. Linkages between OSRM and Surface Ozone Flux model. Some initial calculations.
Section 10 - Other Project Activities	- Project meetings and reports. Conferences and seminar attended and publications. Project website.
Section 11 -References	
Section 12 -Acknowledgements	

2 UK Ozone

2.1 INTRODUCTION

Ozone is a secondary pollutant formed in the lower atmosphere from the sunlight-initiated oxidation of volatile organic compounds (VOCs) in the presence of nitrogen oxides (NO_x). In common with the other key pollutants of current concern (nitrogen dioxide and particulate matter), ozone concentrations do not respond in a simple manner to precursor emission control. Ozone is also present in the unperturbed atmosphere and ground-level concentrations are influenced by input from the stratosphere and by changes occurring at the hemispheric scale (e.g., as a result of climate change).

While the control of VOCs emissions generally improves ozone air quality, the position is more complex for the emissions of oxides of nitrogen (i.e., nitric oxide and nitrogen dioxide). Oxides of nitrogen are involved in both the production of ozone and, at higher concentrations, the loss of ozone. The strong coupling between the concentrations of ozone and oxides of nitrogen (NO_x) and the loss of ozone at higher NO_x concentrations is illustrated in Figure 2.1, adapted from Clapp and Jenkin [2001]. Urban areas generally have higher emissions and hence concentrations of oxides of nitrogen than those of rural areas. Oxides of nitrogen suppress ozone, resulting in lower concentrations in urban areas.

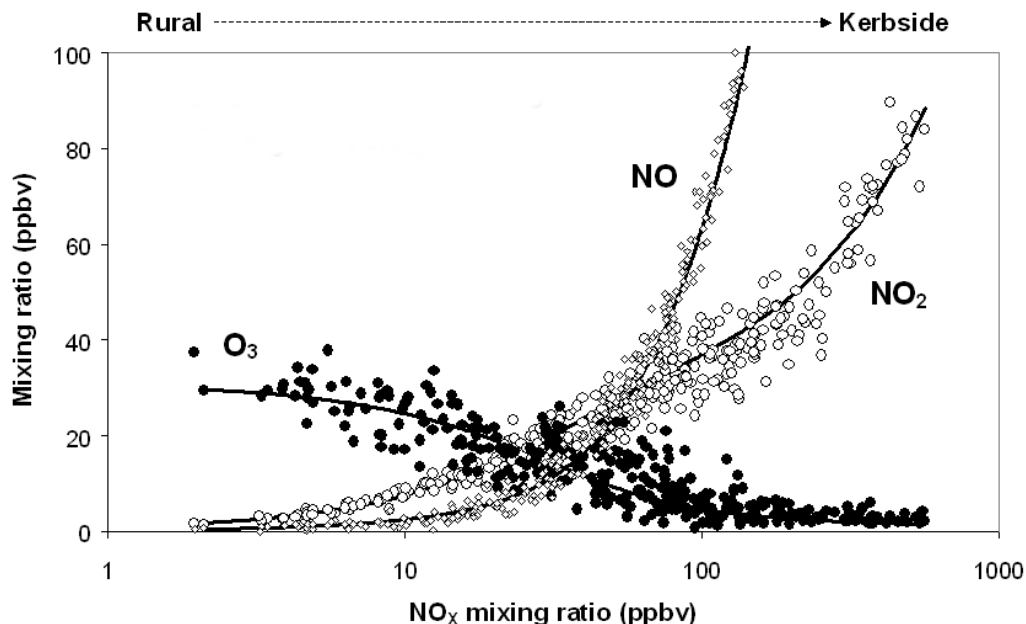


Figure 2.1 *Dependence of the Observed Daylight Average Mixing Ratios of O_3 , NO and NO_2 on the Concentration of NO_x at Six Southern UK Sites (Note that the NO_x axis is logarithmic). The Solid Lines were calculated with the Assumption of the Photostationary State.*

2.2 UK OZONE TRENDS

The frequency distributions of the hourly mean ozone concentrations observed at rural UK ozone monitoring sites, during each year, have changed throughout the period over which monitoring has been carried out. Some years show a greater frequency and intensity of summertime ozone episodes and wintertime depletion events, compared with others. Despite this variability, episodic peak ozone levels have been decreasing at rural sites at about 2-3 ppb ($4-6 \mu\text{g m}^{-3}$) per year during the 1990s, and by about 50-150 ppb ($100-300 \mu\text{g m}^{-3}$) from the early 1970s to the late 1990s. The decreasing intensity of the regional ozone pollution episodes can be illustrated using the annual trends in the maximum 8-hour mean ozone concentrations monitored during each year at a selection of long-running rural UK ozone monitoring sites (see Figure 2.2). The majority of the rural sites show downwards trends in maximum 8-hour mean ozone concentrations that are statistically significant,

reflecting the influence of the Europe-wide controls on the ozone precursor emissions of volatile organic compounds and oxides of nitrogen through the introduction during the 1990s of three-way exhaust gas catalysts to petrol-engined motor vehicles and of canisters to reduce petrol evaporation emissions.

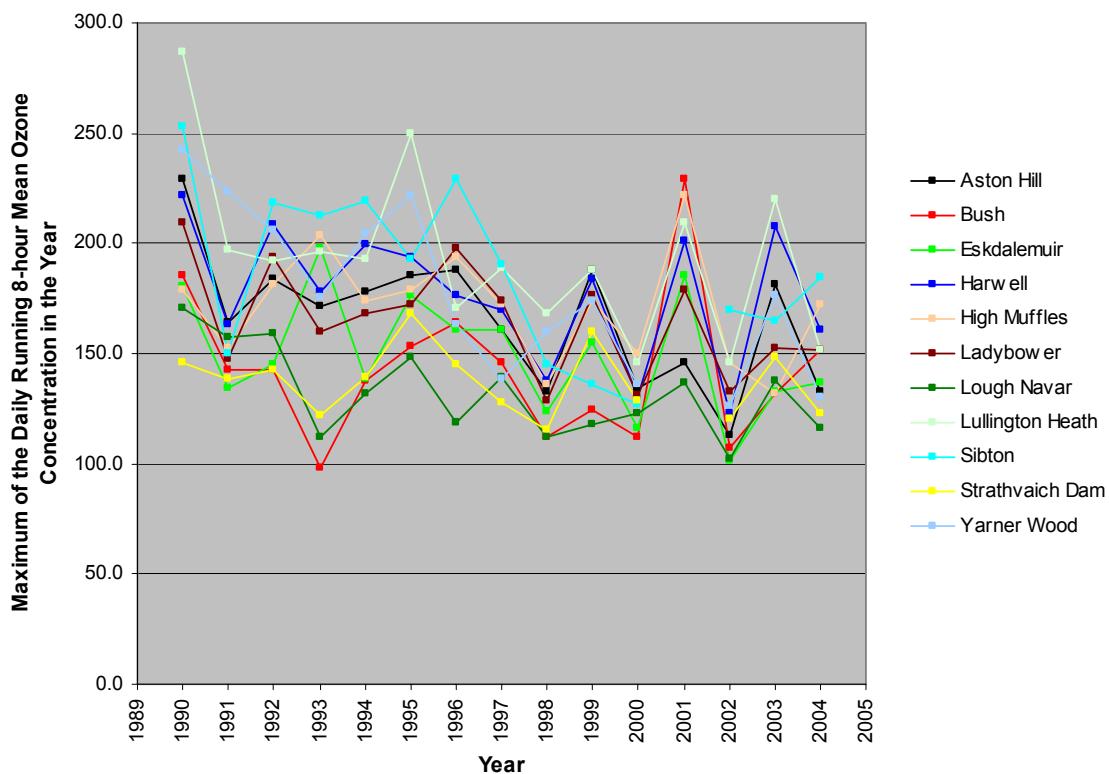


Figure 2.2 Time Series of the Maximum of the Daily Running 8-hour Mean Ozone Concentrations Determined at a Selection of Long-running Rural UK Ozone Monitoring Sites between 1990 and 2004.

Three-way exhaust gas catalysts and measures to reduce NO_x emissions from diesel traffic have also reduced the extent of ozone scavenging by the NO_x emissions from road traffic. As a result, ozone levels in towns and cities have begun to rise back towards the levels found in the surrounding countryside. Wintertime ozone depletion events have become less severe. There has been a tendency, therefore, for levels to rise during much of the year whilst episodic peak levels during summertime have fallen.

There have also been more subtle influences at work on the ozone distribution across north west Europe because of hemispheric scale changes in ozone air quality. For most urban pollutants, the location of major European population and industrial centres on the east of the UK has been an air quality advantage because clean Atlantic Ocean air masses generally bring low pollution levels. However, ozone production from both natural and man-made ozone precursors on the hemispheric scale ensures that these otherwise clean air masses always contain some background or baseline levels of ozone. This is why ozone is almost invariably present in most towns and cities across Europe on almost all days. Over the period from 1987 onwards, ozone levels in these Atlantic Ocean air masses has been observed to be steadily rising, by about 5 ppb ($10 \mu\text{g m}^{-3}$) per decade. Winter and spring levels have been rising somewhat faster than summertime levels. A similar trend has been observed in clean Pacific Ocean air masses entering the North American continent.

To illustrate some of these trends, Figure 2.3 presents a histogram of the hourly ozone mean concentrations measured at an urban background site in central London during 1991 and 1998. There has been a marked shift in the frequency distribution of ozone concentrations between these years bringing a much reduced frequency of low ozone concentrations (<10 ppb $<20 \mu\text{g m}^{-3}$) and a much increased frequency of ozone concentrations in the 10-40 ppb (20 - $80 \mu\text{g m}^{-3}$) range. This is likely to be due mainly to reduced NO_x emissions from petrol-engined vehicles, which deplete urban ozone, but

will also reflect the steadily increasing ozone background, especially during wintertime. Similar behaviour is anticipated in most towns and cities in north west Europe.

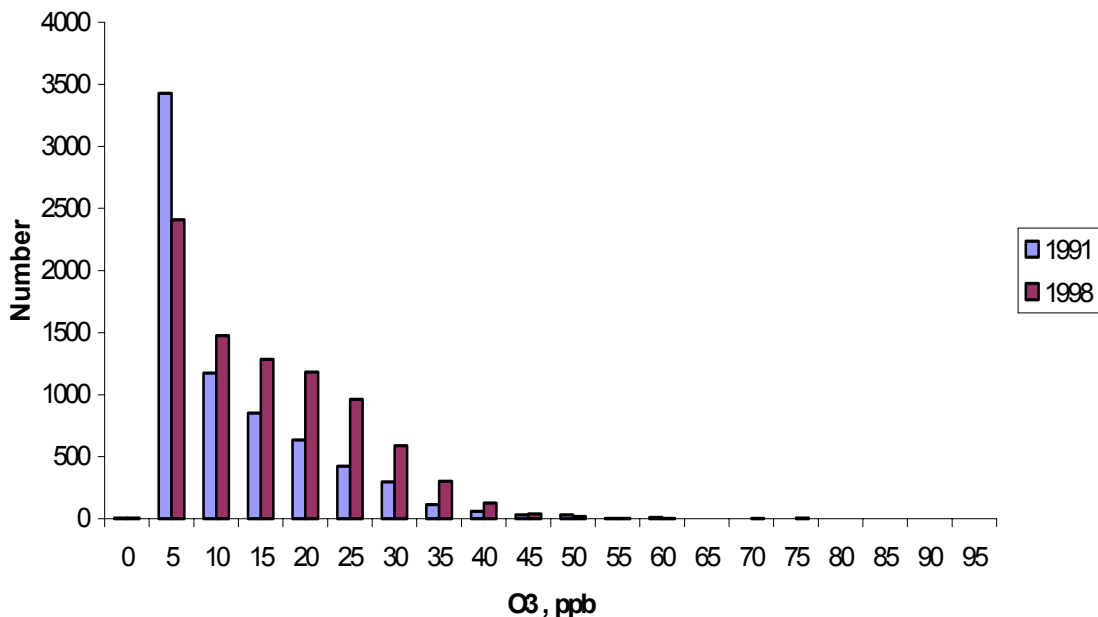


Figure 2.3 Histogram of the Hourly Ozone Concentrations Measured during 1991 and 1998 at a Typical Urban Background Site in Inner London (Bridge Place).

The drivers are further illustrated in Figure 2.4, which shows the temporal trend of the following percentiles – 10th, 30th, 50th, 70th, 90th, 92nd, 94th, 96th, 98th and the maximum – for selected UK rural and London urban sites for the years 1990 to 2003. At all sites and restating the result of Figure 2.2, the maximum hourly ozone concentration shows a downward trend. The upward trend in the maximum hourly concentration at the London North Kensington site is driven by the high value in 2003 (240 $\mu\text{g m}^{-3}$) and its influence on the trend derived from a limited time series. If this measurement were to be excluded, the maximum hourly concentration would show a strong decrease. Upward trends are generally seen in the lower percentiles at all the sites. Although based on fewer years of monitoring, the two London sites show much stronger upward trends in all percentiles up to the 98th percentile.

The analysis of hourly ozone concentrations measured at UK ozone monitoring sites provides clear evidence of a downward trend in the maximum hourly ozone concentration and of percentiles above the 90th to 95th percentile and upward trends in the lower percentiles. These are a result of

- regional controls on NO_x and VOC emissions, reducing peak ozone concentrations (*i.e.*, **reduced photochemical ozone production**)
- a **reduction in the NO_x titration effect**, especially in urban areas, as a result of the control of local NO_x emissions, leading to increased ozone concentrations at lower percentiles
- an **increasing background concentration** arising from global changes in atmospheric composition and hemispheric circulation

Numerical models need to incorporate these features if accurate forecasts of future ozone air quality are to be made and the effectiveness of emission control policies are to be assessed.

2.3 ANALYSIS OF OZONE MONITORING DATA AGAINST A HEALTH PROTECTION METRIC

The annual average of the daily maximum 8-hour mean ozone concentrations is used as an appropriate ozone metric for human health protection. The EMEP ozone database has been recompiled on this basis.

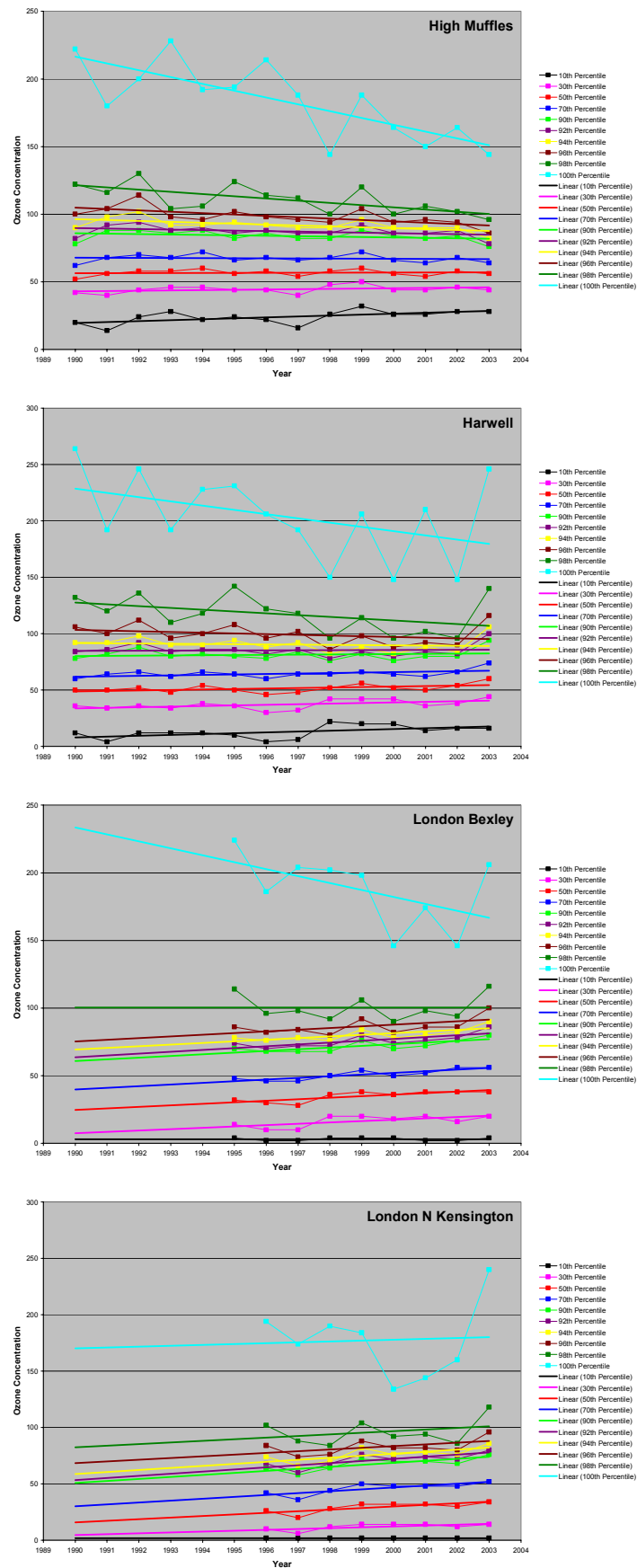


Figure 2.4 The Trend in Ozone Concentration Percentiles between 1990 and 2003 at 4 UK Ozone Monitoring Sites.

There are 46 EMEP rural sites, located below at elevations below 500 metres that have long enough observational records to enable robust trend analysis. Table 2.1 presents an analysis of the trends in the annual averages of daily maximum 8-hour mean ozone concentrations for the period from 1990 through to 2002. The year 2003 was specifically excluded from this analysis because of the unusually severe hot spell of weather that occurred during that year in central Europe. Of the 46 sites in Table 2.1, 17 sites showed downwards trends and 29 sites showed upwards trends. Of these, 11 sites showed highly statistically significant upwards trends and 2 similarly significant downwards trends. Taking all the sites together, the average trend was $0.3 \pm 0.6 \mu\text{g m}^{-3} \text{ yr}^{-1}$ (0.15 ± 0.3) ppb yr^{-1} .

Table 2.1 Trends and their Statistical Significance in the Annual Average Daily Maximum 8-hour Mean Ozone Concentrations for 46 EMEP Rural Sites with elevations below 500 metres over the period from 1990 through to 2002, together with the 1990 values of the Ozone Metric.

Site	Initial value ($\mu\text{g m}^{-3}$)	Slope ($\mu\text{g m}^{-3} \text{ yr}^{-1}$)	Significance	Site	Initial value ($\mu\text{g m}^{-3}$)	Slope ($\mu\text{g m}^{-3} \text{ yr}^{-1}$)	Significance
Illmitz (AT02)	83.6	0.10		Strathvaich Dam (GB15)	74.7	0.17	
Pillersdorf (AT30)	87.7	0.12		Aston Hill (GB31)	78.0	-0.13	
Dunkelsteinerwald (AT45)	75.4	-0.16		Bottesford (GB32)	54.2	1.63	**
Gaenserndorf (AT46)	75.6	0.84	+	Bush (GB33)	67.7	0.21	
Stixneusiedl (AT47)	77.8	-0.03		Glazebury (GB34)	56.5	0.09	
Eupen (BE32)	60.9	1.74	***	Harwell (GB36)	68.5	-0.24	
Vezein (BE35)	74.4	0.83		Lullington Heath (GB38)	81.2	-0.40	
Westerland (DE01)	66.1	1.47	**	Sibton (GB39)	68.2	-0.59	***
Laggenbrügge (DE02)	67.0	0.32		Mace Head (IE31)	76.5	0.39	
Neuglobsow (DE07)	46.1	0.97	+	ISPRA (IT04)	78.3	-0.10	
Zingst (DE09)	60.4	0.93	*	Preila (LT15)	59.6	1.23	
Bassum (DE12)	54.3	0.24		Kollumerwaard (NL09)	76.2	-0.36	
Ueckermunde (DE26)	78.3	0.13		Vreedepel (NL10)	72.6	-0.61	+
Ulborg (DK31)	61.9	0.20		Birkenes (NO01)	67.1	0.00	
Frederiksborg (DK32)	60.6	-0.05		Kárvatn (NO39)	56.4	0.96	**
Lille Varby (DK41)	61.3	-0.10		Prestebakke (NO43)	62.4	1.04	**
Utö (FI09)	73.9	0.23		Jeløya (NO45)	71.5	-0.33	
Virolahti (FI17)	67.1	0.48		Monte Velho (PT04)	65.6	1.81	
Oulanka (FI22)	71.9	-0.18		Rörvik (SE02)	67.8	0.27	
Eskdalemuir (GB02)	68.2	-0.42		Vavihill (SE11)	68.6	0.44	*
Lough Navar (GB06)	64.9	-0.33		Aspvreten (SE12)	69.4	0.82	+
Yarner Wood (GB13)	80.8	-0.49		Norra-Kvill (SE32)	78.7	0.09	
High Muffles (GB14)	66.5	-0.07		Vindeln (SE35)	62.8	0.53	+

Notes: *** implies statistical significance at the 99.9%, ** at the 99%, * at the 95% and + at the 90% levels.

To identify the major influences on the observed long term trends in the annual average daily maximum 8-hour mean ozone concentrations at the EMEP rural sites, the observed trends over the 1990-2002 period were plotted against the initial 1990 value of the ozone metric, as shown in Figure 2.5. Figure 2.5 shows that there is a correlation between the magnitude of the observed ozone trend and the initial 1990 value of the ozone metric. Those EMEP sites with low initial values of the ozone metric, such as those shown in Figure 2.5 in Germany and Belgium, show strong upwards trends in the ozone metric. These are sites that were influenced by traffic emissions initially. As three-way catalysts have been fitted widely across Europe, NO_x -driven depletion of ozone has steadily reduced and levels of the ozone metric have increased. At sites heavily influenced by long range transboundary transport, such as the Netherlands site in Figure 2.5, initial levels of the ozone metric were high because the sites were located away from traffic. Europe-wide measures to reduce ozone precursor VOC and NO_x emissions have steadily reduced levels of the ozone metric, leading to the observed downwards trends over the 1990-2002 period. Sites such as Mace Head, which are on the Atlantic Ocean sea-board of Europe, are strongly influenced by the increasing hemispheric and global ozone baseline and show increasing trends over the 1990-2002 period.

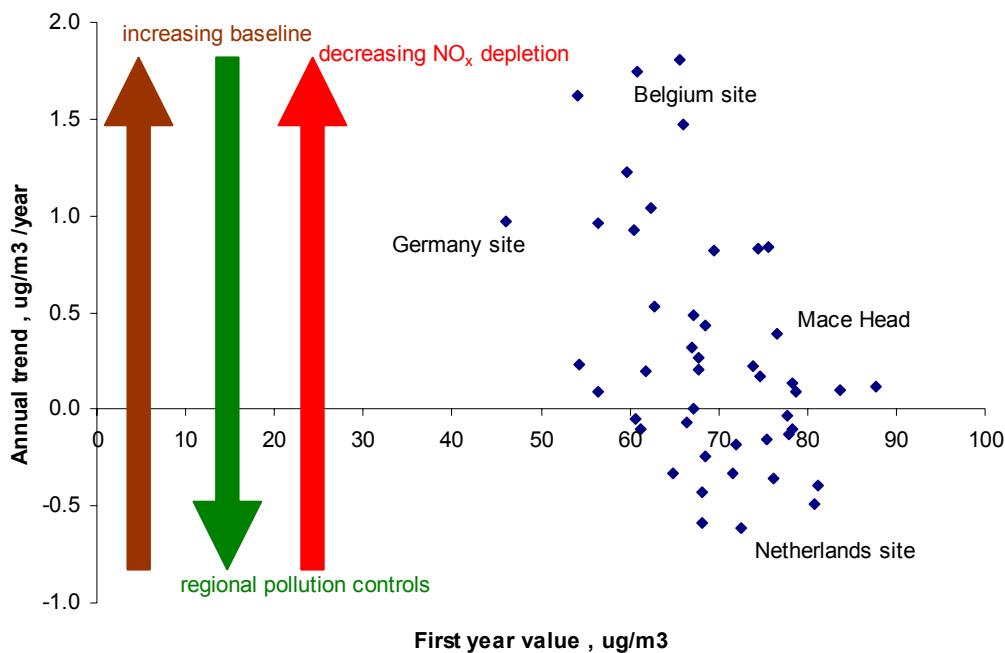


Figure 2.5 A Scatter Plot of the Trends in the Annual Average Daily Maximum 8-hour Mean Ozone Concentrations observed at 46 EMEP Rural Sites over the Period 1990-2002 plotted against the Initial 1990 Value of the Ozone Metric.

As stated before, there are therefore three opposing influences on rural ozone levels in Europe over the period from 1990 through to 2002:

- the decreasing intensity of the regional ozone pollution episodes, tending to reduce the ozone metric;
- the decreasing depletion of ozone by traffic NO_x emissions;
- the growth in hemispheric or global baseline ozone.

Overall, an approximate balance has been maintained between these influences over the 1990-2003 period at the rural EMEP sites.

Although monitoring of the ozone levels in rural locations in Europe began during the 1970s, monitoring in urban locations is a relatively recent activity. There are over 1,000 urban ozone monitoring sites contributing to the AIRBASE database of the EU during the 2000s. With this large increase in urban ozone monitoring, it is clear that urban ozone levels are substantially reduced below rural levels by NO_x -driven depletion processes. This depletion is increasingly more apparent when comparing suburban with urban background and traffic-influenced sites.

In view of the importance of urban exposure levels, a clear understanding of urban ozone trends is required. As an example, the urban ozone trends are examined for the United Kingdom over the period from 1994-2003. It is anticipated that the ozone behaviour found is typical of that experienced in most of the European towns and cities. The trends in the annual average daily maximum 8-hour mean ozone concentration at the UK urban sites are shown in Table 2.2. Upwards trends are found at the vast majority of the urban sites, 47 out of 49, and downwards trends at only 2 sites. A total of 19 sites showed trends that are highly statistically significant (> 90% confidence). The London Marylebone Road site is the most heavily trafficked and most heavily polluted site of all in Table 2.2 and the site which has the lowest annual mean daily maximum 8-hour mean ozone concentrations. The low ozone levels at this site are caused by NO_x depletion and the strong upwards trend of 1.4 µg m⁻³ yr⁻¹ (0.7 ppb yr⁻¹) observed at this site has been caused by the diminution of this NO_x depletion by the reduction of NO_x emissions from petrol-engined vehicles due to the fitting of exhaust gas catalysts. This same influence is apparent across all the other urban sites in Table 2.2.

Table 2.2 Trends and their Statistical Significance in the Annual Mean Daily Maximum 8-hour Mean Ozone Concentrations observed at UK Rural, Suburban, Urban and Roadside sites during the Period from 1990 onwards.

Site	Statistical Significance	Trend (in ppb yr ⁻¹)	Site	Statistical Significance	Trend (in ppb yr ⁻¹)
Urban Sites 1994-2003			Urban Sites 1997-2003		
Belfast Centre		+0.31	Barnsley Gawber		+0.55
Birmingham Centre	*	+0.45	Bolton	+	+0.88
Birmingham East		+0.17	Bradford Centre		+0.85
Bristol Centre		+0.18	Derry		+0.79
Cardiff Centre	+	+0.45	Glasgow Centre	*	+0.58
Edinburgh Centre		+0.32	Leamington Spa		+0.72
Hull Centre		+0.09	London Brent		+0.77
Leeds Centre	*	+0.57	London Eltham		+0.21
Leicester Centre		+0.39	London Hackney		+0.48
Liverpool Centre	+	+0.75	London Haringey		+0.85
London Bexley	**	+0.49	London Hillingdon	+	+0.99
London Bloomsbury	*	+0.40	London N. Kensington		+1.01
Middlesbrough	**	+0.81	London Southwark		+0.68
Southampton Centre		+0.44	London Sutton		+0.54
Swansea	*	+0.54	London Teddington	*	+0.83
Wolverhampton Centre	+	+0.48	London Wandsworth	+	+0.81
Average	+	+0.35	Manchester Piccadilly		+0.34
Roadside Sites 1997-2003			Manchester South	+	+0.65
Bury Roadside	+	+0.55	Newcastle Centre		+0.54
London Marylebone Road	**	+0.71	Norwich Centre		+1.86
			Nottingham Centre		+0.37
			Plymouth Centre		+0.95
			Port Talbot		+0.57
			Reading		-0.40
			Redcar	*	+1.09
			Rotherham Centre		+0.66
			Salford Eccles		+0.31
			Sheffield Centre		+0.34
			Stoke-on-Trent Centre		0
			Swansea		+0.37
			Thurrock		+0.74
			Average		+0.76

Notes: Statistical significance is based on the non-parametric Mann-Kendall test and Sen's slope estimates and is indicated by: ** at the 0.01 level of significance, * at the 0.05 level of significance, + at the 0.1 level of significance and blank means less than the 0.1 level.

The strong upwards trends in the ozone metric observed at almost all of the UK urban sites have been caused by the diminution of the depletion of ozone by chemical reactions with NO_x, which has been caused, in turn, by the reduction of NO_x emissions from petrol-engined vehicles due to the fitting of exhaust gas catalysts. At these urban sites there appears to have been little influence of the decrease in intensity of regional pollution episodes. Similar behaviour is anticipated in most European towns and cities during the 1990s and 2000s.

2.4 OZONE IN 2003

2003 was one of the hottest years on record, with the highest UK temperature (38.1 °C) recorded at Gravesend in Kent on 10th August 2003. It was a photochemically active year with major photochemical episodes in August and July. The peak concentrations during these episodes were 246 $\mu\text{g m}^{-3}$ at Harwell (15th July), 238 $\mu\text{g m}^{-3}$ at London Brent (6th August), 236 $\mu\text{g m}^{-3}$ at London Brent and Lullington Heath (11th August). These were classical UK photochemical ozone episodes: high pressure conditions existed with easterly airflows bringing polluted air to the UK from Europe. Although ozone concentrations were higher than those recorded in more recent years, the episodes were largely limited to the central and southern part of the UK. Figure 2.6 shows a time series from 1990 to 2004 of the two ozone metrics of relevance for the 3rd Daughter Directive for 4 UK monitoring sites – Strathvaich Dam (Scotland), Harwell (Oxfordshire), High Muffles and Leeds Centre (Yorkshire).

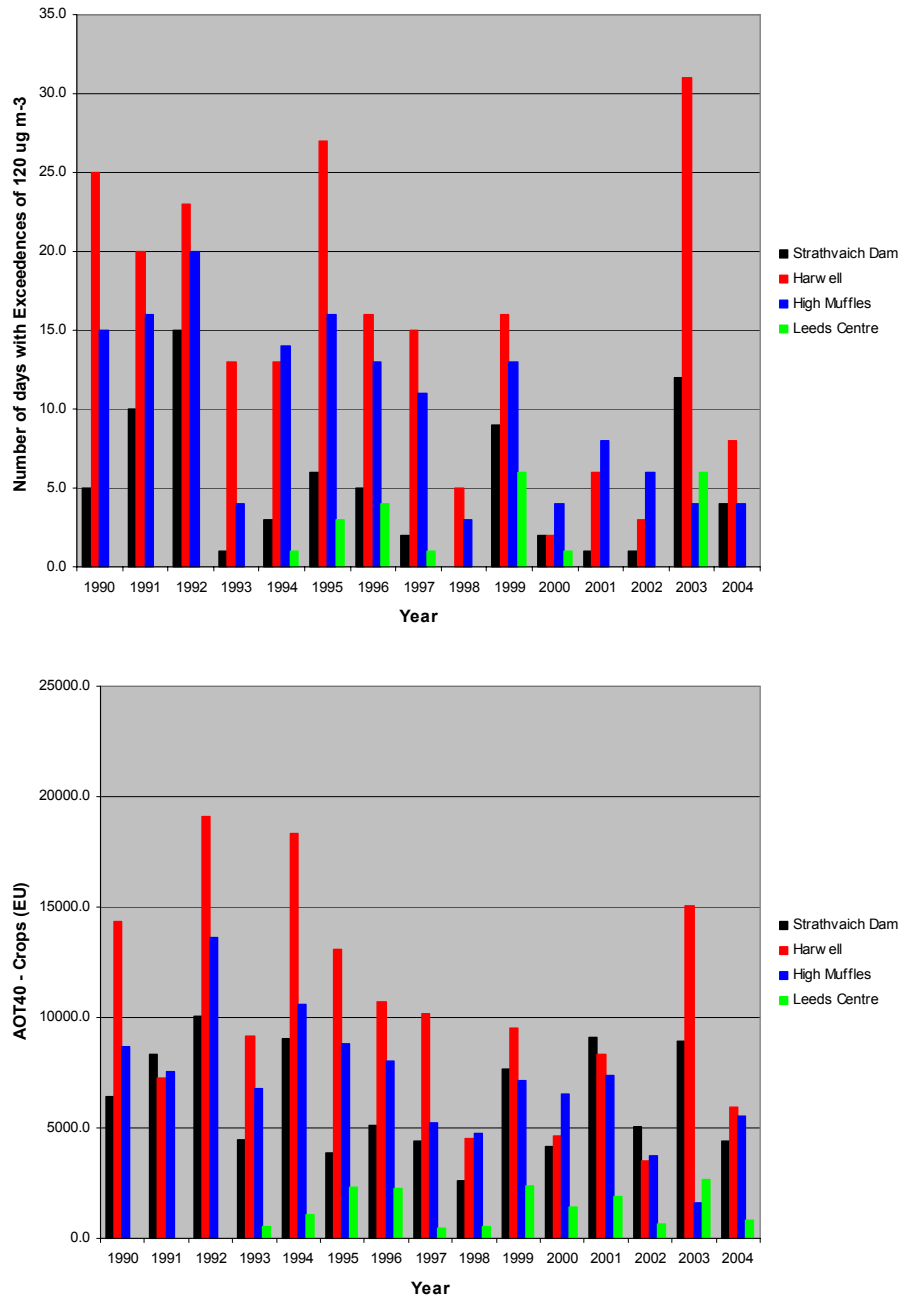


Figure 2.6 Time Series from 1990 to 2004 of the Two Ozone Metrics of Relevance for the 3rd Daughter Directive (Number of Days on which the Maximum Daily Running 8-hour Mean Concentration exceeds 120 $\mu\text{g m}^{-3}$ (upper panel) and AOT40 – Crops (lower panel) for 4 UK monitoring sites.

For Harwell, 2003 had the highest number of days on which the maximum daily running 8-hour mean concentration exceeded $120 \mu\text{g m}^{-3}$. Although AOT40 – Crops was significantly elevated in 2003, it was not the highest recorded in the period between 1990 and 2004. Similarly, AOT40 – Crops was elevated at Strathvaich Dam but it was not the highest value between 1990 and 2004. For these metrics at Leeds Centre, 2003 was a comparable year to 1999. The values of the two metrics calculated for High Muffles for 2003 were lower than those determined for other years.

3 Overview and Key Findings

3.1 PROJECT AIMS AND STRUCTURE

The principal aims of the project are:

- to maintain, develop and apply tools for modelling tropospheric ozone formation over a range of spatial scales
- to support and guide policy on emission reductions and objectives, and to verify compliance

To meet these aims and to address the intended applications, the programme of work has 5 main objectives or tasks:

- Objective 1 - **Development and Application of Ozone Models**
- Objective 2 - **Detailed Assessment of the Relationship between Ozone, NO and NO₂, and Factors Controlling Them**
- Objective 3 - **Policy Development and Scenario Analysis**
- Objective 4 - **Improvements to Photochemical Reaction Schemes**
- Objective 5 - **Development of Stomatal Flux Module for Crops and Semi-natural Vegetation**

There are strong linkages between the project objectives and with Defra's policy requirements, as shown in Figure 3.1.

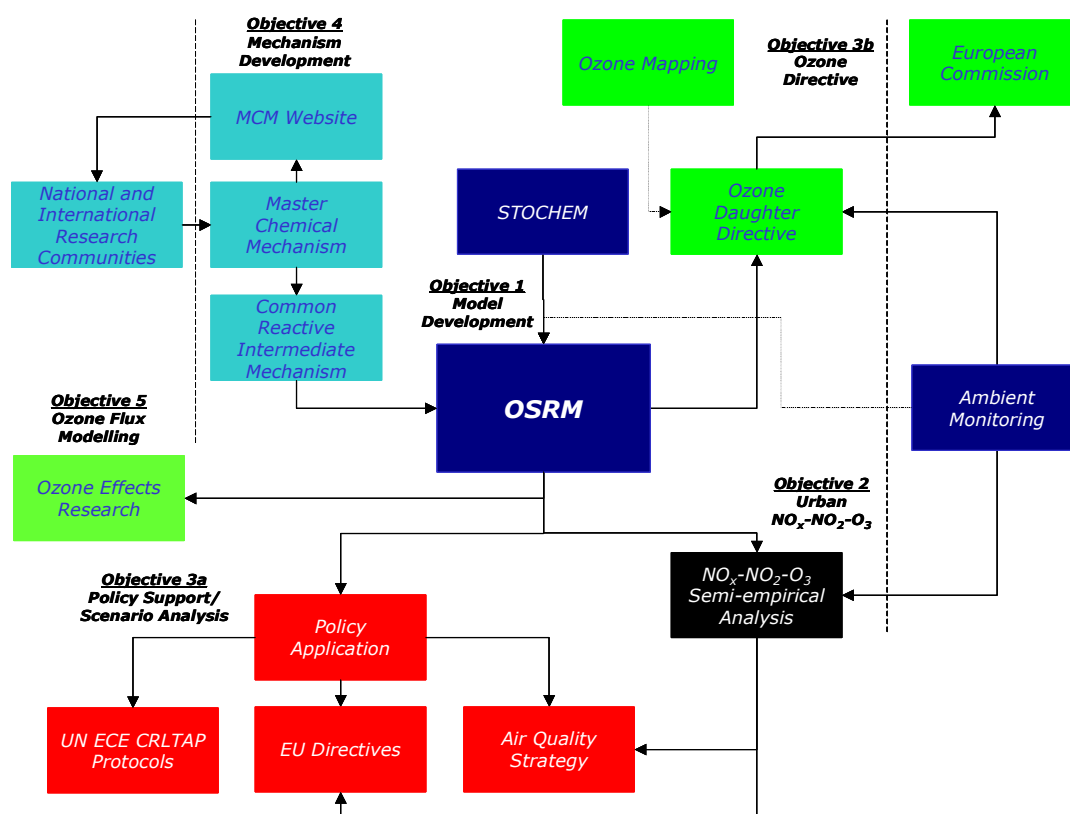


Figure 3.1 Schematic of the Linkages between the Project Objectives and with Defra's Policy Requirements.

The key requirements for the project are:

- an ability to develop and apply numerical models for policy applications;

- an ability to develop tractable chemical mechanisms for policy applications;
- recognised expertise in the chemistry and physics of the lower atmosphere to understand the relationship between ozone and other pollutants of interest;
- detailed understanding of the key policy drivers; and
- networking to ensure timely uptake of the latest results from national and international research programmes.

3.2 PROJECT PARTNERS

The project team led by netcen comprised: Professor Dick Derwent (rdscientific), Dr Mike Jenkin (Imperial College), Professor Mike Pilling (University of Leeds) and Dr Peter Fitzgerald (SERC0 Assurance)¹. The project partners were responsible for delivering specific tasks of the overall work programme, as shown in the schematic presented in Figure 3.2.

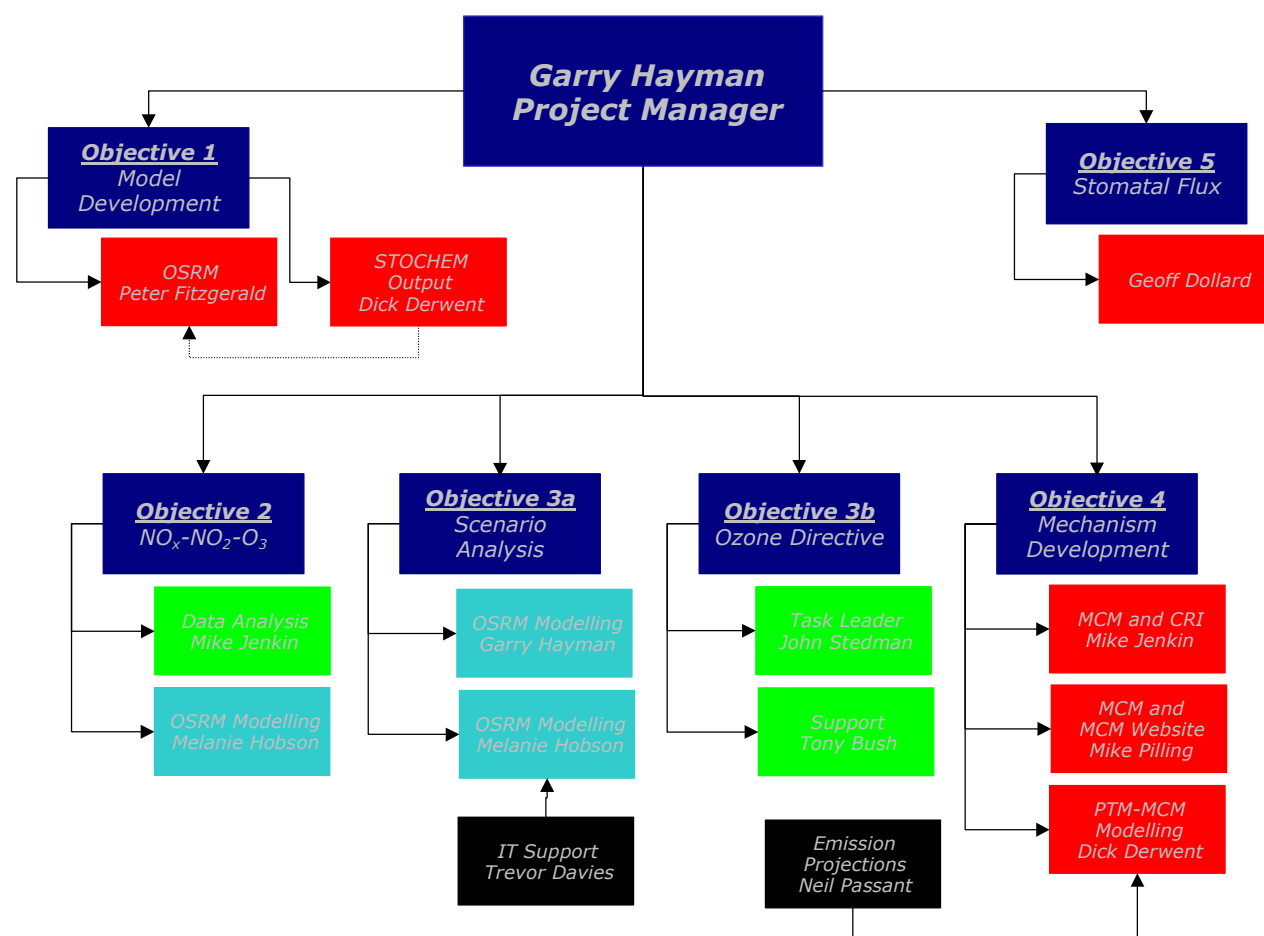


Figure 3.2 Allocation of the Objectives to the Consortium Partners.

3.3 ACHIEVEMENTS AND KEY RESULTS

The project schedule proposed at the start of the project is shown in Figure 3.3.

¹ Peter Fitzgerald completed the initial work on Objective 1. Following his departure from SERCO Assurance, he is no longer involved in the project. Future model development on the OSRM will be undertaken in house.

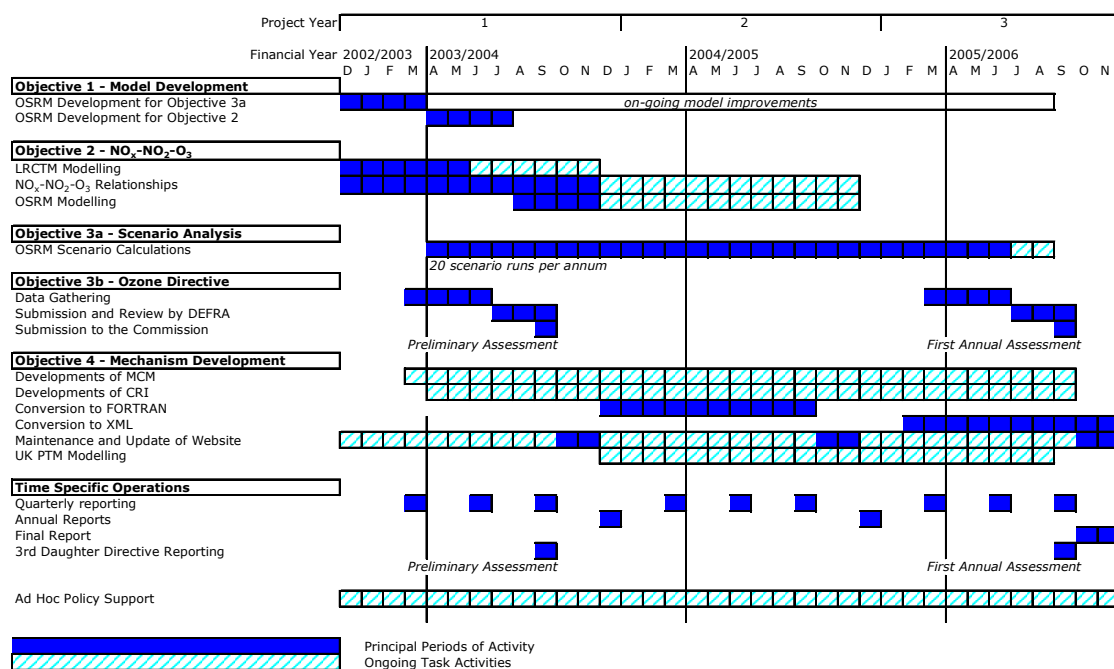


Figure 3.3 Project Schedule.

The programme of work proposed during the tendering phase of the contract is included as Appendix 1. While some of the work could be specified in detail, other elements were more open-ended or ad hoc in nature and were undertaken during the course of the contract to agreed programmes of work and timescales. The most significant deviations from the programme of work were under Objective 3 – Policy Support and Scenario Analysis. The modelling work for the proposed reviews of the UN ECE Gothenburg Protocol and the related National Emission Ceilings Directive of the European Union was not undertaken as the Protocol and Directive did not come into force on the expected timescale, thereby delaying the reviews. Instead, the major element of work under this objective has been the ozone modelling undertaken for the Review of the UK Air Quality Strategy.

A summary of the work undertaken by Objective is given below:

Objective 1: Development and Application of Ozone Models: The Ozone Source-Receptor Model was identified as the primary modelling tool for the current project. While the version of the model (v1.2) available at the commencement was able to reproduce some features of the observed ozone measurements, it was recognised that further development was needed to improve the performance and realism of the model.

A number of developments, improvements or modifications have been made to the OSRM during the course of the contract, such as:

- the length of the trajectory
- the boundary layer depth
- the chemical mechanism
- the initialisation of the trajectory
- the biogenic inventory used
- the treatment of the emissions

The newer versions of the model (versions 1.8) were still found to be producing too much ozone and generated peak ozone concentrations which were two to three times greater than those observed. In addition, these versions were not able to reproduce concentrations of ozone (and oxides of nitrogen) in urban environments. Further work was undertaken, including the development and refinement of a Surface Conversion algorithm, to address this.

The OSRM describes the boundary layer by a single box and assumes that this is well mixed. While this is a reasonable assumption for rural areas, it is less valid in urban areas with high NO_x emissions. In such areas, there will inevitably be a

gradient in the NO_x concentration profile, with higher concentrations at the surface. This will lead to lower ozone concentrations at the surface through reaction with nitric oxide. An algorithm has been developed and implemented in the OSRM post-processor to convert the mid-boundary layer concentrations to surface concentrations. This algorithm uses the meteorological parameters characterising the boundary layer, surface roughness appropriate for the surface types considered, resistance parameters for O_3 and NO_2 , the local NO_x emission rates and a simple $\text{NO-NO}_2\text{-O}_3$ photostationary state chemistry. The performance of the Ozone Source-Receptor Model, especially in urban areas, has been significantly improved through the development and use of this Surface Conversion algorithm.

Further metrics for ozone and oxides of nitrogen have been added to the OSRM post-processor to address the impacts of ozone on human health and ecosystems.

The output of the OSRM has been compared with established models - the UK Photochemical Trajectory and ADMS Urban models – which are widely used in the regulatory and policy context to assess different emission control options. On a like-for-like basis, the OSRM and UK Photochemical Trajectory Model were found to give identical output and responses. The comparison of the OSRM with the ADMS Urban models gave similar overall responses, although there were differences in the detail.

The model developments and comparisons confirm that the latest version of the OSRM is a robust model that can be used to assist the development of policy for not only ozone but also oxides of nitrogen.

Objective 2: Detailed Assessment of the Relationship between Ozone, NO and NO_2 , and Factors Controlling Them: The ambient levels of O_3 and NO_2 are inextricably linked because of the chemical coupling of O_3 and NO_x . As a consequence, the response to reductions in the emissions of NO_x is highly non-linear and any resultant reduction in the level of NO_2 is invariably accompanied by an increase in the level of O_3 . The success of proposed control strategies will depend on a complete understanding of the relationships between O_3 , NO and NO_2 under atmospheric conditions.

In the previous contract (Modelling of Tropospheric Ozone Formation, EPG 1/3/143, see Hayman *et al.* [2005]), monitoring data from a limited number of sites, mainly in Greater London, were analysed and insight was gained into the dependence of the annual mean concentrations of NO_2 on $[\text{NO}_x]$. The concentration of 'oxidant', $[\text{OX}] (= [\text{O}_3] + [\text{NO}_2])$, was found to depend approximately linearly with $[\text{NO}_x]$ over the entire range, such that the level of OX at a given location has a NO_x -independent contribution, and a NO_x -dependent contribution. The former is effectively a 'regional' contribution which equates to the background O_3 level, whereas the latter is effectively a 'local' contribution which correlates with the level of primary pollution. Subsequently, the fractional contribution of NO_2 to OX (*i.e.*, $[\text{NO}_2]/[\text{OX}]$) as a function of the NO_x concentration was determined. In this way, it was possible to rationalise the derived $[\text{NO}_2]$ vs. $[\text{NO}_x]$ relationships, and their site-to-site variations, in terms of sources of OX and well-understood chemical processes.

During this contract, the analysis of the annual mean concentrations (based on data up to 2001) has been extended to 66 automatic sites where O_3 and NO_x are monitored. The analysis showed that the description of annual mean concentrations of NO_2 , and their dependence on $[\text{NO}_x]$, could be improved by the application of empirically-derived relationships between concentrations of O_3 , NO_x and NO_2 . In this way, it was possible to rationalise the variation of $[\text{NO}_2]$ with $[\text{NO}_x]$, and how it varies from one site to another, in terms of sources of OX and well-understood chemical processes. $[\text{NO}_2]$ vs. $[\text{NO}_x]$ relationships were recommended for 56 urban and suburban sites. These analyses have been extended to include the annual mean data at selected sites up to 2004.

The results generally indicated that zones in the southern UK, northeast England and Scotland have slightly higher regional background levels of OX. Previous analyses of

rural O₃ concentrations in the UK have tended to show a similar phenomenon. As found previously, the derived local OX contributions show substantial site-to-site variations. Although there are a small number of outliers, values typically lie in the range 3-17%. Possible reasons for these variations include the fractional contribution of NO₂ to emitted NO_x from differing vehicle fleet compositions (e.g., proportion of diesel vehicles) and driving conditions (e.g., vehicle speed), which are characteristic of each site.

The results were also used to propose representative expressions for different regions of the UK, and were compared with those currently employed in the National Scale Empirical NO₂ modelling activities. The present results broadly support the NO₂ vs. NO_x dependences used in the National Scale Modelling activities, but provide an alternative approach based on understanding of OX sources and the chemical coupling of NO_x and O₃. The present expressions also have the advantage that the possible effects of changes in background OX levels and/or primary NO₂ emissions can be investigated.

The relationships between the annual mean concentrations of NO-NO₂-NO_x-O₃-OX has been included in the work of the Department's Air Quality Expert Group and specifically in its report on Nitrogen Dioxide. The relationships developed above have been incorporated into the empirically-based modelling work undertaken by netcen on other contracts for the Department.

A comprehensive analysis of 1998 and 1999 hourly mean data has been carried out for the site at Marylebone Road. This has provided insights into the seasonal and diurnal dependence of OX sources and their origins, and the conditions under which exceedences of the hourly mean NO₂ limit value (200 µg m⁻³, 104.5 ppb) are more probable. The present analysis demonstrates that the ambient concentration of OX at Marylebone Rd is sensitive to a number of factors, such as primary NO₂ emissions and regional background O₃ concentrations, and that variation in the magnitudes of these factors leads to substantial diurnal and seasonal differences in the level of NO_x required for the hourly mean NO₂ limit value of 104.5 ppb to be exceeded. The factors that cause these differences at an individual site are also likely to contribute to the site-to-site variations in annual mean NO_x thresholds. However, the annual mean local OX contributions for a number of urban background and urban centre sites (i.e., up to ~20%) are significantly greater than the vehicular primary NO₂ fractions derived in the present work. This suggests that either the primary NO₂ fractions are elevated by factors such as traffic congestion, or that the local OX at these sites has additional contributions from local scale chemical processes. As discussed previously by AQEG and the project consortium, a number of thermal and photochemical sources may potentially contribute, through converting NO to NO₂, without associated removal of O₃.

The analysis would also be expected to predict a general lowering of NO_x concentrations required for the hourly mean NO₂ limit value to be exceeded. Support for this conclusion is apparent from the record of exceedences of the NO₂ hourly mean limit value at London AURN sites including Marylebone Rd. Although there is inevitably some year-to-year variation in the number of hours exceedence in each year, a general decrease is apparent in the early part of the time series (1998-2002) consistent with the progressive reduction in NO_x emissions over this period. However, an increase in exceedences is apparent at a number of sites since 2003, most notably Marylebone Rd, which is linked to the abrupt increase in the primary NO₂ emissions fraction in 2003. The data for 2003-2005 further suggest that the situation is progressively worsening at Marylebone Rd, in agreement to the conclusion derived from the annual mean analysis. It is noted, however, that (to date) no London AURN site other than Marylebone Rd has failed the associated objective of ≤ 18 hours exceedence in a given year during this period, although it is quite likely that the A3 roadside site will also fail in 2005.

The OSRM has been used to simulate the 2002 annual mean annual mean concentrations of O₃, NO, NO₂ and Oxidant (= [O₃] + [NO₂]) at background sites in the

London, Kent and Hertfordshire Air Quality Monitoring Networks [Derwent, 2005a]. The comparison of the modelled and measured concentrations shows that the chemistry implemented in the surface conversion algorithm gives NO-NO₂-NO_x-O₃-O_x relationships, which are consistent with those derived from observations. Scatter plots show the good agreement between the modelled and measured concentrations of O₃, NO, NO₂, NO_x and Oxidant for these London and South East sites (Non-Roadside), confirming its suitability for urban ozone modelling.

Objective 3: **Policy Development and Scenario Analysis:** This objective comprises 2 main areas (a) Policy Development and Scenario Analysis and (b) Implementation of the Third Daughter Directive on Ozone.

The UK Photochemical Trajectory Model (PTM) and Ozone Source-receptor Model (OSRM) have been applied to evaluate a number of proposed ozone control measures. In the UK PTM model runs, a single linear trajectory was most often used. The trajectory had been selected to represent the air flow during an idealised photochemical episode over the UK (*i.e.*, anticyclonic meteorological situation of easterly winds, leading to a broad westerly air flow carrying photochemically-aged polluted air masses out of Europe towards the British Isles). This trajectory does not represent the conditions prevailing during a particular photochemical episode but represents a potential worst-case situation. For the OSRM model run, a calendar year is simulated and a wider range of realistic air mass trajectories is sampled, including those from other wind directions. These other trajectories may have little or no photochemical ozone production, especially if the trajectory has mainly passed over low emission areas (*e.g.*, the sea). There will be a chemical titration of the ozone in such air masses when these air masses pass over NO_x emission sources. It is therefore likely that the two models will give different response to NO_x and/or VOC emission controls (particularly NO_x control).

(a.1) Policy Development and Scenario Analysis using the UK Photochemical Trajectory Model (PTM): The UK PTM has been applied to evaluate a number of proposed ozone control measures:

- (i) **Petrol Volatility:** The policy question concerns the likely benefit from a 7 thousand tonne reduction in VOC emissions from petrol evaporation between 1st June and 31st August. Calculations by the UK PTM showed that this measure would have little impact on peak ozone concentrations.
- (ii) **Petrol vs. Diesel:** There is strong pressure for policymakers to increase the penetration of new diesel vehicle technologies into the passenger car and LGV fleets to meet future targets for greenhouse gas emissions. The UK PTM has been used to assess the ozone benefit or dis-benefit to this policy from the implied increased NO_x emissions since the EURO IV emission standards imply higher NO_x emissions per kilometre travelled from diesel-engined cars compared with petrol-engined cars. The model results showed that the evaluation of the ozone benefits or dis-benefits of increasing the penetration of new diesel-vehicle technologies depends markedly on whether just the NO_x emission changes are considered or whether wider issues such organic emissions from petrol-engined vehicles are also taken into account.
- (iii) **Decorative Paints:** The European Commission has proposed a Directive to reduce the VOC content of decorative paints, varnishes and vehicle refinishing products. The OSRM and UK PTM have been used to assess the benefits to the UK of reductions in VOC emissions arising from within UK, and in UK + rest of Europe. Preliminary UK PTM calculations assuming a 40 ktonne per annum reduction in UK VOC emissions and proportional reduction in European emissions gave a noticeable reduction in peak ozone concentrations. OSRM model results, undertaken as part of the Regulatory Impact Assessment, indicated that the UK emission reduction would only be 2 ktonnes per annum over the current NAEI base case projection for 2010. These are significantly smaller than those proposed by the Commission as much of the reduction identified is already included in the current base case

projection. OSRM calculations using the revised VOC emission reduction showed that UK action would have a negligible effect but that EU action would be more effective.

- (iv) **Post-Gothenburg Emission Controls:** The PTM was used to investigate the additional NO_x and VOC emission controls, which would be needed to achieve Ozone air quality standards and objectives beyond those agreed in the EU National Emission Ceilings Directive and the UN ECE Gothenburg Protocol. Three further stages of emission reductions were considered taking emissions below the 2010 levels by 30%, 60% and 90%. In all cases, these emission reductions were applied across-the-board on all source categories and on all countries. For the 30% emission reduction scenarios, the UK PTM is indicating that the arrival point in Wales is still VOC-limited in 2010, because the ozone benefit (74.2 down to 69.6 ppb) from reducing VOC emissions is larger than the ozone benefit (74.2 down to 69.9 ppb) from reducing NO_x emissions. However, looking at the 60% and 90% reductions, the situation reverses and the ozone benefits from NO_x reductions look substantially greater than those from VOC reductions.
- (a.2) **Policy Development and Scenario Analysis using the Ozone Source-receptor Model (OSRM):** Earlier versions of the OSRM were used to assess a number of policy options relating to ozone:
- (i) **Regulatory Impact Assessment of Directive on Decorative Paints:** The European Commission has proposed a Directive to reduce the VOC content of decorative paints, varnishes and vehicle refinishing products. There is a requirement to calculate the benefits to the UK of reductions in VOCs arising from within UK, and in UK + rest of Europe. The Commission have calculated potential emission reductions that would arise from the proposed controls in 2010. UK-scale model runs were undertaken to a 10 km x 10 km grid.
- (ii) **Proposed NO_x Emission Standards for Vehicles (EURO V Standards):** The European Commission are expected to propose new emission standards for vehicles in 2004. The Department and the Department for Transport wish for information on the air quality implications of various scenarios to inform the UK position. Although the main focus to date has been on NO₂ and PM exposure, there is a need to assess the effects on ozone concentrations and hence human exposure. UK-scale model runs were undertaken to a 20 km x 20 km grid for computational reasons.
- (iii) **Regulatory Impact Assessment of Directive on Petrol Vapour Recovery:** OSRM modelling calculations have been undertaken as part of the regulatory impact assessment on petrol vapour recovery (PVR) and possible derogations. UK-scale model runs were undertaken to a 10 km x 10 km grid.
- (iv) **Post-Gothenburg Scenarios:** Assuming full compliance with the UN ECE Gothenburg Protocol and the EU National Emissions Ceilings Directive, the Department is interested the effectiveness of different controls on NO_x and/or VOC emissions to improve ozone air quality after 2010. Four OSRM model runs were undertaken with across-the-board reductions in the emissions of NO_x and/or VOC of 30%. UK-scale model runs were undertaken to a 10 km x 10 km grid.

The above model runs used meteorology for 1999.

The discussion is therefore based on the unconverted outputs. There appeared to be two counteracting effects (a) photochemical production of ozone involving oxides of nitrogen and volatile organic compounds and (b) chemical titration by NO_x removing ozone. These two effects respond differently to emission control. Thus, either VOC emission control alone or combined VOC and NO_x emission

controls are needed to improve ozone air quality. A paper was prepared on these model runs, from which the following are taken:

The surface-conversion algorithm was not available for use in the above OSRM model runs. The discussion is therefore based on the unconverted outputs. There appeared to be two counteracting effects (a) photochemical production of ozone involving oxides of nitrogen and volatile organic compounds and (b) chemical titration by NO_x removing ozone. These two effects respond differently to emission control. Thus, either VOC emission control alone or combined VOC and NO_x emission controls are needed to improve ozone air quality. A paper was prepared on these model runs, from which the following are taken:

- **Trends in Base Case:** The reduction in NO_x emissions between 1999 and 2015 leads to a reduction in NO₂ concentrations by between 30-35% for England and Wales and ~40% for Scotland and Northern Ireland. There is a downward trend in the AOT40 for the protection of crops across the UK although there are still large parts of the country, which are above the threshold of 3,000 ppb hours (6,000 µg m⁻³ hours). The annual mean of the maximum of the 24 possible 8-hour running mean concentrations in each day appears to fall at the extremities of the UK but rise in England where the emissions of nitrogen oxides are higher. However, the annual mean of the maximum of the 24 possible 8-hour running mean concentrations in each day, which are greater than 35 ppb, on the other hand decreases between 1999 and 2005. Thereafter, there is a very slight increase.
 - **Emission Reductions:** NO_x emission reductions alone (e.g., the EURO V Emission Standards) lead to lower NO₂ concentrations but to increases in the population-weighted annual mean of the maximum daily running 8-hour ozone concentrations. On the other hand, VOC emission reductions (Petrol Vapour Recovery and the proposed Directive on Decorative Paints) have little or no effect on the annual mean NO₂ concentration but do lead to lower values of all the ozone metrics considered.
 - **Post-Gothenburg:** A 30% VOC emission reduction improves ozone air quality but a 30% reduction in NO_x emission reduction leads to poorer ozone air quality. Comparison of the scenario in which NO_x and VOC emissions are each reduced by 30% with separate 30% reduction in NO_x or VOC reductions indicates that the counteracting effects of photochemical production of ozone (by NO_x and VOC emissions) and the titration effect of NO_x emissions.
 - **Regional Changes:** Compared to the 1999 model run, the base case runs show an improvement in ozone air quality, as measured by the annual mean of the maximum of the 24 possible 8-hour running mean concentrations in each day, which are greater than 35 ppb, for each region (England, Wales, Scotland and Northern Ireland). On the other hand, there is a reduction in the annual mean of the maximum of the 24 possible 8-hour running mean concentrations in each day for Northern Ireland, little change in this metric for Scotland and Wales and a deterioration for England. The annual mean of the maximum of the 24 possible 8-hour running mean concentrations in each day will be sensitive to all hours and trajectories, including those where the titration effect is dominant. The annual mean of the maximum of the 24 possible 8-hour running mean concentrations in each day will be more sensitive to the higher ozone concentrations, which are more likely to be of a photochemical origin.
- (a.3) Modelling with the Ozone Source-receptor Model (OSRM) for the Review of the Air Quality Strategy: The UK Government and the Devolved Administrations (the Scottish Executive, Welsh Assembly Government and the Department of the Environment Northern Ireland) published an Air Quality Strategy for England, Scotland, Wales and Northern Ireland (AQS) in January 2000. The Government and the Devolved Administrations are currently undertaking a review of the Air Quality Strategy. This review will assess progress towards the achievement of the AQS objectives and assess the costs and benefits of possible additional measures to improve air quality in the UK. The focus of this review of possible

measures will be on the impact of measures on concentrations of particles, nitrogen dioxide and ozone, the pollutants for which the achievement of the objectives is likely to be the most challenging.

The latest version of the OSRM (Version 2.2a with Surface Conversion Algorithm) was used to investigate the impacts of a number of measures being considered for the **Review of the Air Quality Strategy** on future ozone and nitrogen dioxide air quality. A new set of emission projections was developed for the base case and control scenarios for 2010, 2015 and 2020. Model runs were undertaken to a 10 km x 10 km receptor grid covering the UK, mostly using meteorological datasets for 2003. The analysis of the various base case and scenario runs considered seven ozone and one nitrogen dioxide metrics. Population-weighted means were derived for the metrics associated with impacts on human health. Area-weighted means were derived for the non-health effects metrics. The population- and area-weighted means have been determined for the following regions: All UK, Scotland, Wales, Northern Ireland, Inner London, Outer London and the Rest of England.

The key points to note from the model runs are that:

- The base case runs show a progressive worsening of ozone air quality for all metrics from 2003 to 2010 and beyond;
- There is however an improvement in nitrogen dioxide air quality as annual mean concentrations fall, especially for the NO_x control measures;
- The use of population-weighted means focuses the analysis on ozone in urban areas. In addition to the role of NO_x emissions in photochemical ozone production, lower NO_x emissions reduce the chemical titration effect, most notably in urban areas. This causes ozone concentrations to move towards the higher concentrations in surrounding rural areas. The reduced chemical titration is a major factor in the increase in the ozone metrics and the deterioration of ozone air quality;
- A second major factor leading to higher ozone concentrations is changing atmospheric composition arising from climate change. In the absence of such a change, the base case runs would have shown an improvement in ozone air quality for some metrics (AOT40 – Crops and AOT40 – Forests);
- The NO_x control measures generally increase ozone concentrations, although there are instances for some of the measures that ozone air quality is improved in 2020, as evidenced by a lower value of the ozone metric;
- The VOC control measures, on the other hand, lead to an improvement in ozone air quality for all ozone metrics;
- Meteorological effects and year-to-year variability in meteorology can have a larger effect on ozone air quality than some of the emission control measures considered.

As a result of the above, there will be widespread exceedences of ozone air quality standards and objectives in 2010 and beyond.

The model outputs - population- and area-weighted means of seven ozone metrics - were passed to the teams involved in the cost-benefit analysis being carried out for the Review of the Air Quality Strategy. These have been reported as part of other Defra-let contracts.

The model runs described above were largely based on specific emission control measures. The emission reductions implied by the measures were used to prepare the emission inventories for the model runs. Although desirable, the measures by themselves would not necessarily ensure attainment of ozone air quality targets or objectives. As a result, the Department has subsequently commissioned additional site-specific model runs, in which larger reductions of NO_x and/or VOC emissions were made. Six series of OSRM model runs were

undertaken in which the emissions were progressively reduced from 80% to 20% of their 2020 base case values in 10% increments:

- UK NO_x emissions
- UK NO_x and VOC emissions
- UK VOC emissions
- European and UK NO_x emissions
- European and UK NO_x and VOC emissions
- European and UK VOC emissions

The results of these runs will be reported in an addendum to this Final Report.

- (b) *Implementation of the Third Daughter Directive on Ozone:* As required by the Directive, a preliminary assessment report was prepared and submitted to Defra in August 2003. This assessment, largely based on monitoring data, reviewed the current position and the likelihood of achieving the proposed target values and long-term objectives for ozone. The target values for 2010 do not appear particularly stringent but long-term objectives are likely to be more difficult to achieve.

The Directive allows the use of supplementary assessment techniques to reduce the burden of monitoring. Work has been undertaken to assess the relative performance of the 2 ozone modelling techniques and thus to recommend the preferred supplementary assessment technique to be used for the third Daughter Directive on ozone. Outputs from the OSRM (based on Version 2.2 with Surface Conversion Algorithm available at January 2005, *i.e.*, prior to the review of the OSRM and Surface Conversion Algorithm), empirical modelling estimates and measurement data from the AURN have been compared for the two ozone metrics of relevance to the Directive (a) number of days with a running 8-hour ozone concentration greater than 120 µg m⁻³ (averaged over the 3-year period: 2001 to 2003) and (b) AOT40 – Crops (averaged over the 5-year period: 1999 to 2003). From the analysis of the comparative performance of the empirical and OSRM models, it was judged that the empirical modelling approach delivers least uncertainty in the model outputs. It was proposed that the empirical modelling approach should be taken forward as the preferred means of supplementary assessment for the reporting ozone levels in 2004 calendar year. A further recommendation was made to repeat the assessment to take account of updates to the modelling techniques.

2004 is the first year for which an annual air quality assessment for the third Daughter Directive pollutants is required. The questionnaire has been completed for submission to the European Union containing the results of this air quality assessment (along with those required for the first and second Daughter Directives). The assessment takes the form of comparisons of measured and modelled air pollutant concentrations with the target values and long-term objectives set out in the Directives. Maps of background ozone concentrations in 2004 on a 1 km x 1 km grid of the ozone metrics listed above have been prepared using the empirical mapping technique. There are 28 agglomeration zones (large urban areas) and 15 non-agglomeration zones. The status of the zones status has been determined from a combination of monitoring data and model results. The results of this assessment are summarised in the table below, in terms of exceedences of Target Values (TV) and Long-term Objectives (LTO).

Summary Results of Air Quality Assessment relative to the Target Values and Long-term Objectives for Ozone for 2010.

Target Value	Number of Zones exceeding
Max Daily 8-hour mean Target Value	none
AOT40 Target Value	none
Long-term Objective	Number of Zones exceeding
Max Daily 8-hour mean Long-term Objective	43 zones (36 measured + 7 modelled)
AOT40 Long-term Objective	7 zones (5 measured + 2 modelled)

Objective 4: **Improvements to Photochemical Reaction Schemes:** Work has been undertaken on the following topics:

- (a) Updating of the Master Chemical Mechanism: The degradation schemes for four aromatic hydrocarbons - benzene, toluene, *p*-xylene and 1,3,5-trimethylbenzene - have been updated. The performance of these schemes has been evaluated against environmental chamber datasets obtained from the European Photoreactor (EUPHORE). The updated mechanisms show improved ability to simulate some of the observations from the EUPHORE datasets and represent our current understanding of aromatic degradation mechanisms. However, significant discrepancies remain concerning, in particular, ozone formation potential and oxidative capacity of aromatic hydrocarbon systems. The combination of over-prediction of ozone concentration and under-prediction of reactivity poses a problem for mechanism development; a reduction in ozone concentration can be achieved by a reduction in peroxy radical concentration, which limits the NO to NO₂ conversion, but this will also lead to a reduction in OH production and in the oxidative capacity of the system.

Photo-dissociation of atmospheric molecules by solar radiation plays a fundamental role in atmospheric chemistry. The photolysis of trace species such as ozone and formaldehyde contributes to their removal from the atmosphere, but probably the most important role played by these processes is the generation of highly reactive atoms and radicals. Photo-dissociation of trace species and the subsequent reaction of the photo-products with other molecules is the prime initiator and driver for the bulk of tropospheric chemistry. As a polluted air parcel ages, the contribution of the photolysis of oxygenated intermediates becomes the major source of radicals. Therefore it is clear that understanding photolysis processes requires accurate and reliable determination of photolysis frequency data in order to accurately model the total HO_x and NO_x budgets within the troposphere.

As part of the present contract, a thorough survey of literature cross-section and quantum yield data has been carried out in order to review and update the calculation of the photo-dissociation coefficients for organic (and inorganic) species in the MCM and to expand upon the current range of species covered. New photolysis rates have been calculated using the discrete ordinate radiative transfer model *TUV4.2* (Madronich and Flocke [1998]). The use of such a flexible model enables the photolysis rate to be calculated under a variety of atmospheric conditions (*e.g.*, altitude, cloud cover, surface type (albedo)).

Many of the photochemical parameters are temperature and pressure dependent. These dependencies have been quantified in some of the recent literature studies for the first time. One of the future developments of the MCM is to extend its use to the free troposphere. Therefore in order to facilitate this, the photolysis rates are calculated as a function of pressure as well as temperature where appropriate data are available. Such new and improved laboratory measurements has enabled the expansion of the current list of photolysis rates in the MCM. This new data will also enable us to review the surrogate representation for species whose parameters are still not known. For example, the degree to which the contributions of different functional groups within a molecule are additive could be tested if enough data are available on bi-functional groups.

- (b) Verification of the Master Chemical Mechanism: The MCM v3 degradation schemes for butane and isoprene have been evaluated using the large environmental chamber dataset of the Statewide Air Pollution Research Center (SAPRC) at the University of California. The MCM v3 mechanisms for both butane and isoprene were found to provide an acceptable reaction framework for describing the NO_x-photo-oxidation experiments, and generally performed well. A number of parameter refinements were identified which resulted in an improved performance. While the recommended updates are certainly necessary to maintain the MCM fully, it is emphasised that they have only a minor influence on the performance of the butane and isoprene schemes in atmospheric models. Consequently, these evaluation activities provide strong support for the MCM

schemes for butane and isoprene, which are the most abundant components of emissions of anthropogenic and biogenic non-methane VOC, respectively.

- (c) *MCM Website*: The Master Chemical Mechanism (MCM) has been updated to MCM version 3.1. MCM v3.1 now contains 135 primary emitted VOCs which lead to a mechanism containing ca. 5,900 species and 13,500 reactions. As part of the ongoing improvements to the MCM a new version of the website has been developed with the primary objectives of making the website clearer and easier to navigate and of improving access to the MCM itself. The site can be found at the address: <http://mcm.leeds.ac.uk/MCM/>.
- (d) *Code Conversion*: The MCM is now available in several output formats (a) the standard FACSIMILE output, which has been improved, (b) FORTRAN and (c) XML, although work is in progress to develop the most appropriate and useful design for the XML schema and the properties of Chemical Markup Language (CML) are being examined to understand the ways in which XML is currently used to represent chemistry. The FORTRAN and XML formats are more robust than that of FACSIMILE and are more future proof. This should further improve the uptake of the Master Chemical Mechanism.
- (e) *The Common Reactive Intermediate (CRI) Mechanism*: Using the knowledge and understanding gained from developing the MCM, a reduced mechanism - the Common Reactive Intermediate (CRI) mechanism - was derived from the Master Chemical Mechanism. The CRI mechanism treats the degradation of methane and 120 VOC using approximately 570 reactions of 270 species (*i.e.*, about 2 species per VOC). It thus contains < 5% of the number of reactions and < 7% of the number of chemical species in MCM v3.1, providing a computationally attractive mechanism. The CRI mechanism has been benchmarked against the MCM and was shown to produce almost identical concentrations for key species to those calculated using the full Master Chemical Mechanism. Whilst it is recognised that CRI v1 correctly represents ozone formation from the VOC mixture, it may not fully recreate the relative contributions of component VOC or VOC classes within the emitted mixture. A new version of the mechanism is being developed which will treat the degradation of individual classes of VOC (*e.g.*, alkanes, alkenes, aromatics) separately. The work to date has demonstrated that the mechanism is improved by defining separate series of representative intermediates for some VOC classes. This will result in an ultimate increase the size of the mechanism over that of CRI v1, but will allow a more rigorous description of the impact of the different VOC emission sectors, and an improved foundation for the expansion of the mechanism to the treatment of the several hundred minor VOC not currently represented in MCM or CRI.
- (f) *Multi-day Reactivity*: The UK Photochemical Trajectory Model incorporating the Master Chemical Mechanism has been used to investigate how the reactivity of different classes of volatile organic compounds changes with time. The standard idealised trajectory was used, in which an air parcel was followed as it travelled on an easterly wind from Austria across Europe to its arrival point in Wales. The work has now been completed and three mechanisms have been found to account for ozone formation on subsequent days following their emissions. These are (a) the carry over of unreacted VOCs, (b) the formation of peroxyacetylnitrates and (c) the consecutive reactions of aldehyde formation and degradation. From a study of the chemical mechanisms used in most policy models, EMEP included, it is likely that the multi-day formation of ozone from alkenes and carbonyl compounds is underestimated because of the simplifications and approximations made in the compression of the chemical mechanisms.

The use of the MCM v3.1 has resolved some previous anomalies in the behaviour of certain aromatic compounds (*p*-xylene, ethylbenzene, propylbenzene and *i*-propylbenzene). As suspected, there were problems in the detailed mechanisms for these four aromatic species in the previous version of the MCM (v3.0).

- (g) *PTM Modelling of the TORCH Measurements*: The UK Photochemical Trajectory Model (PTM), containing speciated emissions of 124 non-methane VOC and a comprehensive description of the chemistry of VOC degradation (provided by MCM v3.1 and the CRI mechanism), has been used to simulate the measurements made at a site in the southern UK during the NERC Tropospheric Organic Chemistry Experiment (TORCH). The measurement campaign coincided with the August 2003 photochemical pollution episode. The comparison of the simulated and observed distributions of 34 emitted hydrocarbons provides strong support for the VOC speciation used in the NAEI, but is indicative of an under representation of the input of biogenic hydrocarbons, particularly at elevated temperatures. The model calculations also provided detailed distributions of ca. 1250 carbonyl compounds, formed primarily from the degradation of 124 emitted VOC. Although the simulated distributions of four aldehydes and three ketones correlated well with observations for each class of compound, the simulated concentrations of the aldehydes were systematically lower than those observed, whereas those of the higher ketones were systematically higher. The MCM is one of the few chemical mechanisms available to predict the patterns and structures of oxidised products, such as simple and multi-functional carbonyls, thereby allowing a much more detailed examination of atmospheric chemical mechanisms. These model calculations will allow further refinement of the formation routes of these compounds in the MCM.

The work was extended to assess the impact on the daily-average ozone concentration calculated throughout the campaign which resulted from an increase of VOC emissions by 1% from (a) man made and (b) natural sources. The anticyclonic period generally shows the largest increment, because the emissions input was greatest during this period. It was also evident that the biogenic emissions are calculated to make a larger relative contribution at the prevailing higher temperatures. Although the magnitude of biogenic VOC emissions is subject to some uncertainty, these results support an important role for biogenic VOC oxidation in regional-scale ozone formation under heatwave conditions.

A further set of model runs was undertaken using historical emissions of NO_x , anthropogenic VOC, CO and SO_2 appropriate to the years 1990, 1995 and 2000 (based on NAEI and EMEP), and projected emissions for the years 2005, 2010, 2015 and 2020, based on relative UK figures reported in AQEG (2004; 2005). The simulated ozone distributions show that the same episode conditions in earlier years would have been accompanied by broader ozone distributions with greater daytime maxima and increased overnight depletion. The decreasing trend in peak ozone concentrations is driven primarily by reductions in emissions of anthropogenic VOC since 1990, and provides a reasonable description of the observed trend in peak hourly mean ozone concentrations observed at long-running UK rural sites in the heatwave years of 1989, 1990, 1995 and 2003 (defined as years when temperatures $> 34^\circ\text{C}$ were recorded). The increasing (night-time) minima are a consequence of associated NO_x emissions reductions, resulting from decreased local removal of ozone by reaction with NO emitted into the shallow night-time boundary layer.

The effects of 10% incremental reductions in the emissions of NO_x and anthropogenic VOC were examined for the 1990, 2003 and 2020 scenarios, to investigate whether ozone formation is limited by the availability of NO_x or VOC. The 1990 scenario demonstrates strong VOC limitation throughout the campaign period, with NO_x reductions almost always leading to an increase in ozone concentration, such that VOC emissions controls are clearly the favoured option for reducing ozone concentrations. Although the results for the 2003 scenario show that the campaign period is still dominated by VOC-limited conditions, there is a shift towards NO_x -limitation, with an increased number of days (relative to 1990) where the NO_x control leads to a reduction in ozone concentration. The results for the 2020 scenario show that 10% NO_x control leads comparable numbers of days when the ozone concentration is increased and decreased, and a further increase in the number of days (relative to 2003 and 1990) when NO_x control is more beneficial in reducing ozone concentrations than VOC control.

Despite this, VOC reductions remain the favoured option when the whole campaign is considered. The results therefore demonstrate that peak ozone formation for the photochemically-active conditions of this campaign at this location is predominantly VOC-limited for the complete time series, but shows a trend towards NO_x-limitation. Although this is in general agreement with previous assessments for Southeast England, this sensitivity study also shows that VOC- and NO_x-limitation are not intrinsic properties of a location, and that it is possible to get events when either condition prevails.

- (h) Application of a New VOC Speciation: The NAEI project team has provided speciated VOC inventories for the years 2000, 2010 and 2020. The inventory for 2000 contains emissions for 663 individual species, arising from 248 separate man-made emission source categories (excluding emissions from natural sources). The annual VOC emissions could be described by a 248x663 element matrix, with the columns representing the emission source categories and the rows the individual VOC species. Applying a lower emission limit of 10 kg per year, the number of species could be reduced to 445 species

MCM v3.1 provided the complete degradation schemes for 139 species of the 445 species and was able to account for 78.8% of the total mass emission in the NAEI inventory for the year 2000. Chemical degradation mechanisms for an additional 37 VOC species have been constructed using techniques taken from the CRI mechanism. These additional VOC species included (i) 19 alkanes representing C₁₀ to C₁₄, (ii) 12 cycloalkanes, (iii) 4 C₁₀-aromatics and (iv) an alkene (limonene) and an alkyne (propyne). For the long chain alkanes with limited numbers of alkyl substituents, the initiation reactions were represented explicitly but the subsequent degradation was described using the chemistry for the corresponding normal alkane of the same carbon number as a mechanistic surrogate. For the >C₁₂ alkanes, a CRI representation was used for the initiation reactions followed by the formation of MCM intermediates at the earliest opportunity. Propyne was represented explicitly on the basis of reported data. For the cycloalkanes, a CRI method was used to represent the initiation, with an appropriate MCM intermediate generated after ring-opening. Limonene was represented using the chemistry of its isomer, α-pinene, as a mechanistic surrogate. For the C₁₀ aromatics, explicit initiation reactions were included with the subsequent chemistry taken from the MCM scheme for the C₁₀ aromatic, 1,3-dimethyl-5-ethylbenzene.

Attention was then given to the 48 species that are described as unresolved mixtures of compounds in the NAEI inventory, responsible for 180 ktonnes per year (*i.e.*, 12% of the total mass emission). These unresolved mixtures were represented using the available emitted species wherever possible. Where there was no information available, then those mixtures were left unresolved. In this way, the 176 organic compounds considered in the UK PTM using the both the complete MCM v3.1 mechanisms and the CRI-based degradation mechanisms, were able to represent 90% of the total mass emissions of organic compounds in the year 2000 NAEI VOC emission inventory. No ozone production was included from the remaining 10% by mass of the emissions of organic compounds. The latest version of the UK PTM contains as accurate a picture of the emissions of the major organic compounds as can be given with current understanding, for the UK and by assumption, the rest of Europe.

- (i) Contributions from Different Sources of Organic Compounds to Photochemical Ozone Formation: The UK PTM, incorporating MCM v3.1 and degradation schemes for an additional 37 VOCs, was used to describe photochemical ozone formation along the idealised photochemical episode trajectory giving the highest ozone concentration over the UK. The same speciation of the VOC emissions was assumed along the trajectory as that found for the United Kingdom using the 248 x 663 matrix. A series of sensitivity experiments was performed by perturbing slightly this assumed speciation and, in this way, the incremental reactivities were calculated for each of the 248 source categories using the photochemical trajectory model. At each point along the trajectory, a small

fractional change (7.3% was chosen) was made to the instantaneous VOC emissions. This additional VOC emission increased photochemical ozone production over the base case experiment and the ozone increments were determined by subtracting off the ozone concentration at the end point of the base case trajectory. The choice of 7.3% was completely arbitrary and had no policy significance. It was a compromise between the requirement to produce results that were above the noise level in the model but not too large as to take the model out of its linear response range.

The incremental reactivities for each of the 248 VOC emission source categories in the NAEI VOC inventory were evaluated for the year 2000. Using the NAEI emission projections, VOC emissions are available for each source category for 2010 and 2020. Assuming that there is no change in the incremental reactivities, the influence of the changing VOC emissions on peak ozone concentrations can be assessed. On the idealised episode trajectory from Austria to the United Kingdom, the peak ozone concentration was reduced by 12.67 ppb when the 2010 VOC inventory was substituted by that for 2000. The reduction was somewhat smaller at 12.19 ppb when the substitution was made with the 2020 inventory.

The largest contribution to the decline in episodic peak ozone concentrations between the years 2000 and 2010 was 6.6 ppb (*i.e.*, more than 50% of the total) came from the reduction in VOC emissions from the road transport sector. The next largest combined contribution, amounting to about 15% of the ozone decline, came from VOC emission reductions in the stationary source sectors of the chemicals, oil and gas industries. In 2020, because of the marked reductions in VOC emissions in the transport sector, a different range of source categories will be responsible for the bulk of the ozone formation. The major ozone producing sectors in 2020 will be dominated by stationary VOC sources in industries, associated with the chemical, oil and gas industries and the manufacturing industries that use solvents. The only sector listed associated with road transport, is that of petrol stations and the emission of VOC from refuelling motor vehicles with unleaded petrol.

- (j) **Photochemical Ozone Creation Potentials:** As a result of developments to the chemical mechanisms in MCM v3.1 and because of improvements made to the speciation of the VOC emission inventories, a far wider range of organic compounds can now be represented in the UK PTM. The Photochemical Ozone Creation Potentials POCPs have been determined for 177 selected organic compounds using the UK PTM and the standard 5-day trajectory case. The POCPs were determined by increasing the emissions of each organic compound in turn by a fixed mass and determining the increase in mean ozone concentrations averaged over the entire trajectory length over and above the base case with standard emissions. The ozone increments found with each organic compound were then ratioed to that found with ethylene and expressed as an index relative to ethylene = 100. Some of the highest POCPs are found with the alkenes and aromatic compounds. In comparison, the alkanes are significantly less reactive as class. The oxygenated organic compounds tend to overlap the alkanes in reactivity terms, although certain specific oxygenates are found that are highly reactive, including methyglyoxal and some higher aldehydes.

Objective 5: **Development of Stomatal Flux Module for Crops and Semi-natural Vegetation:** The objective is to provide a link between the ozone assessment capability of OSRM and the Surface Ozone Flux Model (SOFM). This will provide the Department with a robust assessment tool that will allow the preparation of UK maps of accumulated stomatal flux for wheat, potatoes and beech trees for use with damage/loss response functions for impact assessment.

Working closely with the Department's contractors on Ozone Effects (Lisa Emberson and Mike Ashmore), a module has been developed to calculate the effects of ozone deposition on crops in the United Kingdom based on predictions of ozone

concentrations made using the Ozone Source Receptor Model (OSRM). The capability of the module to produce UK-scale maps has been demonstrated.

The model predicted that the growth of beech trees in 2001 was affected by ozone deposition, with greater than 5% loss in biomass throughout the country. Ozone deposition to beech trees in much of the southern part of the UK was limited by the availability of soil moisture for plant uptake during the latter part of the growing season. The model predicted that the growth of winter wheat throughout much of England and Wales in 2001 was affected by ozone deposition. Ozone deposition was associated with more than 5% loss in yield in central England. The loss in yield was smaller in cooler areas in Scotland and in coastal areas of England with lower maximum temperatures. The model also predicted that the growth of potatoes was not substantially affected by ozone deposition. Ozone deposition was associated with less than 5% loss in yield throughout the country.

Model predictions of stomatal flux based on ozone concentrations calculated using the OSRM were compared with stomatal flux estimates based on measured ozone concentrations in 2001. The comparison suggested that the OSRM can provide an effective means of predicting accumulated flux over threshold to vegetation types.

Overall, the various studies have more than met the original objectives. The project has provided key technical input to the development of policies related to ozone air quality and has generated new insight into the factors controlling the concentrations of ozone and oxides of nitrogen. The developments made to the Master Chemical Mechanism and its availability in other formats have confirmed its status as a benchmark chemical mechanism for boundary-layer and tropospheric modelling and have improved its uptake. Sections 4 to 9 provide more detailed information on the work undertaken under each Objective.

3.4 POLICY RELEVANCE

The work reported here assists the development of UK actions and policies on ozone as follows:

- The realism and performance of the Ozone Source-receptor Model (OSRM) have been improved significantly through the modifications made to the model and by the introduction of a Surface Conversion algorithm (**Objective 1**). The performance of the OSRM has been compared to other models. These model developments and comparisons confirm that the OSRM is a robust model which can be used to assess the effectiveness of agreed or proposed actions and policies on ozone and oxides of nitrogen;
- Ambient levels of O₃ and NO₂ are strongly coupled (**Objective 2**). Thus, the response to reductions in the emissions of NO_x is highly non-linear. The success of proposed control strategies will depend on a complete understanding of the relationships between O₃, NO and NO₂ under atmospheric conditions. The extension of the previous analysis of O₃, NO and NO₂ measurements at relevant AURN sites to include more recent data has provided clear evidence that the fraction of NO_x emitted as NO₂ has increased significantly from the road vehicle fleets at a number of roadside and kerbside sites. At Marylebone Road, a number of factors may have contributed to the observed effect (such as an increase in the number of buses on routes running on Marylebone Road, and possibly by greater congestion resulting from Marylebone Road lying on the perimeter of the Congestion Charging zone). This will have implications for the attainment of the annual limit value for NO₂ (40 µg m⁻³, 20.9 ppb).

The analysis of hourly mean data for the site at Marylebone Road has provided insights into the seasonal and diurnal dependence of OX sources and their origins, and the conditions under which exceedences of the hourly mean NO₂ limit value (200 µg m⁻³, 104.5 ppb) are more probable. The present analysis demonstrates that the ambient concentration of OX at Marylebone Rd is sensitive to a number of factors, such as primary NO₂ emissions and regional background O₃ concentrations, and that variation in the magnitudes of these factors leads to substantial diurnal and seasonal differences in the level of NO_x required for the hourly mean NO₂ limit value of 104.5 ppb to be exceeded.

- The UK Photochemical Trajectory Model (PTM) was applied to evaluate a number of proposed ozone control measures (**Objective 3a**):

- **Petrol Volatility:** The policy question concerns the likely benefit arising from a 7 thousand tonne reduction in VOC emissions from petrol evaporation between 1st June and 31st August. Calculations by the UK PTM showed that this measure would have little impact on peak ozone concentrations.
 - **Petrol vs. Diesel:** There is strong pressure for policymakers to increase the penetration of new diesel vehicle technologies into the passenger car and LGV fleets to meet future targets for greenhouse gas emissions. The UK PTM has been used to assess the ozone benefit or dis-benefit to this policy from the implied increased NO_x emissions since the EURO IV emission standards imply higher NO_x emissions per kilometre travelled from diesel-engined cars compared with petrol-engined cars. The model results showed that the evaluation of the ozone benefits or dis-benefits depends markedly on whether just the NO_x emission changes are considered or whether wider issues, such the avoided volatile organic emissions from petrol-engined vehicles, are also taken into account.
 - **Decorative Paints:** The European Commission has proposed a Directive to reduce the VOC content of decorative paints, varnishes and vehicle refinishing products. The OSRM and UK PTM have been used to assess the benefits to the UK of reductions in VOC emissions arising from within UK, and in UK + rest of Europe. Preliminary UK PTM calculations assuming a 40 ktonne per annum reduction in UK VOC emissions and proportional reduction in European emissions gave a noticeable reduction in peak ozone concentrations. Work undertaken as part of the Regulatory Impact Assessment indicated that the UK emission reduction would only be 2 ktonnes per annum over the current NAEI base case projection for 2010. These are significantly smaller than those proposed by the Commission as much of the reduction identified is already included in the current base case projection. OSRM calculations using the revised VOC emission reduction showed that UK action would have a negligible effect but that EU action would be more effective.
 - **Post Gothenburg Controls:** Using its idealised episode trajectory, the UK PTM has shown that both VOC and NO_x control are effective in improving ozone air quality beyond 2010. Model runs, in which NO_x and VOC emissions were separately reduced by 30% across-the-board, suggested that the worst-case trajectory to central Wales was still VOC limited (i.e., VOC control was more effective than NO_x control). Larger emission reductions indicated that the trajectory became NO_x limited.
- Earlier versions of the OSRM (Versions 1.8a and 2.2 with Surface Conversion Algorithm) were applied to evaluate a number of proposed ozone control measures (**Objective 3a**):
- (a) Regulatory Impact Assessment of Directive on Decorative Paints (see also above)
 - (b) Proposed NO_x Emission Standards for Vehicles (EURO V Standards)
 - (c) Regulatory Impact Assessment of Directive on Petrol Vapour Recovery
 - (d) Post-Gothenburg Scenarios

These were UK-scale model runs. As the surface-conversion algorithm was not available for use with version 1.8, the conclusions were based on the unconverted mid-boundary layer outputs. There appeared to be two counteracting effects (a) photochemical production of ozone involving oxides of nitrogen and volatile organic compounds and (b) chemical titration by NO_x removing ozone. These two effects respond differently to emission control. VOC emission control always seemed to improve ozone air quality while NO_x emission control gave a more complex response, which was metric and region specific. Generally, NO_x emission control had an adverse effect on ozone air quality. Thus, either VOC emission control alone or combined VOC and NO_x emission controls are needed to improve ozone air quality.

The OSRM outputs for the 2 Regulatory Impact Assessments were given to colleagues at netcen to undertake the cost-benefit analyses. A paper was prepared on all four series of model runs for the first phase of the review of the Air Quality Strategy [Hayman *et al.*, 2004b].

- The latest version of the OSRM (Version 2.2a with Surface Conversion Algorithm) has been applied to evaluate a number of ozone and NO_x control measures for the Review of the Air Quality Strategy (**Objective 3a**). This review will assess progress towards the achievement of the AQS objectives and assess the costs and benefits of possible additional measures to improve air quality in the UK. The focus of this review of possible measures will be on the impact of

measures on concentrations of particles, nitrogen dioxide and ozone, the pollutants for which the achievement of the objectives is likely to be the most challenging.

The base case runs show a progressive worsening of ozone air quality for all metrics from 2003 to 2010 and beyond. The reduced chemical titration, arising from lower NO_x emissions, is a major factor in the increase in the ozone metrics and the deterioration of ozone air quality, especially in urban areas. A second major factor leading to higher ozone concentrations is changing atmospheric composition arising from climate change. There is however an improvement in nitrogen dioxide air quality as annual mean concentrations fall, especially for the NO_x control measures.

The NO_x control measures reduce NO_x emissions by <1 to ~18% and generally increase ozone concentrations, although there are instances for some of the measures that ozone air quality is improved in 2020. The VOC control measures, on the other hand, lead to an improvement in ozone air quality for all ozone metrics. Meteorological effects and year-to-year variability in meteorology can have a larger effect on ozone air quality than some of the emission control measures considered.

As a result of the above, there will be widespread exceedences of ozone air quality standards and objectives in 2010 and beyond.

A paper was prepared on the ozone model runs for the Review of the Air Quality Strategy. This will be published as a supporting document to the Consultation Paper.

The UK-scale model runs undertaken for the Review of the Air Quality Strategy were largely based on specific emission control measures. Although desirable, the measures by themselves would not necessarily ensure attainment of ozone air quality targets or objectives. As a result, the Department has subsequently commissioned additional site-specific model runs, in which larger reductions of NO_x and/or VOC emissions were made. These runs will be reported in an addendum to this Final Report.

- A preliminary assessment has been prepared and submitted to the European Commission to meet the requirements of the third Daughter Directive on ozone (**Objective 3b**).

The Directive allows the use of supplementary assessment techniques to reduce the burden of monitoring. Work has been undertaken to assess the relative performance of the 2 ozone modelling techniques (OSRM and empirical mapping methods) and thus to recommend the preferred supplementary assessment technique to be used for the third Daughter Directive on ozone. From the analysis of the comparative performance of the two techniques, it was judged that the empirical modelling approach delivers least uncertainty in the model outputs. It was proposed that the empirical modelling approach should be taken forward as the preferred supplementary assessment technique for reporting ozone levels in 2004 calendar year.

The first annual air quality assessment for the third Daughter Directive pollutants has been prepared and submitted to the European Union. There are 28 agglomeration zones (large urban areas) and 15 non-agglomeration zones. The status of the zones has been determined from a combination of monitoring data and model results. The results of this assessment are summarised in the table below, in terms of exceedences of Target Values (TV) and Long-term Objectives (LTO).

Summary Results of Air Quality Assessment relative to the Target Values and Long-term Objectives for Ozone for 2010.

Target Value	Number of Zones exceeding
Max Daily 8-hour mean Target Value	none
AOT40 Target Value	none
Long-term Objective	Number of Zones exceeding
Max Daily 8-hour mean Long-term Objective	43 zones (36 measured + 7 modelled)
AOT40 Long-term Objective	7 zones (5 measured + 2 modelled)

- The Chemical Mechanism development (**Objective 4**) has less immediate policy relevance but it underpins the modelling tools used in the contract to assess ozone policy options. The reaction schemes for butane and isoprene in the MCM have been evaluated against chamber data. The evaluations have provided strong support for the MCM schemes for the most abundant components of emissions of anthropogenic and biogenic non-methane VOC, respectively.

The UK Photochemical Trajectory Model, incorporating (i) the Master Chemical Mechanism (v3.1), (ii) the Common Reactive Intermediate (CRI) mechanism or (iii) the Master Chemical Mechanism (v3.1) with the CRI-approach used for 37 new VOCs, has been used in a number of studies:

- Multi-day Reactivity: The results demonstrate the need for a comprehensive chemical mechanism as simplified mechanisms could potentially lead to different ozone source-receptor relationships being used in integrated assessment models.
- Modelling of the 2003 TORCH Campaign: The comparison of the simulated and observed distributions of 34 emitted hydrocarbons provides strong support for the VOC speciation used in the NAEI, but is indicative of an under representation of the input of biogenic hydrocarbons, particularly at elevated temperatures. The MCM is one of the few chemical mechanisms available to predict the patterns and structures of oxidised products, such as simple and multifunctional carbonyls, thereby allowing a much more detailed examination of atmospheric chemical mechanisms. The comparison of modelled and measured products of VOC oxidation (carbonyl compounds) showed that the simulated distributions of four aldehydes and three ketones correlated well with observations for each class of compound. However, the simulated concentrations of the aldehydes were systematically lower than those observed, whereas those of the higher ketones were systematically higher. These results will be used to refine the MCM.

The relative contributions of VOC emissions from (a) man made and (b) natural sources to the modelled daily-average ozone concentration during the campaign was determined. The biogenic emissions were calculated to make a larger relative contribution at the higher temperatures prevailing the episode phase of the campaign. Although the magnitude of biogenic VOC emissions is subject to some uncertainty, these results support an important role for biogenic VOC oxidation in regional-scale ozone formation under heatwave conditions. 2003 may become a more typical year in the future, as a result of climate change.

The effects of 10% incremental reductions in the emissions of NO_x and anthropogenic VOC were examined for the emission years 1990, 2003 and 2020 (all other model parameters were left unchanged) to investigate whether ozone formation is limited by the availability of NO_x or VOC. The 1990 scenario demonstrates strong VOC limitation throughout the campaign period, with NO_x reductions almost always leading to an increase in ozone concentration. The results for 2003 and 2020 indicate that peak ozone formation for the photochemically-active conditions of this campaign is predominantly VOC-limited for the complete time series, but shows a trend towards NO_x-limitation. This sensitivity study also shows that VOC- and NO_x-limitation are not intrinsic properties of a location, and that it is possible to get events when either condition prevails.

- Contribution of Different VOC Source Sectors: Using the new NAEI VOC speciated emission inventories, the UK PTM has been updated and now contains as accurate a picture of the emissions of the major organic compounds as can be given with current understanding for the UK and, by assumption, the rest of Europe. A series of sensitivity experiments was performed to calculate incremental reactivities for each of the 248 VOC source categories in the UK inventory. The largest contribution to the decline in episodic peak ozone concentrations between the years 2000 and 2010 came from the reduction in VOC emissions from the road transport sector. In 2020, because of the marked reductions in VOC emissions in the transport sector, a different range of source categories - chemical, oil and gas industries and the manufacturing industries that use solvents - will be responsible for the bulk of the ozone formation. This points to a major shift in policy if ozone levels are to be reduced beyond 2010 levels so that stationary VOC sources are targeted rather than motor vehicles.
- Photochemical Ozone Creation Potentials: The Photochemical Ozone Creation Potential is an index to rank volatile organic compounds according to their production of ground-level ozone. As a result of developments to the Master Chemical Mechanisms and because of improvements made to the speciation of the VOC emission inventories, updated or new POCPs have been determined for 177 selected organic compounds using the UK PTM and the standard 5-day trajectory scenario.

The work on Objective 4 and the improvements to the MCM website contribute to the Department's desired outcome to maintain the leading position of the Master Chemical Mechanism.

- A module to calculate ozone stomatal fluxes (**Objective 5**) has been developed for use with the OSRM. This will provide the Department with a more realistic tool to evaluate the impact of ozone on crops and vegetation for the forthcoming reviews of the European Union's National Emission Ceilings Directive and the Gothenburg Protocol to the UN ECE Convention on Long-range Transboundary Air Pollution.

The work described above will make an important contribution to the development of UK actions and policies on ozone.

4 Development and Application of Ozone Models (Objective 1)

4.1 INTRODUCTION

The current project has a strong UK focus with national (Objective 3a) and local (Objective 2) scale interests. This is further emphasised by the work needed to provide the preliminary and interim assessments of the 3rd Daughter Directive (Objective 3b). For these reasons, the Ozone Source-Receptor Model (OSRM) was proposed as the primary modelling tool to meet these objectives. The Ozone Source-Receptor Model was developed during the previous Defra project on Modelling of Tropospheric Ozone Formation (EPG 1/3/143) [Hayman *et al.*, 2002].

4.2 BRIEF OVERVIEW OF THE LATEST VERSION OF THE MODEL

The Ozone Source-Receptor Model (OSRM) is a recently developed model to describe photochemical ozone production in the UK [Hayman *et al.*, 2002, 2004a; 2005a]. The OSRM covers the EMEP model domain and uses global meteorological datasets provided by the Met Office to derive 96-hour back trajectories to specified receptor sites (UK/EMEP monitoring sites or a 10km x 10km grid covering the UK). The chemical scheme is based on that used in the STOCHEM model [Collins *et al.*, 1997; 2000; Stevenson *et al.*, 1997]. The mechanism has ~70 chemical species involved in ~180 thermal and photochemical reactions. The mechanism represents ozone formation using 12 VOCs, which provides an appropriate description of ozone formation on the regional scale. The emission inventories are taken from EMEP for Europe with the option to use NAEI emission inventories for the UK, which have been aggregated to 10 km x 10 km and into 8 key sectors.

The OSRM is similar in concept to the UK Photochemical Trajectory Model (UK PTM) Derwent *et al.*, 1998, 2004] in that it simulates the chemical development of species in an air parcel moving along a trajectory and to the ELMO source-receptor model [Metcalf *et al.*, 2002] in that calculations can be undertaken to a 10 km x 10 km grid covering the UK. The OSRM (version 2.2a) has a number of notable enhancements and advantages to these models:

- **Air Mass Trajectories:** Realistic air mass trajectories are derived from wind fields extracted from meteorological datasets. The UK PTM and ELMO model use linear trajectories. Meteorological datasets are available for use with the OSRM for the years 1995 to 2003;
- **Meteorology:** The boundary layer depth and other meteorological parameters characterising the boundary layer are interpolated in space and time from the input meteorological datasets;
- **Chemical Mechanisms:** Three chemical mechanisms have been developed for use in the OSRM (a) the chemical mechanism used in the ELMO or STOCHEM models, (b) a modified and extended version of chemical mechanism used in the ELMO or STOCHEM models. The chemical mechanism has been modified to include the formation of HONO and organic nitrates and a more extensive chemistry of NO₃, and (c) a reduced version of the Common Reactive Intermediate mechanism where the CRI concept has been used for the VOCs used in the mechanism. The modified STOCHEM mechanism is currently used in the OSRM. Table 4.1 provides details of these chemical mechanisms;
- **Photolysis Rates:** Photolysis rates have been calculated off line using a modified version of the PHOTOL code. The input database contains the dependence of photolysis rates for 17 species on zenith angle, cloud cover, land surface type and column ozone;
- **Emissions:** The model uses up-to-date emission inventories for nitrogen oxides, volatile organic compounds, carbon monoxide and sulphur dioxide taken from UK (National Atmospheric Emission Inventory) and European (EMEP) sources. The emissions of each pollutant have been divided into to 8 broad source categories (solvent usage, road transport, industrial processes, power generation, fossil fuel extraction and delivery, domestic combustion, natural and other). The assignment of the ~600 VOCs in the UK speciated VOC emission inventory to the 13 model VOCs was based on reactivity and structural considerations.

Table 4.1 Details of the Modified STOCHEM Chemical Mechanisms used in the OSRM.

	STOCHEM	Modified STOCHEM	Mini-CRI
# of Species	70	70	70
# of Reactions	154	180	198
# of VOCs	10	12	12
Emitted VOCs	<ul style="list-style-type: none"> ➤ alkanes (ethane, propane, <i>n</i>-butane) ➤ alkenes (ethene, propene) ➤ aromatics (toluene, <i>o</i>-xylene) ➤ oxygenated VOCs (methanol, acetone, methyl ethyl ketone) 	<ul style="list-style-type: none"> ➤ alkanes (ethane, propane, <i>n</i>-butane) ➤ alkenes (ethene, propene) ➤ aromatics (toluene, <i>o</i>-xylene) ➤ oxygenated VOCs (methanol, acetone, methyl ethyl ketone, formaldehyde, acetaldehyde) 	<ul style="list-style-type: none"> ➤ alkanes (ethane, propane, <i>n</i>-butane) ➤ alkenes (ethene, propene) ➤ aromatics (toluene, <i>o</i>-xylene) ➤ oxygenated VOCs (methanol, acetone, methyl ethyl ketone, formaldehyde, acetaldehyde)
Biogenic VOCs	Isoprene	isoprene	isoprene
VOC speciation	NAEI 1998	NAEI 1998	NAEI 1998

- **Temporal Emission Factors:** The OSRM converts the annual emission estimates to instantaneous emission rates using temporal profiles for the emissions of NO_x, VOCs, SO₂ and CO generated by Jenkin *et al.* [2000]. These profiles were derived either from real activity data or by using one of small set of default profiles.
- **Biogenic VOC Emissions:** An additional emission term is added to the emission rate of isoprene to represent the natural biogenic emissions from European forests and agricultural crops. The emission estimates can either be the same as those used in the UK PTM and taken from Simpson *et al.* [1995] or the new biogenic inventory produced using the PELCOM land cover dataset and the TNO tree species inventory (see following Section 4.3);
- **Dry Deposition:** Dry deposition processes are represented using a conventional resistance approach, in which the rate of dry deposition is characterised by a deposition velocity. Different deposition velocities are used over land and sea. The ozone deposition velocity over land has an imposed diurnal and seasonal cycle.
- **Initialisation:** The concentrations of O₃, CO, CH₄, C₂H₆, HNO₃ and PAN are initialised on each OSRM trajectory using output from the global tropospheric STOCHEM model (see following Section 4.3).

A single trajectory calculation using the backwards-iterative EULER solver with a chemical timestep of 240s takes ~0.025 s (*i.e.*, ~40 trajectories per second) using a Dell Precision Workstation 650 MiniTower (containing dual Intel® Xeon 3.06GHz processors). Making use of the two available processors on the workstation gives a runtime of ~4.5 days for a UK-scale model run to ~3,000 receptor sites for a calendar year.

4.3 MODEL DEVELOPMENTS

At the start of the contract, the Ozone Source-receptor model was available as version 1.2. While version 1.2 was able to reproduce some features of the observed ozone measurements, it was recognised that further development was needed to improve the performance and realism of the model. The following features of the model were modified:

- the length of the air mass trajectory
- the boundary layer depth
- the initialisation of the trajectory
- exchange with the free troposphere
- the biogenic inventory
- the model runtime

- (1) **Trajectory Length:** The current trajectory length is fixed to a maximum of 96 hours. The trajectory can be shorter if the back trajectory reaches the EMEP model domain boundary before 96 hours. The boundaries of the EMEP model domain had been defined to capture all the significant emitting areas. While the westerly boundary in the middle of the Atlantic was a low emitting region, this was not the case for the easterly boundary.

The code has been modified so that all trajectories, in principle, start from the EMEP model domain boundary. However, it was recognised that under certain meteorological conditions it could take a significant amount of time to reach the model boundary and this could increase the runtime per trajectory. A practical cut-off has been applied in such cases.

- (2) **Initialisation of the Trajectory:** Version 1.2 of the model used the same concentration of ozone and other trace species for each trajectory, irrespective of where it started. To address this and also the issues of the coupling between regional scale ozone production and the hemispheric circulation, the OSRM has been modified so that the concentration of ozone and other key trace species vary with location, time of year, etc.

Output from the global tropospheric STOCHEM model has been used to initialise the OSRM trajectories. Initial conditions have been provided for the species O₃, CO, CH₄, C₂H₆, HNO₃ and PAN. A full set of daily concentration fields have been provided for 2 calendar years, one representing the climatology of the late 1990's (actually 1998) and the second a future atmosphere (IPCC SRES scenarios for 2030). This will allow model runs to be undertaken to assess the effect of climate change on regional ozone concentrations.

- (3) **The Boundary Layer Depth:** The model had adopted the same idealised behaviour of the boundary layer as used in the UK Photochemical Trajectory Model (UK PTM), with the boundary layer represented using two boxes. The height of the lower box varies diurnally and mixing occurs with the upper box when the boundary layer grows. The concentrations of species in the upper box are held constant until reset when the boundary layer collapses.

A boundary layer depth was available as a parameter in the meteorological datasets and this has been interpolated in space and time to give the local boundary layer depth along each trajectory. Mixing between the two boxes occurs whenever the boundary layer height is rising.

- (4) **Biogenic VOC Emission Inventory:** In version 1.2, the OSRM used a biogenic emission inventory produced by Simpson *et al.* [1995]. This inventory provides an annual emission rate of biogenic VOCs as isoprene on the old EMEP 150 km x 150 km grid. As part of another project, a new biogenic inventory had been produced using the PELCOM land cover dataset and the TNO tree species inventory. This emission inventory gives emission potentials aggregated to the EMEP 50 km x 50 km grid for the following VOC species (see Figure 4.1):

- isoprene from deciduous and evergreen trees (both temperature and light² sensitive)
- monoterpenes from deciduous and evergreen trees (both temperature sensitive)
- monoterpenes from deciduous and evergreen trees (both temperature and light sensitive)
- other VOCs (OVOCs) from deciduous and evergreen trees (both temperature sensitive)

The inventory has been introduced into the OSRM and the code modified to calculate the environmental correction factors along the trajectory. These emissions have all been assigned to isoprene as the only biogenic VOC in the STOCHEM mechanism. The monoterpene emissions were scaled to correct for the relative reactivity of isoprene and monoterpenes.

- (5) **Meteorological Data:** Meteorological data have been passed from the Met Office to netcen for all the years from 1995 through to 2003. The data for the years from 1995 through to 1998 have been based on the meteorological analysis fields employed in the global model STOCHEM whereas those from 1999 through to 2003 have been based on the NAME model fields. This has required changes to be made within the OSRM met pre-processor code to accommodate the different formats and coverages of the two sets of meteorological archives.
- (6) **Model Runtime:** Version 1.2 of the OSRM used the variable-order GEAR solver that is also used in the FACSIMILE numerical integration programme. To speed up the OSRM model a search has been made for alternative solvers to replace the Gear's method that was the default option. A backwards-iterative EULER solver, based on that used in the ELMO model, has been provided and it was added into the OSRM code as an alternative during the model development phase.

² This is the photosynthetically active radiation, typically about 45-50% of total global radiation, covering the wavelength range 400-700nm.

A simpler two-step solver, based on the work of Verwer and Simpson [1995], has also been assessed as offering potential further improvements in model runtime. The first version was fast enough but appeared to be unstable in the presence of large NO_x sources. A modified version of the two-step solver was developed using the coding from a QSSA integrator, in which NO and NO_x ($= \text{NO} + \text{NO}_2$) are solved instead of NO and NO_2 separately. This second version of the two-step integrator was assessed but has not been used.

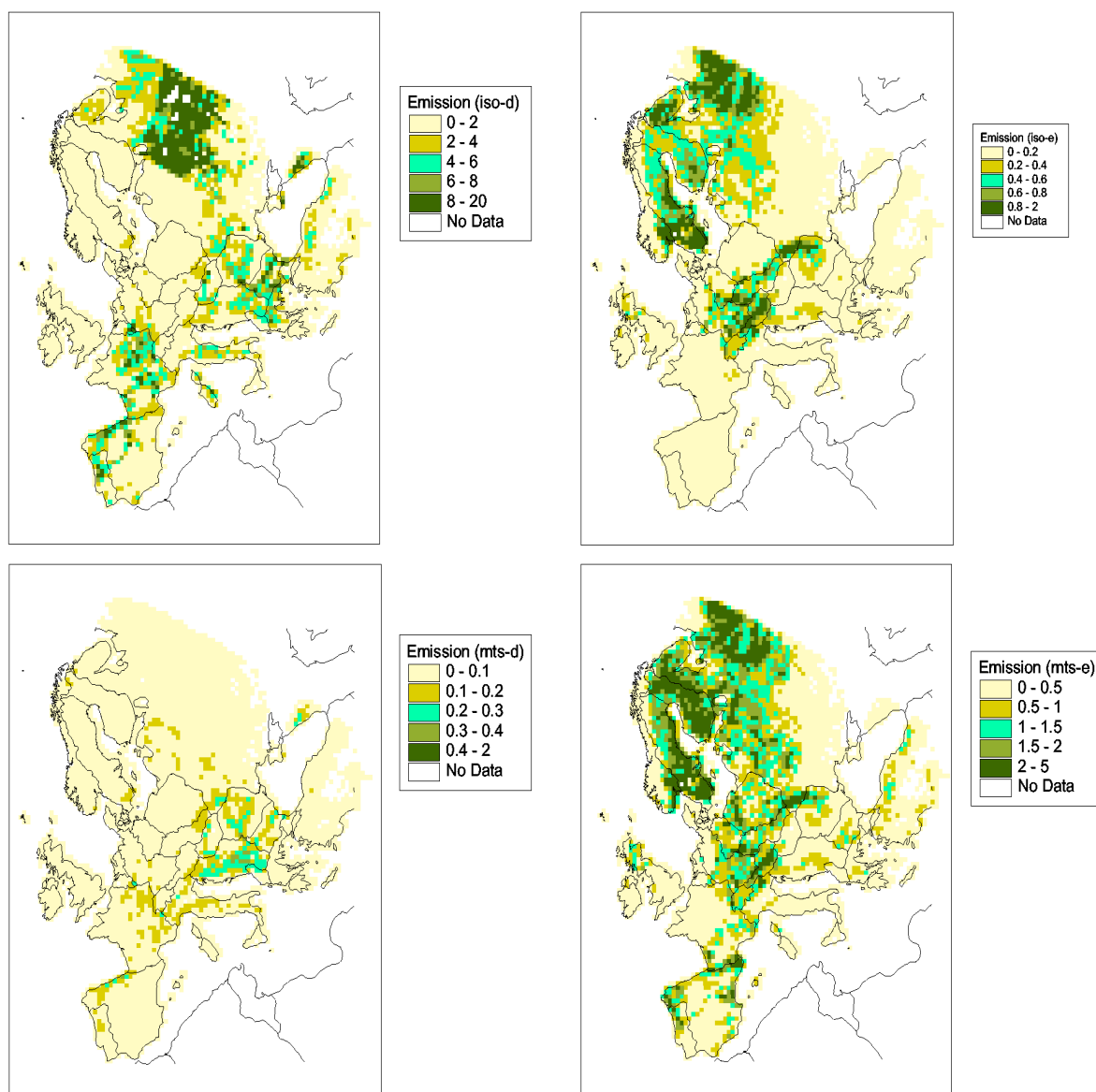


Figure 4.1 Biogenic VOC Emission Potentials for Europe (Upper panels: isoprene emissions from deciduous and evergreen trees; Lower panels: mono-terpene emissions from deciduous and evergreen trees).

Following this initial intense phase of model development, further model developments have taken place during the course of the contract to improve the performance of the OSRM:

- (1) Comparison with the UK Photochemical Trajectory Model: The OSRM was configured, as far as was possible, to be like the UK Photochemical Trajectory Model. Comparison of outputs from box and trajectory model runs resulted in modifications to the OSRM:
 - the STOCHEM chemical mechanism was modified to include the formation of HONO and organic nitrates and a more extensive chemistry of NO_3 and to make it more compatible with the Common Reactive Intermediate mechanism;

- the database of photolysis rates was recalculated using a larger value for the ozone column above the model domain;
 - the calculation of the biogenic emission rates.
- (2) Introduction of a Surface Conversion algorithm: This is discussed later in Section 4.4.2.
- (3) The model had a tendency to over predict ozone concentrations under episode conditions. A number of changes were made to the model to reduce the ozone production rate under such conditions:
- **VOC Emissions:** The VOC emissions were reduced by 10% to account for the formation of secondary organic aerosol;
 - **Biogenic Emissions:** The parameters used to calculate the Environmental Correction Factors (ECFs) were adjusted to values recommended in the CORINAIR Emission Handbook. This had the effect of reducing the biogenic VOC emissions;
 - **Dispersion of Emissions:** To account for the horizontal spread of the air mass as it moved along the trajectory, a greater number of emission grid squares were used to generate the emission rate the further the air mass was from the receptor site;
 - **Time Constant for Mixing of Emissions:** With its single boundary-layer, the OSRM effectively assumes instantaneous mixing of the emissions. An option was included to define a time constant for the mixing of the emissions in the boundary layer (not used);
 - **Temperature:** The surface temperature, which is needed to calculate the ECFs for the biogenic VOC emissions, was also used as the temperature to calculate the photochemical ozone production rates. A switch was incorporated to allow the use of mid-boundary layer temperatures to calculate the photochemical ozone production rates. As mid-boundary layer temperatures are generally a few degrees lower than the surface temperature, the use of mid-boundary layer temperatures would reduce the ozone production rates.

These changes, together with the introduction of a Surface Conversion algorithm (see Section 4.4.2), have led to a significant improvement in the performance of the OSRM, as described in Section 4.5.

4.4 THE OSRM POST-PROCESSOR

4.4.1 Ozone and Nitrogen Oxide Metrics

A post-processor code has also been developed to process the hourly concentrations generated by the OSRM. The post-processor code currently calculates a large number of metrics for ozone and nitrogen dioxide and produces output datafiles for generating maps of these metrics:

- Ozone:**
- (1) annual mean concentration
 - (2) AOT30 for the protection of crops (EU and UN ECE³)
 - (3) AOT30 for the protection of forests (EU and UN ECE)
 - (4) AOT40 for the protection of crops (EU and UN ECE)
 - (5) AOT40 for the protection of forests (EU and UN ECE)
 - (6) AOT60 for the protection of human health (EU and UN ECE)
 - (7) maximum hourly concentration in the year
 - (8) maximum 8-hour running mean concentration in the year
 - (9) annual mean of the maximum of the 24 possible 8-hour running mean concentrations in each day
 - (10) number of days when the maximum of the 24 possible 8-hour running mean concentrations in each day exceeds $100 \mu\text{g m}^{-3}$ (metric in the UK Air Quality Strategy)
 - (11) number of days when the maximum of the 24 possible 8-hour running mean concentrations in each day exceeds $120 \mu\text{g m}^{-3}$ (metric in the EU 3rd Daughter Directive)

³ The EU methodology uses fixed hours (08:00-20:00 Central European Time) during the relative accumulation period, whereas the UN ECE calculation uses daylight hours, defined by the incident UV radiation being greater than 50 mW m^{-2} .

- (12) AOT30 for the protection of horticulture (EU and UN ECE)
 - (13) AOT30 for the protection of semi-natural vegetation (EU and UN ECE)
 - (14) AOT40 for the protection of horticulture (EU and UN ECE)
 - (15) AOT40 for the protection of semi-natural vegetation (EU and UN ECE)
 - (16) annual mean of those maxima of the 24 possible 8-hour running mean concentrations in each day > 35 ppb
 - (17) maximum hourly concentration in the summer
 - (18) annual mean of the difference between the maximum of the 24 possible 8-hour running mean concentrations in each day and 35 ppb (or $70 \mu\text{g m}^{-3}$) for the protection of human health
 - (19) annual mean of the difference between the maximum of the 24 possible 8-hour running mean concentrations in each day and 50 ppb (or $100 \mu\text{g m}^{-3}$) for the protection of human health
- Nitric Oxide:**
- (20) annual mean concentration
- Nitrogen Dioxide:**
- (21) annual mean concentration
 - (22) maximum hourly concentration in the year
 - (23) number of hours in the year when the hourly concentration exceeds $200 \mu\text{g m}^{-3}$

4.4.2 Surface Conversion Algorithm

The OSRM describes the boundary layer by a single box and assumes that this is well mixed. When the model is required to handle and generate concentrations of species near to the surface, account must be taken of surface removal processes (dry deposition and chemical reactions) and emissions that will generate gradients in the concentrations of ozone and oxides of nitrogen. This will result in lower and higher concentrations, respectively, of these species compared to their corresponding mid-boundary layer concentrations. These effects are of particular significance in urban areas.

An algorithm has been developed and implemented in the OSRM post-processor to convert the hourly mid-boundary layer concentrations to surface concentrations. The algorithm uses the meteorological parameters characterising the boundary layer, surface roughness appropriate for the surface types considered, resistance parameters for O_3 and NO_2 , the local NO_x emission rates and a simple $\text{NO}-\text{NO}_2-\text{O}_3$ photostationary state chemistry.

The algorithm solves the following set of coupled differential equations, which presumes mass balance for each species:

$$\text{NO:} \quad \frac{\partial}{\partial z} \left(\frac{ku^* z}{\phi} \frac{\partial[\text{NO}]}{\partial z} \right) - k_1[\text{NO}][\text{O}_3] + J[\text{NO}_2] = 0 \quad (4.1)$$

$$\text{O}_3: \quad \frac{\partial}{\partial z} \left(\frac{ku^* z}{\phi} \frac{\partial[\text{O}_3]}{\partial z} \right) - k_1[\text{NO}][\text{O}_3] + J[\text{NO}_2] = 0 \quad (4.2)$$

$$\text{NO}_2: \quad \frac{\partial}{\partial z} \left(\frac{ku^* z}{\phi} \frac{\partial[\text{NO}_2]}{\partial z} \right) + k_1[\text{NO}][\text{O}_3] - J[\text{NO}_2] = 0 \quad (4.3)$$

The assumption is then made that the stability parameter (ku^*/ϕ), defined by Equation (4.4), is constant throughout surface boundary layer.

$$\frac{ku^*}{\phi} = \frac{1}{R_A} \ln \left(\frac{H/10}{z_0} \right) \quad (4.4)$$

where u^* is the friction velocity and k is the von Karman constant. The differential equations (4.1) to (4.3) are transformed from a height-based co-ordinate system (z) to a resistance-based co-ordinate system (r) using the substitution:

$$r = \frac{\phi}{ku^*} \ln\left(\frac{z}{z_0}\right) \quad (4.5)$$

The differential equations (4.1) to (4.3) can be rewritten as:

$$\frac{\phi}{ku^*} \frac{\partial^2 [NO]}{\partial r^2} - k_1 [NO][O_3]z + J[NO_2]z = 0 \quad (4.6)$$

with corresponding expressions for O₃ and NO₂.

The upper boundary conditions at $r=R_A$ are $[NO] = [NO]_{mbl}$, $[NO_2] = [NO_2]_{mbl}$ and $[O_3] = [O_3]_{mbl}$. The lower boundary conditions at $r=0$ is:

$$\frac{\partial [NO]}{\partial r} = -E_{NO} + v_d [NO] \quad (4.7)$$

where E_{NO} is the emission rate of nitric oxide;
 v_d is the non-aerodynamic deposition velocity ($=1/(r_b+r_{sur})$)

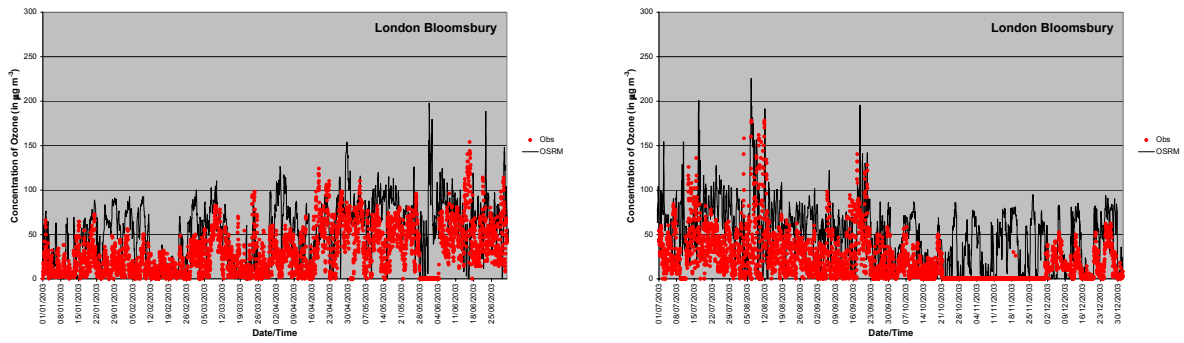
with similar expressions for O₃ and NO₂.

The differential terms in each of the equations are replaced by finite difference approximations and the resulting simultaneous linear equations solved by Gaussian elimination along the tridiagonal. As the chemical reaction term introduces some non-linearity, it is necessary to repeat the calculations a few times to obtain convergence with successive approximations to the non-linear terms. The parameters needed for the conversion are taken from a combination of additional output generated during the OSRM model run and databases calculated using the Surface Ozone Flux Model [Abbott, 2004].

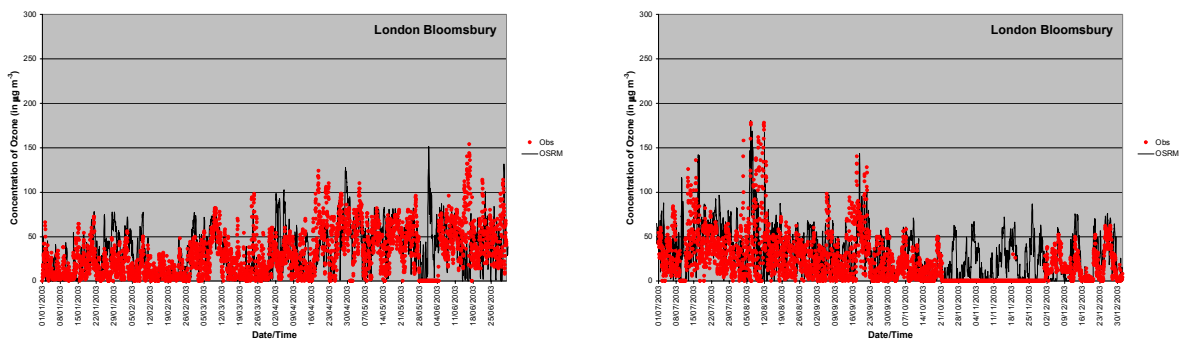
The effect of the surface correction algorithm can be seen in Figure 4.2⁴. These figures compare the hourly concentrations of ozone observed at the London sites of Teddington and Bloomsbury in 2003 with those calculated using the OSRM. Bloomsbury is a site in central London while Teddington is a suburban site to the west of London. Panels (a) and (c) of Figure 4.2 compare the OSRM mid-boundary-layer output against the measurements while Panels (b) and (d) show the surface-corrected results. The effect of the surface conversion algorithm is more noticeable at London Bloomsbury site, which is in an area of higher NO_x emissions. The effect of the surface conversion algorithm is smaller at London Teddington for two reasons (i) the site is in an area of lower emissions and (ii) the ozone measurements are made at 15 m compared to the more typical 2-3 m at other sites.

⁴ These include the modifications made to the surface conversion algorithm, described in the following section (Section 4.4.3).

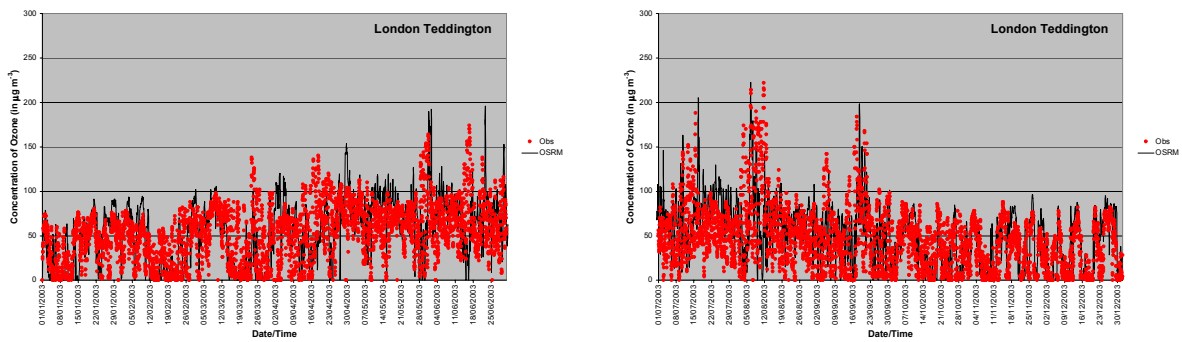
(a) Ozone – No OSRM Post-processor Surface Conversion



(b) Ozone – OSRM Post-processor Surface Conversion



(c) Ozone – No OSRM Post-processor Surface Conversion



(d) Ozone – OSRM Post-processor Surface Conversion

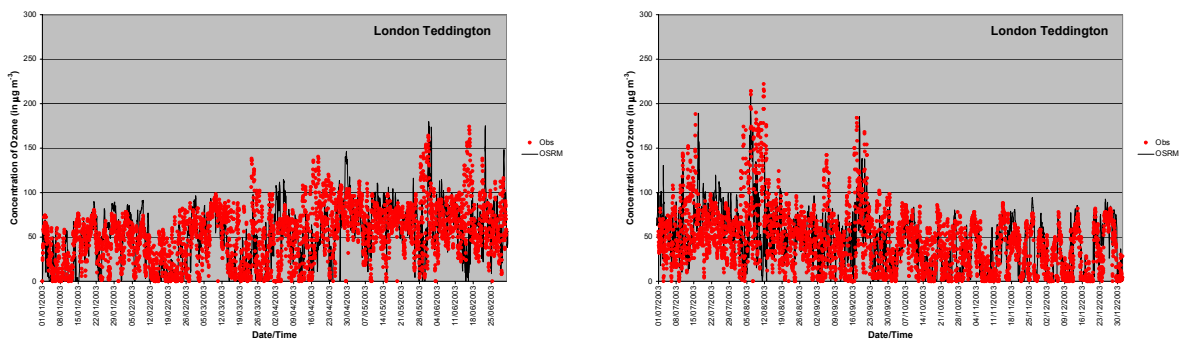


Figure 4.2 Comparison of the Observed and Modelled Hourly Concentrations (in $\mu\text{g m}^{-3}$) of Ozone for the London Bloomsbury and London Teddington Sites in 2003. The Modelled Concentrations are shown with (Panels b and d) and without (Panels a and c) Surface Conversion.

4.4.3 Review of the Surface Conversion Algorithm

A review of the OSRM model system was undertaken in the third year of the contract. As part of that review, the performance of the OSRM was evaluated by comparing model results with observations at urban monitoring sites in the London, Kent and East Hertfordshire Air Quality Networks [Derwent, 2005a]. The comparison showed that the chemistry implemented in the surface conversion algorithm gave identical NO-NO₂-NO_x-O₃-O_x relationships as the observations, as shown in Figure 4.3. However, although the annual mean ozone, nitrogen dioxide and oxidant concentrations were in good agreement with the measurements (see Figure 4.4), there was a tendency for the model to overpredict NO and hence NO_x concentrations by quite a large factor.

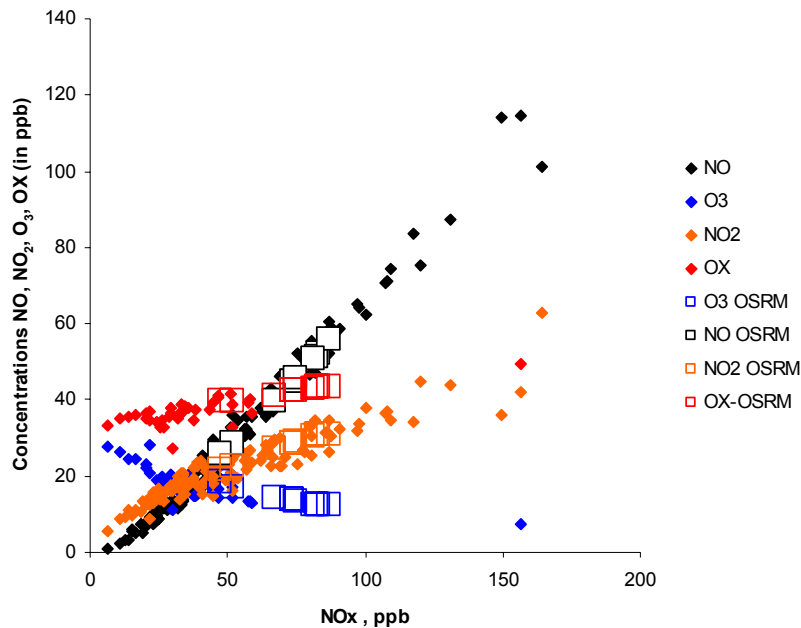


Figure 4.3 Modelled and Measured Concentrations of Ozone, Nitric Oxide, Nitrogen Dioxide and Oxidant ($=[O_3]+NO_2]$) at London Sites in 2002 as a Function of the Modelled or Measured NO_x Concentration.

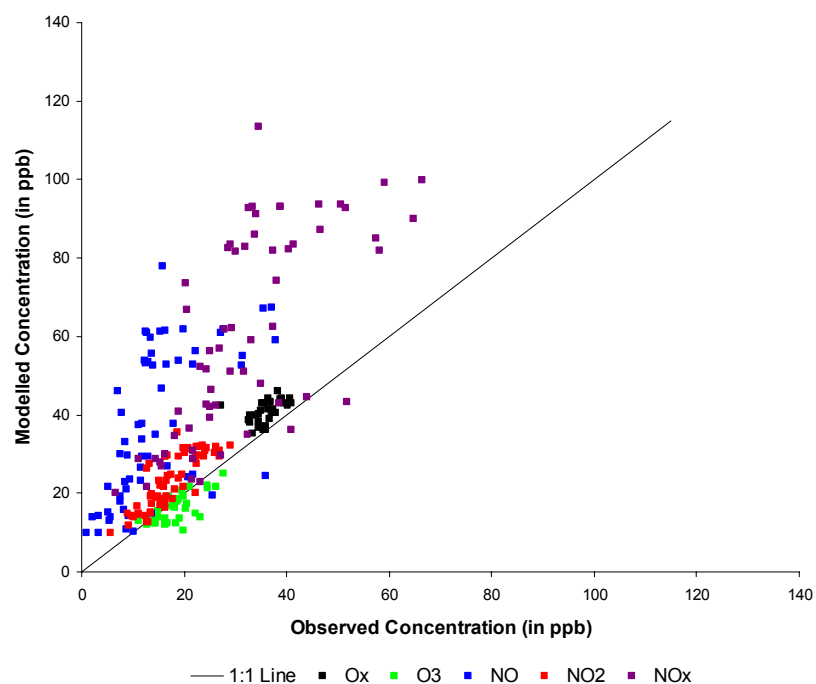


Figure 4.4 Scatter Plot of Modelled vs. Measured Concentrations of Ozone, Nitric Oxide, Nitrogen Dioxide, Oxidant and Oxides of Nitrogen for South East non-Roadside Sites in 2002.

As a result of this review, a number of changes were made to the OSRM post-processor:

- **Allowance for Height of Monitoring Site:** The surface conversion algorithm was originally configured to take the concentrations from the lowest level. Most of the inlet heights at UK monitoring sites are between 2-4 m and close to the lowest level in the surface conversion algorithm. However, at some sites, the inlet heights are significantly higher (e.g., 8 m at Bush and 15 m at London Teddington). The post-processor code has been modified to take account of the height of the sampling site.
- **Use of More Relevant Boundary-layer Parameters:** The surface-conversion algorithm incorporated into the OSRM post-processor needs information on aerodynamic and stomatal resistance parameters on an hour-by-hour basis. These parameters were taken from the OSRM model run and combined with information on local NO_x emissions. At the spatial resolution of the meteorological datasets used in the OSRM, there is no distinction between urban and rural areas. Parameters, such as the surface roughness and Monin-Obukhov length, which describe the boundary layer and its properties, tend to reflect regional rural values rather than those associated with urban surfaces. The aerodynamic resistance (R_a), in particular, tends to be lower in urban areas. The overestimation of the NO_x concentrations is a direct consequence of using higher aerodynamic resistances in urban areas as the surface concentration is proportional to the product of the local emission rate and the aerodynamic resistance. Building on the work to calculate Ozone Stomatal Fluxes (see Section 9), the OSRM post-processor was modified to use databases of resistance parameters generated for each hour of the year for 5 different surface types – urban, grass, wheat, potatoes and beech.
- **Dispersion Kernel for NO_x Emissions:** There are a number of options available in the OSRM post-processor on the form of the NO_x emissions used in the surface-conversion algorithm (10 km x 10 km or 1 km x 1km emission inventories or the emission calculated over the last hour of the OSRM trajectory). The review of the OSRM post-processor indicated a need to take account of the airmass history. This has been addressed through the use of dispersion kernels, an approach widely used within netcen's dispersion modelling studies for the Department, the Environment Agency and local authorities (see, for example, Abbott, Vincent and Stedman [2005]). Instead of simply aggregating the emission rates in the 100 1 km x 1km grid squares within each 10 km x 10 km grid square to give the overall emission rate, the emission rate assigned to each 1 km x 1 km grid square was calculated using weighted contributions from its surrounding 100 1 km x 1 km grid squares. The weights (*i.e.*, dispersion kernels) were calculated on an annual basis from year-specific meteorological datasets.

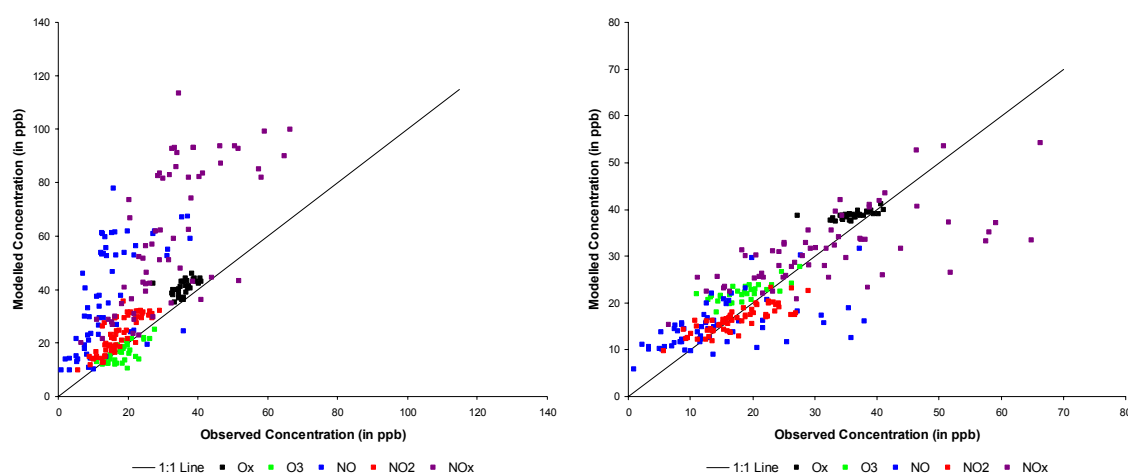


Figure 4.5 Scatter Plots of Modelled vs. Measured Concentrations of Ozone, Nitric Oxide, Nitrogen Dioxide, Oxidant and Oxides of Nitrogen for London Sites (Non-Roadside) in 2002. The Performance is shown Before (Left-hand Panel) and After (Right-hand Panel) the Developments to the OSRM Post-processor.

Figure 4.5 presents scatter plots of the modelled against the measured concentrations of O₃, NO, NO₂, NO_x and Oxidant for sites in the London, Kent and East Hertfordshire Air Quality Networks (Non-Roadside) in 2002 (the left-hand panel is the same as Figure 4.4). The two scatter plots illustrate the

improvement in the performance of the OSRM model system following the developments to the OSRM Post-processor described above.

4.5 OSRM PERFORMANCE

4.5.1 Comparison of Different Versions of OSRM

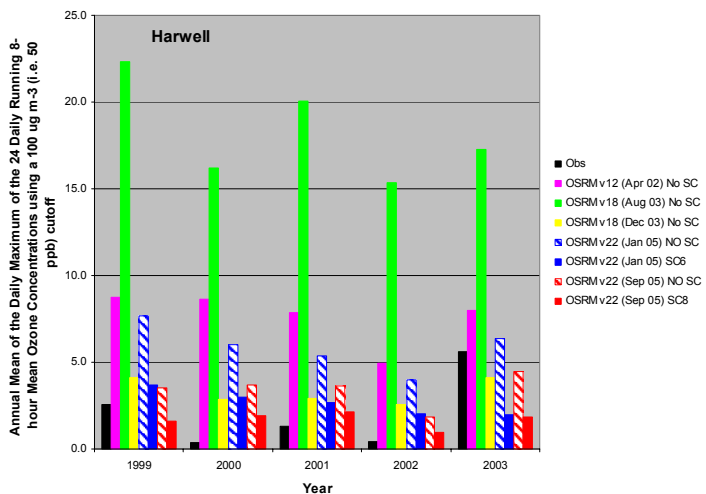
As discussed in Sections 4.3 and 4.4, major changes have been made to the Ozone Source-receptor model throughout the course of the contract to improve its performance, particularly against observations. In Figure 4.6 and Figure 4.7, comparisons are presented of four of the metrics, (a) Annual Mean of the Daily Maximum of the 24 Daily Running 8-hour Mean Ozone Concentrations using a $100 \mu\text{g m}^{-3}$ cutoff, (b) the Number of days with Exceedences of $100 \mu\text{g m}^{-3}$, (c) AOT40 - Forests and (d) Annual Mean NO_2 Concentration (in $\mu\text{g m}^{-3}$), calculated by different versions of the Ozone Source-receptor Model for the Harwell and London Bexley sites respectively for the years 1999 to 2003. The observed values of the metrics are shown as the black bars in these figures.

It is clear that the developments made to the OSRM and the introduction of the surface conversion algorithm has reduced the values of the ozone metrics and brought them into good agreement with the observed values. Versions 1.2 and 1.8 of the model led to a significant overestimation of the hourly ozone concentrations and hence the derived ozone metrics. Versions 2.2 and 2.2a of the model and the application of the surface conversion algorithm (shown as the solid blue and red bars in Figure 4.6 and Figure 4.7) provide a much improved description of the measurements.

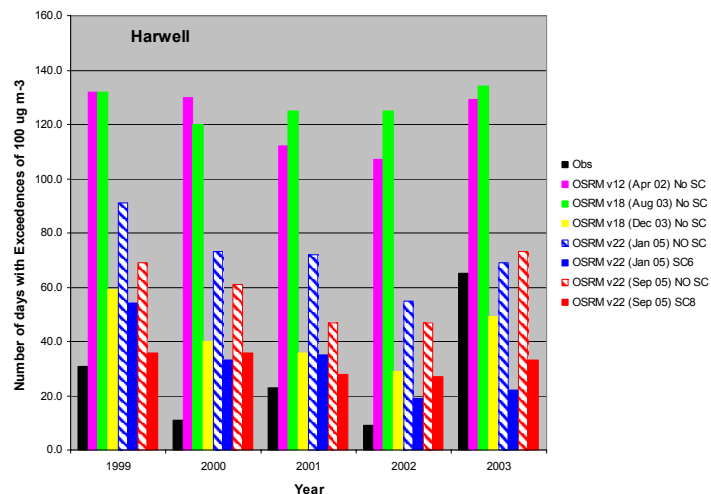
As discussed in the previous section, although the annual mean ozone concentrations were in good agreement with the measurements (see Figure 4.4), there was a tendency for the model to overpredict NO and hence NO_x concentrations by quite a large factor. Modifications were made to the surface conversion algorithm following the review of the algorithm in 2005 and the effect of these changes can be seen in the improved agreement for the annual mean NO_2 concentration.

4.5.2 Comparison with Measurements

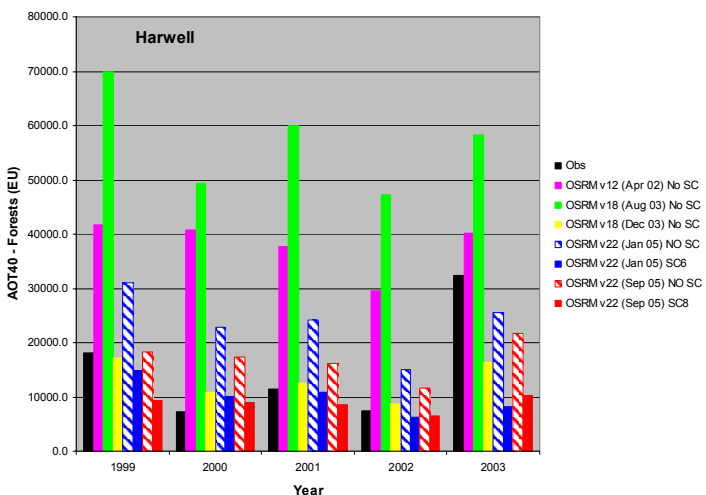
Figure 4.6, Figure 4.7 and Table 4.2 provide visual and numerical comparisons of the performance of the latest version of the OSRM (version 2.2) against observations made at UK ozone monitoring sites. Table 4.2 compares (a) the annual mean of the maximum daily running 8-hour mean ozone concentration ($\mu\text{g m}^{-3}$) and (b) the number of days when the running 8-hour mean ozone concentration exceeds $100 \mu\text{g m}^{-3}$ calculated in 2003 for the selected 41 UK ozone monitoring sites. The table presents the OSRM results for the uncorrected and surface-corrected output. There is a significant improvement in the performance of the OSRM, particularly for the London and other urban sites, when the surface correction is applied. The surface-correction algorithm was therefore used in the processing of all the subsequent OSRM output.



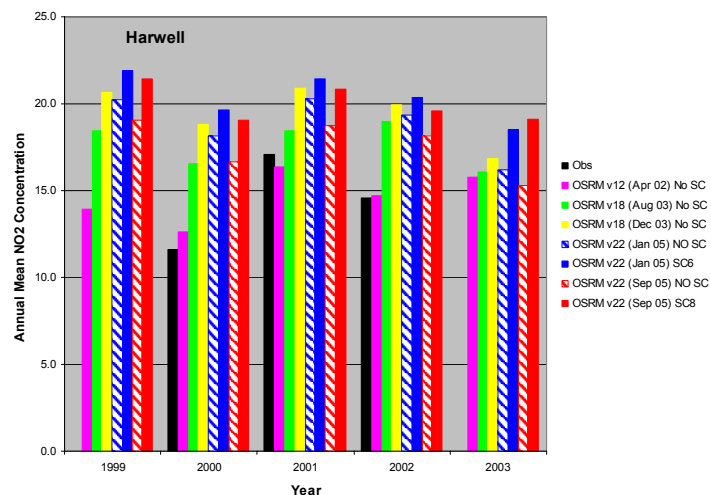
(a)



(b)

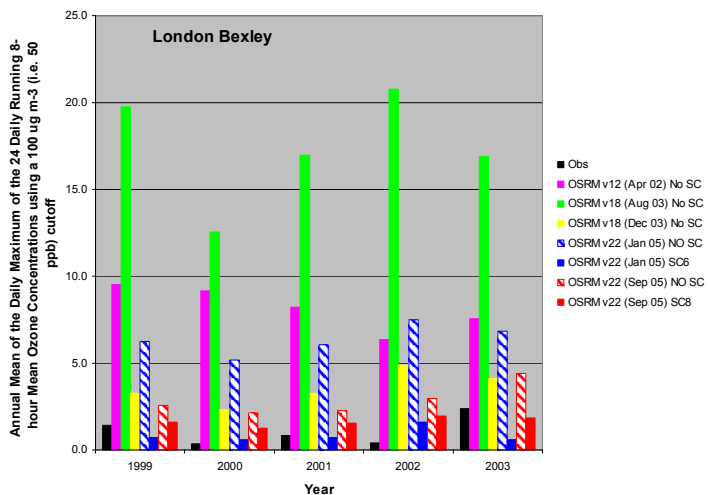


(c)

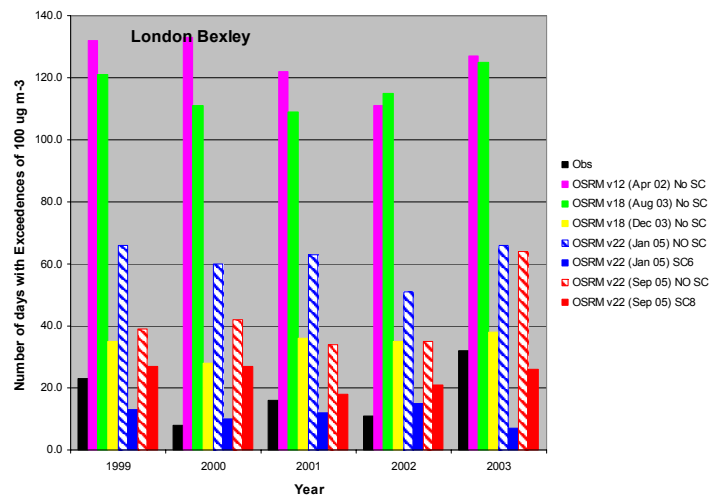


(d)

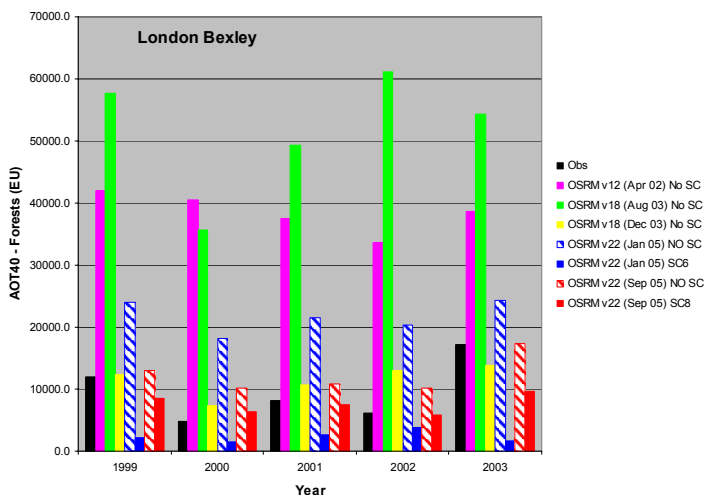
Figure 4.6 Comparison of Different Versions of the Ozone Source-receptor Model for the Metrics – (a) Annual Mean of the Daily Maximum of the 24 Daily Running 8-hour Mean Ozone Concentrations using a $100 \mu\text{g m}^{-3}$ (i.e., 50 ppb) cutoff (in $\mu\text{g m}^{-3}$), (b) Number of days with Exceedences of $100 \mu\text{g m}^{-3}$, (c) AOT40 - Forests (in $\mu\text{g m}^{-3}$ hours) and (d) Annual Mean NO_2 Concentration (in $\mu\text{g m}^{-3}$), Calculated at London Bexley for the Years 1999 to 2003. The Observed Values of the Metrics are shown in Black.



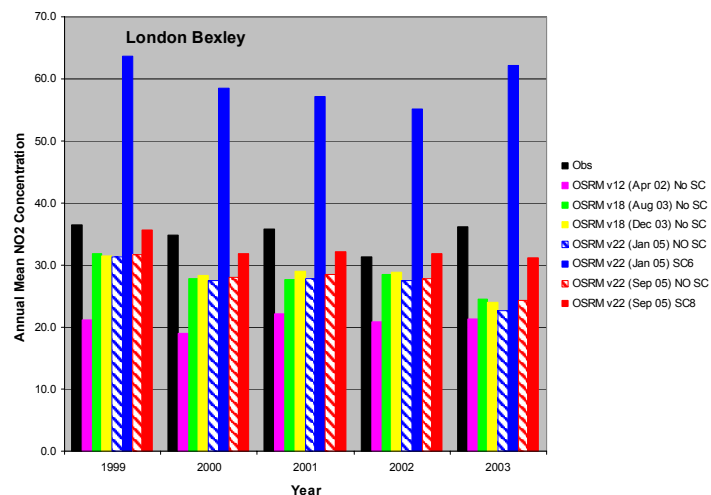
(a)



(b)



(c)



(d)

Figure 4.7 Comparison of Different Versions of the Ozone Source-receptor Model for the Metrics – (a) Annual Mean of the Daily Maximum of the 24 Daily Running 8-hour Mean Ozone Concentrations using a $100 \mu\text{g m}^{-3}$ (i.e., 50 ppb) cutoff (in $\mu\text{g m}^{-3}$), (b) Number of days with Exceedences of $100 \mu\text{g m}^{-3}$, (c) AOT40 - Forests (in $\mu\text{g m}^{-3}$ hours) and (d) Annual Mean NO_2 Concentration (in $\mu\text{g m}^{-3}$), Calculated at London Bexley for the Years 1999 to 2003. The Observed Values of the Metrics are shown in Black.

Table 4.2 Comparison of the Uncorrected and Surface-Corrected OSRM Output for the Annual Mean of Maximum Daily Running 8-Hour Mean Ozone Concentration ($\mu\text{g m}^{-3}$) and the Number of Days when the Running 8-hour Mean Ozone Concentrations exceeds $100 \mu\text{g m}^{-3}$ for 2003 against the Values derived from the Measured Ozone Concentrations.

Site	Annual Mean of the Daily Maximum of the 24 Daily Running 8-hour Mean Ozone Concentrations			Number of days with Exceedences of $100 \mu\text{g m}^{-3}$		
	Obs	OSRM - Without Surface Conversion	OSRM - With Surface Conversion	Obs	OSRM - Without Surface Conversion	OSRM - With Surface Conversion
Strathvaich Dam	83.8	83.2	76.6	45.0	66.0	41.0
Aston Hill	73.6	79.7	72.8	39.0	74.0	41.0
Bush	72.8	79.8	69.9	24.0	61.0	25.0
Eskdalemuir	66.0	80.8	74.9	18.0	61.0	40.0
Great Dun Fell	76.5	80.8	72.9	36.0	62.0	38.0
Harwell	80.3	77.3	65.6	65.0	73.0	33.0
High Muffles	66.0	78.7	73.0	15.0	58.0	42.0
Ladybower	70.9	73.5	65.8	27.0	48.0	27.0
Lullington Heath	81.3	80.9	76.5	57.0	100.0	75.0
Narberth	66.3	85.6	81.2	27.0	97.0	67.0
Rochester	76.8	71.5	66.2	54.0	61.0	38.0
Sibton	73.3	76.1	71.6	37.0	75.0	50.0
Somerton	78.0	83.3	74.9	46.0	88.0	55.0
Wharley Croft	-	80.4	73.2	0.0	62.0	37.0
Wicken Fen	72.0	75.3	67.0	44.0	65.0	30.0
Wray	-	79.1	72.8	0.0	60.0	36.0
Yarner Wood	79.2	86.6	78.7	48.0	102.0	61.0
Bottesford	67.2	74.1	63.6	31.0	47.0	22.0
Glazebury	58.0	72.6	66.9	14.0	42.0	27.0
Lough Navar	-	84.7	80.0	5.0	75.0	49.0
London Bexley	64.0	71.2	60.5	32.0	64.0	26.0
London Bloomsbury	45.8	70.3	46.4	14.0	56.0	11.0
London Brent	66.1	71.5	61.0	39.0	58.0	24.0
London Eltham	60.5	72.2	62.9	31.0	62.0	29.0
London Hackney	52.2	70.4	55.5	21.0	53.0	16.0
London Haringey	58.8	70.9	59.2	32.0	54.0	19.0
London Hillingdon	47.9	72.1	56.6	17.0	56.0	18.0
London North Kensington	58.7	70.5	54.4	29.0	57.0	14.0
London Teddington	71.7	71.3	61.9	49.0	55.0	27.0
London Westminster	50.3	71.0	53.5	19.0	62.0	14.0
Birmingham Centre	57.7	72.9	53.2	18.0	47.0	12.0
Birmingham East	63.2	72.6	60.5	33.0	47.0	20.0
Manchester Piccadilly	46.9	72.7	53.0	11.0	44.0	12.0
Leeds Centre	53.5	72.5	54.2	13.0	48.0	12.0
Newcastle Centre	57.6	79.8	62.9	15.0	54.0	23.0
Bristol Centre	57.1	79.1	62.4	13.0	76.0	24.0
Southampton Centre	60.0	80.4	71.8	26.0	83.0	45.0
Glasgow Centre	50.4	79.5	58.4	3.0	57.0	12.0
Edinburgh Centre	-	79.6	63.0	0.0	64.0	19.0
Belfast Centre	59.7	82.8	69.2	8.0	67.0	24.0
Cardiff Centre	59.0	78.7	63.0	20.0	67.0	24.0

A similar trend is seen when the OSRM model output is compared to measurements for other years (1999-2002).

Figure 4.8 presents regression plots of the modelled against the observed values of the two ozone metrics of relevance for the EU third Daughter Directive on Ozone – AOT40 – Crops and the Number of Days on which the maximum daily running 8-hour mean ozone concentration exceeded 60 ppb (or $120 \mu\text{g m}^{-3}$). The figure also shows the 1:2 line and 2:1 lines, which define the data quality objective. The agreement is better for the AOT40 – Crops metric than for the Number of Days on which the maximum daily running 8-hour mean ozone concentration exceeded 60 ppb (or $120 \mu\text{g m}^{-3}$). The latter metric is more sensitive to peak ozone concentrations and any over prediction of the ozone concentration will affect this metric more than the AOT40 – Crops metric.

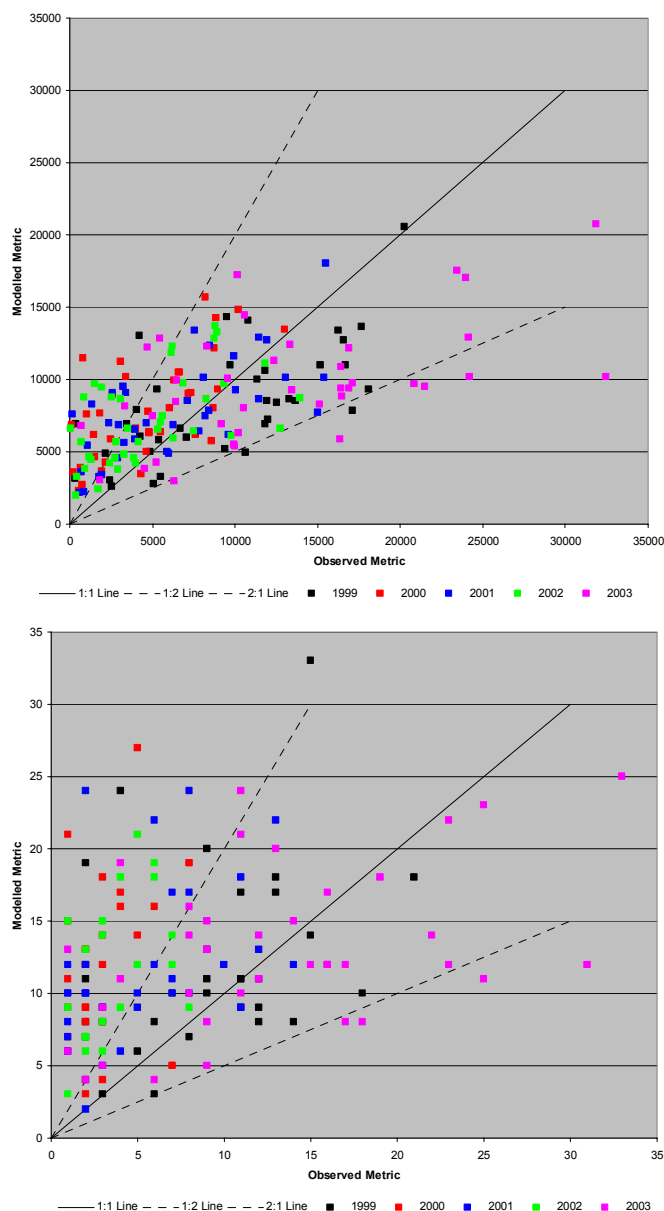


Figure 4.8 Scatter Plots of the Calculated against the Observed Values of the Ozone Metrics - AOT40 – Crops (Upper Panel) and the Number of Days on which the Maximum Daily Running 8-hour Mean Ozone Concentration exceeded 60 ppb (or 120 $\mu\text{g m}^{-3}$) (Lower Panel) for the Years 1999 to 2003.

4.5.3 Comparison with Other Models

The output of the OSRM has been compared with that from the UK Photochemical Trajectory Model and the ADMS Urban Model.

(1) UK Photochemical Trajectory Model

The UK-Photochemical Trajectory Model (PTM) has been used extensively to assist the evaluation of ozone policy options [e.g., Derwent *et al.*, 1998, 2004]. For the comparison, the model calculations used the idealised episode trajectory of the UK PTM from Central Europe to mid-Wales. The OSRM was configured to calculate ozone concentrations along the same linear trajectory. As far as was possible, the two models used (a) the same emission inventories (from EMEP and a biogenic emission inventory with no temporal emission factors), (b) the same VOC speciation and (c) the same treatment and parameter values for the photolysis and dry deposition processes. The remaining differences were the chemical mechanisms and solvers used in the two models (PTM: CRI

Mechanism with a variable order Gear solver; OSRM: the modified STOCHEM mechanism with a backward Euler solver).

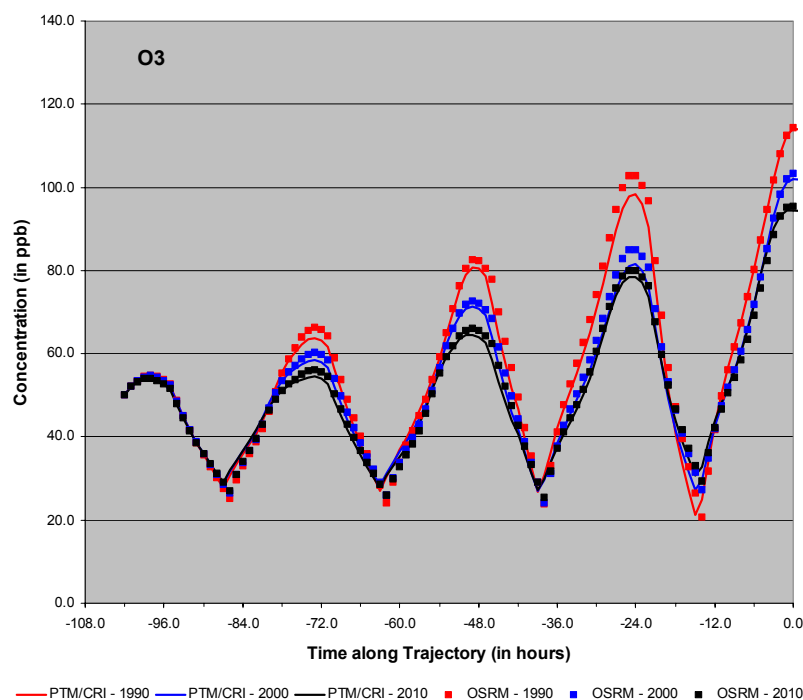


Figure 4.9 Comparison of the Ozone Concentrations Calculated by the OSRM and PTM for Three Different Emission Years along the Idealised Episode Trajectory of the PTM.

Figure 4.9 shows a comparison of the mid-boundary layer ozone concentrations calculated along the idealised episode trajectory by the two models for three different emission years. The peak ozone concentrations in these model runs, together with additional runs in which the VOC and NO_x emissions were reduced by 30% across-the-board, are presented in Table 4.3. The Surface-conversion algorithm was not necessary for this comparison. The agreement between the two models is excellent.

Table 4.3 Comparison of the Peak Ozone Concentrations Calculated by the PTM and OSRM for Different Emission Scenarios along the Idealised Episode Trajectory of the PTM.

Model Run	PTM Peak Ozone (in ppb)	OSRM Peak Ozone (in ppb)
1990 Base Case	114.9	115.1
2000 Base Case	102.6	103.9
2010 Base Case	95.1	96.2
2010 Base Case + 30% NO _x Reduction	92.0	95.2
2010 Base Case + 30% VOC Reduction	86.5	85.2

(2) ADMS Urban

The OSRM has been used to generate maps of ozone and nitrogen dioxide metrics for London for 2010 and a number of current years (1999-2003). Model runs were undertaken to calculate the hourly ozone and nitrogen dioxide concentrations for a model domain covering Outer London using meteorological data and UK and EMEP emission inventories for the relevant years. The model domain used a 1 km x 1 km grid of 1,639 receptor sites. From the hourly concentrations, maps were derived of the annual mean ozone and nitrogen dioxide concentrations. Both surface-converted and unconverted maps were prepared.

Under a separate contract let by Defra and the Devolved Administrations, CERC have used ADMS-Urban to generate concentrations maps of the annual mean ozone and nitrogen dioxide concentrations for the Greater London area for 1999 [CERC, 2003]. These are compared with the

corresponding surface-corrected OSRM maps in Figure 4.10. While the OSRM maps do not have the detailed structure of the ADMS maps, the OSRM maps do show the high concentrations of NO_2 (and low concentrations of O_3) in central London and in the vicinity of Heathrow airport, which reflect the areas of high NO_x emissions in London. There is also evidence of the major London roads (e.g., the M3, M4 and A40 to the west and the North Circular Road). The OSRM NO_2 concentrations are generally lower than those in the ADMS-Urban maps and as a result the OSRM maps show higher O_3 concentrations.

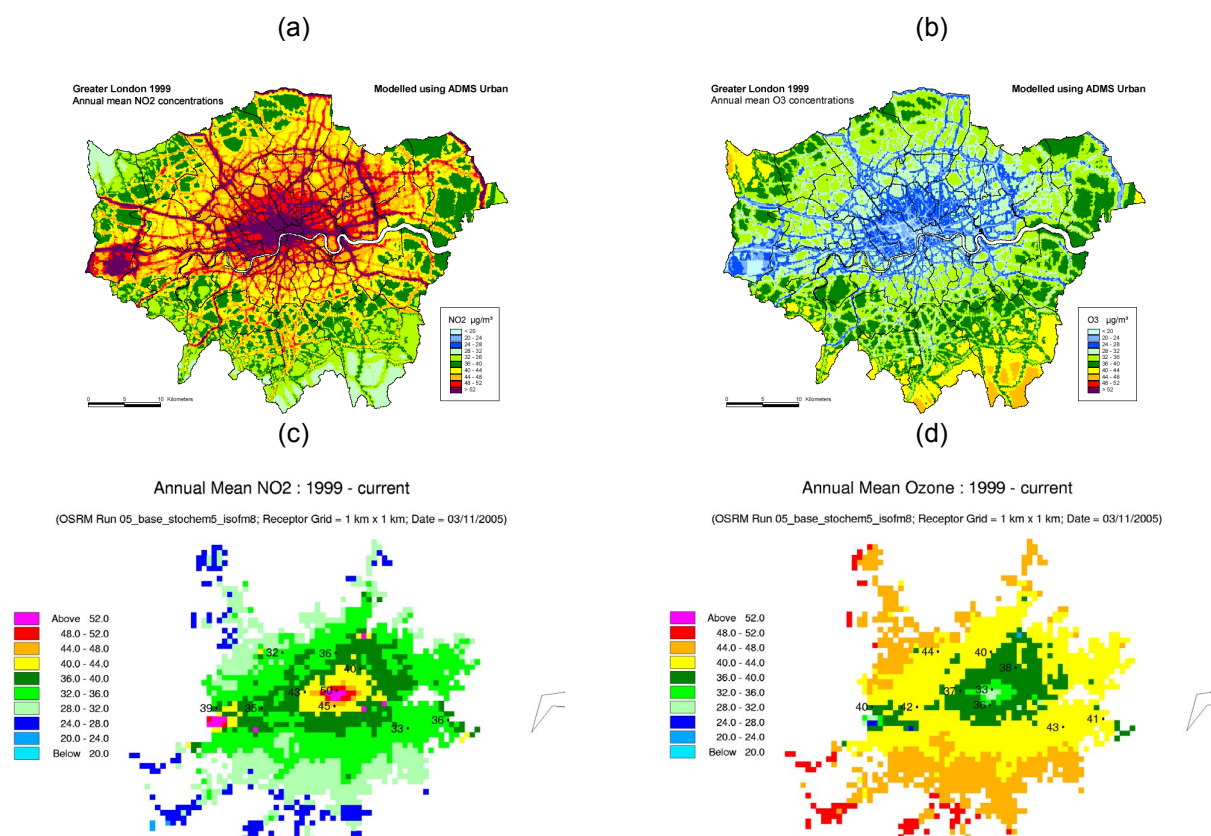


Figure 4.10 Comparison of Maps for Greater London of Annual Mean Concentrations (in $\mu\text{g m}^{-3}$) of NO_2 (left-hand panels) and O_3 (right-hand panels) calculated using ADMS-Urban (panels a and b) and the Ozone Source-receptor (panels c and d) Models for 1999.

Both models show a reduction in the annual mean NO_2 concentration between 1999 and 2010 as the NO_x emissions are lower. There is a corresponding increase in the annual mean ozone concentration as a result of the reduced NO_x titration effect.

4.6 SUITABILITY OF THE OSRM

Overall, the OSRM is a model, which now has a robust and flexible construction that makes it ideal for the demands of assisting in the development of policy. The improvements made to the OSRM during the current contract have produced a model that is able to reproduce boundary-layer concentrations of ozone and oxides of nitrogen, representative of the UK.

In the context of ozone formation, the OSRM and UK Photochemical Trajectory Model were found to give identical output and responses, on a like-for-like basis. For the determination of surface concentrations of ozone and oxides of nitrogen, the OSRM has post-processor options, which take account of local emissions and removal processes. The comparison of the OSRM with the ADMS Urban model gave similar responses and showed similar spatial patterns. These comparisons demonstrate that the OSRM is a robust model which can be used to assist the development of policy.

5 Detailed Assessment of the Relationship between Ozone, NO and NO₂, and Factors Controlling Them (Objective 2)

5.1 INTRODUCTION

Owing to the chemical coupling of O₃ and NO_x, ambient levels of O₃ and NO₂ are inextricably linked. Consequently, the response to reductions in the emissions of NO_x is highly non-linear [e.g., AQEG, 2004], and any resultant reduction in the level of NO₂ is invariably accompanied by an increase in the level of O₃. It is therefore necessary to have a complete understanding of the relationships between O₃, NO and NO₂ under atmospheric conditions, if the success of proposed control strategies is to be fully assessed.

Prior to the current contract, monitoring data from a number of sites in Greater London were analysed to determine whether the description of annual mean concentrations of NO₂, and their dependence on [NO_x], can be improved by the application of empirically-derived relationships between concentrations of O₃, NO_x and NO₂ [Clapp and Jenkin, 2001]. In that study, it was demonstrated that additional insights could be gained by establishing, first, how the concentration of 'oxidant', [OX] (taken to be the sum of [O₃] and [NO₂]), varies with the concentration of NO_x and, secondly, how the fractional contribution of NO₂ to OX (i.e., [NO₂]/[OX]) varies with [NO_x]. In this way, it was possible to rationalise the derived [NO₂] vs. [NO_x] relationships, and their site-to-site variations, in terms of sources of OX and well-understood chemical processes.

In the present contract, the analysis has been extended in a number of ways, as described in detail below. First, a comprehensive analysis has been carried out of data from 65 AURN sites and one additional site where O₃ and NO_x are monitored in 13 UK zones, using annual mean data up to 2001. This has allowed annual mean [NO₂] vs. [NO_x] (and [O₃] vs. [NO_x]) relationships to be recommended for 56 roadside, urban centre, urban background, suburban and urban industrial sites. These results have been used to suggest representative expressions for different regions of the UK, which have subsequently been employed in the National Scale Empirical NO₂ modelling activities. The analysis has also considered annual mean data at selected sites since 2001, which has helped to reveal a significant increase in the local OX source (i.e., due to increased primary NO₂ emissions) at a number of sites since 2003.

In addition, a detailed analysis of 1998 and 1999 hourly mean data has been carried out for Marylebone Rd. This has allowed insights into the seasonal and diurnal dependence of OX sources and their origins, and the conditions under which exceedences of the hourly mean NO₂ limit value (200 µg m⁻³, 104.5 ppb) are more probable. In conjunction with NO_x emissions estimates, based on traffic flow statistics, the data have been used to draw conclusions about the likely fractional contribution of primary NO₂ to NO_x emissions from diesel and petrol-fuelled vehicles at that time.

5.2 THE CHEMICAL COUPLING OF O₃, NO AND NO₂

The interconversion of NO, NO₂ and O₃ under atmospheric conditions is generally dominated by the following reactions:



As a result, the behaviour of NO and NO₂ is highly coupled, and it is convenient to refer to them collectively as NO_x. Because this coupling also involves O₃, however, NO₂ and O₃ are also often collectively defined as 'oxidant (OX)' [e.g., Kley *et al.*, 1994]. Reactions (5.1) and (5.2) are thus a cycle with no net chemistry, which has the overall effect of partitioning NO_x between its component forms of NO and NO₂, and OX between its component forms of O₃ and NO₂, but leaving the total concentration of

both NO_x and OX unchanged. At low levels of NO_x , O_3 is the major component of OX, whereas NO_2 dominates at high levels.

The previous studies [Clapp and Jenkin, 2001] were able to show that the concentration of OX ($[\text{OX}] = [\text{O}_3] + [\text{NO}_2]$) tends to increase linearly with $[\text{NO}_x]$, such that it is made up of two identifiable contributions: a NO_x -independent (or regional) contribution and a NO_x -dependent (or local) contribution. The former equates to the regional background O_3 level, whereas the latter correlates with the level of primary pollution. A significant (sometimes dominant) fraction of this local contribution is likely to result from emission of a fraction of NO_x directly in the form of NO_2 . A number of thermal and photochemical sources also potentially contribute, as also discussed by Clapp and Jenkin [2001]. These are all processes which convert NO to NO_2 without associated removal of O_3 , and are therefore net sources of OX.

5.3 ANALYSIS OF ANNUAL MEAN DATA

5.3.1 Regional OX levels in the UK

Data from AURN sites in 13 UK zones have been used to investigate the relationship between annual mean concentrations of OX and NO_x . Figure 5.1 shows the results for two zones, and the regional and local contributions derived from this analysis for all zones are summarized in Table 5.1. The main purpose of this analysis was to estimate the regional background OX level, and to identify any zonal variations. Although the analysis provides reasonably consistent values across the whole UK (typically in the range 30-35 ppb), and therefore a good first estimate, it is recognized that the combination of sites within a given zone may introduce bias. It will only truly determine the regional background if the local OX contribution is the same at all sites in the zone. The regional background was therefore also estimated from the value at the least polluted site in the zone, with the assumption that the local OX contribution is 10%. Previous work has shown that this is a reasonable average value [Clapp and Jenkin, 2001].

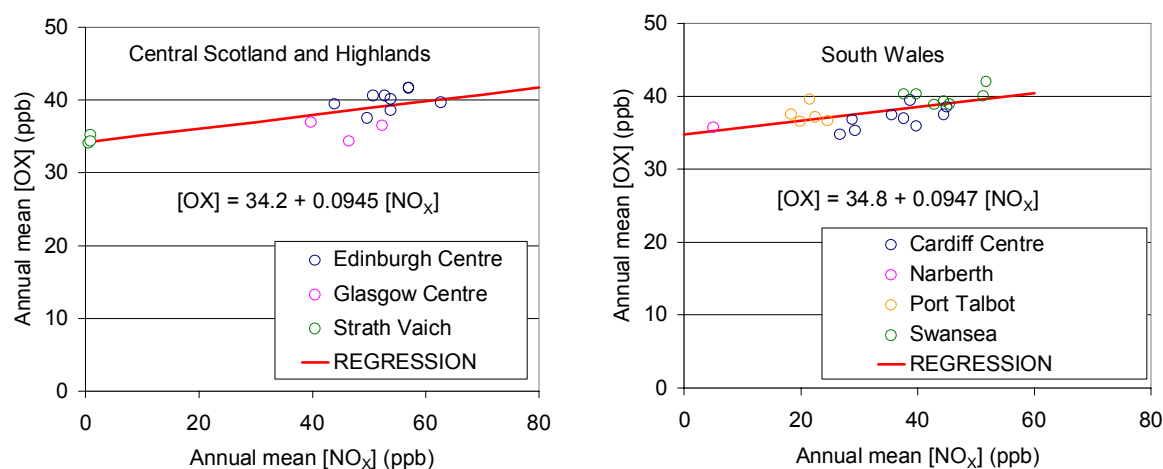


Figure 5.1 Annual mean concentrations of OX as a function of NO_x concentration for AURN sites in Central Scotland and the Highlands, and South Wales. The number of years for which data are available varies with sites. All the displayed data were measured between 1992 and 2001.

The results from both methods (Table 5.1) generally indicate that zones in the southern UK, northeast England and Scotland have slightly higher regional background levels of OX. Previous analyses of rural O_3 concentrations in the UK have tended to show a similar phenomenon [e.g., PORG 1997]. As indicated in Table 5.1, the zones under consideration were placed in four groups, each with a different regional background level determined from the composite results: the Highlands, Central Scotland, Northern Ireland and the North East (34.4 ppb); the North West and Yorkshire and Humberside (33.8 ppb); the West Midlands, East Midlands and the East (32.4 ppb); South Wales, the South West, the South East and London (34.7 ppb).

Table 5.1 Summary of OX Contributions determined from the Analysis of O₃ and NO_x Data in 13 UK zones.

Zone	local OX (% of NO _x)	regional OX (ppb)		
		method 1 ^a	method 2 ^b	assigned value ^c
Central Scotland/Highlands	(9.5 ± 2.3)	(34.2 ± 1.1)	34.4	region 1 = 34.4
Northern Ireland	(18.2 ± 4.3)	(31.5 ± 1.4)	31.9	
North East	(3.7 ± 3.2)	(35.5 ± 0.9)	35.1	
North West	(9.0 ± 1.3)	(33.6 ± 0.8)	32.7	region 2 = 33.8
Yorkshire and Humberside	(8.6 ± 3.4)	(33.9 ± 1.6)	35.9	
West Midlands	(18.1 ± 3.3)	(30.5 ± 1.1)	32.2	region 3 = 32.4
East Midlands	(14.4 ± 2.8)	(32.0 ± 0.8)	33.2	
East	(8.4 ± 3.9)	(31.7 ± 1.9)	31.8	
South Wales	(9.5 ± 2.8)	(34.8 ± 1.0)	35.4	region 4 = 34.7
South West	(14.6 ± 3.5)	(32.7 ± 1.7)	33.4	
South East	(8.0 ± 1.8)	(34.9 ± 0.6)	34.9	
Greater London	(10.3 ± 1.0)	(34.7 ± 0.7)	34.9	

a: regional OX determined from intercept of [OX] vs. [NO_x] plot (e.g., see Figure 5.1); b: regional OX determined from data for least polluted site in zone with the assumption of a local OX contribution of 10% (see text); c: average of method 2 for regions 2, 3 and 4; for region 1, Strath Vaich provides a direct measure at close to zero NO_x (see Figure 5.1) and the value is applied accordingly.

5.3.2 Site-dependent Local OX Contributions

Local OX contributions for each of the monitoring sites were determined from a regression analysis of the measured annual mean [OX] and [NO_x], with the intercepts constrained to the appropriate regional OX value assigned above. This analysis was performed for the 58 non-rural AURN sites and one additional site (Watford Roadside). The derived local OX contributions are summarized in Table 5.2. In the cases of Derry, Coventry Centre and Manchester South, the analysis was found to yield anomalous results with significantly negative values of the local OX contribution. This was found to be particularly severe in the case of Manchester South, where annual mean [OX] values are consistently well below background, with values of ca. 25-26 ppb reported on three occasions. As indicated below, these sites also display anomalies in their [NO₂]/[OX] values.

Table 5.2 Summary of parameters required to define site-dependent annual mean [NO₂] vs. [NO_x] relationships. The threshold annual mean [NO_x] values corresponding to 20.9 ppb (40 μg m⁻³) NO₂, as derived from these relationships, are also shown.

Site	Regional OX (ppb)	Local OX (fraction of NO _x)	[NO ₂]/[OX] Polynomial f(NO _x)	Adjustment Factor	NO _x Threshold (ppb) ^a
	B	A		C	
Central Scotland					
Edinburgh Centre (UC)	34.4	0.105	(ii)	0.951	42.2
Glasgow Centre (UC)	34.4	0.033	(i)	1.042	48.2
Northern Ireland					
Belfast Centre (UC)	34.4	0.108	(ii)	0.973	40.7
North East					
Middlesbrough (UI)	34.4	0.070	(ii)	1.037	39.4
Newcastle Centre (UC)	34.4	0.062	(i)	0.991	49.2
Redcar (S)	34.4	0.141	(ii)	1.036	35.9
North West					
Blackpool (UB)	33.8	0.104	(i)	0.974	47.6
Bolton (UB)	33.8	0.086	(ii)	0.975	42.9
Bury Roadside (UR)	33.8	0.086	(i)	1.003	47.0
Liverpool Centre (UC)	33.8	0.124	(i)	0.963	46.6
Manchester Piccadilly (UC)	33.8	0.037	(ii)	1.052	41.7
Preston (UB)	33.8	0.052	(i)	1.013	49.9
Salford Eccles (UI)	33.8	0.082	(ii)	0.981	42.8
Wirral Tranmere (UB)	33.8	0.041	(ii)	1.006	44.3
Yorkshire and Humberside					
Barnsley Gawber (UB)	33.8	0.208	(i)	0.987	39.7
Bradford Centre (UC)	33.8	0.049	(ii)	0.953	47.4
Hull Centre (UC)	33.8	0.094	(i)	1.012	45.6
Leeds Centre (UC)	33.8	0.104	(i)	1.033	43.4
Rotherham Centre (UC)	33.8	0.008	(i)	1.030	54.7
Sheffield Centre (UC)	33.8	0.083	(i)	0.975	49.6

Table 5.2 Summary of parameters required to define site-dependent annual mean [NO₂] vs. [NO_x] relationships. The threshold annual mean [NO_x] values corresponding to 20.9 ppb (40 µg m⁻³) NO₂, as derived from these relationships, are also shown (continued):

Site	Regional OX (ppb)	Local OX (fraction of NO _x)	[NO ₂] / [OX] Polynomial f(NO _x)	Adjustment Factor	NO _x Threshold (ppb) ^a
	B	A		C	
West Midlands					
Birmingham Centre (UC)	32.4	0.158	(ii)	1.030	37.8
Birmingham East (UB)	32.4	0.087	(ii)	1.016	42.7
Leamington Spa (UB)	32.4	0.143	(ii)	1.115	34.8
Sandwell West Bromwich (UB)	32.4	0.204	(ii)	1.006	36.9
Stoke on Trent Centre (UC)	32.4	0.130	(i)	0.994	46.4
Wolverhampton Centre (UC)	32.4	0.078	(ii)	0.989	45.0
East Midlands					
Leicester Centre (UC)	32.4	0.149	(ii)	1.016	39.0
Nottingham Centre (UC)	32.4	0.097	(ii)	1.058	39.7
East					
Norwich Centre (UC)	32.4	0.118	(ii)	1.062	38.3
Southend-on-Sea (UB)	32.4	0.166	(ii)	0.997	39.0
Stevenage (S)	32.4	0.059	(i)	0.972	56.6
Thurrock (UB)	32.4	0.129	(i)	1.027	44.3
Watford Roadside (UR)	32.4	0.102	(i)	1.051	44.9
South Wales					
Cardiff Centre (UC)	34.7	0.062	(ii)	1.043	39.1
Port Talbot (UB)	34.7	0.131	(i)	0.941	46.1
Swansea Centre (UC)	34.7	0.118	(i)	0.915	49.3
South West					
Bristol Centre (UC)	34.7	0.116	(i)	0.918	49.2
Exeter Roadside (UR)	34.7	0.069	(i)	0.943	52.1
Plymouth Centre (UC)	34.7	0.030	(i)	0.998	51.8
South East					
Reading (UB)	34.7	0.091	(i)	0.982	46.4
Southampton Centre (UC)	34.7	0.074	(i)	1.004	46.3
London					
<i>Outer London</i>					
Bexley (S)	34.7	0.099	(ii)	0.974	40.8
Brent (UB)	34.7	0.071	(ii)	1.036	39.0
Eltham (S)	34.7	0.060	(ii)	1.014	40.9
Hillingdon (S)	34.7	0.039	(i)	1.005	50.0
Sutton (S)	34.7	0.006	(ii)	1.020	44.7
Teddington (UB)	34.7	0.104	(ii)	0.993	39.4
<i>Inner London</i>					
Hackney (UC)	34.7	0.143	(i)	1.035	39.3
Lewisham (UC)	34.7	0.047	(ii)	0.984	43.7
Marylebone Rd (UR)	34.7	0.095	(i)	1.009	44.1
N. Kensington (UB)	34.7	0.105	(ii)	1.037	37.1
Wandsworth (UC)	34.7	0.062	(i)	1.022	46.0
<i>Central London</i>					
Central London (UB)	34.7	0.126	(ii)	1.023	36.8
Bloomsbury (UC)	34.7	0.132	(ii)	1.026	36.4
Bridge Place (UB)	34.7	0.168	(ii)	1.003	35.9
Southwark (UC)	34.7	0.135	(ii)	0.959	39.6

a: [NO₂] for which [NO₂] = 20.9 ppb (40 µg m⁻³). To convert NO_x threshold to µg m⁻³ as NO₂, multiply by 1.913

As found previously [Clapp and Jenkin, 2001], the derived local OX contributions show substantial site-to-site variations. Although there are a small number of outliers, values typically lie in the range 3-17%. Possible reasons for these variations have been discussed by Clapp and Jenkin [2001]. These particularly include variations in the fractional contribution of NO₂ to emitted NO_x, which might accompany the differing vehicle fleet compositions (e.g., proportion of diesel vehicles) and driving conditions (e.g., vehicle speed) characteristic of each site. Recent studies at the Transport Research Laboratory [TRL] have confirmed that diesel engines emit a higher proportion of NO_x as NO₂ than petrol vehicles, and that this proportion increases at lower vehicle speeds [Latham *et al.*, 2001]. It has been recognised for some time that annual average NO₂ concentrations show a distinct variation from one site to another, even for sites for which the annual average NO_x is comparable [e.g., Stedman *et al.*, 2000]. The present analysis clearly demonstrates that the large variation in the local sources of OX from one site to another makes a major contribution to the reported site-to-site variation for NO₂.

5.3.3 Oxidant Partitioning as a Function of NO_x

In conjunction with the $[\text{OX}]$ vs. $[\text{NO}_x]$ relationships defined above, a knowledge of the precise partitioning of OX between its component forms of NO_2 and O_3 , and its dependence on $[\text{NO}_x]$, potentially allows $[\text{NO}_2]$ vs. $[\text{NO}_x]$ and $[\text{O}_3]$ vs. $[\text{NO}_x]$ relationships to be defined. Figure 5.2 shows the fraction of OX, which is in the form of NO_2 , based on the annual average data for the 56 sites in Table 5.2, and the 7 associated rural sites. As expected, the data generally show that a progressively greater proportion of OX is in the form of NO_2 as the level of NO_x increases. Consistent with the analysis [Clapp and Jenkin, 2001], mainly based on London sites, the data appear to fall broadly into two groups. The first is made up of roadside sites, but also includes a large number of additional sites that presumably possess some roadside character. The data for these sites are presented in Figure 5.3. The polynomial expression of Clapp and Jenkin [2001] was obtained from a fit to data for Marylebone Rd and three other sites identified in the figure, using data up to 2000. The present analysis includes 3 further roadside sites (Bury, Exeter and Watford), which are also adequately represented by the previous polynomial expression, which is as follows (applicable range, 10-220 ppb NO_x):

$$[\text{NO}_2]/[\text{OX}] = 8.962 \times 10^{-2} + 1.474 \times 10^{-2} [\text{NO}_x] - 1.290 \times 10^{-4} [\text{NO}_x]^2 + 5.527 \times 10^{-7} [\text{NO}_x]^3 - 8.906 \times 10^{-10} [\text{NO}_x]^4 \quad (i)$$

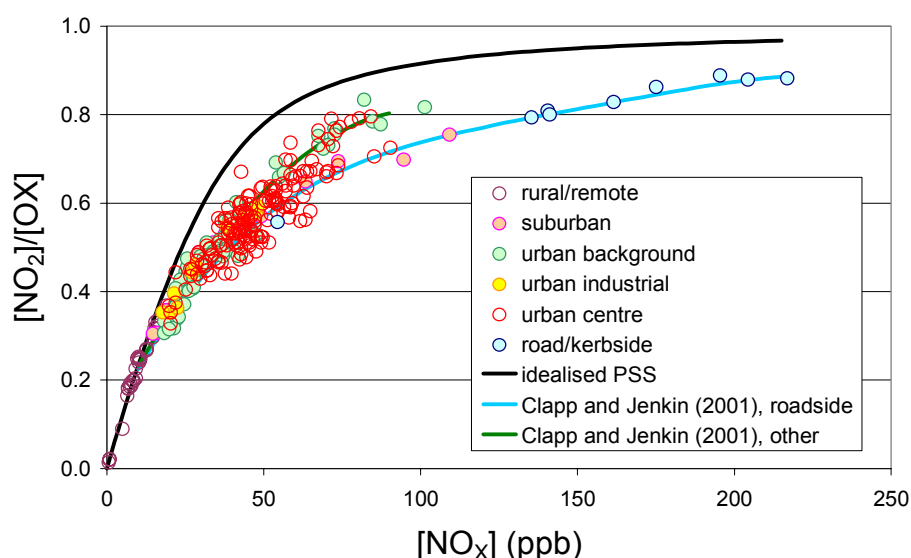


Figure 5.2 Variation of annual mean $[\text{NO}_2]/[\text{OX}]$ as a function of $[\text{NO}_x]$. The black line is the calculated idealised variation based on the assumption of photostationary state. The other lines are fitted polynomial expressions based on data for subsets of sites, reported previously (Clapp and Jenkin, 2001).

The 21 sites in Figure 5.3, which are not nominally roadside sites, are distributed among the nominal urban centre, urban background and suburban categories, but show no particular propensity for any one of these.

The data for the remaining sites (Figure 5.4) are also adequately represented by a second polynomial expression reported by Clapp and Jenkin (applicable range, 10-90 ppb NO_x):

$$[\text{NO}_2]/[\text{OX}] = 1.015 \times 10^{-1} + 1.367 \times 10^{-2} [\text{NO}_x] - 6.127 \times 10^{-5} [\text{NO}_x]^2 - 4.464 \times 10^{-8} [\text{NO}_x]^3 \quad (ii)$$

Once again, this category includes a variety of urban centre, urban background and suburban sites, and also the two urban industrial sites considered in this analysis. Despite the title 'without immediate road influence' given in the figure, it is emphasised that the dominant source of NO_x at these sites is still road transport. It is suggested that, in these cases, a greater time available for conversion of emitted NO to

NO_2 leads to OX partitioning characteristics more associated with urban background locations away from the immediate impact of roads.

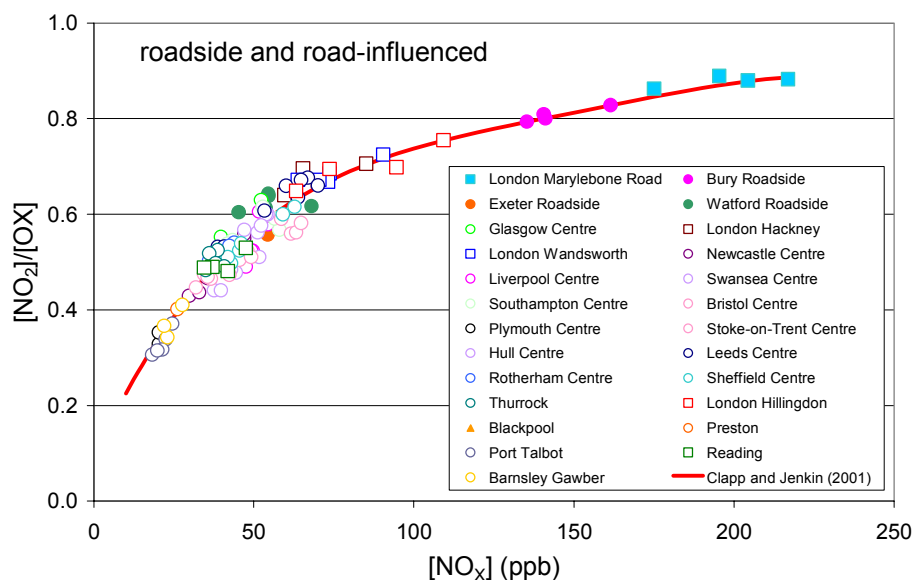


Figure 5.3 Variation of annual mean $[\text{NO}_2]/[\text{OX}]$ as a function of $[\text{NO}_x]$ for sites which are most closely represented by the 'road-influenced' polynomial expression (equation (i) of Clapp and Jenkin [2001]). Square symbols identify the sites which were originally used to define the expression. Filled symbols identify nominal roadside sites.

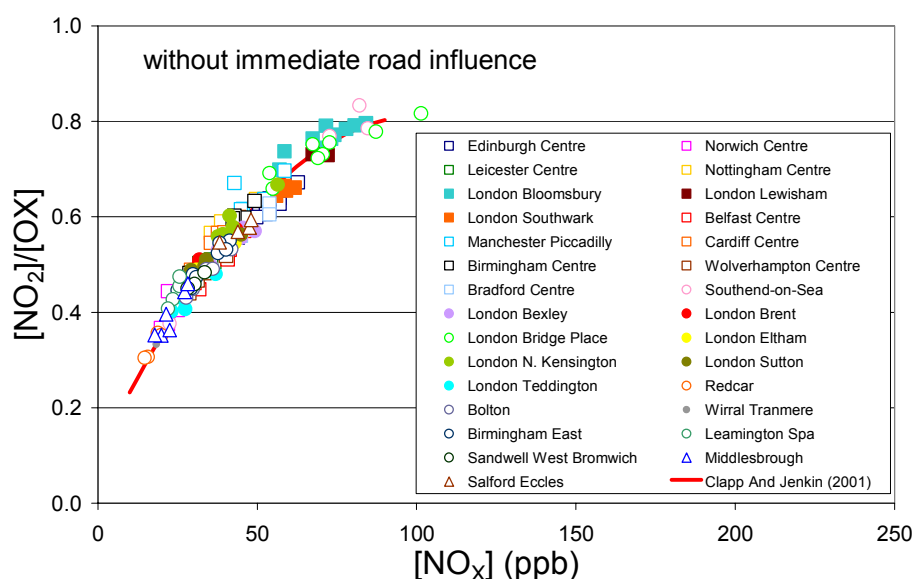


Figure 5.4 Variation of annual mean $[\text{NO}_2]/[\text{OX}]$ as a function of $[\text{NO}_x]$ for sites which are most closely represented by the 'without immediate road influence' polynomial expression (equation (ii) of Clapp and Jenkin [2001]). Filled symbols identify the sites which were originally used to define the expression. Squares are urban centre sites; circles are urban background and suburban sites; triangles are urban industrial sites.

Although equations (i) and (ii) provide a good general description of the variation of $[\text{NO}_2]/[\text{OX}]$ with $[\text{NO}_x]$ for the identified groups of sites, the data for an individual site are clearly not precisely defined by these expressions. Table 5.2 also lists a series of near-unity site-dependent adjustment factors (C) that can be used to scale the polynomial expressions so that they pass through the average of the data for a given site. The mean of these factors is (1.004 ± 0.037) , where the error is one standard deviation. Accordingly, the factors for 95% of the sites (53 out of 56) lie within two standard deviations of the mean, *i.e.*, between 0.930 and 1.078. Because the distinction between the two groups of sites identified above becomes marginal at lower $[\text{NO}_x]$ (*i.e.*, < ca. 25 ppb), it was found that only very small

adjustments (< 5%) were required for a few of the less polluted sites to fit into either of the groups shown in Figures 3 and 4. The assigned group was strictly based on which gave a value of C which is closer to unity, although it is noted that this limited number of sites could reasonably fit into either group.

The $[\text{NO}_2]/[\text{OX}]$ data for the three sites eliminated from the analysis above (Derry, Coventry Centre and Manchester South) were also considered, yielding C values of 0.858, 1.207 and 1.121, respectively, these values being beyond the extremities of the reported range for the other sites. It is suggested that the anomalously low OX concentrations at these sites, discussed above, may be due to systematically low annual mean $[\text{O}_3]$ at Coventry Centre and Manchester South, and systematically low annual mean $[\text{NO}_2]$ at Derry.

5.3.4 Site-dependent $[\text{NO}_2]$ vs. $[\text{NO}_x]$ and $[\text{O}_3]$ vs. $[\text{NO}_x]$ relationships

The parameters listed in Table 5.2 allow expressions for the NO_x -dependence of annual mean $[\text{NO}_2]$ and $[\text{O}_3]$ to be defined (in ppb) for all 56 sites, as follows,

$$\begin{aligned} [\text{NO}_2] &= (A[\text{NO}_x] + B).f(\text{NO}_x).C && \text{(iii)} \\ [\text{O}_3] &= (A[\text{NO}_x] + B).(1-f(\text{NO}_x)).C && \text{(iv)} \end{aligned}$$

where A is the local oxidant contribution, B is the regional oxidant, $f(\text{NO}_x)$ is the appropriate $[\text{NO}_2]/[\text{OX}]$ polynomial (i.e., equation (i) or (ii)) and C is the near-unity adjustment factor. The dependences defined by equation (iii) have been used to calculate the concentration of $[\text{NO}_x]$ at each site, which corresponds to the annual mean $[\text{NO}_2]$ objective of 20.9 ppb ($40 \mu\text{g m}^{-3}$). The resultant values, listed in the ' $[\text{NO}_x]$ threshold' column of Table 5.2, vary over the approximate range 35-55 ppb, and further emphasise the site-to-site variations in the NO_2 vs. NO_x relationship. For the 14 sites where comparison is possible, the $[\text{NO}_x]$ thresholds are generally in good agreement with, but supersede, those that can be calculated from the expressions of Clapp and Jenkin [2001].

The ability of the expressions calculated using equations (iii) and (iv) to describe the NO_x -dependence of annual mean $[\text{NO}_2]$ and $[\text{O}_3]$ can be tested using data from sites which have been in operation for a reasonable number of years, and which ideally cover a wide range of annual mean $[\text{NO}_x]$. Figure 5.5 presents data for NO_2 , O_3 and OX for a number of such urban centre sites (Birmingham, Edinburgh, Belfast, Cardiff and Leeds). In each case, the NO_x dependence is well described by the expressions derived in the present work, despite the substantial differences between the sites. The calculated $[\text{NO}_x]$ thresholds also provide a good indication of the level required for exceedence of the 20.9 ppb ($40 \mu\text{g m}^{-3}$) NO_2 objective to be avoided at each site. However, because of the (albeit small) scatter in the data, minor exceedences have inevitably been observed at NO_x levels below the thresholds calculated here (e.g., see data for Cardiff). It is therefore suggested that practical thresholds of 90% of the present values might be appropriate to allow for such variations.

These five sites are characterized by annual mean NO_2 in 2001 that are either close to or below the annual mean objective value. Of the 56 sites considered in the present analysis, five are estimated to require reductions in $[\text{NO}_x]$ of greater than 20% from 2001 levels for the annual mean NO_2 objective to be achieved. These are Bury Roadside (67%), and the London sites, Hillingdon (21%), Marylebone Road (75%), Wandsworth (35%), Bloomsbury (36%) and Southwark (32%). Figure 5.5 illustrates this for Bloomsbury, Marylebone Road and Hillingdon. These sites might be regarded as being broadly representative of many other UK sites where large NO_x reductions are required, particularly roadside locations (AQEG, 2004), but which are not considered here because O_3 is not monitored.

Because the $f(\text{NO}_x)$ expressions in equations (i) and (ii) are only regarded as valid down to ca. 10 ppb NO_x , it is recommended that, if required, the NO_x -dependence of annual mean $[\text{NO}_2]$ and $[\text{O}_3]$ at lower NO_x levels is based on the idealised behaviour under photostationary state conditions. As shown in Figure 5.2, this gives an acceptable description of the variation observed at rural locations. The corresponding calculated variation for NO_2 and O_3 is illustrated in Figure 5.5 for selected sites. The derivation of the idealised expressions is given in Appendix 1 of Jenkin (2004).

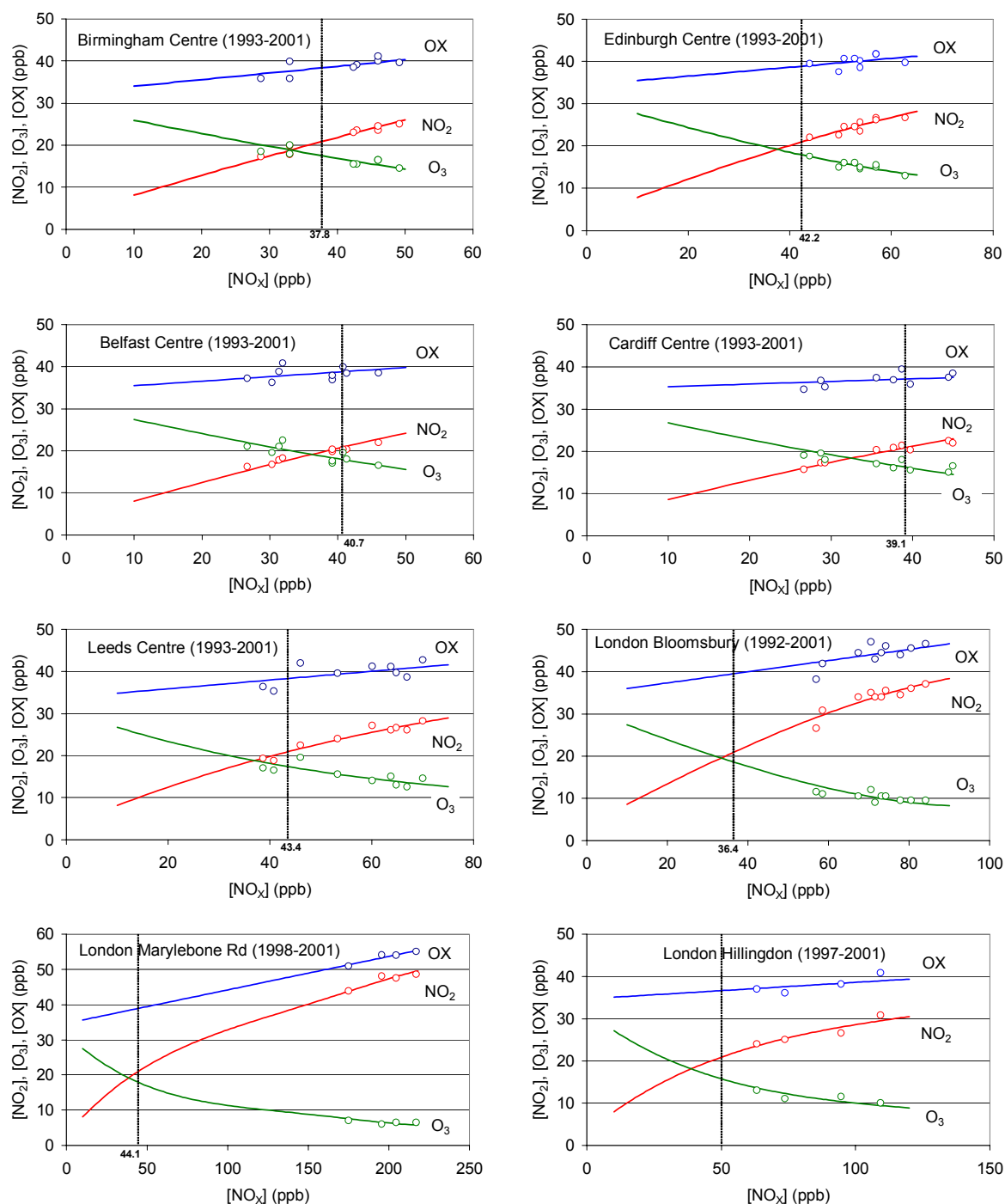


Figure 5.5 Comparison of the NO_x -dependence of annual mean $[\text{NO}_2]$, $[\text{O}_3]$ and $[\text{OX}]$ calculated from the parameters in Table 5.2 with annual mean concentrations observed at a number of sites. The calculated NO_x thresholds, corresponding to 20.9 ppb ($40 \mu\text{g m}^{-3}$) NO_2 , are also indicated.

5.3.5 Representative Expressions for Modelling Applications

The analysis presented above has been concerned with providing a description of the likely NO_x -dependence of annual mean $[\text{NO}_2]$ and $[\text{O}_3]$ at specific monitoring sites. Although this provides insights into the factors controlling ambient levels of these species, the substantial site-to-site variations make the resultant expressions impractical for modelling activities, unless a limited number of sites are specifically being considered.

On the basis of the comparatively large number of sites analysed, it is possible to define average expressions which have greater general applicability (although it is emphasised that such expressions

do not necessarily provide a good description of an individual site). The main feature of any simplification concerns the local oxidant contribution (A), because this parameter accounts for most of the site-to-site variation. Table 5.3 presents a series of average values derived from the data in Table 5.2. The various site classifications are considered for the Central, Inner and Outer London areas and elsewhere. This geographical breakdown was considered to allow comparison with expressions used in the UK national empirical NO₂ modelling activities (see below). The averages in Table 5.3 indicate that the local OX contribution in Central London tends to be higher than in the other areas. As discussed above, this may indicate that NO₂ generally accounts for a greater proportion of vehicular NO_x emissions in Central London, by virtue of a greater contribution of diesel vehicles and/or a greater level of congestion leading to lower average driving speeds. In the other London areas and elsewhere, there is no evidence for substantial differences in the local OX contribution, based on the averages and standard deviations indicated in Table 5.3. The average local OX contribution for all sites in Central London and all sites outside Central London are (0.140±0.019) and (0.093±0.043) ppb/ppb NO_x, respectively. The latter provides some retrospective justification for the generic value of 0.1 used to determine the regional OX levels by 'method 2' above (Table 5.1 and section 5.3.2).

Based on these averages, it is therefore possible to suggest the following generic expressions for the variation of annual mean [NO₂] with [NO_x] (in ppb),

$$\text{Central London:} \quad [NO_2] = (0.140[NO_x] + 34.7).f(NO_x) \quad (v)$$

$$\text{Outside Central London:} \quad [NO_2] = (0.093[NO_x] + B).f(NO_x) \quad (vi)$$

using either equation (i) or (ii) for $f(NO_x)$, to represent directly road-influenced and other sites, respectively. The appropriate values of B given in Table 5.1 can be applied in equation (vi).

Table 5.3 Average local OX contributions (A) for London Areas and Elsewhere, broken down by Site Classification.

	Average local OX contribution (fraction of NO _x)				
	Urban centre	Urban Background	Suburban	Urban Industrial	Roadside
Central London	(0.134±0.002)	(0.147±0.030)	-	-	-
Inner London	(0.084±0.052)	0.105 ^a	-	-	0.095 ^b
Outer London	-	(0.088±0.023)	(0.051±0.039)	-	-
Elsewhere	(0.084±0.048)	(0.104±0.077)	(0.100±0.058)	(0.076±0.008)	(0.086±0.017)

Notes: (a) based on North Kensington; (b) based on Marylebone Road

5.3.6 Analysis of More Recent Annual Mean Data (2002-2005)

More recent annual mean data from a series of urban centre sites (Belfast, Birmingham, Bristol, Cardiff, Leeds and Southampton) and urban background/suburban sites (London N. Kensington and London Bexley) have been analysed. As shown for the examples of Belfast Centre and Leeds Centre in Figure 5.6, the more recent data are generally well described by the semi-empirical NO₂ vs. NO_x expressions derived above from the data up to 2001. At all these sites, the observed NO_x concentrations in 2004 are below the calculated thresholds for exceedence of the annual mean limit value for NO₂ (Table 5.2). Accordingly, the observed annual mean NO₂ concentrations are either less than 20.9 ppb (40 µg m⁻³) or equal to it in the case of N. Kensington. The data for 2005 (based on an average up to the end of August) are also consistent with the observed trend.

Data from a number of more polluted London sites (Bloomsbury, Hillingdon, Wandsworth and Marylebone Road) have also been analysed, as shown in Figure 5.7. These are all sites which for which annual mean NO₂ concentrations are greater than 20.9 ppb (40 µg m⁻³) for all complete years on record. The ability of the semi-empirical NO₂ vs. NO_x expressions derived previously to describe the 2002-2005 data at these sites is variable. The annual mean for 2002 at the kerbside site at Marylebone Rd is also consistent with the previous expressions. In contrast data from 2003 and 2004 (and the first part of 2005) demonstrate a striking discontinuity, consistent with an abrupt increase in the local oxidant source (*i.e.*, primary NO₂) in 2003. The increase is indicative of a change in the primary NO₂ emissions fraction from *ca.* 10% of emitted NO_x to *ca.* 18% in 2003 and the excess oxidant is manifested almost entirely in the form of NO₂. As a result of this change, the projected NO_x annual mean concentration threshold corresponding to 20.9 ppb (40 µg m⁻³) NO₂ has decreased by

nearly 20%, from ca. 44 ppb to ca. 36 ppb. The 2004 and 2005 data provide some evidence that the primary NO_2 fraction has continued to increase, and is probably now over 20 %.

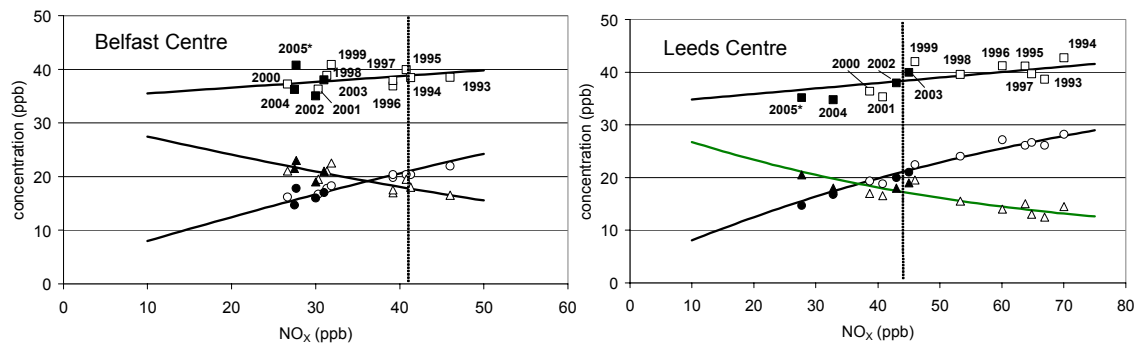


Figure 5.6 Annual Mean Concentration Data for NO_2 (circles) O_3 (triangles) and Oxidant (squares) at Selected Urban Centre Sites. Open Symbols are Data up to 2001: Filled symbols are Data for 2002-2005 (with 2005 based on Data up to the end of August). Lines are the Predicted Concentration Variations with $[\text{NO}_x]$, based on the Semi-empirical Method described above, derived from Data up to 2001. Vertical lines show the Predicted NO_x Concentration which corresponds to 20.9 ($40 \mu\text{g m}^{-3}$) NO_2 .

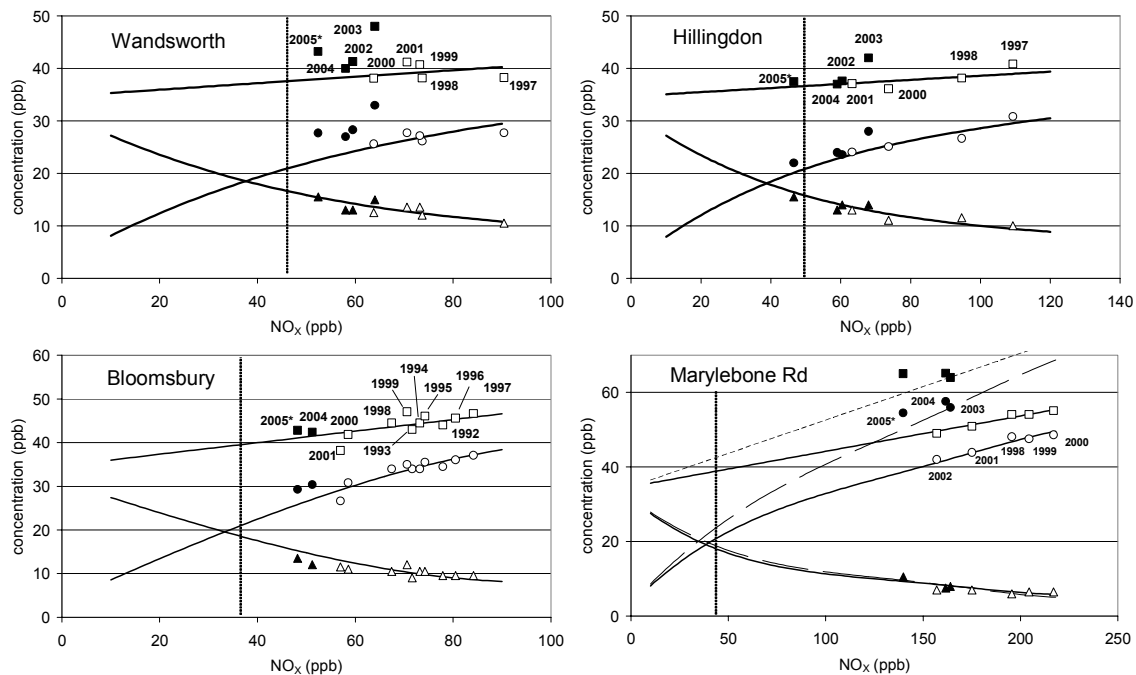


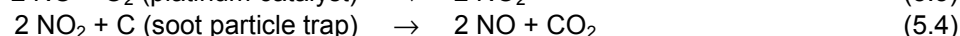
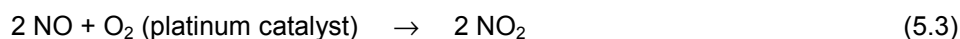
Figure 5.7 Annual Mean Concentration Data for NO_2 (circles) O_3 (triangles) and Oxidant (squares) at Selected London Sites. Open Symbols are Data up to 2001: Filled symbols are Data for 2002-2005 (with 2005 based on Data up to the end of August). Lines are the Predicted Concentration Variations with $[\text{NO}_x]$, based on the Semi-empirical Method described above, derived from Data up to 2001. Vertical lines show the Predicted NO_x Concentration which corresponds to 20.9 ($40 \mu\text{g m}^{-3}$) NO_2 . Broken lines for Marylebone Rd are the predicted concentration variations with $[\text{NO}_x]$, allowing for an increase in local OX to 18 %.

The data from Wandsworth exhibit increases in oxidant (manifested as NO_2) in all the recent years, 2002-2005, even though the annual mean NO_x concentrations are the lowest on record. This is also indicative of a local increase in the fraction of NO_x emitted as NO_2 , with an additional contribution (1-2 ppb) in 2003 probably resulting from an elevated regional oxidant background (as observed in ozone concentrations at a number of rural sites). Again, it is now likely that the estimated NO_x annual mean concentration threshold in Table 5.2 (46 ppb) is now optimistic.

The 2001 data from Bloomsbury show an abrupt decrease in oxidant (manifested as NO₂), which may have been influenced by the relocation of site within Russell Square at that time. However, the 2004 data demonstrate that the oxidant concentration has subsequently increased, with a notable shift in the fraction of oxidant present as NO₂, and this appears to be being maintained in 2005. Because of the unavailability of data for 2002 and 2003, and the now short time series for the site at its new location, it is currently difficult to interpret this variation, or to draw firm conclusions concerning future concentration trends.

The 2002 and 2004 data from Hillingdon are consistent with the semi-empirical NO₂ vs. NO_x expression derived previously, such that the threshold of 50 ppb (Table 5.2) probably remains a reasonable estimate. It is noted, however, that oxidant (and NO₂) in 2003 were significantly elevated, which was probably due (at least partially) to an elevated regional oxidant background.

The data thus provide evidence that the fraction of NO_x emitted as NO₂ has increased significantly from the road vehicle fleets at some locations, with Marylebone Rd providing a particularly dramatic example. At Marylebone Rd, a number of factors may contribute to the observed effect, although further work is required to establish the exact cause. For example, the introduction of central London congestion charging in early 2003 was accompanied by an increase in the number of buses on routes running on Marylebone Rd⁵, and possibly by greater congestion resulting from Marylebone Rd lying on the perimeter of the zone. Based on the diurnal dependence results presented below in Section 5.4.2, both effects would be expected to increase the local oxidant source. In addition to this, the buses have been fitted with oxidising particulate traps which operate by oxidising exhaust NO to NO₂ to promote the oxidation of soot:



Generation of excess NO₂ (*i.e.*, produced by reaction (3), but not destroyed by reaction (4)) therefore leads to an increase in primary NO₂ emissions.

5.4 ANALYSIS OF 1998 AND 1999 HOURLY MEAN DATA AT MARYLEBONE RD

5.4.1 Methodology

The present study considers hourly mean OX and NO_x data for 1998 and 1999, and focuses on weekdays (excluding national holidays). Data for photochemical episode days, when the regional background OX level is elevated, were also excluded from the analysis. These were defined as days between April and September when the daylight mean concentration of OX exceeded 50 ppb at the comparatively unpolluted urban background AURN site at London Teddington [the method also employed by Clapp and Jenkin, 2001]. The data were subdivided by hour of day and month of year, to allow investigation of diurnal and seasonal effects. Because of local one hour changes between Greenwich Mean Time (GMT) and British Summer Time (BST) on the final weekends in March and October, the small amount of data for relevant weekdays at the ends of these months were analysed as part of the April and November data, respectively. As a result of data unavailability in July 1998, and a significant number of photochemical episode days in July 1999, there are insufficient data for meaningful analysis, and July was therefore not considered.

5.4.2 Diurnal and Seasonal Dependence of Local and Regional OX Contributions

The NO_x-dependence of hourly mean OX concentrations was analysed on a month-by-month basis for data recorded in each hour of the day. Example plots of data for the hours ending at 06:00 and 12:00 in the months of March and October are shown in Figure 5.8. For each of these months, regression analysis indicates that the slope of the [OX] vs. [NO_x] plot (*i.e.*, the local OX contribution) is significantly greater for the 1200 hr data than for the 0600 hr data, although the intercept (*i.e.*, the regional OX contribution) in each case is comparable. The corresponding full diurnal variations of the local and regional OX contributions are presented for March and October in Figure 5.9, along with the data for August. Although

⁵ D. Carlaw, personal communication to Mike Jenkin.

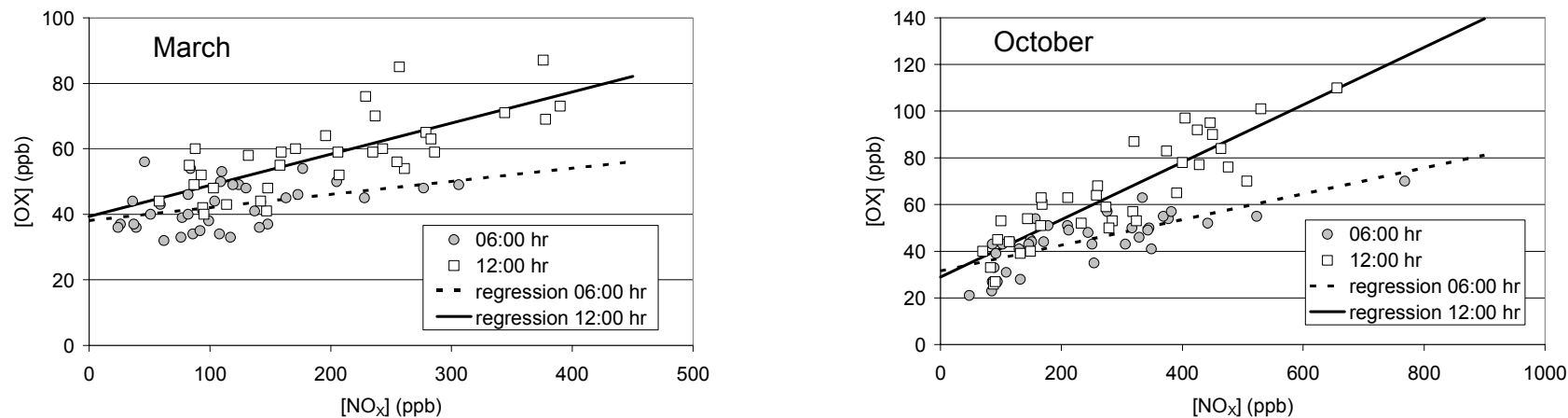


Figure 5.8 The Variation of Hourly Mean [OX] with [NO_x], using Data recorded for the Hours ending 0600 hr and 1200 hr on Weekdays in March and October. Regression Analysis of the March Data yields $[OX] = (0.040 \pm 0.017) \cdot [NO_x] + (38.1 \pm 2.2)$, for 0600 hr, and $[OX] = (0.095 \pm 0.015) \cdot [NO_x] + (39.3 \pm 3.3)$ for 1200 hr. Regression analysis of the October Data yields $[OX] = (0.055 \pm 0.008) \cdot [NO_x] + (31.6 \pm 2.2)$, for 0600 hr, and $[OX] = (0.123 \pm 0.011) \cdot [NO_x] + (28.9 \pm 3.7)$ for 1200 hr.

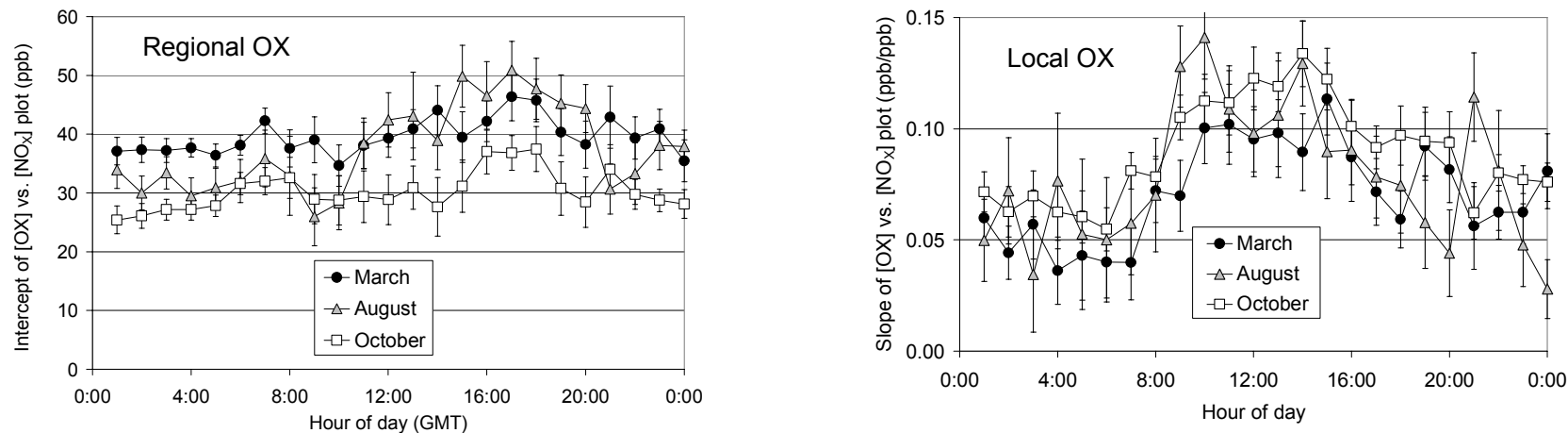


Figure 5.9 The Diurnal Variation of Regional and Local Oxidant Sources in Selected Months, based on Weekday Hourly Mean Data in 1998 and 1999.

there is some scatter (particularly for the August data), a strong diurnal dependence in the local OX contribution is apparent for all three months, with significantly greater values observed during the daytime. This pattern was clearly observable in the data for every month analysed.

In contrast, the regional contributions show only weak diurnal variations, with slightly higher values generally observed during the daytime in each month. It is also clear that the regional OX varies from month to month, with the October values being notably lower than those in March or August. Accordingly, Figure 5.10 shows the full seasonal dependence of the diurnally-averaged regional OX concentration, which is believed to provide an estimate of the regional O₃ background. Also shown in the figure are data presented by Scheel *et al.* (1997) for two sites in the EUROTRAC TOR (Tropospheric Ozone Research) network, namely Mace Head (Ireland) and Kollumerwaard (Netherlands). These sites are low altitude sites in northwest Europe, and therefore the most appropriate for comparison with the present data. The seasonally-varying concentrations derived from the present analysis are clearly in good agreement with those reported from the TOR network. The fact that the regional O₃ background concentrations can be retrieved from analysis of data from one of the most polluted UK sites provides strong support for employed method of data interpretation, *i.e.*, in terms of regional (NO_x-independent) and local (NO_x-dependent) OX contributions.

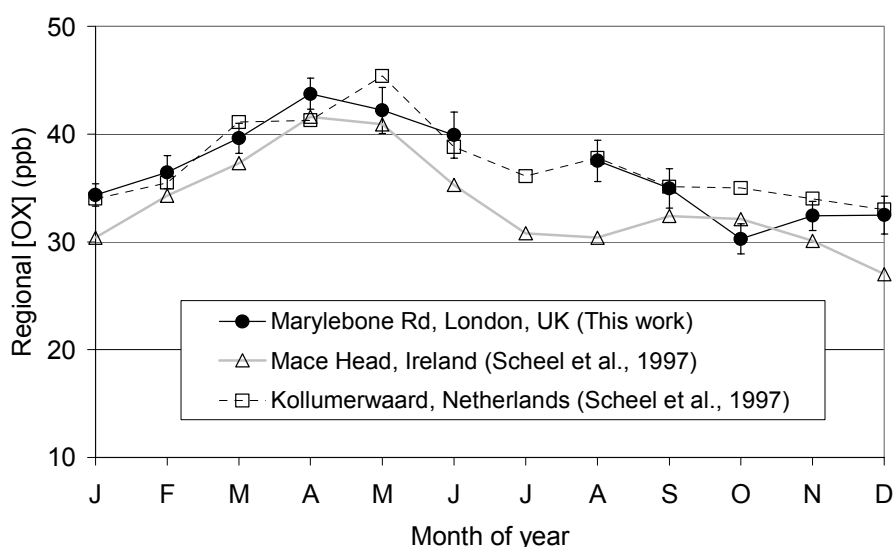


Figure 5.10 Seasonal Variation of Regional [OX] at Marylebone Rd. Also Shown are Data presented by Scheel *et al.* (1997) for Mace Head, Ireland (based on O₃ in Unpolluted Air Masses), and for Kollumerwaard, Netherlands (based on OX in Unpolluted Air Masses).

The diurnal dependences of the local OX contribution were averaged over the months of the year when GMT and BST operate. The corresponding results, shown in Figure 5.11, are denoted 'winter' and 'summer', respectively. A temporal shift between the winter and summer data is clearly apparent, giving a strong indication that the origin of the diurnal variation is related to road transport emissions, specifically an hour-to-hour variation in the fractional contribution of NO₂ to NO_x emissions. The form of the two profiles is very similar, although there is also some evidence that the winter night-time values are slightly higher than those observed in the summertime. The data were further averaged to give the annual mean diurnal profile in Figure 5.12. This was achieved by applying a shift of one hour to the data for the summer months prior to averaging. The resultant profile is therefore believed to represent the annual mean diurnal variation in the primary NO₂ emissions fraction, based on local hour.

5.4.3 Estimation of Primary NO₂ Emissions from Diesel and Petrol Vehicles

The diurnal variation in the primary NO₂ emissions fraction, inferred from the local OX data, is likely to originate from a variation in the vehicle fleet composition and/or driving conditions. Carslaw and Beevers [2004] have recently estimated hourly emissions of NO_x from diesel and petrol vehicles from July 1998 to December 2002, based on automatic and manual traffic flow statistics at Marylebone Rd, and vehicle, fuel and speed-dependent NO_x emission factors recommended by the UK National Atmospheric Emissions Inventory [Goodwin *et al.*, 2001]. On the basis of their data for 1999⁶, Figure 5.12 shows the annual mean

⁶ D. Carslaw, personal communication to Mike Jenkin.

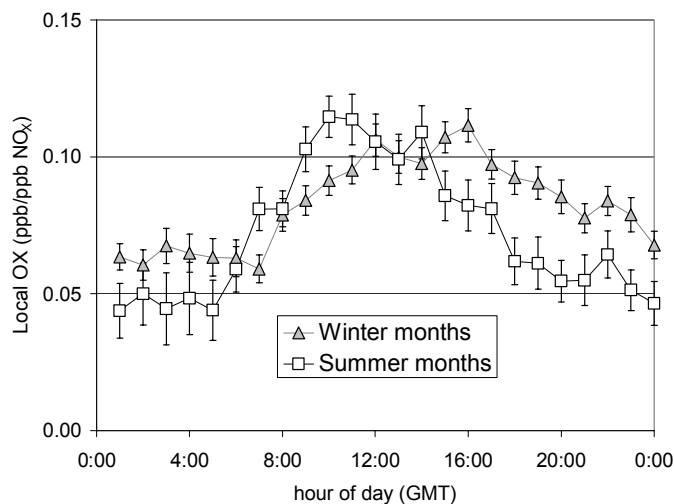


Figure 5.11 The Diurnal Variation of the Local OX, Averaged over Winter and Summer Months.

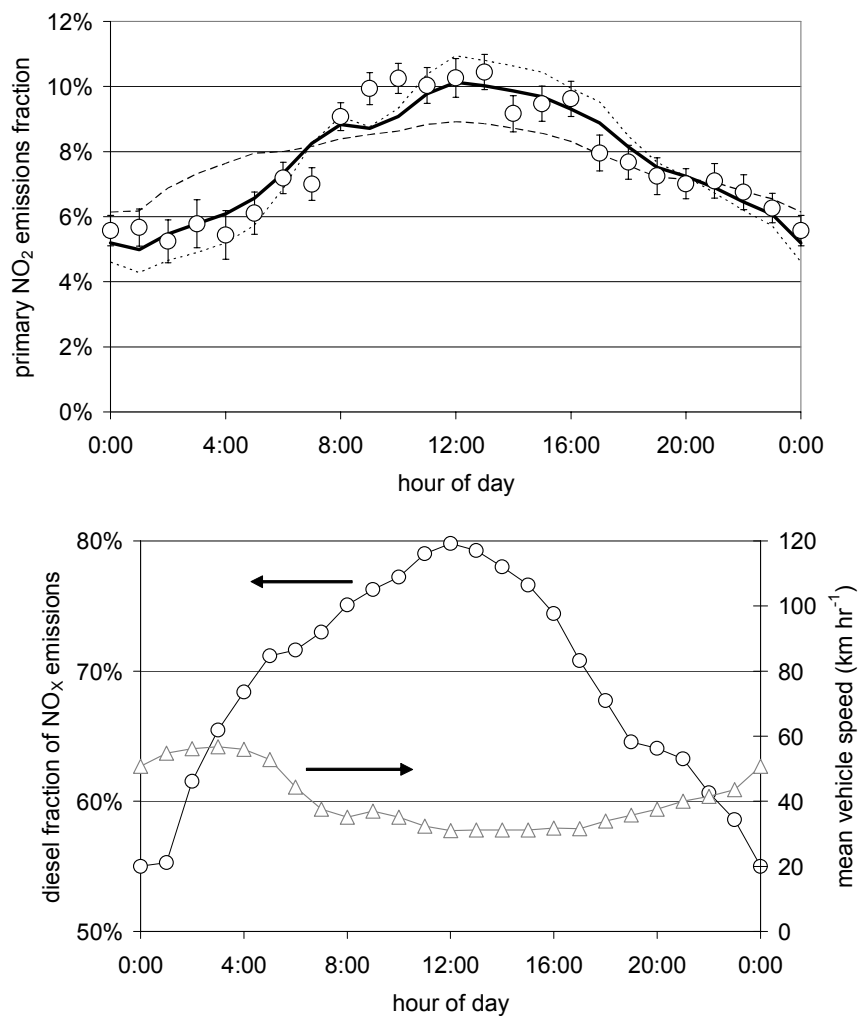


Figure 5.12 Upper Panel - Annual Mean Diurnal Variation of Primary NO₂ emissions, as a Volumetric Fraction of NO_x. Circles are values inferred from the Observed Local OX Contributions: Solid line is the Calculated Variation, based on Equation (i) for Diesel Vehicles. Broken and Dotted Lines are the Calculated Variation, using Speed Exponents of v^0 and v^{-1} , respectively. Lower panel: Annual Mean Diurnal Variation of Hourly Mean Vehicle Speed and Diesel Fractional Contribution to NO_x Emissions, based on Vehicle Flow Data and Emissions Estimates for 1999 reported by Carslaw and Beevers (2004).

diurnal dependence of the NO_x emissions fraction which derives from diesel vehicles. The diesel contribution varies over the approximate range 55-80%, maximizing in the middle of the day, with the balance being due to petrol vehicles. Also shown is the diurnal variation of mean vehicle speed, estimated from the automatic traffic flow data. This shows that the mean speed falls from almost 60 km hr^{-1} overnight to around 30 km hr^{-1} during the middle part of the day.

These data give a clear indication that diesel emissions must make an important contribution to the observed primary NO_2 , as inferred from the local OX measurements in the present study. The emissions and vehicle speed data were used to calculate diurnal variations in the primary NO_2 emissions fraction, as presented in Figure 5.12 (upper panel). By optimizing the calculated profile to the observed primary NO_2 profile (using residual least squares methodology), it was possible to estimate primary NO_2 emissions fractions for diesel and petrol vehicles. In order to recreate the shape of the diurnal profile, however, it was also necessary to take account of the vehicle speed such that the primary NO_2 fraction decreases at higher speeds, using an assumed function. The best fit to the data was obtained with the assumption that primary NO_2 derives wholly from diesel vehicle emissions, with the NO_2 emissions, as a volumetric fraction of NO_x emissions, being well described by the following equation:

$$\text{Diesel primary NO}_2 \text{ fraction} = 0.996 v^{-0.6} \quad (\text{i})$$

where v is the mean vehicle speed in km hr^{-1} . This indicates that NO_2 accounts for 8.5% of NO_x emissions (by volume) from diesel vehicles travelling at a mean speed of 60 km hr^{-1} , increasing to 12.9% at 30 km hr^{-1} . Although this is a comparatively weak dependence, the profile is sensitive to quite small variations in the vehicle speed exponent, as illustrated in Figure 5.12. Because the representation of the speed dependence employed here has no fundamental basis (and is clearly invalid for stationary traffic), this equation can only be regarded as valid over the mean speed range of the data used to derive it, i.e., $30\text{-}60 \text{ km hr}^{-1}$. Allowing for the diurnal variation in the absolute magnitude of the NO_x emissions, the present analysis leads to an integrated diurnal primary NO_2 emission of $(11.8 \pm 1.2) \%$ of NO_x from diesel-fuelled vehicles at Marylebone Rd, where the uncertainty reflects only the scatter and error in the observed local OX contribution data.

Although the data were best described with the assumption that petrol vehicles emit no primary NO_2 , it was possible to get reasonable fits to the observations with primary NO_2 emissions up to about 3% of NO_x , and this upper limit value is therefore suggested on the basis of the present data. At this upper limit value for petrol vehicles, the diesel primary NO_2 fractions optimized simultaneously were about 1% lower than those quoted above.

Table 5.4 Summary of Reported Contributions of NO_2 to NO_x Emissions.

Study	NO_x Emission Source	NO_2/NO_x (Volume %)	Comment
Jimenez <i>et al.</i> , 2000	Diesel truck	5.6 – 10.9	a
Kurtenbach <i>et al.</i> , 2001	Vehicle mix	5.0	b,c
	MAN diesel truck	11.0	b,d
	Petrol car	< 0.2	b,d
	Diesel car	5.9	b,d
Carslaw and Beevers, 2004	Diesel vehicles	(12.7 ± 0.1)	e
	Petrol vehicles	(0.6 ± 0.2)	e
This work	Diesel vehicles	$99.6 v^{-0.6}$	f,g
	Petrol vehicles	(11.8 ± 1.2) < 3	f,h f

a: Operating at ca. 30 km hr^{-1} during mild acceleration. Measurements by TILDAS; b: Kiesbergtunnel, Wuppertal, Germany. Measurements by DOAS; c: traffic mix with $\leq 6\%$ heavy duty trucks, 6% commercial vans, 12.3% diesel cars, 74.7% petrol cars; d: single vehicle experiment, $0\text{-}40 \text{ km hr}^{-1}$; e: Marylebone Rd, London, UK. Derived from differential measurements of [OX] compared to local background site and detailed traffic statistics over period 1998-2002; f: Marylebone Rd., London, UK. Derived from [OX] vs. [NO_x] dependence using 1998-1999 weekday data, and detailed traffic statistics for 1999; g: for $30 < v/\text{km hr}^{-1} < 60$; h: integrated diurnal contribution.

The present results can be compared with a number of other published estimates of primary NO_2 from diesel and petrol vehicles, as summarized in Table 5.4. These studies all indicate that diesel vehicles have a greater propensity to emit NO_x in the form of NO_2 , and reasonably consistent fractional contributions have been reported. In particular, the present results are fully consistent with the diesel and petrol primary emissions fractions reported for Marylebone Rd in the recent study of Carslaw and Beevers

[2004]. In addition to the studies summarized in Table 5.4, recent work at the UK Transport Research Laboratory (TRL) has evaluated NO_2 emissions from a small sample of vehicles over a series of legislative and real-world driving cycles, on a chassis dynamometer [Latham *et al.*, 2001; AQEG, 2004]. The results of that study also suggest that diesel engines emit a higher proportion of NO_x as NO_2 than petrol vehicles, and that this proportion tends to increase at lower vehicle speeds.

As a result of the strong diurnal variation in the local OX contribution, it is clear that the level of NO_x required for OX in the form of NO_2 to exceed the hourly mean limit value of 104.5 ppb is likely to vary dramatically with time of day, under typical conditions. In addition to this, the seasonal dependence of the regional background OX concentration will have a less dramatic, but nonetheless important, influence. Figure 5.13 shows estimated hourly mean NO_x thresholds which correspond to 104.5 ppb OX as a function of season and hour of day, based on the results of the present study. At the NO_x concentrations concerned (\geq ca. 600 ppb), OX is almost exclusively in the form of NO_2 such that the displayed thresholds effectively correspond to the level of NO_x required for exceedence of the hourly mean NO_2 limit value. This illustration demonstrates that the lowest NO_x threshold concentrations are likely to occur in the middle of day, with the lowest calculated values of ca. 600 ppb in the spring. The highest values are calculated to occur in the early hours, maximising at over 1400 ppb in October-December. It should be noted, however, that these illustrative figures are based on average driving conditions for the given hour and month. The actual conditions clearly show some variation about the mean, as demonstrated by the scatter in Figure 5.8.

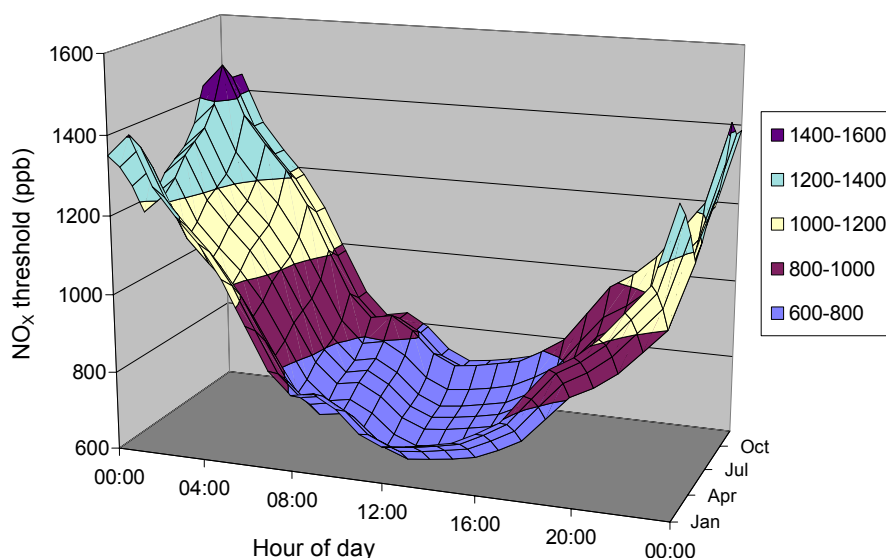


Figure 5.13 Estimated Hourly Mean NO_x Thresholds which correspond to 104.5 ppb OX, based on the Diurnal Local OX contributions in Figure 5.12, and the Seasonal Regional OX concentrations in Figure 5.10 (with the July Value assumed to be the Average of the June and August Values). At these NO_x Concentrations, the Thresholds are an approximation to those required for Exceedence of the Hourly Mean NO_2 Limit Value (104.5 ppb, $200 \mu\text{g m}^{-3}$) to occur (see text).

In addition to this, the analysis presented here specifically does not consider summertime photochemical pollution episode conditions. Under these circumstances, elevated regional OX concentrations would lead to an additional lowering of the NO_x levels required for the hourly mean NO_2 limit value to be exceeded.

5.4.4 Conclusions

The present analysis demonstrates that the ambient concentration of OX at Marylebone Rd is sensitive to a number of factors, such as primary NO_2 emissions and regional background O_3 concentrations, and that variation in the magnitudes of these factors leads to substantial diurnal and seasonal differences in the level of NO_x required for the hourly mean NO_2 limit value of 104.5 ppb to be exceeded. The factors which cause these differences at an individual site are also likely to contribute to the site-to-site variations in annual mean NO_x thresholds, presented above in Section 5.3.

Table 5.5 Number of Exceedences of NO₂ Hourly Mean Limit Value at London AURN sites in Each Year since 1998 (*2005 data up to 21 November).

	1998	1999	2000	2001	2002	2003	2004	2005*
Brentford Roadside							8	2
Camden Kerbside	6	7				2	6	6
Haringey Roadside		1						
Hounslow Roadside	6							
London A3 Roadside		6			6	16	8	17
London Bexley							1	
London Bloomsbury		9						
London Brent						3		
London Bridge Place	1							
London Bromley								1
London Cromwell Road 2	4	12	13	2		6	3	1
London Hackney	3	9	1			5	11	2
London Hillingdon	1							
London Lewisham						1	1	1
London Marylebone Road	71	64	104	60	2	471	542	595
London N. Kensington	2		3	4				
London Wandsworth						8	2	3
London Westminster							3	
Southwark Roadside	3	4				2		
Sutton Roadside				3				
Tower Hamlets Roadside	10	11	3	6	2	6	3	
West London		1					1	1
London total	107	124	124	75	10	520	589	629

The apparent large increase in primary NO₂ since 2003 (discussed above in Section 5.3.6 for annual mean data), would of course influence the results of the analysis presented above. Although the qualitative form of the diurnal and seasonal variations might be expected to remain similar, an analysis of more recent data would be expected to reveal generally higher local OX slopes, with an even greater derived primary NO₂ emissions fraction from diesel vehicles. Accordingly, the analysis would also be expected to predict a general lowering of NO_x concentrations required for the hourly mean NO₂ limit value to be exceeded. Support for this conclusion is apparent from the record of exceedences of the NO₂ hourly mean limit value at London AURN sites including Marylebone Rd. Table 5.5 shows the number of hours exceedence in each year since 1998 at sites where at least one exceedence has been observed. Although there is inevitably some year-to-year variation, a general decrease is apparent in the early part of the time series (1998-2002) consistent with the progressive reduction in NO_x emissions over this period. However, an increase in exceedences is apparent at a number of sites since 2003, most notably Marylebone Rd, which can be explained by an abrupt increase in the primary NO₂ emissions fraction in 2003. The data for 2003-2005 further suggest that the situation is progressively worsening at Marylebone Rd, in agreement to the conclusion derived from the annual mean analysis in Section 5.3.6. It is noted, however, that (to date) no London AURN site other than Marylebone Rd has failed the associated objective of ≤ 18 hours exceedence in a given year during this period, although it is quite likely that the A3 roadside site will also fail in 2005.

5.5 OSRM MODELLING OF URBAN OZONE, NITRIC OXIDE AND NITROGEN DIOXIDE

In Section 4.4.3, modifications made to the OSRM and the surface conversion algorithm were described. In this section, the output from latest version of the OSRM and Surface Conversion Algorithm are compared with observations at urban monitoring sites in the London, Kent and Hertfordshire Air Quality Monitoring Networks [Derwent, 2005a]. Figure 4.3 shows the modelled and measured annual mean concentrations of O₃, NO, NO₂ and Oxidant (= [O₃] + [NO₂]) at background sites

in London and the South East in 2002 as a function of the modelled or measured NO_x concentration. The comparison shows that the chemistry implemented in the surface conversion algorithm gives NO-NO₂-NO_x-O₃-Ox relationships, which are consistent with those derived from observations, as described in previous sections.

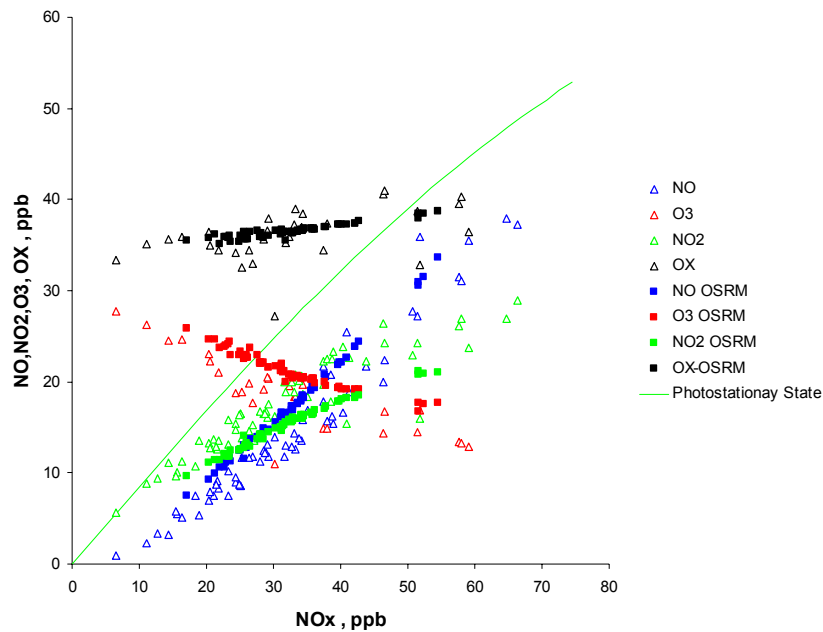


Figure 5.14 Modelled and Measured Concentrations of Ozone, Nitric Oxide, Nitrogen Dioxide and Oxidant (= [O₃] + [NO₂]) at London Sites in 2002 as a Function of the Modelled or Measured NO_x Concentration.

Figure 5.15 presents scatter plots of the modelled against the measured concentrations of O₃, NO, NO₂, NO_x and Oxidant for these London and South East sites (Non-Roadside). The figure shows the good agreement between the modelled and measured concentrations, confirming its suitability for urban ozone modelling.

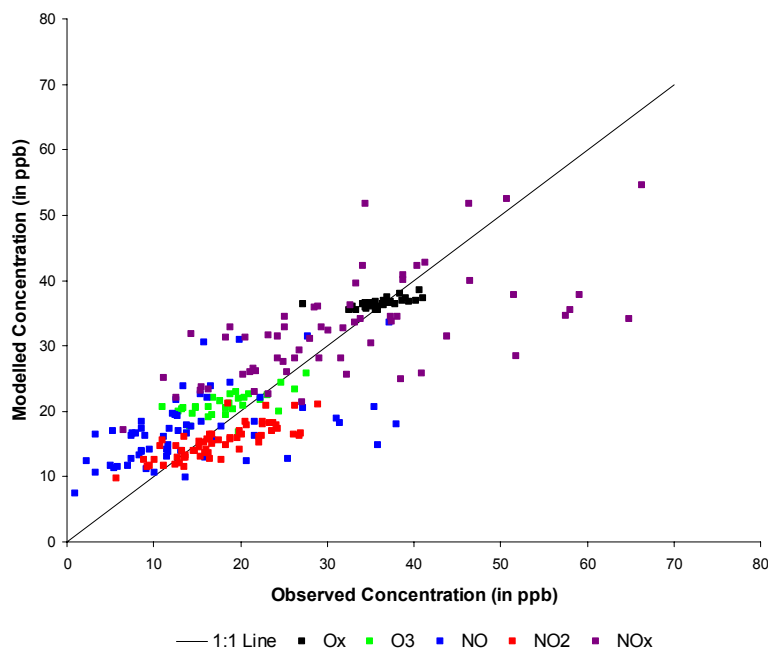


Figure 5.15 Scatter Plot of Modelled vs. Measured Concentrations of Ozone, Nitric Oxide, Nitrogen Dioxide, Oxidant and Oxides of Nitrogen for South East non-Roadside Sites in 2002.

6 Policy Development and Scenario Analysis (Objective 3a)

6.1 INTRODUCTION

In this section of the report, the available modelling tools – the Ozone Source-receptor Model (OSRM) and UK Photochemical Trajectory Model (UK PTM) – have been used to assess a number of policy options relating to ozone:

- (1) **Petrol Volatility:** The policy question concerns the likely benefit from a 7 thousand tonne reduction in VOC emissions from petrol evaporation between 1st June and 31st August [Modelled using UK PTM, OSRM not available];
- (2) **Petrol vs. Diesel:** There is strong pressure for policymakers to increase dramatically the penetration of new diesel vehicle technologies into the passenger car and LGV fleets to meet future targets for greenhouse gas emissions. Since the EURO IV emission standards imply higher NO_x emissions per kilometre travelled from diesel-engined cars (0.40 g/km) as opposed to petrol-engined cars (0.12 g/km), there may well be an ozone dis-benefit to this policy from the implied increased NO_x emissions [Modelled using UK PTM];
- (3) **Regulatory Impact Assessment of Directive on Decorative Paints:** The European Commission proposed a Directive in 2002 to reduce the VOC content of decorative paints, varnishes and vehicle refinishing products. There is a requirement to calculate the benefits to the UK of reductions in VOCs arising from within UK, and in UK + rest of Europe. The Commission have calculated potential emission reductions that would arise from the proposed controls in 2010 [Modelled using OSRM, UK PTM];
- (4) **Proposed NO_x Emission Standards for Vehicles (EURO V Standards):** The European Commission are expected to propose new emission standards for vehicles in 2004. The Department and the Department for Transport wish for information on the air quality implications of various scenarios to inform the UK position. Although the main focus to date has been on NO₂ and PM exposure, there is a need to assess the effects on ozone concentrations and hence human exposure [Modelled using OSRM, UK PTM];
- (5) **Regulatory Impact Assessment of Directive on Petrol Vapour Recovery:** OSRM modelling calculations have been undertaken as part of the regulatory impact assessment on petrol vapour recovery (PVR) and possible derogations [Modelled using OSRM];
- (6) **Post-Gothenburg Scenarios:** Assuming full compliance with the UN ECE Gothenburg Protocol and the EU National Emissions Ceilings Directive, the Department is interested the effectiveness of different controls on NO_x and/or VOC emissions to improve ozone air quality after 2010. Four model runs were undertaken with across-the-board reductions in the emissions of NO_x and/or VOC of 30% [Modelled using OSRM, UK PTM];
- (7) **Review of the Air Quality Strategy:** The OSRM was used to investigate the impacts on ozone of a number of measures being considered as part of the Review of the Air Quality Strategy. Model runs were undertaken to 41 UK receptors sites in urban and rural locations [Modelled using OSRM].

In the UK PTM model runs, a single linear trajectory has been used, which has been selected to represent the air flow during an idealised photochemical episode (*i.e.*, anticyclonic meteorological situation of easterly winds, leading to a broad westerly air flow carrying photochemically-aged polluted air masses out of Europe towards the British Isles). This trajectory does not represent the conditions prevailing during a particular photochemical episode but represents a potential worst-case situation. The trajectory path was selected from the review of meteorological analyses prepared for the PHOXA study covering the period 1980-1985 [Bultjes, 1987; Pankrath, 1989].

In an OSRM model run, a calendar year is simulated and a wider range of realistic air mass trajectories is sampled, including those from other wind directions. These other trajectories may have little or no photochemical ozone production, especially if the trajectory has mainly passed over low

emission areas (e.g., the sea). One can envisage that there will be a chemical titration of the ozone in such air masses when these air masses pass over NO_x emission sources. It is therefore likely that the two models will give different response to NO_x and/or VOC emission controls (particularly NO_x control). NO_x and/or VOC emission control are both effective in reducing episodic ozone concentrations. However, while VOC emission control does improve ozone air quality in the OSRM, the response to NO_x emission control is more complex, but generally causes a worsening in ozone air quality.

6.2 UK PTM MODELLING

6.2.1 Petrol Volatility:

The UK PTM was used to assess the likely benefit that would arise from a 7 thousand tonne reduction in VOC emissions from petrol evaporation between 1st June and 31st August. The UK PTM for 1999 conditions has a n-butane emission of 138.642 thousand tonnes per year. This is the major component of evaporative emissions from petrol. The n-butane emissions were decreased by 7 thousand tonnes per year to 131.642 thousand tonnes per year over the UK and the UK PTM was rerun. The peak ozone concentrations at the arrival point in Wales were as follows:

base case model run	85.52 ppb
base case -7 kilotonnes/year	85.48 ppb
difference	0.039 ppb

which is small and within the noise of the UK PTM.

6.2.2 Petrol vs. Diesel

There is strong pressure for policymakers to act to increase dramatically the penetration of new diesel vehicle technologies into the passenger car and LGV fleets to meet future targets for greenhouse gas emissions. There may well be an ozone dis-benefit to this policy from the implied increased NO_x emissions and increased ozone production in north-west Europe under episode conditions. The UK Photochemical Trajectory Model UK PTM has been employed to assess the magnitude of this likely dis-benefit.

A set of emission scenarios has been developed to examine the impacts on episodic peak ozone concentrations of the increasing penetration of diesel- and petrol-engined vehicle technologies. The base case scenario has been taken to be the year 2010 with Europe meeting the UN ECE Gothenburg Protocol and the EU National Emissions Ceilings Directive. A five-day air parcel trajectory has been followed from Austria through to Wales using the UK PTM and the Master Chemical Mechanism v3.0.

The impact of increasing penetration of new diesel vehicle technologies has been simulated by replacing the EURO IV petrol-engined fleet by diesel vehicles meeting the EURO IV standard, then the EURO III petrol-engined fleet and so on until all EURO I – IV petrol-engined vehicles have been replaced by EURO IV diesel-engined vehicles. The impact of increasing penetration of new petrol vehicle technologies has been simulated by replacing the EURO IV diesel-engined fleet by petrol-engined vehicles meeting the EURO IV standard and so on until all EURO I – IV diesel vehicles have been replaced by EURO IV petrol vehicles. The changes have been applied to both passenger cars and LGVs. The NO_x emissions from road transport corresponding to each scenario are shown in Table 6.1. NO_x emissions from source categories other than road transport were held constant and no changes were made to the emissions from HGVs, buses and motorcycles.

Table 6.1 shows how with increasing penetration of new diesel-vehicle technologies, UK emissions of NO_x from cars and LGVs would increase by close to a factor of two, total road transport NO_x emissions would increase by 45% and total NO_x emissions from all sources by 14%. Whereas with increasing penetration of new petrol-vehicle technologies, UK NO_x emissions from cars and LGVs decreased by close to a factor of two, total road transport emissions would decrease by 26% and total NO_x emissions from all sources by 8%. These same fractional increases in NO_x emissions were implemented across Europe in each scenario.

The impact of increasing the penetration of new diesel-vehicle technologies is to produce an increase in photochemical ozone production across Europe, resulting in a 0.7 ppb increase in the ozone

concentration at the arrival point in Wales, see Table 6.1. The corresponding impact from increased penetration of new petrol-vehicle technologies is a decrease in ozone of about 0.7 ppb. These differences at the 1% level are significant in UK PTM model terms but may not be of policy significance.

Table 6.1 UK Emissions of NO_x from Cars and LGVs and Ozone Concentrations in the UK PTM found at the end of a 5-day trajectory in 2010 for Scenarios of increasing Penetration of Diesel- and Petrol-vehicle Technologies, evaluating only the Changes due to NO_x Emissions.

Scenario	NO _x Emissions from Cars and LGVs ktonnes per annum	Ozone concentration, ppb
Increasing diesel-vehicle technology penetration		
Base case 2010	227	74.19
Replace EURO IV petrol vehicles	411	74.89
Replace EURO III+IV petrol	406	74.89
Replace EURO II+III+IV petrol	403	74.85
Replace EURO I+II+III+IV petrol	398	74.85
Increasing petrol-vehicle technology penetration		
Base case 2010	227	74.19
Replace EURO IV diesel vehicles	203	74.15
Replace EURO III+IV diesel	168	73.80
Replace EURO II+III+IV diesel	129	73.50
Replace EURO I+II+III+IV diesel	119	73.44

Increasing penetration of diesel-vehicle, or petrol-vehicle technologies for that matter, will have ramifications for the emissions of other pollutants, particularly of suspended particulate matter, not considered here and of organic compounds, which are of importance in photochemical ozone formation. Increasing the penetration of diesel-vehicle technologies will decrease the vehicle kilometres travelled by the petrol-engined passenger car fleet, leading to decreased evaporative emissions of organic compounds and to decreased emissions from the distribution of motor spirit. Assuming that these emissions fall in line with the decreasing vehicle kilometres travelled by petrol-engined vehicles, then the emissions of organic compounds in each of the scenarios can be estimated, see Table 6.2. On this basis, total UK emissions of organic compounds may well decrease by 10% with increasing penetration of diesel-vehicle technologies or increase by 10% with increasing penetration of petrol-vehicle technologies. Again, all these fractional changes in organic compound emissions have been implemented across Europe.

Table 6.2 UK Emissions of Volatile Organic Compounds from Cars and LGVs and Ozone Concentrations in the UK PTM found at the end of a 5-day trajectory in 2010 for Scenarios of increasing Penetration of Diesel- and Petrol-vehicle Technologies, evaluating both the NO_x and VOC Emission Changes.

Scenario	VOC Emissions from Cars and LGVs ktonnes per annum	Ozone concentration, ppb
Increasing diesel-vehicle technology penetration		
Base case 2010	110	74.19
Replace EURO IV petrol vehicles	25	72.19
Replace EURO III+IV petrol	17	71.90
Replace EURO II+III+IV petrol	2	71.44
Replace EURO I+II+III+IV petrol	0	71.37
Increasing petrol-vehicle technology penetration		
Base case 2010	110	74.19
Replace EURO IV diesel vehicles	117	74.22
Replace EURO III+IV diesel	121	74.03
Replace EURO II+III+IV diesel	121	73.82
Replace EURO I+II+III+IV diesel	121	73.70

Table 6.2 indicates a clear positive benefit in terms of decreasing photochemical ozone formation from increasing the penetration of new diesel-vehicle technologies. This benefit in episodic peak ozone formation may be up to 2.8 ppb from new diesel-vehicle technologies and may be of significant policy significance. The reduction in organic compound emissions has produced such a large positive benefit that it has overcome the ozone dis-benefit from the increased NO_x emissions. The

corresponding improvement from increasing the penetration of new petrol-vehicle technologies is much smaller at 0.5 ppb, which is significant in UK PTM terms but may be of little policy significance.

In summary, evaluation of the ozone benefits or dis-benefits of increasing the penetration of new diesel-vehicle technologies depends markedly on whether just the NO_x emission changes are considered or whether wider issues such organic emissions from petrol-engined vehicles are also taken into account. On the narrow basis of NO_x emission changes, increasing the penetration of diesel cars would lead to a small deterioration in ozone air quality relative to the base case. Taking into account the decreased evaporative emissions and decreased emissions from petrol distribution, increasing the penetration of diesel cars and LGVs would produce a substantial improvement in ozone air quality in the future. All of this improvement in ozone air quality has come from the petrol-engined vehicle fleet whereas all of the deterioration has come from the diesel-engined vehicle fleet. The ozone benefits could be achieved by other means such reduction of the vapour pressure of petrol or increased vapour recovery at petrol stations rather than through the increased penetration of diesel vehicle technologies.

6.2.3 Decorative Paints

The European Commission has proposed a Directive to reduce the VOC content of decorative paints, varnishes and vehicle refinishing products [EC, 2002a]. There is a requirement to calculate the benefits to the UK of reductions in VOCs arising from within UK, and in UK + rest of Europe. The Commission have calculated potential emission reductions that would arise from the proposed controls in 2010 for member states, as shown in Table 6.3. For the UK, ENTEC calculate the potential UK emission cuts arising from the proposed controls, and these seem lower than the Commission's estimates. ENTEC figures for UK are 9 thousand tonnes per year as against 30 thousand tonnes per year calculated by the European Commission.

Table 6.3 NECD VOC Emission Limits and Proposed Reduction in VOC Emissions from Paints and Varnishes.

Member State	NECD VOC Emission Limit (ktonne per year)	Proposed VOC Reduction (ktonne per year)		
		Solvent-based	Water-based	Total
Austria	159.0	3.0	2.2	5.2
Belgium	139.0	4.1	3.1	7.2
Denmark	85.0	2.7	2.0	4.7
Finland	130.0	1.7	1.3	3.0
France	1050.0	13.1	36.5	49.6
Germany	995.0	35.6	26.5	62.1
Greece	261.0	5.4	4.0	9.4
Ireland	55.0	2.3	1.7	4.0
Italy	1159.0	16.3	12.1	28.4
Luxembourg	9.0	0.2	0.1	0.3
Netherlands	185.0	8.3	6.2	14.5
Portugal	180.0	5.4	4.0	9.4
Spain	662.0	25.9	19.3	45.2
Sweden	241.0	3.2	2.4	5.6
UK	1200.0	17.2	12.8	30.0
European Community	6510.0	144.4	134.2	278.6

The NAEI speciated inventory for 1998 contains the following VOC emissions from paints:

Sector	Emission (ktonne per annum)
coating manufacture – paints	5.784
decorative paint - retail decorative	20.040
- trade decorative	20.040
industrial coatings – automotive	13.444
- coil coatings	0.342
- commercial vehicles	8.400
- marine	4.200
- metal and plastic	34.118
- metal packaging	7.809
- vehicle refinishing	7.560
- wood coating	16.100
Total Paints	138.237

A VOC reduction of 40.48 ktonnes per year was used in the UK PTM for 1999 (out of 1,600 ktonnes per year) to simulate the complete phase-out of decorative paint, both trade and retail. The same reduction was applied across-the-board over all Europe.

At the end of the 5-day trajectory:	O ₃ base case	85.5 ppb
	with VOC reduction	84.8 ppb

and the difference is 0.686 ppb. This is quite a noticeable reduction and well beyond the noise in the model. It should be noted that this is the ozone reduction due to the reduction in mass emissions. No account was taken of the changing reactivity of the stationary source emissions.

6.2.4 Post Gothenburg Emission Control

The UK PTM was set up with the standard trajectory case that starts in Austria and finishes in Wales. This case is meant to represent the worst-case peak episodic conditions of long-range transport into the British Isles. When running using 1999 precursor emissions for the UK and the rest of Europe, the air parcel arrived in Wales with a peak ozone concentration of 85.5 ppb.

The emission conditions were then changed to represent the full implementation of the UN ECE Gothenburg Protocol and the EU National Emissions Ceilings Directive in the year 2010. The peak ozone concentration dropped to 74.2 ppb and these results are shown as 'GP' in Figure 6.1. The reduction in ozone exposures is clearly dramatic following the control measures expected through to the year 2010.

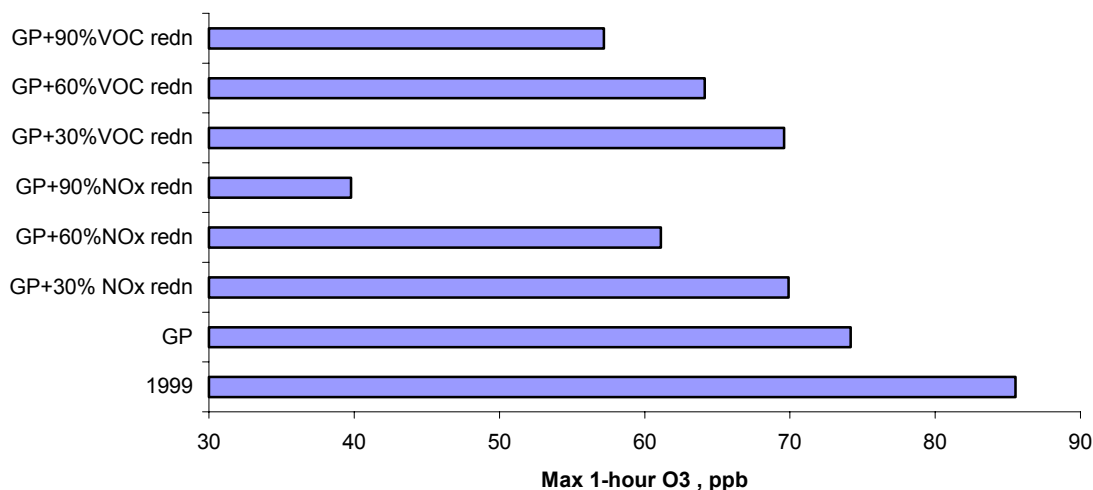


Figure 6.1 The Impact of Various Emission Scenarios on the Peak Ozone Concentrations predicted with the UK PTM for an Arrival Point in Wales.

In a series of model experiments, the impact of further emission controls beyond those envisaged in the UN ECE Gothenburg Protocol and the EU National Emissions Ceilings Directive were examined. Three further stages of emission reductions were considered taking emissions below the 2010 levels by 30%, 60% and 90%. In all cases, these additional percentage reductions were applied across-the-board on all source categories and on all countries. When these further stages were applied to NO_x emissions, peak ozone fell from 74.2 ppb in 2010 to 69.9, 61.1 and 39.8 ppb, respectively. These results are presented in Figure 6.1 as 'GP+30%NO_x redn' and so on. When applied to VOC emissions, peak ozone fell to 69.6, 64.1 and 57.2 ppb, respectively, shown as 'GP+30%VOC redn' in Figure 6.1.

Looking at the 30% reductions beyond the Gothenburg Protocol, the UK PTM is indicating that the arrival point in Wales is still VOC-limited in 2010, because the ozone benefit (74.2 down to 69.6 ppb) from reducing VOC emissions is larger than the ozone benefit (74.2 down to 69.9 ppb) from reducing NO_x emissions. However, looking at the 60% and 90% reductions, the situation reverses and the ozone benefits from NO_x reductions look substantially greater than those from VOC reductions.

6.3 OSRM MODELLING

As described in Section 4, a number of improvements were made to the OSRM during the course of the contract and different versions (version 1.8a without Surface Conversion and version 2.2 with Surface Conversion) were introduced and used for this objective. Details of the OSRM runs, excluding the large number undertaken for the Review of the Air Quality Strategy, are given in Table 6.4. The model runs for the Review of the Air Quality Strategy are described in Section 6.4.

6.3.1 Using OSRM Version 1.8a

The OSRM (version 1.8a without Surface Conversion) was used to investigate the policy measures or scenario analyses listed below. Table 6.4 provides details about the runs (meteorology, emission inventories):

- **Current Ozone:** Three OSRM model runs were undertaken (see Table 6.4) to simulate the current ozone climatology (1998, 1999 and 2001). The model runs used meteorology and emission inventories for the relevant year.
- **Regulatory Impact Assessment of Directive on Decorative Paints:** Work undertaken at netcen for the Regulatory Impact Assessment (RIA) concluded that the effect of the proposed legislation on the VOC content of paints and the emissions from the car-refinishing sector will lead to a further reduction of approximately 2 ktonnes per annum over the current NAEI base case projection for 2010. These are significantly smaller than those proposed by the European Commission [EC, 2002a], as much of the reduction identified by the Commission is now included in the base case projection.

Five OSRM model runs were undertaken (see Table 6.4). The outputs were provided to colleagues at netcen to undertake the Regulatory Impact Assessment. The effects of the emissions reductions on human health (evaluated using the annual mean ozone concentration) and on crops (evaluated using AOT40 for crops) were determined.

- **Proposed EURO V Road Transport Emission Standards:** The European Commission is expected to propose new emission standards for vehicles in 2004. The Department and the Department for Transport wish for information on the air quality implications of various scenarios to inform the UK position. Although the main focus to date has been on NO₂ and PM exposure, there is a need to assess the effects on ozone concentrations and hence human exposure.

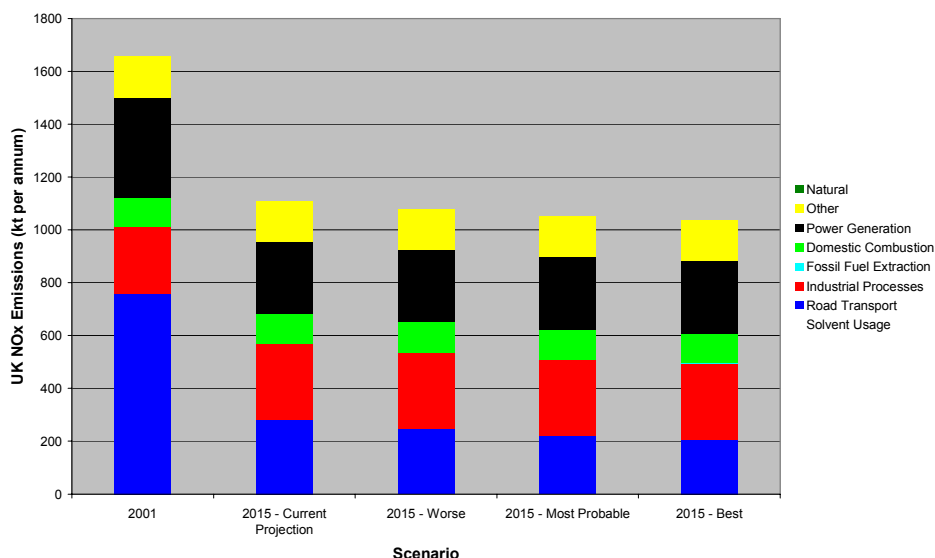


Figure 6.2 Total UK NO_x Emissions and Breakdown by OSRM Source Sector for 2001, 2015 and Possible EURO V Emission Reduction Scenarios.

As the new standards would not take effect until 2010, 2015 was selected for this work as the NO₂ and PM assessments have already been undertaken for this year [Stedman, 2003]. Estimates of the NO_x emissions in 2015 have been developed for a number of possible road transport scenarios [Murrells, 2003]. The base case road transport emissions were projected to be 280.3

Table 6.4 Summary of the Meteorology, Emission Inventories and Emission Reductions used in the OSRM Model Runs.

Policy Option/Model Runs	OSRM Version (1)	Meteorology	Base UK Inventories (2)	Base EMEP Inventories	Emission Control
Current Year - 1998 Base Case - 1999 Base Case - 2001 Base Case	v1.8 (no SC) v1.8 (no SC) v1.8 (no SC)	1998 1999 2001	NAEI 1998 (2001) NAEI 1999 (2001) NAEI 2001 (2001)	EMEP 1997 EMEP 1999 EMEP 2001	Current Year - 1998 Base Case - 1999 Base Case - 2001 Base Case
RIA: VOC from Paints - 2010 Base Case - 2010 Base Case – UK (30 kt pa) - 2010 Base Case – EU (278 kt pa) - 2010 Base Case – UK (2 kt pa) - 2010 Base Case – EU-14 (250 kt pa)	v1.8 (no SC) v1.8 (no SC) v1.8 (no SC) v1.8 (no SC) v1.8 (no SC)	1999 1999 1999 1999 1999	NAEI 2010 (2001)	EMEP 2010	VOC Emission Control - 2001 NAEI Projections - NAEI 2001 spatial maps scaled to 2010 by OSRM sector totals; EMEP 2001 spatial map scaled
EURO V NO _x Scenarios - 2015 Base Case (Road transport = - 2015 Best (Road transport = - 2015 Most Probable (Road transport = - 2015 Worse (Road transport =	v1.8 (no SC) v1.8 (no SC) v1.8 (no SC) v1.8 (no SC)	1999 1999 1999 1999	NAEI 2015 (2001*)	EMEP 2010	NO _x Emission Control - NAEI Projections revised - NAEI 2001 spatial maps scaled to 2015 by OSRM sector totals; EMEP 2001 spatial map scaled
RIA: PVR (March 2004) - 2005 Base Case - 2005 Base Case – PVR1 - 2010 Base Case - 2010 Base Case – PVR2a - 2010 Base Case – PVR2b	v1.8 (no SC) v1.8 (no SC) v1.8 (no SC) v1.8 (no SC) v1.8 (no SC)	1999 1999 1999 1999 1999	NAEI 2005 (2001*) NAEI 2005 (2001*) NAEI 2010 (2001*) NAEI 2010 (2001*) NAEI 2010 (2001*)	EMEP 2010	VOC Emission Control - Point and Area sources for SNAP 5 revised - NAEI 2001 spatial maps scaled to 2010 by OSRM sector totals; EMEP 2001 spatial map scaled - Control on petrol stations with throughput > 3000 m ³ - Control on petrol stations with throughput > 3500 m ³
Post-Gothenburg Scenarios - 2010 Base Case – 30% VOC (including natural) - 2010 Base Case – 30% NO _x - 2010 Base Case – 30% VOC (excluding natural) - 2010 Base Case – 30% VOC and 30% NO _x	v1.8 (no SC) v1.8 (no SC) v1.8 (no SC) v1.8 (no SC)	1999 1999 1999 1999	NAEI 2010 (2001*) NAEI 2010 (2001*) NAEI 2010 (2001*) NAEI 2010 (2001*)	EMEP 2010	NO _x or VOC Control - 30% across the board reduction (including natural) - 30% across the board reduction - 30% across the board reduction - 30% across the board reduction
Current Year - 1997 Base Case - 1998 Base Case - 1999 Base Case - 2000 Base Case - 2001 Base Case - 2002 Base Case - 2003 Base Case	v2.2 (+SC) v2.2(+SC) v2.2(+SC) v2.2(+SC) v2.2(+SC) v2.2(+SC) v2.2(+SC)	1997 1998 1999 2000 2001 2002 2003	NAEI 1997 (2002) NAEI 1998 (2002) NAEI 1999 (2002) NAEI 2000 (2002) NAEI 2001 (2002) NAEI 2002 (2002) NAEI 2003 (2002)	EMEP 1997 EMEP 1997 EMEP 1999 EMEP 2000 EMEP 2001 EMEP 2002 EMEP 2003	
RIA: PVR (March 2005: Repeat) - 2010 Base Case - 2010 Base Case – PVR2a - 2010 Base Case – PVR2b	v2.2 (+SC) v2.2 (+SC) v2.2 (+SC)	2003 2003 2003	NAEI 2010 (2002*) NAEI 2010 (2002*) NAEI 2010 (2002*)	EMEP 2010	VOC Emission Control - See RIA PVR (March 2004) above - Control on petrol stations with throughput > 3000 m ³ - Control on petrol stations with throughput > 3500 m ³

Notes: (1) (+SC) = with Surface Conversion, (no SC) = without Surface Conversion; (2) NAEI 1998 (2001) indicates that the spatial distributions used in the model run were based on the 2001 NAEI inventory year and scaled to the 1998 emission totals.

ktonne per annum reducing to 248.9, 220.8 and 205.4 ktonne per annum in the worse, most probable and best scenarios, respectively (see Figure 6.2). No assessment has been made to date of the effect of these measures on the emissions of other pollutants. The emissions for CO, SO₂ and VOCs for 2015 were taken from the latest NAEI projections (see NAEI emission projections (December 2003) in Hayman *et al.*, 2004b). Four OSRM model runs were undertaken.

➤ **Regulatory Impact Assessment of Directive on Petrol Vapour Recovery:** OSRM modelling calculations were undertaken as part of the regulatory impact assessment on petrol vapour recovery (PVR) and possible derogations:

1. **PVR I Derogation:** Assessment of the unabated emissions and benefits relating to derogation for service stations with thresholds of >100 m³ - <500 m³ petrol throughput per annum in 2005.
2. **PVR II Controls:** Assessment of the costs and benefits of Petrol Vapour Recovery Stage II controls in 2010, using 100% compliance for service stations with thresholds of >3000 m³ and >3500 m³ petrol throughput per annum (PVR II).

Information was provided on the location of UK service stations and their throughputs as part of the regulatory impact assessment. The information was used to refine the VOC emissions for the CORINAIR SNAP 5 emission sector on fossil fuel extraction and distribution. The revised 2001 NAEI projections were used for the other pollutants and emission source sectors. The VOC emissions used in the model runs are shown in Table 6.5.

Table 6.5 VOC and NO_x Emissions Used in the Petrol Vapour Recovery Model Runs.

Scenario	VOC Emission From SNAP 5 (kt per annum)	Total UK VOC Emission (kt per annum)	Total UK NO _x Emission (kt per annum)
Run 1: 2005 Base Case	273.3	1,282.9	1,452.3
Run 2: with no PVR I derogation	273.1	1,282.8	1,452.3
Run 3: 2010 Base Case	281.3	1,214.1	1,221.5
Run 4: with PVR II control on throughputs > 3,000 m ³	256.9	1,189.8	1,221.5
Run 5: with PVR II control on throughputs > 3,500 m ³	259.0	1,191.9	1,221.5

The outputs were provided to colleagues at netcen to undertake the Regulatory Impact Assessment (RIA 2004). The effects of the emissions reductions on human health (evaluated using the annual mean ozone concentration) and on crops (evaluated using AOT40 for crops) were determined. Work is in progress to repeat the PVR II scenarios using new emission data.

➤ **Post-Gothenburg Scenarios:** Assuming full compliance with the UN ECE Gothenburg Protocol and the EU National Emissions Ceilings Directive, the Department is interested the effectiveness of different controls on NO_x and/or VOC emissions to improve ozone air quality after 2010. Four model runs were undertaken with across-the-board reductions in the emissions of NO_x and/or VOC of 30%.

The OSRM calculations described above used the meteorology for 1999, as a typical ozone year, to calculate the hourly ozone concentrations at 2,946 10 km x 10 km (or 836 20 km x 20 km) receptor sites covering the UK. Further details (base case emission inventories, emission control scenarios) about the OSRM model runs can be found in the report prepared by Hayman *et al.* [2004b].

Maps of (a) the annual mean of the maximum of the 24 possible 8-hour running mean concentrations in each day, (b) the annual mean of the maximum of the 24 possible 8-hour running mean concentrations in each day which are greater than 35 ppb, (c) the AOT40 for the protection of crops and (d) the annual mean concentration of nitrogen dioxide for the base case runs (1999 as a current year, 2005, 2010 and 2015) were prepared. Apart from the Post-Gothenburg emission scenarios, the other model runs generally show relatively small changes from the related base case run.

Table 6.6 Summary of the Population-weighted Annual Mean of the Maximum Daily Running 8-hour Mean Ozone Concentration (in $\mu\text{g m}^{-3}$ and as Percentage of the 1999 Values) Calculated in the Various OSRM Scenario Runs for the UK, England, Wales, Scotland and Northern Ireland.

Scenario Run	Year	Annual Mean of the Maximum Daily Running 8-hour Mean Ozone Concentrations > 70 $\mu\text{g m}^{-3}$ (in $\mu\text{g m}^{-3}$)					Annual Mean of the Maximum Daily Running 8-hour Mean Ozone Concentrations > 70 $\mu\text{g m}^{-3}$ (as % of 1999 Value)				
		UK	England	Scotland	Wales	Northern Ireland	UK	England	Scotland	Wales	Northern Ireland
Current											
Current	1998	88.1	88.4	86.2	87.5	87.9	94.9%	94.9%	93.7%	96.7%	98.0%
Current	1999	92.8	93.2	92.1	90.4	89.7	100.0%	100.0%	100.0%	100.0%	100.0%
Current	2001	90.2	90.7	86.9	90.5	86.1	97.2%	97.3%	94.3%	100.1%	96.0%
Petrol Vapour Recovery RIA											
Base Case	2005	91.0	91.1	91.1	89.2	89.0	98.0%	97.8%	98.9%	98.6%	99.2%
PVR I - No Derogation	2005	91.0	91.1	91.1	89.2	89.0	98.0%	97.8%	98.9%	98.6%	99.2%
Base Case	2010	91.3	91.5	91.2	89.5	89.1	98.3%	98.2%	99.0%	98.9%	99.3%
PVR IIa (> 3000 m3)	2010	91.2	91.4	91.1	89.5	89.1	98.3%	98.1%	99.0%	98.9%	99.3%
PVR IIb (> 3500 m3)	2010	91.2	91.4	91.1	89.5	89.1	98.3%	98.2%	99.0%	98.9%	99.3%
Decorative Paints RIA											
Base Case	2010	91.2	91.4	91.1	89.5	89.1	98.3%	98.1%	99.0%	98.9%	99.3%
UK VOC Reduction of 30 ktonne pa	2010	91.0	91.2	91.0	89.3	89.0	98.1%	97.9%	98.8%	98.8%	99.1%
EU + UK VOC Reduction of 278 ktonne pa	2010	91.2	91.4	91.1	89.4	89.0	98.2%	98.1%	98.9%	98.9%	99.2%
EU + UK VOC Reduction of 252 ktonne pa	2010	91.1	91.2	91.0	89.4	89.0	98.1%	97.9%	98.8%	98.8%	99.2%
EU VOC Reduction of 250 ktonne pa	2010	91.1	91.2	91.0	89.4	89.0	98.1%	97.9%	98.8%	98.8%	99.2%
Post-Gothenburg Scenarios											
30% VOC Reduction (including natural)	2010	87.7	87.6	88.9	87.6	87.8	94.5%	94.0%	96.6%	96.9%	97.9%
30% NOx Reduction	2010	92.1	92.3	91.7	90.4	89.3	99.2%	99.1%	99.6%	100.0%	99.5%
30% VOC Reduction	2010	89.7	89.8	90.1	88.6	88.4	96.6%	96.4%	97.9%	97.9%	98.5%
30% VOC/ 30% NOx Reduction	2010	90.4	90.5	90.6	89.0	88.5	97.3%	97.1%	98.4%	98.4%	98.6%
EURO V Emission Standards											
Base Case	2015	91.4	91.6	91.3	89.4	89.1	98.5%	98.3%	99.2%	98.9%	99.2%
EURO V – Worse	2015	91.6	91.8	91.4	89.8	89.1	98.7%	98.6%	99.2%	99.3%	99.3%
EURO V – Most Probable	2015	91.7	91.9	91.5	89.9	89.2	98.8%	98.7%	99.4%	99.4%	99.4%
EURO V – Best	2015	91.8	92.0	91.5	90.0	89.2	98.8%	98.7%	99.4%	99.5%	99.4%

To aid the comparison of the different OSRM scenario runs, the population-weighted values have been derived for the

- annual mean of the maximum of the 24 possible 8-hour running mean concentrations in each day,
- annual mean of the maximum of the 24 possible 8-hour running mean concentrations in each day which are greater than $70 \mu\text{g m}^{-3}$ (i.e., 35 ppb)
- annual mean concentration of nitrogen dioxide

These population-weighted metrics were calculated for the UK and separately for England, Wales, Scotland and Northern Ireland. As an example, Table 6.6 shows how the annual mean of the maximum of the 24 possible 8-hour running mean concentrations in each day which are greater than $70 \mu\text{g m}^{-3}$ responds to the different emission control scenarios. Tables of the other metrics are given in Hayman *et al.* [2004b].

Discussion

Elevated concentrations of ozone over the UK are generally associated with photochemical production and easterly airflows. This is the situation modelled in the UK PTM with its idealised trajectory from central Europe to the UK. It is expected that reduction of NO_x and/or VOC emissions would be effective in reducing ozone. In an OSRM model run, a calendar year is simulated and a wider range of trajectories is sampled, including those from other wind directions. These other trajectories may have little or no photochemical ozone production, especially if the trajectory has mainly passed over low emission areas (e.g., the sea). One can envisage that there will be a chemical titration of the ozone in such air masses when these air masses pass over NO_x emission sources. This seems to be apparent in the maps of annual mean ozone concentrations where the ozone concentrations are suppressed in regions of high NO_x emissions (central and South-East England). As the NO_x emissions are reduced, there will be less titration and hence higher ozone concentrations. This is clearly seen in the increase in the annual mean ozone concentrations.

The total NO_x and VOC emissions for the UK and the EMEP model domain used in the OSRM model run for 1999 and the base case runs for 2005, 2010 and 2015 are shown in Table 6.7. The UK emissions are taken from the latest NAEI projections and include the changes to the NO_x road transport emission projections. The EMEP totals assume full compliance with the UN ECE Gothenburg Protocol and EU National Emission Ceilings Directive. For other part of the EMEP model domain, the time series trends are used to estimate these emissions. The totals shown for the EMEP model domain will not necessarily match emission totals contained in EMEP reports.

Table 6.7 The Total NO_x and VOC Emissions for the UK and the EMEP Model Domain used in the OSRM for 1999 and the Base Case Runs for 2005, 2010 and 2015.

	1999	2005	2010	2015
UK NO_x Emissions (ktonne pa)	1,794.0	1,453.8	1,221.5	1,108.9
% Change on 1999 emissions		-19.0%	-31.9%	-38.2%
UK VOC Emissions (ktonne pa)	1,670.9	1,276.5	1,196.6	1,191.3
% Change on 1999 emissions		-23.6%	-28.4%	-28.7%
EMEP NO_x Emissions	21,559		17,375	
% Change on 1999 emissions			-19.4%	
EMEP VOC Emissions	18,548		13,998	
% Change on 1999 emissions			-24.5%	

Using these emission estimates, the results from the different OSRM model runs, which were presented in Table 6.4 [see also Hayman *et al.*, 2004b and Second Annual Project Report (Hayman *et al.*, 2005a)], suggest that:

- **Trends in Base Case:** The reduction in NO_x emissions between 1999 and 2015 leads to a reduction in NO_2 concentrations by between 30-35% for England and Wales and ~40% for Scotland and Northern Ireland.

There is a downward trend in the AOT40 for the protection of crops across the UK although there are still large parts of the country, which are above the threshold of 3,000 ppb hours ($6,000 \mu\text{g m}^{-3}$)

hours). The annual mean of the maximum of the 24 possible 8-hour running mean concentrations in each day appears to fall at the extremities of the UK but rise in England where the emissions of nitrogen oxides are higher. However, the annual mean of the maximum of the 24 possible 8-hour running mean concentrations in each day, which are greater than 35 ppb, on the other hand decreases between 1999 and 2005. Thereafter, there is a very slight increase.

- **Emission Reductions:** NO_x emission reductions alone (e.g., the EURO V Emission Standards) lead to lower NO₂ concentrations but to increases in the population-weighted annual mean of the maximum daily running 8-hour ozone concentrations. On the other hand, VOC emission reductions have little or no effect on the annual mean NO₂ concentration but do lead to lower values of the ozone metrics.
- **Post-Gothenburg:** Again, a 30% VOC emission reduction improves ozone air quality but a 30% reduction in NO_x emission reduction leads to poorer ozone air quality. Comparison of the scenario in which NO_x and VOC emissions are each reduced by 30% with separate 30% reduction in NO_x or VOC reductions indicates that the counteracting effects of photochemical production of ozone (by NO_x and VOC emissions) and the titration effect of NO_x emissions.
- **Regional Changes:** Compared to the 1999 model run, the base case runs show an improvement in ozone air quality, as measured by the annual mean of the maximum of the 24 possible 8-hour running mean concentrations in each day, which are greater than 35 ppb, for each region (England, Wales, Scotland and Northern Ireland). On the other hand, there is a reduction in the annual mean of the maximum of the 24 possible 8-hour running mean concentrations in each day for Northern Ireland, little change in this metric for Scotland and Wales and a deterioration for England. The annual mean of the maximum of the 24 possible 8-hour running mean concentrations in each day will be sensitive to all hours and trajectories, including those where the titration effect is dominant. The annual mean of the maximum of the 24 possible 8-hour running mean concentrations in each day will be more sensitive to the higher ozone concentrations, which are more likely to be of a photochemical origin.

Thus, there appears to be two counteracting effects (a) photochemical production of ozone involving oxides of nitrogen and volatile organic compounds and (b) chemical titration by NO_x removing ozone. These two effects respond differently to emission control. Either VOC emission control alone or combined VOC and NO_x emission controls are needed to improve ozone air quality.

6.3.2 Using OSRM Version 2.2

The OSRM (version 2.2 with Surface Conversion, available in January 2005 prior to the review of the Surface Conversion Algorithm) was used to investigate the policy measures or scenario analyses listed below. Table 6.4 provides details about the runs (meteorology, emission inventories):

- **Current Ozone:** OSRM model runs were undertaken (see Table 6.4) to simulate the current UK ozone climatology (1997-2003). The model runs used meteorology and emission inventories for the relevant year. The output from these model runs were used to assess the suitability of the OSRM as a supplementary assessment technique for the third Daughter Directive on Ozone (see Section 7.3);
- **Regulatory Impact Assessment (RIA) on Petrol Vapour Recovery (PVR):** As described in the previous section, the OSRM (version 1.8) was used for a Regulatory Impact Assessment (RIA) on Petrol Vapour Recovery (PVR) to assess the effect of selected VOC emission control scenarios on UK ozone concentrations and the impacts on human health, materials and ecosystems resulting from these concentrations changes. In March 2005, the calculations were repeated to account for the increased penetration of diesel-fuelled vehicles in the UK vehicle fleet. This would reduce the throughput of petrol and consequently would result in lower emission abatement from the PVR measures.

As part of the work programme under the RIA contract, the locations of large petrol stations in the UK were compiled and these were used to derive maps of the VOC emissions from this source sector. The abatement in emissions resulting from application of the proposed PVR control scenarios was then used to produce a spatially-disaggregated emission map for each of the PVR scenarios. The VOC emission totals and the abatement achieved for the two control scenarios for the RIA 2004 and RIA 2005 is shown in Table 6.8. The emission estimates for the RIA 2004 were amended as the PVR emission abatement had been applied to the entire fuel throughput and not just the petrol component. The information provided in Table 6.8 illustrates that the effect of the

policy in terms of VOC abatement between is approximately 80% of that estimated in the revised RIA 2004. Although the relationship between ozone formed and the precursor emissions is complex; this overall reduction would be expected to reduce ozone concentrations across the UK – *i.e.*, would reduce the relative impact of the abatement.

Table 6.8 Base Case Sector Emissions and Emission Reduction for the PVR II Scenarios for 2010 for the RIA 2004 and RIA 2005 Base Case Runs.

Scenario	VOC emissions (tonnes per annum)	RIA 2004 (Original)	RIA 2004 (Revised)	RIA 2005
Baseline	TOTAL SECTOR EMISSIONS	37,721	38,196	29,745
	Type 4 emissions (>3,000m ³ and <3,500m ³)	2,889	4,146	3,677
	Type 5 emissions (>3,500m ³)	31,568	19,399	14,763
Scenario 1	Abatement due to PVR at type 5 sites	22,240	16,600	12,380
	CHANGE IN SECTOR EMISSIONS (%)	59%	43%	42%
Scenario 2	Abatement due to PVR at type 4 and 5 sites	24,320	19,900	15,464
	Change in sector emissions (%)	64%	52%	52%

Three model runs were undertaken in March 2005 (2010 base case, 2010 PVR Scenario 1 and 2010 PVR Scenario 2). The other inputs required for these model runs were chosen to be consistent with the other OSRM model runs undertaken at the same time for the Review of the Air Quality Strategy (*e.g.*, the runs used meteorology for 2003, see Section 6.4). The PVR model runs undertaken in March 2005 gave a much smaller response to the control measures than the first set of runs. The March 2005 runs were subsequently repeated (a) to fix the VOC reactivity of the European air mass at the corresponding base case values and (b) using meteorology for other years (1999, 2000, 2001 and 2002). The change in VOC reactivity of the European air mass effectively offset the improvements that resulted from the reduction in VOC mass emissions, which explains some of the much smaller response observed.

Table 6.9 Summary of Benefits (Physical Impacts) from Application of Petrol Vapour Recovery.

(a) Stage II Controls Applied at Service Stations with Petrol throughput > 3,000m³.

Main Benefits	Units	Benefits in the UK in 2010 from UK VOC reductions	Benefits across all UNECE in 2010 (from UK VOC reductions)
Health effects to population due to ozone exposure (COMEAP)	Acute mortality (cases)	9.9	19.4
	Respiratory hospital admissions (cases)	10.6	23.2
Effects to crop production due to ozone exposure	Improved yield, (tonnes spread across all sensitive crops)	4033	<i>not quantified</i>
Effects of ozone on materials		<i>not quantified</i>	<i>not quantified</i>

(b) Stage II Controls Applied at Service Stations with Petrol throughput > 3,500m³.

Main Benefits	Units	Benefits in the UK in 2010 from UK VOC reductions	Benefits across all UNECE in 2010 (from UK VOC reductions)
Health effects to population due to ozone exposure (COMEAP)	Acute mortality (cases)	8.0	15.6
	Respiratory hospital admissions (RHAs) (cases)	8.5	18.6
Effects to crop production due to ozone exposure	Improved yield, (tonnes spread across all sensitive crops)	3207	<i>not quantified</i>
Effects of ozone on materials		<i>not quantified</i>	<i>not quantified</i>

Following this and changes made to the OSRM post-processor (see Section 4.4), it was agreed with the Department that the PVR RIA results should be based on the May 2005 model runs undertaken using the 1999 meteorology and that the surface conversion algorithm should only be applied to urban areas (*i.e.*, the surface conversion algorithm was not used in rural areas). The results of the revised analysis were passed to colleagues in netcen to undertake the cost-benefit analysis. Table 6.9 illustrates the benefits for human health, materials and ecosystems resulting from the PVR controls. These benefits were then monetised and reported to the Department through the RIA contract [Watkiss *et al.*, 2005].

6.4 OSRM MODELLING FOR THE REVIEW OF THE AIR QUALITY STRATEGY

The latest version of the Ozone Source-receptor Model (Version 2.2a with Surface Conversion Algorithm available in September 2005) was used to investigate the impact on ozone and nitrogen dioxide concentrations of various policy measures being considered as part of the Review of the Air Quality Strategy.

Table 6.10 list the emission control measures being considered for the Review of the Air Quality Strategy. The primary focus of most of these measures is to reduce the concentrations of particulate matter and nitrogen dioxide. Measure M (VOC emission control) was the only measure, which was specifically targeted for its impact on ozone. As the control of nitrogen oxide emissions may cause ozone concentrations to increase (through lower chemical titration) or to decrease (through lower photochemical ozone production), a number of other measures were also modelled to assess the benefits/disbenefits of these measures for ozone. The measures modelled using the OSRM are highlighted in bold in Table 6.10. More detailed information on the activity and emission assumptions for these measures can be found in Appendix 1 of the report by Hayman *et al.* [2005b].

Table 6.10 The Measures being Considered as Part of the Review of the Air Quality Strategy with the Measures modelled by the OSRM highlighted in Bold.

Measure	Description
A	Introduction of Euro V/VI Standards (Low Intensity)
B	Introduction of Euro V/VI Standards (High Intensity)
C	Programme of incentives for early uptake of Euro V/VI Standards (Low Intensity)
D	Programme of incentives to phase out most polluting vehicles
E	Programme of incentives to increase penetration of low emission vehicles
F	Impact of All User Road Charging Schemes
G	Extend London Low Emission Zone to London + 7 largest urban areas
H	Retrofit of particulate traps to HDVs and captive fleets
I	Domestic combustion (switch from coal to oil and natural gas)
J & K	Domestic (NO_x Standards for Gas-fired Appliances) and industrial combustion
K	Industrial combustion
L	Small combustion plant
M	VOC emission control at petrol stations and for on and offshore tanker loading operations
N	Shipping measure through IMO
O	Combined scenario for transport (Measures C and E)
P	Combined scenario for transport and industrial measures (Measures C and L)
Q	Combined scenario for transport and industrial measures (Measures C, E and L)
M & Q	Combined scenario for transport and industrial measures (Measures M and Q [=C, E and L])

6.4.1 Key Features of the Model Runs:

The OSRM model runs

- were undertaken for the years 2010, 2015 and 2020;
- were undertaken at 10 km x 10 km resolution to ensure a consistent approach for the determination of the health benefits;
- used the NAEI emission projections developed for the Review of the Air Quality Strategy;
- took the projected national emission totals for European countries developed for the Clean Air for Europe (CAFÉ) programme. A limited number of runs were also undertaken using the emission

totals agreed under the National Emissions Ceilings Directive for the EU member states (except for the UK) and the Gothenburg Protocol for the other UN ECE countries;

- used the meteorology for 2003. Although this was a high ozone year, it would ensure consistency with the NO₂/PM modelling and it could possibly become a typical ozone year in the future as a result of climate change. Sensitivity runs would be undertaken using meteorology for two other years (2000 and 2002);
- included the effects of climate change on atmospheric composition. The effect of climate change on atmospheric composition, especially ozone, was based on the monthly trends derived by Derwent [2005b] for the business-as-usual scenario with climate change (see Section 6.4.1.5).

6.4.1.1 UK Emissions

As part of the Department's National Atmospheric Emission Inventory (NAEI) [Dore *et al.*, 2004] programme and using the latest available information, emission estimates were produced [Hobson, 2005] for the base case scenarios and for the various measures selected for modelling using the OSRM (highlighted in bold in Table 6.10). The total UK NO_x and VOC emissions for the base case runs for 2010, 2015 and 2020 are given in Table 6.11 and for the selected measures in Table 6.12.

Measures A, B, C, E, J, K and L only affected the NO_x emissions. Measure M used the UK VOC cost curve to identify abatement of various on and offshore VOC emission sources. These included the application of petrol vapour recovery from petrol stations with throughputs > 3,000 m³ and abatement of VOC emissions from on and offshore loading of crude oil. A more detailed breakdown of the emissions for the UK used in the OSRM model runs by OSRM source sector can be found in Hayman *et al.* [2005b].

As the VOC emission controls in Measure M were based on specific sectoral activities with localised emissions, separate maps of VOC emissions from petrol stations and on and offshore loading of crude oil were created for 2010 for the OSRM source sector Fossil Fuel Extraction and Distribution and adjusted to produce the corresponding maps for 2015 and 2020. The maps for the other OSRM VOC source sectors were prepared as described previously.

6.4.1.2 Non-UK Emissions: Base Case Runs:

It has long been known that European NO_x and VOC emission contribute to ozone production over the UK. Spatially-disaggregated emission inventories are therefore needed for the non-UK emissions on the OSRM model domain. As part of the UN ECE Convention on Long-range Transboundary Air Pollution, signatory countries are required to submit national emission estimates to EMEP. EMEP have taken these national estimates and used expert judgement to prepare emission inventories for current years (up to 2002) on a 50 km x 50 km grid covering the EMEP model domain (which is also the OSRM model domain). These inventories can be downloaded from the EMEP website [UNECE/EMEP Activity Data and Emission Database, <http://webdab.emep.int/>].

For the base case runs for 2010, 2015 and 2020, two sets of emission scenarios were investigated:

- Scenario 1 - Compliance with the NECD or Gothenburg Protocol:** In this scenario, European countries were assumed to achieve the emission total that was agreed in the National Emissions Ceilings Directive for EU member states (except for the UK) and the Gothenburg Protocol for the other UN ECE countries. These emission limits were then assumed to hold in 2015 and 2020. In other words, no further emission reduction was assumed to occur. The emission totals of other sources (*e.g.*, natural marine emissions, volcanic) were assumed to be unchanged from the current year values.
- Scenario 2 - Emission Projections developed for the CAFÉ programme.** IIASA have developed emission projections for the Clean Air for Europe (CAFÉ) programme for a number of policy options. The country emission totals used in the current work are based on the IIASA RAINS scenario NAT_CLE (Official national energy projections with climate policies). The emission totals of other sources (*e.g.*, natural marine emissions, volcanic) were again assumed to be unchanged from the 2002 values.

For both cases, the base case emission inventories for 2010, 2015 and 2020 were derived from the latest available maps from EMEP (2002 calendar year). The country emission contribution in each

Table 6.11 Summary and Breakdown of the NAEI Emission Projections (in ktonne per annum) Used in the OSRM Current and Base Case Runs.

Pollutant	OSRM_Sector	Annual Emission Estimate (in ktonne per annum)							
		1999	2000	2001	2002	2003	2010	2015	2020
SO _x	Solvent Usage	0.0	0.0	0.0	0.0	0.0	0.0	0.0	0.0
	Road Transport	13.6	6.0	3.4	3.0	3.0	0.8	0.8	0.8
	Industrial Processes (1)	321.0	264.3	274.7	241.8	228.6	238.3	240.0	244.1
	Fossil Fuel Extraction and Distribution	1.2	1.1	0.6	0.6	0.6	0.3	0.3	0.3
	Domestic Combustion	78.3	61.8	63.2	50.3	36.4	11.5	9.1	14.8
	Major Point Sources	776.4	821.0	741.5	680.4	677.2	210.1	123.5	77.1
	Other	38.9	35.0	30.3	26.4	32.8	23.4	23.2	22.6
	Natural	0.0	0.0	0.0	0.0	0.0	0.0	0.0	0.0
	Total	1229.4	1189.2	1113.7	1002.5	978.6	484.4	396.9	359.7
NO _x	Solvent Usage	0.0	0.0	0.0	0.0	0.0	0.0	0.0	0.0
	Road Transport	909.7	826.4	760.3	710.8	632.1	396.2	290.5	267.8
	Industrial Processes (1)	276.2	248.5	243.5	246.2	279.3	219.1	226.1	234.7
	Fossil Fuel Extraction and Distribution	1.2	0.7	0.7	0.7	0.7	0.5	0.5	0.5
	Domestic Combustion	105.1	103.8	106.7	101.6	138.6	96.7	100.6	105.0
	Major Point Sources	338.2	365.5	378.8	379.2	378.5	280.3	248.7	136.7
	Other	179.5	172.7	156.9	143.0	140.5	125.8	125.8	124.5
	Natural	0.0	0.0	0.0	0.0	0.0	0.0	0.0	0.0
	Total	1809.9	1717.6	1646.9	1581.5	1569.7	1118.6	992.2	869.2
VOC	Solvent Usage	461.6	429.1	404.0	389.7	376.6	342.4	357.0	371.7
	Road Transport	369.7	300.1	248.6	211.0	159.6	71.7	56.2	54.2
	Industrial Processes (1)	224.8	218.4	195.1	184.4	186.8	195.7	203.9	213.0
	Fossil Fuel Extraction and Distribution	283.3	289.1	287.5	277.3	259.6	162.6	163.5	163.4
	Domestic Combustion	44.6	35.9	39.0	35.5	30.3	19.6	19.6	23.6
	Major Point Sources	8.0	8.5	8.5	8.9	6.7	10.2	10.3	11.0
	Other	87.2	82.8	82.1	78.8	68.8	46.0	46.2	46.3
	Natural	178.0	178.0	178.0	178.0	178.0	178.0	178.0	178.0
	Total	1657.2	1541.9	1442.8	1363.6	1266.4	1026.2	1034.7	1061.2
CO	Solvent Usage	0.0	0.0	0.0	0.0	0.0	0.0	0.0	0.0
	Road Transport	3034.9	2548.3	2182.9	1915.5	1703.3	633.8	422.5	392.5
	Industrial Processes (1)	714.2	621.3	660.0	574.7	652.2	603.9	616.6	629.6
	Fossil Fuel Extraction and Distribution	1.1	0.7	0.5	0.7	0.7	2.7	2.9	3.1
	Domestic Combustion	262.1	233.0	246.5	224.8	306.5	150.6	159.5	193.8
	Major Point Sources	60.5	69.5	71.7	71.0	70.9	79.2	79.0	79.3
	Other	457.9	455.5	474.6	451.1	443.2	457.8	461.9	465.6
	Natural	0.0	0.0	0.0	0.0	0.0	0.0	0.0	0.0
	Total	4530.7	3928.3	3636.2	3237.8	3176.8	1928.0	1742.4	1763.9

Table 6.12 Total UK NO_x and VOC Emissions for the Base Case and the Measures Modelled using the OSRM for 2010, 2015 and 2020.

Measure(s)	Description	Total UK NO _x Emissions (ktonne per annum)		
		2010	2015	2020
Base	Base case projections	1118.52	992.07	869.12
A	Introduction of EURO V/VI (low reduction scenario)	1115.92	958.31	803.66
B	Introduction of EURO V/VI (high reduction scenario)	1109.58	914.06	727.77
B*	An earlier version of the Introduction of EURO V/VI (high reduction scenario)	1109.58	911.57	712.68
C	Early uptake of EURO V/VI	1107.80	946.47	799.41
E	Introduction of low emission vehicles	1116.98	986.58	857.91
J	Domestic combustion	1115.64	984.32	856.20
K & L	Control on power stations, iron and steel and oil refineries	924.06	795.92	784.95
L	Control on small combustion plant (20-50 MW) (= base case in 2010 as no NO _x emission reduction until 2013)	1118.52	976.43	852.89
M	Petrol vapour recovery from petrol stations and abatement of VOC emissions from on and offshore loading of crude oil (= base case emissions as only VOC emission reduction)	1118.52	992.07	869.12
O	A combination of Measures C and E	1106.35	941.78	790.09
P	A combination of Measures C and L	1107.80	930.83	783.18
Q	A combination of Measures C, E and L	1106.35	926.14	773.86
M & Q	A combination of Measures C, E, L (=Q) and M	1106.35	926.14	773.86
Measure(s)	Description	Total UK VOC Emissions (ktonne per annum)		
		2010	2015	2020
Base	Base Case projections	1026.17	1034.68	1061.25
M	Petrol vapour recovery from petrol stations and abatement of VOC emissions from on and offshore loading of crude oil	952.15	958.42	983.00
M & Q	Combination of selected NO _x and VOC control measures	952.15	958.42	983.00

Note: The above VOC emission totals include a contribution from natural sources of 178 ktonne per annum. This sectoral source was not used and the VOC emissions were generated using a biogenic emission potential inventory (see Section 0).

EMEP grid square was scaled by the ratio of its projected emission total to its total in 2002. The revised country contributions were then summed. Appendix 3 of the report on this modelling [Hayman *et al.* (2005b)] gives the national emission totals used for the two emission cases for the 4 pollutants.

6.4.1.3 Non-UK Emissions: Scenario Runs:

For Measures A, B, C, O, P, Q and the combination of Measures M and Q, the UK emission data were used to derive (a) the fraction of the total NO_x emissions produced by the road transport sector (based on the corresponding base case run) and (b) the scaling factors to reduce the road transport sectoral emissions (see Table 6.13). These two factors were assumed to apply to other European countries and were used to scale the total non-UK NO_x emissions.

Table 6.13 European Emission Scaling Factors for Road Transport NO_x Emissions (as Fraction of Relevant Base Case) for 2010, 2015 and 2020.

Measure(s)	Description	Scaling Factors for Road Transport NO _x Emissions		
		2010	2015	2020
Base	Base Case projections (January 2005)	1.00	1.00	1.00
A	Introduction of EURO V/VI (Low Reduction Scenario)	0.99	0.88	0.76
B	Introduction of EURO V/VI (High Reduction Scenario)	0.98	0.73	0.47
B*	Introduction of EURO V/VI (High Reduction Scenario)	0.98	0.72	0.42
C	Early uptake of Measure 1 + all road user charging schemes	0.99	0.88	0.76
O	Combined Transport Measures (C & E)	0.99	0.88	0.76
P	Combined Transport & Industrial Measures (C & L)	0.99	0.88	0.76
Q	Combined Transport & Industrial Measures (3b, 12 & 21)	0.99	0.88	0.76
M & Q	Combined Transport & Industrial Measures (3b, 12, 13 & 21)	0.99	0.88	0.76

The other measures modelled using the OSRM – the transport measure E, the domestic and industrial (Measures J, K and L) and VOC control (Measure M) measures – were assumed to be UK specific and no reduction was made of the European emissions. Scaling factors of unity were used, as in the base case runs.

6.4.1.4 Biogenic VOCs:

The biogenic VOC emissions were treated differently. The emission potential inventory derived using the PELCOM land cover dataset and the TNO tree species inventory was used, as described in Section 4.3 [see also Dore *et al.*, 2003]. The use of this inventory therefore allows for the effects of year-to-year variations in meteorology.

6.4.1.5 Boundary Conditions:

Output from the global tropospheric STOCHEM model has been used to initialise the OSRM trajectories. Initial conditions have been derived for the species O₃, CO, CH₄, C₂H₆, HNO₃ and PAN from datasets of spatially-disaggregated daily concentration fields. Two datasets have been provided for 2 calendar years, one representing the climatology of the late 1990's (actually 1998) and the second a future atmosphere (IPCC SRES scenarios for 2030). The use of these datasets will enable the OSRM to describe the seasonal cycles in the concentrations of ozone and other trace gases and will make a link between regional scale ozone production and the hemispheric circulation. As described in Section 4.3, the OSRM has been modified so that the concentration of ozone and other key trace species vary with location, time of year, etc.

Table 6.14 Monthly Trends in Ozone Concentrations (in ppb per year) derived for Mace Head from STOCHEM Global Model Output [Derwent, 2005b].

Scenario	Jan	Feb	Mar	Apr	May	Jun	Jul	Aug	Sep	Oct	Nov	Dec
Business-as-Usual	0.084	0.074	0.204	0.185	0.090	0.120	0.118	0.150	0.101	0.025	0.081	0.082
Business-as-Usual with Climate Change	0.085	0.004	-0.074	0.200	0.225	0.039	-0.085	-0.120	0.066	0.086	0.097	0.127
Maximum Feasible Reduction	-0.139	-0.147	-0.117	-0.130	-0.184	-0.073	-0.017	0.026	-0.066	-0.143	-0.107	-0.131
IPCC SRES A2	0.153	0.191	0.214	0.270	0.170	0.158	0.113	0.074	0.177	0.051	0.148	0.146
IPCC SRES A2 with Climate change	0.188	0.263	0.287	0.362	0.150	-0.317	-0.168	-0.019	0.154	0.147	0.162	0.128

Derwent [2005b] has calculated global ozone concentrations using the STOCHEM 3-D tropospheric ozone model for a number of climate-related emission scenarios. The output of the model runs has been used to derive monthly trends in ozone at Mace Head, as shown in Table 6.14. This would cause changes from 2003 concentrations ranging from -0.8 to +1.6 ppb on the initial daily ozone concentrations by 2010 and -1.9 to +3.8 ppb by 2020. Following discussion with the Department and Prof Derwent, it was agreed to use the monthly trends for the Business-as-Usual with Climate Change scenario.

6.4.2 Model Outputs

The OSRM Post-processor was used to process the hourly concentrations calculated by the OSRM to generate UK maps for the 8 ozone and nitrogen dioxide metrics listed below. All the results presented in this report have been derived with the Surface Conversion algorithm activated (see Section 4.4.2).

Health-based Metrics:

- Annual Mean of the Maximum Daily Running 8-hour Average Ozone concentration (*i.e.*, with no cutoff)
- Annual Mean of the Difference between the Maximum Daily Running 8-hour Average Ozone concentration and a 35 ppb (or 70 $\mu\text{g m}^{-3}$) cutoff

Table 6.15 Summary of the Population-Weighted Annual Mean of the Difference (in $\mu\text{g m}^{-3}$) between the Daily Maximum Running 8 Hourly Ozone Concentration and $100 \mu\text{g m}^{-3}$ for the OSRM Runs Undertaken for the Review of the Air Quality Strategy.

Run Description	Population-Weighted Annual Mean of the Difference (in $\mu\text{g m}^{-3}$) between the Daily Maximum Running 8 Hourly Ozone Concentration and $100 \mu\text{g m}^{-3}$						
	All UK	Scotland	Wales	Northern Ireland	Inner London	Outer London	Rest of England
1999 - Current Year	1.75	1.69	2.03	1.88	1.35	1.44	1.79
2000 - Current Year	1.65	1.32	2.24	2.09	1.06	1.07	1.73
2001 - Current Year	1.71	1.22	2.44	0.79	1.62	1.73	1.76
2002 - Current Year	1.47	1.62	1.26	1.41	1.67	1.58	1.44
2003 - Current Year	1.93	1.69	2.73	1.96	1.52	1.53	1.97
2010 - Base Case (NECD)	2.19	1.87	2.97	2.09	1.87	1.83	2.23
2010 - Base Case (CAFÉ)	2.14	1.80	2.89	2.01	1.92	1.86	2.18
2010 - Base Case (CAFÉ) – Current Composition	1.75	1.48	2.37	1.60	1.60	1.55	1.78
2015 - Base Case (NECD)	2.68	2.23	3.53	2.45	2.40	2.36	2.74
2015 - Base Case (CAFÉ)	2.50	2.06	3.34	2.29	2.28	2.23	2.55
2020 - Base Case (NECD)	3.22	2.66	4.22	2.86	2.89	2.86	3.30
2020 - Base Case (CAFÉ)	2.95	2.43	3.96	2.63	2.66	2.61	3.01
2020 - Base Case (CAFÉ) – Current Composition	1.83	1.50	2.46	1.61	1.68	1.64	1.87
2010 - Base Case	2.14	1.80	2.89	2.01	1.92	1.86	2.18
2010 - Measure A	2.15	1.80	2.89	2.01	1.92	1.87	2.19
2010 - Measure B	2.16	1.80	2.90	2.01	1.93	1.88	2.20
2010 - Measure B*	2.16	1.80	2.90	2.01	1.93	1.88	2.20
2010 - Measure C	2.16	1.80	2.90	2.01	1.94	1.89	2.20
2010 - Measure E	2.15	1.80	2.89	2.01	1.92	1.87	2.19
2010 - Measure J	2.15	1.80	2.89	2.01	1.93	1.87	2.19
2010 - Measures K & L	2.30	1.90	3.11	2.09	2.02	1.97	2.36
2010 - Measure L	2.14	1.80	2.89	2.01	1.92	1.86	2.18
2010 - Measure O	2.16	1.81	2.90	2.01	1.94	1.89	2.20
2010 - Measure P	2.16	1.80	2.90	2.01	1.94	1.89	2.20
2010 - Measure Q	2.16	1.81	2.90	2.01	1.94	1.89	2.20
2010 - Measures M & Q	2.15	1.80	2.89	2.00	1.94	1.89	2.19
2010 - Measure M	2.14	1.79	2.88	2.00	1.92	1.86	2.18
Sensitivity to Meteorology							
2010 - Base Case	2.14	1.80	2.89	2.01	1.92	1.86	2.18
2010 - Measure B*	2.16	1.80	2.90	2.01	1.93	1.88	2.20
2010 - Measure B* with 2000 meteorology	1.80	1.08	2.28	1.70	1.61	1.66	1.89
2010 - Measure B* with 2002 meteorology	1.72	1.79	1.58	1.51	1.93	1.87	1.70
2010 - Measure M	2.14	1.79	2.88	2.00	1.92	1.86	2.18
2010 - Measure M with 2000 meteorology	1.77	1.07	2.26	1.69	1.54	1.59	1.85
2010 - Measure M with 2002 meteorology	1.69	1.78	1.57	1.50	1.88	1.82	1.67

Table 6.15 Summary of the Population-Weighted Annual Mean of the Difference (in $\mu\text{g m}^{-3}$) between the Daily Maximum Running 8 Hourly Ozone Concentration and $100 \mu\text{g m}^{-3}$ for the OSRM Runs Undertaken for the Review of the Air Quality Strategy (Continued).

Run Description	Population-Weighted Annual Mean of the Difference (in $\mu\text{g m}^{-3}$) between the Daily Maximum Running 8 Hourly Ozone Concentration and $100 \mu\text{g m}^{-3}$						
	All UK	Scotland	Wales	Northern Ireland	Inner London	Outer London	Rest of England
2015 - Base Case	2.50	2.06	3.34	2.29	2.28	2.23	2.55
2015 - Measure A	2.55	2.08	3.38	2.30	2.34	2.28	2.60
2015 - Measure B	2.60	2.11	3.42	2.31	2.42	2.36	2.66
2015 - Measure B*	2.61	2.11	3.42	2.31	2.42	2.37	2.66
2015 - Measure C	2.57	2.09	3.39	2.30	2.37	2.31	2.62
2015 - Measure E	2.51	2.06	3.35	2.29	2.30	2.24	2.56
2015 - Measure J	2.52	2.07	3.35	2.29	2.32	2.25	2.56
2015 - Measures K & L	2.68	2.19	3.61	2.36	2.42	2.37	2.74
2015 - Measure L	2.52	2.07	3.35	2.29	2.30	2.25	2.57
2015 - Measure O	2.58	2.10	3.40	2.31	2.39	2.33	2.63
2015 - Measure P	2.58	2.10	3.41	2.31	2.40	2.34	2.63
2015 - Measure Q	2.59	2.10	3.41	2.31	2.41	2.35	2.64
2015 - Measures M & Q	2.58	2.09	3.40	2.30	2.41	2.34	2.63
2015 - Measure M	2.50	2.05	3.33	2.28	2.28	2.22	2.55
2020 - Base Case	2.95	2.43	3.96	2.63	2.66	2.61	3.01
2020 - Measure A	3.02	2.45	3.99	2.61	2.77	2.73	3.09
2020 - Measure B	3.08	2.43	3.97	2.53	2.92	2.91	3.15
2020 - Measure B*	3.09	2.42	3.95	2.50	2.95	2.95	3.15
2020 - Measure C	3.03	2.46	4.00	2.61	2.79	2.75	3.10
2020 - Measure E	2.97	2.45	3.97	2.64	2.69	2.64	3.03
2020 - Measure J	2.97	2.45	3.97	2.64	2.73	2.65	3.03
2020 - Measures K & L	3.03	2.49	4.07	2.65	2.74	2.68	3.10
2020 - Measure L	2.97	2.44	3.97	2.63	2.69	2.63	3.03
2020 - Measure O	3.05	2.47	4.01	2.62	2.82	2.78	3.11
2020 - Measure P	3.05	2.46	4.01	2.61	2.82	2.77	3.11
2020 - Measure Q	3.06	2.47	4.02	2.62	2.85	2.80	3.13
2020 - Measures M & Q	3.05	2.46	4.01	2.60	2.84	2.79	3.11
2020 - Measure M	2.94	2.42	3.94	2.62	2.65	2.60	3.00

- (c) Annual Mean of the Difference between the Maximum Daily Running 8-hour Average Ozone concentration and a 50 ppb (or $100 \mu\text{g m}^{-3}$) cutoff
- (d) Number of Days when the maximum of the 24 possible 8-hour running mean concentrations in each day exceeds $100 \mu\text{g m}^{-3}$ (metric in the UK Air Quality Strategy)
- (e) Annual Mean NO_2 concentration

Non Health-based Metrics:

- (f) Annual Mean O_3 concentration
- (g) AOT40 for crops
- (h) AOT40 for forests

Population-weighted means were derived for the metrics associated with impacts on human health. Area-weighted means were derived for the non-health effects metrics. The population- and area-weighted means were determined for the following regions: All UK, Scotland, Wales, Northern Ireland, Inner London, Outer London and the Rest of England. An example of the output is shown in Table 6.15. The complete set of the ozone and nitrogen dioxide metrics calculated by the OSRM for the current year, base case and scenario runs are given in Appendix 4 of Hayman *et al.* [2005b].

These statistics were then used within the cost-benefit analysis being carried out for the Review of the Air Quality Strategy [AQS, 2005; IGCP, 2005]. The ozone metrics (a), (b) and (c) have been used to assess the benefits/disbenefits to human health of the measures modelled by the OSRM. The metrics (f), (g) and (h) have been used to assess the non-health benefits/disbenefits for materials, crops and vegetation.

6.4.2.1 Base Case Runs

Overview

Overall, the base case runs show a progressive increase in the ozone metrics (*i.e.*, a decline in ozone air quality) from the current year to 2010 and beyond. This is shown in Figure 6.3 where maps of three of the seven ozone metrics used for the Review of the Air Quality Strategy (see previous Section) are presented for 2003, 2010, 2015 and 2020. There is generally a progressive reduction in the annual mean NO_2 concentration from the current year to 2010 and beyond (*i.e.*, an improvement in NO_2 air quality). The response of the annual mean NO_2 concentration to the different emission projections is generally in the opposite sense to the ozone metrics.

Elevated concentrations of ozone over the UK are generally associated with summertime photochemical production and easterly airflows. This is the situation modelled in the UK Photochemical Trajectory Model with its idealised trajectory from central Europe to the UK (and the OSRM when configured to use this idealised trajectory). Reduction of NO_x and/or VOC emissions are effective in reducing peak ozone concentrations [see Hayman *et al.*, 2004a,b; 2005a]. In an OSRM model run, however, a calendar year is simulated and a wider range of trajectories is sampled, including those from other wind directions. These other trajectories may have little or no photochemical ozone production, especially if the trajectory has mainly passed over low emission areas (*e.g.*, the sea). It is likely that there will be a chemical titration of the ozone in such air masses when these air masses pass over NO_x emission sources (the same mechanism explains the lower ozone concentrations observed in urban centres). As the NO_x emissions are reduced, there will be less titration and hence higher ozone concentrations result.

In previous OSRM scenario calculations, VOC emission reductions alone led to an improvement in ozone air quality for all the ozone metrics calculated by the OSRM post-processor. NO_x emission reduction scenarios gave a more complex response, reflecting their role in the formation and removal of ozone. The response depended on the choice of ozone metric and could show regional differences for a given metric. Generally, there was a deterioration in ozone air quality if NO_x emissions alone were controlled. When both VOC and NO_x emissions are reduced, as occurs in the current base case emission projections, these two effects compete and the overall response depends on the relative changes in emissions. In the present base case runs, the UK emission projections show a

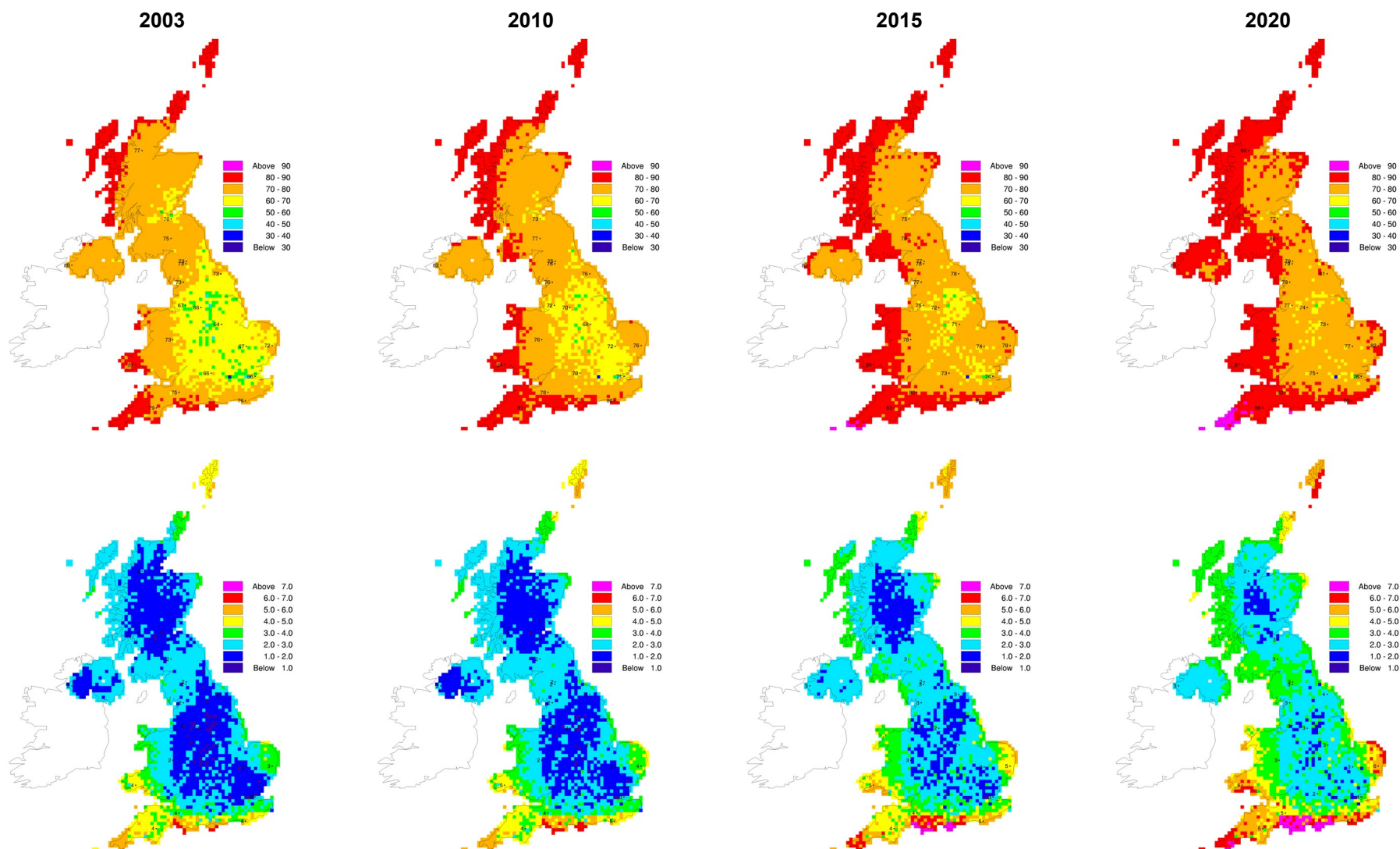


Figure 6.3 UK-scale Maps of generated from the OSRM Base Case Runs for 2003, 2010, 2015 and 2020 for the Metrics: Annual Mean of the Maximum Daily Running 8-hour Average Ozone concentration (i.e., with no cutoff) [Upper Panels] and Annual Mean of the Difference between the Maximum Daily Running 8-hour Average Ozone concentration and a 50 ppb (or 100 µg m⁻³) cutoff [Lower Panels].

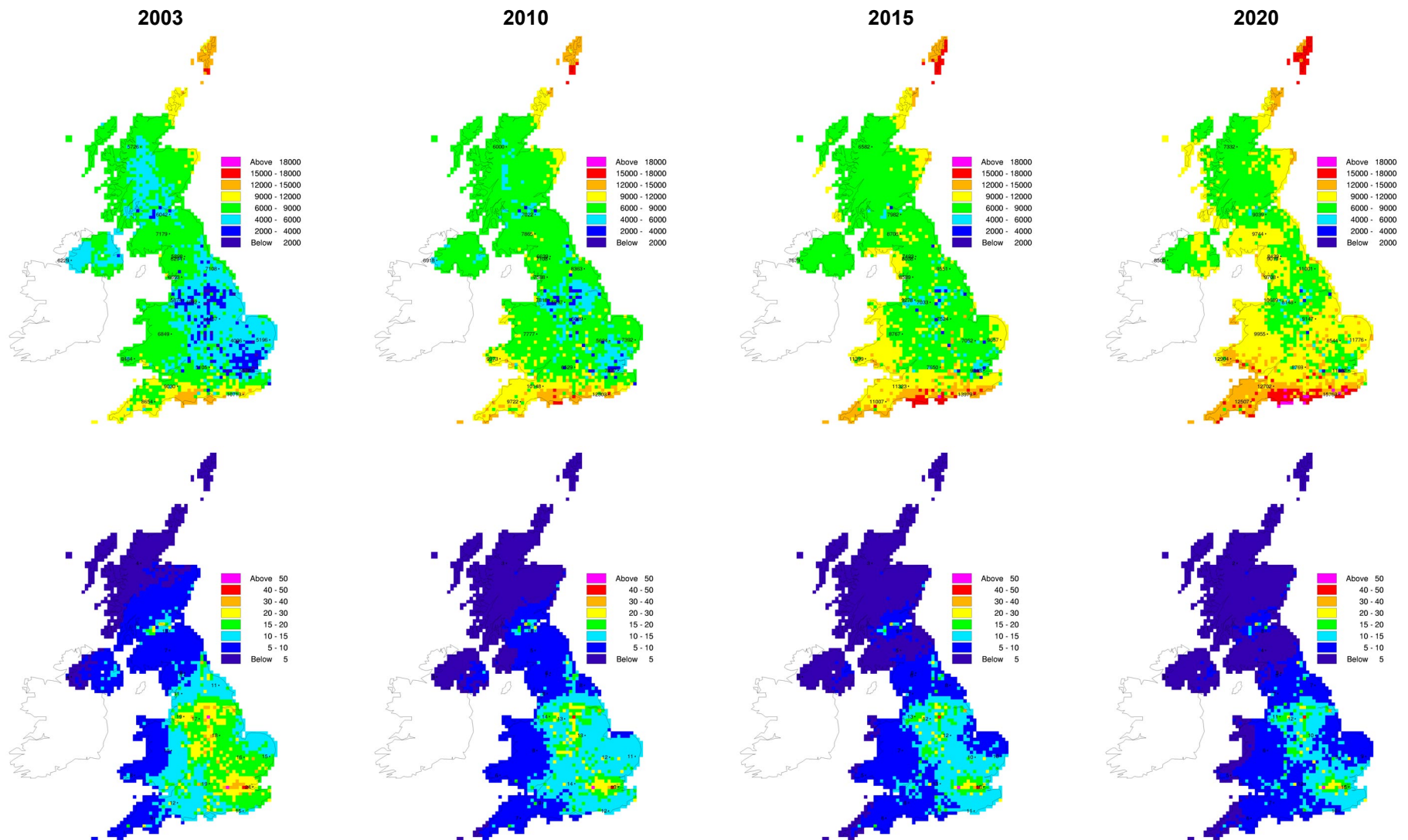


Figure 6.3 UK-scale Maps of generated from the OSRM Base Case Runs for 2003, 2010, 2015 and 2020 for the Metrics: AOT40 - Crops [Upper Panels] and Annual Mean Nitrogen Dioxide Concentration [Lower Panels].

greater decrease in the NO_x emissions out to 2020 than in the VOC emissions. Indeed, the 2020 total UK VOC emissions are actually higher than those in 2015 for both emission projections. In terms of emissions from other European countries, there are comparable changes in the NO_x and VOC emissions. Overall, there is a proportionately greater reduction in the emissions of NO_x, suggesting a smaller NO_x titration effect and thus poorer ozone air quality, as evidenced by the increases in the ozone metrics.

The other major driver for the deterioration in ozone air quality is changing atmospheric composition. The OSRM base case runs described here have applied a ramp to the initial ozone concentrations, based on the monthly trends in ozone concentrations derived for a global business-as-usual scenario with climate change. Sensitivity runs were undertaken to investigate the effects of the changing atmospheric composition and these are discussed later in this section.

6.4.2.2 Sensitivity Runs

A limited number of model runs were undertaken to assess the sensitivity to changes in (1) the non-UK emission assumptions and (2) atmospheric composition.

1. NECD against CAFÉ Emission Projections: The majority of the OSRM runs for the years 2010, 2015 and 2020 made use of projected national emission totals for European countries developed for the Clean Air for Europe (CAFÉ) programme. A limited number of runs were also undertaken using the emission totals agreed under the National Emissions Ceilings Directive for the EU member states (except for the UK) and the Gothenburg Protocol for the other UN ECE countries.

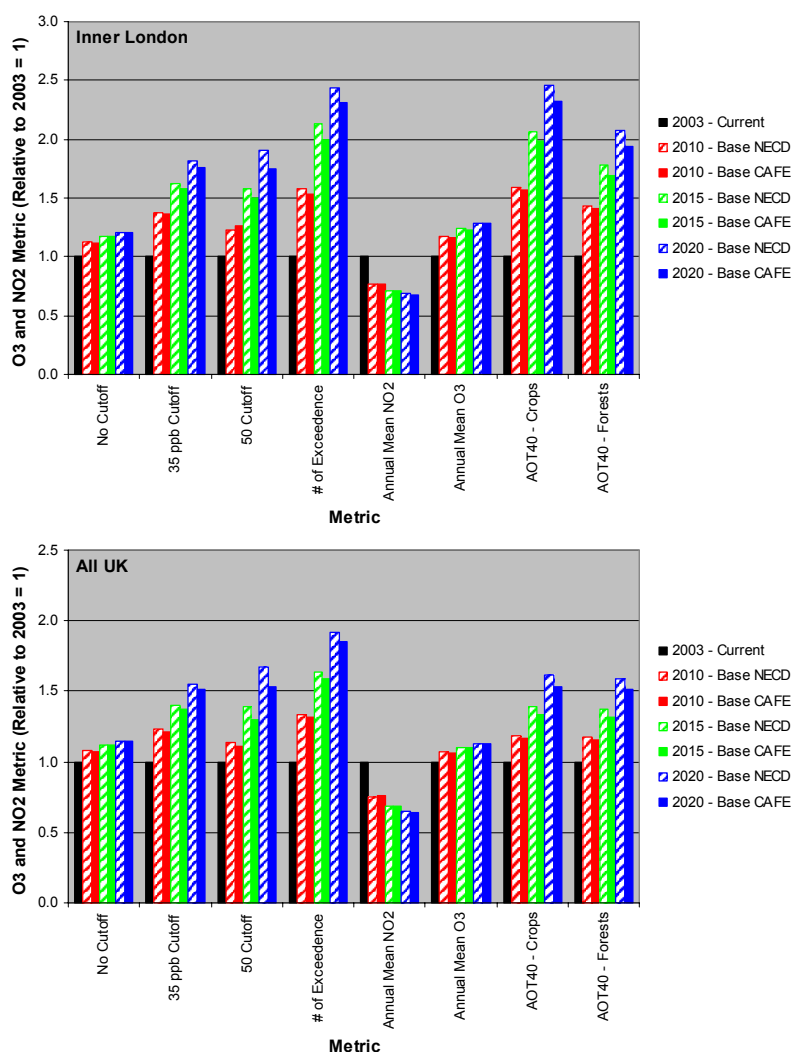


Figure 6.4 *The Sensitivity of the Different Ozone and Nitrogen Dioxide Metrics Calculated by the OSRM for the 2010, 2015 and 2020 Base Case Runs Relative to 2003 (=1) for Inner London (Upper Panel) and the UK (Lower Panel).*

Figure 6.4 shows the sensitivity of the different population and area-weighted ozone and nitrogen dioxide metrics for Inner London and the UK for the 2010, 2015 and 2020 base case runs (relative to 2003 metrics = 1) using these two emission projections.

The base case runs based on the NECD emission limits effectively used the same emission totals for 2010, 2015 and 2020 for all other European countries, whereas there was a progressive and comparable decline in the NO_x and VOC emissions in the CAFÉ projections. As noted earlier, the model runs using NECD emission projections for 2015 and 2020 give higher values, especially for the ozone metrics sensitive to peak ozone concentrations, than the corresponding model runs undertaken using the CAFÉ emission projections. The peak ozone concentrations are more likely to be associated with photochemical events (and 2003 was a photochemically-active year) and in this case the NO_x and VOC emission reductions are both likely to improve ozone air quality.

2. Changing Atmospheric Composition: The changes in atmospheric composition assumed will lead to higher ozone concentrations and hence a deterioration in ozone air quality. Sensitivity runs were undertaken for the CAFÉ emission projections for 2010 and 2020 with a current atmosphere (2003) and future atmospheric composition based on the business-as-usual scenario with climate change (see Section 6.4.1.5), as shown in Figure 6.5.

The model runs illustrated in Figure 6.5 differed in initial concentrations used for ozone and other key species. A ramp was applied to the initial ozone concentration, based on the monthly trends in ozone concentrations at Mace Head derived for a global business-as-usual scenario with climate change. The effect of this ramp was to change ozone concentrations from their 2003 values by -0.8 to +1.6 ppb in 2010 (depending on the month) and by -1.9 to +3.8 ppb in 2020.

It is interesting to note that the runs without climate change would have led to lower values of the O₃ metrics in both 2010 and 2020 for the UK for the annual mean of the maximum daily running 8-hour average ozone concentration with a 50 ppb (or 100 µg m⁻³) cut-off and the two AOT40 metrics. This is also seen in Figure 6.6, which shows the sensitivity of the different population and area-weighted ozone and nitrogen dioxide metrics for Inner London and the UK for the 2010 and 2020 base case runs, with and without changing atmospheric composition, relative to the 2003 current year (=1).

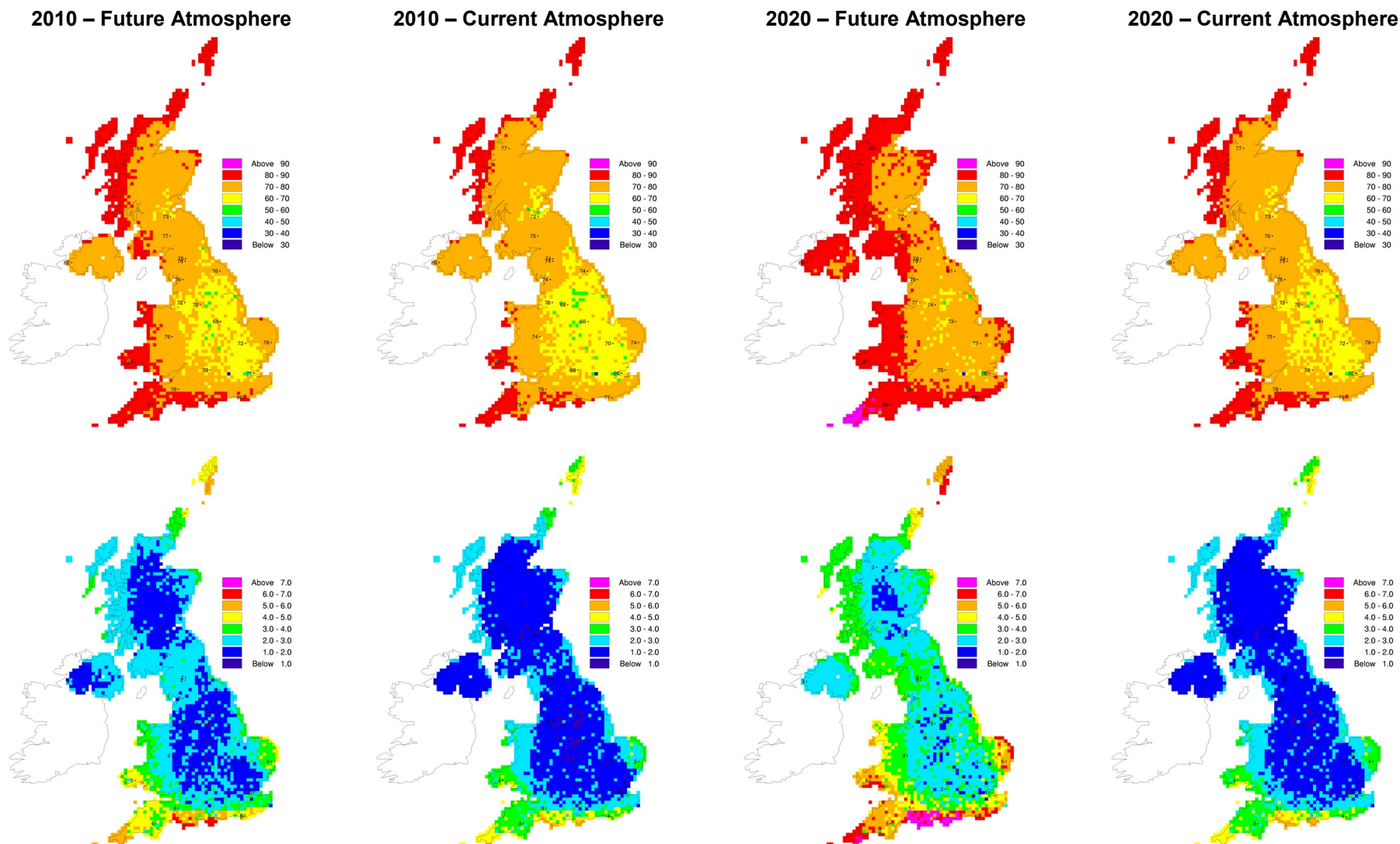


Figure 6.5 UK-scale Maps of generated from the OSRM Base Case Runs for 2010 and 2020 (with Future and Current Atmospheric Compositions) for the Metrics: Annual Mean of the Maximum Daily Running 8-hour Average Ozone concentration (i.e., with no cutoff) [Upper Panels] and Annual Mean of the Difference between the Maximum Daily Running 8-hour Average Ozone concentration and a 50 ppb (or 100 µg m⁻³) cutoff [Lower Panels].

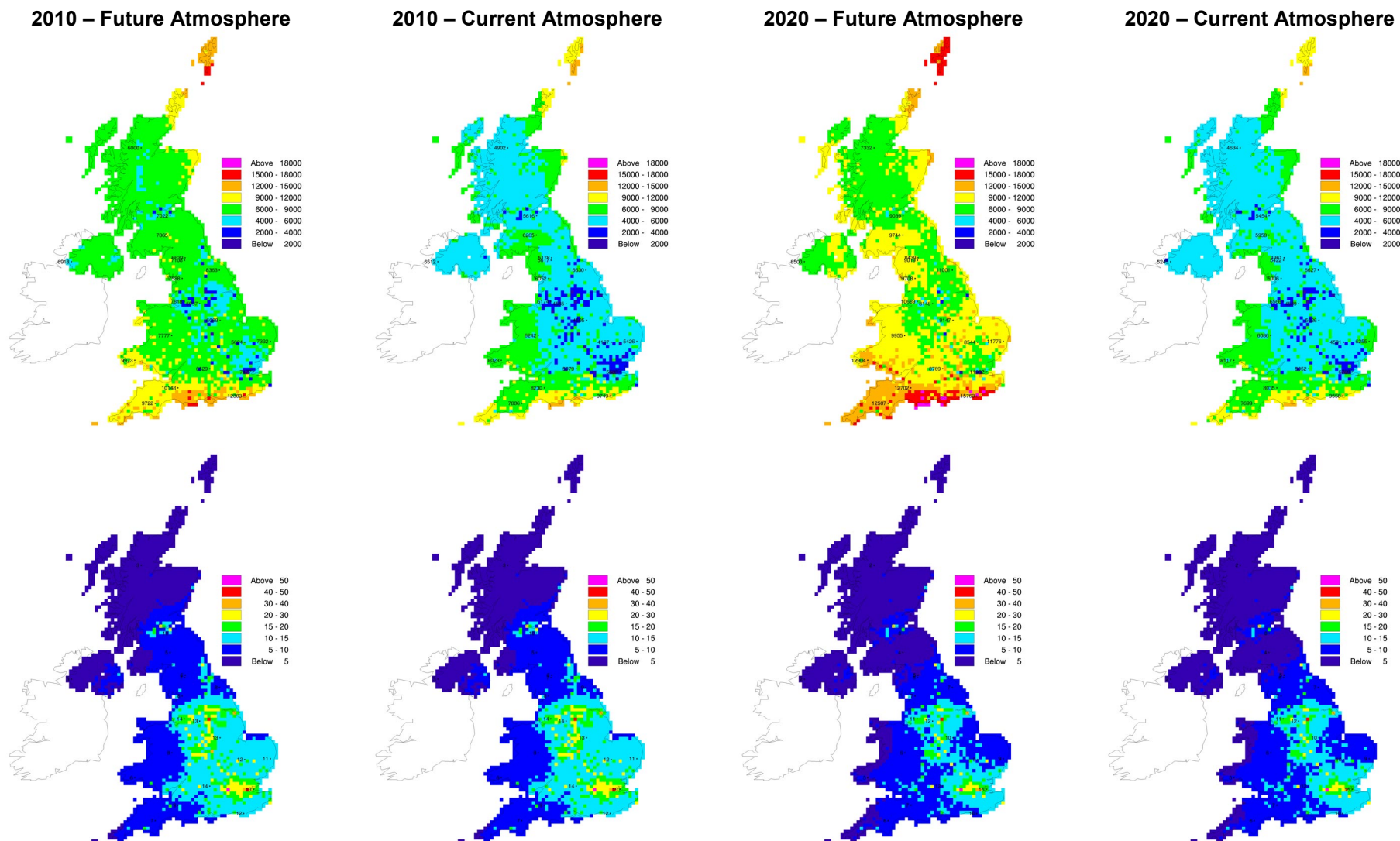


Figure 6.5 UK-scale Maps of generated from the OSRM Base Case Runs for 2010 and 2020 (with Future and Current Atmospheric Compositions) for the Metrics: AOT40 - Crops [Upper Panels] and Annual Mean Nitrogen Dioxide Concentration [Lower Panels].

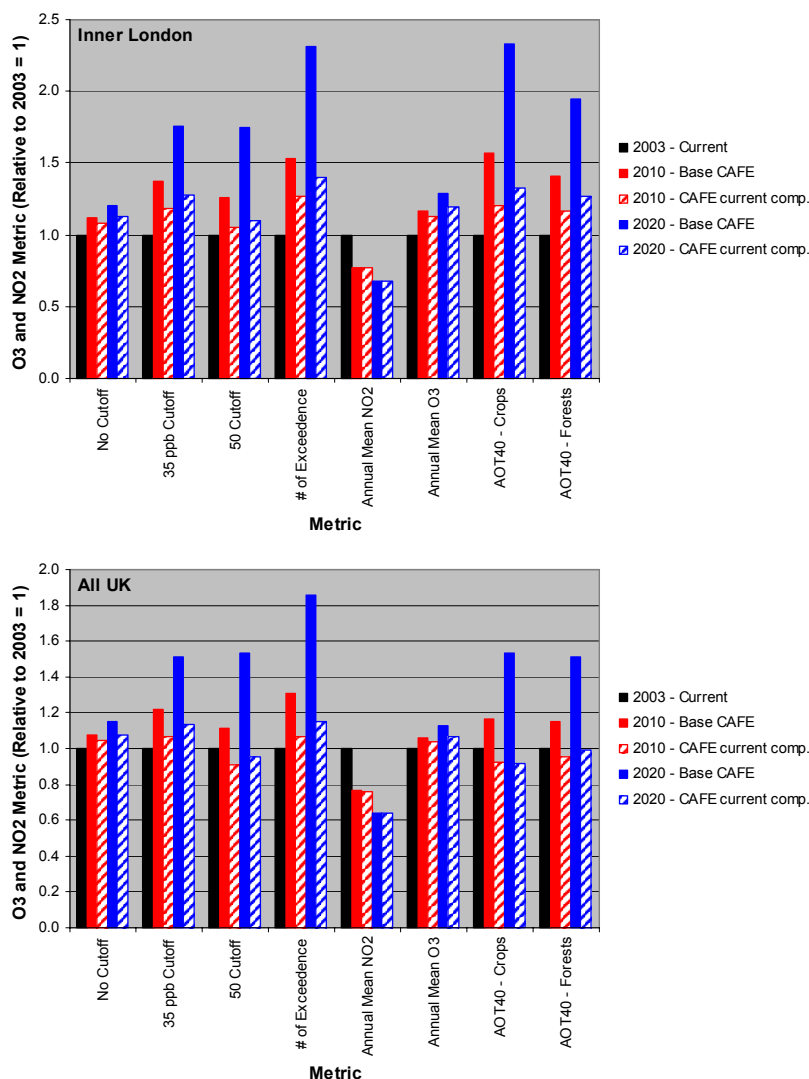


Figure 6.6 The Sensitivity of the Different Ozone and Nitrogen Dioxide Metrics Calculated by the OSRM for the 2010 and 2020 Base Case Runs (With and Without Changing Atmospheric Composition) Relative to 2003 (=1) for Inner London (Upper Panel) and the UK (Lower Panel).

There are significant and increasing differences for the ozone metrics between the runs undertaken with the current atmospheric composition and a future atmospheric composition based on the business-as-usual scenario with climate change. The greatest differences occur for the ozone metrics with an exceedence of a threshold, *i.e.*, annual mean of the maximum daily running 8-hour average ozone concentration with a 35 ppb (or 70 $\mu\text{g m}^{-3}$) or 50 ppb (or 100 $\mu\text{g m}^{-3}$) cut-off, the number of days when the maximum of the 24 possible 8-hour running mean concentrations in each day exceeds 100 $\mu\text{g m}^{-3}$ and the two AOT40 metrics. There is little effect on the annual mean NO₂ concentrations between the runs with and without a changing atmospheric composition.

6.4.2.3 Scenario Runs

NO_x Emission Control Measures

The OSRM (v2.2a with surface conversion algorithm) was used to model the impact on ozone concentrations across the UK of selected road transport and other NO_x abatement measures (Measures A, B, C, E, J and L) and of combinations of these measures (Measures K & L, O, P and Q). Table 6.12 provided information on the total UK NO_x emissions for the selected measures for 2010, 2015 and 2020. The complete set of the ozone and nitrogen dioxide metrics calculated by the

OSRM for the current year, base case and scenario runs are given in Appendix 2 (and Appendix 4 of Hayman *et al.* [2005b]). An example of the output is shown in Table 6.15.

Figure 6.7 shows the fractional response (relative to the corresponding base case =1) of the ozone and nitrogen dioxide metrics for the 2010 and 2020 base case and scenario runs for the UK and Inner London. As the emission controls of the measures are generally small compared to the changes in the base case emissions from the current year to 2010 and beyond, there is an overall progressive increase in all of the ozone metrics (*i.e.*, a decline in ozone air quality). There is a significant shift in the impact of the different NO_x measures between 2010 and 2020, reflecting the large effect of the short-term component of Measure K.

As the emissions of oxides of nitrogen have been reduced in these measures, there is generally a progressive reduction in the annual mean NO₂ concentration from the current year to 2010 and beyond (*i.e.*, an improvement in NO₂ air quality). The annual mean NO₂ concentration follows the emission reductions in the different scenarios and the response is most often in the opposite sense to that of the ozone metrics.

The impacts of the selected measures are as follows:

- **Measure A - Introduction of EURO V/VI (Low Reduction Scenario):** There appears to be little, if any, change from the corresponding base case runs for all 8 metrics for the 2010 and 2015 model runs. This is not surprising given the relatively small reductions in the NO_x emissions. There is a slight change for the 2020 model runs, with an improvement in the annual mean nitrogen dioxide concentration and a general worsening of ozone air quality (*i.e.*, the ozone metrics have increased). The largest relative changes occur in London where the road transport NO_x emissions represent a higher proportion of the total emissions for the regions considered.
- **Measure B - Introduction of EURO V/VI (High Reduction Scenario):** There appears to be little, if any, change from the corresponding base case runs for all 8 metrics for the 2010 model run. This is again not surprising given the relatively small reductions in the NO_x emissions (2% on road transport emissions). There is a slightly larger change for the 2015 and 2020 model runs. The largest relative changes occur in London. There is an improvement in the annual mean nitrogen dioxide concentration and a worsening of ozone air quality (*i.e.*, the ozone metrics have increased). However, there are some ozone metrics (AOT40 – Crops), which show a decrease in 2020 for some regions, indicating that NO_x emission control leads not to an increase but a decrease in ozone concentrations.
- **Measure C – Early Uptake of EURO V/VI (Low Reduction Scenario):** This measure is an earlier implementation of Measure A and therefore has slightly larger NO_x emission reductions. As a result, the responses of the two Measures follow the same pattern with a slightly larger response for Measure C.
- **Measure E – Low Emission Vehicles:** This measure has relatively small but increasing emission reductions compared to the corresponding base case projection. The responses follow the usual pattern of improving air quality for nitrogen dioxide and a deterioration in ozone air quality. The 2010 runs show little difference from the base case run. There is a slightly larger response in 2020, reflecting the proportionately larger emission reductions.
- **Measure J - Domestic Combustion:** The emission reductions of this measure are relatively small, increasing from ~3 ktonne per annum in 2010 to 13 ktonne per annum (see Table 6.12). As a result, there appears to be little, if any, change from the corresponding base case run. The largest relative changes occur in London.
- **Measures K and L - Controls on Power Stations, Iron and Steel, Oil refineries and Small Combustion Plants:** Measure K has two components: a short-term component leading to significant emission reductions between 2010 and 2016 and a smaller, long-term component. As a result, this combination of measures differ from the other measures considered above as a significant uptake is expected by 2010 resulting in the largest emission reduction in 2010. Thus, these measures have the greater impact on the ozone metrics in 2010, as can be seen in Figure 6.7. The other measures become more effective in 2020.

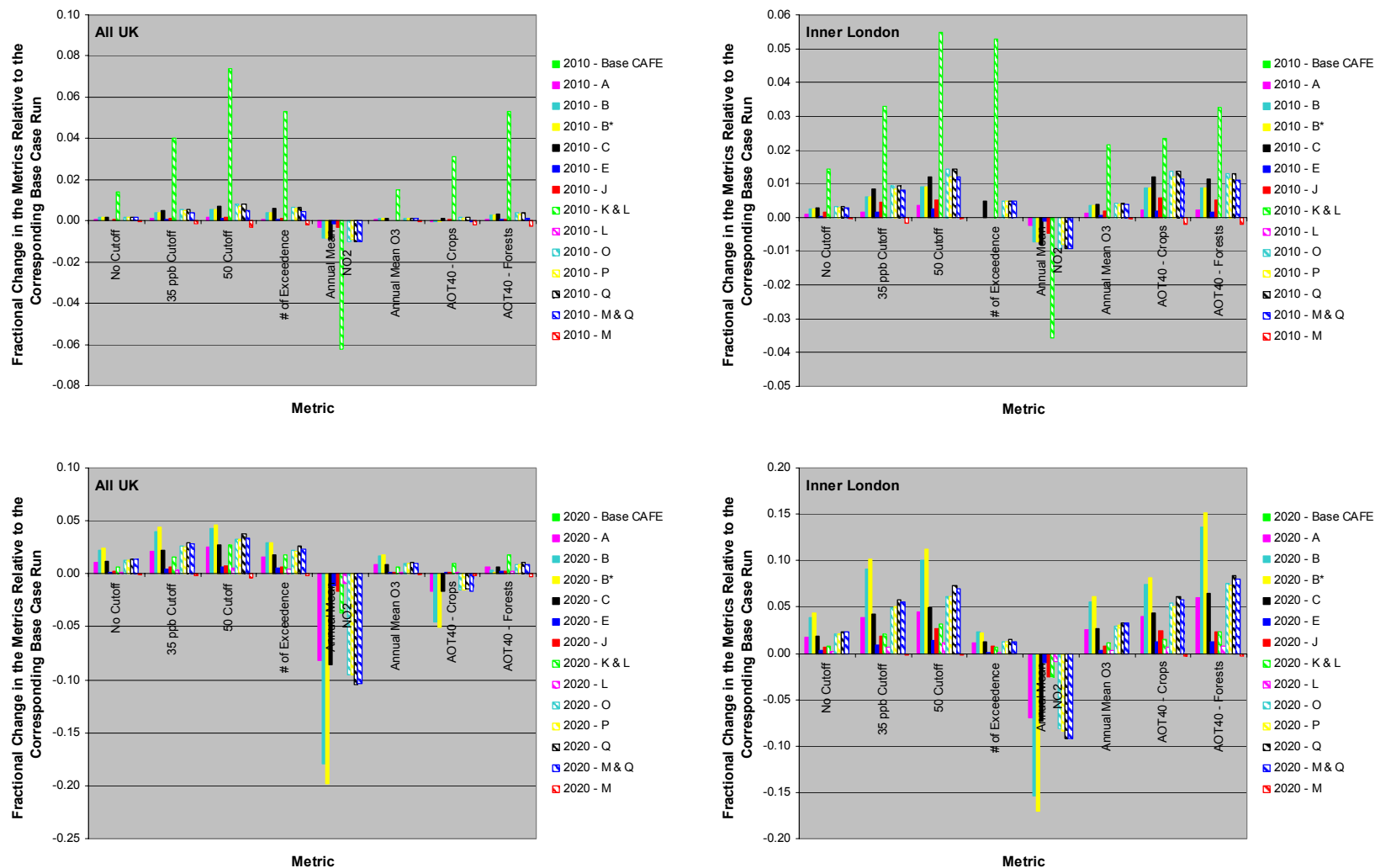


Figure 6.7 The Fractional Response of the Different Ozone and Nitrogen Dioxide Metrics Calculated by the OSRM for the Base Case and Scenario Runs for the UK (Left-hand Panels) and Inner London (Right-hand Panels) in 2010 (Upper Panels) and 2020 (Lower Panels).

- **Measure L - Controls on Small Combustion Plants:** As this measure is implemented after 2010, there is no difference from the 2010 base case. The emission reductions of this measure are relatively small, ~16-17 ktonne per annum in 2015 and 2020 (see Table 6.12). As a result, there appears to be little, if any, change from the corresponding base case run. The largest relative changes occur in London.
- **Measure O (Combination of Measures C and E):** The emission reduction in this combination of road transport NO_x measures is dominated by those of Measure C. As a result, the response of the different ozone and nitrogen dioxide metrics for this combination of measures is very similar to, but slightly larger than, that of Measure C.
- **Measure P (Combination of Measures C and L):** As Measure L (NO_x reduction from small combustion plant) is only implemented after 2010, the response of the ozone and nitrogen dioxide metrics in 2010 are the same as those for Measure C. After 2010, Measure L provides a further abatement of 13 ktonne per annum. As a result, the response of the different ozone and nitrogen dioxide metrics for this combination of measures is similar to, but larger than, that of Measure C and also of Measure O.
- **Measure Q (Combination of Measures C, E and L):** As Measure L (NO_x reduction from small combustion plant) is only implemented after 2010, the response of the ozone and nitrogen dioxide metrics in 2010 are the same as those for Measure O and similar to that of Measure C. After 2010, Measure L provides a further abatement of 13 ktonne per annum. As a result, the response of the different ozone and nitrogen dioxide metrics for this combination of measures is similar to, but larger than, that of Measure P and also of Measures C and O.

Ranking the measures in terms of increasing response, the order would be:

All UK – 2010 (Note 1):	Base Case < E < A ~ J < B < C = P < O = Q < K & L
All UK - 2020:	Base Case < L < E < J < K & L < A < C < O ~ P < Q < B
Inner London – 2010 (Note 1)	Base Case < E < A ~ J < B < C = P < O = Q < K & L
Inner London - 2020	Base Case < L < E < J < K & L < A < C < O ~ P < Q < B

Note 1: Measure L is implemented after 2010.

Clearly, the ordering reflects the relative emission reductions of the different measures in 2010 and 2020 and their spatial distribution. For both Inner London and the UK as a whole, the industrial measures have the larger impact in 2010 but the road transport measures have the larger impact for the 2020 model runs.

VOC Emission Control Measures

The OSRM was also used to model the impact on ozone concentrations across the UK of a VOC abatement measure (Measure M) and a combination of VOC and NO_x abatement measures (Measures M and Q). Table 6.12 provided information on the total UK NO_x and VOC emissions for the measures for 2010, 2015 and 2020. The complete set of the ozone and nitrogen dioxide metrics calculated by the OSRM for the current year, base case and scenario runs are given in Appendix 2 (and Appendix 4 of Hayman *et al.* [2005b]). An example of the output is shown in Table 6.15.

Figure 6.7 shows the fractional response (relative to the corresponding base case =1) of the ozone and nitrogen dioxide metrics for the 2010 and 2020 base case and scenario runs for the UK and Inner London. As the VOC emission controls in Measure M are based on specific sectoral activities with localised emissions, separate maps of VOC emissions from petrol stations and on and offshore loading of crude oil were created for 2010 and adjusted to produce the corresponding maps for 2015 and 2020. Consistent with previous work, VOC emission control led to an improvement in all the ozone metrics considered (*i.e.*, an improvement in ozone air quality) compared to the corresponding base case. The improvements in ozone air quality over the base case run were modest. This reflects the relatively small emission changes and the specific regions where the VOC emissions were controlled. There is little or no effect on the annual mean NO₂ concentration of the VOC control measure. As the emission controls of the measures are generally small compared to the changes in the base case emissions from the current year to 2010 and beyond, there is an overall progressive

increase in all of the ozone metrics (*i.e.*, a decline in ozone air quality). The VOC emission reductions in Measure M do not offset this overall decline.

As for Measure M, the combination of NO_x and VOC control measures (M and Q) gave a similar small improvement in ozone air quality compared to the corresponding set of measures without the VOC control (*i.e.*, Measure Q). The improvement does not offset the effects of the NO_x emission reductions in this combination of measures, which led to poorer ozone air quality (*i.e.*, increases in the ozone metrics) compared to the corresponding base case and Measure M runs. Again, there does not appear to be any notable regional variations.

Two sets of additional model runs were undertaken to assess the response of Measure M. The first set of model runs used the same overall reduction in UK VOC emissions achieved by Measure M (~9% excluding the natural contribution) but assumed that the emission reduction was spread equally across all the UK non-natural OSRM source sectors. Model runs were undertaken for 2010, 2015 and 2020 and only UK VOC emissions were affected. The second set of runs applied the same emission reduction to the European VOC emissions as well. Figure 6.8 shows the response and fractional response of the AOT40 – Forests metric for the UK.

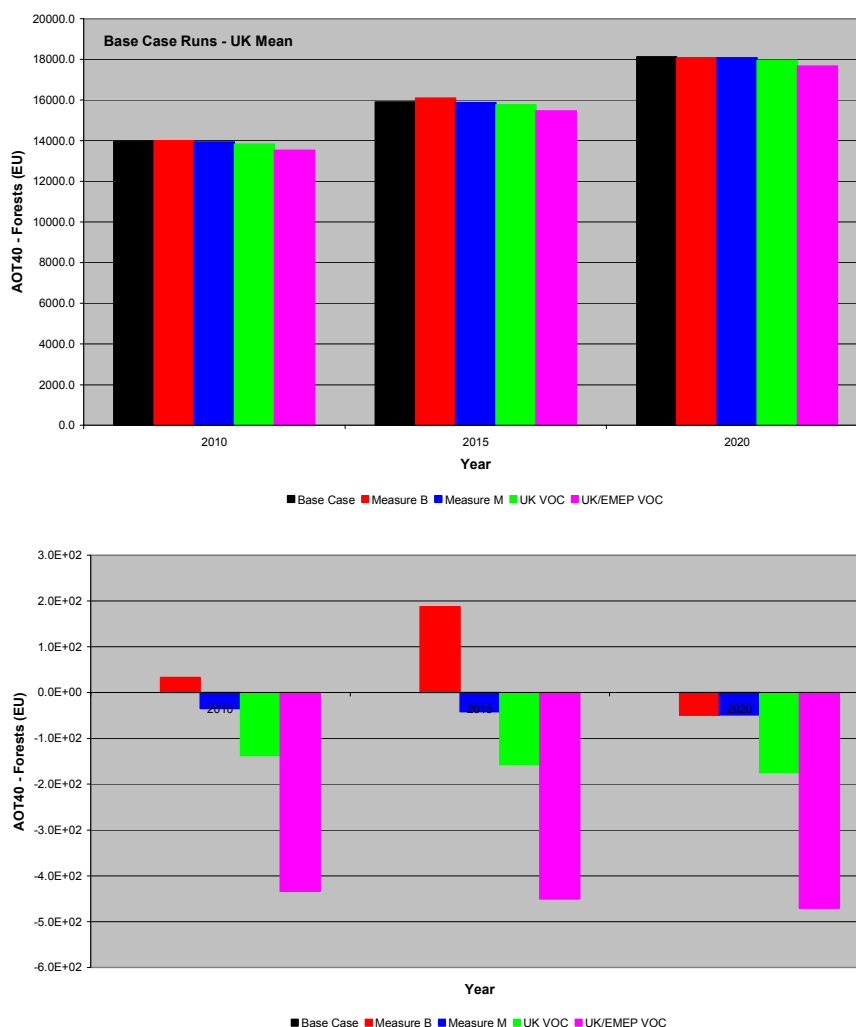


Figure 6.8 The Response (Upper Panel) and Fractional Response (Relative to Base Case =1, Lower Panels) of the AOT40 – Forests Metric Calculated by the OSRM for the Base Case and Scenario Runs for the UK.

Included in the figure is the response for Measure B for comparison. The results show that the response of Measure M is smaller than the response for an equivalent across-the-board emission reduction. The spatial location of the emission sources is significant. As expected, there is a larger response when both UK and European VOC emissions are controlled. It is also interesting to note

that the sign of the response changes for the NO_x emission reductions of Measure B between 2015 and 2020.

6.4.2.4 Sensitivity to Meteorology

The base case and scenario model runs have used the meteorology for 2003. The highest UK temperature was recorded in 2003 and it was a photochemically-active year with major several episodes of elevated ozone concentrations, especially in South-East England, in July and August (see Section 2.4). It could therefore become a typical ozone year in the future as a result of climate change. Sensitivity runs were undertaken using meteorology for 2002 (a current typical ozone year) and 2000 (a low ozone year, considering the headline air quality indicator). The model runs used the same emission scenarios.

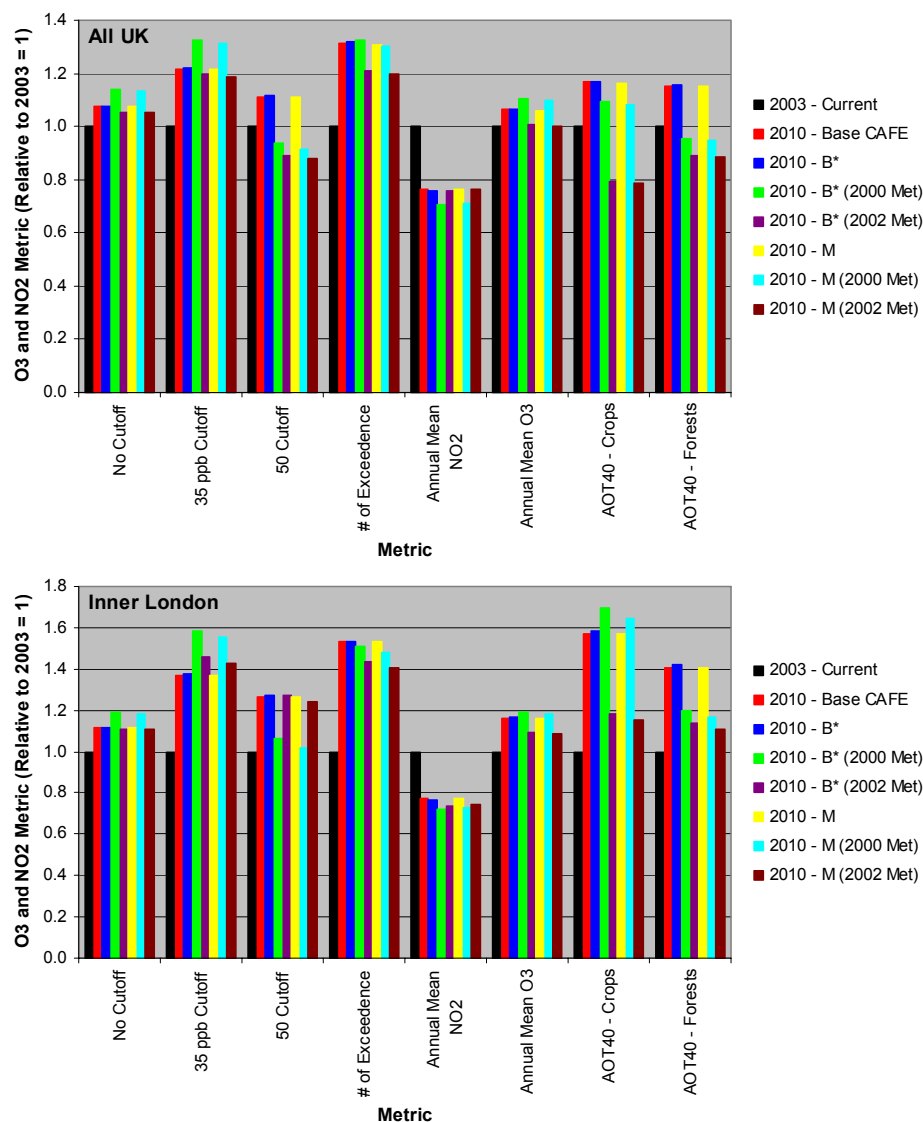


Figure 6.9 The Sensitivity of Different Ozone and Nitrogen Dioxide Metrics Calculated by the OSRM for Various Current and Future Base Case and Scenarios Runs to Meteorology for the UK (Upper Panel) and Inner London (Lower Panel).

Figure 6.9 shows the sensitivity of the different O₃ and NO₂ metrics to meteorology for Inner London and the UK for Measures B* (an earlier version of Measure B) and M. For the UK as a whole (see upper panel of Figure 6.9), 2003 gave the highest values of the following ozone metrics: Annual Mean of the Difference between the Maximum Daily Running 8-hour Average Ozone concentration and a 50 ppb (or 100 $\mu\text{g m}^{-3}$) cutoff, the Number of Days when the maximum of the 24 possible 8-hour running mean concentrations in each day exceeds 100 $\mu\text{g m}^{-3}$, AOT40 – Crops and AOT40 – Forests. These

metrics are sensitive to elevated peak ozone concentrations and also extended photochemical episodes such as those that occurred in July and August 2003. Clearly, the meteorology in 2000, 2002 and 2003 will undoubtedly affect the trajectories, emission history and chemical evolution of the air masses arriving at the OSRM receptor sites.

The ozone metrics calculated for Inner London (see lower panel of Figure 6.9) show more variation and do not follow the same pattern as for the UK. There are some interesting features, in that the 2000 meteorology gave the higher value of the metric, AOT40 for crops, whereas the 2003 meteorology gave the higher values for the metric, AOT40 – Forests. As these metrics accumulate ozone concentrations for different times of the year, the results indicate the differing levels and distributions of photochemical activity and model performance for the years, 2000, 2002 and 2003.

A further observation to make is that the ozone metrics show (a) as much sensitive to meteorology as to the emission changes in the runs between 2000 and 2010 and (b) greater sensitivity to meteorology than to the changes associated with the emission reductions of Measures B and M. The annual mean nitrogen dioxide concentration is less sensitive than the ozone metrics to meteorology. Again, the sensitivity of the annual mean nitrogen dioxide concentration to meteorology is as great as the emission changes associated with the measures.

6.4.3 Comparison with Air Quality Objectives

The Air Quality Strategy, the EU 3rd Daughter Directive and the UN ECE define air quality objectives and target values for ozone for the protection of human health and ecosystems, as shown in Table 6.16. This table also includes limit values, objective and target values for nitrogen dioxide.

Table 6.16 Air Quality Limit Values, Objectives and Target Values for O₃ and NO₂.

Metric	Limit Value/ Objective/Target	Limit Value/ Objective/Target
Annual mean ozone concentration (materials)		40 µg m⁻³
AOT30 – crops (ecosystems)	UN ECE	8,000 µg m ⁻³ hours
AOT40 – crops (ecosystems)	3DD LTO	6,000 µg m⁻³ hours
AOT40 – crops (ecosystems)	3DD Target Value	18,000 µg m⁻³ hours
AOT40 – forests (ecosystems)	UN ECE	20,000 µg m⁻³ hours
AOT60 (human health)	UN ECE	5,800 µg m⁻³ hours
Number of days when the daily maximum running 8-hour mean ozone concentration > 100 µg m⁻³ (human health)	Air Quality Strategy Objective	10
Number of days when the daily maximum running 8-hour mean ozone concentration > 100 µg m ⁻³ (human health)	EPAQS	0
Number of days when the daily maximum running 8-hour mean ozone concentration > 120 µg m⁻³ (human health)	3DD Target Value	25
Number of days when the daily maximum running 8-hour mean ozone concentration > 120 µg m ⁻³ (human health)	3DD LTO	0
Annual mean nitrogen dioxide concentration (human health)	Limit Value/ Air Quality Strategy Objective	40 µg m⁻³
Annual mean NO _x concentration (ecosystem)	Limit Value/ Air Quality Strategy Objective	30 µg m ⁻³
Number of hours when the hourly nitrogen dioxide concentration > 200 µg m⁻³ (human health)	Limit Value/ Air Quality Strategy Objective	18

Table 6.17 summarises the number of 10 km x 10 km grid squares where the objective or target value for the metrics highlighted in bold are exceeded. There are 2,946 grid squares in total. The total shows that there are widespread exceedences of the objectives and target values for (a) annual mean O₃ concentrations, (b) AOT40 - Crops (long-term objective) and (c) the number of days when the daily maximum running 8-hour average ozone concentration exceeds 100 µg m⁻³ is greater than zero or 10 (not shown for no exceedences as almost all the grid squares have one or more exceedences).

The response to the different emission control and sensitivity runs gives a similar picture to that described earlier.

Table 6.17 Number of OSRM 10 km x 10km Grid Squares which have Exceedences of the O₃ or NO₂ Air Quality Objective or Target Value.

Run	Metric	Annual Mean O ₃ Concentration	AOT40 - Crops	AOT40 - Crops	AOT40 - Forests	AOT60	# of days when the daily maximum running 8-hour mean O ₃ concentration > 100 µg m ⁻³	Number of days when the daily maximum running 8-hour mean O ₃ concentration > 120 µg m ⁻³	Annual Mean NO ₂ Concentration	# of hourly NO ₂ concentrations > 200 µg m ⁻³
	Objective	40 µg m ⁻³	6000 µg m ⁻³ hr	18000 µg m ⁻³ hr	20000 µg m ⁻³ hr	5800 µg m ⁻³ hr	10	25	40 µg m ⁻³	18
1999 – Current Year		2921	1319	0	46	0	2936	141	6	0
2000 – Current Year		2928	1796	0	23	3	2928	119	3	0
2001 – Current Year		2902	1308	0	0	0	2940	75	3	0
2002 – Current Year		2905	379	0	21	0	2917	64	2	0
2003 – Current Year		2920	1862	0	134	2	2936	166	4	43
2010 – NECD Projections		2943	2645	0	239	1	2943	270	3	17
2010 – CAFE Projections		2941	2611	0	215	0	2943	232	3	17
2010 – CAFE Projections - Current Atmospheric Composition		2939	1175	0	70	0	2940	91	3	14
2010 – Measure(s) A (CAFE Projections)		2941	2609	0	214	0	2943	235	3	17
2010 – Measure(s) B (CAFE Projections)		2942	2613	0	214	0	2943	238	3	17
2010 – Measure(s) B* (CAFE Projections)		2942	2617	0	214	0	2943	235	3	16
2010 – Measure(s) C (CAFE Projections)		2941	2612	0	215	0	2943	232	3	16
2010 – Measure(s) E (CAFE Projections)		2943	2733	0	278	0	2944	307	2	17
2010 – Measure(s) J (CAFE Projections)		2941	2611	0	215	0	2943	232	3	17
2010 – Measure(s) K & L (CAFE Projections)		2941	2611	0	215	0	2943	232	3	17
2010 – Measure(s) L (CAFE Projections)		2942	2621	0	214	0	2943	235	3	17
2010 – Measure(s) O (CAFE Projections)		2942	2621	0	214	0	2943	235	3	17
2010 – Measure(s) P (CAFE Projections)		2942	2617	0	214	0	2943	235	3	16
2010 – Measure(s) Q (CAFE Projections)		2942	2613	0	214	0	2943	238	3	17
2010 – Measure(s) M and Q (CAFE Projections)		2941	2612	0	214	0	2943	233	3	17
2010 – Measure(s) M (CAFE Projections)		2940	2608	0	211	0	2943	230	3	17
2010 – Measure B* (CAFE Projections)		2942	2613	0	214	0	2943	238	3	17
2010 – Measure B* (CAFE Projections) + 2000 Meteorology		2943	1944	0	88	0	2943	116	1	0
2010 – Measure B* (CAFE Projections) + 2002 Meteorology		2941	688	0	45	0	2942	91	2	0
2010 – Measure M (CAFE Projections)		2940	2608	0	211	0	2943	230	3	17
2010 – Measure M (CAFE Projections) + 2000 Meteorology		2943	1917	0	77	0	2943	109	1	0
2010 – Measure M (CAFE Projections) + 2002 Meteorology		2941	680	0	43	0	2942	81	2	0

Note: A total of 2,946 10 km x 10 km grid squares were used in the OSRM model runs.

Table 6.17 Number of OSRM 10 km x 10km Grid Squares which have Exceedences of the O3 or NO2 Air Quality Objective or Target Value.
(Continued)

Run	Metric	Annual Mean O ₃ Concentration	AOT40 - Crops	AOT40 - Crops	AOT40 - Forests	AOT60	# of days when the daily maximum running 8-hour mean O ₃ concentration > 100 µg m ⁻³	Number of days when the daily maximum running 8-hour mean O ₃ concentration > 120 µg m ⁻³	Annual Mean NO ₂ Concentration	# of hourly NO ₂ concentrations > 200 µg m ⁻³
	Objective	40 µg m ⁻³	6000 µg m ⁻³ hr	18000 µg m ⁻³ hr	20000 µg m ⁻³ hr	5800 µg m ⁻³ hr	10	25	40 µg m ⁻³	18
2015 - NECD Projections	2944	2863	2	527	29	2945	483	3	10	
2015 - CAFE Projections	2944	2843	1	449	4	2945	420	3	9	
2015 - Measure(s) A (CAFE Projections)	2944	2851	0	466	7	2945	428	3	9	
2015 - Measure(s) B (CAFE Projections)	2944	2855	0	484	14	2945	439	2	6	
2015 - Measure(s) B* (CAFE Projections)	2944	2854	0	472	8	2945	429	3	8	
2015 - Measure(s) C (CAFE Projections)	2944	2846	1	452	4	2945	422	3	9	
2015 - Measure(s) E (CAFE Projections)	2944	2868	1	542	18	2945	464	1	9	
2015 - Measure(s) J (CAFE Projections)	2944	2845	1	456	4	2945	422	3	10	
2015 - Measure(s) K & L (CAFE Projections)	2944	2845	1	452	4	2945	422	3	10	
2015 - Measure(s) L (CAFE Projections)	2944	2856	0	472	8	2945	428	3	8	
2015 - Measure(s) O (CAFE Projections)	2944	2859	0	476	9	2945	430	2	6	
2015 - Measure(s) P (CAFE Projections)	2944	2856	0	475	9	2945	430	2	8	
2015 - Measure(s) Q (CAFE Projections)	2944	2855	0	484	14	2945	439	2	6	
2015 - Measure(s) M and Q (CAFE Projections)	2944	2857	0	473	8	2945	428	1	8	
2015 - Measure(s) M (CAFE Projections)	2944	2842	1	443	4	2945	414	3	10	
2020 - NECD Projections	2944	2921	31	916	62	2945	770	2	10	
2020 - CAFE Projections	2944	2906	15	732	33	2945	646	2	9	
2020 - CAFE Projections - Current Composition	2943	1051	0	81	0	2943	81	2	8	
2020 - Measure(s) A (CAFE Projections)	2944	2915	7	752	41	2945	636	2	5	
2020 - Measure(s) B (CAFE Projections)	2945	2924	2	763	52	2945	578	2	4	
2020 - Measure(s) B* (CAFE Projections)	2945	2915	7	756	41	2945	638	2	4	
2020 - Measure(s) C (CAFE Projections)	2944	2909	15	738	35	2945	648	2	9	
2020 - Measure(s) E (CAFE Projections)	2945	2911	16	788	38	2945	673	2	9	
2020 - Measure(s) J (CAFE Projections)	2944	2907	15	739	36	2945	648	2	10	
2020 - Measure(s) K & L (CAFE Projections)	2944	2909	14	740	36	2945	647	2	8	
2020 - Measure(s) L (CAFE Projections)	2945	2918	7	762	42	2945	643	2	5	
2020 - Measure(s) O (CAFE Projections)	2945	2918	7	768	43	2945	644	1	5	
2020 - Measure(s) P (CAFE Projections)	2945	2917	7	764	42	2945	643	1	5	
2020 - Measure(s) Q (CAFE Projections)	2945	2921	2	765	51	2945	579	2	5	
2020 - Measure(s) M and Q (CAFE Projections)	2945	2918	7	762	42	2945	639	1	6	
2020 - Measure(s) M (CAFE Projections)	2944	2906	15	718	32	2945	640	2	9	

Note: A total of 2,946 10 km x 10 km grid squares were used in the OSRM model runs.

6.4.4 Calculation of Benefits

The population- and area-weighted means of the ozone metrics were passed to the teams involved in the cost-benefit analysis being carried out for the Review of the Air Quality Strategy [AQS, 2005; IGCP, 2005]. Three of the ozone metrics [metric (a), (b) and (c) below] were used to assess the benefits/disbenefits to human health of the measures modelled by the OSRM. Another three of the metrics [metrics (f), (g) and (h) below] were used to assess the non-health benefits/disbenefits for materials, crops and vegetation.

6.4.5 Summary

The Ozone Source-receptor model has been used to determine ozone air quality for future years and to assess the effectiveness of control measures on ozone precursor emissions (NO_x and VOC emissions) being considered for the Review of the Air Quality Strategy.

Population-weighted means were derived for the metrics associated with impacts on human health. Area-weighted means were derived for the non-health effects metrics. The population- and area-weighted means have been determined for the following regions: All UK, Scotland, Wales, Northern Ireland, Inner London, Outer London and the Rest of England.

The key points to note from the model runs are that:

- The base case runs show a progressive worsening of ozone air quality for all metrics from 2003 to 2010 and beyond;
- There is however an improvement in nitrogen dioxide air quality as annual mean concentrations fall, especially for the NO_x control measures;
- The use of population-weighted means focuses the analysis on ozone in urban areas. In addition to the role of NO_x emissions in photochemical ozone production, lower NO_x emissions reduce the chemical titration effect, most notably in urban areas. This causes ozone concentrations to move towards the higher concentrations in surrounding rural areas. The reduced chemical titration is a major factor in the increase in the ozone metrics and the deterioration of ozone air quality;
- A second major factor leading to higher ozone concentrations is changing atmospheric composition arising from climate change. In the absence of such a change, the base case runs would have shown an improvement in ozone air quality for some metrics (AOT40 – Crops and AOT40 – Forests);
- The NO_x control measures generally increase ozone concentrations, although there are instances for some of the measures that ozone air quality is improved in 2020, as evidenced by a lower value of the ozone metric;
- The VOC control measures, on the other hand, lead to an improvement in ozone air quality for all ozone metrics;
- Meteorological effects and year-to-year variability in meteorology can have a larger effect on ozone air quality than some of the emission control measures considered.

As a result of the above, there will be widespread exceedences of ozone air quality standards and objectives in 2010 and beyond.

7 Ozone Daughter Directive (Objective 3b)

7.1 INTRODUCTION

The Air Quality Assessment and Management Framework Directive [EC, 1996] provides a mechanism to establish limit values or target values for specified ambient air pollutants within the EU. The 3rd Daughter Directive [EC, 2002b] sets target values and long-term objectives for ozone using the following metrics:

- Number of days above $120 \mu\text{g m}^{-3}$ in 2003
- Number of days above $120 \mu\text{g m}^{-3}$ between 2001-2003
- AOT40 wheat crops in 2003
- AOT40 wheat crops between 1999-2003

Under Article 5 of The Framework Directive, a requirement has been placed upon Member States to undertake a preliminary investigation of ambient air quality, prior to the implementation of the Daughter Directive relating to ozone. The objectives of this assessment are to establish estimates of the overall distribution and levels of ozone, and to identify additional monitoring requirements, which may be necessary in order to fulfil obligations in the Framework and 3rd Daughter Directive.

Monitoring of air quality in the UK is carried out through national networks of air quality monitoring stations (e.g., the Automatic Urban and Rural Networks and hydrocarbon networks). In addition, local authority funded monitoring activities operate throughout the UK, although in general, these are not combined with the national network. This report describes how the national monitoring networks are to be expanded to meet the requirements of the Framework Directive and 3rd Daughter Directive on ozone. This expansion will be achieved in many cases by the incorporation of local authority monitoring stations into the national network.

This section provides a brief summary of

- The Preliminary Assessment (Bush and Kent [2003])
- The Evaluation of Possible Supplementary Assessment Techniques (Targa and Bush [2005])
- The Supporting Document on the Supplementary Modelling for the Questionnaire on the 2004 Calendar Year (Bush, Traga and Stedman [2005])

7.2 PRELIMINARY ASSESSMENT

For the purpose of the preliminary assessment, levels of ozone throughout the UK were assessed using measurement data for 2001 from the UK's national Automatic Urban and Rural Networks (AURN). Information provided by this monitoring network has also been supplemented by high resolution empirical model outputs, based upon the techniques used by UK expert advisory groups [NEG-TAP, 2001] and developed by the Centre for Ecology and Hydrology [Coyle *et al.*, 2002]. The empirical model outputs have been used as a screening tool to inform on the general levels and distribution of ozone in locations with no monitoring. The models draw heavily upon measurement data from the UK's automatic urban and rural network (AURN), and are calibrated to these networks.

This approach, which combines highly accurate measured data and information from screening tools provides a comprehensive and consistent means of estimating pollutant concentrations throughout the whole of the UK. In order to check that the modelled exceedence statistics provided by this approach have not been systematically underestimated, a comparison with measured exceedence data for the 2000 calendar year has been performed at sites within the current AURN [Bush and Kent, 2003]. Agreement between modelled exceedences at each monitoring location and measured exceedence statistics is generally good.

The UK has been divided into 16 zones and 28 agglomerations (areas of urban population > 250,000). Measured and modelled ozone concentrations within each zone and agglomeration have been compared with the relevant long-term objectives and target values, defined in the 3rd Daughter Directive and summarised in Table 7.1 below. Areas requiring additional monitoring have been identified by an exceedence of the long-term objective and an examination of the coverage provided by the current automatic monitoring network of these areas. The number of additional monitoring sites required has been calculated from the population of the individual zones and agglomerations.

Table 7.1 Summary of Target Values and Long-term Objectives for Ozone under the 3rd Daughter Directive.

	Parameter	Target/Objective
1. Target value for the protection of human health for 2010	Maximum daily 8-hour mean	120 $\mu\text{g m}^{-3}$ not to be exceeded on more than 25 days per calendar year averaged over three years
2. Target value for the protection of vegetation for 2010	AOT40, calculated from 1h values from May to July	18,000 $\mu\text{g/m}^3\cdot\text{h}$ averaged over five years
1. Long-term objective for the protection of human health	Maximum daily 8-hour mean within a calendar year.	120 $\mu\text{g/m}^3$
2. Long-term objective for the protection of vegetation	AOT40, calculated from 1h values from May to July	6,000 $\mu\text{g/m}^3\cdot\text{h}$

Annex V of the 3rd Daughter Directive presents the minimum monitoring requirements assuming fixed monitoring as the sole source of information. However, Article 9 of the Directive also recognises the value of supplementary information sources (models, emissions inventories, indicative monitoring) and specifies that the overall monitoring burden can be reduced where such techniques are available, provided that;

1. Supplementary techniques provide adequate level of information for assessment of air quality in relation to target, information and alert thresholds.
2. The number of monitoring stations, in combination with other assessment techniques, fulfil the Data Quality Objectives (DQOs) outlined in Sections I and II of Annex VII of the Directive.
3. At least 1 monitoring station is deployed per 2,000,000 inhabitants of a zone or agglomeration, or 1 per 50,000 km^2 whichever results in the most sites.
4. Each zone/agglomeration has at least 1 monitoring station.
5. NO_2 is measured at all remaining monitoring stations except rural background locations.

Based on the availability of supplementary assessment techniques in the UK (the empirical maps of ozone presented in this report and the OSRM), it has been assumed that the minimum requirements laid out in Section I Annex V of the Directive are superseded by those presented by paragraphs 1 (a-e) of Article 9 and summarised in bullets 1-5 above.

7.2.1 Supplementary Information Techniques in the UK

The empirical model outputs presented in this report provide a useful screening tool for an assessment of the general levels and distribution of ozone. However it is recognised that the approach used by these models may over simplify the mechanisms effecting ozone levels and as a result may be subject to uncertainties that are as yet unquantified.

Ozone concentrations throughout the UK have been assessed using measurements from the AURN and modelled data at locations away from busy roads, which characterise urban and rural background conditions. Modelled estimates of ozone concentrations in 2001 have been derived using empirical models [Coyle, 2003] for both the maximum daily 8-hour mean and AOT40 metrics. Automatic monitoring data are incorporated into the empirical models used. Measured and modelled levels have been compared with the long-term objectives for ozone within each agglomeration and non-agglomeration zone within the UK. Where exceedence of a long-term objective was identified this triggered the requirement to monitor in each agglomeration and non-agglomeration zone. Exceedence of the target values have also been calculated for information only, exceedences of the target values do not impact on the monitoring required for compliance with the Directive.

- (a) Exceedences relative to Long-term Objectives: Maps showing measured and modelled exceedences of the long-term objectives have been compiled for the UK. Measurements and modelled concentrations are presented for non-roadside/kerbside locations. Figure 7.1 presents the measured and modelled estimates of the number of days exceeding the maximum daily 8-hour mean long-term objective for ozone ($120 \mu\text{g m}^{-3}$ as a maximum daily 8-hour mean). Figure 7.2 presents similar plots of measured and modelled values for the AOT40 long-term objective for the protection of vegetation and ecosystems.

Figure 7.2 shows that measured exceedence of the long-term objective for the protection of vegetation and ecosystems was widespread throughout England during 2001. A total of 23 monitoring station measured levels in excess of the AOT40 long-term objective ($6,000 \mu\text{g/m}^{-3}\cdot\text{h}$). Highest levels were measured in the South East at Teddington in London ($12,118 \mu\text{g m}^{-3} \text{ h}$), Lullington Heath ($11,580 \mu\text{g m}^{-3} \text{ h}$) and Rochester ($10,470 \mu\text{g m}^{-3} \text{ h}$). Figure 7.2 also presents the modelled AOT40 metric and indicates that zones and agglomerations in southern and eastern areas of England and Wales and eastern areas of Scotland are likely to have AOT40 levels in excess of the long-term objective for the protection of vegetation and ecosystems.

A single measured or modelled exceedence of either the long-term objective for the protection of human health or vegetation and ecosystems triggers a requirement to monitor ozone.

- (b) Exceedences relative to target values: The measured target values for the protection of human health and for the protection of vegetation and ecosystems are shown in Figure 7.3. Target value exceedences are based on an average number of exceedences per year, over 3 and 5-year period, for human health and vegetation/ecosystems protection respectively.

The target value for the protection of human health allows for no more than 25 exceedences of $120 \mu\text{g m}^{-3}$ (as a maximum daily running 8-hour mean) per calendar year (averaged over 3 years). Figure 7.3, presents the average number days exceeding $120 \mu\text{g m}^{-3}$ per year between 1999 and 2001 for background monitoring stations in the AURN. On average, levels were highest at Lullington Heath where $120 \mu\text{g m}^{-3}$ was exceeded on 13 days a year between 1999 and 2001. Levels of exceedence of this magnitude are well below the target value of 25 days.

Similarly, the measured data indicate that levels throughout the UK are below the target value for the protection of vegetation and ecosystems, as also illustrated by Figure 7.3. The highest 5-year average of AOT40 measured between 1997 and 2001 was also measured at Lullington Heath ($9,091 \mu\text{g m}^{-3} \text{ h}$), approximately 50% of the target value of $18,000 \mu\text{g m}^{-3} \text{ h}$.

7.2.2 Additional Monitoring Requirements

In Agglomerations

The minimum number of monitoring stations required within agglomerations defined by Annex V of the Daughter Directive on Ozone assumes that fixed monitoring is the sole source of information. Based on the guidance presented by Annex V and the exceedences of the long-term objective presented in Figure 7.1 and Figure 7.2, the minimum number of monitoring stations required in UK agglomerations, is presented in by the '*Minimum Number of Stations A*' statistic.

Article 9 of the Directive sets out the minimum monitoring requirement in agglomerations where supplementary sources of information on ozone levels are also available. Article 9 sets out a requirement within agglomerations of 1 co-located ozone and NO_x monitoring station per 2 million inhabitants, provided that other criteria are also met (see Section 7.2). Based on guidance provided by Article 9 and the exceedences of the long-term objective presented in Figure 7.1 and Figure 7.2, the minimum number of monitoring stations required in UK agglomerations is presented in Table 7.2 by the '*Minimum Number of Stations B*' statistic. All monitoring must be located at urban background or suburban locations, away from major emissions sources, which may be expected to effect ozone levels.

Table 7.2 identifies the agglomeration zones with measured or modelled exceedences of the long-term objectives. Additional monitoring required for agglomerations with exceedences of the long-term objectives have been calculated based on the population of the agglomeration and coverage from the monitoring network as of January 2003.

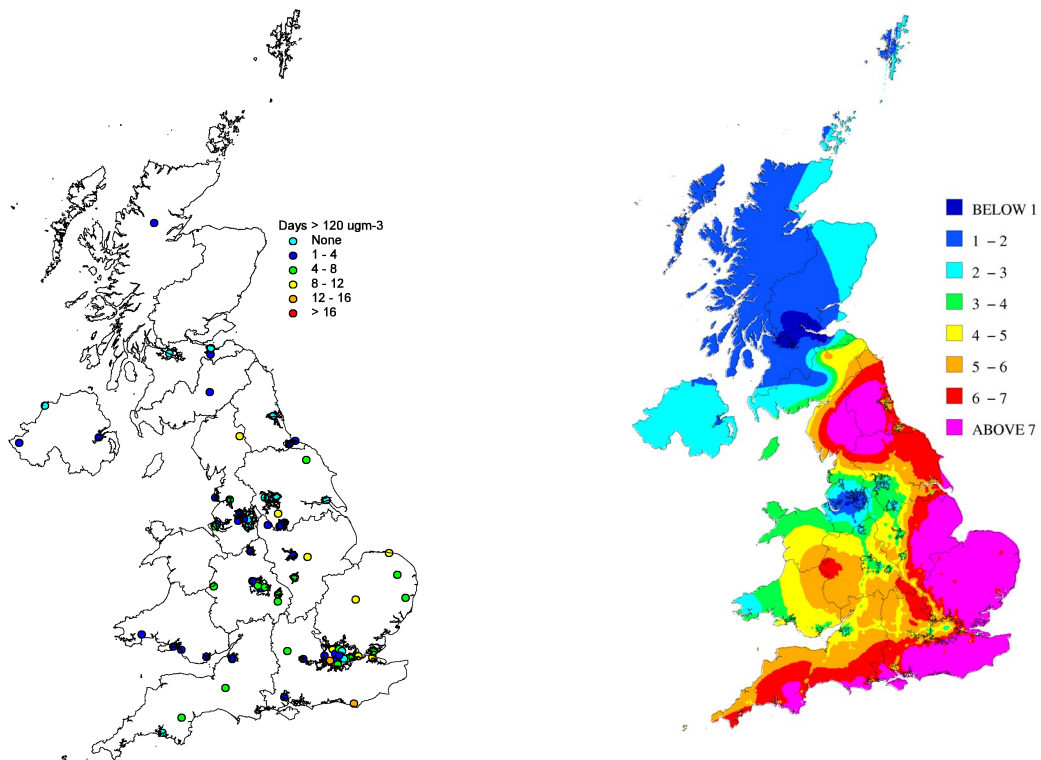


Figure 7.1 Measured (at all non-roadside/kerbside sites in UK, left-hand panel) and Modelled (right-hand panel) Long-term Objectives for the Protection of Human Health (Days > 120 $\mu\text{g m}^{-3}$ as a Maximum Daily 8-hour mean) in 2001.

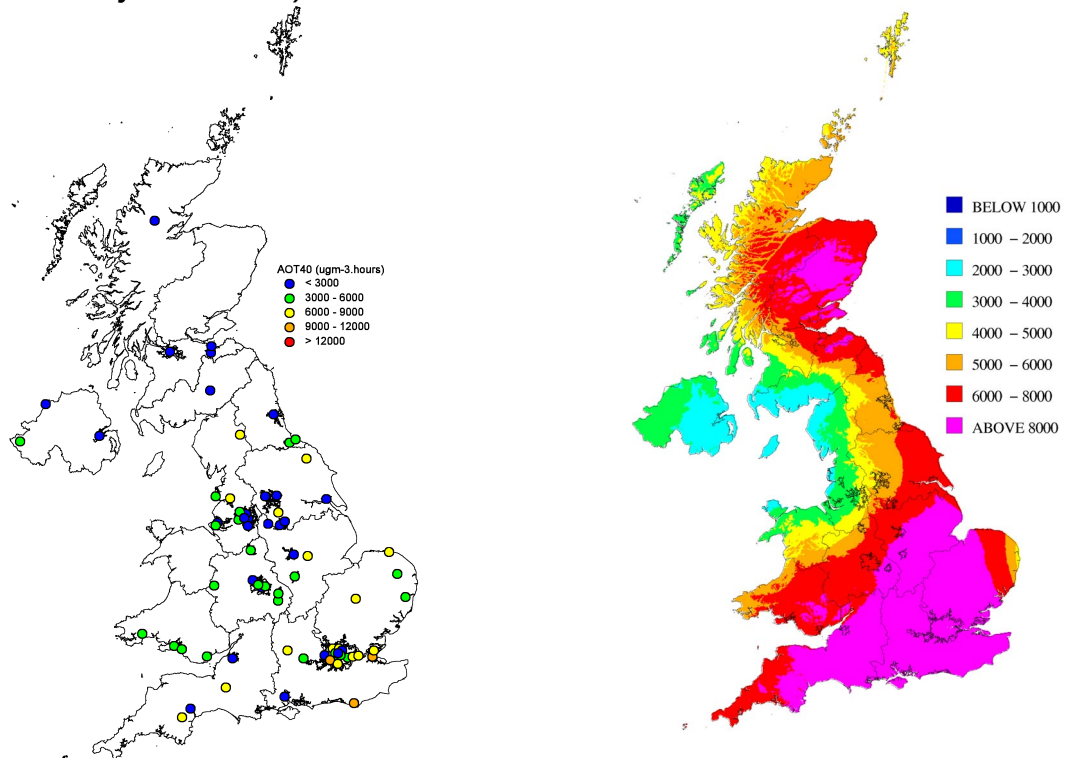


Figure 7.2 Measured (at all non-roadside/kerbside sites in UK, left-hand panel) and Modelled (right-hand panel) Long-term Objectives for the Protection of Vegetation and Ecosystems in 2001 (AOT40 $\mu\text{g m}^{-3} \cdot \text{hours}$) for 2001.

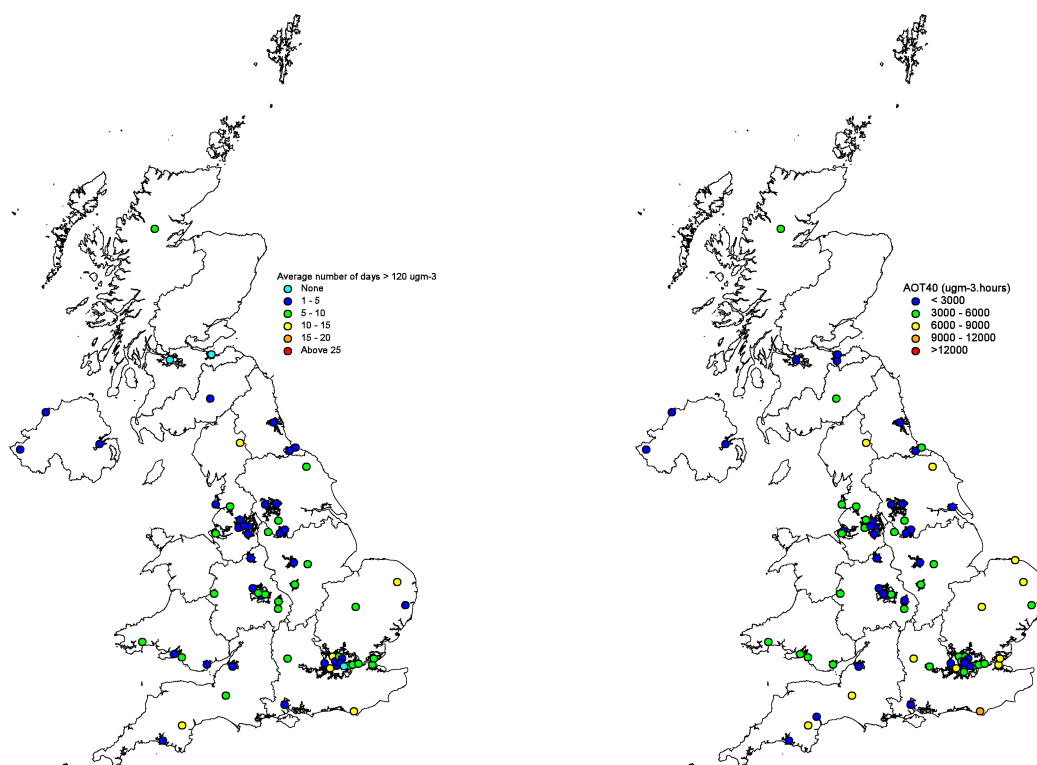


Figure 7.3 Measured Target Values for the Protection of Human Health (Days > 120 $\mu\text{g m}^{-3}$ as a Maximum Daily 8-hour mean; left-hand panel) for 1999-2001 and the Protection of Vegetation and Ecosystems (AOT40 $\mu\text{g m}^{-3}$ hours; right-hand panel) for 1997-2001 at all non-roadside/kerbside sites in UK.

Table 7.2 shows that when the current network of automatic monitoring stations and the supplementary assessment methods are taken into account, a total of 3 additional co-located NO_2 and ozone monitoring stations and the recommissioning of the monitoring station in the Reading agglomeration are required for compliance with the Directive. There are no additional monitoring requirements for agglomeration zones in Scotland, Wales and Northern Ireland.

In Non-agglomeration Zones

The amount of monitoring required within non-agglomeration zones in the UK is regulated by the same criteria specified for agglomeration zones under Article 9 of the Directive. However, within non-agglomeration zones, co-located NO_2 and ozone monitoring stations must be located at suburban and rural background locations. A minimum requirement of 1 co-located station per 2 million inhabitants of a zone remains or 50,000 km^2 whichever yields the greatest number of sites.

Table 7.3 identifies non-agglomerations zones with measured or modelled exceedences of the long-term objectives. The current number of co-located NO_2 and ozone monitoring stations⁷ which meet the suburban and rural background siting criteria specified by Annex IV of the Directive are also indicated. As for agglomerations zones, the minimum monitoring requirement assuming fixed monitoring as the sole source of information is presented by the 'Minimum Site Number A' statistic. Monitoring requirements taking into account supplementary assessment techniques are presented by the 'Minimum Site Number B' statistic. Table 7.3 shows that when the current network of automatic monitoring stations and the supplementary assessment methods are taken into account, a total of 8 additional co-located NO_2 and ozone monitoring stations are required for compliance with the Directive within non-agglomerations zones in England. A further 4 monitoring stations are required in Scotland and 2 in Wales. No additional monitoring requirements were identified for Northern Ireland.

⁷ Based on AURN network statistics January 2003.

Table 7.2 Monitoring Stations for Proposed Urban and Suburban Ozone Network in Agglomerations.

Zone	Population*	Long-term objective exceeded? **		Minimum number of stations		Existing urban background & suburban co-located NO ₂ /O ₃ stations	Additional Monitoring required
		Max daily 8-hour	AOT40	A	B		
Greater London Urban Area	7650944	Yes	Yes	6	4	13	-
West Midlands Urban Area	2296180	Yes	Yes	4	2	4	-
Greater Manchester Urban Area	2277330	Yes	No	4	2	4	-
West Yorkshire Urban Area	1445981	Yes	No	3	1	2	-
Glasgow Urban Area	1315544	Yes	Yes	3	1	1	-
Tyneside	885981	Yes	Yes	2	1	1	-
Liverpool Urban Area	837998	Yes	No	2	1	1	-
Sheffield Urban Area	633362	Yes	Yes	2	1	2	-
Nottingham Urban Area	613726	Yes	Yes	2	1	1	-
Bristol Urban Area	522784	Yes	Yes	2	1	1	-
Belfast Urban Area	475987	Yes	No	1	1	1	-
Brighton/Worthing/Littlehampton	437592	Yes	Yes	1	1	None	1 ^a
Leicester Urban Area	416601	Yes	Yes	1	1	1	-
Edinburgh Urban Area	416232	Yes	Yes	1	1	1	-
Portsmouth Urban Area	409341	Yes	Yes	1	1	None	1 ^b
Teesside Urban Area	369609	Yes	Yes	1	1	2	-
The Potteries	367976	Yes	Yes	1	1	1	-
Bournemouth Urban Area	358321	Yes	Yes	1	1	None	1 ^c
Reading/Wokingham Urban Area	335757	Yes	Yes	1	1	None	1 ^d
Coventry/Bedworth	331248	Yes	Yes	1	1	1	-
Kingston upon Hull	310636	Yes	Yes	1	1	1	-
Cardiff Urban Area	306904	Yes	Yes	1	1	1	-
Southampton Urban Area	276752	Yes	Yes	1	1	1	-
Swansea Urban Area	272456	Yes	Yes	1	1	1	-
Birkenhead Urban Area	270207	Yes	No	1	1	1	-
Southend Urban Area	266749	Yes	Yes	1	1	1	-
Blackpool Urban Area	261355	Yes	No	1	1	1	-
Preston Urban Area	256411	Yes	Yes	1	1	1	-

a. Requires additional NO_x, ozone and monitoring enclosure

b. Ozone monitor required at existing NO_x station(s)

c. Affiliate existing ozone monitor

d. Relocation of existing monitoring station

* Population statistics based on the 1991 National Census

** Exceedence category based on measured and modelled data

Table 7.3 Additional Monitoring Stations for Proposed Rural and Suburban Ozone Network in Zones.

Zone	Population*	Long-term objective exceeded? **		Minimum number of stations		Existing suburban & rural background co-located NO ₂ /O ₃ stations	Additional Monitoring required
		Max daily 8-hour	AOT40	A	B		
Eastern	4788766	Yes	Yes	6	3	4	-
South West	3728319	Yes	Yes	5	2	None	2 ^a
South East	3702634	Yes	Yes	5	2	3	-
East Midlands	2923045	Yes	Yes	5	2	1	1 ^d
North West & Merseyside	2823559	Yes	Yes	5	2	None	2 ^{a,b}
Yorkshire & Humberside	2446545	Yes	Yes	4	2	1	1 ^a
West Midlands	2154783	Yes	Yes	4	2	1	1 ^e
Central Scotland	1628460	Yes	Yes	3	1	None	1 ^c
South Wales	1544120	Yes	Yes	3	1	None	1 ^d
North East	1287979	Yes	Yes	3	1	None	1 ^e
Northern Ireland	1101868	Yes	No	3	1	1	-
North East Scotland	933485	Yes	Yes	2	1	None	1 ^b
North Wales	582488	Yes	Yes	2	1	None	1 ^a
Highland	364639	Yes	Yes	2	1	None	1 ^e
Scottish Borders	246659	Yes	Yes	1	1	None	1 ^a

- a. NO_x monitors required at existing ozone station(s)
- b. Ozone monitor required at existing NO_x station(s)
- c. Affiliate existing NO_x monitoring
- d. Affiliate existing ozone monitoring
- e. Requires additional NO_x, ozone and monitoring enclosure

* Population statistics based on the 1991 National Census

** Exceedence category based on measured and modelled data

At Rural Background Locations

Annex V of the Daughter Directive for ozone presents a requirement for monitoring of ozone at rural background locations. Section I Annex V of the Directive specifies that 1 measurement station must be located in a rural background locations for every 50,000 km² of land mass. The UK covers approximately 244,767 km², as a result 5 monitoring locations are required in rural background locations for compliance with the Directive. Table 7.4 presents the monitoring stations in the UK network for compliance with rural background monitoring requirements. The location types described as rural background by the Directive have historically been known as 'remote' locations within the UK.

Table 7.4 Monitoring Stations proposed for Rural Background Monitoring.

Site	Pollutants Measured
Strath Vaich	O ₃
Great Dun Fell	O ₃
Lough Navar	O ₃
Narberth	O ₃ , SO ₂ , PM10 and NO _x
Sibton	O ₃

Automatic monitoring of NO₂ at rural background location is not required.

Monitoring Requirements for Ozone Precursors

Article 9 (3) of the Directive requires Members States to measure a suite of ozone precursors in at least 1 urban background location within their territory. Ozone precursors are defined as NO_x and volatile organic compounds (VOC) and recommendations on the type of compounds to be measured are provided in Annex VI of the Directive.

There is currently one location within the UK's benzene monitoring network (London Marylebone Road) which is capable of measuring 27 out of the 31 recommended VOC presented in Annex VI of the Directive. However, the Marylebone Road is located at the roadside and the specified siting criteria for the precursor monitoring station is urban background. As a result monitoring of precursors will be recommissioned at the Eltham AURN urban background monitoring station. In addition to the sites presented above, a further 3 automatic stations measure a smaller suite of VOC (benzene, 1-3 butadiene, toluene, m p and o xylenes and ethylbenzene). These monitoring stations are located at the Harwell (rural), Cardiff Centre and Glasgow Centre (urban background) AURN stations.

7.2.3 Achieving Compliance

Ozone levels have been assessed throughout the UK using measured and modelled data. On the basis of the assessments and analyses presented in this report, the minimum number of additional automatic monitoring stations has been identified for areas with measured or modelled exceedences of the long-term objectives for ozone. The recommendations for additional monitoring are summarised in Table 7.5. Fixed monitoring will be supplemented by information from other sources (empirical maps, OSRM etc.) in all zones and agglomerations. Monitoring stations already available in the current monitoring network have also been taken into account.

Table 7.5 Summary of Monitoring Requirements for Minimum Compliance with the Ozone Directive

Additional monitoring stations	3
Additional NO ₂ analysers in existing monitoring stations	11
Additional O ₃ analysers in existing monitoring stations	10
Additional VOC monitoring	1

By implementing the NO₂ and ozone monitoring presented in Table 7.5, a total of 18 additional co-located monitoring stations will be commissioned. The additional monitoring needed for formal compliance with the Directive will be satisfied by a process of affiliation of existing local authority monitoring stations and also by direct funding of new monitoring sites from the UK Government.

7.3 EVALUATION OF SUPPLEMENTARY ASSESSMENT TECHNIQUES

In implementing the Directive, Member States were required to submit a 'preliminary assessment' of ozone levels within their territory to identify current levels of ozone and the level of monitoring and/or other assessment techniques to be commissioned in order to fulfil obligations to the 3rd Daughter Directive. Within the UK, a combination of measurements and model based assessments were proposed to achieve the most practicable and cost-effective assessment of ozone levels relative to the Target Values and Long-term objectives [Bush and Kent, 2003]⁸.

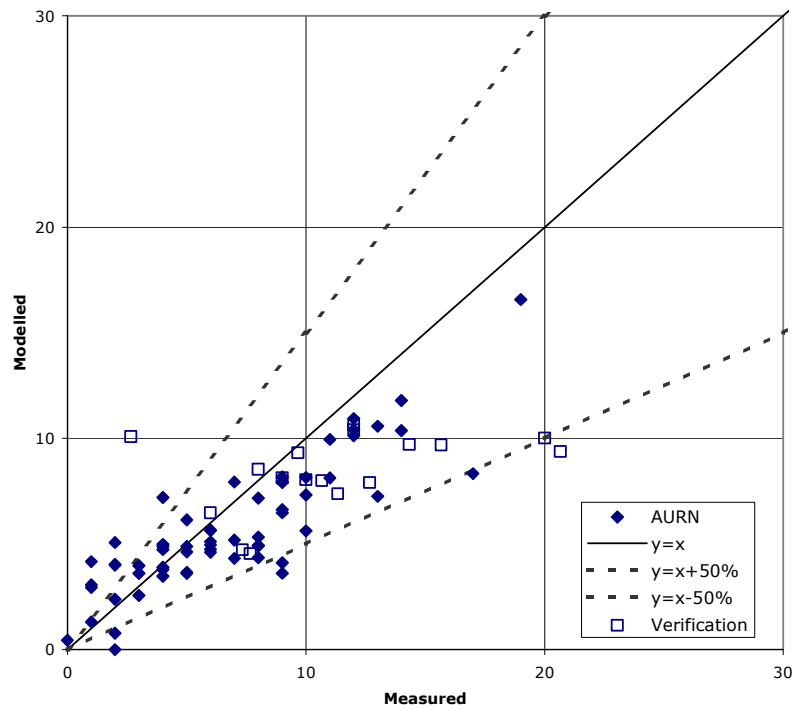
In addition to measurements, 2 models were identified as potential candidates to be the supplementary assessment - the OSRM and empirical mapping models. At the time of publication of the UK's preliminary assessment, it was not possible to recommend a specific modelling technique, owing to continued development of the candidate methods. As a result, it was proposed that the performance of candidate methods would be compared at a later date, in order to provide information to select the most appropriate method for the regulatory use with the 3rd Daughter Directive.

Work was undertaken to assess the relative performance of the 2 ozone modelling techniques and thus to recommend the preferred supplementary assessment technique to be used for the third Daughter Directive on ozone [Targa and Bush, 2005]. Outputs from the OSRM (Version 2.2 with Surface Conversion Algorithm available at January 2005), empirical modelling estimates and measurement data from the AURN were compared. Examples of the comparison of the two models are shown in Figure 7.4 and Figure 7.5 for the number of days with a running 8-hour ozone concentration greater than 120 $\mu\text{g m}^{-3}$ (averaged over the 3-year period: 2001 to 2003) and AOT40 – Crops (averaged over the 5-year period: 1999 to 2003).

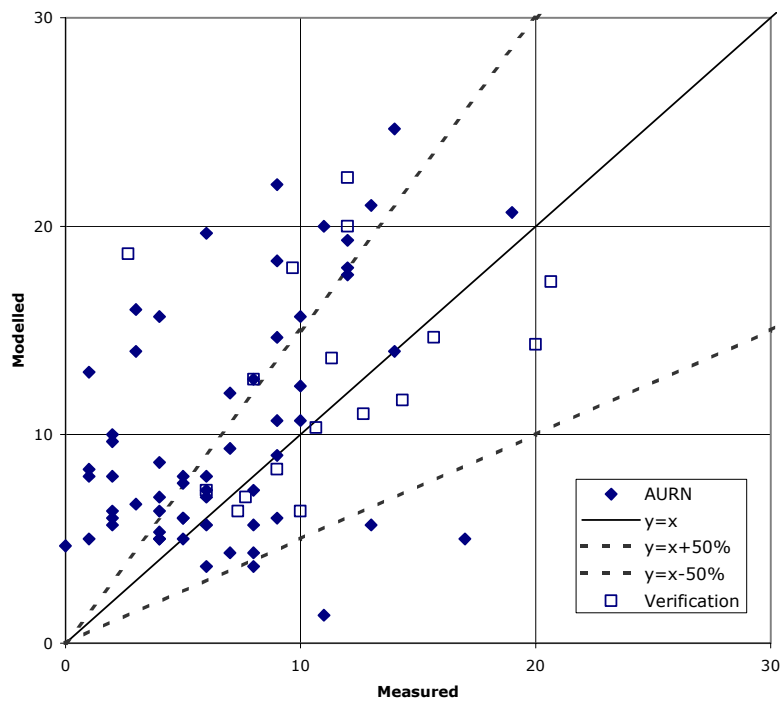
From the analysis of the comparative performance of the empirical and OSRM models, it was judged that the empirical modelling approach delivers least uncertainty in the model outputs [Targa and Bush, 2005]. It was proposed, therefore, that the empirical modelling approach should be taken forward as the preferred means of supplementary assessment for the reporting ozone levels in 2004 calendar year. A further recommendation was made however, to simultaneously undertake the same assessment using the OSRM in order to reassess the performance of both models in the light of updates to the modelling techniques.

It was also noted that the prediction of exceedences of the Long-term Objectives and Target Values was not particularly sensitive to the model used. This is a result of the combined effective of the general levels of ozone experienced in the UK at present and the relative laxity of the Directives Target Values and the stringency of the Long-term Objectives.

⁸ The report is available from http://www.airquality.co.uk/archive/reports/reports.php?report_id=349.

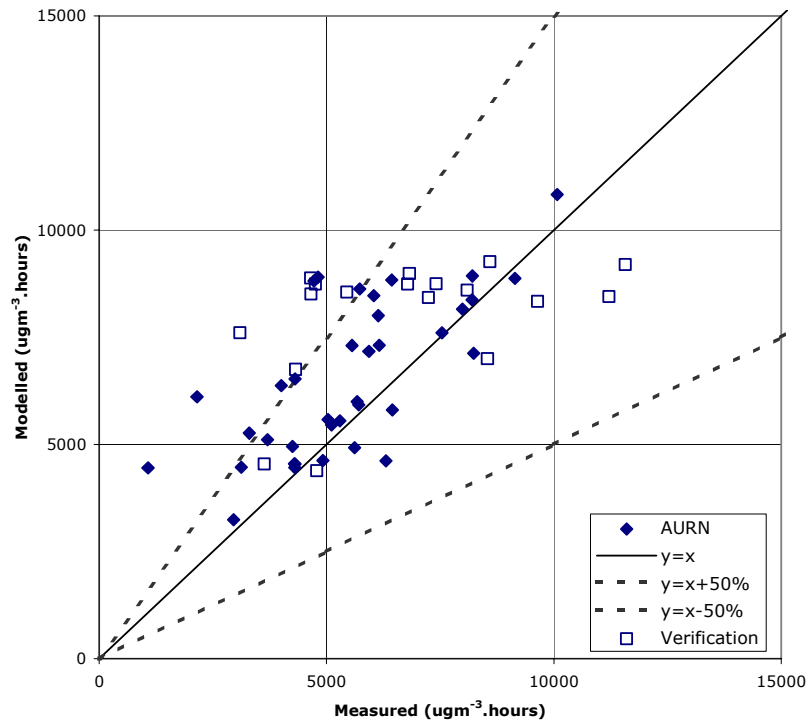


Days greater than 120 $\mu\text{g m}^{-3}$ in 2001-2003. Measured vs Empirical

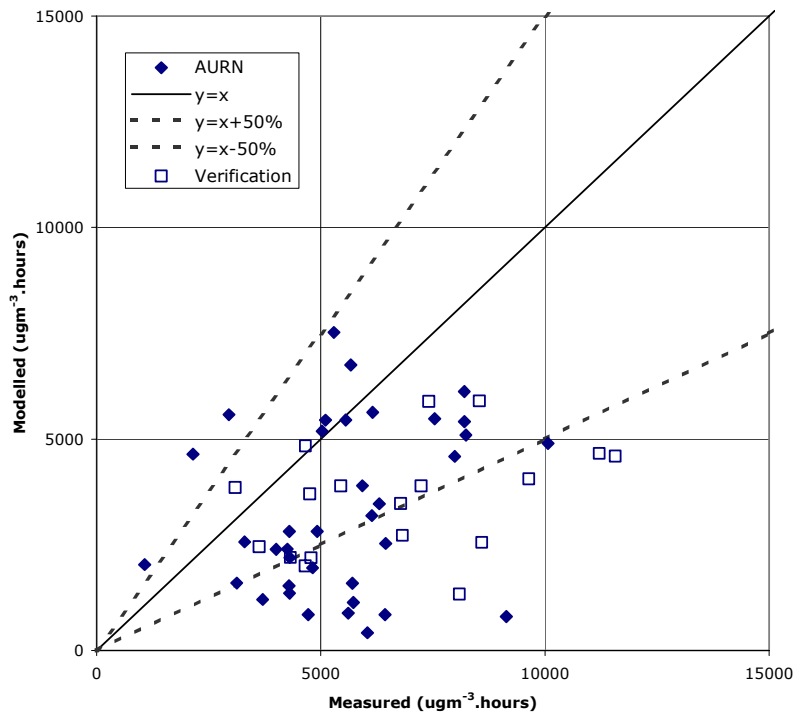


Days greater than 120 $\mu\text{g m}^{-3}$ in 2001-2003. Measured vs OSRM

Figure 7.4 Average Number of Days in 2001-2003 with a Running 8-Hour Ozone Concentration greater than 120 $\mu\text{g m}^{-3}$. Comparison between Measured and Modelled Data.



AOT40 wheat crop in 1999-2003. Measured vs Empirical



AOT40 wheat crop in 1999-2003. Measured vs OSRM

Figure 7.5 AOT40 - Crops in 1999-2003. Comparison between Measured and Modelled Data.

7.4 SUPPORTING DOCUMENTATION FOR THE QUESTIONNAIRE

2004 is the first year for which an annual air quality assessment for the third Daughter Directive pollutants is required. During the present reporting period, colleagues at netcen have completed the questionnaire for submission to the EU containing the results of this air quality assessment along with those required for the first and second Daughter Directives. The assessment takes the form of comparisons of measured and modelled air pollutant concentrations with the target values and long-term objectives set out in the Directives. Air quality modelling has been carried out under this contract to supplement the information available from the UK national air quality monitoring networks.

Following the assessment of the ozone modelling techniques (see Section 7.3 and Targa and Bush [2005]), maps of background ozone concentrations in 2004 on a 1 km x 1 km grid of the ozone metrics listed above have been prepared using the preferred empirical mapping technique [Bush, Targa and Stedman, 2005]. These are shown in Figure 7.6 and Figure 7.7. Verification plots against independent measurements are presented in the report. The UK has been divided into 43 zones for air quality assessment. There are 28 agglomeration zones (large urban areas) and 15 non-agglomeration zones. The status of the zones status has been determined from a combination of monitoring data and model results. The results of this assessment are summarised in Table 7.6, in terms of exceedences of Target Values (TV) and Long-term Objectives (LTO).

Table 7.6 Summary Results of Air Quality Assessment relative to the Target Values and Long-term Objectives for Ozone for 2010.

Target Value	Number of Zones exceeding
Max Daily 8-hour mean Target Value	none
AOT40 Target Value	none
Long-term Objective	Number of Zones exceeding
Max Daily 8-hour mean Long-term Objective	43 zones (36 measured + 7 modelled)
AOT40 Long-term Objective	7 zones (5 measured + 2 modelled)

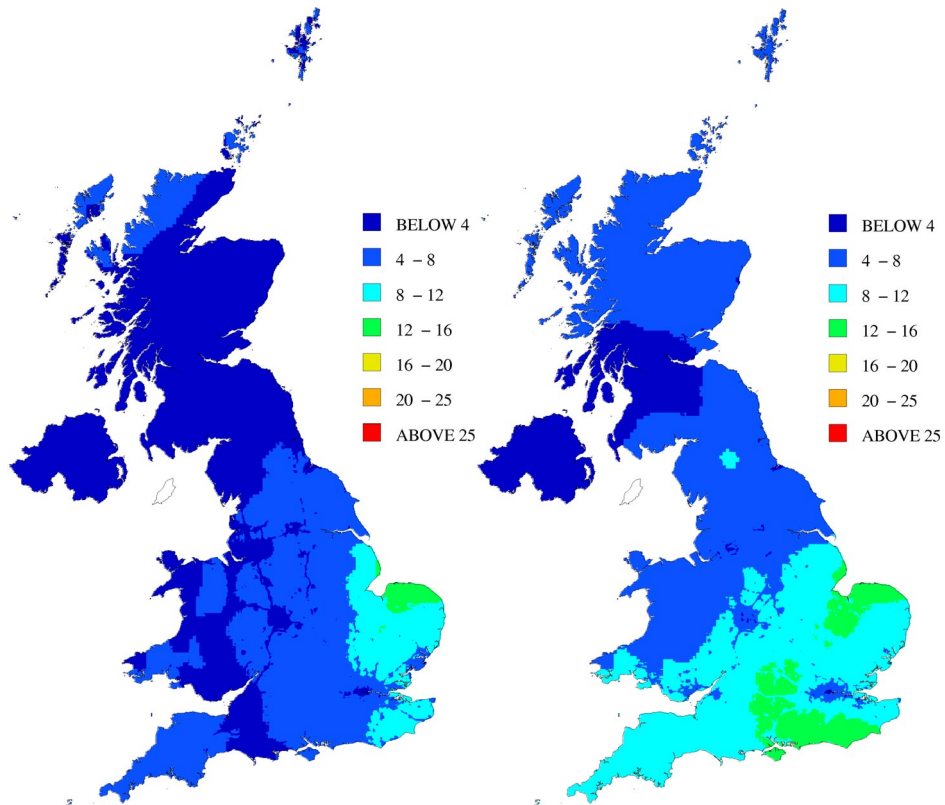


Figure 7.6 *Estimated Number of Days above 120 µg m⁻³ in 2004 (Left-hand Panel) and Estimated Average Number of Days above 120 µg m⁻³, 2002 to 2004 (Right-hand Panel).*

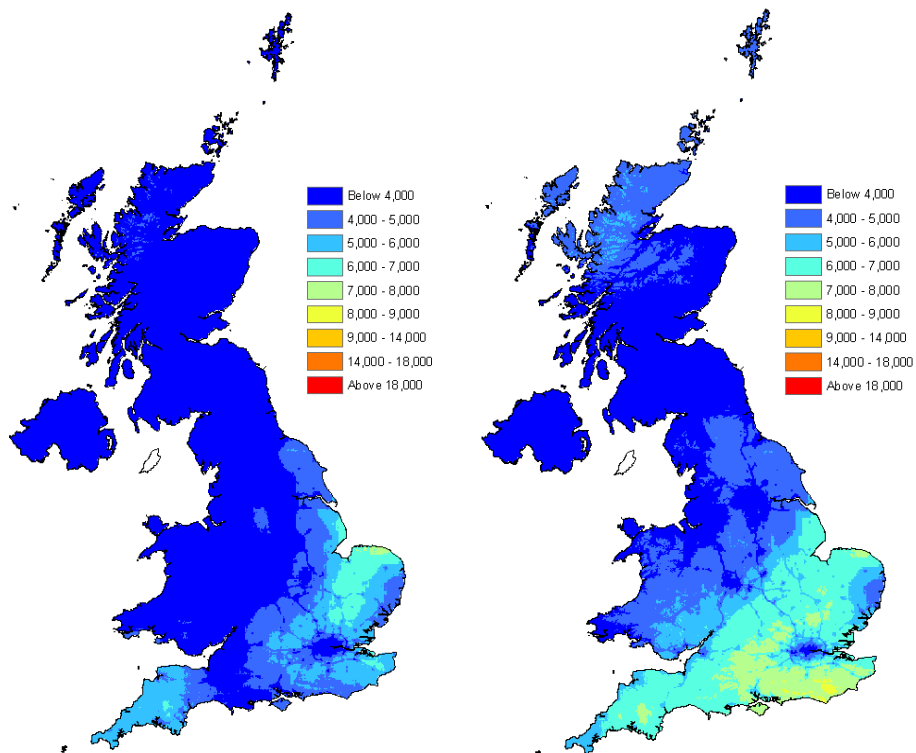


Figure 7.7 *Estimated AOT40 Crops in 2004 (µg m⁻³ hours, Left-hand Panel) and Estimated AOT40 Crops, averaged 2000–2004 (µg m⁻³ hours, Right-hand Panel).*

8 Improvements to Photochemical Reaction Schemes (Objective 4)

8.1 MECHANISM DEVELOPMENT

8.1.1 Update of the Master Chemical Mechanism to MCMv3.1

The Master Chemical Mechanism (MCM) has been updated to MCMv3.1. The major updates in MCMv3.1 include an extensive update to the aromatic mechanisms, which are important in the photochemistry of the polluted boundary layer, and also the addition of a number of new degradation schemes of some important biogenic species. MCMv3.1 now contains 135 primary emitted VOCs, which lead to a mechanism containing ca. 5,900 species and 13,500 reactions.

8.1.2 Development and Evaluation of a Detailed Mechanism for the Atmospheric Oxidation of Aromatic Hydrocarbons

The degradation schemes for four aromatic hydrocarbons; benzene, toluene, *p*-xylene and 1,3,5-trimethylbenzene, have been updated on the basis of new kinetic and mechanistic data from current literature and conference proceedings. The performance of these schemes concerning ozone formation from tropospheric aromatic oxidation has been evaluated using detailed environmental chamber datasets from the EU EXACT measurement campaigns, which took place in the European Photoreactor (EUPHORE). This comprehensive databank includes photochemical smog chamber studies on the four classes of mono-aromatic compounds above (carried out under suitable atmospheric conditions) as well as a series of experiments looking into specific key areas of aromatic photo-oxidation, focussing on subsets of the toluene system. Results from this system can be transferred to other aromatics as the mechanisms are expected to be similar. Where appropriate, results from this database have been used to refine the mechanisms.

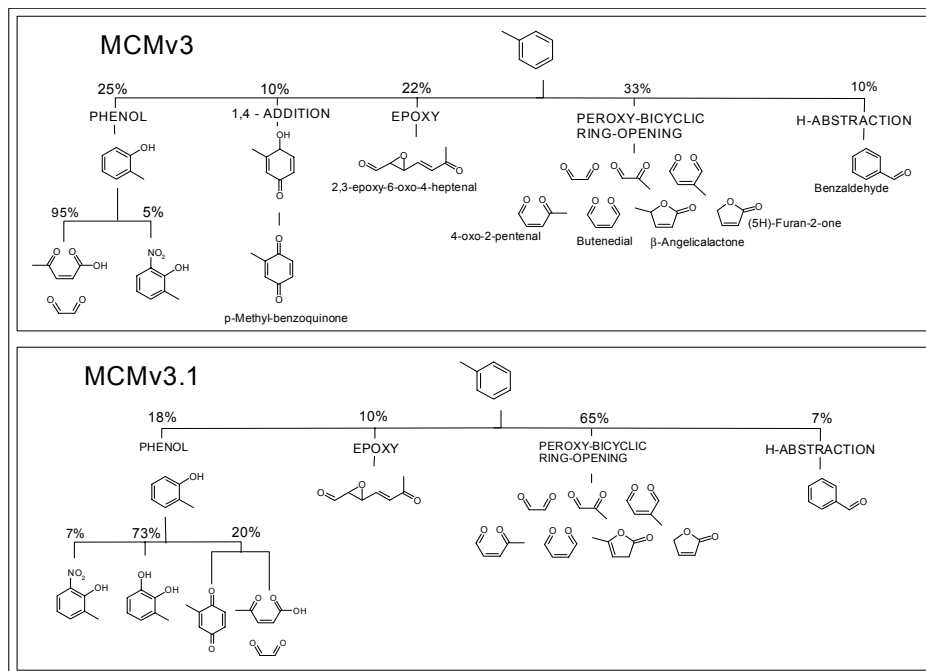


Figure 8.1 Schematic Representations of Toluene Oxidation Mechanisms. Upper Panel MCMv3, Lower Panel MCMv3.1.

The oxidation pathways of toluene as implemented in the original mechanism (MCMv3) and the updated mechanism (MCMv3.1) are shown in Figure 8.1. The key areas in which the aromatic mechanisms have been changed are:

- Benzaldehyde yield is slightly lower in the toluene system in MCMv3.1 than MCMv3 in order to better represent the more recent data at low NO_x levels (Calvert *et al.* [2002]).
- Photolysis rates of unsaturated γ -dicarbonyls (an important source of radicals) have been adjusted according to Thuener *et al.* [2003] for butenedial and 4-oxo-2-pentenal, and Graedler and Barnes [1997] for 3-hexene-2,5-dione. The photolysis rates of the epoxydicarbonylene products have also been increased as they were originally estimated by analogy with the unsaturated γ -dicarbonyls.
- The breakdown of the carbon skeleton for 2(5H)-furanone (also a photolysis product of butenedial) has been updated and β -angelica lactone has been replaced by α -angelica lactone to reduce secondary glyoxal formation. These changes were prompted by findings of Volkamer *et al.* [2001] that secondary glyoxal formation in the toluene system is negligible.
- New phenol-type chemistry has been implemented reflecting the lower yield for the ring-opening channel reported by Olariu *et al.* [2002], and the need for reduced ozone formation found in a cresol photo-smog experiment at EUPHORE.
- Branching ratios for the different oxidation routes of aromatics have been adjusted to reflect the reported yields of glyoxal and of phenol-type compounds at NO_x levels appropriate to the atmosphere (Volkamer *et al.* [2001]; Volkamer *et al.* [2002]).

A comparison of modelled and measured concentrations from a photo-smog experiment on butenedial is shown in Figure 8.2. This experiment and similar studies on 4-oxo-2-pentenal indicated a number of shortcomings in the mechanisms. NO₂ concentration-time profiles are poorly simulated for all experiments, and the differences between experiments under different initial conditions are not well represented. It is clear that the NO_x budget is not well understood. The simulated OH and HO₂ radical concentrations are significantly lower than the observed values and it seems that a large radical source is missing from the mechanism. However, very low HO₂ radical concentrations were measured in γ -dicarbonyl photolysis experiments in the absence of NO_x but these measured concentrations were much lower than HO₂ concentrations simulated by MCMv3.1. This important issue so far remains unresolved.

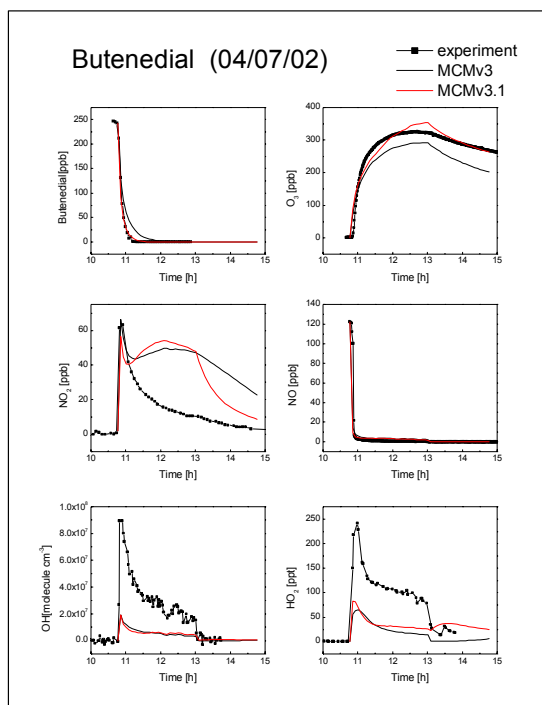


Figure 8.2 Butenedial Experiment - Comparison of Modelled and Measured Concentrations of Parent Compound, O₃, NO_x and HO_x.

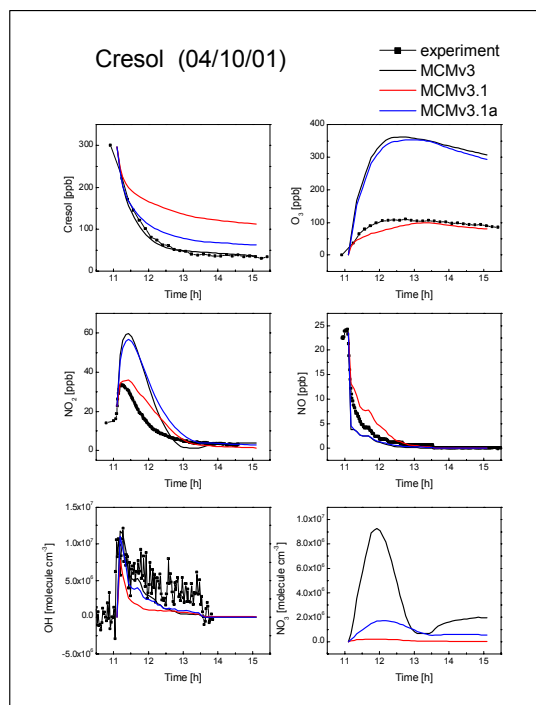


Figure 8.3 Cresol Experiment - Comparison of Modelled and Measured Concentrations of Cresol, O₃, NO_x and OH with MCMv3, MCMv3.1 and MCMv3.1a. Also shown are modelled concentrations of NO₃.

The results from a chamber experiment on the photo-oxidation of *o*-cresol are illustrated in Figure 8.3. These results were used to adjust the representation of hydroxyarene degradation in MCMv3.1 (see also Figure 8.1). The peak O₃ concentration is well simulated by MCMv3.1, and the representation of the NO and NO₂ concentration-time profiles is improved from MCMv3. However, the simulated radical yield is too low and the rate of cresol oxidation is therefore underestimated. In Figure 8.3, MCMv3.1a differs from MCMv3.1 in that the first generation ring retaining products are treated in the same way as the original cresol, *i.e.*, assuming the same branching ratios as for the original initial oxidation channels. The second generation ring retained products are then assumed to undergo ring opening.

Figure 8.4 and Figure 8.5 show example aromatic model-measurement comparisons for benzene and toluene respectively. The O₃ peak in the benzene system is greatly reduced in MCMv3.1 compared to MCMv3, and is in good agreement with the measurements, as shown in Figure 8.4. This substantial improvement is mainly a result of an increased phenol channel yield implemented in MCMv3.1 and an increased ring-retaining product yield in that channel. However, this increase in ring-retaining yield and consequent decrease in radical production leads to a reduction in OH production and oxidative capacity of the system (which was better simulated by MCMv3). This is indicative of a general problem with the mechanisms; over-prediction of the ozone concentration but under-prediction of the reactivity of the system.

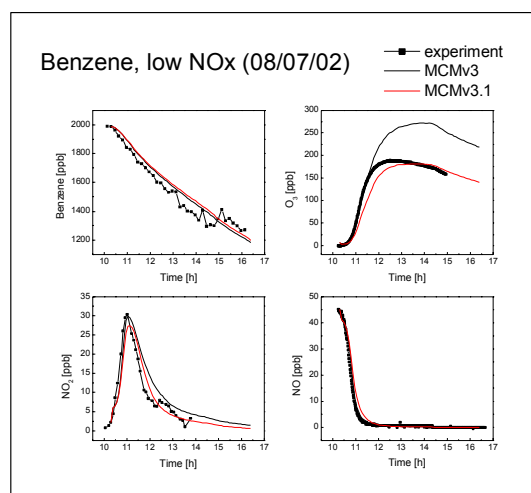


Figure 8.4 Model-Measurement comparison for Benzene, O₃, NO₂ and NO in a EUPHORE Benzene Photo-smog Experiment.

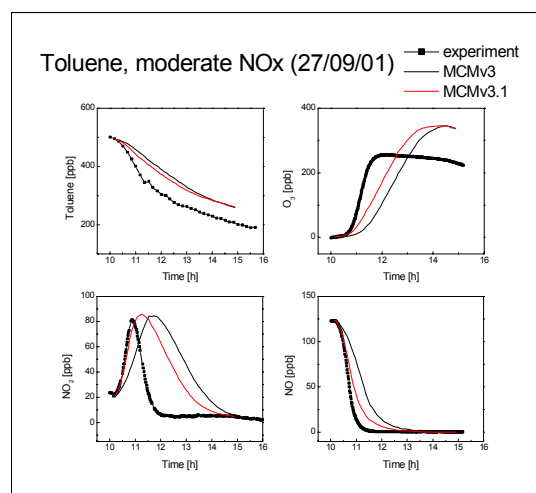


Figure 8.5 Model-Measurement comparison for Benzene, O₃, NO₂ and NO in a EUPHORE Toluene Photo-smog Experiment.

For the toluene system, model-measurement agreement in terms of O₃ concentration and NO oxidation is improved in MCMv3.1 but the maximum O₃ is still over estimated as shown in Figure 8.5. This mechanism has an increased branching ratio for ring opening in toluene oxidation, and a slightly decreased cresol yield (see Figure 8.1). These changes, along with the increased photolysis rates of the unsaturated dicarbonyl compounds, tend to increase radical production, particularly early in the experiment, and hence increase O₃ generation. However, changes to the substituted phenol (cresol) chemistry, analogous to those discussed above for the benzene system, decrease O₃ formation and reduce radical production in the middle of the experiment. The changes balance out in such a way that some decrease in O₃ formation is achieved while increasing the radical production in the early stages of the experiment. However, the amount of “missing” OH needed for the model to reproduce the observed decay of the primary aromatic was calculated over the whole course of the experiment, and in general is higher for the MCMv3.1 simulations indicating an overall reduction in oxidative capacity for this mechanism consistent with the reduced ozone formation potential.

In general the updated mechanism, MCMv3.1, shows improved ability to simulate some of the observations from the EXACT EUPHORE datasets and represents our current understanding of aromatic degradation. However, significant discrepancies remain concerning, in particular, ozone formation potential and oxidative capacity of aromatic hydrocarbon systems:

- The peak ozone concentration in the benzene experiments is well simulated but for the substituted aromatics the simulations generally over-estimate the peak ozone concentration.

- The OH radical production in the mechanisms is too low to account for the OH concentration inferred from the rate of loss of the parent aromatic. The simulations under-estimate the oxidative capacity of the aromatic systems.
- For the majority of the experiments the simulations under-predict the NO oxidation rate, which is used as a measure of the timing of the simulations. This parameter is closely related to the processes responsible for the production of ozone and the reactivity of the system.

The combination of over-prediction of ozone concentration and under-prediction of reactivity poses a problem for mechanism development; a reduction in ozone concentration can be achieved by a reduction in peroxy radical concentration, which limits the NO to NO₂ conversion, but this will also lead to a reduction in OH production and in the oxidative capacity of the system.

A number of possible mechanistic fixes have been investigated and a number of strategies for resolving some of these issues have been proposed.

- An increase in OH yield without additional NO to NO₂ conversion would improve the simulated concentration-time profiles. A potential OH regeneration channel has been identified, but there is no firm evidence for its occurrence.
- Conversion of NO₃ to HO₂ by a dummy reaction in the model decreases O₃ yields but does not significantly affect the aromatic decay rate.
- A modelled conversion of NO₂ to HONO on the secondary organic aerosol has been shown to improve model-measurement agreement for O₃, NO_x and toluene decay. However, the relatively high HONO concentrations generated have not been observed experimentally, and the reactive uptake coefficient required is much higher than the upper limits for such processes suggested by the work of Broske *et al.* [2003].
- A sensitivity analysis is planned, to investigate the effect of the uncertainty in the rate of radical generation on ozone formation in the standard photochemical trajectory model (see next section). In an environment with many VOC species and radical precursors, this uncertainty may be less significant.

The development work discussed here on aromatic degradation schemes has been extended to update the degradation schemes of twelve other mono-aromatics in the MCM with saturated alkyl side chains.

In addition to the extensive work carried out on the aromatic systems, a new degradation scheme has been constructed for the biogenic hydrocarbon 2-methyl-3-buten-2-ol (MBO). This scheme introduces 89 new reactions to the MCM and includes 29 new species, though most of the major oxidation products of MBO were already in the mechanism. Further additions to the MCM include an extended list of chloro- and hydrochlorocarbons and two hydrobromocarbons. The list of primary VOCs included in MCMv3.1 is now 135.

8.1.3 Update to the Treatment of Photolysis Reactions in the MCM

Photo-dissociation of atmospheric molecules by solar radiation plays a fundamental role in atmospheric chemistry. The photolysis of trace species such as ozone and formaldehyde contributes to their removal from the atmosphere, but probably the most important role played by these processes is the generation of highly reactive atoms and radicals. Photo-dissociation of trace species and the subsequent reaction of the photo-products with other molecules is the prime initiator and driver for the bulk of tropospheric chemistry. As a polluted air parcel ages, the contribution of the photolysis of oxygenated intermediates becomes the major source of radicals. Therefore it is clear that understanding photolysis processes requires accurate and reliable determination of photolysis frequency data in order to accurately model the total HO_x and NO_x budgets within the troposphere.

In MCMv3.1, photolysis reactions are considered for photo-labile carbonyl species such as aldehydes, ketones and α -dicarbonyls (*e.g.*, Glyoxal) (Jenkin *et al.* [1997a]). Such species are emitted directly as primary pollutants (combustion, vegetation) or produced as degradation intermediates. Photolysis reactions are also considered for more complex carbonyls, hydroperoxides and organic nitrates which are all generated in the NO_x-mediated oxidation of volatile organic compounds (VOCs). However, the database in MCM v3.1 is, in some respects, both limited and out of date.

In order to calculate a tropospheric photolysis rate coefficient (also referred to as a j -value, units of s^{-1}), the following equation can be evaluated for each photo-labile molecule:

$$j = \int_{\lambda_{\min}}^{\lambda_{\max}} \sigma(\lambda, T) \phi(\lambda, T) F(\lambda) d\lambda$$

where σ is the **absorption cross section** of the molecule and ϕ is the **quantum yield** for the photo-process (both σ and ϕ can be both temperature (T) and pressure (p) dependent). The final term, $F(\lambda)$, is the **spectral actinic flux**, which quantifies the *in situ* radiation available to a molecule from all directions for the initiation of a photo-dissociation process (e.g., see Madronich and Flocke [1998]). Actinic fluxes can be either measured *in-situ* by spectral radiometers or calculated using radiative transfer models.

In MCM v3.1, photolysis rates for 26 core reactions whose σ and ϕ are known have been determined as a function of solar zenith angle (SZA) using the *PHOTOL* two stream isotropic scattering model (on the 1st July (clear sky) at 0.5 km, latitude 45°N) [Jenkin *et al.* (1997a)]. Variation of J with SZA is described well by the following expression:

$$j = (\cos \chi)^m \exp(-n \cdot \sec \chi)$$

14 surrogate parameters are also used to define the photolysis rate of several thousand related species whose photolysis parameters are not known. However, the current cross-sections and quantum yields employed in the definition of these parameters have not been substantially updated since 1997. Subsequently, new and updated laboratory measurements (higher resolution, better wavelength coverage) have become available in the literature.

Therefore, as part of the ongoing evolution of the MCM a thorough survey of literature cross-section and quantum yield data has been carried out in order to review and update the calculation of the photo-dissociation coefficients for organic (and inorganic) species in the MCM and to expand upon the current range of species covered. New photolysis rates have been calculated using the discrete ordinate radiative transfer model *TUV4.2* (Madronich and Flocke [1998]) which is freely available online (www.acd.ucar.edu/Science/Models/TUV/index.shtml). The use of such a flexible model enables the photolysis rate to be calculated under a variety of atmospheric conditions (e.g., altitude, cloud cover, surface type (albedo)). Initial calculations were performed on the 1st July, 45°N latitude at a height of 500 m asl using an ozone column of 300 DU and a surface albedo of 0.1.

As well as the latest evaluations from IUPAC (www.iupac-kinetic.ch.cam.ac.uk/) and JPL, (<http://jpldataeval.jpl.nasa.gov/>), which only currently include evaluated data for relatively short chain photo-labile organic species, primary literature data sources used include the new and comprehensive MPI-Mainz database of absorption cross sections for gaseous molecules and radicals, which is also available on the web (www.atmosphere.mpg.de/enid/2295). This database currently contains about 4000 data files for nearly 600 species. Also, the results of citable chamber studies such as the EU Evaluation of radical sources in atmospheric chemistry through chamber and laboratory studies (RADICAL) project (Moortgat *et al.* [2000]) and the work of Pinho *et al.* [2005], have been considered particularly for photolysis rates with highly uncertain parameters. As quantum yields are particularly difficult parameters to measure accurately, such chamber studies have been used to define a so called “effective” quantum yield, ϕ_{eff} , which is defined as the average quantum yield over the entire absorption region at wavelengths over 295 nm (Moortgat *et al.* [2000]). ϕ_{eff} is calculated as the ratio of the measured photolysis frequency under natural sunlight conditions to the theoretical decomposition rate calculated using the measured actinic fluxes and a $\phi = 1$.

As already mentioned many of the σ and ϕ are temperature and pressure dependent with some of the recent literature studies quantifying these dependencies for the first time. One of the future developments of the MCM is to extend its use to the free troposphere. Therefore in order to facilitate this, the photolysis rates are calculated as a function of pressure as well as temperature where appropriate data are available.

Such new and improved laboratory measurements enabled the expansion of the current list of photolysis rates in the MCM. This new data will also enable us to review the surrogate representation for species whose parameters are still not known. For example, the degree to which the contributions of different functional groups within a molecule are additive could be tested if enough data are available on bi-functional groups.

In order to demonstrate the expansion and update of the photochemical scheme used in the MCM specific highlights are given below:

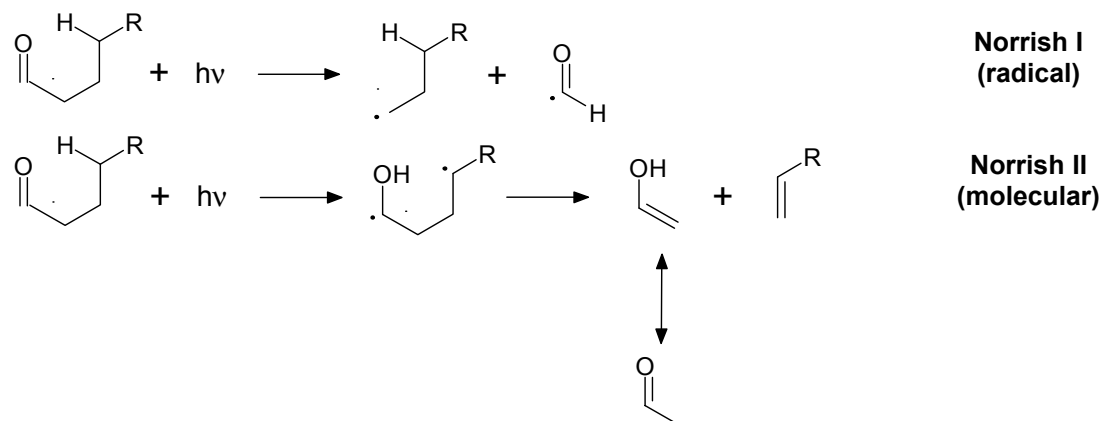
(1) Photolysis of Long-chain and Branched Aldehydes

The photolysis of oxygenated intermediates is one of the major uncertainties in atmospheric gas-phase VOC oxidation chemistry and hence is currently not well defined in the MCM. In MCMv3.1 the parameterisations that describe the photolysis of *n*-butanal (C₃H₇CHO) and *i*-butanal ((CH₃)₂CHCHO) are assigned as surrogates to describe the photolysis of longer chained (> C₄) aldehydes. However, a relatively large database of literature cross-sections for long chain and branched C₂-C₇ aldehydes has become available since the MCM photolysis rates were last assessed.

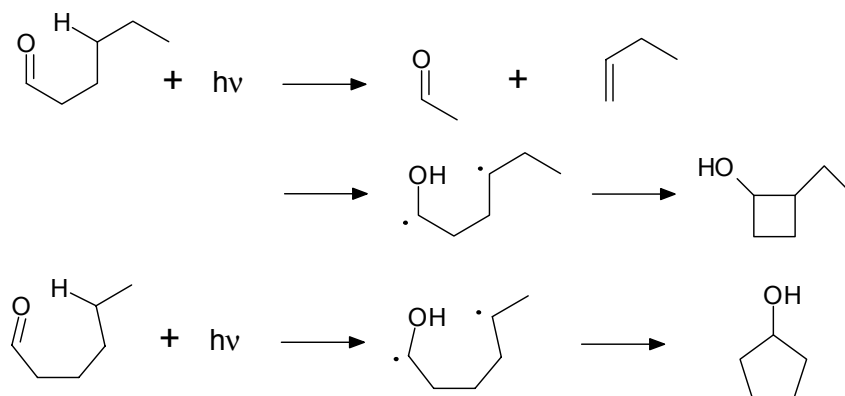
The main atmospheric degradation processes of aldehydes are reaction with OH and photolysis. The photo-dissociation of aliphatic aldehydes is a potentially important source of HO₂ radicals in the troposphere (Zhu *et al.* [1999]). In general, the photolysis of aliphatic aldehydes can occur through the following fragmentation channels:

The Norrish-Type I reaction occurs *via* the α -cleavage of the photo-excited carbonyl leading to an acyl-alkyl radical pair. The HCO radical will go on to react with molecular oxygen to form HO₂ and CO. The Norrish-Type II reaction involves an intermolecular abstraction of a γ -hydrogen to produce a 1,4-biradical which will then fall apart to give acetaldehyde (rapidly formed from the tautomerism of the initial enol product) and an alkene.

The relative quantum yield branching ratio for the two Norrish processes described above depends on the structure of the aldehyde in question and also whether a γ -hydrogen is available for abstraction in the case of branched aldehydes. For example, the Norrish-Type I (radical) process is the dominant pathway for *n*-butanal photolysis (*ca.* 68 %). In contrast, the Norrish-Type II (molecular) channel is the main decomposition pathway for *n*-pentanal (*ca.* 80 %) (Tadic *et al.* [2001a]).



There is also literature evidence for the formation of cyclic alcohols in the photolysis of longer chain *n*-aldehydes (C₄-C₇) (Tadic *et al.* [2002]). For example for *n*-hexanal:



The longer the alkyl side chain, the more cyclic alcohols (4, 5 and 6 membered rings) can be produced.

The latest literature cross-section and (pressure dependent) quantum yields have been used to calculate new photolysis rates for *n*- (and branched) long chain aldehydes using TUV4.2. In general, the calculations show that the relative importance of the radical (Norrish I) channel generally *decreases* with respect to the molecular channel (Norrish II) with increasing *n*-aldehyde length. This can be explained by looking more closely at the σ and ϕ used.

The left-hand panel of Figure 8.6 shows a plot of the C₁-C₇ *n*-aldehyde cross-sections that are available in the updated model. The right-hand panel of Figure 8.6 shows the C₃-C₇ *n*-aldehyde HCO radical (Norrish I) quantum yields available in the updated model.

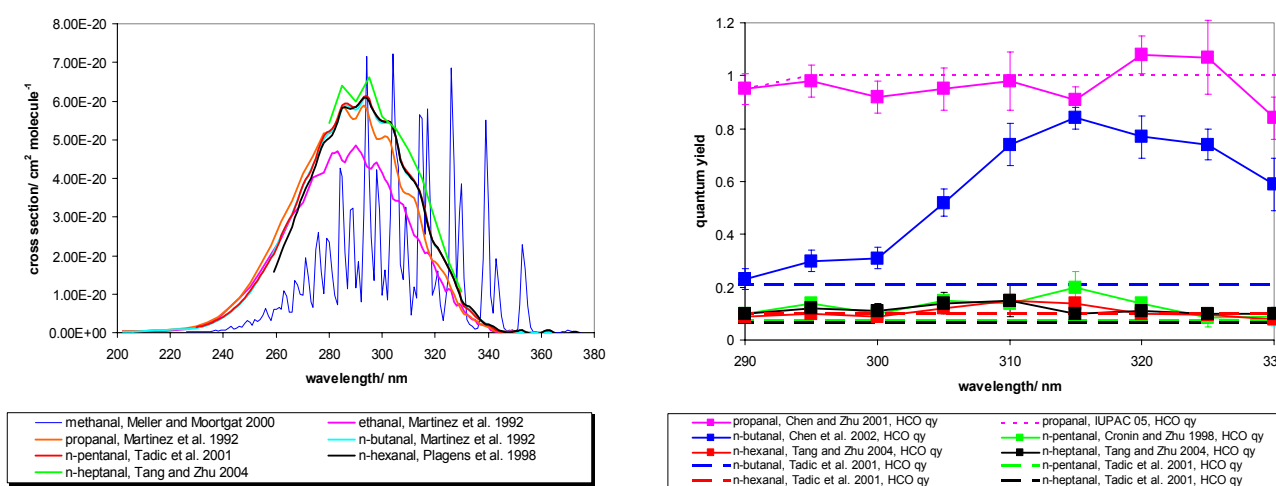


Figure 8.6 C₁-C₇ *n*-aldehyde Cross-sections (Left-hand Panel) and C₃-C₇ *n*-aldehyde HCO Radical (Norrish I) Quantum Yields (Right-hand Panel) available in the updated TUV4.2 model.

As shown in the left-hand panel of Figure 8.6, the cross-sections for the C₃-C₅ *n*-aldehydes are similar in shape and magnitude, exhibiting a broad bell shape with a maximum centred at ca. 290 nm of about 6×10^{-20} cm² molecule⁻¹. The cross-section for acetaldehyde (ethanal) is of a similar shape but only has a maximum of about 4.75×10^{-20} cm² molecule⁻¹. The cross-section for formaldehyde (methanal) extends to longer wavelengths and is highly structured. right-hand panel of Figure 8.6 shows that, in general, the radical quantum yield from C₃-C₇ *n*-aldehydes decrease with alkyl chain length, with *n*-propanal exhibiting a radical ϕ of ca. 1.0 (the Norrish II pathway is not open to this aldehyde). There are generally two literature values available for the quantum yields of each *n*-aldehyde in the updated model. These come from recent measurements made by the groups of Zhu and Moortgat. Zhu and co-workers use a laser light source to photolyse the aldehyde of interest and measure the ϕ for the production of HCO radicals directly in these studies using cavity ringdown spectroscopy (e.g., Cronin and Zhu, [1998]). However, Moortgat and co-workers generally use a continuous broad band photolysis source (with FTIR detection of the photo-products) in their studies,

hence they can only determine an integral effective ϕ for the photoactive spectral region (e.g., Tadic *et al.* [2001b]). This would go some way to explain the difference between the two ϕ_{HCO} measurements for *n*-butanal and *n*-pentanal shown in Figure 8.6.

Figure 8.7 shows a plot of relative product channel yield vs. carbon number. The radical channel (Norrish I) generally decreases from C₃ to C₇ as the molecular channel (Norrish II) increases. Also, as the aldehyde increases in length the more cyclic alcohols can be formed hence the yield of cyclic alcohols increases with length from C₄-C₇ at the expense of the Norrish II molecular channel. Until now these types of compounds have not been considered in atmospheric models. Therefore new chemistry will have to be added to the MCM to account for their atmospheric degradation.

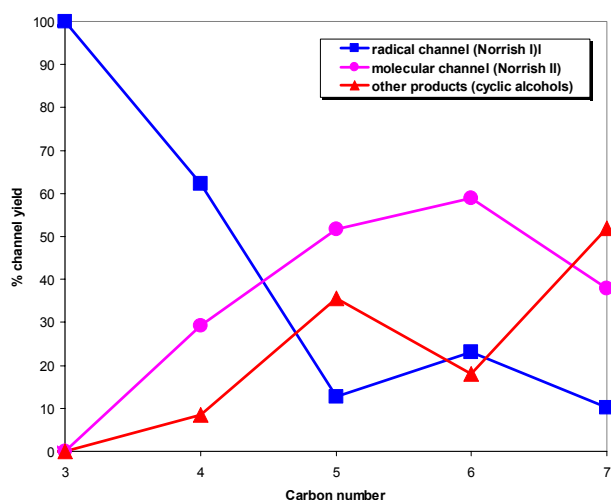


Figure 8.7 Relative Product Yields from the Photolysis of C₃-C₇ *n*-aldehydes.

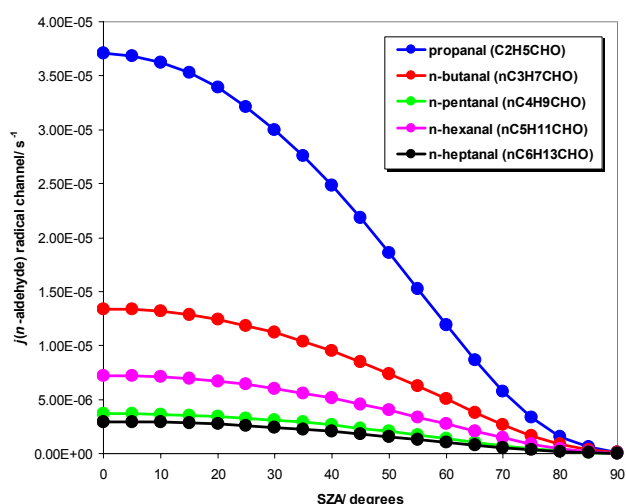


Figure 8.8 $J(n\text{-aldehyde})$ Values for the Norrish I Radical Channel as a Function of SZA as calculated using the Updates TUV4.2 Model.

Figure 8.8 shows calculated $j(n\text{-aldehyde})$ values for the radical channel with respect to solar zenith angle as calculated by the updated TUV4.2 model. As the aldehyde alkyl chain length increase $j(n\text{-aldehyde})_{\text{radical}}$ decrease as we would expect. In MCMv3.1 the parameterisation for $j(n\text{-C}_3\text{H}_7\text{CHO})$ is used as a surrogate for all longer chain ($> \text{C}_4$) *n*-aldehydes. This will obviously lead to an over estimation of the radical yields from $> \text{C}_4$ *n*-aldehyde photolysis.

(2) Glyoxal Photolysis

The cross-sections and quantum yields for glyoxal have been updated with the relative contributions of the photolysis branching ratios being better defined than previously.

The α -dicarbonyl compound glyoxal (CHOCHO) is predominantly formed in the oxidation of biogenic and anthropogenic hydrocarbons although small amounts are emitted directly from vehicle exhausts. In particular, glyoxal is an important ring opening product in the OH initiated oxidation of aromatics (see Figure 1.1). Glyoxal is also formed in the reaction of OH and O₃ with alkenes and unsaturated aliphatic aldehydes. Like the majority of atmospheric aldehydic species glyoxal is predominantly removed from the atmosphere by photolysis and reaction with OH.

In MCMv3.1 the photolysis pathways of glyoxal are:

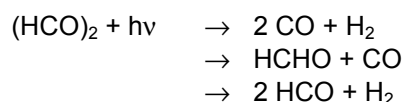


Figure 8.9 shows a plot of the glyoxal cross-sections that are available in the updated TUV4.2 model. There are two absorption bands, one in the UV (Left-hand Panel) and the other in the visible (Right-hand Panel).

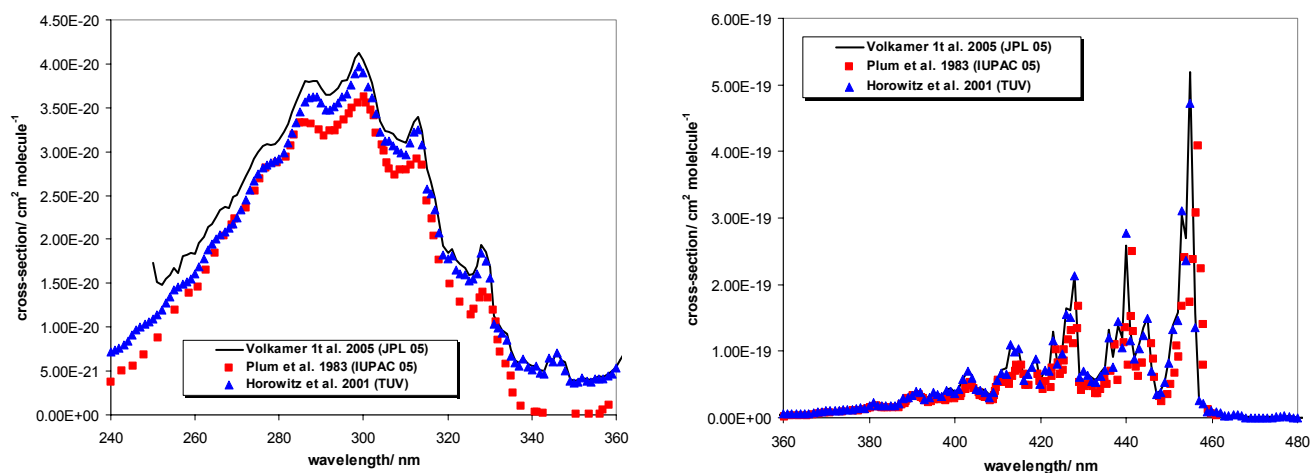


Figure 8.9 UV (Left-hand Panel) and Visible (Right-hand Panel) Component of the Glyoxal Cross-sections available in the Updated TUV4.2 Model.

From a closer inspection of the UV area of the spectrum (Left-hand panel of Figure 8.9) we can see that the recent measurements by Volkamer *et al.* [2005], which are the data recommended by JPL 2005 (not yet published) are higher than those of Plum *et al.* [1983], as recommended by IUPAC 2005, and Horowitz *et al.* [2001]. This manifests itself as a 5 % increase in total $j(\text{glyoxal})$ at a SZA of 0° .

In MCMv3.1 the ϕ for the three photolysis process were taken from the IUPAC 1992 recommendation. The model has been updated using the ϕ as listed in Table 8.1. The ϕ recommended by Calvert *et al.* [2000] has a cut off at 417 nm because Chen and Zhu [2003] suggest the energetic threshold (for the formation of 2 HCO) is 417 nm.

Table 8.1 Quantum Yields for the Photo-process involved in the Photolysis of Glyoxal.

Reaction	Calvert <i>et al.</i> [2002] 417 nm cut off	RADICAL Project (Moortgat <i>et al.</i> [2000]) Model Yields
H ₂ + 2CO	–	0.0044
HCHO + CO	0.089	0.026
2HCO	0.028	0.0044
Total	0.117	0.035

The ϕ from the RADICAL project (Moortgat *et al.* [2000]) are calculated using product studies and a measured ϕ_{eff} of 0.035 (defined as RADICAL v2 in Figure 8.11). Also during the RADICAL project absolute and the relative glyoxal quantum yields were measured in the laboratory, with the distribution of the absolute quantum yields for each photo-dissociation process deduced as shown in Figure 8.10 (defined as RADICAL v1 in Figure 8.11).

The photolysis rate of glyoxal was calculated using the cross-sections of Volkamer *et al.* [2005] and the various quantum yields listed above, the results of which are shown in Figure 8.11. The upper left hand panel of Figure 8.11 shows that the new photolysis rate calculations using the new measured and model RADICAL quantum yields are higher than both the MCMv3.1 parameterisation and $j(\text{glyoxal})$ calculated using the ϕ recommended by Calvert *et al.* [2002]. However, all the calculated photolysis rates are in agreement with the measurement of Klotz *et al.* [2000] of $\text{ca. } 1 \times 10^{-4} \text{ s}^{-1}$ at a SZA of 25° within error. However, the photolysis rates of the individual photo-processes are quite different depending on which quantum yields are used. For example, for $j(\text{glyoxal})$ calculations of the HCHO + CO channel (bottom right hand panel in Figure 8.11) calculation using the measured RADICAL quantum yield (RADICAL v1) gives a j -value that is much greater than that calculated using the MCMv3.1 parameterisation. Conversely, calculations of $j(\text{glyoxal})$ for the radical 2HCO channel (bottom left hand panel of Figure 8.11) show that the RADICAL v1 calculation gives a much lower radical yield than the calculation using the MCMv3.1 parameterisation.

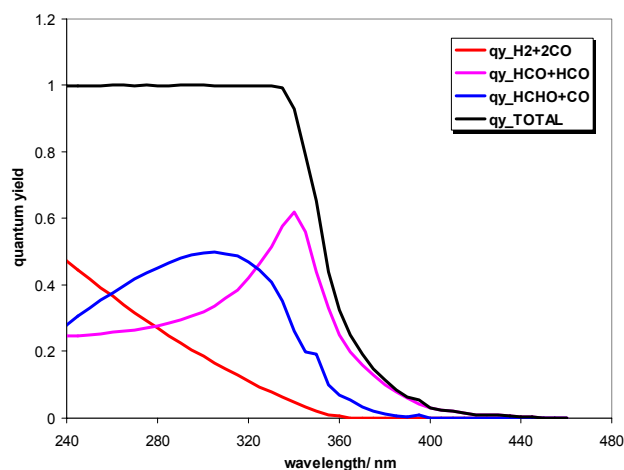


Figure 8.10 Absolute Quantum Yield and Relative Yields of the Different Decomposition Processes involved in the Photolysis of Glyoxal [Moortgat *et al.*, 2000].

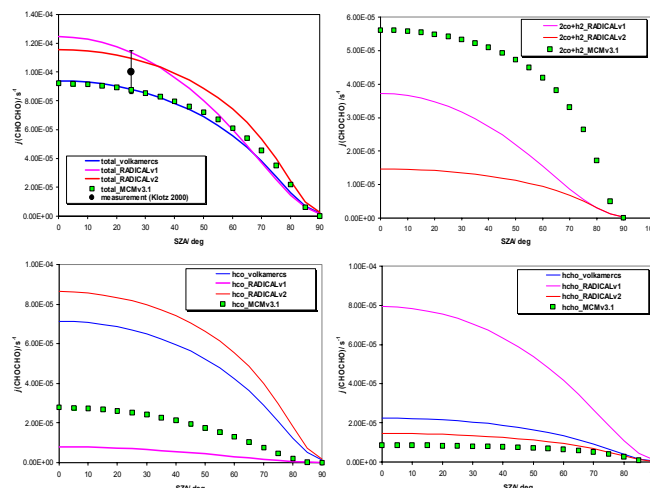


Figure 8.11 J (glyoxal) Calculations (total, radical and molecular channels) using the Cross-sections of Volkamer *et al.* (2005) and the various Quantum Yields as defined in the Text and Available in the updated TUV4.2 model. Also shown is J (glyoxal) calculated using the MCMv3.1 Parameterisation.

(3) Photolysis Overview

The way in which photolysis rates are represented in the MCM has been reviewed, updated and expanded. An extensive literature survey of cross-section and quantum yield data has been carried out in order to update the photolysis rate parameters currently in the MCM. The list of photolysis rates has been expanded through new literature data and this has enabled the choice and representation of surrogate parameters to be reviewed. All new and updated photolysis rates have been calculated using the discrete ordinate radiative transfer model *TUV4.2* (Madronich and Flocke [1998]).

The photolysis rates of ketones have also been extensively updated. New temperature and pressure dependent cross-sections (Gierczak *et al.* [1998]) and quantum yields (Blitz *et al.* [2004]) for acetone have been added to the model. A new acetone photolysis channel has been added which forms $2\text{CH}_3 + \text{CO}$ (threshold 299 nm) which becomes significant under upper tropospheric conditions. The photolysis of methyl ethyl ketone ($\text{CH}_3\text{C}(\text{O})\text{CH}_2\text{CH}_3$), methyl vinyl ketone ($\text{CH}_3\text{C}(\text{O})\text{CH}=\text{CH}_2$) (and the unsaturated aldehyde methacrolein ($\text{CH}_2=\text{C}(\text{CH}_3)\text{CHO}$)) have been updated using the lower quantum yields suggested by Pinho *et al.* [2005] in their evaluation of the MCM against SAPRC chamber experiments (see Imperial College contribution to Task 4 for more details). New data on the photolysis of specific carbonyl products formed in the oxidation of various biogenic VOCs have been added namely pinonaldehyde, pivalaldehyde, crotonaldehyde, glycolaldehyde and acrolein.

The complete overview of photolysis rates will be made available via the MCM website (<http://mcm.leeds.ac.uk>) and published as a review protocol. Recommended σ and ϕ parameters will be available as a function of wavelength and as a function of pressure and temperature in order to extend the MCM for use under free tropospheric conditions.

The new photolysis rate calculations will be made available in a similar parameterised form as the current MCM photolysis rates. Calculations of photolysis rates (with respect to SZA) will also be carried out under various representative atmospheric conditions (altitude, cloud cover, surface albedo) which will also be made available. However, by using a freely available program such as *TUV*, we will be able to make the updated model available on the website so that the user can calculate their own photolysis rates, either using our recommended σ and ϕ or any of the other literature selection which are also available in the model, for a particular atmospheric scenario of their choice.

Some of the new and updated data have opened up new photo-dissociation pathways not currently covered in the MCM (*e.g.*, cyclic alcohol formation in the photolysis of $> \text{C}_4$ *n*-aldehydes). Therefore new chemistry will need to be added to the MCM in order to accommodate these new species.

8.1.4 Evaluation of Master Chemical Mechanism (MCM v3) using Environmental Chamber Data

Introduction and Methodology

In collaboration with Paulo de Pinho and Professor Casimiro Pio (University of Aveiro, Portugal) and Professor William Carter (University of California, Riverside, USA), the MCM v3 degradation schemes for butane and isoprene have been evaluated using the large environmental chamber dataset of the Statewide Air Pollution Research Center (SAPRC) at the University of California [Carter *et al.*, 1995]. In addition to evaluation using butane-NO_x and isoprene-NO_x photo-oxidation experiments, this work has made use of experiments involving the major degradation products of butane (methyl ethyl ketone, MEK, acetaldehyde, CH₃CHO, and formaldehyde, HCHO), and of isoprene (methyl vinyl ketone, MVK, methacrolein, MACR, and formaldehyde, HCHO). The formation of MEK, CH₃CHO and HCHO from the degradation of butane is shown schematically in Figure 8.12, illustrating the participation of the carbonyl products in the degradation of butane to CO₂. In cases of both butane and isoprene, a procedure was adopted in which the experiments for the carbonyl products were used to test the corresponding subsets of the parent hydrocarbon mechanism, prior to evaluation of the full scheme. This step-by-step approach is advantageous, because it allows any compensating errors in the sub-mechanisms to be identified.

The full evaluation considered 46 butane-NO_x-air, 6 MEK-NO_x-air, 11 CH₃CHO-NO_x-air, 24 HCHO-NO_x-air, 9 isoprene-NO_x-air, 8 MACR-NO_x-air and 5 MVK-NO_x-air experiments (*i.e.*, 109 experiments in total). The ranges of reagent concentrations are presented in Table 8.2. Throughout the study, the performance of the MCM v3 chemistry was simultaneously compared with that of the corresponding chemistry in the SAPRC-99 mechanism, which was developed and optimised in conjunction with the chamber datasets [Carter, 2000].

Table 8.2 Ranges of Reagent Concentrations for the Considered Experiments.

	Butane	MEK	CH ₃ CHO	HCHO/NO _x	Isoprene	MACR	MVK
[VOC] (ppm)	1.47– 4.95	7.83– 9.49	0.44– 1.67	0.29– 1.01	0.27– 1.00	1.53– 4.41	0.87– 2.00
[NO _x] (ppm)	0.09– 0.66	0.09– 0.29	0.14– 0.28	0.16– 0.54	0.15– 0.60	0.24– 0.57	0.51– 0.60
[VOC]/[NO _x]	5.22– 39.89	26.61– 99.44	1.71– 11.73	1.00– 3.40	0.62– 2.08	3.57– 9.19	1.73– 3.72

Results and Conclusions

The MCM v3 mechanisms for both butane and isoprene were found to provide an acceptable reaction framework for describing the NO_x-photo-oxidation experiments, and generally performed well (*e.g.*, Figure 8.13 shows results for selected butane experiments). A number of parameter refinements were identified which resulted in an improved performance, the refined mechanism being denoted MCM v3a. The refinements all relate to the magnitude of sources of free radicals from organic chemical process, such as carbonyl photolysis rates and the yields of radicals from the reactions of O₃ with unsaturated oxygenates, which are under review in MCM development activities. Specifically, recommendations have been made [Pinho *et al.*, 2005] to update the photolysis parameters for HCHO, MEK, MACR and MVK, and the OH yields from the reactions of O₃ with MACR and MVK, either in line with data reported since the MCM mechanism development protocol [Jenkin *et al.*, 1997b], or on the basis of optimisation in the current study.

While the recommended updates are certainly necessary to maintain the MCM fully, it is emphasised that they have only a minor influence on the performance of the butane and isoprene schemes in atmospheric models. Consequently, these evaluation activities provide strong support for the MCM schemes for butane and isoprene, which are the most abundant components of emissions of anthropogenic and biogenic non-methane VOC, respectively.

The MCM v3.1 degradation mechanisms for ethene, propene, 1-butene, 1-hexene, α -pinene and β -pinene have also been evaluated. The mechanisms have been found to provide a good reaction framework for describing the NO_x-photo-oxidation experiments on these systems, and the work is currently being written up for publication.

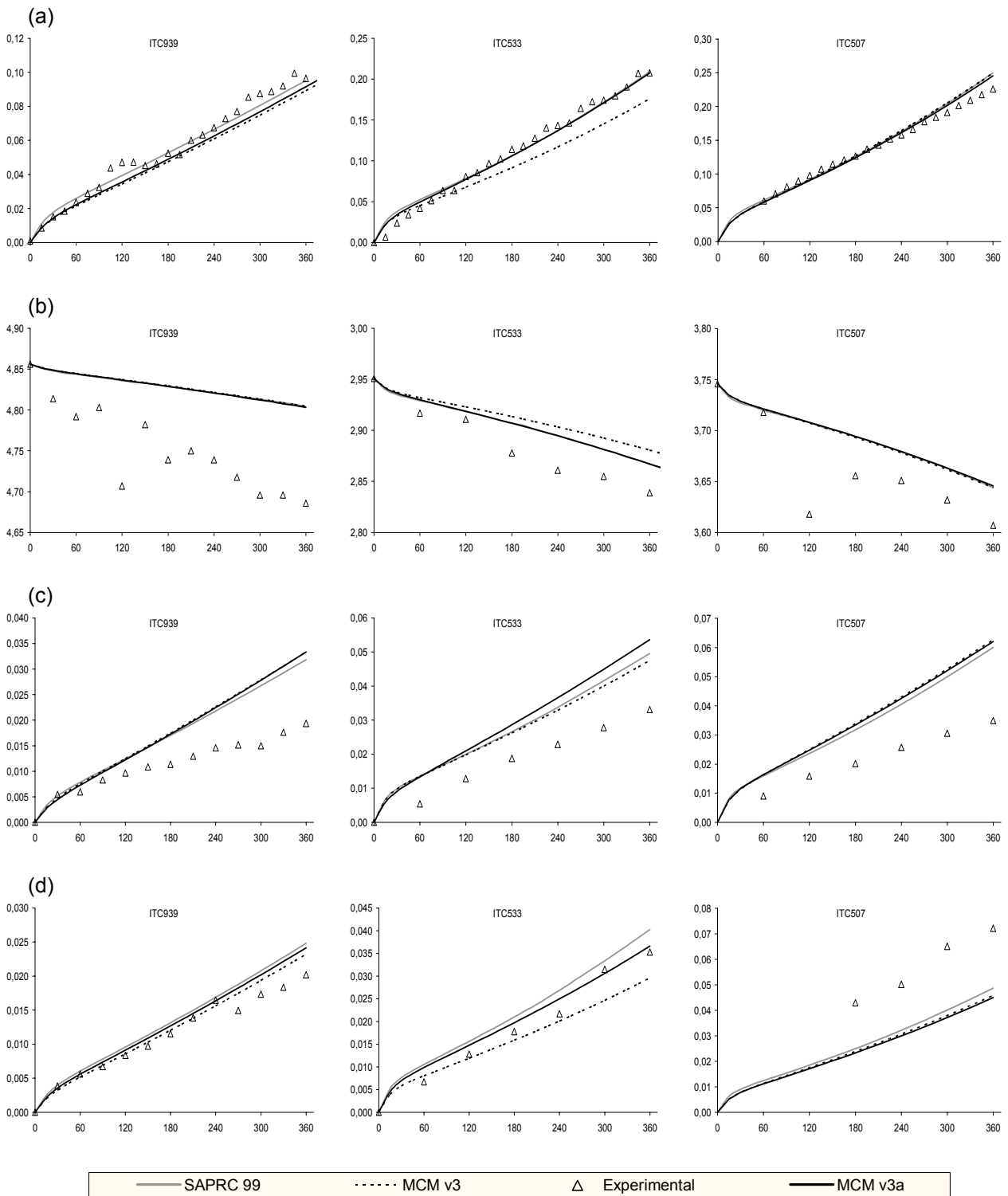
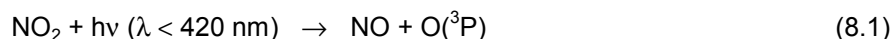


Figure 8.13 Observed and Calculated $\Delta(O_3-NO)$ (ppm) vs. Time (min) (Top Row of Panels), Butane vs. Time (min) (Second Row of Panels), CH_3CHO (ppm) vs. Time (min) (Third Row of Panels) and MEK (ppm) vs. Time (min) (Third Row of Panels) for the Same Selected butane/ NO_x /Air Experiments.

8.1.5 The Common Representative Intermediates (CRI) Mechanism

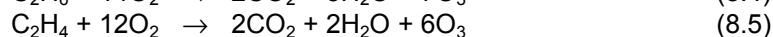
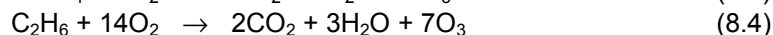
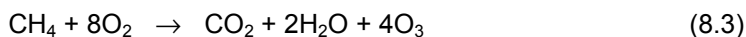
Introduction

The complete oxidation of a given VOC though to CO₂ and H₂O normally proceeds via a series of intermediate oxidised products. At each stage, the chemistry is propagated by reactions of free radicals leading to the oxidation of NO to NO₂ and resultant formation of O₃ as a by-product, following the photolysis of NO₂:



The total quantity of O₃ potentially generated is therefore dependent on the number of NO to NO₂ conversions which can occur during the degradation, but is restricted by the time available for the chemistry to occur. Consequently, the O₃ forming ability of VOC has sometimes been expressed in terms of 'kinetic' and 'mechanistic' or 'structure-based' components [e.g., Carter, 1994; Derwent *et al.*, 1998].

On the basis of understanding of the detailed chemistry for simple hydrocarbons such as methane, ethane and ethene, the total quantity of O₃ potentially formed as a by-product of the complete OH-initiated and NO_x-catalysed oxidation to CO₂ and H₂O can be represented by the following overall equations:



In the case of ethane, for example, this is based on the oxidation via CH₃CHO, HCHO and CO as intermediate oxidised products, as shown in Figure 8.14. According to equations (8.3) - (8.5), therefore, the complete oxidation of one molecule of each of these compounds leads to the production of 4, 7 and 6 molecules of O₃ respectively. Logically, the number of O₃ molecules produced in each case (*i.e.*, the number of NO to NO₂ conversions) is equivalent to the number of reactive bonds in the parent molecule, that is the number of C-H and C-C bonds which are eventually broken during the complete oxidation to CO₂ and H₂O.

Construction of the CRI Mechanism

In the CRI mechanism, this simple rule is used to define a series of generic intermediate radicals and products, which mediate the breakdown of larger VOC into smaller fragments (*e.g.*, HCHO), the chemistry of which is treated explicitly [Jenkin *et al.*, 2002]. Version 1 of the CRI mechanism treats the degradation of methane and 120 emitted VOC using about 570 reactions of 250 species (*i.e.*, an average of about 2 species per VOC). It thus contains <5% of the number of reactions and <7% of the number of chemical species in MCM v3.1, providing a computationally economical alternative. The mechanism was previously optimised through comparison with the MCM, by adjusting the reactivity of representative intermediate carbonyl products, such that it was able to generate concentrations of ozone, OH, peroxy radicals, NO and NO₂ which were in excellent agreement with those calculated using the MCM, in simulations using the PTM on a standard trajectory [Jenkin *et al.*, 2002].

Testing of Version 1 of the CRI Mechanism

Whilst it is recognised that CRI v1 correctly represents ozone formation from the VOC mixture on the standard trajectory, it is recognised that it may not fully recreate the relative contributions of component VOC or VOC classes within the emitted mixture, and that there may be other ambient scenarios for which its performance is less good. In view of this, a programme of validation and testing activities has been carried out.

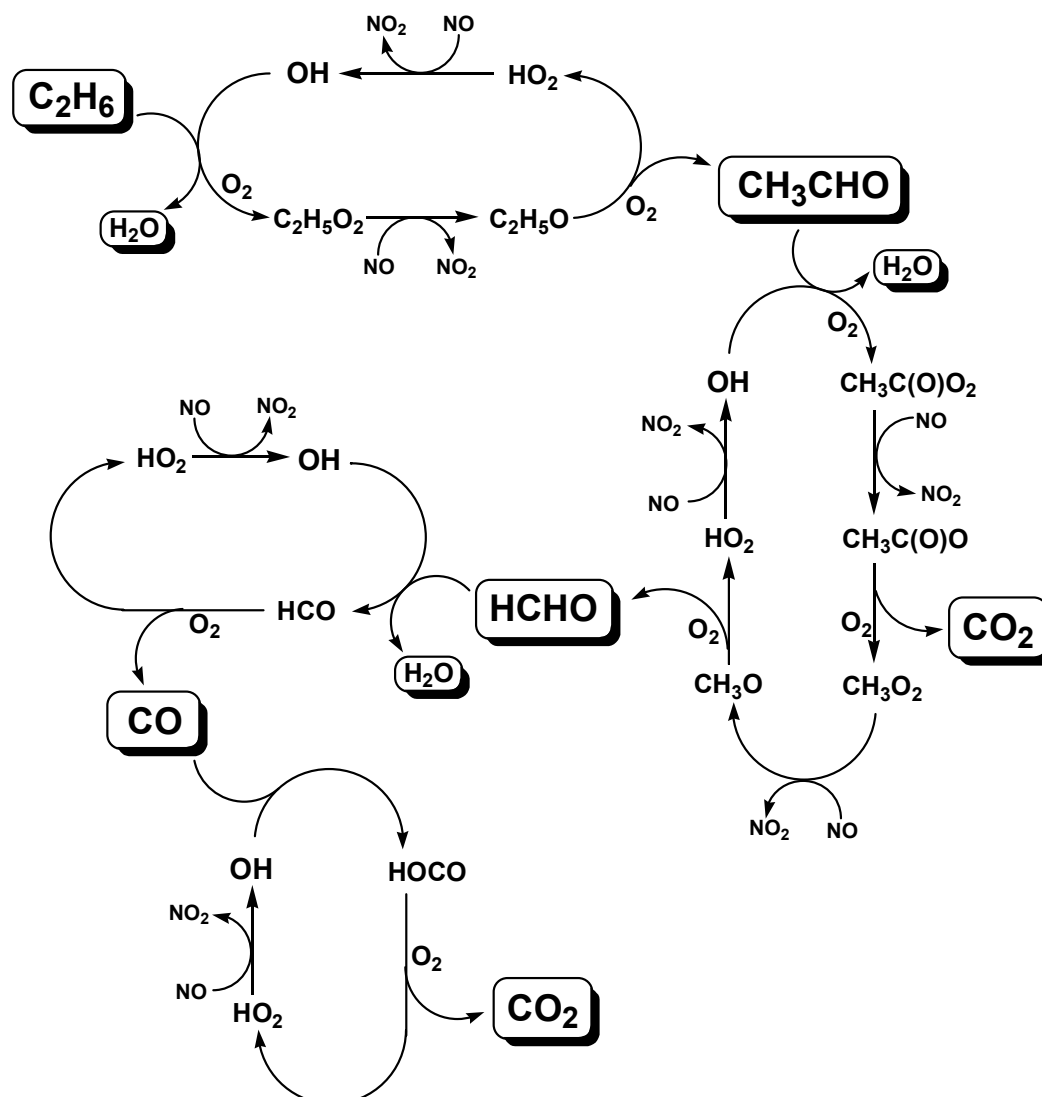


Figure 8.14 Schematic Representation of the Reactions involved in the OH initiated, NO_x catalysed Oxidation of Ethane to CO_2 . The Reaction Sequence shows the Formation of Acetaldehyde (CH_3CHO), Formaldehyde (HCHO) and CO as Intermediate Oxidised Products. The Complete Sequence results in 7 NO to NO_2 conversions. Subsequent photolysis of NO_2 regenerates NO and leads to Ozone Formation (Reactions (8.1) and (8.2)), with the Net Overall Chemistry as shown in Reaction (4). (N.B. The Oxidation of CO to CO_2 partially proceeds via $\text{OH} + \text{CO} \rightarrow \text{H} + \text{CO}_2$, followed by $\text{H} + \text{O}_2 + \text{M} \rightarrow \text{HO}_2 + \text{M}$, which has the Same Overall Chemistry as that displayed above, i.e., $\text{OH} + \text{CO} + \text{M} \rightarrow \text{HOCO} + \text{M}$, followed by $\text{HOCO} + \text{O}_2 \rightarrow \text{HO}_2 + \text{CO}_2$).

The performance of CRI v1 was initially tested for the conditions of the first campaign of the Tropospheric Organic Chemistry Experiment (TORCH) in August 2003, which is described in more detail below (Section 8.4). The PTM-CRI v1 and PTM-MCM v3.1 were both used to simulate the chemical development of air parcels travelling along 16 96-hour case study trajectories, prior to arrival at the TORCH campaign site at Writtle, near Chelmsford in Essex. Figure 8.15 shows that the ozone concentrations simulated with PTM-CRI v1 at the arrival point were generally in very good agreement with those simulated with PTM-MCM v3.1, indicating that the reduced mechanism captures the major features of the chemistry of regional-scale ozone formation. In one case study (9 August), however, the PTM-CRI v1 simulates a significantly lower ozone concentration, suggesting that the performance is not so good under specific conditions. Inspection of the associated trajectory reveals that, in this one case, the air mass was almost stationary over the Greater London conurbation for the final day of the simulation, prior to travelling to the receptor in the final 3 hours, such that the conditions tended towards those of an urban simulation.

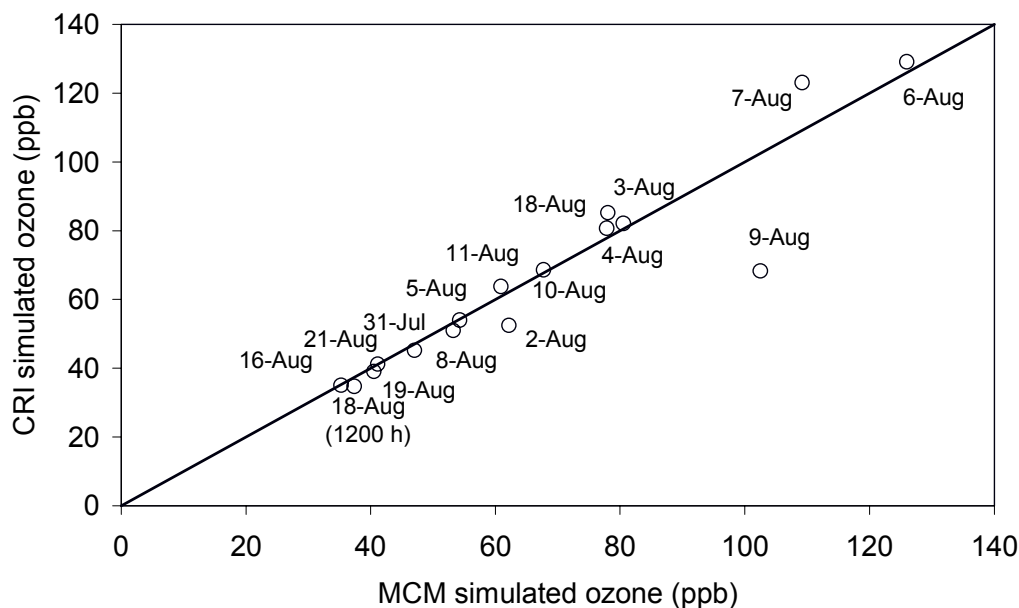


Figure 8.15 Comparison of Ozone Concentrations simulated with PTM-CRI v1 and PTM-MCM v3.1 at the Receptor Site of the TORCH 2003 campaign (Writtle, Essex) for 16 Case Study Events. Unless otherwise stated, the arrival time was 18:00h.

Further examination of CRI v1, in comparison with MCM v3.1, has been carried out in collaboration with Laura Watson and Dr Dudley Shallcross (University of Bristol), using a boundary layer box model collecting emissions of VOC, NO_x, methane, CO and SO₂ at average UK rates (based on 2001 NAEI data), but with diurnal variations applied. Simulations carried out over a four day period with the full VOC speciation have demonstrated that the two mechanisms generally perform comparably, as shown in Figure 8.16.

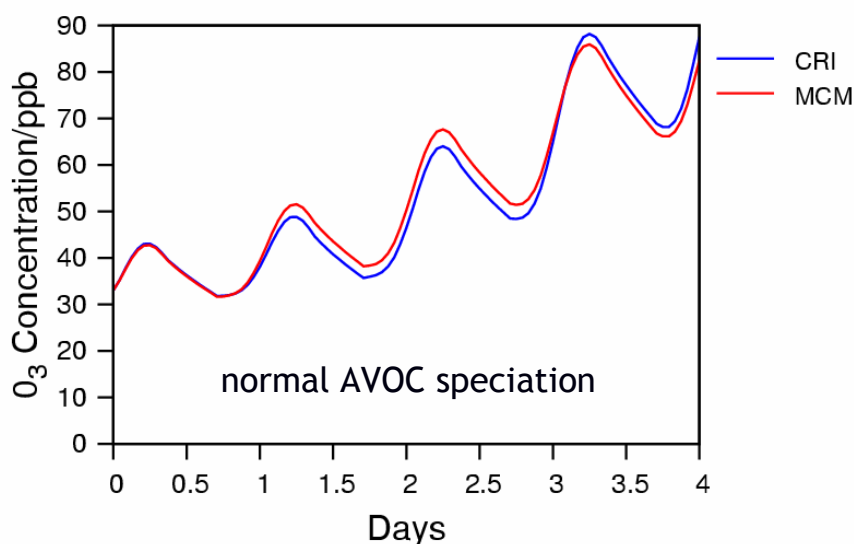


Figure 8.16 Comparison of Ozone Concentrations simulated with CRI v1 and MCM v3.1 over a Four-day Period in a Boundary Layer Box model with Average UK Emissions (21 June, 51.5°N). Calculations performed in Collaboration with Laura Watson and Dr Dudley Shallcross (University of Bristol).

The results show that the CRI under-simulates ozone formation slightly in the early stages of the simulation, but simulates similar ozone concentrations to MCM v3.1 on the final day. The performance has been examined further by emitting VOC entirely as individual classes, namely as alkenes, alkenes, oxygenates and aromatics. In each case, the relative speciation within the given

class is the same as in the base case simulation, but the total emissions of that class are scaled to represent the total VOC emissions. The results (shown in Figure 8.17) demonstrate that the CRI v1 chemistry for alkenes, alkenes and oxygenates performs comparably with MCM v3.1. However, the CRI v1 aromatic simulation seriously underestimates ozone formation in the early stages, although the final ozone concentration after four days approaches that simulated with MCM v3.1, indicating some longer timescale recovery. Given that aromatic chemistry is particularly important on the urban scale, it is clear that shortcomings in its representation contribute to the under-simulation of CRI v1 in the TORCH 9 August case study (Figure 8.15). The main conclusion, therefore, is that CRI v1 generally performs extremely well in comparison with MCM v3.1 for simulation of regional scale ozone formation on trajectories to rural receptors, but may be less adequate for urban simulations.

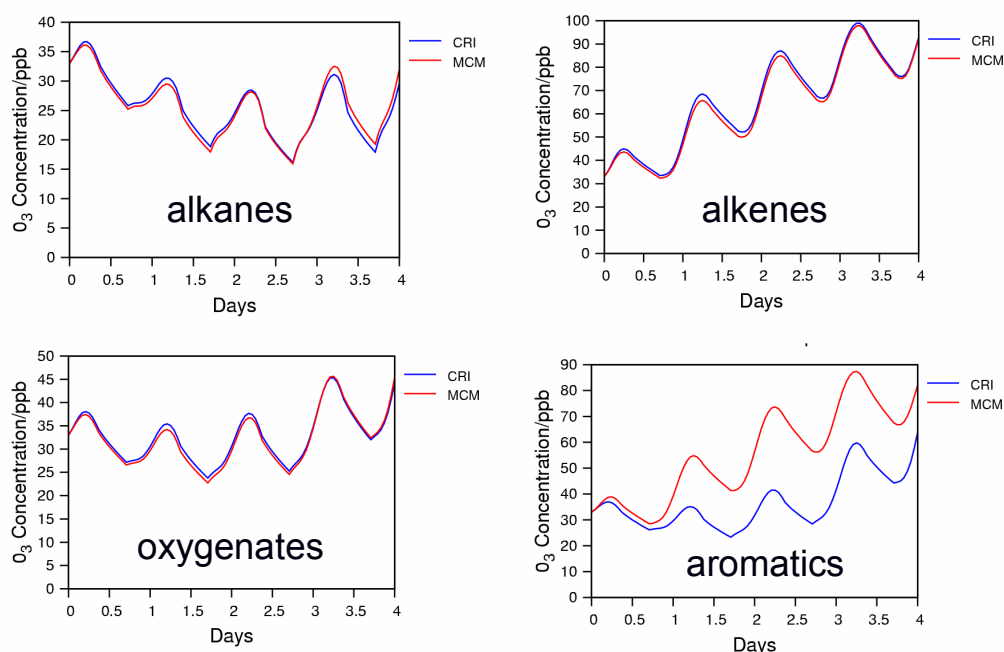


Figure 8.17 As Figure 8.16, but with VOC emitted entirely as the Individual VOC Classes, Alkanes, Alkenes, Oxygenates and Aromatics (see text).

Development of Version 2 of the CRI Mechanism

Based on the above appraisal, development activities for CRI v2 for have therefore focussed on the treatment of the degradation of classes of VOC. A procedure has been adopted in which each individual VOC in a given class has been considered separately, and validated using the representation in MCM v3.1. This has demonstrated that the mechanism is improved by defining separate series of representative intermediates for some VOC classes. This leads to an ultimate increase the size of the mechanism over that of CRI v1, but allows a more rigorous description of the impact of the different VOC emission sectors, and an improved foundation for the expansion of the mechanism to the treatment of the many minor VOC not previously represented in MCM or CRI.

The construction and optimisation procedure makes use of reference simulations of ozone concentrations, using the MCM v3.1 version of the boundary layer box model described above. The model is run with VOC emissions entirely in the form of an individual VOC. Although the studies described above indicate that the alkane, alkene and oxygenate classes perform well when the complete speciation within a given class is used, the possibility of compensating errors exists in the representations of the chemistry of the individual VOC. Thus, the systematic procedure is applied to all VOC classes.

The results for a series of alkanes (Figure 8.18) demonstrate that different amounts of ozone are generated with each different VOC. Starting with the smallest alkane, simulations are performed with the CRI mechanism, and the reactivity of appropriate intermediate products is varied to optimise ozone formation in comparison with MCM v3.1, and the procedure is repeated in turn for the larger alkanes. To illustrate this, Figure 8.19 shown a portion of the mechanism in which pentane is

degraded until an intermediate is generated, which also formed from the degradation of butane. Given that the representation of butane degradation is already optimised, optimisation of the pentane scheme can be achieved through variation of the reactivity of the intermediate 'CARB13' (Figure 6). In this way, the mechanism for complete classes of VOC is built up and optimised.

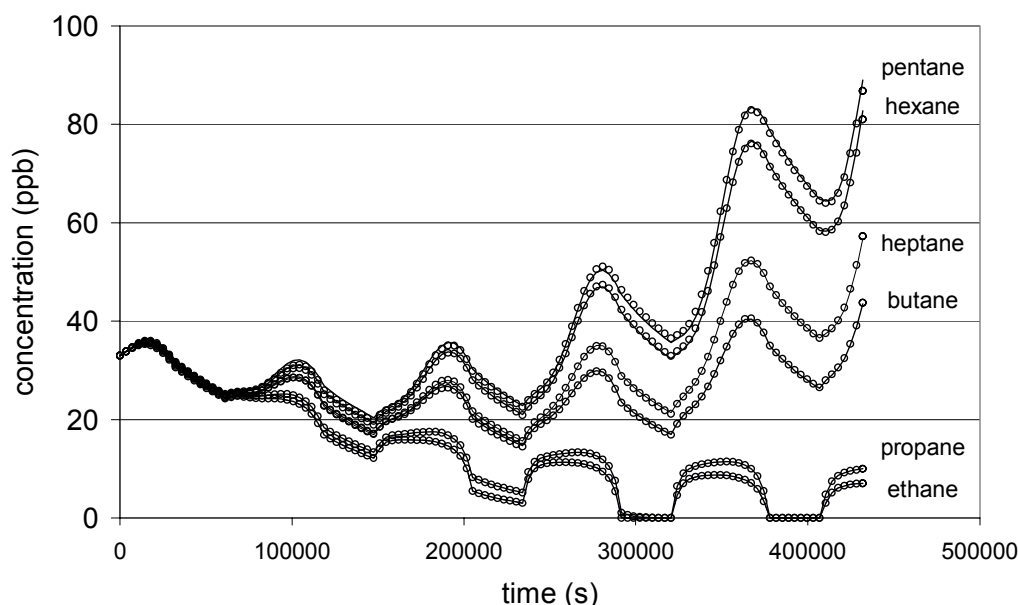


Figure 8.18 Comparison of Ozone Concentrations simulated with MCM v3.1 (open circles) and Optimised CRI v2 (lines) over a Five-day Period in a Boundary Layer Box Model with Average UK Emissions (21 June, 51.5°N). In each case, VOC are emitted in the form of the Single Alkane identified in the Figure.

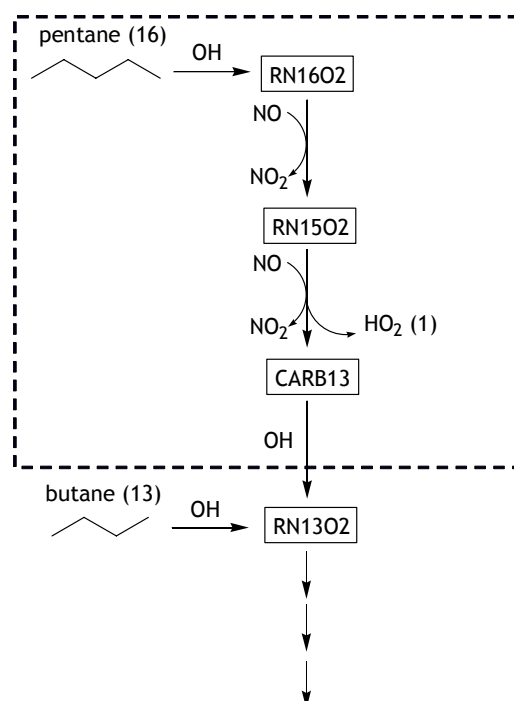


Figure 8.19 Schematic Representation of a Portion of the Degradation Chemistry in CRI v2, showing the Degradation of Pentane and how it feeds into the Butane Degradation Mechanism. The Index assigned (in brackets) to each Alkane is the Total Number of C-H and C-C bonds it contains. The Indices within the Generic Radicals and Carbonyls (e.g., '16' in RN16O₂ and '13' in CARB13), thus represent the Number of NO to NO₂ Conversions which can result from the Subsequent Complete Degradation.

Within the course of the current contract, the above procedure has been carried out for the non-aromatic VOC classes, such that the associated chemistry provides a rigorously tested reduced mechanism. Optimisation of the reduced aromatic chemistry is in progress, and will yield a mechanism in which the common intermediates cover a much wider reactivity range than represented in CRI v1. This will facilitate improved representation of the chemistry close to source, and a mechanism applicable to a wider range of scenarios.

Development of a CRI-based annex to MCM v3.1

The common representative intermediates (CRI) approach has also been used to develop a representation of the degradation of 38 additional VOC from the NAEI speciation. The species, listed in Table 8.3, are mainly large alkanes, cycloalkanes and aromatics which are collectively significant components of 'white spirit' and 'kerosene', but which individually make comparatively small contributions to the overall NAEI speciation.

Table 8.3 Additional VOC Species treated in the CRI-based Annex to MCM v3.1, and the Unspeciated Mixtures for which Emissions Representations have been recommended.

Speciated

Alkanes (C₈-C₁₄)	2,6-dimethyloctane	methylcyclohexane	Aromatics (C₆-C₁₂)
2-methylheptane	2-methyl-3-ethylheptane	ethylcyclohexane	1,2,3,5-tetramethylbenzene
3-methylheptane	2,2,3,3-tetramethylhexane	propylcyclohexane	1,2,4,5-tetramethylbenzene
2-methyloctane	2-methyldecane	i-propylcyclohexane	p-cymene
3-methyloctane	3-methyldecane	1,2,3-trimethylcyclohexane	1-methyl-3-i-propylbenzene
4-methyloctane	4-methyldecane	butylcyclohexane	i-propylcyclohexane
3,4-dimethylheptane	5-methyldecane	i-butylcyclohexane	Alkenes & Alkynes (C₃-C₁₀)
2-methylnonane	tridecane	1-methyl-3-propylcyclohexane	dipentene
3-methylnonane	tetradecane	1-methyl-4-i-propylcyclohexane	propyne
4-methylnonane	Cycloalkanes (C₆-C₁₂)	pentylcyclohexane	
2,5-dimethyloctane	methylcyclopentane	hexylcyclohexane	

Unspeciated

Unspeciated Mixtures	C ₁₃₊ alkanes	other alkenes	Aromatics
Alkanes	Alkenes	Cycloalkanes	C ₁₀ aromatics
C ₇ alkanes	C ₆ alkenes	C ₇ cycloalkanes	C ₁₁ aromatics
C ₈ alkanes	C ₇ alkenes	C ₈ cycloalkanes	C ₁₂ aromatics
C ₁₀ alkanes	C ₈ alkenes	C ₉ cycloalkanes	C ₁₃₊ aromatics
C ₁₁ alkanes	C ₉ alkenes	C ₁₀ cycloalkanes	other aromatics
C ₁₂ alkanes	C ₁₀ alkenes	C ₁₁ cycloalkanes	
C ₁₃ alkanes	C ₁₂ alkenes	other cycloalkanes	

The applied methodology has involved explicit representation of the reactions which initiate degradation, to produce radical products which possess the appropriate CRI index. The subsequent chemistry of these radicals feeds into the MCM v3.1 chemistry at the earliest possible opportunity, by generating MCM species which possess the correct CRI index (*i.e.*, based on the number of C-H and C-C bonds). Because the MCM usually includes a wide variety of species of the same index, the selected species is generated from the degradation of a related VOC, where possible. In this way, portions of the existing MCM chemistry are able to act as 'mechanistic surrogates' for the degradation of the additional compounds.

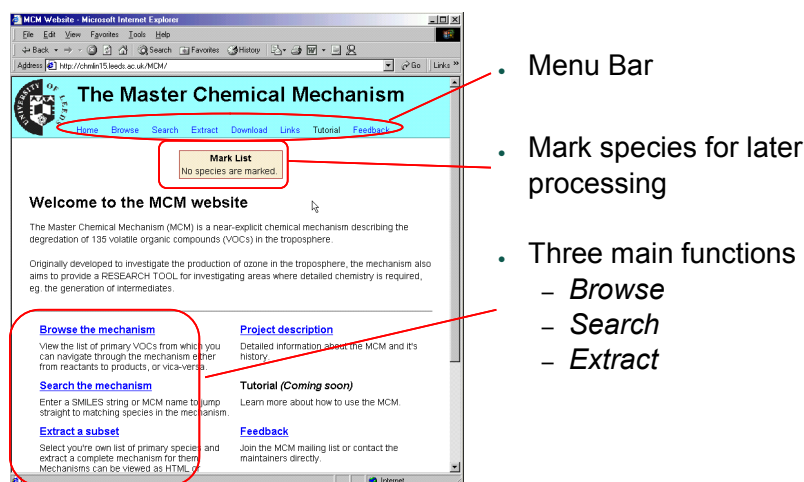
A representation of 25 VOC unspeciated mixtures has also been recommended, based on the species currently treated in MCM v3.1 and the additional 38 VOC in the CRI annex. These mixtures are also listed in Table 8.3.

8.2 THE NEW MCM WEBSITE

As part of the ongoing improvements to the MCM a new version of the website has been developed with the primary objectives of making the website clearer and easier to navigate and of improving access to the MCM itself. The new site is available at the following address: <http://mcm.leeds.ac.uk/MCM/>.

8.2.1 New Layout and Web Tools

The new site has three main self-explanatory functions; **Browse**, **Search** and **Extract** as shown in Figure 8.20.



- Menu Bar
- Mark species for later processing
- Three main functions
 - Browse
 - Search
 - Extract

Figure 8.20 The New MCMv3.1 Homepage.

Also illustrated in Figure 8.20 is the permanently displayed **Mark List** which is effectively a “shopping basket” for collecting species of interest as you browse around the MCMv3.1 ready for mechanism extraction. The **Browse** facility enables the user to look through the MCMv3.1 by category in a similar way to the old site except the species now have structures associated with them. Figure 8.21 shows the **Browse** web page. All 135 primary VOCs are listed by category along with the inorganic chemistry (gas and particle reactions and photolysis rates) as well as listings for the generic rate coefficients used throughout MCMv3.1 including the photolysis rate parameterisations.

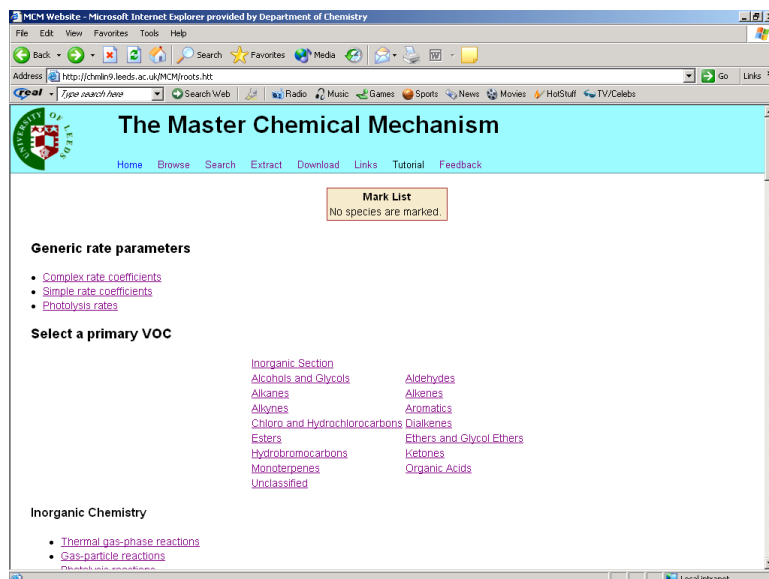


Figure 8.21 MCMv3.1 Browse Facility.

Alternatively the **Search** function allows the user to search the MCMv3.1 either by SMILES string (tutorial on SMILES linked to website) or by MCM species name as shown in Figure 8.22. For example, in the case of isoprene (2-methyl-1,3-butadiene) if either the SMILES string (C=C(C)C=C) or MCM species name (C5H8) is entered as a query then the search results should return the structure of the species and the MCM name as seen in Figure 8.23.

Enter SMILES string
– e.g. isoprene: C=C(C)C=C

Enter a MCM species name
– e.g. n-butane: NC4H10

Figure 8.22 MCMv3.1 Search Facility.

Structure image linked to reaction listing.

Figure 8.23 MCMv3.1 Search Results.

If the MCM species name is then clicked upon then the user will be lead to its degradation scheme (with reactant and product structural information) as illustrated in Figure 8.24, again for isoprene. Each individual reaction within the reaction listing displays its rate constant and branching ratio. Any generic rate constants and photolysis rates are directly linked to an appropriate table which list the equations and parameters used to calculate their value. Each reaction product's degradation scheme can be accessed in a similar fashion by clicking on its MCM species name. Also individual reactants and products have an associated “mark” button so that they can be added to (and displayed in) the *Mark List* for complete mechanism extraction later.

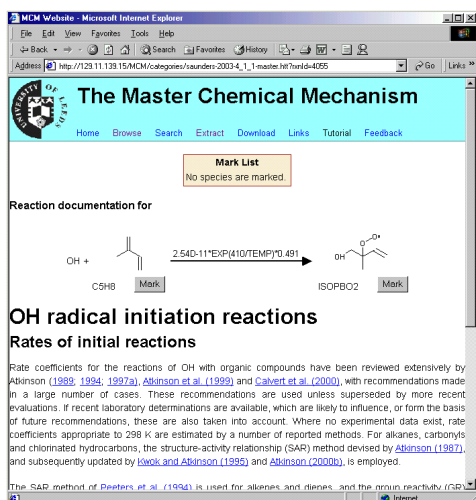
Reaction source information

Add species to Mark List

Figure 8.24 MCMv3.1 Degradation Scheme for Isoprene.

To the right of each equation is the “doc” link (see Figure 8.24). This leads to a webpage containing contextual information from the MCM protocols [Jenkin *et al.* 1997b, Saunders *et al.* 2003] on where

the rate constants and branching ratios come from or how they were calculated (from a suitable structure activity relationship) as shown in Figure 8.25.



- Information based on Protocol papers
- Hyperlinked citations

Figure 8.25 Contextual Information on Reaction of Interest.

The protocol web pages are linked to a central citations database, which contains a list of references complete with abstract (where available). Figure 8.26 shows a flow diagram breakdown of the MCM by reaction category along with the protocol section references used to construct the contextual web pages.

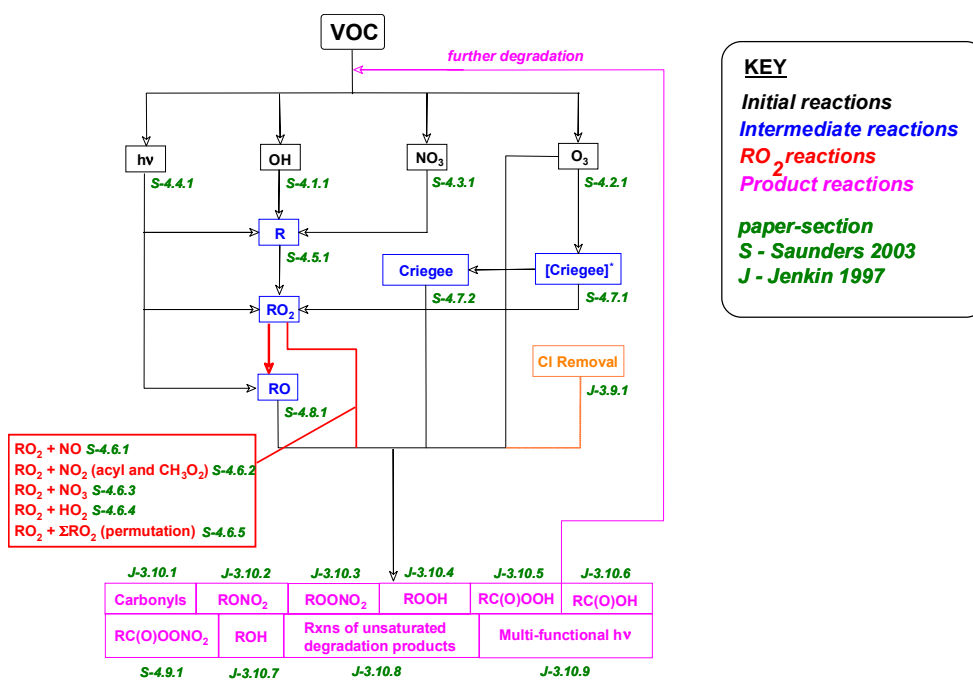
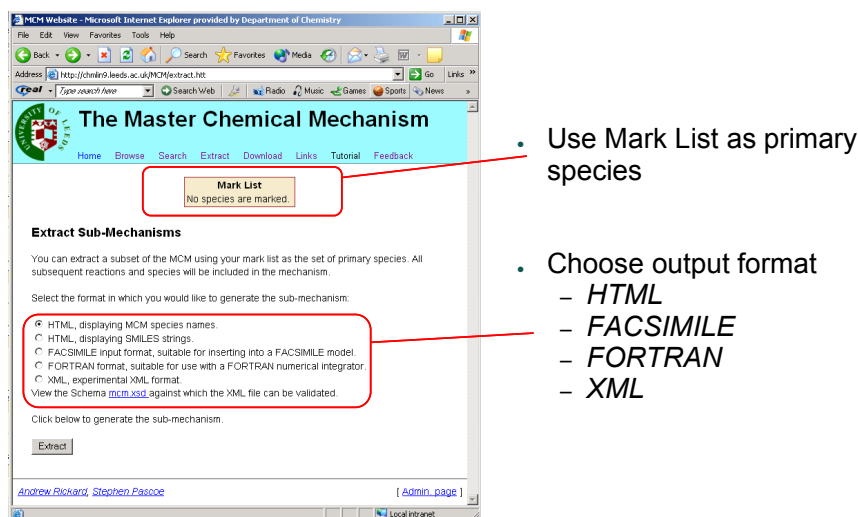


Figure 8.26 Flow Chart showing the Major MCM reaction Categories considered in the MCM Protocols.

As already mentioned the new *Extract* web-tool can extract complete subset mechanisms of the MCMv3.1 for the species listed in the *Mark list*. The MCM is primarily set up for use with the FACSIMILE integrator. In order to encourage the MCM's wider use within the modelling community several extraction output formats and options are now available as shown in Figure 8.27 and listed below:



- Use Mark List as primary species

- Choose output format
 - HTML
 - FACSIMILE
 - FORTRAN
 - XML

Figure 8.27 The MCMv3.1 Extract Tool and Output Options.

- (1) The FACSIMILE output has been improved by additionally including a list of species variables and a peroxy radical summation list so that the mechanism can be more easily integrated into a FACSIMILE box model.
- (2) A FORTRAN subset extractor option is available which directly interprets the material retrieved from the database by the subset extractor and produces the files needed to run the subset with a FORTRAN solver. The reactions are produced in a numerical format which can be easily read into the user's own numerical integrator. Details of rate coefficients for each reaction are also output in a FORTRAN subroutine which includes all the expressions for the calculation of the complex rate coefficients and photolysis rates. A further FORTRAN subroutine is output which can be used to calculate the right hand side of the rate equations of the subset.
 A converter which will allow users to convert their own mechanisms from a standard FACSIMILE format to FORTRAN format is also available on the website. This allows the user to generate all the data files described above for any existing FACSIMILE file. This code only extracts the reaction structure from the file, it is then up to the user to adapt the output files to allow simulation of the required conditions.
- (3) XML versions of the subsets can also be extracted. This extractor has been updated so that subsets are accurately produced in full in a developmental XML format. Work is continuing to develop the most appropriate and useful design for the XML schema and the properties of Chemical Markup Language (CML) are being examined to understand the ways in which XML is currently used to represent chemistry. We are currently liaising with modellers who are interested in using the MCM in this format as to what is the best design scenario. This on-going research will lead to the production of a simple but flexible method by which extracted subsets can be displayed and analysed.
- (4) A trial KPP version of the subsets can now be extracted. KPP (Kinetic PreProcessor, Damian *et al.* [2002]) is a software package for the numerical integration of chemical mechanisms (<http://people.cs.vt.edu/~asandu/Software/kpp/>). It is similar in format to FACSIMILE but is available freely on the internet and the resulting code is much easier to incorporate into other (e.g., global) models. This version of the extractor will produce a representation of the subset in KPP format and a full species listing. A subroutine which can be used for the calculation of rate coefficients is also available for download. Thanks to Rolf Sander at MPI-Mainz for his help with the development of the KPP extractor.

All the above formats are more robust than FACSIMILE and are more future proof, their availability should encourage the wider use of the MCM in a greater variety of applications. Complete FACSIMILE MCMv3.1 box models are available in the "Download" section of the website in both PC and UNIX versions. A new mailing list option has been added to the site in order that users can give feedback on the MCMv3.1 and the site, report errors and receive regular updates.

8.2.2 Mechanism Reduction using the CRI mechanism

There is also on-going work developing techniques which can be used to generate mechanisms of reduced dimension in a more automatic fashion (Whitehouse *et al.* 2004a, 2004b). In particular work is in progress using the CRI mechanism ("CRIMECH", see Section 8.1.5 earlier) to create a lower dimension mechanism using the automatic lumping of species with similar lifetimes. Groups of species which have the potential to be successful lumps can be identified using an algorithm based on the type of reaction rates. CRIMECH is an ideal candidate for the application of this due to the large numbers of identical reaction rates. A preliminary investigation using a subset of CRIMECH has led to a 70 % reduction in the number of species in the mechanism. This work will be continued using the full mechanism.

8.2.3 Under the Hood: New Design and Interactive Database

Fundamentally important to the new website design/operation was the conversion of the central MCM database (where the basic reaction and species information is stored) to just one MySQL integrated and interactive database on the web server. The online MySQL database essentially consists of three tables containing information on the species, reactions and generic rate parameters, from which the website representation of the MCMv3.1 is constructed. The updating and maintenance of the MySQL database is facilitated *via* ODBC (open database connectivity) through the usual Access/Accord front end. A simple flow chart illustrating the connectivity between the online and offline central MCM databases is shown in Figure 8.28.

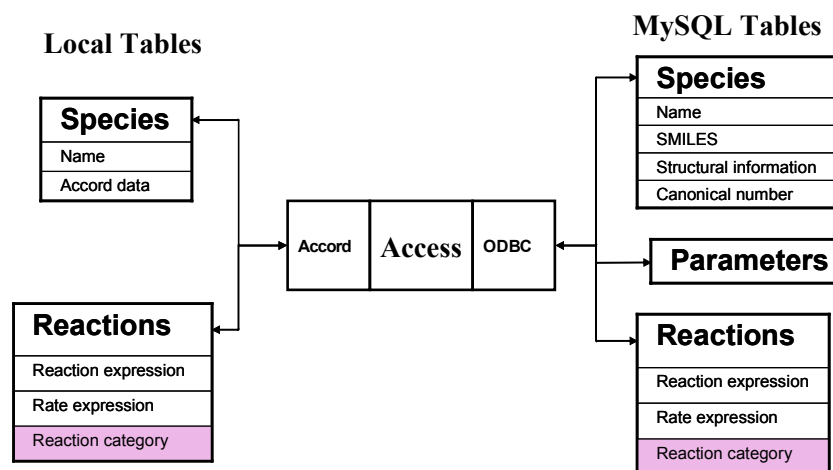


Figure 8.28 Flow Chart for the Central MCM Database.

Accord structural information stored in the local species table is converted and stored as Cartesian coordinates in the online MySQL table. Programs embedded within the MCM website then use this information to construct the reactant and product structures when called upon and these images are then stored in a cache file for future use. The unique conical numbers (derived from the structural information) and SMILES string information in the MySQL species table are used by the website for efficient searching of the MCM database. The reaction category in the local and MySQL reactions tables store the web links to pages containing contextual information on each reaction (*e.g.*, Figure 8.25). The inner workings of the new website are summarised in Figure 8.29.

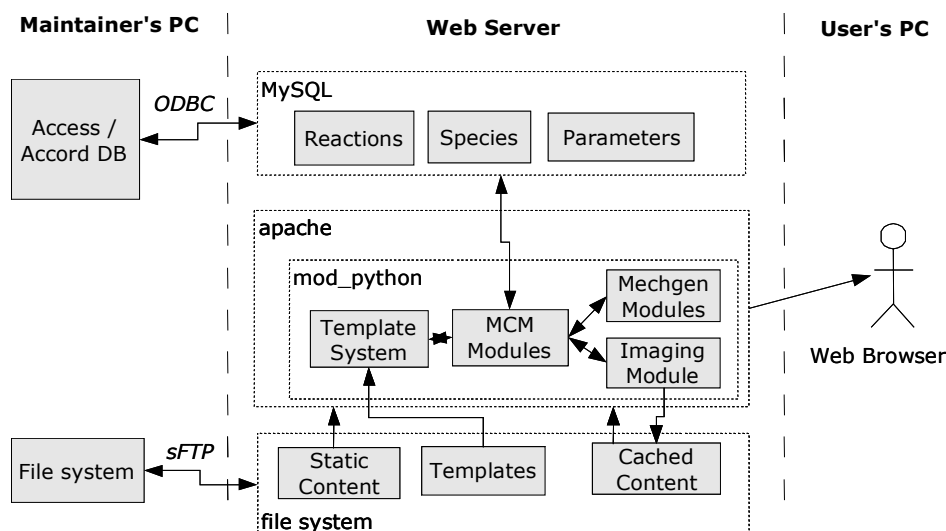


Figure 8.29 Design Layout of the new MCM Website.

For future mechanism development new reactions and updated rate data will be added to an offline development version of the database in order to test self-consistency prior to addition to an offline “master” database. This master database will be an identical mirror of the online MySQL version and would serve as a back up facility. The new mechanisms and updated data will be transferred to the online database approximately every 6 months and information regarding the changes documented and made available on the website.

8.3 MULTI-DAY REACTIVITY SCALES DETERMINED BY THE UK PTM

8.3.1 Model Set-up

In this study, the UK PTM⁹ was used to follow an air parcel as it travelled on an easterly wind from its trajectory release point in Austria across Europe to its arrival point at the England-Wales border. The air parcel picked up emissions of NO_x, SO₂, CO, methane, isoprene and 120 man-made organic compounds en route. The chemical reactions occurring in the air parcel were represented using the Master Chemical Mechanism v3.0. In the base case model experiment, ozone concentrations steadily built up from 50 ppb at the trajectory release point to 90 ppb at the arrival point.

After the air parcel had been travelling for 69 hours, whilst the air parcel was over Northern France, a spike or pulse of a single organic compound was injected into the air parcel by increasing the emission rate of that organic compound over a one-hour period. The spike was exactly the same magnitude for each organic compound, namely 2.3 ppb. The chosen size of the spike was quite arbitrary, being small enough not to disturb significantly the photochemistry in the air parcel but large enough to produce detectable changes in the chemistry over and above the noise in the model. All of the experimental results were generated by subtracting the species concentrations from each of the spiked experiments from those in the base case experiment.

8.3.2 Aldehydes

Table 8.4 presents the integrated ozone production during the first day following the emission of the spike of each aldehyde. Because of their rapid reactions with OH radicals and because of the number of NO to NO₂ oxidation steps in their degradation pathways, significant ozone production was found during the first day. Expressing the integrated ozone production in ppb normalised by the magnitude of the concentration spike in ppb for each aldehyde species, then first day ozone production varied from about 1.6 to -0.3 ppb/ppb across the aldehyde class from formaldehyde to benzaldehyde, see Table 8.4. The behaviour of benzaldehyde marks it out as distinctly different from the other aldehydes as a class in that less ozone was formed following the emission of its spike, rather than more.

⁹ See Appendix 2 for a general description of the model.

Table 8.4 Integrated Ozone Production on the First and Second days following a Spike in the Emissions of each Aldehyde Species.

Species	First day ozone production in ppb/ppb	Second day ozone production in ppb/ppb
Formaldehyde	1.663	-0.139
Acetaldehyde	1.624	0.415
Propionaldehyde	1.437	0.688
Butyraldehyde	1.197	0.707
i-propionaldehyde	1.099	0.084
Pentanal	1.232	0.584
Benzaldehyde	-0.344	0.131

A surprising feature of Table 8.4 is that the aldehyde spike also stimulates additional ozone production on the second day, despite the short lifetime of the aldehydes as a class and the almost complete decay of the spike during the first day. Second day production was particularly large for propionaldehyde, butyraldehyde and acetaldehyde lying in the range 0.4 to 0.7 ppb/ppb. It was significantly smaller for i-propionaldehyde and benzaldehyde and non-existent for formaldehyde. The explanation lay in the production of peroxyacetyl nitrates during the first day, which survived through the night and decomposed during the second day. This decomposition generated additional NO_x and peroxy radicals, which stimulated further ozone production on the second day.

Formaldehyde is unable to form a peroxyacetyl nitrate of sufficient stability to survive into the second day and so showed no second day ozone production whatsoever. i-propionaldehyde, on the other hand, formed peroxy-i-propionyl nitrate during the first day and this survived into the second day. When it thermally decomposed, however, the peroxy-i-propionyl radical reacted to form acetone, an unreactive carbonyl compound, which halted the generation of additional ozone. In contrast, the peroxyacetyl nitrates formed on the first day from acetaldehyde, propionaldehyde and butyraldehyde decompose on the second day to form formaldehyde, acetaldehyde and propionaldehyde, carbonyl compounds with short lifetimes, and so were able to stimulate additional ozone formation on the second day.

To demonstrate that the second day ozone production was driven by the carry-over of peroxyacetyl nitrates from the first day, a spike of peroxyacetyl nitrate PAN itself was added to the base case model experiment at the end of the first day and the integrated ozone production was followed during the second day. A 0.4 ppb spike of PAN gave 2.68 ppb integrated ozone production during the second day, equivalent to 6.7 ppb ozone production per ppb of PAN.

8.3.3 Ketones

Table 8.5 describes the first and second day integrated ozone productions following the emission of a spike in the emission of each ketone. Acetone is the least reactive of the ketones and shows similarly small ozone productions on the first and second days. In contrast, methyl-i-butylketone shows a large production on the first day of about 1.4 ppb/ppb and hexan-3-one shows a large second day production of about 0.8 ppb/ppb.

Table 8.5 Integrated Ozone Production on the First and Second days following a Spike in the Emissions of each Ketone Species.

Species	First day ozone production in ppb/ppb	Second day ozone production in ppb/ppb
Acetone	0.137	0.100
methyl ethylketone	0.514	0.412
methyl i-butylketone	1.359	0.261
methyl propylketone	0.937	0.635
diethylketone	0.489	0.555
methyl i-propylketone	0.566	0.428
hexan-2-one	0.748	0.617

The appreciable second-day ozone productivities found for the ketones appear to arise through at least two mechanisms. The first mechanism involves the carry-over of unreacted parent VOCs or ketone oxidation products which have survived the first day's chemistry and can then react on the

second and subsequent days. This is undoubtedly the mechanism that explains the behaviour found for acetone. The second mechanism involves the formation of peroxyacylnitrates during the first day's chemistry that can react on the second day to form ozone.

8.3.4 Alkenes

The alkenes are as a class, the most reactive of all the organic compounds considered in this study as is shown by the values of the integrated ozone formation following the emission of a spike of each alkene, see Table 8.6. As with the aldehydes, appreciable ozone production was observed on the second day with the majority of the alkenes, despite their short lifetimes and the almost complete decay of each spike during the first day. Integrated ozone productions on the first and second day's are compiled in Table 8.6. As a class, the alkenes show between 1.8 and 3.5 ppb integrated ozone production per ppb spike during the first day. The butenes lie at the top end of the range and 1-hexene at the bottom of the range. On the second day, integrated ozone productions were in the range from close to zero up to over 0.7 ppb. At the top end of the range, second day ozone production was about one third of the first day, despite there being almost no alkene left to react on the second day. At the bottom end of the range, virtually no second day ozone production was found with butylene. The spike of butylene decayed away quickly to form acetone which is highly unreactive and did not stimulate any significant second day ozone production.

Table 8.6 Integrated Ozone Production on the First and Second days following a Spike in the Emissions of each Alkene Species.

Species	First day ozone production in ppb/ppb	Second day ozone production in ppb/ppb
ethylene	3.197	0.318
propylene	3.261	0.512
but-1-ene	2.490	0.701
cis but-2-ene	3.409	0.517
trans but-2-ene	3.530	0.412
cis pent-2-ene	2.903	0.670
trans pent-2-ene	2.908	0.704
1-pent-ene	2.010	0.741
2-methylbut-1-ene	1.913	0.278
3-methylbut-1-ene	2.032	0.090
2-methylbut-2-ene	2.791	0.046
butylene	2.014	-0.024
isoprene	3.077	0.441
1-hexene	1.845	0.630
cis hex-2-ene	2.434	0.717
trans hex-2-ene	2.434	0.681
1,3-butadiene	2.270	0.260

At least two mechanisms have been established for VOCs to produce ozone during subsequent days following their emission. The first mechanism involved the carry over into subsequent days of any unreacted VOC. This is clearly the most important mechanism for ketones, such as acetone, that are of low reactivity. The second mechanism involved the formation of peroxyacylnitrates during the first day. Such species may be an important source of ozone formation on the second day because they can survive the first night and decompose to NO_x and peroxy radicals during the second day thereby stimulating additional ozone formation. This appears to be an important route for second day ozone formation with many of the alkenes, aldehydes and ketones.

From plots of second day ozone production vs. nighttime PAN concentrations, it is apparent that the above mechanisms are not the only mechanisms that drive second day ozone production. A further mechanism has been investigated involving the formation of aldehydes and ketones during the first day and their survival through the first night to stimulate second day ozone production. To this end, Table 8.7 presents the nighttime concentrations of a selection of aldehyde and ketone products following the emission pulses of a selection of highly reactive olefins.

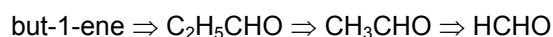
Following the emission of a 1 ppb pulse of ethylene, 0.41 ppb of formaldehyde survives during the first night to stimulate ozone formation on the second day. Because of the chemical structure of

ethylene, no production of aldehydes and ketones beyond formaldehyde is to be expected and, indeed, none is seen in Table 8.6.

Table 8.7 The Concentrations (in ppb) of a Selection of Aldehydes and Ketones during the First Night following the Emission of a Pulse of a Selection of Different Olefins.

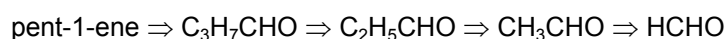
Olefins	HCHO	CH ₃ CHO	C ₂ H ₅ CHO	<i>i</i> -C ₃ H ₇ CHO	Acetone	MEK
Ethylene	0.41	-0.01	0.00	0.00	0.01	0.00
Propylene	0.25	0.04	0.00	0.00	0.00	0.00
but-1-ene	0.18	0.15	0.01	0.00	0.00	0.00
cis but-2-ene	0.22	0.02	0.00	0.00	0.01	0.00
trans but-2-ene	0.21	0.01	0.00	0.00	0.01	0.01
cis pent-2-ene	0.20	0.09	0.00	0.00	0.01	0.00
trans pent-2-ene	0.20	0.09	0.00	0.00	0.01	0.00
pent-1-ene	0.14	0.14	0.07	0.00	-0.01	0.00
2-methylbut-1-ene	0.11	0.03	0.00	0.00	0.01	0.69
3-methylbut-1-ene	0.04	0.00	0.00	0.00	0.81	0.00
2-methylbut-2-ene	0.08	-0.01	0.00	0.00	0.74	0.01
Butylene	0.04	-0.01	0.00	0.00	1.19	0.00

Propylene is more reactive than ethylene and so its oxidation products, formaldehyde and acetaldehyde are produced earlier in the day and hence they have less chance to survive into the first night. But-1-ene is yet more reactive than propylene and virtually none of its C₂H₅CHO product survives into the first night. The major oxidation product of C₂H₅CHO is acetaldehyde and significantly more of the acetaldehyde from but-1-ene oxidation survives into the first night than from propylene. This apparently contradictory results is a consequence of the consecutive nature of the kinetic system which is operating here:

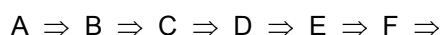


The consecutive nature of the kinetic system, delays the production of the subsequent oxidation products and thus enables their survival into the first night.

The influence of the delay mechanism that results from the consecutive nature of the kinetic system is apparent with 1-pentene, see Table 8.6, where it is an important source of night-time formaldehyde, acetaldehyde and propionaldehyde, despite its exceptionally short lifetime.



For a series of consecutive reactions where, for the sake of simplicity, each species has the same first order removal coefficient, k :



Then it can be shown that the time of the concentration maximum of B following the emission pulse of A, occurs after $1/k$. The concentration maximum of C occurs after $2/k$, that of D after $3/k$ and so on. So the maximum concentrations are delayed by the consecutive reaction system, despite each member being highly reactive.

The rapid reactions of olefins and their aldehyde oxidation products in a consecutive kinetic system, provides an important mechanism for short-chain aldehydes to survive through to the second day to stimulate ozone production. This second day ozone production mechanism is thus an important feature of the Master Chemical Mechanism and is a consequence of its explicit representation of the degradation pathways for olefins, aldehydes and ketones.

In all, three mechanisms have been found to account for ozone formation on subsequent days, following their emissions. These are:

- the carry over of unreacted VOCs,
- the formation of peroxyacetyl nitrates
- the consecutive reactions of aldehyde formation and degradation.

From a study of the chemical mechanisms used in most policy models, EMEP included, it is likely that the multi-day formation of ozone from alkenes and carbonyl compounds is underestimated because of the simplifications and approximations made in the compression of the chemical mechanisms.

8.3.5 Multi-day Ozone Formation from Alkanes

The left-hand panel of Figure 8.30 shows how, in response to the spike, each alkane stimulated additional ozone production on the first and second day. Ozone productivities for the short chain alkanes, ethane and propane, are low because of their slow reactions with OH radicals and hence they are positioned close to the origin of the plot in Figure 8.30. Neo-pentane is found close to them appearing to be unreactive because it contains only primary C-H bonds. With increasing carbon chain length and hence increasing numbers of secondary C-H bonds, OH reactivity increases steadily through n-butane and n-pentane and together with it, both first and second day's ozone productivities.

First- and second-day ozone formation increases steadily with increasing carbon number with both reaching their respective maxima with the C₆ alkanes: 2- and 3-methylpentane and 2,3-dimethylbutane. As carbon number increases beyond C₆, first-day reactivity collapses whilst second-day reactivity increases slightly. This behaviour results directly from the increasing formation of alkyl nitrate from the reaction of organic peroxy radicals with NO and from the increasing propensity of oxy radicals to undergo 1,5 H-atom isomerisation reactions with carbon numbers beyond C₆.

The detailed reaction pathways anticipated for the alkanes and represented in the MCM therefore exert an important influence on their reactivities on the regional scale and their propensities to form ozone on multi-day timescales.

8.3.6 Multi-day Ozone Formation from Aromatic VOCs

The right-hand panel of Figure 8.30 shows how, in response to the spike, each aromatic compound stimulated additional ozone production on the first and second day using MCM v3.1. For the large part, this figure shows monotonically increasing trends in first and second day ozone productivities. This behaviour is markedly different to the corresponding plot found with the MCM v3.0 in which anomalous behaviour was found for p-xylene, ethylbenzene, propylbenzene and i-propylbenzene. All four compounds now lie in the same region of the plot as the remaining aromatic compounds, see Figure 8.30. This confirms what had been suspected, that there were problems in the detailed mechanisms for these four aromatic species in MCMv3.0. Further work is now planned to understand the mechanisms that control first and second day ozone production following the emission of a spike in each aromatic compound.

8.4 MODELLING THE AMBIENT DISTRIBUTION OF ORGANIC COMPOUNDS USING THE UK PTM

8.4.1 Introduction

Modelling studies using detailed emitted VOC speciation and comprehensive descriptions of the chemistry of VOC degradation are able to quantify the roles played by individual VOC in atmospheric chemistry generally, and in ozone formation in particular. Furthermore, they allow the prediction of the patterns and structures of oxidised products, such as simple and multifunctional carbonyls, thereby allowing a much more detailed examination of atmospheric chemical mechanisms.

In this section, the results of detailed simulations of the ambient distributions of organic compounds are described. The UK PTM containing speciated emissions of 124 non-methane VOC (based on the NAEI), and a comprehensive description of the chemistry of VOC degradation (provided by MCM v3.1 and the CRI mechanism), has been used to simulate the chemical evolution of boundary layer air masses arriving at a field campaign site in the southern UK, during the August 2003 photochemical pollution episode. No adjustment was made to other model parameters (e.g., those characterising the evolution of the boundary layer or dry deposition) from the values used for describing an idealised photochemical episode over the UK.

The simulated concentrations and distributions of organic compounds at the arrival location (Writtle College, near Chelmsford) were compared with observations of a series of hydrocarbons and selected carbonyl compounds, which were measured as part of the first campaign of the Tropospheric Organic

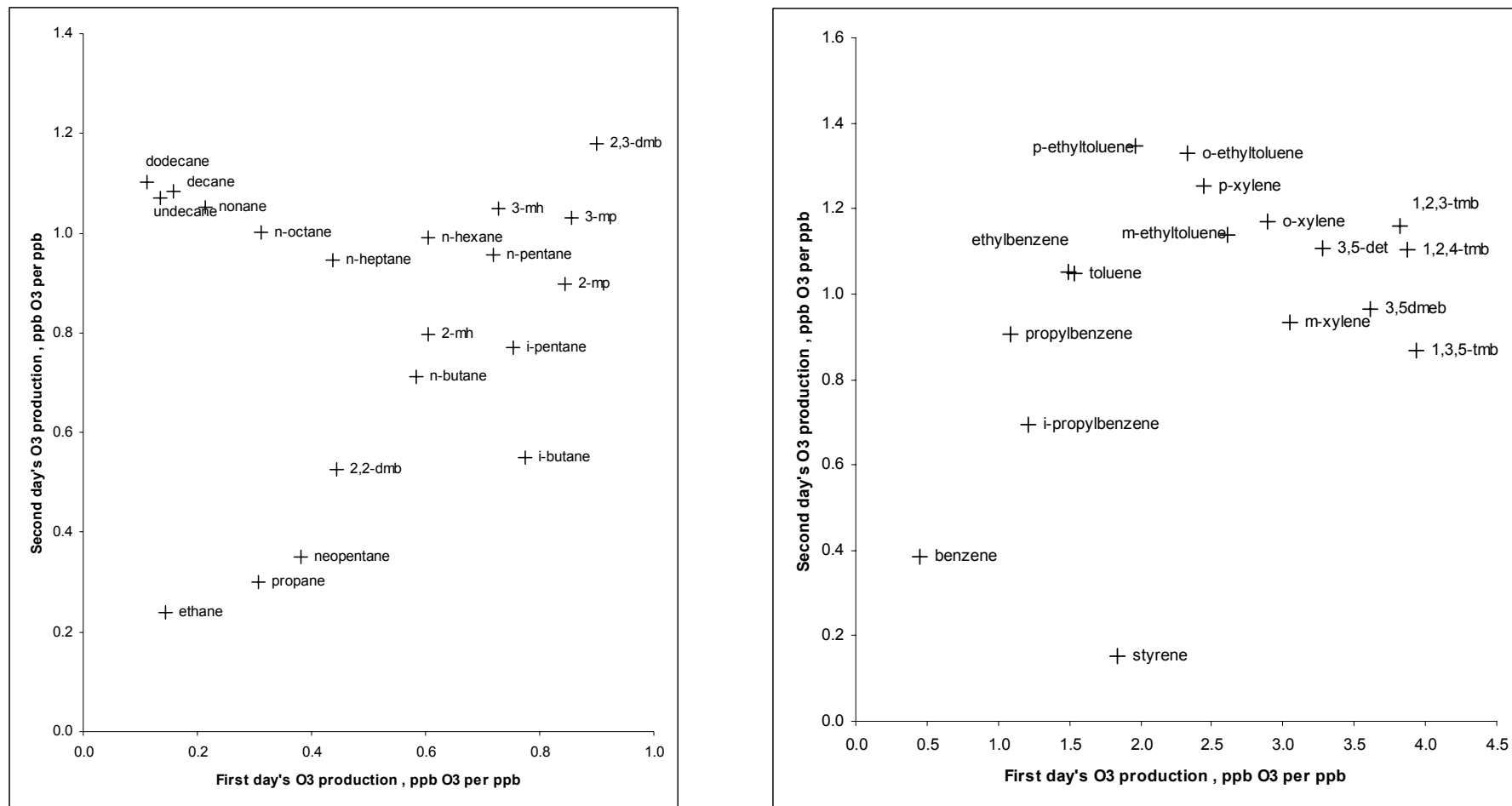


Figure 8.30 The First and Second Day's Additional Ozone Production following the Emission of a Spike of each Alkane (Left-hand Panel) and of each Aromatic (Right-hand Panel).

Chemistry Experiment (TORCH). The organic compounds were measured using GC-FID and multidimensional GC methods by the University of York, as reported by Utembe *et al.* [2005]. The results of the model-measurement comparison are discussed in terms of the magnitude and speciation of emitted VOC, the distribution of simple and multifunctional carbonyls formed as degradation products, and the impacts of these carbonyls on free radical formation.

8.4.2 Speciation and Temporal Variation of non-methane VOC Emissions

The speciation of the emitted anthropogenic VOC was based on the NAEI, which identifies *ca.* 650 individual species. To allow coupling with the chemical mechanisms, the speciation was represented by the 124 species identified in Figure 8.31, which collectively account for *ca.* 70 % of the NAEI emissions, by mass. The outstanding > 500 species, which each makes a small contribution to the remaining 30%, were emitted in the form of appropriate surrogates, which were assigned on the basis of chemical class and reactivity. For example, the longer chain *n*-alkanes $\geq C_8$ were generally used to represent alkanes isomers of the same carbon number, dodecane was used to represent all alkanes $\geq C_{12}$, and cyclohexane was used to represent all cycloalkanes. Biogenic VOC were emitted as isoprene (50 %) and the monoterpenes α -pinene (30 %) and β -pinene (20 %).

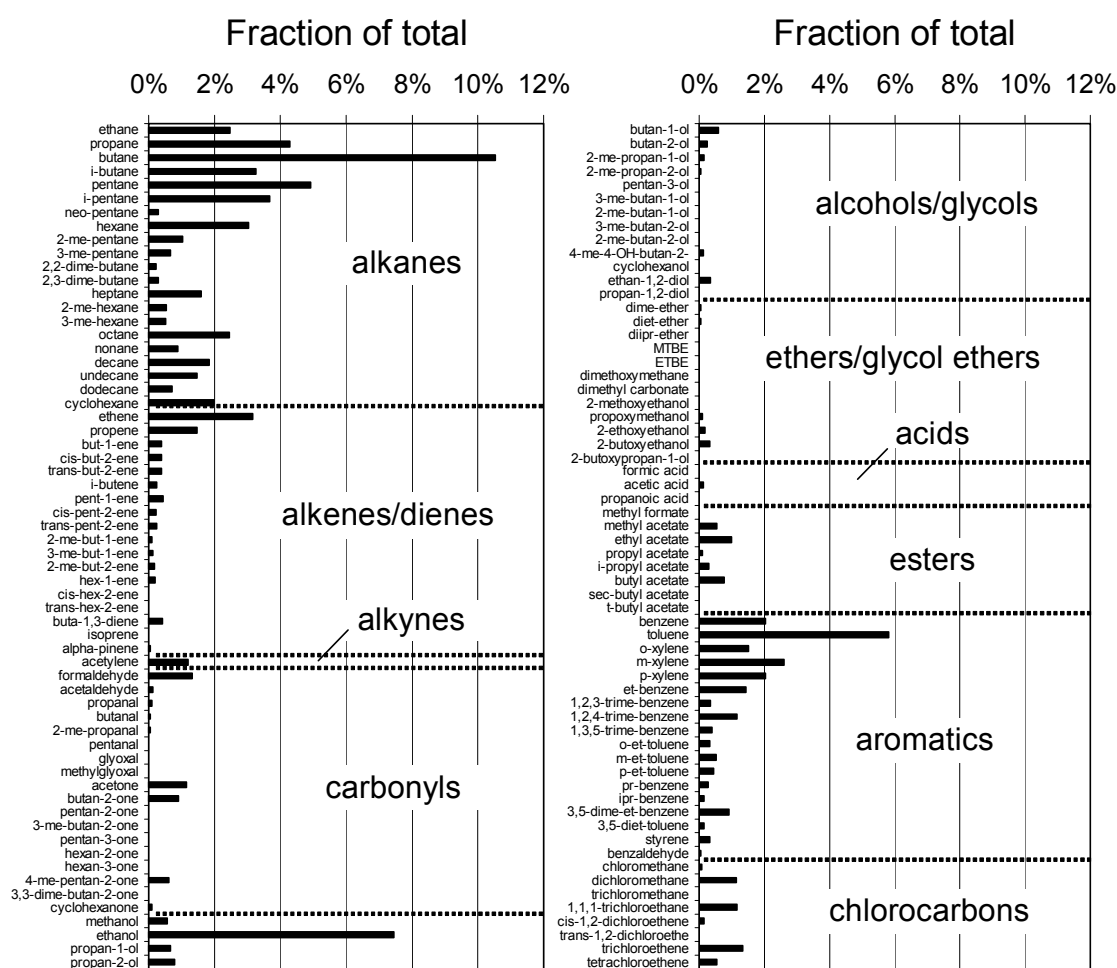


Figure 8.31 Speciation of Anthropogenic non-methane VOC Emissions used in PTM (see text).

The temporal variations applied to the emissions of VOC and NO_x were based on those estimated for the UK by Jenkin *et al.* [2000]. In that study, single representative profiles describing the seasonal, day-of-week and hour-of-day variations in emissions were assigned to each of over 180 source categories included in the NAEI. Where possible, the profiles were based on available temporally resolved data (e.g., fuel consumption, electricity generation, traffic volume statistics), which can be related to emissions. The temporal variation of biogenic VOCs takes account of typical seasonal and diurnal variations in photosynthetically active radiation (PAR) and temperature, and were determined using the methodology of Guenther *et al.* [1994] as also discussed for Europe by Simpson *et al.* [1995].

8.4.3 Simulations of Emitted Hydrocarbons using the CRI Mechanism

The PTM-CRI was used to simulate the chemical evolution of air parcels arriving at the Writtle site at six-hourly resolution for the entire TORCH-1 campaign. Comparisons of the simulated and observed concentrations of a series of 34 emitted hydrocarbons are presented in Figure 8.32 to Figure 8.34.

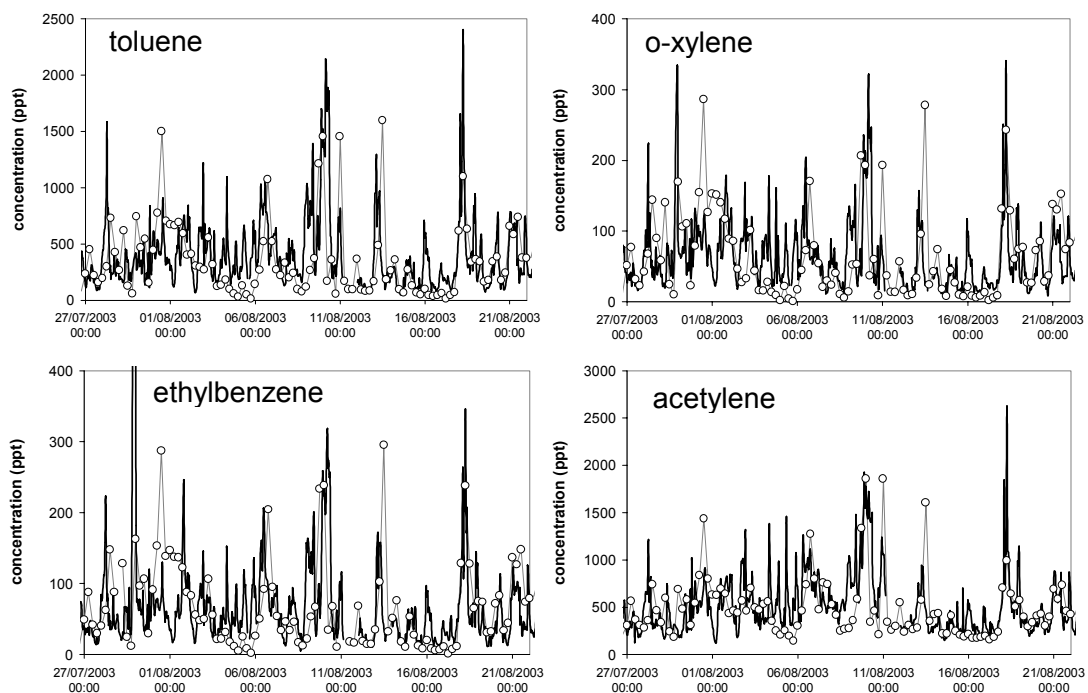


Figure 8.32 Comparison of Observed and Simulated Concentrations of Selected Aromatic Hydrocarbons and Acetylene. The Heavy Black Lines represent the Observed Concentrations. The Points are the Simulated Concentrations at Six-hourly Intervals.

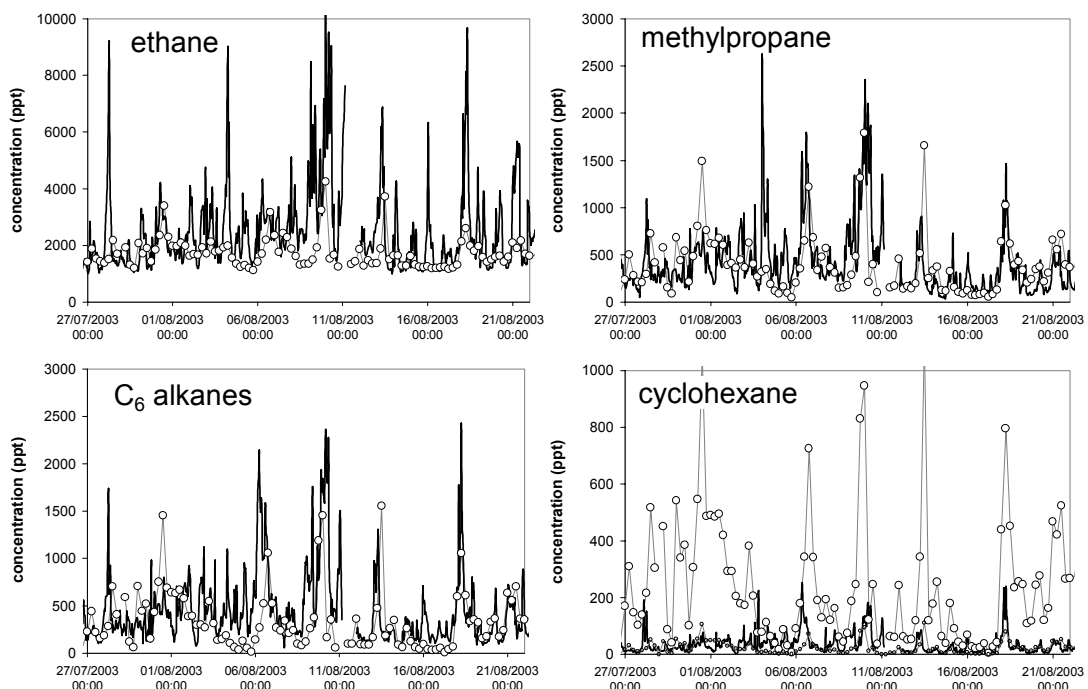


Figure 8.33 Comparison of Observed and Simulated Concentrations of Selected Alkanes. C₆-Alkanes are Hexane, Methylpentane Isomers and Dimethylbutane Isomers. The Heavy Black Lines represent the Observed Concentrations. The Points are the Simulated Concentrations at Six-hourly Intervals. The Smaller Points on the Cyclohexane plot are 10% of the Simulated Concentrations (see text).

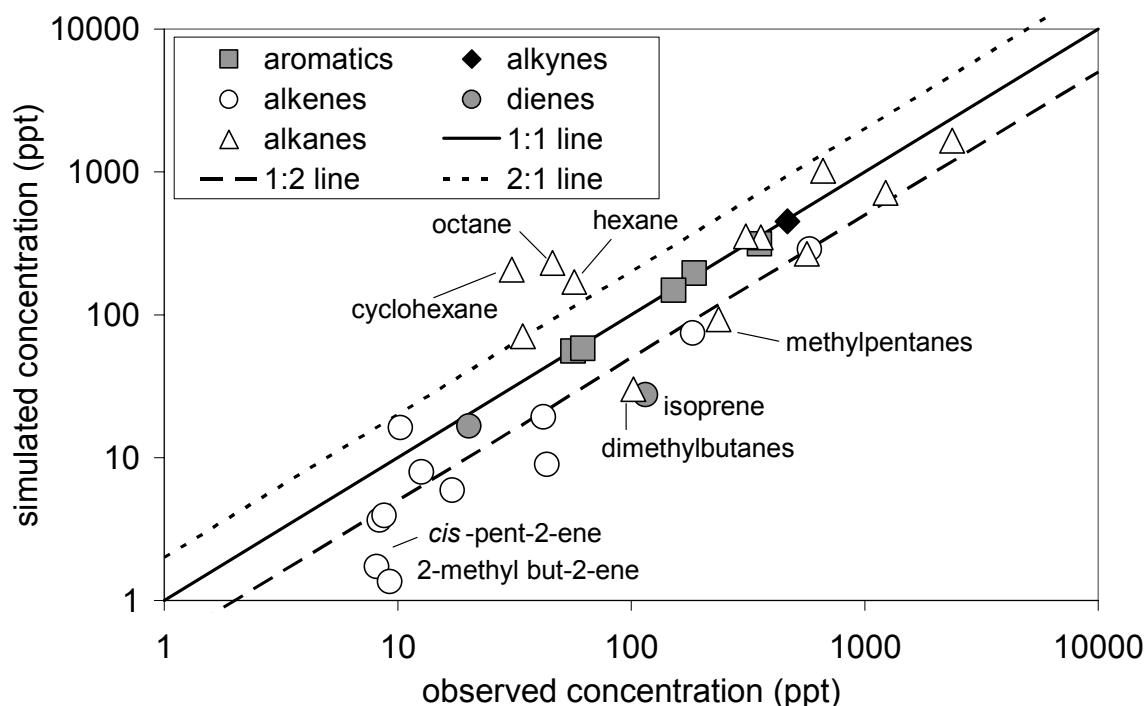


Figure 8.34 Comparison of Observed and Simulated Campaign Mean Concentrations of 34 Emitted Hydrocarbons.

This provides a test of a combination of aspects of the model, *i.e.*, the emissions speciation of the hydrocarbons, their lifetimes under the prevailing conditions and the quantity collected along the applied trajectory paths. The simulated concentrations generally recreate the overall features of the campaign (Figure 8.32 and Figure 8.33). The correlation of the campaign mean concentrations (Figure 8.33) also demonstrates that the simulated concentrations of the majority of hydrocarbons were within a factor of *ca.* 2 of those observed. The model generally provides a good description of the observed concentrations of anthropogenic hydrocarbons. As shown in Figure 8.32 and Figure 8.34, the concentration variation and mean concentrations of aromatic hydrocarbons, buta-1,3-diene and acetylene are in very good agreement with observations.

The concentrations of C₄ alkanes (butane and methylpropane) are also reasonably well described, although the smaller alkanes (ethane and propane) tend to be slightly underestimated by the model. The comparison for C₅-C₇ aliphatic alkanes tends to show scatter around the 1:1 line, although the simulated and observed total concentrations for a given carbon number are generally in reasonable agreement. For example, Figure 8.34 shows that the mean concentration of hexane is overestimated by the model, whereas the concentrations of the methylpentane and dimethylbutane isomers are underestimated. As shown in Figure 8.33, however, the concentration sum of these C₆ alkanes agrees reasonably well with the observations. It is likely that the inventory speciation within a given carbon number tends to overestimate the contribution of the *n*-alkanes, since information supplied to inventory compilers often includes nominal components such as 'hexane', when it is probable that a mixture of hexane isomers is actually emitted.

The simulated concentrations of longer-chain alkanes (*e.g.*, octane) and cyclohexane are typically overestimated by the model, mainly due to these species being used as surrogates for other long-chain alkanes which are not included in the chemical mechanisms. This is demonstrated for cyclohexane (see Figure 8.33), which, as indicated above, is used as a surrogate for all cycloalkanes in the NAEI inventory, even though it only accounts for *ca.* 10 % of cycloalkane emissions. Consequently, the simulated concentrations are about an order of magnitude greater than those observed.

The simulated concentrations of the alkenes are typically lower than those observed, particularly for some of the larger species (*e.g.*, *cis*-2-pentene and 2-methyl-but-2-ene), with a similar effect also

observed for isoprene (see Figure 8.34). This may be indicative of under representation in the emissions speciation. However, the larger alkenes and isoprene are generally the most reactive hydrocarbons, and are therefore most prone to underestimation if there are sources comparatively local to the measurement site. The local representation of emissions in the model is based on the average over the 10 km square containing the measurement site, and the simulated concentrations also assume rapid vertical mixing within the boundary layer. Because the lifetimes of the larger alkenes and isoprene are typically of the order of 10-30 minutes under the prevailing daytime conditions, the ambient concentrations would be expected to show horizontal and vertical variations which may not be captured by the model. This would lead to a bias towards underestimation by the model if local sources are greater than the 10 x 10 km average, and a bias toward overestimation if local sources are below the average.

The extent of under simulation for isoprene was found to be greatest (*i.e.*, typically a factor of ca. 10) during the most severe period of the photochemical episode (6th-11th August), when the highest temperatures (> 30 °C) were also observed. This suggests that the representation of biogenic emissions, based on mean monthly and diurnal temperatures, may be inadequate, and work is currently in progress to implement biogenic emissions based on trajectory-specific meteorological conditions. The discrepancies between simulated and observed concentrations of the larger alkenes also tend to be greater during the high temperature period, suggesting that there could be a biogenic input of these hydrocarbons. Support for this is provided by the measurements of Klemp *et al.* [1997] at Schauinsland, Germany. They observed evidence for biogenic sources of larger alkenes (specifically the butene isomers in their study), which displayed a clear dependence of temperature.

8.4.4 Simulations of Carbonyl Distributions with the MCM

The PTM-MCM v3.1 was used to simulate the detailed chemical composition of the air parcels travelling along five case study trajectories, allowing calculated concentration distributions of organic species which are produced by chemical processing of the emitted VOC. The resultant information for carbonyl compounds at the arrival point is shown in Table 8.8.

Simulated concentration data for ca. 1250 compounds containing the carbonyl functionality were obtained. This includes both simple carbonyls (*i.e.*, aldehydes and ketones), and carbonyls containing one or more additional functional groups (*e.g.*, carbonyl; hydroxyl). The simulated concentrations of 61 selected aldehydes, ketones and bifunctional carbonyls for each of the five case study trajectories are given in Table 8.8. These species collectively account for between 88 and 91% of the simulated total molecular concentrations of carbonyl species. Additional small contributions were made by species such as methacrolein, methylvinyl ketone, pinonaldehyde and nopinone, which are derived from the biogenic precursors isoprene, α -pinene and β -pinene. The balance was made up of almost 1200 carbonyl species individually making very small contributions, but collectively accounting for up to ca. 10% of the total carbonyl concentration.

The simulated concentrations of the carbonyl compounds are dominated by their secondary formation from the degradation of emitted VOC, with primary emissions of the limited number of carbonyls (Figure 8.31) making only very small contributions to their concentrations at the arrival point. Accordingly, the total carbonyl concentrations given in Table 8.8 broadly correlate with the integrated VOC emissions along the corresponding trajectory. The simulated distributions for each class of carbonyl compound shows a general decrease in concentration as carbon number increases, consistent with a progressively smaller number of precursor VOC being available: and also because larger carbonyls are generally degraded to form smaller ones, as illustrated for aldehydes by Derwent *et al.* (2005). The results of the simulations are therefore in broad agreement with reported trends in ambient distributions of carbonyl compounds with size [*e.g.*, Andreini *et al.*, 2000; Christensen *et al.*, 2000; Possanzini *et al.*, 2000; Grosjean *et al.*, 2002; Bakeas *et al.*, 2003]. Figure 8.35 shows a comparison of the simulated concentrations for seven aldehyde and ketone species with observed concentrations measured using the GCxGC technique, for the arrival hour of four of the case study trajectories. It is apparent that the relative concentration variation for aldehydes and ketones shows a good degree of consistency, although there are systematic discrepancies in the absolute concentrations.

Table 8.8 Simulated Concentrations (in ppt by volume)^a of Selected Carbonyls at Arrival Point for 5 Case Study Trajectories (2nd, 4th, 6th, 7th and 31st August 2003, respectively).

	Trajectory number				
	1	2	3	4	5
Total carbonyl species^b	11,321	3,788	13,127	9,432	6,573
Simple aldehydes (≤ C₆)	4,072 (36.0 %)	1,540 (40.7 %)	6,150 (46.9 %)	3,347 (33.9 %)	3,116 (47.4 %)
formaldehyde	2,988 (26.4 %)	1,283 (33.9 %)	3,852 (29.3 %)	2,480 (26.3 %)	2,205 (34.6 %)
acetaldehyde	901 (7.96 %)	216 (5.71 %)	1,773 (13.5 %)	737 (7.81 %)	729 (11.1 %)
propanal	138 (1.22 %)	28 (0.74 %)	413 (3.15 %)	90 (0.95 %)	143 (2.18 %)
butanal	20 (0.17 %)	6 (0.15 %)	50 (0.38 %)	17 (0.18 %)	17 (0.27 %)
2-methylpropanal	9 (0.08 %)	2 (0.06 %)	21 (0.16 %)	7 (0.08 %)	8 (0.12 %)
pentanal	4 (0.03 %)	2 (0.05 %)	5 (0.04 %)	5 (0.05 %)	2 (0.03 %)
2-methylbutanal	1 (0.01 %)	-	4 (0.03 %)	2 (0.02 %)	2 (0.03 %)
hexanal	6 (0.05 %)	2 (0.05 %)	7 (0.06 %)	6 (0.06 %)	3 (0.05 %)
acrolein	5 (0.05 %)	1 (0.03 %)	25 (0.19 %)	3 (0.04 %)	7 (0.11 %)
Simple ketones (≤ C₆)	5,139 (45.4 %)	1,728 (45.6 %)	4,467 (34.0 %)	4,544 (48.2 %)	2,211 (33.6 %)
acetone	4,371 (38.6 %)	1,340 (35.4 %)	3,118 (23.8 %)	3,374 (35.8 %)	1717 (26.2 %)
butanone	436 (3.85 %)	278 (7.35 %)	793 (6.04 %)	745 (7.89 %)	273 (4.16 %)
pentan-2-one	21 (0.19 %)	11 (0.28 %)	33 (0.25 %)	30 (0.32 %)	13 (0.20 %)
pentan-3-one	54 (0.48 %)	28 (0.73 %)	89 (0.68 %)	84 (0.89 %)	33 (0.50 %)
3-methyl-butan-2-one	44 (0.39 %)	19 (0.51 %)	71 (0.54 %)	65 (0.69 %)	26 (0.40 %)
hexan-2-one	4 (0.03 %)	2 (0.06 %)	7 (0.05 %)	6 (0.07 %)	2 (0.04 %)
hexan-3-one	12 (0.10 %)	5 (0.13 %)	18 (0.14 %)	15 (0.16 %)	7 (0.11 %)
4-methyl-pentan-2-one	8 (0.07 %)	3 (0.08 %)	35 (0.27 %)	65 (0.69 %)	11 (0.17 %)
3-methyl-pentan-2-one	3 (0.02 %)	1 (0.03 %)	4 (0.03 %)	3 (0.03 %)	2 (0.03 %)
2-methyl-pentan-3-one	6 (0.05 %)	2 (0.06 %)	9 (0.07 %)	7 (0.08 %)	4 (0.06 %)
cyclohexanone ^c	180 (1.59 %)	39 (1.03 %)	290 (2.21 %)	150 (1.58 %)	123 (1.88 %)
Dicarbonyls (≤ C₆)	394 (3.48 %)	87 (2.30 %)	599 (4.56 %)	277 (2.94 %)	246 (3.74 %)
glyoxal	183 (1.62 %)	31 (0.82 %)	219 (1.66 %)	110 (1.17 %)	99 (1.51 %)
methylglyoxal	76 (0.67 %)	14 (0.38 %)	197 (1.50 %)	44 (0.46 %)	65 (0.99 %)
malonaldehyde	34 (0.30 %)	3 (0.08 %)	10 (0.08 %)	11 (0.12 %)	17 (0.26 %)
ethylglyoxal	14 (0.12 %)	5 (0.12 %)	36 (0.27 %)	11 (0.12 %)	11 (0.16 %)
3-oxo-butanal	14 (0.13 %)	4 (0.10 %)	22 (0.16 %)	14 (0.15 %)	9 (0.14 %)
propylglyoxal	1 (0.01 %)	-	1 (0.01 %)	1 (0.01 %)	-
i-propylglyoxal	-	-	1 (0.01 %)	-	-
3-oxo-pentanal	18 (0.16 %)	3 (0.07 %)	27 (0.21 %)	12 (0.12 %)	13 (0.19 %)
4-oxo-pentanal	10 (0.09 %)	2 (0.06 %)	13 (0.10 %)	9 (0.10 %)	6 (0.09 %)
4-oxo-hexanal	7 (0.06 %)	1 (0.04 %)	9 (0.07 %)	6 (0.06 %)	5 (0.07 %)
buta-2,3-dione	4 (0.04 %)	2 (0.05 %)	13 (0.10 %)	4 (0.04 %)	4 (0.05 %)
penta-2,3-dione	-	-	1 (0.01 %)	-	-
penta-2,4-dione	14 (0.12 %)	13 (0.35 %)	23 (0.18 %)	31 (0.33 %)	7 (0.11 %)
hexa-2,4-dione	-	3 (0.07 %)	1 (0.01 %)	-	-
hexa-2,5-dione	19 (0.17 %)	6 (0.16 %)	26 (0.20 %)	24 (0.26 %)	10 (0.16 %)
Hydroxycarbonyls (≤ C₆)	305 (2.69 %)	77 (2.03 %)	483 (3.68 %)	254 (2.69 %)	209 (3.18 %)
glycolaldehyde	92 (0.81 %)	24 (0.64 %)	133 (1.01 %)	78 (0.82 %)	61 (0.93 %)
2-hydroxypropanal	-	-	1 (0.01 %)	1 (0.01 %)	-
3-hydroxypropanal	21 (0.18 %)	5 (0.13 %)	31 (0.24 %)	18 (0.19 %)	15 (0.23 %)
2-hydroxybutanal	1 (0.01 %)	1 (0.02 %)	1 (0.01 %)	2 (0.02 %)	-
3-hydroxybutanal	2 (0.02 %)	1 (0.02 %)	3 (0.03 %)	3 (0.03 %)	1 (0.02 %)
4-hydroxybutanal ^d	14 (0.13 %)	3 (0.09 %)	25 (0.19 %)	13 (0.14 %)	10 (0.16 %)
2-hydroxypentanal	1 (0.01 %)	1 (0.02 %)	1 (0.01 %)	2 (0.02 %)	-
3-hydroxypentanal	1 (0.01 %)	-	1 (0.01 %)	1 (0.01 %)	-
4-hydroxypentanal ^d	10 (0.08 %)	2 (0.06 %)	15 (0.11 %)	8 (0.08 %)	7 (0.11 %)
4-hydroxyhexanal ^d	7 (0.06 %)	1 (0.04 %)	10 (0.07 %)	5 (0.05 %)	5 (0.08 %)
4-hydroxy-4-methylpentanal ^d	3 (0.03 %)	1 (0.01 %)	7 (0.05 %)	2 (0.02 %)	3 (0.04 %)
hydroxyacetone	11 (0.10 %)	7 (0.19 %)	18 (0.13 %)	13 (0.14 %)	8 (0.12 %)
1-hydroxybutan-2-one	4 (0.04 %)	2 (0.06 %)	8 (0.06 %)	7 (0.07 %)	3 (0.05 %)
3-hydroxybutan-2-one	2 (0.02 %)	1 (0.03 %)	4 (0.03 %)	3 (0.03 %)	1 (0.02 %)
4-hydroxybutan-2-one	13 (0.11 %)	5 (0.12 %)	20 (0.15 %)	9 (0.10 %)	9 (0.14 %)
1-hydroxypentan-2-one	1 (0.01 %)	-	1 (0.01 %)	1 (0.01 %)	-
3-hydroxypentan-2-one	-	-	1 (0.01 %)	-	-
5-hydroxypentan-2-one ^d	62 (0.55 %)	12 (0.32 %)	99 (0.76 %)	52 (0.55 %)	42 (0.65 %)
5-hydroxyhexan-2-one ^d	22 (0.19 %)	3 (0.08 %)	37 (0.28 %)	14 (0.14 %)	16 (0.25 %)
6-hydroxyhexan-3-one ^d	27 (0.24 %)	5 (0.12 %)	44 (0.34 %)	19 (0.20 %)	19 (0.29 %)
4-hydroxy-4-methylpentan-2-one ^d	7 (0.06 %)	2 (0.05 %)	16 (0.12 %)	-	6 (0.09 %)
5-hydroxy-3-methylpentan-2-one	4 (0.04 %)	1 (0.02 %)	7 (0.06 %)	3 (0.03 %)	3 (0.05 %)
Aromatic aldehydes (≤ C₈)	21 (0.19 %)	26 (0.68 %)	53 (0.40 %)	12 (0.13 %)	20 (0.30 %)
benzaldehyde	14 (0.12 %)	26 (0.68 %)	36 (0.28 %)	8 (0.09 %)	13 (0.20 %)
2-methylbenzaldehyde	1 (0.01 %)	-	3 (0.02 %)	1 (0.01 %)	1 (0.02 %)
3-methylbenzaldehyde	2 (0.02 %)	-	5 (0.04 %)	1 (0.01 %)	2 (0.03 %)
4-methylbenzaldehyde	4 (0.04 %)	-	9 (0.07 %)	2 (0.02 %)	4 (0.05 %)

Notes: (a) Concentrations are rounded to the nearest ppt. A missing entry indicates a sub-ppt concentration. Percentage contribution to total (rounded to nearest 0.01% for less abundant species), is given in brackets. (b) Concentration sum of species containing one or more carbonyl groups. (c) Concentrations for cyclohexanone should be regarded as indicative of total anthropogenically-derived cycloalkane concentrations. (d) Concentrations for 1,4-hydroxycarbonyls notionally include contributions from isomeric cyclic hemiacetals (see text)

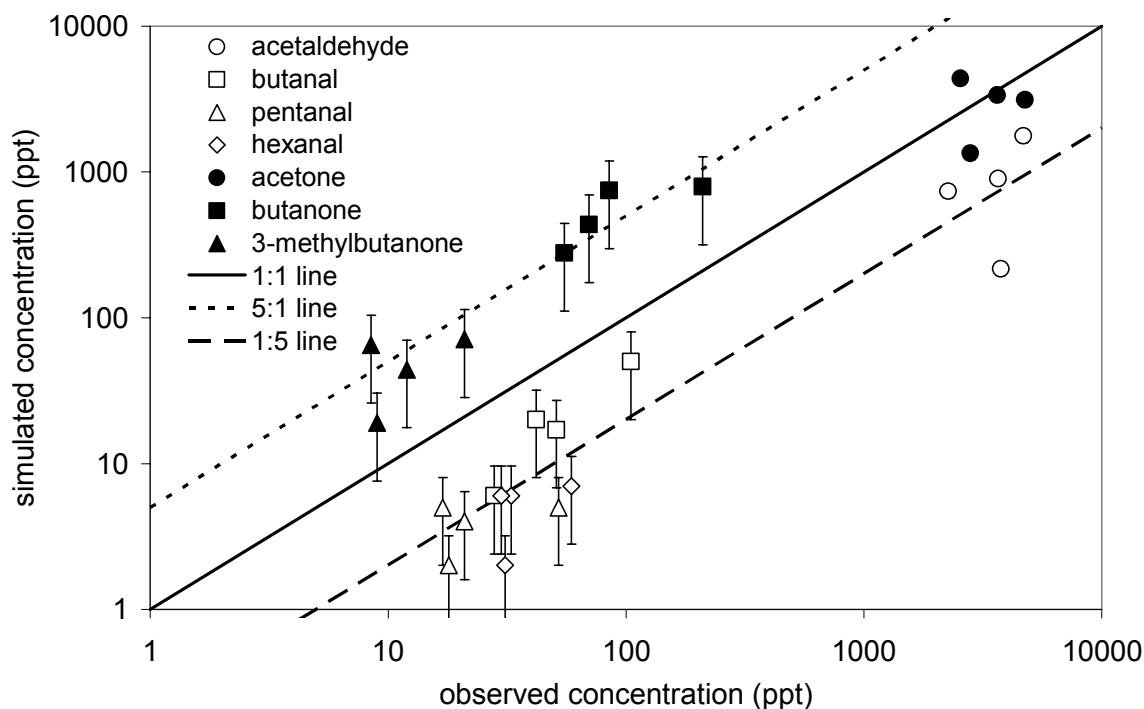


Figure 8.35: Comparison of Observed and Simulated Concentrations of 7 Carbonyls for the Arrival Hour of Trajectories 1-4. Open symbols are Aldehydes; Filled Symbols are Ketones.

8.4.5 Conclusions

The comparison of the simulated and observed distributions of 34 emitted hydrocarbons provides support for the magnitude and applied emissions speciation of anthropogenic hydrocarbons (based primarily on the NAEI), but is indicative of an under representation of the input of biogenic hydrocarbons, particularly at elevated temperatures. Simulations of the detailed distribution of ca. 1250 carbonyl compounds, formed primarily from the degradation of 124 emitted VOC, focus on 61 aldehydes, ketones, and bifunctional carbonyls which collectively account for ca. 90 % of the simulated total molar concentration of carbonyls. The simulated distributions of four aldehydes and three ketones correlated well with observations for each class of compound. However, the simulated concentrations of the aldehydes were systematically lower than those observed, whereas those of the higher ketones were systematically higher.

8.5 UK PTM ANALYSIS OF OZONE FORMATION IN THE AUGUST 2003 HEATWAVE: SENSITIVITY TO CHANGES IN OZONE PRECURSOR EMISSIONS

8.5.1 Introduction

The UK PTM-CRI described in the previous section (Section 8.4), but with an updated representation of biogenic VOC emissions, has also been used to investigate various features of ozone formation during the August 2003 heatwave for the conditions of the TORCH 2003 campaign. In this appraisal, the emissions of NO_x and VOC (and CO and SO_2) have been varied to simulate over the time frame 1990-2020 to examine the relative severity of the episode if it occurred in other years. The relative impacts of incremental NO_x and VOC emission controls have also been examined for the years 1990, 2003 and 2020, to investigate whether ozone formation is VOC- or NO_x limited, and to quantify the relative contributions to ozone formation made by anthropogenic and biogenic VOC.

For this appraisal, the representation of biogenic VOC emissions was based on the method described by Dore *et al.* [2003]. Emissions of isoprene, monoterpenes and 'other biogenic VOC' were thus described in terms of mapped emissions potentials (see Section 4.3), and environmental correction factors incorporating the influence of variations in surface temperature and photosynthetically active

radiation (PAR) along the applied trajectory paths. This allowed a more rigorous representation of the magnitudes and temporal variations of the biogenic VOC emission rates relevant to the TORCH 2003 campaign period.

The model was used to simulate the chemical development over a 96 hour period along 150 trajectories arriving at the site of the TORCH-2003 campaign at Writtle in Essex. The trajectories corresponded to arrival times of 00:00, 06:00, 12:00 and 18:00 hr for the period 26 July – 31 August 2003. Figure 8.36 shows a comparison of the simulated ozone concentrations at the arrival point with those observed. This demonstrates that the model broadly recreates the observations, including the generally elevated concentrations during the anticyclonic period, which persisted from 3-12 August.

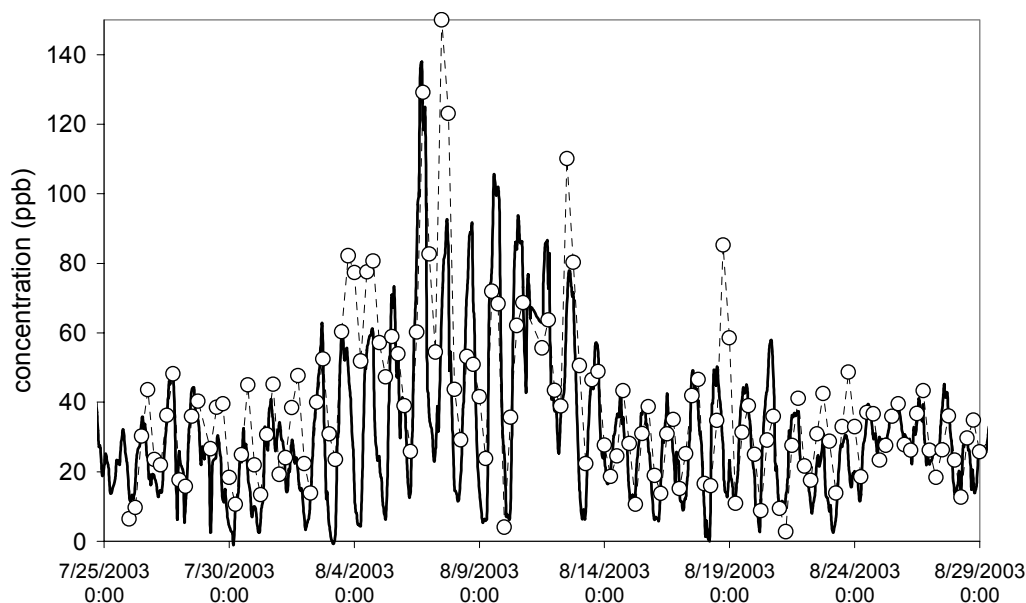


Figure 8.36 Comparison of Observed Hourly Mean Ozone Concentrations (lines) with those Simulated at Six-hourly Intervals (points) for the Entire TORCH-2003 Campaign.

8.5.2 Contributions of Anthropogenic and Biogenic VOC to Ozone Formation

Figure 8.37 shows the change in simulated daily-average ozone concentration throughout the campaign resulting from increasing VOC emissions by 1%. The anticyclonic period generally shows the largest increment, because the emissions input was greatest during this period. However, it is also clear that the biogenic emissions are calculated to make a larger relative contribution at the prevailing higher temperatures. During the anticyclonic (heatwave) period, biogenic VOC emissions are thus calculated to account for 33% of regional scale ozone formation on average, and typically 40-45 % on the highest temperature days. This can be compared with a simulated contribution of about 20 % during the remainder of the campaign. Although it is recognised that the magnitude of biogenic VOC emissions is subject to some uncertainty, these results support an important role for biogenic VOC oxidation in regional-scale ozone formation under heatwave conditions.

8.5.3 Sensitivity to Anthropogenic Emissions Variations over the Period 1990-2020

The 2003 campaign has been simulated using historical emissions of NO_x , anthropogenic VOC, CO and SO_2 appropriate to the years 1990, 1995 and 2000 (based on NAEI and EMEP), and projected emissions for the years 2005, 2010, 2015 and 2020, based on relative UK figures reported in AQEG (2004; 2005). *All other model parameters were left unchanged from the standard values and no change in atmospheric composition was assumed.* Figure 8.38 shows the trend in the simulated ozone distribution, which indicates that the same conditions in earlier years would have been accompanied by broader ozone distributions with greater daytime maxima and increased overnight depletion. The decreasing trend in the top-end ozone concentrations is driven primarily by reductions in emissions of anthropogenic VOC since 1990, and provides a reasonable description of the observed trend in peak hourly mean ozone concentrations observed at long-running UK rural sites in the heatwave years of 1989, 1990, 1995 and 2003 (defined as years when temperatures $> 34^\circ\text{C}$ were recorded). The increasing (night-time) minima

are a consequence of associated NO_x emissions reductions, resulting from decreased local removal of ozone by reaction with NO emitted into the shallow night-time boundary layer.

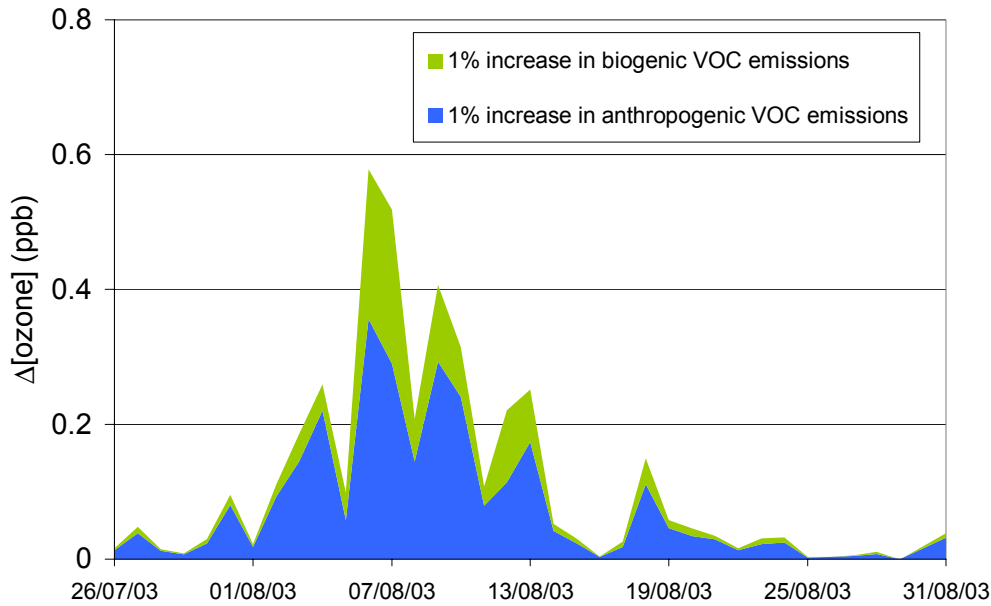


Figure 8.37 Simulated Increase in Ozone Concentrations at the Arrival Point (Writtle, Essex) resulting from an Incremental Increase of 1% in VOC Emissions.

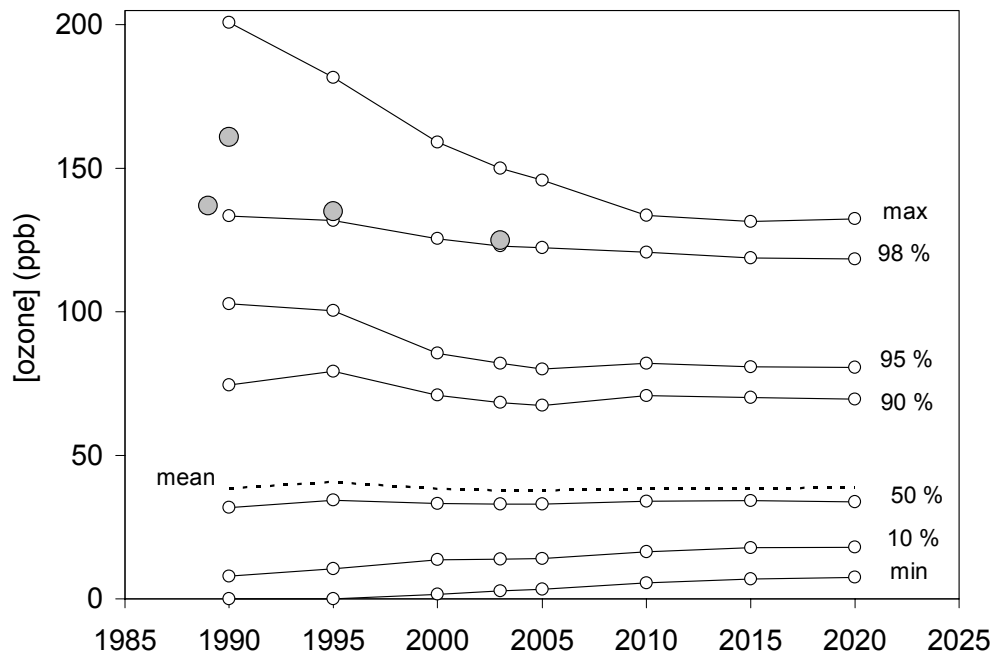


Figure 8.38 Open points: Simulated Trend in Ozone Distribution Statistics for the August 2003 Episode at Writtle (Essex) as a Function of Emissions for the Period 1990-2020. Filled Grey Points: Observed Maximum Hourly Mean Ozone Concentrations in Heatwave Years at Long-running UK Rural Sites (i.e., based on Data from Aston Hill, Bottesford, Bush, Eskdalemuir, Glazebury, Harwell, High Muffles, Ladybower, Lough Navar, Lullington Heath, Sibton, Strath Vaich and Yarner Wood).

Figure 8.39 presents the same data in terms of the AOT (accumulated ozone over threshold) metric, for a variety of thresholds. The results for each threshold are presented relative to the reference 2003 simulation. Once again, the metrics related to severe ozone events (AOT-120 and AOT-90) show a clear decreasing trend over the historical time period 1990-2003, and some continued reduction in the future.

The remainder (AOT-60, AOT-50 and AOT-40) show a modest historical trend, but little variation in the future. Figure 8.40 shows that the historical AOT-90 and AOT-120 values display a similar trend to that observed for information threshold (90 ppb) exceedence statistics at long-running UK rural sites, particularly for the heatwave years. The present simulations for the conditions of the August 2003 episode therefore suggest that the observed downward trend in statistics related to severe ozone events in the UK is a direct consequence of emissions reductions for anthropogenic VOC.

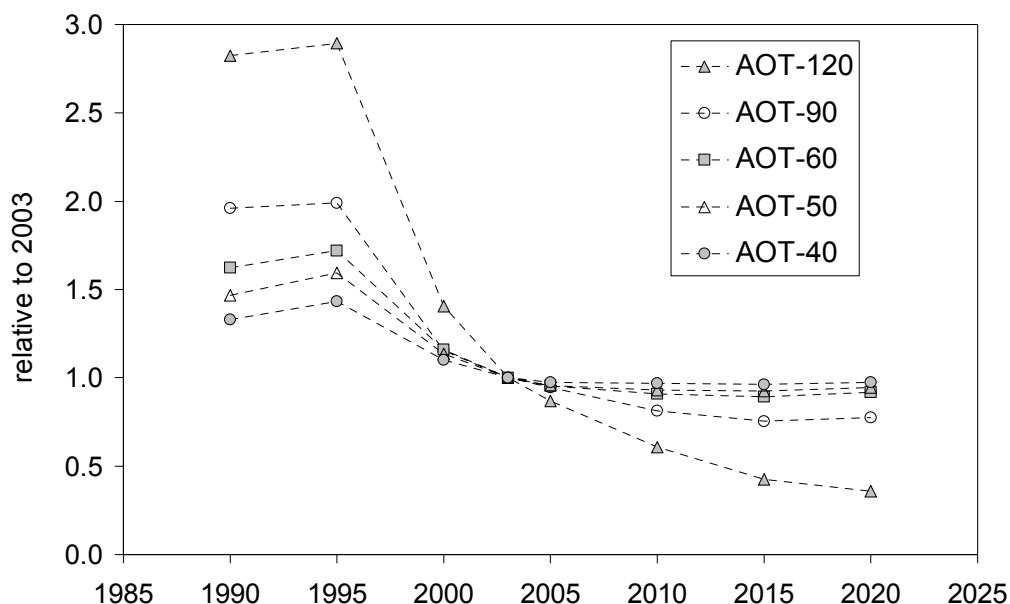


Figure 8.39 Simulated Trends in Selected AOT Metrics for the August 2003 episode at Writtle (Essex) as a Function of Emissions for the Period 1990-2020. Data are Presented Relative to the Value Simulated in the Reference 2003 Case.

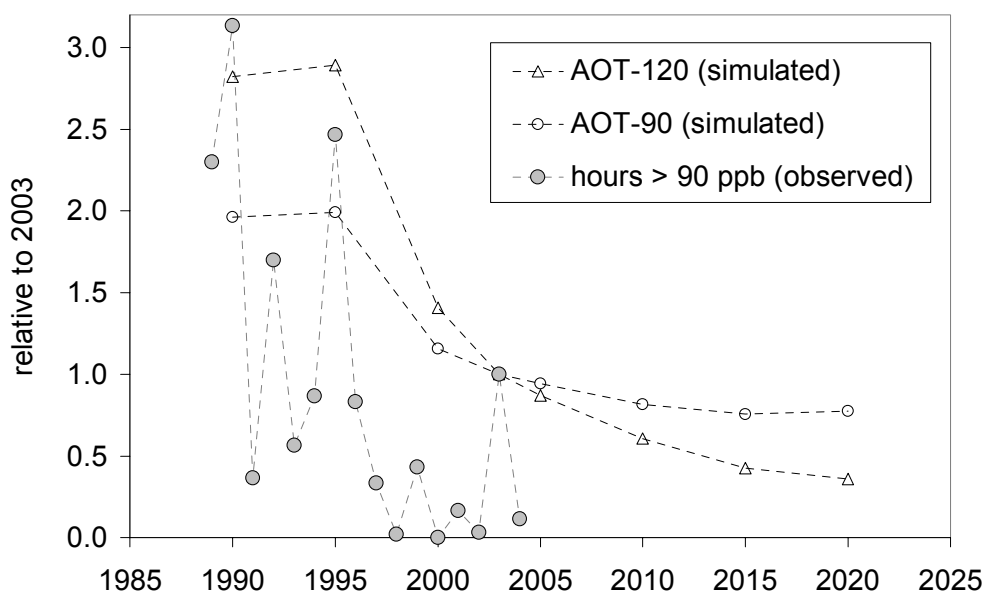


Figure 8.40 Simulated Trends in AOT-120 and AOT-90 for the August 2003 Episode at Writtle (Essex) as a Function of Emissions for the Period 1990-2020, compared with Observed Exceedences of 90 ppb at Long-running UK Rural Sites (identified in Figure 8.38 caption) for the period 1989-2004. Data are presented relative to the Value Simulated or Observed in the Reference 2003 case.

8.5.4 Effects of Incremental NO_x and VOC Emission Reductions

The effects of 10% incremental reductions in the emissions of NO_x and anthropogenic VOC have been examined for the 1990, 2003 and 2020 scenarios, to investigate whether ozone formation is limited by the availability of NO_x or VOC. Figure 8.41 shows the resultant simulated changes in ozone concentrations for the three scenarios.

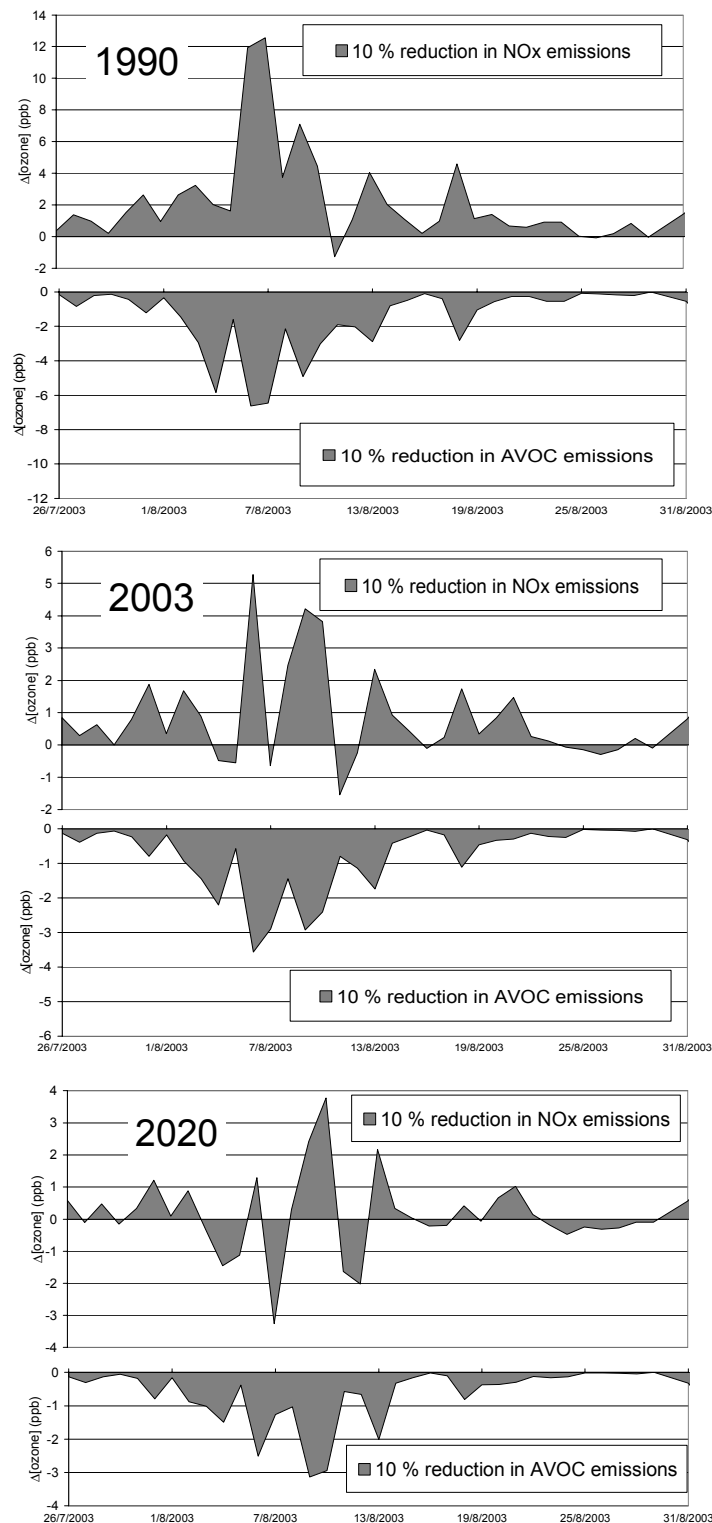


Figure 8.41 Simulated Change in Ozone Concentration at the Arrival Point (Writtle, Essex) resulting from an Incremental Decrease of 10% in Emissions of NO_x and Anthropogenic VOC (AVOC) for the 1990 (Upper Panel), 2003 (Middle Panel) and 2020 (Lower Panel) Emission Scenario.

The 1990 scenario demonstrates strong VOC limitation throughout the campaign period, with NO_x reductions almost always leading to an increase in ozone concentration, such that VOC emissions controls are clearly the favoured option for reducing ozone concentrations. The approximately compensating influences of VOC and NO_x reductions also qualitatively explain the small change in the simulated AOT statistics in the early part of the time series (Upper and Middle Panels of Figure 8.41).

The results for the 2003 scenario demonstrate a shift towards NO_x-limitation, with an increased number of days (relative to 1990) where the NO_x control leads to a reduction in ozone concentration. Although there are two days within the campaign period where 10% NO_x control leads to slightly greater ozone reduction than 10% VOC control, it is clear that the campaign period is still dominated by VOC limited conditions.

The results for the 2020 scenario show that 10% NO_x control leads comparable numbers of days when the ozone concentration is increased and decreased, and a further increase in the number of days (relative to 2003 and 1990) when NO_x control is more beneficial in reducing ozone concentrations than VOC control. Despite this, VOC reductions remain the favoured option when the whole campaign is considered.

The results therefore demonstrate that ozone formation for the conditions of this campaign at this location is predominantly VOC-limited for the complete time series, but shows a trend towards NO_x-limitation. Although this is in general agreement with previous assessments for Southeast England, this sensitivity study also shows that VOC- and NO_x-limitation are not intrinsic properties of a location, and that it is possible to get events when either condition prevails.

8.6 IMPLEMENTATION OF DEFRA'S VOC PROJECTIONS

8.6.1 Updating the UK PTM with the NAEI Speciated VOC Inventory

The NAEI speciated VOC inventories for the years 2000, 2010 and 2020 have been provided by netcen. The inventory for 2000 gives emissions for 663 individual species, arising from 248 separate man-made emission source categories, the entry for natural sources having been deleted. The emissions of VOCs from 248 individual source categories were handled using source profiles, which represented the fraction by mass of the total VOC emission attributed to each organic compound. In principle, each source profile could contain the fractions of up to 663 compounds but, in practice, there are less than a 100 entries on average. The annual VOC emissions were thus described by a 248 x 663 element matrix, with the columns representing the emission source categories and the rows the individual VOC species. The elements of the matrix were the emission of a particular VOC species from a particular emission source category. By summing across the rows, the total would be the annual emission of a particular VOC species and by summing down the columns, the total would be the emission from that particular source category. A *de minimis* lower emission limit of 10 kg per year was set for any species and source category. This led to the deletion of 218 species, leaving 445 species, and reduced the total VOC emission from 1,365.76 thousand tonnes per year to 1365.28 thousand tonnes per year. The MCMv3.1 thus provided the complete degradation schemes for 139 species of the 445 species and was able to account for 78.8 % of the total mass emission in the NAEI inventory for the year 2000.

Chemical degradation mechanisms for an additional 37 VOC species have been constructed using techniques taken from the CRI mechanism, as described in Section 8.1.5. These additional VOC species include:

- 19 alkanes representing C₁₀ to C₁₄
- 1 alkyne, propyne
- 12 cycloalkanes
- 4 aromatics representing C₁₀
- 1 alkene, limonene.

For the long chain alkanes with limited numbers of alkyl substituents, the initiation reactions were represented explicitly but the subsequent degradation was described using the chemistry for the corresponding normal alkane of the same carbon number as a mechanistic surrogate. For the >C₁₂

alkanes, a CRI representation was used for the initiation reactions followed by the formation of MCM intermediates at the earliest opportunity. Propyne was represented explicitly on the basis of reported data. For the cycloalkanes, a CRI method was used to represent the initiation, with an appropriate MCM intermediate generated after ring-opening. Limonene was represented using the chemistry of its isomer, alpha-pinene, as a mechanistic surrogate. For the C₁₀ aromatics, explicit initiation reactions were included with the subsequent chemistry taken from the MCM scheme for the C₁₀ aromatic, 1,3-dimethyl-5-ethylbenzene.

In the next stage, attention was given to the 48 species that are described as unresolved mixtures of compounds in the NAEI inventory, responsible for 180 thousand tonnes per year, 12% of the total mass emission. These unresolved mixtures were represented using the available emitted species wherever possible. Where there was no information available, then those mixtures were left unresolved. In this way, the 176 organic compounds considered in the UK PTM using the both the complete MCM v3.1 mechanisms and the CRI-based degradation mechanisms, were able to represent 90% of the total mass emissions of organic compounds in the year 2000 NAEI VOC emission inventory. No ozone production was included from the remaining 10% by mass of the emissions of organic compounds. The latest version of the UK PTM contains as accurate a picture of the emissions of the major organic compounds as can be given with current understanding, for the UK and by assumption, the rest of Europe.

8.6.2 Contributions from Different Sources of Organic Compounds to Photochemical Ozone Formation

The UK PTM, incorporating the sophisticated, explicit chemical mechanism described in the previous section and highly detailed emission inventories, was used to describe photochemical ozone formation along the idealised photochemical episode trajectory giving the highest ozone concentration over the UK [see Appendix 3]. The contribution made by 176 individual organic compounds arising from 248 separate emission source categories have been assessed at the most detailed level available for north west Europe.

The UK PTM utilises emission inventories at various spatial resolutions to estimate the instantaneous emissions at each point in time along the trajectory path. As in previous studies [Derwent *et al.*, 1998] gridded emissions of methane, CO, NO_x, SO₂ and VOCs were utilised at 150 km x 150 km, 50 km x 50 km and 10 km x 10 km resolution. The emissions in each grid square for each pollutant were updated to 1999 using data from the European Monitoring and Evaluation Programme [EMEP, 2001]. Natural biogenic isoprene emissions were taken from Simpson [1995]. The VOC speciation depended upon the conversion of estimates of the total VOC emissions into estimates of the emissions of 663 organic species for 248 man-made source categories, using profiles that contained estimates of the fraction by mass of total VOC emissions from that source category that are emitted as each individual organic species [Passant, 2002]. The source categories were taken from the UN ECE/CORINAIR methodology at the Selected Nomenclature for Air Pollution SNAP level 3. The assumption was made that the speciation profiles for the UK could be applied across Europe without further adjustment. This was considered a reasonable assumption because vehicle exhaust emissions, fuel evaporative emissions and solvents are likely to have similar profiles across north west Europe. No treatment was given for the natural biogenic emissions of terpenes, though the man-made emissions of α -pinene, β -pinene and limonene were included in the model.

Initial concentrations for NO_x, SO₂, CO, CH₄, HCHO, O₃ and H₂ were set at realistic tropospheric baseline levels as described previously [Derwent *et al.*, 1998]. Dry deposition of O₃, HNO₃, SO₂, NO₂, H₂O₂, organic peroxides and PANs was included as previously. In the base case model experiment, the air parcel travelled across Europe from Austria to Wales and the instantaneous emissions were taken from the EMEP and NAEI inventories. Ozone concentrations calculated in the base case started off at 50 ppb with the air parcel in central Europe and rose to 54 ppb during the first afternoon. On subsequent days, the mid-afternoon maxima rose from 57 ppb, to 63 ppb, 72 ppb and to 88 ppb by which time the air parcel had reached the England-Wales border.

The same speciation of the VOC emissions was assumed along the trajectory as that found for the United Kingdom using the 248 x 663 matrix. A series of sensitivity experiments was performed by perturbing slightly this assumed speciation and, in this way, the incremental reactivities were calculated for each of the 248 source categories using the photochemical trajectory model. At each point along the trajectory, a small fractional change was made to the instantaneous VOC emissions.

In each sensitivity experiment, the VOC emissions were increased by a nominal fraction (7.3% was chosen) and this additional emission was given the speciation of one of the 248 source categories. This additional VOC emission increased photochemical ozone production over the base case experiment and the ozone increments were determined by subtracting off the ozone concentration at the end point of the base case trajectory. The choice of 7.3% was completely arbitrary and had no policy significance. It was a compromise between the requirement to produce results that were above the noise level in the model but not too large as to take the model out of its linear response range. The 5-day trajectory model was then rerun 248 times, once for each VOC source category, and the ozone concentrations at the trajectory endpoint were recalculated for each sensitivity experiment. No other model parameters were changed in the sensitivity experiments from their values in the base case experiment. The additional ozone present at the end-point of the trajectory was taken as a measure of the propensity for regional scale ozone formation from that source category.

Table 8.9 lists the source categories studied, together with the percentage of the total VOC emissions in that source category and the incremental reactivity estimated for that source category for the top 20 ozone-forming VOC source sectors. Appendix 4 extends Table 8.9 to the entire 248 VOC source sectors in the NAEI.

Table 8.9 Percentage Contribution to Emissions, Incremental Reactivity and the Photochemical Ozone Formation by VOC Source Sector along a 5-day Trajectory for the Top 20 Ozone-forming VOCs.

	Source Category	Percentage of total Emissions	Incremental Reactivity	Ozone Production, ppb
1	Road transport (cars without catalysts)_Petrol	11.524	41.387	4.769
2	Road transport (cars with catalysts)_Petrol	5.264	41.578	2.189
3	Onshore loading of crude oil	5.098	31.532	1.608
4	Chemical industry	5.364	28.337	1.520
5	Offshore loading of crude oil	3.739	31.026	1.160
6	Spirit manufacture (maturation)	3.401	30.890	1.051
7	Refineries (process fugitives)	2.091	41.291	0.863
8	Petrol stations (vehicle refuelling unleaded petrol)	2.709	31.327	0.849
9	Other solvent use	3.370	20.229	0.682
10	Gas leakage	4.648	13.527	0.629
11	Decorative paint (trade decorative)	1.811	31.395	0.569
12	Industrial coatings (metal & plastic)	1.627	34.835	0.567
13	Aerosols (cosmetics and toiletries)	1.883	28.638	0.539
14	Decorative paint (retail decorative)	1.669	31.313	0.523
15	Industrial adhesives	1.822	28.569	0.520
16	Road transport (articulated HGVs)_DERV	1.084	46.014	0.499
17	Other industrial (off-road)_Petrol	1.087	43.762	0.476
18	Road transport (rigid HGVs)_DERV	1.013	46.151	0.468
19	Aerosols (car care products)	1.465	28.187	0.413
20	Road transport (LGVs without catalysts)_Petrol	0.923	41.905	0.387

The incremental reactivity of a source category was defined as the ozone increment over the base case for the fractional (7.3%) increase in VOC emissions, divided by the fractional increase in VOC emissions. By multiplying the fraction of the VOC emissions in that source category by the incremental reactivity, a measure was obtained of the contribution to regional scale ozone formation from each of the source categories. These measures summed to 31 ppb over the 248 emission source categories. This is close to the ozone production found in the base case experiment, that is, $87.8 - 50 = 37.8$ ppb. On this basis, we have determined the contribution from each of the 248 source categories to the ozone formation in the base case with reasonable precision. The entries in Table 8.9 have been ranked in order of this contribution.

The source category that made the largest contribution to photochemical ozone formation was road transport, cars without catalysts, with road transport, cars with catalysts, the second largest. These categories were in first and second places by virtue of their large percentage contributions to total VOC emissions and their relatively high incremental reactivities (41.4-41.6). The source category with

the largest incremental reactivity (53.8) was chemical waste incineration but, because of its relatively low percentage contribution to total VOC emissions, it contributed little to ozone formation.

8.6.3 Application to Policy and the Defra VOC Projections to 2010 and 2020

In Section 8.6.2 above, incremental reactivities for each of the 248 VOC emission source categories in the NAEI VOC inventory were evaluated for the year 2000. Using the Defra emission projections, VOC emissions are available for each source category for 2010 and 2020. Assuming that there is no change in the incremental reactivities, the influence of the changing VOC emissions on peak ozone concentrations can be assessed straightforwardly. On the standard base case UK PTM model trajectory from Austria to the United Kingdom, peak ozone was reduced by 12.67 ppb when the 2010 VOC inventory was substituted by that for 2000. The reduction was somewhat smaller at 12.19 ppb when the substitution was made with the 2020 inventory.

Table 8.10 gives the VOC emission source categories that contributed most to the decline in episodic peak ozone concentrations between the years 2000 and 2010 using the Defra VOC emission projections. By far the largest contribution to the decline in ozone of 6.6 ppb, or more than about one half of the total, came from the reduction in VOC emissions in the road transport sector. The next largest combined contribution, amounting to about 15% of the ozone decline, came from VOC emission reductions in the stationary source sectors of the chemicals, oil and gas industries.

Table 8.10 The VOC Emission Source Categories that gave the Greatest Contributions to the Decline in Episodic Peak Ozone Concentrations between the years 2000 and 2010.

Source Category	Contribution to the Decrease in Peak Ozone Concentrations between 2000 and 2010 (in ppb)
Road transport cars without catalysts	4.8
Road transport cars with catalysts	1.1
Onshore loading of crude oil	0.7
Offshore loading of crude oil	0.5
Road transport LGVs without catalysts	0.4
Surface cleaning with trichloroethylene	0.3
Road transport rigid HGVs	0.3
Domestic combustion of coal	0.3
Offshore oil & gas industries	0.3
Chemical industry	0.3
Decorative paint trade decorative	0.3
Gas leakage	0.3
House & garden machinery	0.3

Table 8.11 The VOC Emission Source Categories that gave the Greatest Contributions to Episodic Peak Ozone Concentrations in 2020.

Source Category	Contribution to Peak Ozone Concentrations in 2020 (in ppb)
Chemical industry	1.6
Spirit manufacture (maturation)	1.1
Onshore loading of crude oil	0.9
Road transport cars with catalysts	0.7
Refineries (process fugitives)	0.7
Industrial adhesives	0.7
Petrol stations (vehicle refuelling with up)	0.7
Offshore loading of crude oil	0.7
Industrial coatings (metal plastic)	0.6
Aerosols (cosmetics and toiletries)	0.6
Other solvent use	0.6
Aerosols (car care)	0.5

Notes: ulp = unleaded petrol

In 2020, because of the marked reductions in VOC emissions in the transport sector, a different range of source categories will be responsible for the bulk of the ozone formation. Table 8.11 shows, in order of importance, the major ozone producing sectors in 2020. The entries are dominated by stationary VOC sources in industries, associated with the chemical, oil and gas industries and the

manufacturing industries that use solvents. The only sector listed associated with road transport, is that of petrol stations and the emission of VOC from refuelling motor vehicles with unleaded petrol.

Table 8.11 points to a major shift in policy if ozone levels are to be reduced beyond 2010 levels so that stationary VOC sources are targeted rather than motor vehicles.

8.7 PHOTOCHEMICAL OZONE CREATION POTENTIALS POCPs

As a result of developments to the chemical mechanisms in MCMv3.1 and because of improvements made to the speciation of the VOC emission inventories, a far wider range of organic compounds can now be represented in the UK PTM. The Photochemical Ozone Creation Potentials POCPs have therefore been determined for 177 selected organic compounds using the UK PTM and the standard 5-day trajectory case in which the ozone chemical development is followed in an air parcel travelling from Austria to Wales.

The POCPs were determined by increasing the emissions of each organic compound in turn by a fixed mass and determining the increase in mean ozone concentrations averaged over the entire trajectory length over and above the base case with standard emissions. The ozone increments found with each organic compound were then ratioed to that found with ethylene and expressed as an index relative to ethylene = 100. The resulting POCP values are given in Table 8.12.

Some of the highest POCPs are found with the alkenes and aromatic compounds. In comparison, the alkanes are significantly less reactive as class. The oxygenated organic compounds tend to overlap the alkanes in reactivity terms, although certain specific oxygenates are found that are highly reactive, including methyglyoxal and some higher aldehydes.

Table 8.12 Photochemical Ozone Creation Potentials (POCP) for 154 Selected Organic Compounds determined over a Five-day Trajectory and expressed relative to Ethylene with a POCP = 100.

Volatile Organic Compound	POCP	Volatile Organic Compound	POCP	Volatile Organic Compound	POCP	Volatile Organic Compound	POCP
alkanes		methylcyclopentane		aromatics		sec-butanol	40
ethane	8	cyclohexane	49	benzene	10	t-butanol	2
propane	14	methylcyclohexane	28	toluene	44	3-methyl-1-butanol	44
butane	31	ethylcyclohexane	65	o-xylene	78	phenol	-5
i-butane	28	propylcyclohexane	63	m-xylene	86	o-cresol	19
pentane	40	1,2,3-trimethylcyclohexane	60	p-xylene	72	2,5-xylenol	55
i-pentane	34	i-propylcyclohexane	57	ethylbenzene	46	2,4-xylenol	54
neopentane	18	butylcyclohexane	60	propylbenzene	38	2,3-xylenol	34
hexane	40	i-butylcyclohexane	59	l-propylbenzene	32	cyclohexanol	45
2-methylpentane	41	1-methyl-3-propylcyclohexane	59	1,2,3-trimethylbenzene	105	diacetone alcohol	29
3-methylpentane	43	1-methyl-4-propylcyclohexane	60	1,2,4-trimethylbenzene	110	acetone	6
2,2-dimethylbutane	22	pentylcyclohexane	56	1,3,5-trimethylbenzene	107	methylethylketone	32
2,3-dimethylbutane	50	hexylcyclohexane	56	o-ethyltoluene	73	methyl-i-butylketone	52
heptane	35	methylene dichloride	56	m-ethyltoluene	78	cyclohexanone	29
2-methylhexane	32	ethyl chloride	3	p-ethyltoluene	63	methyl formate	3
3-methylhexane	42	alkenes	11	3,5-dimethylethylbenzene	104	methyl acetate	7
octane	34	ethylene		3,5-diethyltoluene	98	ethyl acetate	19
2-methylheptane	34	propylene	100	1,2,3,5-tetramethylbenzene	104	i-propyl acetate	21
3-methylheptane	37	but-1-ene	117	1,2,4,5-tetramethylbenzene	100	butyl acetate	26
nonane	34	cis-but-2-ene	104	1-methyl-4-i-propylbenzene	75	sec-butyl acetate	0
2-methyloctane	34	trans-but-2-ene	113	1-methyl-3-i-propylbenzene	88	n-propyl acetate	24
3-methyloctane	34	butylene	116	styrene	5	formic acid	3
4-methyloctane	37	1,3-butadiene	63	oxygenates		acetic acid	9
3,4-dimethylheptane	36	cis-pent-2-ene	89	formaldehyde	46	propanoic acid	13
decane	36	trans-pent-2-ene	109	acetaldehyde	55	dimethylether	18
2-methylnonane	35	1-pentene	111	propionaldehyde	72	diethylether	46
3-methylnonane	39	2-methylbut-1-ene	95	i-propionaldehyde	50	di-i-propylether	44
4-methylnonane	35	3-methylbut-1-ene	75	butyraldehyde	70	ethylene glycol	33
2,5-dimethyloctane	38	2-methylbut-2-ene	73	pentanal	71	propylene glycol	39
2,6-dimethyloctane	36	isoprene	82	3-methylbutanal	41	2-butoxyethanol	45
2-methyl-3-ethylheptane	34	hex-1-ene	114	benzaldehyde	-19	1-methoxy-2-propanol	34
2,2-dimethyl-3,3-dimethylhexane	19	cis-hex-2-ene	88	2-methylbenzaldehyde	-28	2-methoxyethanol	29
undecane	36	trans-hex-2-ene	104	3-methylbenzaldehyde	-18	2-ethoxyethanol	37
2-methyldecane	34	alpha-pinene	102	4-methylbenzaldehyde	5	acrolein	54
3-methyldecane	36	beta-pinene	68	methanol	13	methacrolein	92
4-methyldecane	36	limonene	33	ethanol	34	glyoxal	22
5-methyldecane	35	tetrachloroethylene	71	propanol	48	methylglyoxal	101
dodecane	33	trichloroethylene	1	i-propanol	18	other VOCs	
tridecane	42	ethylidene dichloride	29	butanol	52	acetylene	7
tetradecane	46		54	i-butanol	36	propyne	73

9 Development of Stomatal Flux Module for Crops and Semi-natural Vegetation (Objective 5)

9.1 BACKGROUND

The impact of ozone on vegetation are assessed by comparison with critical levels above which direct adverse effects may occur according to present knowledge. To date, the main method to assess the impact of ozone on vegetation has been the concentration-based (AOTx) approach. Separate concentration-based critical levels have been set for agricultural crops, horticultural crops, semi-natural vegetation and forest trees. A short-term critical concentration level has also been set for visible injury to plants.

It is now widely believed that the plant response to ozone is more closely related to the flux of ozone to the plant. Flux-based critical levels based on accumulated stomatal flux of ozone have been set for wheat, potato and provisionally for sensitive deciduous tree species. The Department has funded work through its research programme at the University of Bradford, Stockholm Environment Institute (SEI, University of York) and CEH Edinburgh in support of the development of the EMEP Surface Ozone Flux model.

Objective 5 of the current project requires the integration of the ozone assessment capability of OSRM, *i.e.*, scenarios for precursor reduction and subsequent impact on surface ozone concentrations, to allow the production of critical levels maps of ozone for the UK using the flux-based approach. An initial workshop was held in York in May 2003, which was attended by personnel from Defra and the Devolved Administrations as well as contractors working on the Department and DAs' ozone research programme. A number of specific actions were identified and netcen was tasked to develop a programme of work. Following meetings with SEI and discussions at a subsequent workshop in November 2003, the preferred approach was to develop a postprocessor code to derive ozone fluxes from the ozone concentrations calculated by the OSRM and the resistance components provided by a Surface Ozone Flux model (SOFM). A schematic of this modelling framework is shown in Figure 9.1.

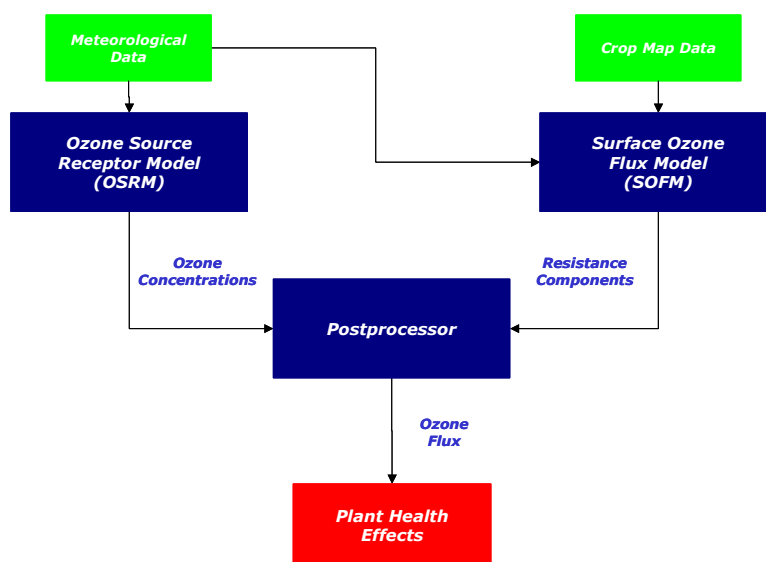


Figure 9.1 Modelling Framework to Calculate Stomatal Ozone Fluxes.

During the second year of the project, a Surface Ozone Flux Model (SOFM) has been developed at netcen, which incorporates the algorithms for the calculation of stomatal flux developed by Emberson *et al.* [2000] and those included in the UNECE mapping manual [UN ECE, 2003]. The Surface Ozone Flux Model was then used to calculate stomatal ozone fluxes for beech, winter wheat and potatoes at four UK locations. This was subsequently extended to the UK scale.

9.2 MODEL COMPONENTS

9.2.1 Surface Ozone-Flux Model

The Surface Ozone Flux Model has primarily been developed to use output generated by the Ozone Source-Receptor Model, although it can also use ambient ozone monitoring data.

The algorithms used in the Surface Ozone Flux Model are based the resistance analogue model, which is shown schematically in Figure 9.2. The purpose of the Surface Ozone Flux Model is to calculate the values of component resistances to the ozone flux between a reference height and the bulk canopy, the upper canopy leaves or flag leaves and the ground. For beech and potatoes, the critical leaves are the uppermost canopy leaf whereas the flag leaf is the most relevant leaf for wheat. The surface area of the individual upper canopy leaf or flag leaf is very small so that it has little effect on the ozone concentrations. The ozone concentrations in the canopy are dominated by the fluxes to the canopy and to the ground. However, the yield loss in crops or the loss of biomass in woodlands is related to the ozone flux to the upper canopy leaf or the flag leaf. It is therefore necessary to calculate the ozone flux to the whole canopy in order to determine the flux to the most sensitive leaves.

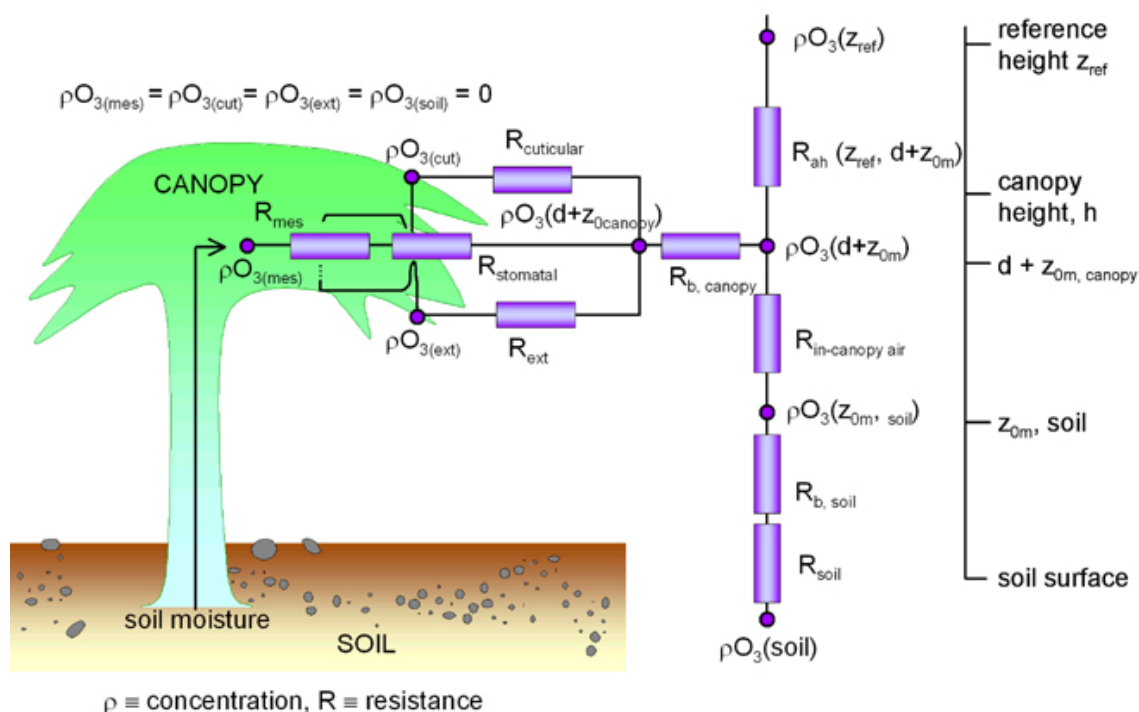


Figure 9.2 Resistance Analogue of Ozone Transfer between the Atmospheric Surface Layer and Terrestrial Ecosystems [taken from NEGTA, 2001].

The component resistances are:

- aerodynamic resistance from a specified reference height to the canopy displacement height
- stomatal resistance of the bulk canopy
- the external resistance to external plant tissue in the canopy
- the quasi-laminar resistance to the canopy
- the in-canopy air resistance below the displacement height
- the ground surface resistance
- stomatal resistance to the upper canopy/flag leaf
- the external resistance to external plant tissue of the leaf
- the quasi-laminar resistance to the leaf

The UNECE mapping manual describes the methods to calculate the stomatal resistance, external resistance and quasi-laminar resistance to the upper canopy leaf: these methods have been implemented within the surface ozone flux model for winter wheat, potatoes and beech trees.

Methods to calculate the bulk canopy resistances are not specified in the mapping manual. The methods used in the Surface Ozone Flux Model have been developed from those reported by Emberson *et al.* [2000] and presented in the EMEP Unified Model description [Simpson *et al.*, 2003]. The model developments at netcen have involved extensive detailed discussions with Dr Emberson and have included the intercomparison of model outputs.

The stomatal conductances are calculated using a multiplicative algorithm with the following formulation:

$$g_{sto} = g_{max} \times [\min(f_{phen}, f_{O3})] \times f_{light} \times [\max(f_{min}, (f_{temp} \times f_{VPD} \times f_{SWP}))]$$

where g_{sto} is the actual stomatal conductance and g_{max} is the species specific maximum stomatal conductance. The parameters f_{phen} , f_{O3} , f_{light} , f_{temp} , f_{VPD} and f_{SWP} are factors in the range 0-1 that take account of the effect of plant phenology, ozone-induced senescence, light levels, temperature, water vapour pressure deficit and soil water pressure.

The vapour pressure deficit is calculated in the Surface Ozone Flux Model using an analogous bulk canopy stomatal flux model adapted for water vapour. The soil water pressure is estimated using a simple box model taking account of precipitation, evaporation from leaf surfaces and evapotranspiration through the plant stomata. As the actual soil water pressure will depend to a great extent on the type of soil and the soil structure, it is not possible to make general predictions about the soil water pressure without detailed data on soil types. However, model predictions for a characteristic soil type (loam) are made in order to assess the potential effect of water stress on ozone fluxes.

The Surface Ozone Flux Model calculates the resistances of each of the components. Details of the calculation methods are provided in Abbott [2004]. A combined surface resistance, R_{sur} , is calculated that includes the contributions from each of the bulk canopy component resistances. Key model outputs include:

- the aerodynamic resistance, R_{aero} ,
- the laminar canopy resistance
- the surface resistance, R_{sur}
- the upper leaf/flag leaf stomatal surface deposition velocity, F_{st}/c_i where F_{st} is the stomatal flux and c_i is the ozone concentration at the interface node.

9.2.2 Meteorological Pre-processor

The Ozone Source Receptor Model and the Surface Ozone Flux Model make use of the same Numerical Weather Prediction data provided by the Meteorological Office. Use of the same meteorological data set for both models takes account of possible correlations between weather conditions and ozone concentrations and between weather conditions and stomatal resistances. However, the data are provided at 1° latitude and 1° longitude intervals every 6 hours throughout the year. The Ozone Source Receptor Model requires data at the nodes of the EMEP grid at one hour intervals. The meteorological preprocessor interpolates the data both in time and space. It scales and formats the data. It also derives a grid-square average estimate of the aerodynamic resistance from the meteorological data. Details of the meteorological pre-processor can be found in Appendix 1 of the report by Abbott [2004].

9.2.3 Ozone Flux Post-processor

The purpose of the ozone flux post-processor is to calculate the flux of ozone to the stomata of the upper canopy leaf for beech and potatoes and the flag leaf for winter wheat from the outputs of the OSRM and SOFM models. It calculates the ozone concentration at the interface node from the mid-boundary layer height concentration calculated by OSRM. It then multiplies this value by the upper leaf/flag leaf stomatal surface deposition velocity, F_{st}/c_i to give the calculated stomatal flux. The

accumulated stomatal flux are calculated using the algorithms specified in the UNECE mapping manual. Details of the program can be found in the report by Abbott [2004].

9.3 OZONE FLUX CALCULATIONS

Selected model outputs are presented in this section. Upper leaf surface conductances were predicted for winter wheat, potatoes and beech at four selected sites in the UK throughout the growing season (day 90-270) for 2001:

- 55.5°N, 3.5°W (near Edinburgh);
- 52.5°N, 2.5°W (in the border area between Wales and England);
- 52.5°N, 1.5°W (in the Midlands);
- 52.5°N, 1.5°E (in East Anglia, near Lowestoft).

Accumulated ozone fluxes to the three vegetation types were derived at UK monitoring sites using ozone concentrations calculated by the OSRM and the fluxes were compared with those based on measured ozone concentrations. Finally, maps of accumulated ozone flux over threshold and crop yields are presented based on OSRM model runs at 10 km resolution.

9.3.1 Upper-leaf Surface Conductance

The upper leaf surface conductance is calculated as the ratio of the ozone flux to the upper leaf or flag leaf per unit projected leaf area to the ozone concentration at the displacement height, F_{st}/c .

- **Winter Wheat:** The maximum daily stomatal conductances for winter wheat were calculated at the four sites for the accumulation period specified in the UNECE mapping manual. The upper panel of Figure 9.3 shows the stomatal fluxes calculated for winter wheat at a location in the Midlands (52.0°N, 1.5°W) in 2001. The accumulation period for winter wheat is based on phenological models and so the accumulation occurs much earlier in the year in southern England than it does further north.

The maximum daily stomatal conductance approached 8 mm s^{-1} . This may be compared with the species specific maximum conductance, g_{\max} for wheat of $450 \text{ mmol m}^{-2} \text{ PLA s}^{-1}$ or 11 mm s^{-1} . The predicted maximum daily conductance in East Anglia (at 52.5°N, 1.5°E) was rather less than that predicted in more northerly and westerly locations. This occurred because the temperatures at this near coastal location were influenced by the presence of the sea. Relatively mild temperatures in the early part of the year brought forward the growing season but maximum daily temperatures were rather less than those inland.

- **Potatoes:** The maximum daily predicted stomatal conductance for potatoes were calculated at the same sites for the accumulation period specified in the UNECE mapping manual, based on a fixed emergence data of day 146. The accumulation period for potatoes is based on phenological models and the accumulation period is rather shorter in southern England than it is further north.

The maximum daily stomatal conductance approached 10 mm s^{-1} . This may be compared with the species specific maximum conductance, g_{\max} for potatoes of $750 \text{ mmol m}^{-2} \text{ PLA s}^{-1}$ or 18.3 mm s^{-1} . The predicted maximum daily conductance at the site in East Anglia was rather less than that predicted in more northerly and westerly locations because the maximum daily temperatures are affected by the sea at this near coastal location.

- **Beech:** The maximum daily stomatal conductance approached 3 mm s^{-1} . This may be compared with the species-specific maximum conductance, g_{\max} for beech of $134 \text{ mmol m}^{-2} \text{ PLA s}^{-1}$ or 3.3 mm s^{-1} . The modelled maximum daily conductance for the site in the Midlands and to a lesser extent in East Anglia decreased sharply in the latter part of the growing season. This occurred because of the lower predicted soil water pressure in inland areas in the south eastern part of the UK.

9.3.2 Upper Leaf Stomatal Fluxes

The upper leaf surface conductance is calculated as the ratio of the ozone flux to the upper leaf or flag leaf per unit projected leaf area to the ozone concentration at the displacement height, F_{st}/c . The upper leaf stomatal flux is then the product of the upper leaf surface conductance (F_{st}/c) and the ozone concentration at displacement height. The ozone concentration at displacement height was calculated from the OSRM mid-boundary layer height using a height correction factor calculated for each hour and crop type by the Surface Ozone Flux Model.

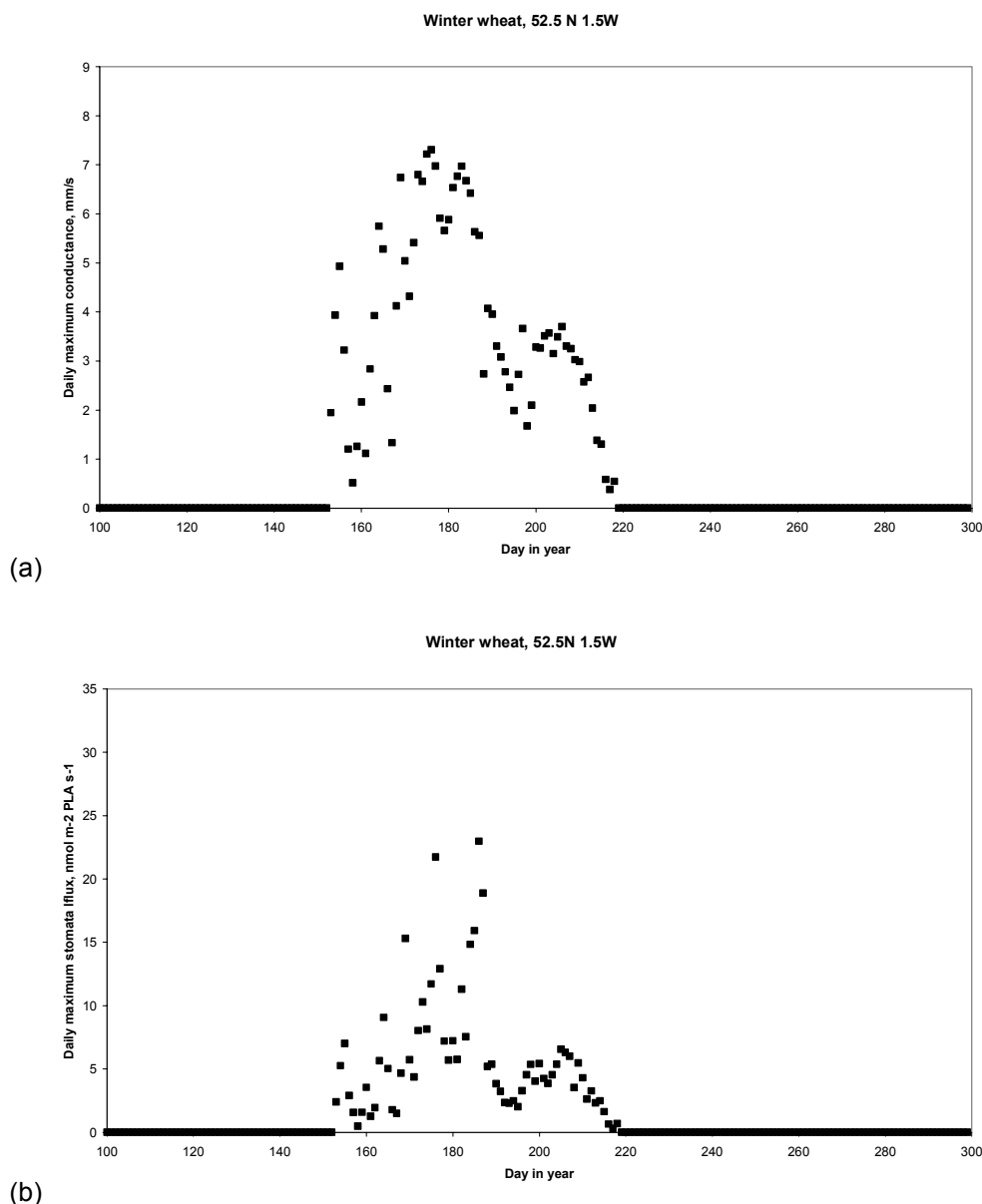


Figure 9.3 Maximum Daily Stomatal Conductance (Left-hand Panel) and Maximum Daily Stomatal Ozone Flux (Right-hand Panel) Calculated for Winter Wheat for 2001 at a Location in the Midlands using the Ozone Source-receptor and Surface Ozone Flux Models.

- Winter Wheat: The lower panel of Figure 9.3 shows the stomatal fluxes calculated for winter wheat at a location in the Midlands (52.0°N, 1.5°W) in 2001. The maximum daily stomatal flux in 2001 was calculated to exceed the threshold value of $6 \text{ nmol m}^{-2} \text{ PLA s}^{-1}$ specified in the UNECE mapping manual on relatively few days throughout the accumulation period.

- **Potatoes:** The maximum daily stomatal flux in 2001 was calculated to exceed the threshold value of $6 \text{ nmol m}^{-2} \text{ PLA s}^{-1}$ specified in the UNECE mapping manual for on relatively few days throughout the accumulation period.
- **Beech:** The maximum daily stomatal flux in 2001 was calculated to exceed the threshold value of $1.6 \text{ nmol m}^{-2} \text{ PLA s}^{-1}$ specified in the UNECE mapping manual for much of the accumulation period. However, predicted stomatal flux during the latter part of the accumulation period at the two more south-easterly sites was restricted by the limited soil moisture content.

9.3.3 Accumulated Ozone fluxes at UK Monitoring sites

The accumulated ozone stomatal flux over threshold was calculated as the sum of the calculated hourly ozone stomatal flux above threshold values, over an accumulation period specified in the UNECE mapping manual. Table 9.1 shows the calculated stomatal fluxes over threshold for beech, winter wheat and potatoes using OSRM-derived hourly ozone concentrations at rural ozone monitoring sites in the UK Automatic Urban and Rural Network.

Table 9.1 Accumulated Ozone Stomatal Fluxes over Threshold at UK Rural Monitoring Sites: Comparison of Predictions based on OSRM Ozone Concentrations with Predictions based on Measured Ozone Concentrations.

Site	Accumulated Ozone Stomatal Flux over Threshold ($\text{mmol m}^{-2} \text{ PLA}$)					
	Using OSRM O ₃ concentrations			Using Measured O ₃ Concentrations		
	Beech	Winter Wheat	Potatoes	Beech	Winter Wheat	Potatoes
Aston Hill	6.14	2.04	2.61	*	*	*
Bush Estate	5.97	0.86	0.95	5.83	0.32	0.41
Eskdalemuir	6.12	1.07	0.97	5.19	0.64	0.62
Great Dun Fell	5.89	2.48	2.31	7.92	2.96	2.80
Harwell	3.39	2.45	3.61	4.38	3.37	4.93
High Muffles	5.28	3.13	2.90	*	*	*
Ladybower	3.05	2.31	3.02	*	*	*
Lullington Heath	5.89	0.20	2.05	7.55	0.21	1.53
Narbeth	9.53	0.02	0.62	10.23	0.01	0.41
Rochester	2.43	1.05	3.33	4.72	1.74	3.44
Sibton	6.65	0.38	1.69	6.92	0.08	0.90
Somerton	5.22	2.35	3.54	6.32	2.74	4.06
Wicken Fen	2.96	2.06	3.71	4.13	3.61	5.66
Yarner Wood	4.41	1.82	3.16	5.92	2.64	3.27
Bottesford	4.16	2.13	2.82	5.75	3.25	4.41

Note * less than 90% data capture

The OSRM-derived accumulated ozone stomatal fluxes were then compared with stomatal flux estimates based on measured ozone concentrations. These estimates are also shown in Table 9.1. As shown in Figure 9.4, there appears to be a good correlation between the two sets of ozone fluxes: to some extent this is inevitable because the same meteorological data were used in both cases. Nevertheless, the comparison suggests that OSRM can provide an effective means of predicting accumulated flux over threshold to vegetation types.

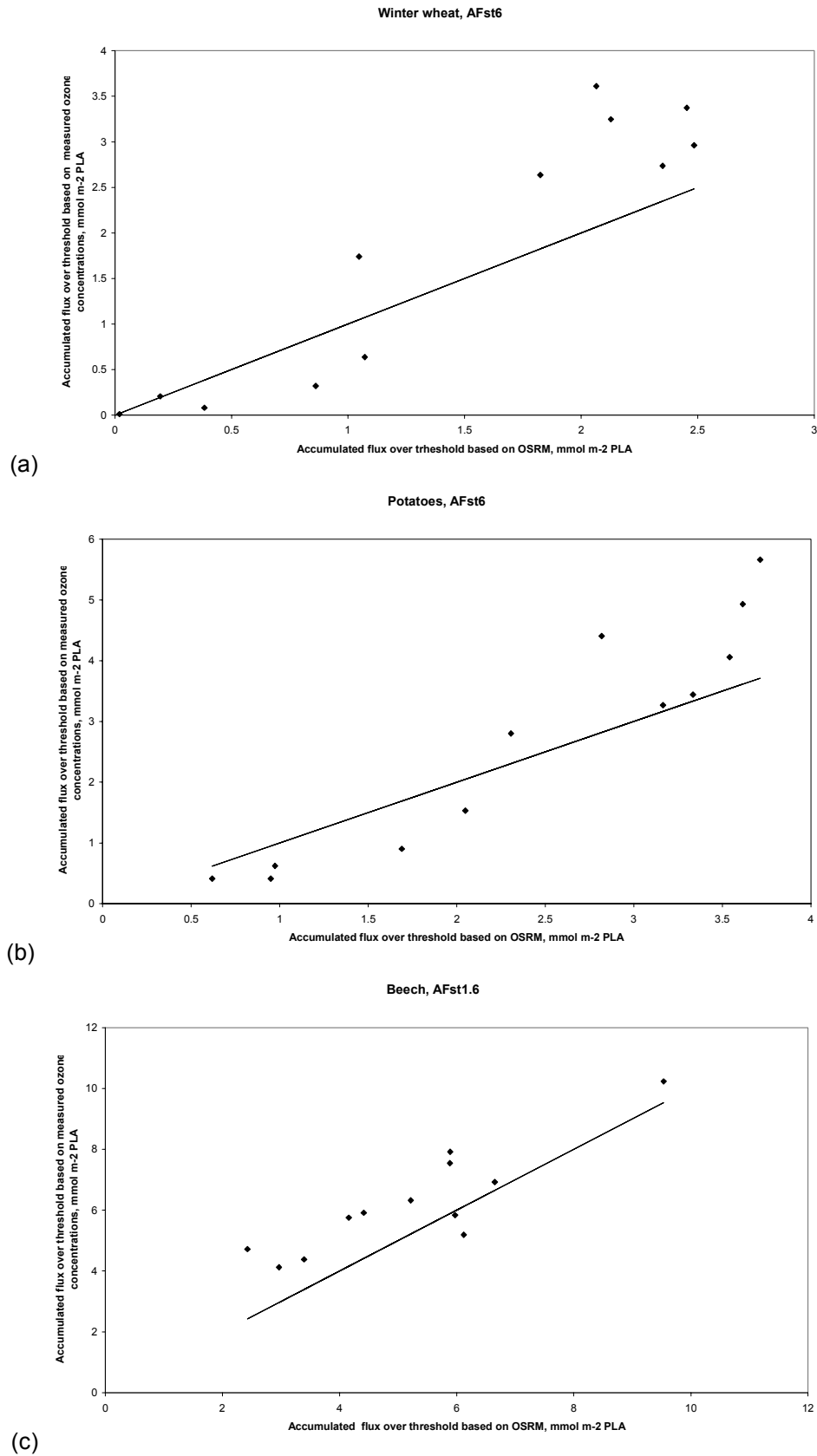


Figure 9.4 Predicted Accumulated Ozone Fluxes over Threshold for Winter Wheat (Panel a), Potatoes (Panel b) and Beech Trees (Panel c) at UK Rural Ozone Monitoring Sites for 2001: Comparison of Predicted Fluxes based on OSRM-derived and Measured Ozone Concentrations.

9.3.4 UK MAPs of Accumulated Fluxes

The Surface Ozone Flux Model was used to calculate UK maps of the accumulated ozone stomatal fluxes in 2001 to beech, winter wheat and potatoes. Panels (a) and (b) of Figure 9.5 show maps of these fluxes to winter wheat and potatoes at a 10 km resolution throughout the UK. The maps of winter wheat, potatoes and also beech show that

- the accumulated flux over threshold, AF_{st6} for winter wheat exceeded the critical value of $1 \text{ mmol m}^{-2} \text{ PLA}$ (projected sunlit leaf area) over much of England and Wales. The critical value corresponds to a 5% loss of yield. The accumulated flux was below the critical value over most of Scotland and Northern Ireland and in coastal areas in England and Wales. The accumulated flux in these areas was limited to some extent by lower maximum temperatures.
- the accumulated flux over threshold, AF_{st6} for potatoes did not exceed the critical value of $5 \text{ mmol m}^{-2} \text{ PLA}$ (projected sunlit leaf area) in the UK in 2001. The critical value corresponds to a 5% loss of yield. The accumulated flux was smallest in Scotland and Northern Ireland and in coastal areas in England and Wales. The accumulated flux in these areas is limited to some extent by lower maximum temperatures.
- the accumulated flux over threshold, $AF_{st1.6}$ for beech exceeded the critical value of $4 \text{ mmol m}^{-2} \text{ PLA}$ (projected sunlit leaf area) over much of the UK. The critical value corresponds to a 5% loss of biomass. The accumulated flux was below the critical value in an area extending north-west from London and covering much of the Midlands. However, the stomatal conductance was limited in this area by soil moisture potential during the latter part of the accumulation period. Trees on soil with better water retention in this area than the loam used in the assessment would have been affected by ozone to a greater extent.

The UNECE mapping manual provides simple statistical relationships between the crop yield for wheat and potatoes affected by ozone uptake as a fraction of the unaffected yield and the accumulated ozone flux over threshold, AF_{st6} . For wheat, the relationship is $\text{Yield} = 1.0 - 0.048 AF_{st6}$ and for potatoes, the corresponding relationship is $\text{Yield} = 1.01 - 0.013 AF_{st6}$.

Panels (c) and (d) of Figure 9.5 show the percentage yield for wheat and potatoes calculated for 2001 at locations throughout the UK. Panel (c) indicates that there was more than 15% loss in wheat yield in a small area in the north-east of England, and more than 10% loss in yield over much of central England. Panel (d) suggests that there was less than 5% loss in the yield of potatoes throughout the UK.

The UN ECE mapping manual recommends that similar maps should not be prepared for forest trees.

9.4 SUMMARY

The feasibility of preparing maps that show the effects of ozone deposition on crops in the United Kingdom based on predictions of ozone concentrations made using the Ozone Source Receptor Model (OSRM) has been demonstrated. Computer programs have been prepared that implement the algorithms for the calculation of stomatal flux, developed by Emberson *et al.* (2000) and those included in the UNECE mapping manual.

Model predictions of stomatal flux based on ozone concentrations calculated using the OSRM were compared with stomatal flux estimates based on measured ozone concentrations. The comparison suggested that the OSRM can provide an effective means of predicting accumulated flux over threshold to vegetation types.

The model predicted that the growth of beech trees in 2001 was affected by ozone deposition, with greater than 5% loss in biomass throughout the country. Ozone deposition to beech trees in much of the southern part of the UK was limited by the availability of soil moisture for plant uptake during the latter part of the growing season.

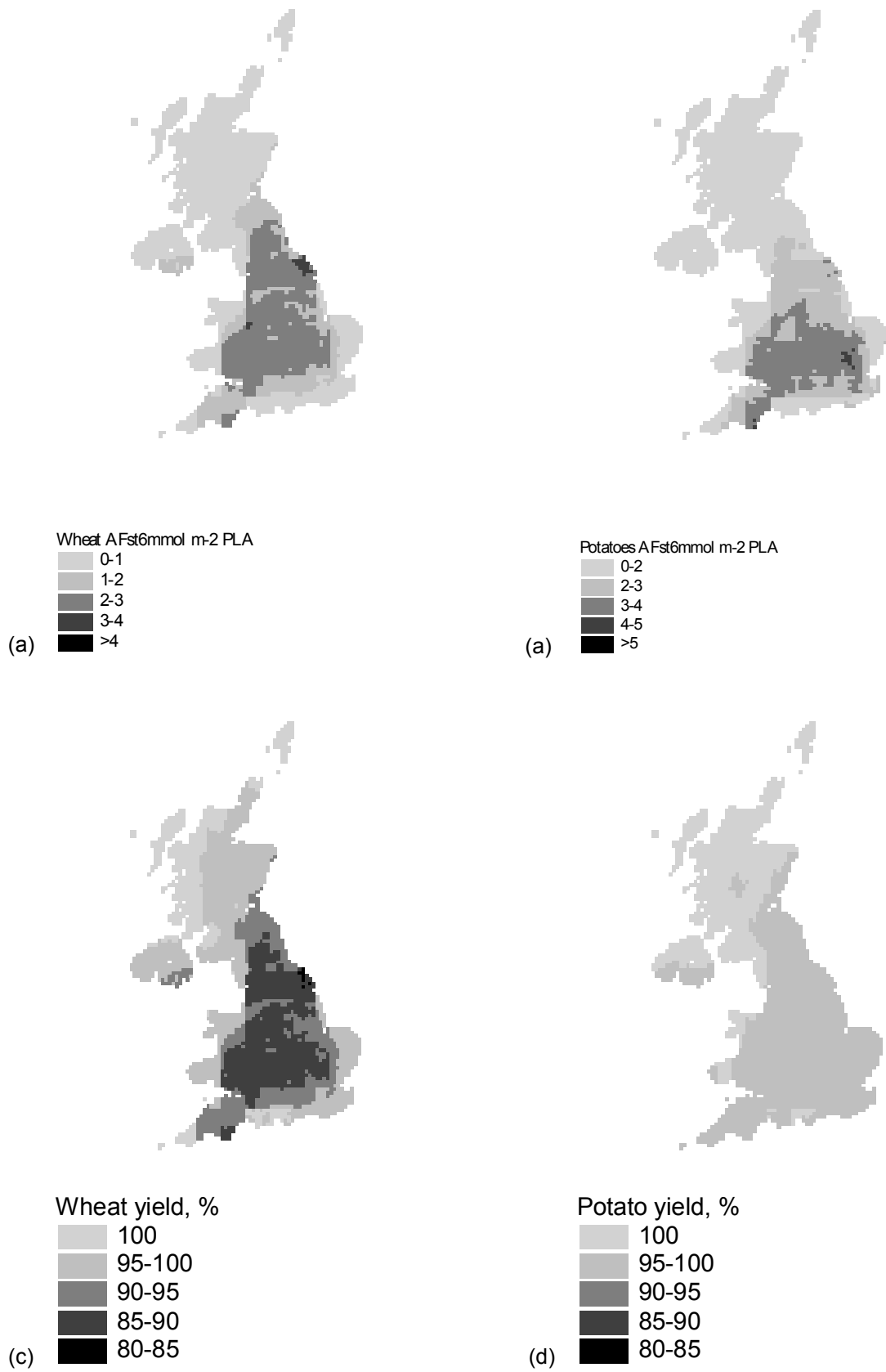


Figure 9.5 Predicted Accumulated Stomatal Fluxes over Threshold (Upper Panels) and Yields (Lower Panels) for Winter Wheat and Potatoes for 2001.

The model predicted that the growth of winter wheat throughout much of England and Wales in 2001 was affected by ozone deposition. Ozone deposition was associated with more than 5% loss in yield in central England. The loss in yield was smaller in cooler areas in Scotland and in coastal areas of England with lower maximum temperatures. The model also predicted that the growth of potatoes was not substantially affected by ozone deposition. Ozone deposition was associated with less than 5% loss in yield throughout the country.

10 Other Project Activities

10.1 PROJECT MEETINGS

The following progress meetings were held in London, with attendance from Defra and the project consortium members:

- Kick-off meeting on 22nd January 2003
- 6-monthly progress meeting on 17th July 2003
- 6-monthly progress meeting on 20th January 2004
- 6-monthly progress meeting on 16th September 2004
- Progress meeting on 11th August 2005

A series of presentations were given on (a) the key policy issues, (b) an overview of the project and (c) work undertaken on the project objectives by members of the project consortium.

Other project meetings of the project partners have been held during the current reporting period on specific project objectives:

➤ **Objective 1: Model Development:**

- An initial meeting was held at Culham in December 2002 to define in detail the model developments needed for the Ozone Source-receptor Model. Further meetings were held during March and April 2003 to review progress;
- A meeting was held in July with Dick Derwent to discuss (a) the developments to the OSRM which form part of **Model Development (Objective 1)**, (b) the chemical solver used in the OSRM and (c) the approach to be used for the **Ozone Flux Modelling (Objective 5)**.

➤ **Objective 3: Scenario Analysis and Policy Support**

- An **Ozone Science-Policy Meeting** was held in London in March 2004 with attendance from Defra, the Devolved Administrations and the project consortium members. A series of presentations were given on recent issues and the policy relevance of ozone and nitrogen dioxide on (a) the urban, (b) the national and (c) regional and global scales;
- A second **Ozone Science-Policy Meeting** was held in London in June 2004 with attendance from Defra and members of the project consortium. A series of presentations were given on recent issues and the policy relevance of ozone and nitrogen dioxide on (a) the urban, (b) the national and (c) regional and global scales;
- The project manager attended a meeting at Defra in June 2004 related to **Preliminary Scenario Modelling of Non-transport Measures for the Review of the Air Quality Strategy**. At the meeting, the non-transport measures were reviewed and the programme of ozone model runs was defined;
- The project manager attended meeting at Defra in December 2004 to discuss **Ozone Modelling for the Review of the Air Quality Strategy**. At the meeting, the proposed measures were reviewed and the programme of ozone model runs was defined;
- A meeting on the OSRM Modelling for the PVR RIA and for the Review of the Air Quality Strategy was held at Defra in May 2005. A follow-up meeting on the OSRM Modelling for the PVR RIA and for the Review of the Air Quality Strategy was held in June 2005.

➤ **Objective 4: Chemical Mechanism Development:**

- A meeting on **Photolysis Rates and Photochemical Parameters (Objective 4)** was held at Culham in February 2003;
- An inaugural meeting of developers and users of the MCM took place at the University of Leeds, 2-3 December 2004. Participants from University of Leeds, Imperial College London,

University of York, University of Aveiro (Portugal) and the Rutherford Appleton Laboratory attended. The full programme and copies of the majority of the presentations are available on the MCM website.

➤ **Objective 5: Ozone Flux Modelling**

- A workshop on **Ozone Flux Modelling (Objective 5)** was held at York in May 2003. The workshop was attended by Defra and DA personnel, as well as contractors working on the Department and DAs' ozone research programme. The agenda comprised presentations on the different contracts followed by discussion on the approach which should be adopted to calculate exposure using ozone fluxes and their response to emission controls. Further meetings of the group were held in York in November 2003 and April 2004;
- A meeting was held at the Met Office in September 2003 to discuss provision of the meteorological and other parameters needed for the **Ozone Flux Modelling (Objective 5)**.

➤ **Related Meetings**

- A presentation on the Modelling of Tropospheric Ozone was given at the **Department's Air Quality Research Seminar**, which was held in London in January 2004, with attendance from Defra and the Devolved Administrations.
- A meeting on Ozone Modelling was held in London in January 2005 with attendance from Defra, project consortium members and other Defra contractors involved in the Department's Ozone Research programme. A series of presentation were given by Defra and its contractors which summarised the key policy issues and provided overviews of the different contracts, their current status and future work programmes. This meeting provided a useful forum to identify synergies and interactions. The Department intends to convene further meetings in the future.

10.2 PROJECT OUTPUTS

In addition to progress and annual reports, the following reports have also been produced:

- T. Bush and A. Kent (August 2003) **Preliminary Assessment of Ozone Levels in the UK**. Report prepared for the Department for Environment, Food and Rural Affairs and the Devolved Administrations (AEA Technology Report AEAT/ENV/R/1528).
- G. D. Hayman (April 2004) **Observed and Modelled Trends in Ground-level Ozone**.
- G. D. Hayman, C. Thomson and R. G. Derwent (May 2004) **Summary and Interpretation of Recent Ozone Modelling Runs**.
- G. D. Hayman and J. Abbott (June 2004) **OSRM Modelling of Ozone in London**.
- G. D. Hayman, J. Abbott and C. Thomson (July 2004) **OSRM Modelling of Ozone for the Review of the Air Quality Strategy**.
- J. A. Abbott (2004) **Development of an Ozone Surface Flux Model**.
- G Hayman, J Abbott, G Dollard and T Davies (July 2005) **Modelling of Tropospheric Ozone: Feasibility Assessment – Integration of Ozone Flux Calculations into the OSRM**. A report prepared for the Department for Environment, Food and Rural Affairs and the Devolved Administrations (AEA Technology Report AEAT/ENV/R/1987).
- J. Targa and T. Bush (June 2005) **Ozone Mapping Techniques for the 3rd Daughter Directive; OSRM vs. Empirical modelling Comparison**. Report prepared for the Department for the Environment, Food and Rural Affairs and the Devolved Administrations (AEA Technology Report AEAT/ENV/R/2006).
- G. Hayman (September 2005) **Impact of Model Developments and Input Data Changes on OSRM Output**.
- T. Bush, J. Targa and J. Stedman (October 2005) **UK Air Quality Modelling for Annual Reporting 2004 on Ambient Air Quality Assessment under Council Directives 96/62/EC and 2002/3/EC relating to Ozone in Ambient Air**. Report prepared for the Department for

Environment, Food and Rural Affairs and the Devolved Administrations (AEA Technology Report AEAT/ENV/R/2053).

- G Hayman, C Thomson, J Abbott and T Bush (November 2005) **Ozone Modelling for the Review of the Air Quality Strategy**. A report prepared for the Department for Environment, Food and Rural Affairs and the Devolved Administrations (AEA Technology Report AEAT/ENV/R/2092).

10.3 PROJECT WEBSITE

A simple, password-protected project website has been set-up to be an archive of project outputs (reports, datasets, etc) and to facilitate the dissemination of these outputs to stakeholders. The address is www.aeat.co.uk/com/tropozone and the home page is shown in Figure 10.1.

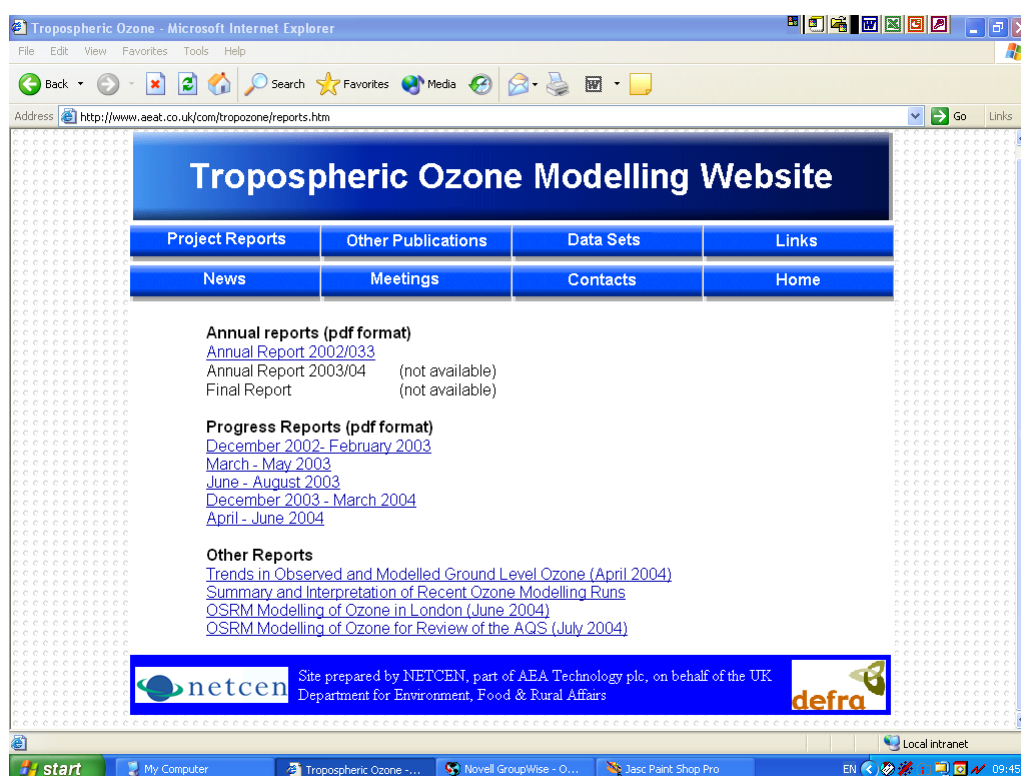


Figure 10.1 Home Page of the Project Website.

10.4 PUBLICATIONS

10.4.1 Journal Publications

The following papers have been produced by the project consortium for publication in the scientific literature:

- C. Bloss, V. Wagner, A. Bonzanini, M.E. Jenkin, K. Wirtz, M. Martin-Reviejo and M.J. Pilling (2005) **Evaluation of Detailed Aromatic Mechanisms (MCM v3 and MCM v3.1) against Environmental Chamber Data**. Atmospheric Chemistry and Physics, **5**, 623-639.
- C. Bloss, V. Wagner, M.E. Jenkin, R. Volkamer, W.J. Bloss, J.D. Lee, D.E. Heard, K. Wirtz, M. Martin-Reviejo, G. Rea, J.C. Wenger and M.J. Pilling (2005) **Development of a Detailed Chemical Mechanism (MCM v3.1) for the Atmospheric Oxidation of Aromatic Hydrocarbons**. Atmospheric Chemistry and Physics, **5**, 641-644.
- R. G. Derwent, P.G. Simmonds and A.J. Kent (2002) **Key Pollutants – Ground-level Ozone. Part 2 2002-2052**. In: The Clean Air Revolution: 1952-2052. pp 42-48. National Society for Clean Air, Brighton.

- R. G. Derwent, M.E. Jenkin, S.M. Saunders, M.J. Pilling, P.G. Simmonds, N.R. Passant, G.J. Dollard and A.J. Kent (2003) **Photochemical Ozone Formation in North West Europe and its Control**. *Atmospheric Environment*, **37**, 1983-1991, (2003).
- R. G. Derwent, M.E. Jenkin, S.M. Saunders, M.J. Pilling and N.R. Passant (2005) **Multi-day Ozone Formation for Alkenes and Carbonyls Investigated with a Master Chemical Mechanism under European Conditions**. *Atmospheric Environment*, **39**, 625-625.
- M.E. Jenkin, S.M. Saunders, V. Wagner and M.J. Pilling (2003) **Protocol for the Development of the Master Chemical Mechanism, MCM v3 (Part B): Tropospheric Degradation of Aromatic Volatile Organic Compounds**. *Atmospheric Chemistry and Physics*, **3**, 181-193.
- M. E. Jenkin (2004) **Analysis of the Sources and Partitioning of Oxidant in the UK. Part 1: The NO_x-dependence of Annual Mean Concentrations of Nitrogen Dioxide and Ozone**. *Atmospheric Environment*, **38**, 5117-5129.
- M. E. Jenkin (2004) **Analysis of the Sources and Partitioning of Oxidant in the UK. Part 2: Contributions of Nitrogen Dioxide Emissions and Background Ozone at Kerbside Locations in London**. *Atmospheric Environment*, **38**, 5131-5138.
- P.G. Pinho, C.A. Pio and M.E. Jenkin (2005) **Evaluation of Isoprene Degradation in the Detailed Tropospheric Chemical Mechanism, MCM v3, using Environmental Chamber Data**. *Atmospheric Environment*, **39**, 1303-1322.
- P.G. Pinho, C.A. Pio and M.E. Jenkin (2004) **Evaluation of Alkene Degradation in the Detailed Tropospheric Chemical Mechanism, MCM v3, using Environmental Chamber Data**. Submitted to *Journal of Atmospheric Chemistry*.
- S.M. Saunders, M.E. Jenkin, R.G. Derwent and M.J. Pilling (2003) **Protocol for the Development of the Master Chemical Mechanism, MCM v3 (Part A): Tropospheric Degradation of Non-aromatic Volatile Organic Compounds**. *Atmospheric Chemistry and Physics*, **3**, 161-180.
- S.M. Saunders, S. Pascoe, A.P. Johnson, M.J. Pilling and M.E. Jenkin (2003) **Development and Preliminary Test Results of an Expert System for the Automatic Generation of Tropospheric VOC Degradation Mechanisms**. *Atmospheric Environment*, **37**, 1723-1735.
- S. R. Utembe, M.E. Jenkin, R.G. Derwent, A.C. Lewis, J.R. Hopkins and J.F. Hamilton (2005) **Modelling the Ambient Distribution of Organic Compounds during the August 2003 Ozone Episode in the Southern UK**. *Faraday Discussions*, **130**, 311-326.
- V. Wagner, M.E. Jenkin, S.M. Saunders, J. Stanton, K. Wirtz and M.J. Pilling (2003) **Modelling of the Photooxidation of Toluene: Conceptual ideas for Validating Detailed Mechanisms**. *Atmospheric Chemistry and Physics*, **3**, 89-106.
- A. Volz-Thomas *et al.* (2003) **Tropospheric Ozone and its Control**. Chapter 3. pp73-122. *Towards Cleaner Air for Europe. Science, Tools and Applications. Part 1*. Margraf Publishers, Leiden, The Netherlands, (2003).
- L. Whitehouse, A. R. Rickard, S. Pascoe, C. Bloss, S. M. Saunders, M. E. Jenkin and M. J. Pilling (2005) **The Master Chemical Mechanism –Version 3.1**, *Faraday Discussion 130: Atmospheric Chemistry*, Leeds, April 2005.
- L. Whitehouse, A. S. Tomlin and M. J. Pilling (2004) **Systematic Reduction of Complex Tropospheric Chemical Mechanisms, Part 1: Sensitivity and Time-Scale Analysis**. *Atmospheric Chemistry and Physics*, **4**, 2025-2056.
- L. Whitehouse, A. S. Tomlin and M. J. Pilling (2004) **Systematic Reduction of Complex Tropospheric Chemical Mechanisms, Part 2: Lumping using a Time-Scale Based Approach**, *Atmospheric Chemistry and Physics*, **4**, 2057-2081.

10.4.2 Other Publications

Members of the project consortium contributed to the following reports:

- AQEG (2004) **Nitrogen Dioxide in the United Kingdom**. Report of the UK Air Quality Expert Group. Prepared at the request of the Department for Environment Food and Rural Affairs, London, PB9025.

- AQEG (2005) **Particulate Matter in the United Kingdom**. Report of the UK Air Quality Expert Group. Prepared at the request of the Department for Environment Food and Rural Affairs, London, PB10580 ISBN 0-85521-143-1.

10.5 CONFERENCES/SEMINARS ATTENDED

Presentations describing work carried out under this contract were given at the following conferences and seminars:

- R G Derwent: **The Great London Smog – Fifty Years On**. London School of Hygiene and Tropical Medicine, December 2002.
- M E Jenkin: UK EUROTRAC workshop, University of East Anglia, January 2003.
- M E Jenkin: NCAS modelling workshop, Imperial College London, March 2003.
- M E Jenkin: European Air Pollution Workshop, Wengen, Switzerland, May 2003.
- R G Derwent: **External Influences on Europe's Air Quality Targets**, European Academies' Scientific Advisory Council, Athens, October 2003.
- M E Jenkin: NCAS Aerosol Workshop, Abingdon November 2003.
- M E Jenkin: Defra-NERC Ozone Workshop, London February 2004.
- G D Hayman: A presentation on the Modelling of Tropospheric Ozone project and related activities was given at the **Joint Defra-NERC TORCH Meeting**, which was held in London in February 2004.
- M J Pilling: **Developing and Using Mechanisms for the Oxidation of Organic Compounds in the Atmosphere**, ACS, *Molecular Modeling and Reaction Chemistry*, Anaheim, March, 2004
- M J Pilling and M.E. Jenkin: **Chemical Mechanisms and Timescales for the Oxidation of Biogenic Compounds**, *Gordon Conference*, Barga, Italy, May 2004
- S M Saunders, M.E. Jenkin, C. Bloss, V. Wagner, A.R. Rickard, L. Whitehouse, S. Pascoe and M.J Pilling: **The Master Chemical Mechanism – Latest Improvements (MCMv3.1)**, *Poster Presentation, 18th International Symposium on Gas Kinetics*, Bristol, August 2004.
- M E Jenkin: European Air Pollution Workshop Venice, Italy October 2004.
- M J Pilling: **Aromatic Hydrocarbon Oxidation: The Contribution of Chamber Photo-oxidation Studies**, *NATO Meeting*, Zakopane, Poland, October 2004
- M E Jenkin: Centre for Atmospheric Science, University of Cambridge, November 2004.
- M J Pilling: **A Master Chemical Mechanism (MCM): Approaches to its Use in CTMs**, *German Chemical Societies*, Frankfurt, November 2004
- M J Pilling: **Atmospheric Chemistry and Chemical Kinetics**, University of Sheffield, November 2004
- C Bloss, A R Rickard, L Whitehouse, S Pascoe, M E Jenkin, S M Saunders, V Wagner, R G Derwent and M J Pilling: **Gas-phase MCM Development Activities at Leeds**, *MCM Developer and User Workshop*, Leeds, December 2004.
- S Pascoe, A R Rickard, L Whitehouse, C Bloss, S M Saunders, M E Jenkin and M J Pilling: **MCM Website Developments**. MCM Developers and Users Meeting, University of Leeds, December 2004.
- M E Jenkin: **History of the MCM and Mechanism Development Protocols**. MCM Developers and Users Meeting, University of Leeds, December 2004.
- M E Jenkin: **CRI Mechanism Development**. MCM Developers and Users Meeting, University of Leeds, December 2004.
- S R Utembe: **Trajectory Modelling in TORCH**. MCM Developers and Users Meeting, University of Leeds, December 2004.

- M E Jenkin: **Chemistry, Origin and Trends in Photochemical Pollution Episodes in the UK**. Invited seminar, University of Cambridge, December 2004.
- M E Jenkin: **The Master Chemical Mechanism: a User and Supplier of Physico-chemical Data**. ACCENT WP5 Workshop on access to Laboratory Data, University of Cambridge, December 2004.
- M E Jenkin: UKCA workshop, University of Leeds, February 2005.
- M E Jenkin: Faraday Discussion 130, University of Leeds, April 2005.
- M E Jenkin: DIAC Research Meeting, University of Leeds, April 2005.
- M J Pilling: **Photochemistry and Kinetics for Atmospheric Applications**, DIAC Research Meeting, University of Leeds, April 2005.
- M J Pilling: **Chemical Kinetics in Atmospheric Chemistry**, Easter Conference, Cardiff University, April 2005.
- M.J. Pilling: **Photochemistry and Kinetics for Atmospheric Applications**, University of Edinburgh, May 2005
- M E Jenkin: Meteorological Office, Exeter, June 2005.
- M J Pilling: **Interpretation of Field Experiments using a Detailed Chemical Mechanism**, Aeronomy Lab, NOAA, August, 2005.
- M J Pilling: **Some 'Elementary' Reactions in the Troposphere**, Reading Gas Kinetics Group Meeting, September 2005.
- M J Pilling: Laboratory and Chamber Measurements of Tropospheric Chemistry, Gordon Research Conference, Montana, September 2005.
- M E Jenkin: European Air Pollution Workshop, Munich, Germany, October 2005.
- M E Jenkin: ACCENT Workshop on Oxidised Nitrogen, Rutland Water, November 2005.
- M E Jenkin: Paul Scherrer Institute, Villigen, Switzerland, December 2005*.
- M E Jenkin: INTROP/ACCENT workshop on organic oxidation, Alpe Huez, France, January 2006*
- M E Jenkin: Department of Physical Chemistry, University of Cambridge, February 2006*.
- M E Jenkin: DIAC/UKAAN Workshop on Regional Aerosol, Exeter, March 2006*.

11 References

- AQEG (2004) **Nitrogen Dioxide in the United Kingdom**. First report of the Air Quality Expert Group. Prepared at the request of the Department of the Environment Food and Rural Affairs, London.
- AQS (2005) **Review of the Air Quality Strategy for England, Scotland, Wales and Northern Ireland**. Consultation paper to be published by Department of the Environment, Transport and the Regions, The Scottish Executive, The National Assembly for Wales and The Department of the Environment in Northern Ireland in early 2006.
- CERC (2003) **Modelling Air Quality for London using ADMS-Urban**. Final report on the contract EPG 1/3/176 for Defra and the Devolved Administrations.
- DETR (2000) **The Air Quality Strategy for England, Scotland, Wales and Northern Ireland**. Department of the Environment, Transport and the Regions, The Scottish Executive, The National Assembly for Wales and The Department of the Environment in Northern Ireland, January 2000.
- EC (1996) Council Directive 96/62 EC, of 27 September 1996 on **Ambient Air Quality Assessment and Management (The Framework Directive)**. From the Official Journal of the European Communities, 21.11.1996, En Series, L296/55.
- EC (2002a) **The Costs and Benefits, The Reduction of Volatile Organic Compounds from Paints**, prepared by Directorate-General Environment, Air and Noise Unit, 2 May 2002.
- EC (2002b) Council Directive 2002/3/EC, of 12 February 2002 relating to **Ozone in Ambient Air (The 3rd Daughter Directive)**. From the Official Journal of the European Communities, 9.3.2002. En series, L67/14.
- EMEP (2003) **Transboundary Acidification, Eutrophication and Ground Level Ozone in Europe: PART III - Source-receptor Relationships**. By L. Tarrason, J. E. Jonson, H. Fagerli, A. Benedictow, P. Wind, D. Simpson and H. Klein, EMEP Report 1/2003, August 2003 (ISSN 0806-4520).
- IGCB (2005) Report of the Intergovernmental Working Group on Costs and Benefits prepared as a Supporting Document for the **Review of the Air Quality Strategy for England, Scotland, Wales and Northern Ireland**, Department of the Environment, Transport and the Regions, The Scottish Executive, The National Assembly for Wales and The Department of the Environment in Northern Ireland.
- NEGTA (2001) **Transboundary Air Pollution: Acidification, Eutrophication and Ground-level ozone in the UK** (ISBN 1 870393 61 9). Prepared by the National Expert Group on Transboundary Air Pollution (NEGTA) on behalf of the Department for Environment, Food and Rural Affairs, the Scottish Executive, Welsh Assembly Government and the Department of the Environment in Northern Ireland.
- PORG (1997) **Ozone in the United Kingdom**. Fourth Report of the UK Photochemical Oxidants Review Group, prepared for the Department of the Environment, Transport and the Regions, London. Published by the Institute of Terrestrial Ecology (now Centre for Ecology and Hydrology), Bush Estate, Penicuik, Midlothian, EH26 0QB, UK. ISBN: 0-870393-30-9 (available at <http://www.edinburgh.ceh.ac.uk/pollution/docs/PORGiv.htm>).
- UN ECE (2003) see <http://www.oekodata.com/pub/mapping/manual/mapman3.pdf>.
- Abbott, J.A. (2004) **Development of an Ozone Surface Flux Model**. Report in preparation.
- Abbott, J.A., Vincent, K. and Stedman, J. R. (2005) **Annual Audits of the Contribution to Pollutant Concentrations from Processes Regulated by the Environment Agency: Method Development**. Report prepared for the Environment Agency (of England and Wales) on contract R&D Project No. P4-120/4.

- Andreini B. P., Baroni R., Galimberti E. and Sesana G. (2000) **Aldehydes in the Atmospheric Environment: Evaluation of Human Exposure in the North-west Area of Milan.** *Microchemical Journal*, **67**, 11-19.
- Bakeas E.B., Argyris D. I. and Siskos P. A. (2003) **Carbonyl Compounds in the Urban Area of Athens Greece.** *Chemosphere*, **52**, 805-813.
- Blitz, M. A., Heard, D. E., Pilling, M. J., Arnold, S. R. and Chipperfield, M. P. (2004) **Pressure and Temperature-dependent Quantum Yields for the Photo-dissociation of Acetone between 279 and 327.5 nm.** *Geophys. Res. Letts.*, **31**, L06111, doi:10.1029/2003GL018793.
- Broske, R., Kleffmann, J. and Wiesen, P. (2003) **Heterogeneous Conversion of NO₂ on Secondary Organic Aerosol Surfaces: A Possible Source of Nitrous Acid (HONO) in the Atmosphere?** *Atmos. Chem. Phys.* **3**, 469-474.
- P J H Builtjes (1987) **Photochemical Oxidant and Acid Deposition Model (PHOXA). Calculation and Evaluation of the Photochemical Episode of July 22-26 1980.** TNO Report 87-278. Apeldoorn, The Netherlands.
- Bush, T. and Kent, A. (2003) **Preliminary Assessment of Ozone Levels in the UK.** Report (AEAT/ENV/R/1528 Issue 1) prepared for Department of the Environment, Transport and the Regions, The Scottish Executive, The National Assembly for Wales and The Department of the Environment in Northern Ireland.
- Bush, T., Targa, J. and Stedman, J. R. (2005) **UK Air Quality Modelling for Annual Reporting 2004 on Ambient Air Quality Assessment under Council Directives 96/62/EC and 2002/3/EC relating to Ozone in Ambient Air.** Report (AEAT/ENV/R/2053 Draft) prepared for Department of the Environment, Transport and the Regions, The Scottish Executive, The National Assembly for Wales and The Department of the Environment in Northern Ireland.
- Calvert, J. G., Atkinson, R., Kerr, J. A., Madronich, S., Moortgat, G. K., Wallington, T. J. and Yarwood, G. (2000) **The Mechanisms of Atmospheric Oxidation of Alkenes.** Oxford University Press.
- Calvert, J. G., Atkinson, R., Becker, K. H., Kamens, R. M., Seinfeld, J. H., Wallington, T. J. and Yarwood, G. (2002) **The Mechanisms of Atmospheric Oxidation of Aromatic Hydrocarbons.** Oxford University Press.
- Carslaw D.C. and Beevers S.D. (2004) **Investigating the Potential Importance of Primary NO₂ Emissions in a Street Canyon.** *Atmospheric Environment*, **38**, 3585-3594.
- Carter W.P.L. (1994) **Development of Ozone Reactivity Scales for Volatile Organic Compounds.** *Journal of the Air and Waste Management Association*, **44**, 881-899.
- Carter W. P. L., Luo D., Malkina I. L., Fitz D., (1995) **The University of California, Riverside Environmental Chamber Data Base for Evaluating Oxidant Mechanisms: Indoor Chamber Experiments Through 1993.** EPA/600/SR-96/078, U.S. Environmental Protection Agency, Research Triangle Park, NC.
- Carter W. P. L. (2000) **Documentation of the SAPRC-99 Chemical Mechanism for VOC reactivity Assessment.** Final Report to California Air Resources Board Contract 92-329 and Contract 95-308, Air Pollution Research Center and College of Engineering Center for Environmental Research and Technology University of California Riverside, California.
- Chen, Y. and Zhu, L. (2003) **Wavelength-dependent Photolysis of Glyoxal in the 290-420 nm Region.** *J. Phys. Chem. A.*, **107**, 4643-4651.
- Christensen C. S., Skov H., Nielsen T. and Lohse C. (2000) **Temporal Variation of Carbonyl Compound Concentrations at a semi-rural site in Denmark.** *Atmospheric Environment*, **34**, 287-296.
- Clapp L.J. and Jenkin M.E. (2001) **Analysis of the Relationship between Ambient Levels of O₃, NO₂ and NO as a function of NO_x in the UK.** *Atmospheric Environment*, **35**, 6391-6405.
- Collins W.J., Stevenson D.S., Johnson C.E., Derwent R.G. (1997) **Tropospheric Ozone in a Global-scale Three-dimensional Lagrangian model and its Response to NO_x Emission Controls.** *Journal of Atmospheric Chemistry*, **26**, 223-274.

- Collins W.J., Stevenson D.S., Johnson C.E., Derwent R.G. (2000) **The European Regional Ozone Distribution and its Links with the Global Scale for the Years 1992 and 2015.** *Atmospheric Environment*, **34**, 255-267.
- Coyle M, Smith R, Stedman J, Weston K and Fowler D (2002) **Quantifying the Spatial Distribution of Surface Ozone Concentration in the UK.** *Atmospheric Environment*, **36**, 1013-1024.
- Coyle, M. (2003) Personal communication with Mhairi Coyle, Centre for Ecology and Hydrology, Penicuik, Scotland.
- Cronin, T. and Zhu, L. (1998) **Dye Laser Photolysis of *n*-Pentanal from 280 to 330 nm.** *J. Phys. Chem. A.*, **102**, 10274-10279.
- Damian, V., Sandu, A., Damian, M., Potra, F., and Carmichael, G.R. (2002) **The Kinetic PreProcessor KPP - A Software Environment for Solving Chemical Kinetics.** *Computers and Chemical Engineering*, **26**, 1567-1579.
- Derwent R.G., M.E. Jenkin, S.M. Saunders and M.J. Pilling. (1998) **Photochemical Ozone Creation Potentials for Organic Compounds in North West Europe Calculated with a Master Chemical Mechanism.** *Atmospheric Environment*, **32**, 2419-2441.
- Derwent R. G., Jenkin M. E., Saunders S. M., Pilling M. J. and Passant N. R. (2004) **Multi-day Ozone Formation of Alkenes and Carbonyls investigated with a Master Chemical Mechanism under European conditions.** *Atmospheric Environment*, **39**, 627-635.
- Derwent, R. G. (2005a) Provision of 2002 Air Quality Data from the London, Kent and East Hertfordshire Air Quality Networks.
- Derwent, R. G. (2005b) Presentation on **Current and Modelled Future Ozone Trends at Mace Head.**
- Dore, C. J., Hayman, G., Scholefield, P., Hewitt, N., Winiwarter, W. and Kressler, F. (2003) Mapping of Biogenic VOC Emissions in England and Wales. Final Project on the Environment Agency R&D Project E1-122.
- Dore, C. J., Watterson, J.D., Goodwin, J.W.L., Murrells, T.P. Passant, N.R., Hobson, M.M., Baggott, S.L. Thistlewaite, G., Coleman, P.J., King, K.R., Adams, M. and Cumine, P. (2004) **UK Emissions of Air Pollutants 1970-2002.** AEAT/ENV/R/1933. ISBN 0954713648.
- Emberson, L. D., D. Simpson, J.-P. Tuovinen, M. R. Ashmore and H. M. Cambridge (2000) **Towards a Model of Ozone Deposition and Stomatal Uptake over Europe.** Research Note No. 42. EMEP/MSC-W 2000.
- Gierczak, T., Burkholder, J.B., Bauerle, S. and Ravishankara, A.R. (1998) **Photochemistry of Acetone under Atmospheric Conditions.** *Chem. Phys.* **231**, 229-244.
- Goodwin J.W.L., Salway A.G., Murrells T.P., Dore C.J., Passant N.R., King K.R., Coleman P.J., Hobson M.M., Pye S.T. and Watterson J.D. (2001) **The UK Emissions of Air Pollutants 1970-1999.** AEA Technology Report AEAT/ENV/R/0798, ISBN 1-85580-031-4.
- Graedler, F. and Barnes, I. (1997) **Photolysis of *Z*-*E*-3-Hexenedione.** EUPHORE Annual Report 1997, 148.
- Grosjean D., Grosjean E. and Moreira L. F. R. (2002) **Speciated Ambient Carbonyls in Rio de Janeiro, Brazil.** *Environmental Science and Technology*, **36**, 1389-1395.
- Guenther, A., Zimmerman, P. and Wildermuth, M. (1994) **Natural Volatile Organic Compound Emission Rate Estimates for US Woodland Landscapes.** *Atmospheric Environment*, **28**, 1197-1210.
- Hayman, G. D., Jenkin, M. E., Pilling, M. J. and Derwent, R. G. (2002) **Modelling of Tropospheric Ozone Formation.** A Final Project Report produced for the Department for Environment, Food and Rural Affairs and Devolved Administrations on Contract EPG 1/3/143.
- Hayman, G. D., Bush, A., Kent, A., Derwent, R. G., Jenkin, M. E., Pilling, M. J. and Abbott, J. (2004a) **Modelling of Tropospheric Ozone.** First Annual Report produced for the Department for Environment, Food and Rural Affairs and the Devolved Administrations on Contract EPG 1/3/200.

- Hayman, G. D., Thomson, C. and Derwent, R. G. (2004b) **Summary and Interpretation of Recent Ozone Modelling Runs**. Note to Defra, May 2004.
- Hayman, G. D., Abbott, J., Thomson, C., Bush, T., Kent, A., Derwent, R. G., Jenkin, M. E., Pilling, M. J., Rickard, A., and Whitehead, L. (2005a) **Modelling of Tropospheric Ozone**. Second Annual Report produced for the Department for Environment, Food and Rural Affairs and the Devolved Administrations on Contract EPG 1/3/200.
- Hayman, G. D., Thomson, C., Abbott, J. A. and Bush T. (2005b) **Ozone Modelling for the Review of the Air Quality Strategy**. Report (AEAT/ENV/R/2092 Issue 1) prepared for Department of the Environment, Transport and the Regions, The Scottish Executive, The National Assembly for Wales and The Department of the Environment in Northern Ireland.
- Hobson, M.M. (2005) **Emission Projections**. AEA Technology, National Environmental Technology Centre.
- Horowitz, A., Meller, R. and Moortgat, G.K. (2001) **The UV-VIS Absorption Cross-sections of the α -Dicarbonyl Compounds: Pyruvic Acid, Biacetyl and Glyoxal**. *J. Photochem. Photobiol. A: Chem.* **146**, 19-27.
- Jenkin, M. E., Hayman, G. D., Derwent, R. G., Saunders, S. M., and Pilling, M. J. (1997a) **Tropospheric Chemistry Modelling: Improvements to Current Models and Application to Policy Issues**. *AEA Technology Technical Report, AEA/RAMP/20150/R001 Issue 1*.
- Jenkin M.E., Saunders S.M and Pilling M.J. (1997) **The Tropospheric Degradation of Volatile Organic Compounds: A Protocol for Mechanism Development**. *Atmospheric Environment*, **31**, 81-104.
- Jenkin M.E., Murrells T.P. and Passant N.R. (2000) **The Temporal Dependence of Ozone Precursor Emissions: Estimation and Application**. AEA Technology report AEAT/R/ENV/0355 Issue 1. Prepared for Department of the Environment, Transport and the Regions.
- Jenkin, M. E., S. M. Saunders, R. G. Derwent and M. J. Pilling (2002) **Development of a Reduced Speciated VOC Degradation Mechanism for Use in Ozone Models**, *Atmospheric Environment*, **36**, 4725-4734.
- Jenkin M.E. (2004) **Analysis of Sources and Partitioning of Oxidant in the UK. Part 1: The NO_x -Dependence of Annual Mean Concentrations of Nitrogen Dioxide and Ozone**. *Atmospheric Environment*, **38**, 5117-5129.
- Jimenez J.L., McCrae G.J., Nelson D.D., Zahniser M.S. and Kolb C.E. (2000) **Remote Sensing of NO and NO_2 emissions from Heavy-duty Diesel Trucks using Tunable Diode Lasers**. *Environmental Science and Technology*, **34**, 2380-2387.
- Jones, G. and Pye, S. (2004) Personal Communication.
- Klemp D., Kley D., Kramp F., Buers H. J., Pilwat G., Flocke F., Patz H. W. and Volz-Thomas A. (1997). **Long-term Measurements of Light Hydrocarbons (C_2 - C_5) at Schauinsland (Black Forest)**. *Journal of Atmospheric Chemistry*, **28**, 135-171.
- Kley D., Geiss H. and Mohnen V.A. (1994) **Tropospheric Ozone at Elevated Sites and Precursor Emissions in the United States and Europe**. *Atmospheric Environment*, **28**, 149-158.
- Klotz, B., Graedler, F., Sorensen, S., Barnes, I. and Becker, K-H. (2001) **A Kinetic Study of the Atmospheric Photolysis of α -Dicarbonyls**. *Int. J. Chem. Kinet.*, **10**, 9-20.
- Kurtenbach, R., K. H. Becker, J. A. G. Gomes, J. Kleffmann, J. C. Lorzer, M. Spittler, P. Wiesen, R. Ackermann, A. Geyer and U. Platt (2001) **Investigations of Emissions and Heterogeneous Formation of HONO in a Road Traffic Tunnel**. *Atmospheric Environment*, **35**, 3385-3394.
- Latham, S., S. Kollamthodi, P. G. Boulter, P. M. Nelson and A. J. Hickman (2001) **Assessment of Primary NO_2 Emissions, Hydrocarbon Speciation and Particulate Sizing on a Range of Road Vehicles**. Report PR/SE/353/2001, Transport Research Laboratory (TRL), Crowthorne, Berkshire, UK.
- Leighton, P.A. (1961) **Photochemistry of Air Pollution**. Academic Press, New York.

- Madronich, S. and Flocke, S. (1998) **The Role of Solar Radiation in Atmospheric Chemistry**, in *Handbook of Environmental Chemistry* (P. Boule, ed.), Springer-Verlag, Heidelberg, 1998, pp. 1-26.
- Metcalfe, S.E., Whyatt, J.D., Derwent, R.G. and O'Donoghue (2002) **The Regional Distribution of Ozone Across the British Isles and its Response to Control Strategies**. *Atmospheric Environment*, **36**, 4045-4055.
- Moortgat, G. K. *et al.* (2000): Final report on the EU fourth framework project "**Evaluation of Radical Sources in Atmospheric Chemistry through Chamber and Laboratory Studies, RADICAL**". European Communities Report EUR 20254 EN., MPI Mainz, Germany.
- Murrells, T. P. (2003) Personal communication with Tim Murrells, netcen.
- Olariu, R.I., Klotz, B., Barnes, I., Becker, K.H. and Mocanu, R. (2002) **FT-IR Study of the Ring-retaining Products from the Reaction of OH Radicals with phenol, o-, m-, and p-cresol**. *Atmospheric Environment* **36**(22), 3685-3697.
- Pankrath, J. (1989) **Photochemical Oxidant Model Application within the Framework of Control Strategy Development in the Dutch/German programme PHOXA In Atmospheric Ozone Research and its Policy Implications**; Elsevier Science Publishers BV: Amsterdam, The Netherlands, p 633.
- Passant N.R. (2002) Personal communication with Neil Passant, netcen.
- Plum, C. N., Sanhueza, E., Atkinson, R., Carter, W. P. L. and Pitts, Jr., J. N. (1983) **OH Radical Rate Constants and Photolysis Rates of α -Dicarbonyls**. *Environmental Science and Technology* **17**, 479-484.
- Pinho P.G., Pio C.A. and Jenkin M.E. (2004) **Evaluation of Isoprene Degradation in the Detailed Tropospheric Chemical Mechanism, MCM v3, using Environmental Chamber Data**. *Atmospheric Environment*, **39**, 1303-1322.
- Possanzini M., Di Palo V., Brancaleoni E., Frattoni M. and Ciccioli P. (2000) **A Train of Carbon and DNPH-coated Cartridges for the Determination of Carbonyls from C₁ to C₁₂ in Air and Emission Samples**. *Atmospheric Environment*, **34**, 5311-5318.
- Saunders, S. M., Jenkin, M. E., Derwent, R. G. and Pilling, M. J. (2003) **Protocol for the Development of the Master Chemical Mechanism, MCM v3 (Part A): Tropospheric Degradation of Non-aromatic Volatile Organic Compounds**. *Atmospheric Chemistry and Physics*, **3**, 161-180.
- Scheel H.E., Areskoug H., Geiss H., Gomiscek B., Granby K., Haszrpa L., Klasnic L., Kley D., Laurila T., Lindskog A., Roemer M., Schmitt R., Simmonds P., Solberg S. and Toupance G. (1997) **On the Spatial and Seasonal Variation of Lower-troposphere Ozone over Europe**. *Journal of Atmospheric Chemistry*, **28**, 11-28.
- Simpson, D., Guenther, A., Hewitt, C.N., Steinbrecher, R. (1995) **Biogenic Emissions in Europe 1. Estimates and Uncertainties**. *J. Geophys. Res.*, **100**, 22875-22890.
- Simpson, D., H. Fagerli, H. E. Jonson, S. Tsyro, P. Wind and J.-P. Tuovinen (2003) **Transboundary Acidification, Eutrophication and Ground Level Ozone in Europe. Part 1. Unified EMEP Model Description**. EMEP Status report 2003.
- Stevenson, D.S., Collins, W.J., Johnson, C.E., Derwent, R.G (1997) **Tropospheric Ozone in a Global-Scale Three-Dimensional Lagrangian Model and its Response to NO_x Emission Control**. *Journal of Atmospheric Chemistry*, **26**, 223-274.
- Stedman J.R., Bush T. and Linehan E.B. (2000) **The 10-year Transport Plan. Site Specific Analyses of Ambient NO₂ and PM₁₀ Concentrations**. AEA Technology, National Environmental Technology Centre Report AEAT/R/ENV/0166, available at: www.aeat.co.uk/netcen/airqual/reports/home.html.
- Stedman J.R. (2003) Personal communication with John Stedman, netcen.
- Tadic, J., Juranic, I. and Moortgat, G.K. (2001a) **Pressure Dependence of the Photo-oxidation of Selected Carbonyl Compounds in Air: *n*-Butanal and *n*-Pentanal**. *Journal of Photochemistry and Photobiology A: Chemistry*, **143**, 169-179.

- Tadic, J., Juranic, I. and Moortgat, G.K. (2001b) **Photooxidation of *n*-Hexanal in Air**. *Molecules*, **6**, 287–299.
- Tadic, J., Juranic, I. and Moortgat, G.K. (2002) **Photooxidation of *n*-Heptanal in Air: Norrish Type I and II Processes and Quantum Yield Total Pressure Dependency**. *Journal of the Chemical Society, Perkin Transactions 2*, 135–140.
- Targa, J. and Bush T. (2005) **Ozone Mapping Techniques for the 3rd Daughter Directive; OSRM vs. Empirical Modelling Comparison Report**. Report (AEAT/ENV/R/2006 Draft for Comment) prepared for Department of the Environment, Transport and the Regions, The Scottish Executive, The National Assembly for Wales and The Department of the Environment in Northern Ireland.
- Thuener, L. P., Rea, G. and Wenger, J. (2003) **Photolysis of Butenedial and 4-oxo-2-pentenal**. EUPHORE Annual Report 2001.
- Utembe S.R., Jenkin M.E., Derwent R.G., Lewis A.C., Hopkins J.R. and Hamilton J.F. (2004). **Modelling the Ambient Distribution of Organic Compounds during the August 2003 Ozone Episode in the Southern UK**. *Faraday Discussions*, **130**, 311-326.
- Verwer, J.G. and Simpson, D. (1995) **Explicit Methods for Stiff ODEs from Atmospheric Chemistry**. *Applied Numerical Mathematics*, **18**:413–430, 1995.
- Volkamer, R., Platt, U. and Wirtz, K. (2001) **Primary and secondary glyoxal formation from aromatics: Experimental evidence for the bicycloalkyl-radical pathway from benzene, toluene, and *p*-xylene**. *Journal of Physical Chemistry A* **105**(33), 7865-7874.
- Volkamer, R., Klotz, B., Barnes, I., Imamura, T., Wirtz, K., Washida, N., Becker, K.H. and Platt, U. (2002) **OH-initiated Oxidation of Benzene - Part I. Phenol Formation under Atmospheric Conditions**. *Phys. Chem. Chem. Phys.* **4**(9), 1598-1610.
- Volkamer, R., Spietz, P., Burrows, J. and Platt, U. (2005) **High-resolution Absorption Cross-section of Glyoxal in the UV-vis and IR Spectral Ranges**. *Journal of Photochemistry and Photobiology A: Chemistry*, **172**, 35-46.
- Watkiss, P., Jones, G., Pye, S., Passant, N., Hayman, G., Hunt, A., Searle, A. and Holland, M. (2005) **Regulatory Impact Assessment: Stage II Petrol Vapour Recovery**. Report (AEAT/ED48740 Issue 5) produced for the Department for Environment, Food and Rural Affairs on Task WP2-SPU13.
- Zhu, L., Cronin, T. and Narang, A. (1999) **Wavelength-Dependent Photolysis of *i*-Pentanal and *t*-Pentanal from 280 to 330 nm**. *Journal of Physical Chemistry*, **103**, 7248-7253.

12 Acknowledgements

The consortium partners acknowledge the support provided by the Department for Environment, Food and Rural Affairs (Defra) and the Devolved Administrations (the Scottish Executive, the Welsh Assembly Government and the Department of the Environment Northern Ireland) under contract EPG 1/3/200.

We would also like to express our thanks to Professor Derwent and the Met Office for the provision of meteorological and other datasets used as input in the OSRM.

Appendices

CONTENTS

- | | |
|------------|--|
| Appendix 1 | Work Programme from Proposal |
| Appendix 2 | Population or Area-weighted Means of the Selected O ₃ and NO ₂ Metrics |
| Appendix 3 | Description of the UK Photochemical Trajectory Model |
| Appendix 4 | Percentage Contribution to Emissions, Incremental Reactivity and Photochemical Ozone Formation by VOC Source Sector. |

Appendix 1

Programme of Work from Proposal

CONTENTS

Appendix 1 – Proposed Programme of Work

In this section, we provide a detailed description of the programme of work needed to meet the project objectives. There are 4 main objectives in the core programme of work:

- Objective 1 - **Development and Application of Ozone Models**
- Objective 2 - **Detailed Assessment of the Relationship between Ozone, NO and NO₂, and Factors Controlling Them**
- Objective 3 - **Policy Development and Scenario Analysis**
- Objective 4 - **Improvements to Photochemical Reaction Schemes**

A fifth objective **Development of Stomatal Flux Module for Crops and Semi-natural Vegetation** is included. This particular objective has been included as an option by the Department as it depends on progress made in other UK and European research programmes.

A1.1 Objective 1 - Development and Application of Ozone Models

The focus of the proposed project is to model ozone production in the UK on both national and local scales. It is therefore proposed to use the Ozone Source-Receptor Model (OSRM) as the primary model tool to achieve this objective.

The Ozone Source-Receptor Model uses the EMEP region as its model domain. Our previous work using the EUROSTOCHEM model has demonstrated the coupling of the regional and global scales and the need to initialise the model for each day. To address these issues and to allow for changes to atmospheric composition arising from climate change, it is proposed to use the STOCHEM global tropospheric model to generate concentration fields of O₃, CO and NO_y which would be used to initialise the OSRM. These concentration fields would be generated for each day of the year for years representative of the atmospheric composition in the mid 1990's and of the composition calculated for a future atmosphere in 2030.

As described in Section 2, the OSRM and STOCHEM models use a common chemical mechanism to represent ozone production and destruction. This mechanism considers 10 emitted VOCs producing 70 chemical species involved in 154 thermal and photochemical reactions. The VOCs have been selected to capture the structural features and the range of reactivity present in the MCM as well as broadly representing the main features of photochemical ozone formation on the regional scale with a spatial scale of 20 km through to about 200 km. As the CRI is derived from the MCM, has been shown to reproduce the behaviour of the MCM and considers the emissions of many more VOCs directly, it is proposed in principle to make the CRI mechanism the default mechanism in the OSRM. The benefits will be a direct link to the MCM and the ability to determine the contribution of individual or classes of organic compounds. The introduction of the CRI mechanism will however depend on the progress made under Objective 4, its conversion into a FORTRAN code and the assumption that it does not adversely affect the runtime.

In addition to modifications required to enable the integration of the STOCHEM concentration fields into the OSRM, a number of other improvements have been identified. All the suggested modifications are listed in Table A1.1.

The benefits of these model improvements will be

- a more realistic treatment of the boundary layer, thereby improving the ability of the OSRM to simulate the diurnal behaviour of ozone
- the ability of the OSRM to include the impact of (a) the hemispheric circulation on the hemispheric scale and (b) climate change on future atmospheric composition
- the use of a biogenic emission inventory based on emission potentials which will allow the emission rates to respond to changes in meteorology
- use of a chemical mechanism derived from the MCM and able to treat compounds in the UK VOC emission inventory more directly

Table A1.1 Summary of Proposed Modifications to the OSRM.

Modification	Present Treatment	Proposed
the trajectory length	Each trajectory is of 96 hours duration unless it would be outside the EMEP model grid	All trajectories will start from the boundary of the EMEP model grid
initialisation of O ₃ , CO and NO _y	The initial concentration of these species on each trajectory is the same	Allow for daily variation in the boundary concentrations of O ₃ , CO and NO _y
the boundary layer depth	The diurnal variation in the boundary layer depth has an idealised behaviour	Use the meteorological dataset to determine the maximum and minimum height for each day
exchange with the free troposphere	No exchange with the free troposphere	Allow for exchange with the free troposphere
chemical mechanism	Uses the STOCHEM mechanism, involving 70 chemical species involved in 154 thermal and photochemical reactions and 10 emitted VOCs	Replace the STOCHEM chemical mechanism with the CRI mechanism (provided that this does not extend the runtime significantly)
biogenic VOC emission inventory	Uses an inventory produced in 1995. This has a fixed annual emission for each 150 km x 150 km grid square	Incorporate a new inventory of emission potentials provided on an EMEP 50 km x 50 km grid for isoprene, monoterpenes and other VOCs.

The work on chemical mechanism development may allow the formation of secondary organic aerosol formation to be calculated. If the mechanism incorporated into the OSRM has this capability, the mass of secondary organic aerosol formed can be derived.

The work on this objective will be led by **netcen** with advice, assistance and provision of datasets from Dick Derwent. The major part of the model development will occur in the initial part of the project with further smaller developments throughout the life of the project.

Further development of the OSRM to allow its use for Objective 2 are described in the next section.

A1.2 Objective 2 - Detailed Assessment of the Relationship between Ambient Levels of Ozone, Nitrogen Oxide and Nitrogen Dioxide, and factors controlling them

In the recently concluded project, monitoring data from a selection of southern UK sites were used to investigate the relationships between ambient levels of O₃, NO and NO₂ as a function of NO_x, for levels of NO_x ranging from those typical of UK rural sites to those observed at polluted urban kerbside sites. The emphasis of the work was to establish how the level of 'oxidant', OX (equal to the sum of O₃ and NO₂) varied with the level of NO_x, and therefore to gain some insight into the atmospheric sources of OX, particularly at polluted urban locations, as described in Box A1.1.

A1.2.1 Development of a Combined Semi-Empirical and Modelling Approach

It is proposed to extend the above analysis for sites in the SouthEast to consider data from the 81 UK monitoring sites¹⁰ where there are co-located measurements of O₃ and NO_x. The main aim of the work will be to establish regional and local-scale inputs to OX at each of the sites, and to determine how the partitioning of OX between its component forms of O₃ and NO₂ varies as a function of NO_x. This information will be used to derive algebraic expressions which describe the variation of annual mean NO₂ with NO_x at each of the sites, and therefore the NO_x threshold corresponding to the Air Quality Strategy objective and EU limit value of 21 ppb NO₂. The results will be compared with the NO₂/NO_x partitioning calculated using the empirical approach of the National Modelling of NO₂, undertaken by John Stedman at **netcen**.

Although the methodology will primarily consider sites where measurements of O₃ and NO_x are co-located, selected additional sites possessing similar characteristics (*e.g.*, local traffic flows and vehicle

¹⁰ 65 of these are funded directly by DEFRA.

fleet composition), but where O₃ is not measured, will be investigated to see if the NO₂ vs. NO_x dependence may be adequately represented by inference. The methodology also potentially enables predictions that take account of future changes in regional OX (*i.e.*, the background O₃ level), or local OX inputs which might arise, for example, from modifications in vehicle emissions control technologies. The influence of such changes on the calculated NO_x threshold corresponding to the Air Quality Strategy objective and EU limit value for NO₂ will also be investigated.

Box A1.1 - Analysis of Ambient Measurements of NO_x, NO₂ and O₃

Ambient monitoring data from a selection of southern UK sites were analysed to understand the relationships between ambient levels of O₃, NO and NO₂ as a function of NO_x, for levels of NO_x ranging from those typical of UK rural sites to those observed at polluted urban kerbside sites. The analysis showed that total OX appeared to increase linearly with NO_x over the entire range considered (see Figure A1.1). The NO_x-independent contribution could be identified as a *regional* contribution, equal to the regional background O₃ level, whereas the NO_x-dependent contribution was effectively a *local* contribution which

correlated with the level of primary pollution. The analysis was extended to consider each month of the year, using 1998 and 1999 data combined. A similar dependence of OX on NO_x was observed, although the data from the 'photochemical season' (April–September) showed significantly greater scatter than the winter months owing to a variation in the regional contribution resulting from periodically elevated levels of O₃ during regional-scale photochemical events.

The seasonal variation of the regional and local contributions, shown in Figure A1.2, indicates that the regional contribution shows a seasonality with the characteristic springtime maximum observed for 'background' O₃ in the northern hemisphere. The local contribution shows remarkably little variation with season, and amounts to about 10% of the NO_x level throughout the year.

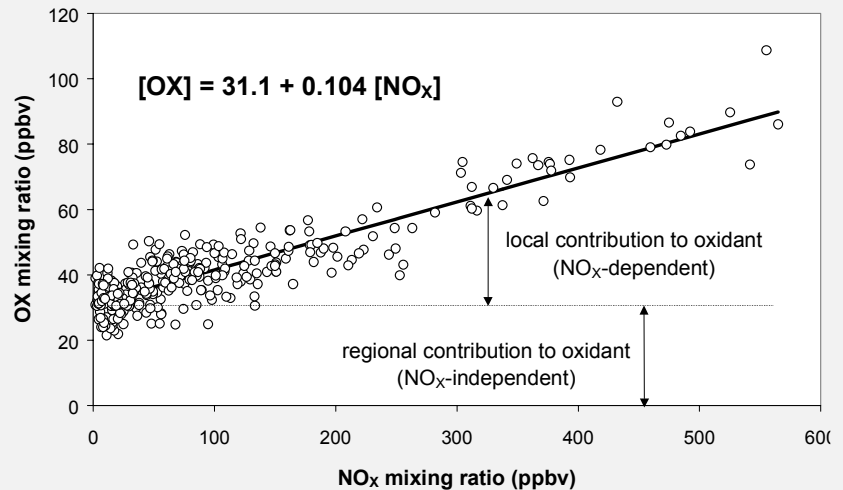


Figure A1.1 Variation of daylight average mixing ratio of OX with level of NO_x. Data are presented for each day of November 1998 and 1999 at 6 sites.

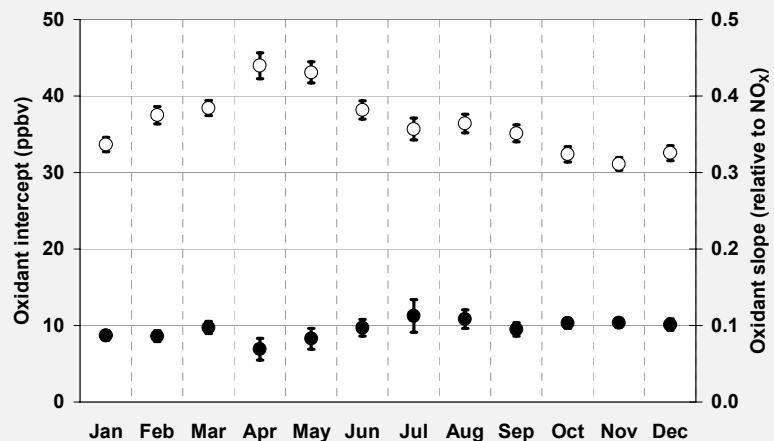


Figure A1.2 Seasonal variation of regional OX sources (OX intercept = open circles) and local OX sources (OX slope = filled circles). O₃ episode days (daylight average OX > 50 ppbv at Teddington) have been excluded from the analysis.

The results of the semi-empirical analysis will also be compared with the NO₂/NO_x partitioning calculated using the OSRM and LRCTM for the present day, and potential improvements to the semi-empirical treatment will be identified and implemented.

The OSRM has the capability to simulate ozone production at higher spatial resolution in urban areas, simply by using a denser network of receptor sites for such areas. In addition to the major developments to the OSRM identified under Objective 1, some specific developments will be needed to ensure efficient model runtimes to a receptor network on a 1 km x 1km scale of all major urban areas in the UK.

As the OSRM will be initialised by concentration fields taken from the STOCHEM model, the impact of climate change on the attainment of the NO₂ air quality standard can also be assessed. The oxidant fields needed as input for the semi-empirical modelling will be provided by the OSRM.

The semi-empirical analysis will be undertaken by Mike Jenkin (Imperial College) and the modelling work using the OSRM by **netcen**.

A1.2.2 Modelling using the London Routine Column Trajectory Model

A recommendation was made in the final report on the previous project that there was a need to find a new approach to the use of the London Routine Column Trajectory Model for the detailed modelling of urban NO₂ and ozone. However, there is some important and relevant on-going short term work which needs to be concluded using the London Routine Column Trajectory Model.

The aim of this work would be three-fold:

1. to provide some theoretical underpinning for the empirical modelling approach of John Stedman for London. London is likely to provide the greatest challenges for meeting the annual mean NO₂ air quality standard. It is vital that the empirical approach is backed up by a theoretical approach to provide some explanation for the relationships found.
2. the greatest weakness in the empirical approach is the assumption that correlation implies cause and effect and that the relationships will hold up into the future. It is likely that the changing fraction of NO_x emitted as NO₂ and the influence of climate change and the global increase in baseline ozone levels will change the empirical relationships in the future. These impacts can only be tested with models.
3. there is a requirement within the City-Delta Model intercomparison exercise of the EU CAFE process to examine the relationship between the ozone distribution in London, and hence the population weighted-ozone exposure, and the 50 km x 50 km NO_x emission for the EMEP grid squares containing London and the EMEP model regional ozone level.

This work will be undertaken by Dick Derwent.

A1.3 Objective 3a - Policy Development and Scenario Analysis

A1.3.1 UK Scale Modelling

As specified in the Invitation to Tender, scenario analysis is needed to assess the impact of planned or proposed policies on ozone concentrations, against agreed air quality standards and objectives. The OSRM will be used to support policy developments relating to

- The Review of the First Daughter Directive of the Air Quality Framework Directive. This Daughter Directive has defined objectives and limit values for NO₂. A review of the Directive is expected at the end of 2003.
- The Review of the Göthenburg Protocol to the UN ECE Convention on Long-range Transport of Air Pollution and European Union's National Emission Ceilings Directive. The protocol and Directive have defined emission limits for SO₂, NO₂, VOCs and NH₃ for European countries to be attained by 2010. A review of the Protocol and Directive is expected in 2004/2005.

The OSRM has been designed to calculate ozone concentrations to a network of receptor grids covering the UK. The spatial resolution can be increased by using a higher density of receptor sites although this will be at the expense of the model runtime. As the OSRM considers trajectories covering the EMEP model domain, it can in principle calculate ozone concentrations at any receptor site on the EMEP model grid. As the development of optimal strategies to maximise reductions in ozone and NO₂ may include differential actions within Europe and the British Isles, it is proposed that a

limited number of additional receptor sites covering Europe should be included to check for adverse outcomes in Europe as opposed to the British Isles. These receptor sites could be ozone monitoring sites in the EMEP network.

The OSRM work will be undertaken by **netcen**.

Model Scenarios

It is expected that the major emphasis of the scenario calculations will be to investigate the impact of medium to long-term national and European policies associated with transport and electricity generation. The OSRM has the facility to allow the user to investigate the effect of differential emission reduction from 8 key sectors by adjusting simple scale factors. The sectors considered are shown in Table A1.2. The table also shows the relationship to the CORINAIR SNAP codes and the pollutants affected.

Table A1.2 Summary of Composite Emission Sectors for CO, NO_x, SO₂ and VOC in the OSRM, and their relation to SNAP Codes.

OSRM code	8 composite sectors represented		SNAP code	Pollutant
01	SU	Solvent Use	6	VOC
02	RT	Road Transport	7	CO,NO _x ,SO ₂ ,VOC
03	IP	Industry/Processes	1*, 3, 4	CO,NO _x ,SO ₂ ,VOC
04	FF	Fossil Fuel Distribution	5	CO,NO _x ,SO ₂ ,VOC
05	DC	Domestic Combustion	2	CO,NO _x ,SO ₂ ,VOC
06	PG	Power Generation	1*	CO,NO _x ,SO ₂ ,VOC
07	OT	Other	8, 9	CO,NO _x ,SO ₂ ,VOC
08	NA	Natural	11	VOC

* PG includes 'power stations' contribution to SNAP code 1: other contributions are in IP

Depending on the nature of the emission scenario considered, work may be required to make projections of future activity and to prepare customised emission inventories. Once the scenario run has been completed, man-time will be required to post-process the large volume of OSRM output to calculate the specific ozone metrics of interest (e.g., AOT40, number of days with running 8 hour means above 50 ppb).

Meteorological Datasets

The OSRM uses global meteorological datasets provided by the Met Office. Datasets have been provided for each year from 1995 to 1998. Although Dick Derwent will be leaving the Meteorological Office during Spring 2003, he will be maintaining his scientific contacts with the Met Office. He has confirmed that the project consortium will have continued access to the STOCHEM model and to the meteorological fields required for the OSRM and STOCHEM models. Meteorological datasets will be supplied for the years 1999, 2000, 2001 and 2002. Should there be additional requirements for Met Office products to meet particular DEFRA requirements that cannot be currently envisaged, then these would be taken up with the Met Office at that point in time.

A1.3.2 VOC Reactivity

In Section 3.1, it was proposed in principle to replace the chemical mechanism currently used in the OSRM with the latest version of the CRI mechanism. This will enable the OSRM to cover any significant changes in VOC reactivity that result from planned or proposed policies. Furthermore, the extent and location of controls required to meet ozone standards at a particular location may also entail some shift in overall VOC reactivity. Again, the OSRM incorporating the CRI mechanism will be suitable to cover such changes in reactivity.

If there is a need to undertake modelling runs before the CRI mechanism has been incorporated into the OSRM, we propose to use the UK Photochemical Trajectory Model for a limited number of trajectories to handle potential changes in VOC reactivity.

This work will be undertaken by Dick Derwent.

A1.4 Objective 3B - Policy Development and Scenario Analysis

The main task under this objective is to provide technical support for the implementation of the 3rd Daughter Directive. This work will be undertaken by **netcen**.

A1.4.1 Preliminary Assessment of Air Quality in Relation to the 3rd Daughter Directive

Under Article 5 and 11(1)d of the Framework Directive (Directive 96/62/EC) Member States are required to conduct a preliminary assessment of air quality in relation to Daughter Directives set in place subsequent to the Framework Directive. We propose to use a modelling-based approach for the preliminary assessment to reduce monitoring effort needed for formal compliance with the Directive.

We propose to evaluate the suitability of both the OSRM and empirical models for this purpose. The empirical models will be developed from a combination of monitoring data, emission inventories and other relevant information, such as altitude. They will build upon the empirical mapping work undertaken for the department at both **netcen** and CEH. We will compare the results from the empirical and OSRM models and select the most representative technique for reporting to the Commission.

After selection of the most appropriate source of supplementary information, we propose to update the current documentation relating to a preliminary assessment on for the 3rd Daughter Directive and consolidate this information in a formatted report suitable for submission to the Commission.

The report will detail:

1. Definition of the geographical extent of zones and agglomerations and populations
2. Extent of the current monitoring network
3. A description of the approach to supplementary assessment and identification of monitoring requirements in conjunction with the Directive guidance
4. A description of the supplementary assessment techniques used
 - i. OSRM
 - ii. Empirical models
5. Measured and/or modelled exceedence of the following by zone and agglomeration based on 2002 measured data
 - i. Target values for the protection of human health
 - ii. Target values for the protection of vegetation
 - iii. Long-term objectives for the protection of human health
 - iv. Long-term objectives for the protection of vegetation
6. Recommendations for additional monitoring for compliance with the 3rd Daughter Directive in relation to
 - i. Ozone
 - ii. NO_x
 - iii. VOC ozone precursor species

The preliminary assessment of air quality for the 3rd Daughter Directive is required to be submitted to the Commission by 9 September 2003. It is proposed that a draft copy of the report, incorporating ratified monitoring data for 2002, shall be submitted to DEFRA by 1st July 2003.

A1.4.2 Calculation of Modelled Exceedence of Targets and Long-term Objectives for reporting to the Commission

Article 10 (2)b and Annex III and VI of the 3rd Daughter Directive specify the annual reporting requirements for measured ozone and ozone precursors. It is proposed that, the preferred supplementary assessment technique will be used to predict exceedence of the target vales and long-term objective for human health and vegetation protection. Based on our experience of reporting requirements of the 1st Daughter Directive it is proposed that the following predictions be made for each zone and agglomeration:

1. Maximum exceedence of the target vales and long-term objective for human health and vegetation protection
2. Area of exceedence of the target vales and long-term objective for human health and vegetation protection
3. Population exposed to exceedence of the target vales and long-term objective for human health and vegetation protection

The spatial resolution at which predictions will be made will be agreed in conjunction with the Department.

Our experience with the reporting requirements for the 1st Daughter Directive, we anticipate that Defra and the devolved administrations will request **netcen** to carry out the tasks outline below:

1. Compilation of the modelling results from supplementary assessment techniques
2. Completion of the questionnaire specified by the Commission

Our budgeting of these tasks assumes that monitoring data and statistics will be available in correct formats from the Department's relevant contractors.

The first calendar year of measurements for which reporting is required is 2004, the timescale for reporting of these data is by 30 September 2005.

A1.5 Objective 4 - Improvements to Photochemical Reaction Schemes

The current consortium has previously developed the Master Chemical Mechanism (MCM) and the Common Representative Intermediates (CRI) mechanism. The current version of the MCM (v3) provides a near-explicit representation of the degradation of 125 VOC (Saunders *et al.*, 2002¹¹; Jenkin *et al.*, 2002¹²) and the associated formation of ozone and many other secondary pollutants. The CRI mechanism is a computationally-efficient, fully compatible alternative to the MCM, which currently treats the degradation of 121 VOC and the associated formation of ozone (Jenkin *et al.*, 2002b¹³). The represented VOC in both mechanisms represent about 70% of the mass emissions in the NAEI speciated inventory (Goodwin *et al.*, 2001¹⁴).

The proposed chemical mechanism development work will focus primarily on the expansion and maintenance of both the MCM and CRI mechanism in a number of areas. Emphasis is placed on aspects of the mechanisms where the representation is currently not fully adequate in terms chemical species coverage or newly reported mechanistic data.

A1.5.1 Development of the Master Chemical Mechanism

The following tasks will be performed to develop the Master Chemical Mechanism:

1. The degradation schemes for the 18 aromatic hydrocarbons will be updated in line with the significant new body of kinetic and mechanistic data which have been recently produced. As far as possible, the schemes will be validated on the basis of highly detailed environmental chamber data which are currently emerging (EUPHORE, 2002¹⁵). By virtue of their generally high reactivity and emissions, the oxidation of aromatic hydrocarbons is believed to make a substantial contribution to the formation of ozone on local and regional scales (*e.g.*, Calvert *et al.*, 2002¹⁶).

¹¹ Saunders S.M., Jenkin M.E., Derwent R.G., Pilling, M.J., (2002) **Protocol for the Development of the Master Chemical Mechanism, MCM v3 (Part B): Tropospheric Degradation of Non Aromatic Volatile Organic Compounds**. Submitted to Atmospheric Chemistry and Physics.

¹² Jenkin, M.E., Saunders, S.M., Wagner, V., Pilling, M.J. (2002a) **Protocol for the Development of the Master Chemical Mechanism, MCM v3 (Part B): Tropospheric Degradation of Aromatic Volatile Organic Compounds**. Submitted to Atmospheric Chemistry and Physics.

¹³ Jenkin M.E., Saunders S.M., Derwent R.G., Pilling, M.J (2002b) **Development of a Reduced Speciated VOC Degradation Mechanism for Use in Ozone Models**. Atmospheric Environment, **36**, 4725-4734.

¹⁴ Goodwin, J.W.L., Salway, A.G., Murrells, T.P., Dore, C.J., Passant, N.P., King, K.R., Coleman, P.J., Hobson, M.H., Pye, S.T. and Watterson, J.D. (2001) **UK Emissions of Air Pollutants: 1970-1999**. Report (AEAT/ENV/R/0798) prepared for DEFRA.

¹⁵ EUPHORE (2002) **Experiments performed at the European Photoreactor as part of the EU EXACT programme**. Information available at http://www.gva.es/ceam/euphore_i.htm

¹⁶ Calvert, J.G., Atkinson, R., Becker K.H., Kamens R.M., Seinfeld J.H., Wallington, T.J., Yarwood, G. (2002) **The Mechanisms of Atmospheric Oxidation of Aromatic Hydrocarbons**. Oxford University Press, New York. ISBN 0-19-514628-X.

2. The degradation mechanism for cyclohexane will be reviewed, and a new scheme will be written for methylcyclohexane as an example of an alkyl-substituted cycloalkane. A large number of cycloalkanes (each with a very small emission) make a major contribution to the 30% mass emissions not currently covered by the MCM.
3. Degradation schemes will be constructed for additional biogenic hydrocarbons with significant emissions, including limonene and 2-methyl-3-buten-2-ol (MBO).
4. Absorption cross-section and quantum yield data will be reviewed to assist the updating of the photolysis rates for inorganic and organic species.
5. The MCM website will be maintained and revised to include the updated MCM when completed.

These tasks will be undertaken by Imperial College and the University of Leeds with assistance from Dick Derwent. The MCM web-site will continue to be located at the University of Leeds.

A1.5.2 Development of the Common Reactive Intermediates Chemical Mechanism

The following tasks will be performed for the CRI mechanism:

1. The representation of a number of VOC classes will be reviewed, in particular, those of the aromatic hydrocarbons, cycloalkanes and monoterpenes. The construction methodology will be validated, using MCM v3 as a reference benchmark.
2. The mechanism will be expanded to include a large number of additional species, including large alkanes, alkyl-substituted cycloalkanes and alkyl-substituted aromatics not treated in the MCM. Consideration will also be given to heteroatomic organic species for which no evaluation has been made.

The entire mechanism will be made available as CRI mechanism, version 2 by Imperial College. The chemistry for the additional species identified above will also form a fully-compatible, modular add-on to the MCM to expand its capability to represent the degradation of VOC emissions from a wide variety of detailed source sectors.

This task will be led by Imperial College with support from the University of Leeds.

A1.5.3 Conversion of the MCM and CRI Codes

The current MCM and CRI mechanisms are written using the language of the FACSIMILE numerical integration program. The FACSIMILE program has a major advantage in that the thermal and photochemical reactions can be written in a natural style (*i.e.*, $\text{OH} + \text{NO}_2 + \text{M} = \text{HNO}_3 + \text{M}$) and the program internally generates the flux terms for each chemical species, which are then solved. As the FACSIMILE program is a commercially-available software code, its use by the wider research community is limited and this has affected the uptake and use of the Master Chemical Mechanism.

The next few years will see a considerable expansion of computationally driven collaborative work through the potential that will be provided web and grid based technologies. It will become feasible for experimental and modelling groups in different locations to work together more directly and to develop models and understanding of complex problems, especially problems which are computationally intensive and data rich. In order to take advantage of these developments, the MCM will need to be written and mounted on the web in XML (extensible mark up language).

It is therefore proposed to convert the Master Chemical Mechanism into FORTRAN- and XML-based versions to improve the uptake of the mechanism. The key coding issues will be to ensure that:

- the number of continuation lines available for species involved in many reactions (such as OH) do not exceed the maximum number available;
- each species remains uniquely identified if fewer significant characters are available in FORTRAN compared to FACSIMILE;

This work will be undertaken by the University of Leeds and Dick Derwent. A Fortran version will be made available in September 2004 and an XML version in December 2005

A1.5.4 Use of the MCM and CRI Mechanism in the Photochemical Trajectory Model

Dick Derwent will incorporate the latest version of the Master Chemical Mechanism into the Photochemical Trajectory Model and use the PTM to investigate the reactivity concept and in particular to extend the POCP concept to the consideration of first day vs. second day reactivity.

The developments proposed above for the MCM and the CRI will allow the direct incorporation of the speciated NAEI VOC inventory into the PTM so that the contribution of each of the 212 VOC source sectors to ozone production can be assessed. Further, it is proposed to implement the VOC emission projections for the 212 VOC source sectors and evaluate the likely benefits of the EU NECD and UN ECE Gothenburg Protocol.

A1.6 Objective 5 - Development of Stomatal Flux Module for Crops and Semi-Natural Vegetation

We believe that the requirement to develop the surface flux module for this option can be met through a two stage process involving:

- (1) **review** and **consultation** with the current active critical loads community in the UK and Europe – here EMEP is the current primary focus; followed by,
- (2) the **development of a module** on an appropriate scale from UK regional, through UK national to the UNECE European region.

Extensive experience in micrometeorological flux gradient work, modelling and mapping of deposition coupled with long standing relationships with the active community research community makes **netcen** well placed to carry out the work and deliver the stomatal flux module for use in the Department's response to decisions within UNECE on the level 2 approach. Additionally, a potentially valuable **netcen** expertise for development of the surface flux model and the subsequent mapping will be the use of remote-sensed or earth observation data, for example to determine species distribution and phenological information - of key importance for mapping.

A1.7 Ad hoc Support

Guidance, information and advice will be provided to DEFRA and the Devolved Administrations on matters relevant to the contract work during the contract period. Provision has been made for 20 days ad hoc support in each project year. If further support is required by the Department over and above this level, the Department will be advised of this by the project manager.

Appendix 2

Population or Area-weighted Means of the Selected O₃ and NO₂ Metrics

CONTENTS

Table A2-1	Population-Weighted Annual Means of Daily Maximum Running 8 Hourly Ozone Concentration (in $\mu\text{g m}^{-3}$) for the OSRM Runs Undertaken for the Review of the Air Quality Strategy.
Table A2-2	Population-Weighted Annual Mean of the Difference (in $\mu\text{g m}^{-3}$) between the Daily Maximum Running 8 Hourly Ozone Concentration and $70 \mu\text{g m}^{-3}$ for the OSRM Scenario Runs Undertaken for the Review of the Air Quality Strategy.
Table A2-3	Population-Weighted Annual Mean of the Difference (in $\mu\text{g m}^{-3}$) between the Daily Maximum Running 8 Hourly Ozone Concentration and $100 \mu\text{g m}^{-3}$ for the OSRM Runs Undertaken for the Review of the Air Quality Strategy.
Table A2-4	Population-Weighted Number of Days when the Daily Maximum Running 8 Hourly Ozone Concentration exceeds $120 \mu\text{g m}^{-3}$ for the OSRM Runs Undertaken for the Review of the Air Quality Strategy.
Table A2-5	Population-Weighted Annual Mean Nitrogen Dioxide Concentration (in $\mu\text{g m}^{-3}$) for the OSRM Scenario Runs Undertaken for the Review of the Air Quality Strategy.
Table A2-6	Area-Weighted Annual Mean Ozone Concentration (in $\mu\text{g m}^{-3}$) for the OSRM Scenario Runs Undertaken for the Review of the Air Quality Strategy.
Table A2-7	Area-Weighted AOT40 - Crops (in $\mu\text{g m}^{-3}$ hours) for the OSRM Scenario Runs Undertaken for the Review of the Air Quality Strategy
Table A2-8	Area-Weighted AOT40 - Forests (in $\mu\text{g m}^{-3}$ hours) for the OSRM Scenario Runs Undertaken for the Review of the Air Quality Strategy

Table A2-1: Summary of the Population-Weighted Annual Means of Daily Maximum Running 8 Hourly Ozone Concentration (in $\mu\text{g m}^{-3}$) for the OSRM Runs Undertaken for the Review of the Air Quality Strategy.

Run Description	Population-Weighted Annual Means of Daily Maximum Running 8 Hourly Ozone Concentration (in $\mu\text{g m}^{-3}$)						
	All UK	Scotland	Wales	Northern Ireland	Inner London	Outer London	Rest of England
1999 - Current Year	67.77	73.48	76.77	77.62	58.40	59.43	67.58
2000 - Current Year	67.86	73.95	76.89	79.06	59.95	60.50	67.37
2001 - Current Year	63.62	68.70	72.03	71.56	55.93	56.88	63.34
2002 - Current Year	63.62	68.01	70.57	70.97	57.71	58.22	63.28
2003 - Current Year	65.14	69.79	73.21	73.96	58.52	59.13	64.75
2010 - Base Case (NECD)	70.32	73.17	77.09	76.54	65.73	65.98	70.02
2010 - Base Case (CAFÉ)	69.96	73.03	76.73	76.42	65.30	65.51	69.65
2010 - Base Case (CAFÉ) – Current Composition	68.02	71.35	74.76	74.72	63.30	63.51	67.67
2015 - Base Case (NECD)	72.76	74.96	79.18	78.06	68.66	68.91	72.53
2015 - Base Case (CAFÉ)	72.58	74.85	79.01	77.96	68.40	68.62	72.34
2020 - Base Case (NECD)	74.88	76.61	81.28	79.54	70.83	71.10	74.71
2020 - Base Case (CAFÉ)	74.72	76.46	81.16	79.39	70.62	70.88	74.57
2020 - Base Case (CAFÉ) – Current Composition	70.16	72.56	76.51	75.49	65.85	66.13	69.93
2010 - Base Case	69.96	73.03	76.73	76.42	65.30	65.51	69.65
2010 - Measure A	70.00	73.04	76.76	76.43	65.35	65.56	69.69
2010 - Measure B	70.07	73.08	76.81	76.46	65.46	65.67	69.77
2010 - Measure B*	70.07	73.08	76.81	76.46	65.46	65.67	69.77
2010 - Measure C	70.08	73.09	76.81	76.46	65.48	65.68	69.77
2010 - Measure E	69.98	73.04	76.74	76.43	65.32	65.53	69.66
2010 - Measure J	70.00	73.05	76.75	76.44	65.39	65.58	69.68
2010 - Measures K & L	70.95	73.68	77.75	76.87	66.23	66.41	70.71
2010 - Measure L	69.96	73.03	76.73	76.42	65.30	65.51	69.65
2010 - Measure O	70.10	73.10	76.82	76.47	65.50	65.71	69.79
2010 - Measure P	70.08	73.09	76.81	76.46	65.48	65.68	69.77
2010 - Measure Q	70.10	73.10	76.82	76.47	65.50	65.71	69.79
2010 - Measures M & Q	70.07	73.08	76.79	76.45	65.48	65.69	69.77
2010 - Measure M	69.94	73.00	76.71	76.40	65.27	65.49	69.62
Sensitivity to Meteorology							
2010 - Base Case	69.96	73.03	76.73	76.42	65.30	65.51	69.65
2010 - Measure B*	70.07	73.08	76.81	76.46	65.46	65.67	69.77
2010 - Measure B* with 2000 meteorology	74.05	76.78	80.93	81.19	69.58	69.94	73.70
2010 - Measure B* with 2002 meteorology	68.73	70.74	74.10	73.15	64.99	65.35	68.54
2010 - Measure M	69.94	73.00	76.71	76.40	65.27	65.49	69.62
2010 - Measure M with 2000 meteorology	73.88	76.69	80.83	81.15	69.29	69.66	73.52
2010 - Measure M with 2002 meteorology	68.54	70.66	73.99	73.10	64.70	65.07	68.35

Table A2-1: Summary of the Population-Weighted Annual Means of Daily Maximum Running 8 Hourly Ozone Concentration (in $\mu\text{g m}^{-3}$) for the OSRM Runs Undertaken for the Review of the Air Quality Strategy (Continued).

Run Description	Population-Weighted Annual Means of Daily Maximum Running 8 Hourly Ozone Concentration (in $\mu\text{g m}^{-3}$)						
	All UK	Scotland	Wales	Northern Ireland	Inner London	Outer London	Rest of England
2015 - Base Case	72.58	74.85	79.01	77.96	68.40	68.62	72.34
2015 - Measure A	73.01	75.05	79.29	78.05	69.04	69.26	72.79
2015 - Measure B	73.57	75.29	79.63	78.16	69.88	70.11	73.37
2015 - Measure B*	73.60	75.30	79.64	78.16	69.93	70.16	73.40
2015 - Measure C	73.14	75.12	79.37	78.10	69.23	69.45	72.92
2015 - Measure E	72.63	74.89	79.05	77.98	68.48	68.71	72.40
2015 - Measure J	72.68	74.93	79.06	78.00	68.65	68.81	72.43
2015 - Measures K & L	73.62	75.51	80.07	78.40	69.47	69.64	73.45
2015 - Measure L	72.66	74.90	79.07	77.98	68.54	68.74	72.43
2015 - Measure O	73.19	75.15	79.40	78.11	69.31	69.53	72.97
2015 - Measure P	73.22	75.17	79.43	78.12	69.38	69.57	73.01
2015 - Measure Q	73.28	75.20	79.46	78.13	69.46	69.65	73.06
2015 - Measures M & Q	73.25	75.17	79.43	78.11	69.44	69.62	73.03
2015 - Measure M	72.55	74.82	78.98	77.94	68.37	68.60	72.31
2020 - Base Case	74.72	76.46	81.16	79.39	70.62	70.88	74.57
2020 - Measure A	75.53	76.76	81.61	79.50	71.87	72.14	75.40
2020 - Measure B	76.40	77.01	82.01	79.52	73.37	73.61	76.31
2020 - Measure B*	76.56	77.05	82.07	79.52	73.66	73.90	76.47
2020 - Measure C	75.57	76.78	81.64	79.51	71.94	72.20	75.45
2020 - Measure E	74.85	76.52	81.23	79.43	70.81	71.06	74.69
2020 - Measure J	74.90	76.58	81.24	79.45	71.06	71.20	74.72
2020 - Measures K & L	75.18	76.73	81.60	79.57	71.16	71.37	75.05
2020 - Measure L	74.82	76.51	81.22	79.41	70.78	71.01	74.66
2020 - Measure O	75.67	76.84	81.70	79.54	72.10	72.36	75.55
2020 - Measure P	75.66	76.83	81.70	79.53	72.11	72.33	75.54
2020 - Measure Q	75.76	76.88	81.76	79.56	72.27	72.49	75.64
2020 - Measures M & Q	75.73	76.85	81.73	79.54	72.24	72.45	75.61
2020 - Measure M	74.69	76.43	81.13	79.37	70.59	70.85	74.54

Table A2-2: Summary of the Population-Weighted Annual Mean of the Difference (in $\mu\text{g m}^{-3}$) between the Daily Maximum Running 8 Hourly Ozone Concentration and $70 \mu\text{g m}^{-3}$ for the OSRM Scenario Runs Undertaken for the Review of the Air Quality Strategy.

Run Description	Population-Weighted Annual Mean of the Difference (in $\mu\text{g m}^{-3}$) between the Daily Maximum Running 8 Hourly Ozone Concentration and $70 \mu\text{g m}^{-3}$						
	All UK	Scotland	Wales	Northern Ireland	Inner London	Outer London	Rest of England
1999 - Current Year	9.68	10.94	14.16	13.10	6.42	6.75	9.61
2000 - Current Year	9.33	10.59	13.63	13.30	6.46	6.66	9.20
2001 - Current Year	8.19	8.34	12.27	8.96	5.90	6.20	8.22
2002 - Current Year	8.67	9.76	11.55	10.67	6.80	6.95	8.56
2003 - Current Year	9.14	9.63	13.38	11.51	6.77	6.93	9.09
2010 - Base Case (NECD)	11.23	11.18	15.26	12.81	9.29	9.38	11.22
2010 - Base Case (CAFÉ)	11.10	11.10	15.07	12.73	9.26	9.31	11.08
2010 - Base Case (CAFÉ) – Current Composition	9.75	9.87	13.50	11.40	8.04	8.08	9.70
2015 - Base Case (NECD)	12.77	12.40	16.79	13.92	10.95	11.09	12.79
2015 - Base Case (CAFÉ)	12.51	12.21	16.51	13.73	10.70	10.80	12.52
2020 - Base Case (NECD)	14.20	13.59	18.41	15.04	12.28	12.46	14.27
2020 - Base Case (CAFÉ)	13.82	13.29	18.02	14.73	11.87	12.03	13.88
2020 - Base Case (CAFÉ) – Current Composition	10.41	10.28	14.15	11.56	8.68	8.80	10.41
2010 - Base Case	11.10	11.10	15.07	12.73	9.26	9.31	11.08
2010 - Measure A	11.12	11.10	15.08	12.73	9.28	9.33	11.09
2010 - Measure B	11.15	11.12	15.10	12.74	9.32	9.37	11.12
2010 - Measure B*	11.15	11.12	15.10	12.74	9.32	9.37	11.12
2010 - Measure C	11.16	11.13	15.11	12.75	9.34	9.39	11.13
2010 - Measure E	11.11	11.10	15.07	12.73	9.28	9.32	11.09
2010 - Measure J	11.12	11.11	15.08	12.74	9.30	9.34	11.09
2010 - Measures K & L	11.55	11.43	15.67	12.95	9.57	9.64	11.56
2010 - Measure L	11.10	11.10	15.07	12.73	9.26	9.31	11.08
2010 - Measure O	11.17	11.13	15.11	12.75	9.35	9.40	11.14
2010 - Measure P	11.16	11.13	15.11	12.75	9.34	9.39	11.13
2010 - Measure Q	11.17	11.13	15.11	12.75	9.35	9.40	11.14
2010 - Measures M & Q	11.15	11.12	15.09	12.73	9.34	9.39	11.12
2010 - Measure M	11.09	11.08	15.05	12.71	9.25	9.30	11.06
Sensitivity to Meteorology							
2010 - Base Case	11.10	11.10	15.07	12.73	9.26	9.31	11.08
2010 - Measure B*	11.15	11.12	15.10	12.74	9.32	9.37	11.12
2010 - Measure B* with 2000 meteorology	12.12	11.80	15.88	14.43	10.72	10.89	12.03
2010 - Measure B* with 2002 meteorology	10.96	11.02	13.31	11.77	9.84	10.05	10.93
2010 - Measure M	11.09	11.08	15.05	12.71	9.25	9.30	11.06
2010 - Measure M with 2000 meteorology	12.01	11.74	15.81	14.40	10.53	10.72	11.92
2010 - Measure M with 2002 meteorology	10.86	10.98	13.26	11.75	9.68	9.90	10.83

Table A2-2: Summary of the Population-Weighted Annual Mean of the Difference (in $\mu\text{g m}^{-3}$) between the Daily Maximum Running 8 Hourly Ozone Concentration and $70 \mu\text{g m}^{-3}$ for the OSRM Scenario Runs Undertaken for the Review of the Air Quality Strategy (Continued).

Run Description	Population-Weighted Annual Mean of the Difference (in $\mu\text{g m}^{-3}$) between the Daily Maximum Running 8 Hourly Ozone Concentration and $70 \mu\text{g m}^{-3}$						
	All UK	Scotland	Wales	Northern Ireland	Inner London	Outer London	Rest of England
2015 - Base Case	12.51	12.21	16.51	13.73	10.70	10.80	12.52
2015 - Measure A	12.67	12.28	16.60	13.72	10.93	11.04	12.69
2015 - Measure B	12.88	12.36	16.71	13.71	11.23	11.38	12.91
2015 - Measure B*	12.89	12.36	16.71	13.71	11.25	11.39	12.92
2015 - Measure C	12.74	12.32	16.65	13.75	11.03	11.14	12.76
2015 - Measure E	12.54	12.23	16.53	13.74	10.75	10.85	12.56
2015 - Measure J	12.56	12.25	16.54	13.75	10.83	10.89	12.57
2015 - Measures K & L	13.01	12.56	17.16	13.93	11.13	11.22	13.05
2015 - Measure L	12.56	12.24	16.55	13.74	10.78	10.86	12.57
2015 - Measure O	12.76	12.34	16.67	13.75	11.07	11.18	12.79
2015 - Measure P	12.78	12.34	16.69	13.75	11.11	11.21	12.80
2015 - Measure Q	12.81	12.36	16.70	13.76	11.15	11.25	12.83
2015 - Measures M & Q	12.79	12.34	16.68	13.75	11.13	11.23	12.81
2015 - Measure M	12.49	12.19	16.49	13.71	10.69	10.79	12.50
2020 - Base Case	13.82	13.29	18.02	14.73	11.87	12.03	13.88
2020 - Measure A	14.11	13.35	18.13	14.66	12.33	12.54	14.18
2020 - Measure B	14.38	13.33	18.11	14.48	12.95	13.18	14.46
2020 - Measure B*	14.43	13.32	18.10	14.44	13.08	13.31	14.51
2020 - Measure C	14.13	13.37	18.15	14.67	12.37	12.58	14.20
2020 - Measure E	13.89	13.33	18.07	14.75	11.97	12.13	13.94
2020 - Measure J	13.90	13.36	18.07	14.76	12.10	12.20	13.95
2020 - Measures K & L	14.04	13.42	18.30	14.81	12.11	12.26	14.11
2020 - Measure L	13.87	13.32	18.06	14.74	11.95	12.09	13.93
2020 - Measure O	14.18	13.39	18.18	14.68	12.46	12.67	14.26
2020 - Measure P	14.18	13.38	18.18	14.67	12.46	12.65	14.25
2020 - Measure Q	14.23	13.41	18.21	14.69	12.55	12.74	14.30
2020 - Measures M & Q	14.21	13.39	18.18	14.67	12.53	12.72	14.28
2020 - Measure M	13.80	13.27	18.00	14.71	11.85	12.01	13.85

Table A2-3: Summary of the Population-Weighted Annual Mean of the Difference (in $\mu\text{g m}^{-3}$) between the Daily Maximum Running 8 Hourly Ozone Concentration and $100 \mu\text{g m}^{-3}$ for the OSRM Runs Undertaken for the Review of the Air Quality Strategy.

Run Description	Population-Weighted Annual Mean of the Difference (in $\mu\text{g m}^{-3}$) between the Daily Maximum Running 8 Hourly Ozone Concentration and $100 \mu\text{g m}^{-3}$						
	All UK	Scotland	Wales	Northern Ireland	Inner London	Outer London	Rest of England
1999 - Current Year	1.75	1.69	2.03	1.88	1.35	1.44	1.79
2000 - Current Year	1.65	1.32	2.24	2.09	1.06	1.07	1.73
2001 - Current Year	1.71	1.22	2.44	0.79	1.62	1.73	1.76
2002 - Current Year	1.47	1.62	1.26	1.41	1.67	1.58	1.44
2003 - Current Year	1.93	1.69	2.73	1.96	1.52	1.53	1.97
2010 - Base Case (NECD)	2.19	1.87	2.97	2.09	1.87	1.83	2.23
2010 - Base Case (CAFÉ)	2.14	1.80	2.89	2.01	1.92	1.86	2.18
2010 - Base Case (CAFÉ) – Current Composition	1.75	1.48	2.37	1.60	1.60	1.55	1.78
2015 - Base Case (NECD)	2.68	2.23	3.53	2.45	2.40	2.36	2.74
2015 - Base Case (CAFÉ)	2.50	2.06	3.34	2.29	2.28	2.23	2.55
2020 - Base Case (NECD)	3.22	2.66	4.22	2.86	2.89	2.86	3.30
2020 - Base Case (CAFÉ)	2.95	2.43	3.96	2.63	2.66	2.61	3.01
2020 - Base Case (CAFÉ) – Current Composition	1.83	1.50	2.46	1.61	1.68	1.64	1.87
2010 - Base Case	2.14	1.80	2.89	2.01	1.92	1.86	2.18
2010 - Measure A	2.15	1.80	2.89	2.01	1.92	1.87	2.19
2010 - Measure B	2.16	1.80	2.90	2.01	1.93	1.88	2.20
2010 - Measure B*	2.16	1.80	2.90	2.01	1.93	1.88	2.20
2010 - Measure C	2.16	1.80	2.90	2.01	1.94	1.89	2.20
2010 - Measure E	2.15	1.80	2.89	2.01	1.92	1.87	2.19
2010 - Measure J	2.15	1.80	2.89	2.01	1.93	1.87	2.19
2010 - Measures K & L	2.30	1.90	3.11	2.09	2.02	1.97	2.36
2010 - Measure L	2.14	1.80	2.89	2.01	1.92	1.86	2.18
2010 - Measure O	2.16	1.81	2.90	2.01	1.94	1.89	2.20
2010 - Measure P	2.16	1.80	2.90	2.01	1.94	1.89	2.20
2010 - Measure Q	2.16	1.81	2.90	2.01	1.94	1.89	2.20
2010 - Measures M & Q	2.15	1.80	2.89	2.00	1.94	1.89	2.19
2010 - Measure M	2.14	1.79	2.88	2.00	1.92	1.86	2.18
Sensitivity to Meteorology							
2010 - Base Case	2.14	1.80	2.89	2.01	1.92	1.86	2.18
2010 - Measure B*	2.16	1.80	2.90	2.01	1.93	1.88	2.20
2010 - Measure B* with 2000 meteorology	1.80	1.08	2.28	1.70	1.61	1.66	1.89
2010 - Measure B* with 2002 meteorology	1.72	1.79	1.58	1.51	1.93	1.87	1.70
2010 - Measure M	2.14	1.79	2.88	2.00	1.92	1.86	2.18
2010 - Measure M with 2000 meteorology	1.77	1.07	2.26	1.69	1.54	1.59	1.85
2010 - Measure M with 2002 meteorology	1.69	1.78	1.57	1.50	1.88	1.82	1.67

Table A2-3: Summary of the Population-Weighted Annual Mean of the Difference (in $\mu\text{g m}^{-3}$) between the Daily Maximum Running 8 Hourly Ozone Concentration and $100 \mu\text{g m}^{-3}$ for the OSRM Runs Undertaken for the Review of the Air Quality Strategy (Continued).

Run Description	Population-Weighted Annual Mean of the Difference (in $\mu\text{g m}^{-3}$) between the Daily Maximum Running 8 Hourly Ozone Concentration and $100 \mu\text{g m}^{-3}$						
	All UK	Scotland	Wales	Northern Ireland	Inner London	Outer London	Rest of England
2015 - Base Case	2.50	2.06	3.34	2.29	2.28	2.23	2.55
2015 - Measure A	2.55	2.08	3.38	2.30	2.34	2.28	2.60
2015 - Measure B	2.60	2.11	3.42	2.31	2.42	2.36	2.66
2015 - Measure B*	2.61	2.11	3.42	2.31	2.42	2.37	2.66
2015 - Measure C	2.57	2.09	3.39	2.30	2.37	2.31	2.62
2015 - Measure E	2.51	2.06	3.35	2.29	2.30	2.24	2.56
2015 - Measure J	2.52	2.07	3.35	2.29	2.32	2.25	2.56
2015 - Measures K & L	2.68	2.19	3.61	2.36	2.42	2.37	2.74
2015 - Measure L	2.52	2.07	3.35	2.29	2.30	2.25	2.57
2015 - Measure O	2.58	2.10	3.40	2.31	2.39	2.33	2.63
2015 - Measure P	2.58	2.10	3.41	2.31	2.40	2.34	2.63
2015 - Measure Q	2.59	2.10	3.41	2.31	2.41	2.35	2.64
2015 - Measures M & Q	2.58	2.09	3.40	2.30	2.41	2.34	2.63
2015 - Measure M	2.50	2.05	3.33	2.28	2.28	2.22	2.55
2020 - Base Case	2.95	2.43	3.96	2.63	2.66	2.61	3.01
2020 - Measure A	3.02	2.45	3.99	2.61	2.77	2.73	3.09
2020 - Measure B	3.08	2.43	3.97	2.53	2.92	2.91	3.15
2020 - Measure B*	3.09	2.42	3.95	2.50	2.95	2.95	3.15
2020 - Measure C	3.03	2.46	4.00	2.61	2.79	2.75	3.10
2020 - Measure E	2.97	2.45	3.97	2.64	2.69	2.64	3.03
2020 - Measure J	2.97	2.45	3.97	2.64	2.73	2.65	3.03
2020 - Measures K & L	3.03	2.49	4.07	2.65	2.74	2.68	3.10
2020 - Measure L	2.97	2.44	3.97	2.63	2.69	2.63	3.03
2020 - Measure O	3.05	2.47	4.01	2.62	2.82	2.78	3.11
2020 - Measure P	3.05	2.46	4.01	2.61	2.82	2.77	3.11
2020 - Measure Q	3.06	2.47	4.02	2.62	2.85	2.80	3.13
2020 - Measures M & Q	3.05	2.46	4.01	2.60	2.84	2.79	3.11
2020 - Measure M	2.94	2.42	3.94	2.62	2.65	2.60	3.00

Table A2-4: Summary of the Population-Weighted Number of Days when the Daily Maximum Running 8 Hourly Ozone Concentration exceeds 100 µg m⁻³ for the OSRM Runs Undertaken for the Review of the Air Quality Strategy.

Run Description	Population-Weighted Number of Days when the Daily Maximum Running 8 Hourly Ozone Concentration exceeds 120 µg m ⁻³						
	All UK	Scotland	Wales	Northern Ireland	Inner London	Outer London	Rest of England
1999 - Current Year	34.69	34.26	55.68	44.31	24.82	26.41	34.44
2000 - Current Year	29.73	32.69	44.04	44.37	23.25	22.80	28.97
2001 - Current Year	27.62	25.51	38.60	23.09	19.60	20.58	28.57
2002 - Current Year	26.19	31.55	35.70	34.08	20.31	21.35	25.47
2003 - Current Year	29.73	28.16	48.34	35.88	22.03	21.66	29.77
2010 - Base Case (NECD)	39.75	34.27	58.96	42.82	34.72	34.42	39.86
2010 - Base Case (CAFÉ)	38.99	34.11	57.89	42.98	33.71	34.28	38.96
2010 - Base Case (CAFÉ) – Current Composition	31.80	28.78	48.66	34.18	27.98	26.91	31.69
2015 - Base Case (NECD)	48.63	41.89	68.10	49.69	46.94	45.62	48.50
2015 - Base Case (CAFÉ)	47.23	41.27	66.84	49.00	44.09	43.20	47.17
2020 - Base Case (NECD)	56.99	50.43	78.33	56.43	53.73	52.97	56.97
2020 - Base Case (CAFÉ)	55.14	49.47	76.92	55.18	51.04	49.78	55.17
2020 - Base Case (CAFÉ) – Current Composition	34.16	30.28	51.77	33.80	30.76	30.06	34.09
2010 - Base Case	38.99	34.11	57.89	42.98	33.71	34.28	38.96
2010 - Measure A	39.01	34.10	57.87	42.92	33.71	34.32	38.99
2010 - Measure B	39.15	34.24	57.97	42.93	33.71	34.37	39.16
2010 - Measure B*	39.15	34.24	57.97	42.93	33.71	34.37	39.16
2010 - Measure C	39.22	34.24	58.00	42.98	33.88	34.66	39.21
2010 - Measure E	39.01	34.11	57.91	43.03	33.71	34.28	38.98
2010 - Measure J	39.03	34.14	57.94	43.03	33.71	34.35	39.00
2010 - Measures K & L	41.06	35.64	61.50	43.70	35.50	35.80	41.12
2010 - Measure L	38.99	34.11	57.89	42.98	33.71	34.28	38.96
2010 - Measure O	39.25	34.25	58.10	42.89	33.88	34.66	39.24
2010 - Measure P	39.22	34.24	58.00	42.98	33.88	34.66	39.21
2010 - Measure Q	39.25	34.25	58.10	42.89	33.88	34.66	39.24
2010 - Measures M & Q	39.15	34.19	57.96	42.78	33.88	34.64	39.13
2010 - Measure M	38.92	34.03	57.74	42.92	33.71	34.19	38.89
Sensitivity to Meteorology							
2010 - Base Case	38.99	34.11	57.89	42.98	33.71	34.28	38.96
2010 - Measure B*	39.15	34.24	57.97	42.93	33.71	34.37	39.16
2010 - Measure B* with 2000 meteorology	39.34	34.57	55.12	46.99	33.23	36.24	39.23
2010 - Measure B* with 2002 meteorology	36.03	37.76	45.32	39.38	31.56	32.76	35.68
2010 - Measure M	38.92	34.03	57.74	42.92	33.71	34.19	38.89
2010 - Measure M with 2000 meteorology	38.78	34.26	54.74	46.88	32.67	35.28	38.65
2010 - Measure M with 2002 meteorology	35.53	37.57	45.20	39.11	30.96	31.78	35.17

Table A2-4: Summary of the Population-Weighted Number of Days when the Daily Maximum Running 8 Hourly Ozone Concentration exceeds 100 µg m⁻³ for the OSRM Runs Undertaken for the Review of the Air Quality Strategy (Continued).

Run Description	Population-Weighted Number of Days when the Daily Maximum Running 8 Hourly Ozone Concentration exceeds 120 µg m ⁻³						
	All UK	Scotland	Wales	Northern Ireland	Inner London	Outer London	Rest of England
2015 - Base Case	47.23	41.27	66.84	49.00	44.09	43.20	47.17
2015 - Measure A	47.84	41.66	67.27	47.85	45.39	43.97	47.83
2015 - Measure B	48.35	41.90	67.32	46.72	45.39	44.56	48.49
2015 - Measure B*	48.39	41.92	67.30	46.67	45.39	44.70	48.52
2015 - Measure C	48.11	41.96	67.46	47.79	45.90	44.41	48.08
2015 - Measure E	47.38	41.44	66.97	49.00	44.31	43.40	47.31
2015 - Measure J	47.44	41.55	67.04	49.09	44.75	43.56	47.32
2015 - Measures K & L	49.25	43.70	69.98	49.55	44.90	44.34	49.29
2015 - Measure L	47.41	41.48	67.11	48.98	44.31	43.37	47.34
2015 - Measure O	48.24	42.09	67.46	47.92	45.90	44.53	48.23
2015 - Measure P	48.33	42.22	67.65	47.77	45.90	44.76	48.30
2015 - Measure Q	48.44	42.32	67.77	47.91	46.18	44.78	48.42
2015 - Measures M & Q	48.33	42.13	67.61	47.79	45.90	44.68	48.32
2015 - Measure M	47.11	41.16	66.69	48.94	44.09	43.07	47.03
2020 - Base Case	55.14	49.47	76.92	55.18	51.04	49.78	55.17
2020 - Measure A	56.04	49.87	76.11	52.98	51.65	51.57	56.29
2020 - Measure B	56.74	49.35	75.05	49.41	52.25	52.90	57.36
2020 - Measure B*	56.77	49.23	74.63	48.87	52.19	53.01	57.46
2020 - Measure C	56.12	49.96	76.10	52.97	51.65	51.79	56.37
2020 - Measure E	55.43	49.81	77.07	55.16	51.05	50.12	55.49
2020 - Measure J	55.49	49.78	77.06	55.21	51.46	50.48	55.51
2020 - Measures K & L	56.11	50.60	78.07	55.14	51.38	50.39	56.22
2020 - Measure L	55.36	49.56	77.11	55.13	51.05	50.03	55.43
2020 - Measure O	56.36	50.07	76.28	52.96	51.65	52.19	56.63
2020 - Measure P	56.31	50.05	76.12	52.94	51.65	52.08	56.59
2020 - Measure Q	56.58	50.26	76.38	52.93	51.81	52.64	56.85
2020 - Measures M & Q	56.42	50.04	76.22	52.90	51.65	52.51	56.69
2020 - Measure M	55.03	49.34	76.79	55.12	51.04	49.78	55.04

Table A2-5: Summary of the Population-Weighted Annual Mean Nitrogen Dioxide Concentration (in $\mu\text{g m}^{-3}$) for the OSRM Scenario Runs Undertaken for the Review of the Air Quality Strategy.

Run Description	Population-Weighted Annual Mean Nitrogen Dioxide Concentration (in $\mu\text{g m}^{-3}$)						
	All UK	Scotland	Wales	Northern Ireland	Inner London	Outer London	Rest of England
1999 - Current Year	22.85	12.07	14.70	7.89	37.05	34.72	23.11
2000 - Current Year	21.20	11.13	13.29	7.50	33.70	31.77	21.56
2001 - Current Year	21.69	11.91	14.70	8.61	33.70	31.63	22.02
2002 - Current Year	21.01	11.71	14.36	8.32	31.73	30.06	21.43
2003 - Current Year	20.86	12.47	13.51	8.82	33.27	30.99	20.97
2010 - Base Case (NECD)	15.64	9.12	9.85	6.28	25.34	23.68	15.71
2010 - Base Case (CAFÉ)	15.93	9.24	10.14	6.50	25.70	24.03	16.01
2010 - Base Case (CAFÉ) – Current Composition	15.90	9.24	10.17	6.52	25.57	23.91	15.99
2015 - Base Case (NECD)	14.31	8.27	8.99	5.70	23.54	21.85	14.34
2015 - Base Case (CAFÉ)	14.26	8.19	8.94	5.66	23.52	21.82	14.28
2020 - Base Case (NECD)	13.56	7.81	8.32	5.35	22.89	21.11	13.54
2020 - Base Case (CAFÉ)	13.33	7.61	8.11	5.16	22.67	20.89	13.29
2020 - Base Case (CAFÉ) – Current Composition	13.30	7.62	8.18	5.20	22.46	20.72	13.28
2010 - Base Case	15.93	9.24	10.14	6.50	25.70	24.03	16.01
2010 - Measure A	15.88	9.22	10.11	6.48	25.64	23.96	15.96
2010 - Measure B	15.79	9.16	10.05	6.44	25.51	23.84	15.87
2010 - Measure B*	15.79	9.16	10.05	6.44	25.51	23.84	15.87
2010 - Measure C	15.79	9.16	10.05	6.44	25.49	23.83	15.87
2010 - Measure E	15.91	9.23	10.13	6.49	25.68	24.00	15.99
2010 - Measure J	15.88	9.21	10.12	6.48	25.59	23.94	15.97
2010 - Measures K & L	14.94	8.63	9.20	6.06	24.78	23.11	14.93
2010 - Measure L	15.93	9.24	10.14	6.50	25.70	24.03	16.01
2010 - Measure O	15.77	9.14	10.04	6.43	25.47	23.81	15.85
2010 - Measure P	15.79	9.16	10.05	6.44	25.49	23.83	15.87
2010 - Measure Q	15.77	9.14	10.04	6.43	25.47	23.81	15.85
2010 - Measures M & Q	15.77	9.14	10.04	6.43	25.47	23.80	15.85
2010 - Measure M	15.93	9.24	10.14	6.50	25.70	24.03	16.01
Sensitivity to Meteorology							
2010 - Base Case	15.93	9.24	10.14	6.50	25.70	24.03	16.01
2010 - Measure B*	15.79	9.16	10.05	6.44	25.51	23.84	15.87
2010 - Measure B* with 2000 meteorology	14.67	7.34	9.00	4.86	24.07	22.44	14.89
2010 - Measure B* with 2002 meteorology	15.82	8.63	10.75	6.19	24.51	23.02	16.08
2010 - Measure M	15.93	9.24	10.14	6.50	25.70	24.03	16.01
2010 - Measure M with 2000 meteorology	14.79	7.41	9.08	4.91	24.25	22.61	15.01
2010 - Measure M with 2002 meteorology	15.95	8.71	10.84	6.24	24.70	23.20	16.21

Table A2-5: Summary of the Population-Weighted Annual Mean Nitrogen Dioxide Concentration (in $\mu\text{g m}^{-3}$) for the OSRM Scenario Runs Undertaken for the Review of the Air Quality Strategy (Continued).

Run Description	Population-Weighted Annual Mean Nitrogen Dioxide Concentration (in $\mu\text{g m}^{-3}$)						
	All UK	Scotland	Wales	Northern Ireland	Inner London	Outer London	Rest of England
2015 - Base Case	14.26	8.19	8.94	5.66	23.52	21.82	14.28
2015 - Measure A	13.72	7.86	8.59	5.41	22.74	21.06	13.74
2015 - Measure B	13.00	7.43	8.13	5.09	21.70	20.04	13.01
2015 - Measure B*	12.96	7.41	8.10	5.07	21.64	19.98	12.97
2015 - Measure C	13.56	7.77	8.50	5.35	22.51	20.83	13.58
2015 - Measure E	14.19	8.15	8.90	5.63	23.42	21.72	14.22
2015 - Measure J	14.13	8.09	8.88	5.60	23.19	21.58	14.17
2015 - Measures K & L	13.18	7.55	7.98	5.22	22.40	20.76	13.12
2015 - Measure L	14.14	8.14	8.87	5.63	23.32	21.67	14.17
2015 - Measure O	13.50	7.73	8.47	5.32	22.42	20.74	13.52
2015 - Measure P	13.45	7.71	8.43	5.32	22.30	20.67	13.46
2015 - Measure Q	13.39	7.67	8.39	5.30	22.21	20.58	13.40
2015 - Measures M & Q	13.39	7.67	8.39	5.30	22.21	20.59	13.40
2015 - Measure M	14.26	8.19	8.94	5.66	23.52	21.82	14.28
2020 - Base Case	13.33	7.61	8.11	5.16	22.67	20.89	13.29
2020 - Measure A	12.25	6.96	7.41	4.68	21.09	19.34	12.19
2020 - Measure B	10.94	6.18	6.59	4.11	19.18	17.46	10.86
2020 - Measure B*	10.69	6.03	6.44	4.00	18.80	17.09	10.60
2020 - Measure C	12.19	6.93	7.38	4.66	21.00	19.26	12.13
2020 - Measure E	13.19	7.52	8.02	5.10	22.45	20.68	13.15
2020 - Measure J	13.11	7.45	8.01	5.07	22.09	20.47	13.10
2020 - Measures K & L	12.83	7.32	7.69	4.98	22.10	20.36	12.76
2020 - Measure L	13.21	7.55	8.03	5.14	22.45	20.73	13.17
2020 - Measure O	12.07	6.85	7.31	4.61	20.82	19.07	12.00
2020 - Measure P	12.07	6.86	7.30	4.63	20.78	19.09	12.00
2020 - Measure Q	11.94	6.79	7.23	4.58	20.59	18.90	11.88
2020 - Measures M & Q	11.94	6.79	7.24	4.58	20.59	18.90	11.88
2020 - Measure M	13.33	7.61	8.11	5.16	22.66	20.89	13.29

Table A2-6: Summary of the Area-Weighted Annual Mean Ozone Concentration (in $\mu\text{g m}^{-3}$) for the OSRM Scenario Runs Undertaken for the Review of the Air Quality Strategy.

Run Description	Area-Weighted Annual Mean Ozone Concentration (in $\mu\text{g m}^{-3}$)						
	All UK	Scotland	Wales	Northern Ireland	Inner London	Outer London	Rest of England
1999 - Current Year	58.99	65.18	63.90	66.65	40.54	41.18	53.91
2000 - Current Year	59.77	66.27	64.38	67.54	42.49	42.86	54.51
2001 - Current Year	54.85	60.04	59.75	60.60	39.46	40.09	50.52
2002 - Current Year	54.59	59.44	58.61	60.56	40.42	40.73	50.59
2003 - Current Year	57.91	63.02	61.89	63.56	43.18	43.46	53.81
2010 - Base Case (NECD)	61.84	65.54	65.52	66.18	50.77	50.57	58.74
2010 - Base Case (CAFÉ)	61.48	65.34	65.13	65.98	50.19	50.01	58.27
2010 - Base Case (CAFÉ) – Current Composition	59.91	63.94	63.49	64.54	48.52	48.36	56.60
2015 - Base Case (NECD)	63.58	66.81	67.17	67.49	53.53	53.33	60.81
2015 - Base Case (CAFÉ)	63.50	66.76	67.11	67.47	53.30	53.11	60.70
2020 - Base Case (NECD)	65.32	68.15	68.88	68.82	55.53	55.36	62.81
2020 - Base Case (CAFÉ)	65.34	68.14	68.94	68.84	55.47	55.30	62.86
2020 - Base Case (CAFÉ) – Current Composition	61.67	64.88	65.12	65.52	51.45	51.35	58.93
2010 - Base Case	61.48	65.34	65.13	65.98	50.19	50.01	58.27
2010 - Measure A	61.51	65.36	65.15	66.00	50.25	50.07	58.31
2010 - Measure B	61.56	65.38	65.20	66.02	50.37	50.18	58.38
2010 - Measure B*	61.56	65.38	65.20	66.02	50.37	50.18	58.38
2010 - Measure C	61.56	65.38	65.19	66.02	50.38	50.19	58.37
2010 - Measure E	61.49	65.35	65.14	65.99	50.22	50.03	58.28
2010 - Measure J	61.50	65.35	65.14	65.99	50.28	50.07	58.29
2010 - Measures K & L	61.48	65.34	65.13	65.98	50.19	50.01	58.27
2010 - Measure L	62.42	65.92	65.98	66.47	51.27	51.06	59.48
2010 - Measure O	61.57	65.38	65.20	66.03	50.40	50.21	58.39
2010 - Measure P	61.56	65.38	65.19	66.02	50.38	50.19	58.37
2010 - Measure Q	61.57	65.38	65.20	66.03	50.40	50.21	58.39
2010 - Measures M & Q	61.55	65.36	65.18	66.01	50.39	50.19	58.36
2010 - Measure M	61.46	65.33	65.11	65.97	50.17	49.99	58.25
Sensitivity to Meteorology							
2010 - Base Case	61.48	65.34	65.13	65.98	50.19	50.01	58.27
2010 - Measure B*	61.56	65.38	65.20	66.02	50.37	50.18	58.38
2010 - Measure B* with 2000 meteorology	63.83	68.14	68.16	69.91	51.45	51.64	60.05
2010 - Measure B* with 2002 meteorology	58.13	61.44	61.68	62.68	47.24	47.49	55.23
2010 - Measure M	61.46	65.33	65.11	65.97	50.17	49.99	58.25
2010 - Measure M with 2000 meteorology	63.73	68.10	68.07	69.86	51.22	51.42	59.90
2010 - Measure M with 2002 meteorology	58.02	61.39	61.60	62.63	46.99	47.24	55.08

Table A2-6: Summary of the Area-Weighted Annual Mean Ozone Concentration (in $\mu\text{g m}^{-3}$) for the OSRM Scenario Runs Undertaken for the Review of the Air Quality Strategy (Continued).

Run Description	Area-Weighted Annual Mean Ozone Concentration (in $\mu\text{g m}^{-3}$)						
	All UK	Scotland	Wales	Northern Ireland	Inner London	Outer London	Rest of England
2015 - Base Case	63.50	66.76	67.11	67.47	53.30	53.11	60.70
2015 - Measure A	63.79	66.87	67.37	67.60	54.01	53.81	61.12
2015 - Measure B	64.16	67.00	67.68	67.76	54.96	54.74	61.65
2015 - Measure B*	64.18	67.00	67.70	67.76	55.01	54.79	61.68
2015 - Measure C	63.86	66.90	67.42	67.64	54.21	54.00	61.21
2015 - Measure E	63.53	66.77	67.14	67.49	53.39	53.19	60.75
2015 - Measure J	63.55	66.78	67.15	67.50	53.56	53.29	60.76
2015 - Measures K & L	63.57	66.79	67.17	67.50	53.47	53.24	60.79
2015 - Measure L	64.46	67.31	67.98	67.95	54.54	54.29	61.96
2015 - Measure O	63.89	66.91	67.44	67.65	54.29	54.08	61.25
2015 - Measure P	63.92	66.92	67.48	67.66	54.39	54.14	61.30
2015 - Measure Q	63.95	66.94	67.50	67.68	54.47	54.22	61.34
2015 - Measures M & Q	63.93	66.92	67.48	67.66	54.45	54.20	61.32
2015 - Measure M	63.48	66.74	67.09	67.46	53.28	53.09	60.68
2020 - Base Case	65.34	68.14	68.94	68.84	55.47	55.30	62.86
2020 - Measure A	65.87	68.31	69.39	69.05	56.89	56.70	63.64
2020 - Measure B	66.42	68.44	69.83	69.24	58.54	58.33	64.50
2020 - Measure B*	66.52	68.45	69.91	69.27	58.85	58.64	64.65
2020 - Measure C	65.89	68.32	69.41	69.06	56.96	56.77	63.68
2020 - Measure E	65.40	68.17	68.99	68.88	55.66	55.49	62.95
2020 - Measure J	65.41	68.18	69.00	68.88	55.92	55.62	62.96
2020 - Measures K & L	65.40	68.17	69.00	68.87	55.66	55.45	62.95
2020 - Measure L	65.74	68.36	69.30	69.04	56.08	55.85	63.40
2020 - Measure O	65.94	68.33	69.44	69.09	57.12	56.92	63.75
2020 - Measure P	65.95	68.34	69.46	69.09	57.15	56.92	63.76
2020 - Measure Q	66.00	68.36	69.50	69.11	57.31	57.07	63.84
2020 - Measures M & Q	65.98	68.34	69.48	69.10	57.28	57.05	63.81
2020 - Measure M	65.32	68.12	68.92	68.83	55.45	55.28	62.83

**Table A2-7: Summary of the Area-Weighted AOT40 - Crops (in $\mu\text{g m}^{-3}$ hours)
for the OSRM Scenario Runs Undertaken for the Review of the Air Quality Strategy.**

Run Description	Area-Weighted AOT40 - Crops (in $\mu\text{g m}^{-3}$ hours)						
	All UK	Scotland	Wales	Northern Ireland	Inner London	Outer London	Rest of England
1999 - Current Year	5808	4694	6769	4778	4921	4896	6469
2000 - Current Year	6353	6240	6847	6177	3573	3685	6396
2001 - Current Year	5692	5010	6797	2863	3790	3952	6281
2002 - Current Year	4061	4183	4144	2861	2241	2475	4152
2003 - Current Year	6385	6690	7222	5824	3877	3772	6181
2010 - Base Case (NECD)	7555	7374	8545	6763	6144	5883	7634
2010 - Base Case (CAFÉ)	7456	7249	8451	6706	6094	5836	7544
2010 - Base Case (CAFÉ) – Current Composition	5925	5874	6761	5290	4680	4446	5928
2015 - Base Case (NECD)	8881	8399	9962	7845	7989	7711	9147
2015 - Base Case (CAFÉ)	8525	8003	9626	7593	7705	7407	8799
2020 - Base Case (NECD)	10342	9565	11563	9013	9528	9265	10794
2020 - Base Case (CAFÉ)	9769	8944	11028	8557	9027	8750	10231
2020 - Base Case (CAFÉ) – Current Composition	5868	5580	6757	5179	5134	4910	6004
2010 - Base Case	7456	7249	8451	6706	6094	5836	7544
2010 - Measure A	7452	7242	8443	6704	6107	5847	7542
2010 - Measure B	7455	7236	8440	6704	6147	5884	7549
2010 - Measure B*	7455	7236	8440	6704	6147	5884	7549
2010 - Measure C	7466	7244	8453	6711	6166	5903	7563
2010 - Measure E	7459	7250	8453	6708	6105	5847	7548
2010 - Measure J	7460	7250	8453	6708	6130	5860	7549
2010 - Measures K & L	7456	7249	8451	6706	6094	5836	7544
2010 - Measure L	7690	7367	8734	6860	6237	5997	7848
2010 - Measure O	7469	7245	8455	6712	6177	5913	7567
2010 - Measure P	7466	7244	8453	6711	6166	5903	7563
2010 - Measure Q	7469	7245	8455	6712	6177	5913	7567
2010 - Measures M & Q	7453	7230	8441	6700	6164	5900	7551
2010 - Measure M	7441	7235	8436	6694	6081	5823	7528
Sensitivity to Meteorology							
2010 - Base Case	7456	7249	8451	6706	6094	5836	7544
2010 - Measure B*	7455	7236	8440	6704	6147	5884	7549
2010 - Measure B* with 2000 meteorology	6979	5732	7863	5767	6561	6660	7726
2010 - Measure B* with 2002 meteorology	5049	4874	4890	3247	4595	4732	5411
2010 - Measure M	7441	7235	8436	6694	6081	5823	7528
2010 - Measure M with 2000 meteorology	6917	5728	7801	5739	6373	6472	7628
2010 - Measure M with 2002 meteorology	5024	4870	4891	3249	4480	4623	5367

**Table A2-7: Summary of the Area-Weighted AOT40 - Crops (in $\mu\text{g m}^{-3}$ hours)
for the OSRM Scenario Runs Undertaken for the Review of the Air Quality Strategy (Continued).**

Run Description	Area-Weighted AOT40 - Crops (in $\mu\text{g m}^{-3}$ hours)						
	All UK	Scotland	Wales	Northern Ireland	Inner London	Outer London	Rest of England
2015 - Base Case	8525	8003	9626	7593	7705	7407	8799
2015 - Measure A	8477	7915	9541	7533	7893	7581	8778
2015 - Measure B	8409	7798	9430	7440	8137	7805	8747
2015 - Measure B*	8404	7790	9422	7433	8149	7816	8743
2015 - Measure C	8496	7916	9555	7540	7998	7678	8809
2015 - Measure E	8534	8004	9633	7597	7753	7452	8814
2015 - Measure J	8535	8004	9633	7597	7821	7484	8815
2015 - Measures K & L	8538	8006	9635	7601	7758	7446	8819
2015 - Measure L	8763	8110	9910	7714	7913	7617	9122
2015 - Measure O	8503	7917	9560	7543	8039	7717	8821
2015 - Measure P	8507	7919	9563	7546	8052	7717	8827
2015 - Measure Q	8515	7919	9569	7549	8094	7756	8839
2015 - Measures M & Q	8497	7903	9552	7536	8075	7738	8819
2015 - Measure M	8508	7987	9609	7580	7688	7390	8780
2020 - Base Case	9769	8944	11028	8557	9027	8750	10231
2020 - Measure A	9607	8703	10780	8344	9383	9068	10128
2020 - Measure B	9331	8345	10400	7997	9699	9348	9918
2020 - Measure B*	9273	8271	10321	7925	9761	9402	9872
2020 - Measure C	9612	8702	10783	8345	9424	9106	10137
2020 - Measure E	9787	8943	11040	8561	9136	8851	10260
2020 - Measure J	9785	8944	11039	8561	9251	8894	10257
2020 - Measures K & L	9782	8945	11036	8561	9090	8795	10251
2020 - Measure L	9861	8970	11128	8588	9163	8864	10366
2020 - Measure O	9622	8698	10789	8346	9513	9188	10157
2020 - Measure P	9621	8699	10788	8346	9487	9150	10153
2020 - Measure Q	9630	8695	10793	8347	9576	9232	10172
2020 - Measures M & Q	9610	8678	10774	8333	9552	9209	10149
2020 - Measure M	9749	8926	11009	8543	9005	8729	10208

**Table A2-8: Summary of the Area-Weighted AOT40 - Forests (in $\mu\text{g m}^{-3}$ hours)
for the OSRM Scenario Runs Undertaken for the Review of the Air Quality Strategy.**

Run Description	Area-Weighted AOT40 - Forests (in $\mu\text{g m}^{-3}$ hours)						
	All UK	Scotland	Wales	Northern Ireland	Inner London	Outer London	Rest of England
1999 - Current Year	10183	9652	12175	8372	7644	7552	10456
2000 - Current Year	10100	9907	11547	9672	5754	5717	10094
2001 - Current Year	9223	8101	11757	5922	6839	6949	9909
2002 - Current Year	8848	9286	9288	7811	5972	6042	8701
2003 - Current Year	11830	11011	13854	11349	8423	8432	12113
2010 - Base Case (NECD)	13938	12423	16151	12461	12024	11733	14706
2010 - Base Case (CAFÉ)	13634	12198	15772	12462	11837	11559	14329
2010 - Base Case (CAFÉ) – Current Composition	11321	10183	13186	10416	9807	9549	11847
2015 - Base Case (NECD)	16225	14149	18643	14131	15053	14766	17356
2015 - Base Case (CAFÉ)	15608	13674	17997	13794	14297	14017	16628
2020 - Base Case (NECD)	18780	16173	21517	16047	17507	17269	20250
2020 - Base Case (CAFÉ)	17855	15438	20566	15371	16359	16137	19190
2020 - Base Case (CAFÉ) – Current Composition	11785	10301	13813	10290	10694	10466	12552
2010 - Base Case	13634	12198	15772	12462	11837	11559	14329
2010 - Measure A	13644	12199	15781	12458	11864	11584	14347
2010 - Measure B	13671	12207	15806	12461	11941	11657	14388
2010 - Measure B*	13671	12207	15806	12461	11941	11657	14388
2010 - Measure C	13680	12214	15815	12472	11972	11688	14398
2010 - Measure E	13641	12201	15779	12464	11857	11579	14339
2010 - Measure J	13643	12202	15781	12466	11899	11601	14342
2010 - Measures K & L	13634	12198	15772	12462	11837	11559	14329
2010 - Measure L	14360	12692	16657	12803	12223	11972	15215
2010 - Measure O	13687	12216	15821	12474	11992	11706	14407
2010 - Measure P	13680	12214	15815	12472	11972	11688	14398
2010 - Measure Q	13687	12216	15821	12474	11992	11706	14407
2010 - Measures M & Q	13652	12183	15780	12450	11967	11681	14371
2010 - Measure M	13599	12165	15731	12437	11813	11534	14294
Sensitivity to Meteorology							
2010 - Base Case	13634	12198	15772	12462	11837	11559	14329
2010 - Measure B*	13671	12207	15806	12461	11941	11657	14388
2010 - Measure B* with 2000 meteorology	11286	9464	13456	9671	10118	10041	12235
2010 - Measure B* with 2002 meteorology	10547	10368	10729	8587	9568	9497	10898
2010 - Measure M	13599	12165	15731	12437	11813	11534	14294
2010 - Measure M with 2000 meteorology	11194	9445	13366	9620	9859	9782	12095
2010 - Measure M with 2002 meteorology	10473	10342	10699	8569	9321	9276	10782

**Table A2-8: Summary of the Area-Weighted AOT40 - Forests (in $\mu\text{g m}^{-3}$ hours)
for the OSRM Scenario Runs Undertaken for the Review of the Air Quality Strategy (Continued).**

Run Description	Area-Weighted AOT40 - Forests (in $\mu\text{g m}^{-3}$ hours)						
	All UK	Scotland	Wales	Northern Ireland	Inner London	Outer London	Rest of England
2015 - Base Case	15608	13674	17997	13794	14297	14017	16628
2015 - Measure A	15717	13671	18070	13715	14726	14450	16827
2015 - Measure B	15843	13647	18141	13598	15349	15067	17072
2015 - Measure B*	15848	13643	18142	13589	15385	15102	17085
2015 - Measure C	15771	13691	18119	13732	14915	14631	16905
2015 - Measure E	15634	13684	18021	13802	14381	14098	16665
2015 - Measure J	15635	13685	18021	13804	14496	14154	16666
2015 - Measures K & L	15652	13698	18045	13810	14403	14100	16687
2015 - Measure L	16382	14176	18927	14132	14885	14588	17592
2015 - Measure O	15792	13698	18139	13739	14989	14704	16936
2015 - Measure P	15814	13713	18165	13747	15026	14718	16962
2015 - Measure Q	15835	13720	18184	13753	15101	14791	16992
2015 - Measures M & Q	15792	13681	18134	13726	15064	14754	16947
2015 - Measure M	15565	13634	17948	13766	14264	13983	16584
2020 - Base Case	17855	15438	20566	15371	16359	16137	19190
2020 - Measure A	17963	15287	20542	15119	17344	17097	19503
2020 - Measure B	17909	14927	20264	14673	18582	18259	19697
2020 - Measure B*	17879	14841	20182	14577	18830	18487	19712
2020 - Measure C	17979	15290	20554	15124	17421	17169	19528
2020 - Measure E	17906	15452	20612	15388	16554	16323	19267
2020 - Measure J	17900	15453	20605	15389	16741	16396	19255
2020 - Measures K & L	17900	15458	20614	15388	16488	16236	19253
2020 - Measure L	18171	15612	20923	15507	16729	16454	19604
2020 - Measure O	18014	15294	20581	15134	17589	17328	19583
2020 - Measure P	18016	15301	20590	15136	17556	17272	19583
2020 - Measure Q	18050	15305	20614	15146	17724	17431	19637
2020 - Measures M & Q	18001	15264	20561	15115	17673	17381	19582
2020 - Measure M	17805	15393	20510	15340	16315	16093	19137

Appendix 3

Description of UK Photochemical Trajectory Model

CONTENTS

Appendix 3 - UK Photochemical Trajectory Model

The UK Photochemical Trajectory model has been developed to describe regional scale ozone, PAN and hydrogen peroxide formation over Europe [Hough and Derwent, 1987; Derwent and Jenkin, 1989; Derwent and Davies, 1994; Derwent *et al.*, 1998, 2004]. The same basic model formulation is adopted and the chemical development in air parcels is followed as they travel across from continental Europe to the UK in a broadly westerly direction. The air parcel extends from the earth's surface up to the top of boundary layer and its horizontal dimensions are 10 km x 10 km. The depth of the model boundary layer starts off at 300 m at 06.00 hr and rises throughout the morning, reaching a height of 1300 m by 14.00 hr [Smith and Hunt, 1978].

The chemical development of the species in the air parcel is described by a series of differential equations of the form of equation (6.1) below:

$$\frac{dC_i}{dt} = P_i + \frac{E_i}{h} - L_i \cdot C_i - \frac{V_i C_i}{h} - (C_i - B_i) \frac{1}{h} \frac{dh}{dt} \quad (\text{A3.1})$$

where C_i is the concentration of species i in the air parcel,
 P_i is the instantaneous production from photochemistry,
 E_i is the local emission rate from pollution sources, and,
 h is the time-dependent boundary layer depth,
 $L_i \cdot C_i$ is the instantaneous loss rate by photochemistry,
 V_i is the species-dependent dry deposition velocity,
 B_i the background concentration of the species aloft.

The mechanism used has been compared with 25 other chemical mechanisms, available in the literature, under the hydrocarbon-limited conditions used in this study, and close agreement between the peak ozone concentrations has been recorded [Derwent, 1990; 1993]. Included in this large range of mechanisms are several which have either been developed from smog chamber studies or have highly compact and parameterised representations of the chemical processes occurring.

A3.1. Treatment of Emissions

The model utilises the following four coordinate systems to identify the location of the air parcel at any point in time:

1. latitude and longitude (also used to fix solar zenith angle),
2. UN ECE EMEP 150km x 150km coordinates,
3. EC CORINAIR 50km x 50km coordinates,
4. UK Ordnance Survey National Grid 10km x 10km eastings and northings.

From the location of the air parcel in each emission grid, the local instantaneous emission rates, E_i , in molecule $\text{cm}^{-2} \text{s}^{-1}$ were calculated for each pollutant, i , assuming that all emission rates were constant throughout the year. The speciation of the total VOC emissions into 95 individual hydrocarbons (comprising 24 alkanes, 11 alkenes, 1 alkyne, 17 aromatic compounds, 8 alcohols, 7 aldehydes, 4 ketones, 3 organic acids, 2 ethers, 6 esters, 9 chlorinated hydrocarbons and 3 other oxygenated compounds) and methane was obtained using species emission profiles for each of the nine major source categories identified in the UK non-methane VOC emission inventory [PORG, 1993]:

- chemical and industrial processes
- stationary combustion
- natural gas leakage
- disposal of industrial and residential waste
- use of solvents
- petrol-engined motor vehicle exhaust
- diesel-engined motor vehicle exhaust
- petrol evaporation from motor vehicles
- petrol evaporation from storage, distribution and sale

The overall percentage emission by mass of each hydrocarbon was obtained by multiplying the species profiles by the UK total VOC emissions from that source category and summing over all the

above nine source categories. In the absence of similar detail for other European countries, the same speciation has been adopted throughout the model domain.

An additional emission term was added to equation (A3.1) for isoprene to represent the natural biogenic emissions from European forests and agricultural crops. These emission estimates were prepared on a 150km x 150km grid by Simpson [1994] using meteorological data from numerical weather prediction models to give temperatures and solar radiation on an hourly basis, together with the BEIS approach [Pierce and Waldruff, 1991].

A3.2. Chemical Mechanism

The chemical mechanism employed in the photochemical trajectory model uses the Master Chemical Mechanism developed by Derwent *et al.* [1998, 2004] to describe the oxidation of methane, 123 additional hydrocarbons, carbon monoxide, sulphur dioxide and NO_x. The mechanism was constructed using a protocol formulated by Jenkin, Saunders and Pilling [1997] and Saunders *et al.* [2003]. It was written specifically to describe the contribution to ozone and PAN formation from a large number of individual hydrocarbon species and their degradation products.

The chemical mechanism contains a number of identifiable and separate elements:

- the inorganic chemistry of the simple atoms and radicals derived from O, H, N, S and CO. These comprise 48 thermal chemical reactions which have been identified in previous modelling studies as important. All rate coefficients have been taken from recent evaluations [Atkinson *et al.*, 1992; De More *et al.*, 1992; De More *et al.*, 1994] and their full temperature and pressure dependences have been treated.
- the photolysis reactions of the photochemically-labile species. These comprise 2,395 time-of-day dependent photochemical processes involving inorganic species, aldehydes, ketones and organic hydroperoxides. For the inorganic species and organic species containing C₃ or less, quantum yield and cross-section data were taken from the recent evaluations [Atkinson *et al.*, 1992; De More *et al.*, 1992; De More *et al.*, 1994]. Additional information was obtained from several publications containing more recent data, particularly for larger molecules [Foreteg, Dobe and Berces, 1978; DeSai *et al.*, 1987; Martinez *et al.*, 1992; Raber and Moortgat, 1994]. Generic photolysis rates were used for the vast majority of the photochemical processes.

Solar actinic fluxes were calculated using a two-stream multiple scattering approach from the solar spectrum at the top of the atmosphere [Hough, 1988]. The J-values for each process at each zenith angle were obtained by convoluting the solar actinic fluxes with the quantum yield and absorption cross-sections over the wavelength range from 200-700 nm.

$$J(X) = \int \phi(\lambda, X) \phi(\lambda) I(\lambda) d\lambda \quad (\text{A3.2})$$

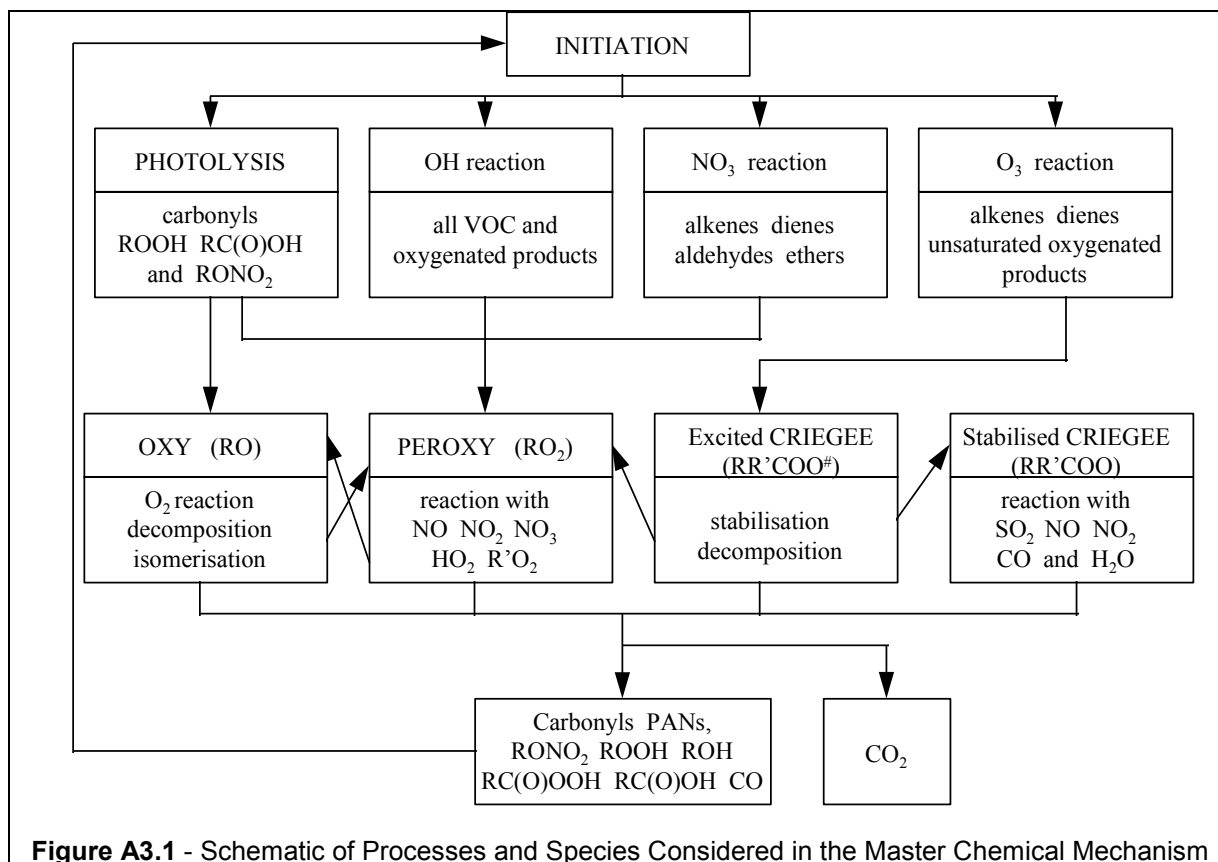
For daylight hours (*i.e.*, for solar zenith angles less than 90°), the time-of-the-day dependence of the photolysis rates was described by calculating the instantaneous solar zenith angle, X, and using expressions of the form (A3.3) below to estimate the photolysis rate, J, for a particular photochemical process:

$$J = I [\cos(X)]^m \exp[-n \sec(X)] \quad (\text{A3.3})$$

During the night (*i.e.*, for solar zenith angles greater than 90°), the photolysis frequencies were set to a low value, close to zero, so that these processes were effectively “switched off”.

The coefficients *I*, *m* and *n* were determined for each process by fitting the J-values calculated using the two stream scattering model of Hough [1988] to the functional form given in expression (III). The difference between the fitted and calculated photolysis frequencies was less than 0.5% for solar zenith angles close to 30° but increased to 5% for a solar zenith angle of 70°. The difference was significantly larger for those photolysis processes having a strong dependence on the solar zenith angle. In these cases however, the photolysis frequencies calculated for solar zenith angles close to 90° were many orders of magnitude smaller than those calculated for smaller zenith angles. With such low photolysis frequencies, these processes will make a negligible contribution to the overall photochemistry.

- the atmospheric degradation of methane and 123 additional hydrocarbons. The oxidation of each hydrocarbon is followed to its complete conversion to CO₂ (see Figure A3.1). The approach used in the Master Chemical Mechanism is not to consider the degradation of all conceivable products or processes but to define criteria for which of these should be included or omitted. Reaction rates are adjusted as appropriate to maintain the overall carbon balance and oxidation rates.



The mechanism comprise 13,500 thermal chemical reactions following the photolysis or attack by hydroxyl radicals (OH), nitrate radicals (NO₃) or ozone on the emitted organic species or their degradation products. The rates of these initiation reactions were either based on laboratory measurements, as reviewed by Atkinson [Atkinson, 1989, 1990, 1994], calculated using structure-reactivity methods developed by Atkinson [1986, 1987] or simply assigned generic values derived from compounds containing the same functionalities for which kinetic and mechanistic data are available.

A strategic simplification is introduced in the treatment of the peroxy radical permutation reactions (RO₂ + R'O₂). The treatment of the peroxy radical chemistry used in the master chemical mechanism is to define a pool of peroxy radicals with which the individual peroxy radicals react. The concentration of the peroxy radical pool is simply the sum of the concentrations of the individual peroxy radicals and is taken to be constant over a given timestep. The products formed are assumed to come from the individual peroxy radical and not the peroxy radical pool. This approach avoids the significant increase in the number of peroxy reactions to consider when a large number of peroxy radicals are present and avoids the possibility of artificially enhancing the concentrations of products and hence the oxidation rate.

The unstable peroxy nitrates, which are formed by the reaction of peroxy radicals with NO₂, are omitted as they have short lifetimes (typically minutes) for the temperatures, close to 288K, which are observed in the boundary layer. They therefore rapidly decompose to give back the original reactants. However, the reactions of acyl peroxy radicals with NO₂ to give peroxy acyl nitrates, which have longer atmospheric lifetimes, were included.

Version 3.1 of the Master Chemical Mechanism has recently been released and is available from <http://mcm.leeds.ac.uk/MCM/>. The major updates in MCMv3.1 include an extensive update to the aromatic mechanisms, which are important in the photochemistry of the polluted boundary layer, and

also the addition of a number of new degradation schemes of some important biogenic species. MCM v3.1 now contains 135 primary emitted VOCs, including isoprene and the two terpenes, α -pinene and β -pinene. The mechanism contains ca. 5,900 species and 13,500 reactions.

A3.3. Numerical Methods

The resulting system of 5,900 simultaneous stiff differential equations was integrated with a variable order Gear's method [FACSIMILE, Curtis and Sweetenham, 1987] on a UNIX workstation. The initial concentrations for most species were set to zero. For a small number of species, initial concentrations were set at realistic tropospheric baseline levels for a polluted boundary layer situation. These were: NO 2 ppb, NO₂ 6 ppb, SO₂ 5 ppb, CO 120 ppb, methane 1700 ppb, formaldehyde 2 ppb, ozone 50 ppb and hydrogen 550 ppb. Aloft concentrations for each species, B_i , were set at the levels reached in the model during the previous early evening and held constant during the intervening night. Aloft concentrations for the first day were taken to be the initial model concentrations.

A3.4. The Base Case Model

In the base case model, the highly idealised anticyclonic meteorological situation of easterly winds, leading to a broad westerly air flow carrying photochemically-aged polluted air masses out of Europe towards the British Isles, was adopted. Windspeeds and directions of 4 m s⁻¹ and 100° (from grid north) were taken across the entire model domain. Air parcels arriving in the south west of the British Isles on the afternoon of the fifth day of photochemistry had started off on the first day in Austria. By the mid-afternoon of the second day, they had passed over south east Germany, north west Germany on the third day, Belgium and northern France on the fourth and over south east England on the fifth day. In contrast, air parcels arriving in central Scotland on the afternoon of the fifth day had started off in Poland and travelled over the Baltic and North Seas and over Denmark. This highly idealised meteorological situation is a broad generalisation of the Germany-Ireland emission scenario case that has been employed in previous studies [Derwent and Jenkin, 1989; Derwent and Davies, 1994; Derwent *et al.*, 1996, 1998, 2004]. The time-integrated NO_x and hydrocarbon emissions amounted to 103 and 115 kg km⁻² respectively, in this base case calculation.

This base case model experiment does not represent the conditions prevailing during a particular photochemical episode. Such an exercise would require the detailed preparation of emissions and meteorological fields which is far beyond our present capabilities. Some of the difficulties experienced in formulating episode-specific data for this photochemical trajectory model have been described elsewhere [Derwent, 1989]. The emission scenarios have been carefully chosen to reflect some form of worst case situation. The trajectory path was selected from the review of meteorological analyses prepared for the PHOXA study covering the period 1980-1985 [Bultjes, 1987; Pankrath, 1989]. Such trajectory paths are frequently associated with elevated ozone concentrations over the Netherlands and the United Kingdom. The scenario is not the worst ever case but is meant to be relevant for the study of regional scale ozone formation and its control.

A3.4. Photochemical Ozone Creation Potentials

The Photochemical Trajectory Model has been used to calculate Photochemical Ozone Creation Potentials (POCPs) for the 135 volatile organic compounds considered in the Master Chemical Mechanism. POCPs are calculated from the results of separate model runs, each a variant on the base case scenario. In each separate model run, an additional emission of 1 ktonne per 50x50 km² per annum was added to the emission of the VOC of interest across the entire model domain. The emission stimulated additional ozone formation over the base case and this incremental ozone amount could be defined for a particular point along the trajectory or integrated over the entire trajectory length. These ozone increments were compared with the corresponding increments for a reference hydrocarbon, taken to be ethylene (ethene). The POCP for a particular hydrocarbon, i , was accordingly defined in equation (A3.4) as:

$$\text{POCP}_i = \frac{\text{Ozone Increment with the } i\text{th hydrocarbon}}{\text{Ozone Increment with ethylene}} \times 100 \quad (\text{A3.4})$$

for the same incremental integrated emission. Ethylene is assigned a POCP of 100.

A3.4. References

- R Atkinson (1987) **A Structure-activity Relationship for the Estimation of Rate Constants for the Gas-phase Reactions of OH Radicals with Organic Compounds**. International Journal of Chemical Kinetics, **19**, 799-828.
- R Atkinson (1989) **Kinetics and Mechanisms of the Gas-phase Reactions of the Hydroxyl Radical with Organic Compounds**. Journal of Physical and Chemical Reference Data, Monograph 1.
- R Atkinson (1990) **Gas-phase Tropospheric Chemistry of Organic Compounds: a Review**. Atmospheric Environment, **24A**, 1-41.
- R Atkinson (1991) **Kinetics and Mechanisms of the Gas-phase Reactions of the Nitrate Radical with Organic Compounds**. Journal of Physical and Chemical Reference Data, **20**, 459.
- R Atkinson (1994) **Gas-phase Tropospheric Chemistry of Organic Compounds**. Journal of Physical and Chemical Reference Data, Monograph 2.
- R Atkinson, D L Baulch, R A Cox, R F Hampson, J A Kerr and J Troe (1992) **Evaluated Kinetic and Photochemical Data for Atmospheric Chemistry: Supplement IV**. Journal of Physical and Chemical Reference Data, **21**, 1125-1592.
- P J H Buitjes (1987) **Photochemical Oxidant and Acid Deposition Model (PHOXA). Calculation and Evaluation of the Photochemical Episode of July 22-26 1980**. TNO Report 87-278. Apeldoorn, The Netherlands.
- A R Curtis and W P Sweetenham (1988) **FACSIMILE/CHEKMAT Users Manual**. AERE-R12805, Harwell Laboratory, Oxfordshire, UK.
- W B DeMore, S P Sander, D M Golden, R F Hampson, M J Kurylo, C J Howard, A R Ravishankara, C E Kolb and M J Molina (1992) **NASA Panel for Data Evaluation. Chemical Kinetic and Photochemical Data for Use in Stratospheric Modelling**, Rep. JPL 92-20, Jet Propulsion Laboratory, Pasadena, California, USA.
- W B DeMore, S P Sander, D M Golden, R F Hampson, M J Kurylo, C J Howard, A R Ravishankara, C E Kolb and M J Molina (1994) **NASA Panel for Data Evaluation. Chemical Kinetic and Photochemical Data for Use in Stratospheric Modelling**, Rep. JPL 94-26, Jet Propulsion Laboratory, Pasadena, California, USA.
- R G Derwent (1989) **A Comparison of Model Photochemical Ozone Formation Potential with Observed Regional Scale Ozone Formation over the United Kingdom in April 1987**. Atmospheric Environment **23**, 1361-1371.
- R G Derwent (1990) **Evaluation of a Number of Chemical Mechanisms for their Application in Models describing the Formation of Photochemical Ozone in Europe**. Atmospheric Environment **24A**, 2615-2624.
- R G Derwent (1993) **Evaluation of the Chemical Mechanism employed in the EMEP Photochemical Oxidant Model**. Atmospheric Environment **27A**, 277-279.
- R G Derwent and M E Jenkin (1991) **Hydrocarbons and the Long-range Transport of Ozone and PAN across Europe**. Atmospheric Environment, **25A** 1661-1678.
- R G Derwent and T J Davies (1994) **Modelling the Impact of NO_x or Hydrocarbon Control of Photochemical Ozone Formation in Europe**. Atmospheric Environment, **28**, 2039-2052.
- R G Derwent, M E Jenkin and S M Saunders (1996) **Photochemical Ozone Creation Potentials for a Large Number of Reactive Hydrocarbons under European Conditions**. Atmospheric Environment, **30**, 181-199.
- R G Derwent, M E Jenkin, S M Saunders and M J Pilling (1998) **Photochemical Ozone Creation Potentials for Organic Compounds in North West Europe calculated with a Master Chemical Mechanism**. Atmospheric Environment, **32** 2429-2441.
- R.G. Derwent, M.E. Jenkin, S.M. Saunders and M.J. Pilling. (1998) **Photochemical Ozone Creation Potentials for Organic Compounds in North West Europe Calculated with a Master Chemical Mechanism**. Atmospheric Environment, **32**, 2419-2441.

- R. G. Derwent, Jenkin M. E., Saunders S. M., Pilling M. J. and Passant N. R. (2004) **Multi-day Ozone Formation of Alkenes and Carbonyls investigated with a Master Chemical Mechanism under European conditions.** Atmospheric Environment, **39**, 627-635.
- J DeSai, J Heicklen, A Bahta and R Simonaitis (1987) **The Photo-oxidation of i-C₃H₇CHO Vapour.** Journal of Photochemistry and Photobiology. **34**, 137-164.
- S Förgeteg, S Dóbe and T Bérces (1978) **Effect of Pressure on the Primary Photochemical Processes of n-butylaldehyde at 313 nm.** Reaction Kinetics and Catalysis Letters **9**, 331-336.
- A M Hough and R G Derwent (1987) **Computer Modelling Studies of the Distribution of Photochemical Ozone Production between Different Hydrocarbons.** Atmospheric Environment, **21**, 2015-2033.
- A.M. Hough (1988) **The Calculation of Photolysis Rates for Use in Global Tropospheric Modelling Studies.** AERE-R13259, Her Majesty's Stationary Office, London, UK.
- P D Lightfoot, R A Cox, J N Crowley, M Destriau, G D Hayman, M E Jenkin, G K Moortgat and F Zabel (1992) **Organic Peroxy Radicals: Spectroscopy, Kinetics and Tropospheric Chemistry.** Atmospheric Environment, **26A**, 1805-1961.
- M E Jenkin, S M Saunders and M J Pilling (1997) **The Tropospheric Degradation of Volatile Organic Compounds: a Protocol for Mechanism Development.** Atmospheric Environment, **31** 81-104.
- R D Martinez, A A Buitrago, N W Howell, C H Hearn and J A Joens (1992) **The Near UV Absorption Spectra of Several Aliphatic Aldehydes and Ketones at 300K.** Atmospheric Environment, **26A**, 785-792.
- J Pankrath (1989) **Photochemical Oxidant Model Application within the Framework of Control Strategy Development in the Dutch/German programme PHOXA In Atmospheric Ozone Research and its Policy Implications;** Elsevier Science Publishers BV: Amsterdam, The Netherlands, p 633.
- T E Pierce and P S Waldruff (1991) **PC-BEIS: A Personal Computer Version of the Biogenic Emission Inventory System.** Journal of the Air and Waste Management Association, **41**, 937-941.
- PORG (1993) **Ozone in the United Kingdom.** Third Report of UK Photochemical Oxidants Review Group: Harwell Laboratory, Oxfordshire, UK.
- W H Raber and G K Moortgat (1994) **Photo-oxidation of Selected Carbonyl Compounds in Air: methylethylketone, methylvinyl ketone, methacrolein and methyl glyoxal** In *Current Problems and Progress in Atmospheric Chemistry*; Barker, J. R., Ed.; In Press, 1994.
- Saunders, S. M., Jenkin, M. E., Derwent, R. G. and Pilling, M. J. (2003) **Protocol for the Development of the Master Chemical Mechanism, MCM v3 (Part A): Tropospheric Degradation of Non-aromatic Volatile Organic Compounds.** Atmospheric Chemistry and Physics, **3**, 161-180.
- D Simpson (1994). **Biogenic VOC Emissions in Europe Part 1: Emissions and Uncertainties.** EMEP/MSC-W Note 5/94. Norwegian Meteorological Institute, Oslo, Norway.
- F B Smith and R D Hunt (1978) **Meteorological Aspects of the Transport of Pollution over Long Distances.** Atmospheric Environment, **12**, 461-477.

Appendix 4

Percentage Contribution to Emissions,
Incremental Reactivity and Photochemical
Ozone Formation by VOC Source Sector.

CONTENTS

Percentage Contribution to Emissions, Incremental Reactivity and the Photochemical Ozone Formation by VOC Source Sector along a 5-day Trajectory.

	Source Category	Percentage of total Emissions	Incremental Reactivity	Ozone Production, ppb		Source Category	Percentage of total Emissions	Incremental Reactivity	Ozone Production, ppb
1	Road transport (cars without catalyts)_Petrol	11.524	41.387	4.769	30	Non-aerosol cosmetics & toiletries	0.938	27.423	0.257
2	Road transport (cars with catalyts)_Petrol	5.264	41.578	2.189	31	Oil terminal storage	0.806	31.340	0.252
3	Onshore loading of crude oil	5.098	31.532	1.608	32	Offshore oil & gas (venting)	0.799	31.381	0.251
4	Chemical industry	5.364	28.337	1.520	33	Non-aerosol automotive products	1.965	12.708	0.250
5	Offshore loading of crude oil	3.739	31.026	1.160	34	Other industrial (off-road)_Gas oil	0.535	46.041	0.246
6	Spirit manufacture (maturation)	3.401	30.890	1.051	35	Industrial coatings (wood)	0.852	28.692	0.244
7	Refineries (process fugitives)	2.091	41.291	0.863	36	Wood impregnation (LOSP)	0.678	35.463	0.241
8	Petrol stations (vehicle refuelling unleaded petrol)	2.709	31.327	0.849	37	Road transport (LGVs)_DERV	0.508	44.185	0.224
9	Other solvent use	3.370	20.229	0.682	38	Industrial coatings (high performance)	0.531	42.219	0.224
10	Gas leakage	4.648	13.527	0.629	39	Industrial coatings (automotive)	0.651	31.436	0.205
11	Decorative paint (trade decorative)	1.811	31.395	0.569	40	Road construction	0.571	35.135	0.201
12	Industrial coatings (metal & plastic)	1.627	34.835	0.567	41	Refineries (tankage)	0.399	42.151	0.168
13	Aerosols (cosmetics and toiletries)	1.883	28.638	0.539	42	Aerosols (household products)	0.586	28.651	0.168
14	Decorative paint (retail decorative)	1.669	31.313	0.523	43	Domestic combustion_Natural gas	0.615	26.959	0.166
15	Industrial adhesives	1.822	28.569	0.520	44	Road transport (4-stroke motorcycles, >50cc)_Petrol	0.387	42.806	0.166
16	Road transport (articulated HGVs)_DERV	1.084	46.014	0.499	45	Industrial coatings (metal packaging)	0.471	34.302	0.161
17	Other industrial (off-road)_Petrol	1.087	43.762	0.476	46	Printing (overprint varnishes)	0.613	26.085	0.160
18	Road transport (rigid HGVs)_DERV	1.013	46.151	0.468	47	Industrial coatings (vehicle refinishing)	0.499	31.941	0.159
19	Aerosols (car care products)	1.465	28.187	0.413	48	Coating manufacture (paint)	0.414	36.623	0.152
20	Road transport (LGVs without catalyts)_Petrol	0.923	41.905	0.387	49	Road transport (buses)_DERV	0.331	44.745	0.148
21	Surface cleaning (hydrocarbons)	1.046	36.186	0.379	50	Petrol stations (delivery of unleaded petrol)	0.433	31.723	0.137
22	Surface cleaning (trichloroethylene)	1.496	24.720	0.370	51	Film coating	0.389	35.190	0.137
23	Refineries (drainage)	0.826	41.865	0.346	52	Offshore flaring	0.881	14.633	0.129
24	Offshore oil & gas industry	1.100	30.931	0.340	53	Road transport (2-stroke motorcycles, >50cc)_Petrol	0.290	43.079	0.125
25	Domestic combustion_Coal	1.015	33.415	0.339	54	Road transport (2-stroke motorcycles, <50cc)_Petrol	0.283	43.298	0.122
26	Printing (flexible packaging)	1.186	27.314	0.324	55	Domestic combustion_Wood	0.356	31.968	0.114
27	Non-aerosol household products	0.849	37.920	0.322	56	Landfill	0.399	28.419	0.113
28	Paint thinners	0.880	35.940	0.316	57	Agricultural power units_Gas oil	0.248	45.427	0.112
29	House & garden machinery_Petrol	2.142	14.592	0.313	58	Agrochemicals use	0.256	42.875	0.110

	Source Category	Percentage of total Emissions	Incremental Reactivity	Ozone Production, ppb		Source Category	Percentage of total Emissions	Incremental Reactivity	Ozone Production, ppb
59	Industrial coatings (commercial vehicles)	0.333	31.641	0.105	92	Printing (heatset web offset)	0.052	46.983	0.024
60	Road transport (cars)_DERV	0.214	43.639	0.093	93	Blast furnaces	0.096	23.642	0.023
61	Power stations_Natural gas	0.406	21.867	0.089	94	Refineries (flares)	0.150	14.701	0.022
62	Petrol terminal storage (unleaded petrol)	0.254	31.900	0.081	95	Petrol terminals (tanker loading of unleaded petrol)	0.069	31.764	0.022
63	Industrial coatings (marine)	0.174	46.533	0.081	96	Paper coating	0.222	9.801	0.022
64	Petrol station storage tanks (unleaded petrol)	0.248	31.422	0.078	97	Domestic combustion_Coke	0.052	39.926	0.021
65	Domestic combustion_SSF	0.178	40.868	0.073	98	Printing (newspapers)	0.060	34.248	0.020
66	Seed oil extraction	0.171	39.544	0.068	99	Power stations_landfill gas	0.104	19.328	0.020
67	Petrol stations (vehicle refuelling with leaded petrol)	0.202	33.361	0.067	100	Other food (malting)	0.127	15.534	0.020
68	Bread baking	0.210	29.962	0.063	101	Printing (other flexography)	0.073	26.795	0.020
69	Printing (screen printing)	0.158	38.875	0.061	102	Industrial coatings (aircraft)	0.064	30.317	0.020
70	Industrial coatings (agricultural & construction)	0.169	35.094	0.059	103	Printing (publication gravure)	0.057	33.374	0.019
71	Surface cleaning (other)	0.224	25.498	0.057	104	Aircraft (domestic TOL)_Aviation turbine fuel	0.054	34.971	0.019
72	Other rubber products	0.146	37.415	0.055	105	Miscellaneous_Natural gas	0.067	27.764	0.019
73	Animal carcase incineration	0.147	35.777	0.052	106	Coating manufacture (glue)	0.065	28.501	0.018
74	Petrol stations (spillages of unleaded petrol)	0.165	31.518	0.052	107	Refineries_OPG	0.061	30.030	0.018
75	Aircraft (International TOL_Aviation turbine fuel)	0.141	35.599	0.050	108	Shipping (naval)_Gas oil	0.045	40.240	0.018
76	Coastal shipping_Gas oil	0.124	39.967	0.049	109	Aircraft (military)_Aviation turbine fuel	0.045	36.364	0.017
77	Tyre manufacture	0.127	36.828	0.047	110	Spirit manufacture (fermentation)	0.049	30.713	0.015
78	Domestic combustion_Anthracite	0.114	40.076	0.046	111	Other industrial combustion_Wood	0.044	32.842	0.014
79	Road transport (coaches)_DERV	0.096	46.014	0.044	112	Public services_Natural gas	0.050	28.010	0.014
80	Other food (cakes, biscuits and cereals)	0.141	29.784	0.042	113	Railways (Freight)_Gas oil	0.030	46.178	0.014
81	Other industrial combustion_Natural gas	0.150	27.819	0.042	114	Domestic adhesives	0.049	27.928	0.014
82	Brewing (barley malting)	0.243	15.684	0.038	115	Iron & steel industry_Coke-oven gas	0.028	48.908	0.013
83	Coating manufacture (ink)	0.108	34.152	0.037	116	Printing (print chemicals)	0.082	15.411	0.013
84	Power stations_Coal	0.084	42.192	0.035	117	Dry cleaning	0.349	3.180	0.011
85	Railways (intercity)_Gas oil	0.077	45.659	0.035	118	Petrol stations (delivery of leaded petrol)	0.032	33.088	0.011
86	Textile coating	0.181	17.595	0.032	119	Agricultural power units_Petrol	0.024	43.557	0.011
87	Industrial coatings (drum)	0.063	47.516	0.030	120	Petroleum processes	0.665	1.570	0.010
88	Industrial adhesives (pressure sensitive tapes)	0.100	28.433	0.028	121	Autogenerators_Natural gas	0.049	21.280	0.010
89	Road transport (LGVs with catalysts)_Petrol	0.065	40.704	0.027	122	Coke production_Coke-oven gas	0.026	40.650	0.010
90	Spirit manufacture (barley malting)	0.154	16.066	0.025	123	Offshore oil & gas industry_Natural gas	0.036	27.655	0.010
91	Refineries (road/rail loading of unleaded petrol)	0.077	31.805	0.024	124	Chemical waste incineration	0.018	53.808	0.010

	Source Category	Percentage of total Emissions	Incremental Reactivity	Ozone Production, ppb		Source Category	Percentage of total Emissions	Incremental Reactivity	Ozone Production, ppb
125	Offshore oil & gas (well testing)	0.064	14.483	0.009	157	Other industrial combustion Burning oil	0.008	23.874	0.002
126	Wood impregnation (creosote)	0.183	4.723	0.009	158	Blast furnaces_Blast furnace gas	0.007	26.959	0.002
127	Spirit manufacture (spent grain drying)	0.053	15.902	0.008	159	Coke production	0.014	13.718	0.002
128	Spirit manufacture (distillation)	0.024	30.822	0.008	160	Power stations_MSW	0.005	35.094	0.002
129	Fishing vessels_Gas oil	0.018	40.431	0.007	161	Refineries (road/rail loading of leaded petrol)	0.006	32.596	0.002
130	Wood products manufacture	0.017	41.182	0.007	162	Leather degreasing	0.010	18.018	0.002
131	Leather coating	0.027	25.935	0.007	163	Petrol terminals (tanker loading of leaded petrol)	0.005	33.033	0.002
132	Industrial coatings (coil)	0.025	24.584	0.006	164	Gasification processes	0.009	18.987	0.002
133	Petrol station storage tanks (leaded petrol)	0.019	32.842	0.006	165	Refineries_Petroleum coke	0.005	29.962	0.002
134	Iron & steel industry_Natural gas	0.022	28.133	0.006	166	Wine manufacture	0.005	30.562	0.001
135	Petrol terminal storage (leaded petrol)	0.018	33.047	0.006	167	Railways (Regional)_Gas oil	0.003	45.168	0.001
136	Printing (other offset)	0.017	34.616	0.006	168	Other industrial combustion_LPG	0.005	28.078	0.001
137	Sinter plant_Coke	0.019	29.252	0.006	169	Solvent & oil recovery	0.026	5.324	0.001
138	Domestic combustion_Burning oil	0.024	21.499	0.005	170	Public services_Sewage gas	0.007	19.328	0.001
139	Ship purging	0.139	3.385	0.005	171	Autogenerators_Coal	0.003	42.370	0.001
140	Sewage sludge incineration	0.012	36.077	0.004	172	Public services_Gas oil	0.006	23.915	0.001
141	Cement (Non-decarbonising)	0.101	4.245	0.004	173	Other industrial combustion_Coal	0.004	30.016	0.001
142	Petrol stations (spillages of leaded petrol)	0.012	33.006	0.004	174	Refineries_Natural gas	0.003	28.092	0.001
143	House & garden machinery_DERV	0.009	45.127	0.004	175	Glass (glass wool)	0.010	9.528	0.001
144	Iron & steel industry_Blast furnace gas	0.015	23.696	0.004	176	Ammonia combustion_Natural gas	0.003	27.587	0.001
145	Power stations_Sewage gas	0.017	19.683	0.003	177	Miscellaneous_Gas oil	0.003	24.352	0.001
146	Printing (metal decorating)	0.007	47.133	0.003	178	Other industrial combustion_Fuel oil	0.004	19.206	0.001
147	Spirit manufacture (casking)	0.010	30.262	0.003	179	Other industrial combustion_Coke-oven gas	0.002	48.867	0.001
148	Surface cleaning (tetrachloroethylene)	0.098	3.085	0.003	180	Glass (continuous filament glass fibre)	0.004	18.878	0.001
149	Aircraft support_Gas oil	0.006	45.591	0.003	181	Iron & steel (Flaring)_Coke-oven gas	0.001	48.976	0.001
150	Blast furnaces_Coke-oven gas	0.006	49.495	0.003	182	Gas separation plant_OPG	0.002	30.453	0.001
151	Coastal shipping_Fuel oil	0.007	40.090	0.003	183	Lime production_Natural gas	0.002	27.723	0.001
152	Refineries_Fuel oil	0.013	19.574	0.003	184	Railways (Stationary sources)_Natural gas	0.002	27.628	0.001
153	Other industrial combustion_Gas oil	0.010	24.529	0.002	185	Iron & steel (Flaring)_Blast furnace gas	0.002	23.533	0.001
154	Brewing (fermentation)	0.008	30.044	0.002	186	Other industrial combustion_OPG	0.002	30.248	0.001
155	Surface cleaning (dichloromethane)	0.057	3.959	0.002	187	Domestic combustion_LPG	0.002	27.532	0.001
156	Gas production_Natural gas	0.007	27.846	0.002	188	Other industrial combustion lubricants	0.002	24.447	0.000

	Source Category	Percentage of total Emissions	Incremental Reactivity	Ozone Production, ppb		Source Category	Percentage of total Emissions	Incremental Reactivity	Ozone Production, ppb
189	Iron & steel industry_Fuel oil	0.003	19.642	0.000	219	SSF production_Coke	0.000	29.648	0.000
190	Agriculture_Natural gas	0.001	27.191	0.000	220	Other industrial combustion_Colliery methane	0.000	27.587	0.000
191	Miscellaneous_Landfill gas	0.002	19.874	0.000	221	Iron & steel industry_Coke	0.000	30.139	0.000
192	Power stations_Sour gas	0.002	20.830	0.000	222	Railways (Stationary sources)_Burning oil	0.000	24.447	0.000
193	Domestic combustion_Gas oil	0.001	22.045	0.000	223	Public services_Burning oil	0.000	24.297	0.000
194	Public services_Fuel oil	0.002	19.274	0.000	224	Miscellaneous_Burning oil	0.000	23.942	0.000
195	Public services_Coal	0.001	29.429	0.000	225	Agriculture_Fuel oil	0.000	19.997	0.000
196	Power stations_Fuel oil	0.002	19.465	0.000	226	Miscellaneous_Coal	0.000	29.757	0.000
197	Agriculture_Gas oil	0.001	23.969	0.000	227	Collieries_Coal	0.000	30.098	0.000
198	Iron & steel industry_Gas oil	0.001	23.956	0.000	228	Agriculture_Coal	0.000	30.044	0.000
199	Cider manufacture	0.001	30.685	0.000	229	Lime production_Coke	0.000	29.825	0.000
200	Other industrial combustion_Coke	0.001	30.207	0.000	230	Domestic combustion_Fuel oil	0.000	21.731	0.000
201	Power stations_Gas oil	0.001	24.625	0.000	231	Coke production_Natural gas	0.000	27.942	0.000
202	Coal, tar & bitumen processes	0.003	7.330	0.000	232	Iron & steel industry_Coal	0.000	29.962	0.000
203	Coke production_Blast furnace gas	0.001	22.782	0.000	233	Gas separation plant_LPG	0.000	27.805	0.000
204	Blast furnaces_Natural gas	0.001	27.764	0.000	234	Collieries_Natural gas	0.000	27.914	0.000
205	Miscellaneous_MSW	0.000	35.299	0.000	235	Agriculture_Straw	0.125	0.000	0.000
206	SSF production	0.001	18.810	0.000	236	Crematoria	0.000	0.000	0.000
207	Clinical waste incineration	0.000	36.213	0.000	237	Electric arc furnaces	0.023	0.000	0.000
208	Refineries_Gas oil	0.000	23.874	0.000	238	Power stations_Poultry litter	0.002	0.000	0.000
209	Miscellaneous_Fuel oil	0.001	19.629	0.000	239	Printing (other inks)	0.022	0.000	0.000
210	Collieries_Colliery methane	0.000	27.805	0.000	240	Brewing (wort boiling)	0.002	0.000	0.000
211	Gas production_LPG	0.000	27.491	0.000	241	Fletton brick manufacture	0.126	0.000	0.000
212	Refineries_LPG	0.000	27.873	0.000	242	Other food (animal feed manufacture)	0.725	0.000	0.000
213	Other industrial combustion_SSF	0.000	39.708	0.000	243	Other food (coffee roasting)	0.004	0.000	0.000
214	Refineries_Naphtha	0.000	30.289	0.000	244	Other food (margarine & other solid fats)	0.383	0.000	0.000
215	Domestic combustion_Burning oil (premium)	0.000	21.704	0.000	245	Other food (meat, fish & poultry)	0.079	0.000	0.000
216	Lime production_Coal	0.000	29.839	0.000	246	Other food (sugar production)	0.002	0.000	0.000
217	Iron & steel industry_LPG	0.000	27.477	0.000	247	Rolling mills (cold rolling)	0.007	0.000	0.000
218	Refineries_Refinery miscellaneous	0.000	30.248	0.000	248	Rolling mills (hot rolling)	0.001	0.000	0.000

Note: Incremental reactivity is the increase in ozone following the fractional increase in VOC emissions divided by the fractional increase in VOC emissions.